

Phytochemical Investigations of Costa Rican Marcgraviaceae and
Development of Insecticide Synergists

Ana Francis Carballo-Arce

Lic., Universidad Nacional Autónoma de Costa Rica, Costa Rica. 2005

Thesis submitted to the
Faculty of Graduate and Postdoctoral Studies
in partial fulfillment of the requirements
for the Doctorate in Philosophy degree in Chemistry

Chemistry Department

Faculty of Science

University of Ottawa

Dedication

....To my family

Table of contents

AKNOGWLEDGMENTS	i
List of figures	iii
List of Schemes	viii
List of tables	ix
List of abbreviations and Symbols	xi
Abstract	xiii
1 Abstract	xv
1 General Introduction and Literature Review.....	1
1.1 Natural products as a source of inspiration for chemistry	1
1.2 Plant derived drugs and medicinal chemistry	6
1.3 Natural Health Products	9
1.4 References	12
2 Phytochemistry of the family Marcgraviaceae.....	15
2.1 Introduction.....	15
2.2 A validated HPLC-APCI-MS/MS method for the quantification of pentacyclic triterpenes of <i>Souroubea sympetala</i>	22
2.2.1 Introduction	22
2.2.2 Results and discussion	22
2.2.3 Experimental	39
2.2.4 References	41
2.3 Untargeted metabolomic analysis of <i>Souroubea sympetala</i> and <i>Souroubea gilgii</i> , by UPLC-QTOF	44

2.3.1	Introduction	44
2.3.2	Results and discussion	48
2.3.3	Experimental	55
2.3.4	Future work.....	57
2.3.5	References	57
2.4	Characterization of Marcgraviaceae species from Costa Rica	59
2.4.1	Introduction	59
2.4.2	Results and discussion	60
2.4.3	Experimental	72
2.4.4	Conclusions and future work	74
2.4.5	References	75
2.5	Bioassay guided isolation of a bacterial quorum sensing inhibitor from <i>Marcgravia nervosa</i> (Marcgraviaceae) from Costa Rica	77
2.5.1	Introduction	77
2.5.2	Results and Discussion	80
2.5.3	Experimental Section.	94
2.5.4	Conclusion and future work.....	97
2.5.5	References	98
3	Section II: Organic synthesis.....	102
3.1	Synthesis of Dillapiol analogs as potential synergists for pesticides	102
3.1.1	Introduction	102
3.1.2	Results and discussion	109
3.1.3	Experimental	157
3.1.4	References	194

4.1 Towards the design of Cx30, Cx36 and Cx43 blockers as potential spinal cord injury treatments	199
4.1.1 Introduction	199
4.1.2 Results and Discussion	202
4.1.3 Conclusions and further work.....	213
4.1.4 Experimental	215
4.1.5 References:	220
Claims to Original Research.....	222
Appendix	224

AKNOGWLEDGMENTS

Foremost, I would like to express my sincere gratitude to my advisors Prof. Tony Durst and Prof. John Thor Arnason for the continuous support of my Ph.D. study and research, for their patience, motivation, enthusiasm, and immense knowledge. Their guidance and help during all the time of my research and the writing of this thesis.

I will like to thank, the multiple collaborators in my research: Professor Zul Merali and Msc. Chris Cayer (Institute of Mental Health Research) for all the bioassays in animal models for the antianxiety test. Dr. Ian Scott (Agricultural Canada) and PhD candidate Suqi Liu for all the bioassay results with CYP 3A4 inhibition, and the *in vivo* test with insects, which has helped in the optimization of a more potent dillapiol analog. Professors Marco Otarola, Luis Poveda, and Pablo Sanchez (Universidad Nacional Autonoma de Costa Rica), for the collection and identification of all the plants from Costa Rica, without their valuable knowledge and enthusiasm my plant collection would not have been possible. PhD. Candidate Marco Rocha (Universidade Federal do Rio doe Janeiro) for bringing his Marcgraviaceae samples from Brazil and the collaboration doing all the chemometric work on this family of plants. Professor Stephanie Bennett and M.Sc. Student Matthew Cooke for all the work on the bioassays for the connexin blockers project, their serendipity finding of the unique activity of one of our library compounds has led to a very interesting project. Dr. Ammar Saleem for all his instuction in analytical techniques and metabolomics.

Dr. Kim Colson, Dr. Jimmy Yuk and all the other members of the team, (R&D division of Bruker BioSpin) for all their help and training for the use of NMR techniques in the quantification of metabolites and plant metabolomics. Rui Liu, for all his help in the bioassays and in the use of HPLC equipment. Dr. Antonio Guerrero, for all the teachings on phytochemistry and being there went I needed someone to talk. Dr. Asim Muhamad, for training in synthesis.

To all the Durst group members: Linda, Ana, Christine, Daria, Ousamma, Karen, Ana Maria, Victoria, Diddier, Anthony, Sherif, Hudda, Jeremie, Emma, Trevor, Irene and Amanda. To all the

members of Dr. Arnson group: Chieu Anh, Brendan, Caroline, Martha, Andrew, Fida, Jonathan, San, Jake and Gabriel.

Special thanks to Ana G. for reading my entire thesis more than once, and be always there went I needed, to Christine to run the last yard by my side. Luis and Ata for listening and support. Mary Durst for her hospitality and support.

I have to thank all my sponsors without their funding my studies and research would not have been possible: Consejo Nacional de Ciencia y tecnologia, CONICIT, Costa Rica. Universidad Autonoma de Costa Rica, UNA. Organizacion de Estados Americanos (American State Organization) OEA. The CREATE- NSERC program. Bioniche, Bruker, BASF,

Lastly, I will like to thank my husband Greg for always being there no matter what, and even learn how to use chemistry software, my wonderfull son Andres for his encouragement and understanding.

For holding my hand:

"Trust in the Lord with all your heart, and lean not on your own understanding; in all your ways acknowledge Him, and He shall direct your paths."

(Proverbs 3:5-6)

List of figures

Figure 1.1: Drugs obtained by rational design.....	1
Figure 1.2: Nature as a source of inspiration of unique hit compounds	4
Figure 1.3: All New Chemical Entities, 01/1981-06/2006, by source (N=1184).	5
Figure 1.4: Chemical process for natural product discovery ¹⁵	7
Figure 1.5: Plant drug development from medicinal chemistry perspective ³⁴	8
Figure 2.1: Phylogenetic of Marcgraviaceae, adapted from Ward et Al. ³	16
Figure 2.2: Geographical distribution for the plant collection in Costa Rica	18
Figure 2.3: Pentacyclic triterpenes identified in <i>Souroubea sympetala</i>	19
Figure 2.4: Chromatographic separation of selected triterpenes of <i>S. sympetala</i> . Positive ionisation A (1-2) detection. B Negative ionization (3-5)	24
Figure 2.5: Chromatographic separation of marker compounds in a crude extract of leaf <i>S. sympetala</i> . Negative ionization A (3-5), Positive ionization B (1-2) detection.	31
Figure 2.6: Mean content of five triterpenes in A. stems, B. Leaf of <i>S. sympetala</i> from two different locations in Costa Rica (n=5)	32
Figure 2.7: Chromatographic separation of marker compounds in a crude extract of leaf <i>S. gilgii</i> . Negative ionization A (3-5), Positive ionization B (1-2) detection.....	33
Figure 2.8: HPLC-DAD profiles of leaf extracts of <i>Souroubea</i> spp.	34
Figure 2.9: Mean content of five pentacyclic triterpenes in stem (A) and leaf (B) of <i>Souroubea gilgii</i>	35
Figure 2.10: Content of betulinic acid in two species of <i>Souroubea</i> from two locations from Costa Rica	36
Figure 2.11: Comparison of relative sensitivities of various analytical techniques used in metabolomic experiments ³ . L.I.F (Laser induced fluorescence).....	46
Figure 2.12: LC-DAD profile of crude leaf extracts of <i>Souroubea</i> spp.	47
Figure 2.13: Geographical distribution of the plant collection for <i>Souroubea</i> spp.	48
Figure 2.14: Variation of the production of metabolites in <i>S. sympetala</i> according with the collection season, using HPLC-DAD as analytical method	50

Figure 2.15: OPLS-DA score plot of twenty-four samples of <i>Souroubea</i> spp. samples. Group A corresponds to <i>S. gilgii</i> samples, group B to <i>S. sympetala</i> samples	51
Figure 2.16: OPLS-DA score plot of twenty four samples of <i>Souroubea</i> spp. samples.....	52
Figure 2.17: Score plot of the OPLS-DA scores for the two clusters corresponding to two <i>Souroubea</i> species.....	54
Figure 2.18: S-plot for the corresponding OPLS-DA loadings calculated for the <i>Souroubea</i> spp. samples.....	55
Figure 2.19: Distribution of metabolite SGN1 in <i>Souroubea</i> spp. samples.....	55
Figure 2.20: Example of a characteristic HPLC-UV herbal fingerprint of pericarpium <i>Citrus reticulatae</i> with some identified marker compounds.....	60
Figure 2.21: Standard mix of six pentacyclic triterpenes used in the development of fingerprints of Marcgraviaceae members. The extracts were separated on a Kinetex C18 column using a linear gradient of 30-100% acetonitrile in water	63
Figure 2.22: Fingerprints of six different Marcgraviaceae species.....	64
Figure 2.23: Comparison of the metabolic profiles of two species of <i>Schwartzia</i> from Costa Rica	65
Figure 2.24: Comparison of the metabolic profiles of three species of <i>Souroubea</i> from Costa Rica	66
Figure 2.25: Comparison of the metabolic profile of two samples: red un-identified sample, and green: <i>M. globulosomarginata</i>	66
Figure 2.26: Standard mix chromatogram with the incorporation of four new standards	68
Figure 2.27: OPLS-DA score plot for the Marcgraviaceae samples the circles indicate species pairs that were similar and submitted for S plot identification of unique phytochemical markers	68
Figure 2.28: S-plots for Marcgraviaceae species that cluster together in the OPLS-DA score plot.	69
Figure 2.29: Content of pentacyclic triterpenes in leaf extracts of eleven genera of Marcgraviaceae: A. Betulin, B. Ursolic acid, C. Lupeol, D. α -Amyrin, E. Betulinic acid, F. β -Amyrin,	

Betulinic acid and the Amyrins have been linked to the bioactivity observed in Souroubea extracts ^{9,12}	71
Figure 2.30: Comparison of mean content of betulinic acid, β -Amyrin and α - Amyrin in thirteen species of Marcgraviaceae	72
Figure 2.31: Leaf and flower of <i>M. nervosa</i> 1-3.....	77
Figure 2.32: Essential steps in biofilm formation ¹	79
Figure 2.33: Fractionation of <i>M. nervosa</i> leaf	81
Figure 2.34: Effect of leaf extracts of <i>Marcgravia nervosa</i> in the anti-Quorum sensing and antifungal bioassay at a maximum concentration of (1mg /disc), tested in disc diffusion assay in <i>C. violaceum</i> and anti- fungal activity in <i>S. cerevisiae</i> . Each value is the mean \pm SEM (n=3) in each group.....	82
Figure 2.35: Quorum sensing and antifungal activity of <i>M. nervosa</i> extracts, (1mg/disc) Photographs by Chieu Ahn Ta.	83
Figure 2.36: ¹ H NMR, spectrum of 2-methoxy-1,4-naphthoquinone isolated from <i>M. nervosa</i> (400MHz, CDCl ₃)	84
Figure 2.37: ¹³ C NMR, spectrum of 2-methoxy-1,4-naphthoquinone isolated from <i>M. nervosa</i> (400MHz, CDCl ₃)	84
Figure 2.38: Triterpenoid metabolites from <i>M. nervosa</i> leaf extract.....	88
Figure 2.39: Mean content of pentacyclic triterpenes in ethanolic leaf extracts of <i>M. nervosa</i> ..	91
Figure 2.40: NMR analysis of crude extracts of three different plant collections of <i>M. nervosa</i> , at two locations in Costa Rica.....	92
Figure 2.41: UPLC-DAD-MS data of the ethanolic extract of <i>M. nervosa</i> leaf from Rio Pacuare, dry season	93
Figure 2.42: Halogenated furanones in <i>D. pulchra</i> ³⁴	98
Figure 3.1 : Active metabolites in some of the commonly used botanical pesticides.....	104
Figure 3.2: Other bioactive secondary metabolites present in <i>Piper</i> species	105
Figure 3.3: A. geographical distribution of <i>Piper aduncum</i> L., B. Leaves and fruit of <i>Piper aduncum</i> L.	106
Figure 3.4: Methylenedioxyphenyl compounds used as pesticide synergists.....	107

Figure 3.5: Schematic representation of pesticide resistance development in insect populations. This phenomenon is known as the “pesticide treadmill”	108
Figure 3.6: Safrol analogs used as pyrethrines synergists	110
Figure 3.7: IUPAC numbering system for the benzo-1,3- dioxole group.	114
Figure 3.8: ^1H -NMR spectrum of “crude” essential oil-mainly dillapiol 400MHz, CDCl_3	115
Figure 3.9: 300 MHz ^1H -NMR Spectrum of compound 2 in CDCl_3	120
Figure 3.10: Dillapiol esters synthesized by the two methods described in	122
Figure 3.11: 400 MHz ^1H -NMR Spectrum of compound 22 in CDCl_3	124
Figure 3.12: A ABX system in dillapiol analogs B, AB systems over the benzo-1,3- dioxole group	125
Figure 3.13: 400 MHz ^1H -NMR Spectrum of compound 30 in CDCl_3	126
Figure 3.14: 400 MHz ^1H -NMR Spectrum of compound 35 in CDCl_3	128
Figure 3.15: 400 MHz ^{13}C -NMR Spectrum of compound 35 in CDCl_3	129
Figure 3.16: 400 MHz ^1H -NMR Spectrum of compound 14 in CDCl_3	130
Figure 3.17: 400 MHz ^1H -NMR Spectrum of compound 16 in CDCl_3	131
Figure 3.18: 400 MHz ^1H -NMR Spectrum of compound 33 in CDCl_3	133
Figure 3.19: Esters of the corresponding sesamol alcohols in Table 3.1.2.3	138
Figure 3.20: 400 MHz ^1H -NMR Spectrum of compound 56 in CDCl_3	140
Figure 3.22: 400 MHz ^1H -NMR Spectrum of compound 58 in CDCl_3	142
Figure 3.23: Results for the <i>in vivo</i> bioassays A. Topical application of selected analogs, B. Ingested application of selected analogs.	155
Figure 3.24: Selected MDP analogs for <i>in vivo</i> model using Colorado Potato Beetle (<i>L. decemlineata</i>)	156
Figure 3.25: Compounds that will be evaluated for anti-cancer activity.....	157
Figure 3.26: Clevenger apparatus - volatile Oil Distilling Apparatus (Heavier than Water)	159
Figure 4.1: A. schematic representation of the gap junction B. Topological model of a connexin. Figure from ref ⁶	199
Figure 4.2: Effect of compound 187 on connexin channel function in NT2/D1 cells. (A) The parachute assay was used to assess gap junctional intercellular communication (GJIC). (B)	

Connexin hemichannel (single membrane channel) function was assessed by measuring the number of cells capable of spontaneous uptake of Lucifer yellow through hemi-channels in a low calcium medium. The image belongs to Mathew Cook's MSc. thesis research¹³205

Figure 4.3: 400 MHz ¹H-NMR Spectrum of compound **3** in CDCl₃208

Figure 4.4: The correct structure for compound **3** (187) according to the x-ray analysis. Appendix 4A209

Figure 4.5: 400 MHz ¹³C-NMR Spectrum of compound **3** in CDCl210

Figure 4.6: Bioassay result summary, A. Change in gap junctional intercellular communication, B Anionic activity in hemi-channels, C Cationic activity in hemi-channels.213

List of Schemes

Scheme 3.1: General detoxification pathways for most insecticides ³²	108
Scheme 3.2: Oxidations of MDP compounds by CYP-450 enzymes.	109
Scheme 3.3: Synthesis of dillapiol analogs 2, 3 and 4.	116
Scheme 3.4: Proposed mechanism for the formation of compound 5.	118
Scheme 3.5: Synthesis of compound 6 and 7.	119
Scheme 3.6: Synthesis of alcohols 8 and 9	121
Scheme 3.7: Esterification via acyl chloride intermediates	121
Scheme 3.8: Steglich Esterification.....	122
Scheme 3.9: Synthesis of dillapiol derived ethers	132
Scheme 3.10: Synthesis of dillapiol analogs 33 and 34	134
Scheme 3.11: Dillapiol and safrol analogs obtained by hydroformylation.....	134
Scheme 3.12: General mechanism for hydroxiformylation of terminal alkenes according with Rosales and co-workers ⁵⁰	135
Scheme 3.13: Synthesis of allyl intermediates from sesamol	136
Scheme 3.14: Synthesis of piperonal analog 55	139
Scheme 3.15: Synthesis of piperonal analogs 56 and 57.....	141
Scheme 3.16: Synthesis of compounds 58	142
Scheme 3.17: Formation of fluorescein benzyl ester by CYP metabolism ⁵⁶	143
Scheme 4.1: Synthesis of compound 187.....	203
Scheme 4.2: Synthesis of analog 3	209
Scheme 4.3: Synthesis of compounds 7 and 8.	211

List of tables

Table 2.2.1.1: Distribution of Marcgraviaceae species in the Neotropics ²	15
Table 2.2.2.1: Structural family, functional groups and molecular weight of the pentacyclic triterpenes quantified in stem and leaf of <i>S. sympetala</i>	23
Table 2.2.2.2: Chromatographic and spectrometric data of pentacyclic triterpenes.....	25
Table 2.2.2.4: Linearity and range of the calibration curve of triterpenes under study	25
Table 2.2.2.5: Limits of detection (LOD, 3:1 signal to noise) and limits of quantification (LOQ, 10:1 signal to noise), of each marker on column (6 x standard deviation) in leaf and stem of <i>S. sympetala</i>	26
Table 2.2.2.6: Recovery of selected pentacyclic triterpenes from leaves and stems of <i>S. sympetala</i>	27
Table 2.2.2.7: Intraday and interday variation in quantitative results.....	27
Table 2.2.2.8: Collection sites for <i>Sourobea sympetala</i> samples included in the study (vouchers are held at JVR herbarium, Universidad national, Heredia, Costa Rica).....	29
Table 2.2.2.9: Quantification (mg of compound/g of dried plant) of five pentacyclic triterpenes in leaf and stems of representative <i>S. sympetala</i> accessions.....	30
Table 2.2.2.10: Physical description of the two collection sites.....	32
Table 2.2.2.11: Mean and SEM (mg of compound/g of dried plant) of five pentacyclic triterpenes in leaf and stems of representative <i>S. gilgii</i> accessions.....	37
Table 2.2.2.12: Collection sites for <i>Sourobea gilgii</i> samples included in the study (vouchers are held at JVR herbarium, Universidad national, Heredia, Costa Rica).....	38
Table 2.3.2.1: Sample information for sample collection of <i>Sourobea</i> spp.....	49
Table 2.3.2.2: Putative markers found in <i>S. gilgii</i>	54
Table 2.4.2.1: Meta data for the Marcgraviaceae plant collection	62
Table 2.5.2.1: Marcgraviaceae species evaluated in the bioassays.....	80
Table 2.5.2.2: Proton (¹ H) and carbon ¹³ C data for bioactive compound isolated from <i>M. nervosa</i> . Comparison with data published for 4-methoxy-1,4-naphthoquinone, 1.	86
Table 2.5.2.3: Meta data for the plant collection of <i>M. nervosa</i>	89

Table 2.5.3.1: Percentage yield of extraction for different <i>M. nervosa</i> collection using ethanol:water (9:1)	95
Table 2.5.3.2: Column chromatography of ethanolic partition of <i>M. nervosa</i> leaf (MNE). Crude extract applied in column 14.67g.	95
Table 3.1.1.1: Major botanical products use for pest control	103
Table 3.1.2.1: Yield of extraction for fresh <i>P. aduncum</i> tissues, all samples were collected during dry season 2011	113
Table 3.1.2.2: Reaction yields for the ester analogs of dillapiol.....	123
Table 3.1.2.3: Reaction yields of sesamol alcohol analogs.....	137
Table 3.1.2.4: IC ₅₀ values for 5-alkoxy-6-allyl sesamol derivatives arranged in order if increasing log P.....	145
Table 3.1.2.5: IC ₅₀ values for alkyl esters from dillapiol arranged in order of increasing IC ₅₀	147
Table 3.1.2.6: IC ₅₀ values for benzylic and aromatic esters from dillapiol arranged in order of increasing IC ₅₀	149
Table 3.1.2.7: IC ₅₀ values for benzylic and aromatic esters from dillapiol arranged in order of increasing IC ₅₀	151
Table 3.1.2.8: IC ₅₀ values for the best analogs developed	153
Table 3.1.3.1: Voucher number for <i>P. aduncum</i> sample collection	159
Table 4.1.1.1: Roles played by hemi-channels, connexins and Gap-junction in different organs, adapted from <i>Kar et Al. 2012</i> ⁸	201

List of abbreviations and Symbols

Ac	acetyl
Ac ₂ O	Acetic anhydride
ACN	acetonitrile
APCI	Atmospheric Pressure chemical ionization
Br	broad
°C	degrees celcius
¹³ C NMR	Carbon-13 Nuclear Magnetic Resonance
CH ₂ Cl ₂ , DCM	Dichloromethane
Cx	Connexin
DCC	Dicyclohexylcarbodiimide
Dd	doublet of doublets
DEPT	Distortionless Enhancement Polarization Transfer
DMAP	4-Dimethylaminopyridine
DMF	Dimetyl formamide
DMSO	Dimethyl sulfoxide
Dt	doublet of triplets
ECB	Europena Corn Borer
EI	electronic ionization
EPM	Elevated Plus-maze
equiv.	equivalents
Et ₂ O	diethyl ether
Et ₃ N	triethylamine
EtOAc	Ethyl acetate
EtOH	ethanol
GJ	Gap Junction
GJIC	Gap Junction intercellular communication
h	hours
¹ H NMR	Proton Nuclear Magnetic Resonance
HPLC	high Performance liquid Chromatography
HRMS	High resolution Mass spectroscopy
Hz	Hertz
IC ₅₀	half maximal inhibitory concentration
J	coupling constant
LOD	limit of detection
LOQ	limit of quantification
meOH	methanol
M	Multiplet
Ph	Phenyl
PMSO	Plosubstrate monooxygenase

ppm	parts per million
q	Quartet
QS	Quorum sensing
QSAR	Quantitative Structure-Activity relationship Study
QTOF	Quadrupole Time of Flight
RT	room temperature
s	Singlet
SAR	Structure-Activity relationship Study
spp.	Species
t	Triplet
TEA	triethanol amine
THF	tetra Hydrofuran
TLC	thin Layer Chromatography
WHO	World Health Organization

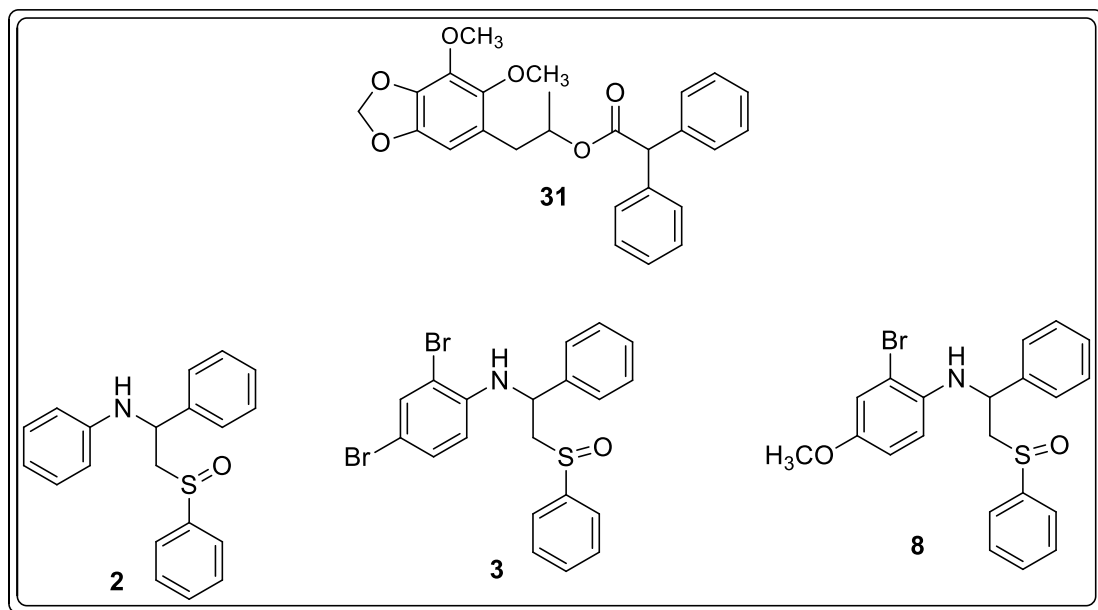
Abstract

Substances of natural and synthetic origin were studied using analytical, bioassay guided isolation, metabolomics and medicinal chemistry techniques. In a section focused on the plant family Marcgraviaceae, a validated method for the quantification of six pentacyclic triterpenes (α and β Amyrin lupeol, ursolic acid, betulin and betulinic acid) in the *Souroubea* spp was developed. Quantification of the triterpenes in the crude extracts was achieved using HPLC-APCI mass selective detection. The calibration curves for the five triterpenes evaluated were highly linear ($r^2 > 0.993$) and percentage recovery from spiked samples were greater than 94% for all compounds. The LOD for betulinic acid was 0.01 μg for betulinic acid on column and LOQ was 0.03 μg . The method was successfully applied to 41 crude extracts from leaf and stem of *Souroubea* spp, from two locations in Costa Rica. The method is suitable for quality control of raw materials used in the manufacture of natural health products. The use of modern metabolomic techniques, UHPLC-QTOF allowed the identification of five putative makers that can potentially be used in distinguishing between the two *Souroubea* species.

The validated method was used in the quantification of the above triterpenes in a total of thirteen Marcgraviaceae species collected in Costa Rica. It was established that betulinic acid and β - Amyrin could be used as makers for this family of tropical vines. These same thirteen plants extracts were evaluated in antifungal and quorum sensing inhibition bioassays. *Marcgravia nervosa* was the only species that showed significant activity in both bioassays. Bioassay guided fractionation of the crude ethanolic extract of *M. nervosa* led to the identification of 2-methoxynaphthoquinone as the bioactive compound responsible for the bioactivity. The crude leaf ethanolic extract from *M. nervosa* showed a significant inhibition of QS comparable or somewhat better than *D. pulchra* extracts with the *M. nervosa* extract showing stronger inhibiting QS with a halo of 21.8mm, more than *D. pulchra* extracts which generated a halo of 15.9mm. The active quinone has a MIC of 85 μM against *Saccharomyces cerevisia*BY4741 (haploid) and 100 μM against *Saccharomyces cerevisiae* BY4743 (diploid) compared to berberine (positive control) with a MIC 600 μM for both strains. This quinone is not present in any of the other twelve species of Marcgraviaceae available to us.

In work focusing on organic synthesis, a total of 57 semi-synthetic derivatives of dillapiol, safrol and piperonal were prepared and evaluated for their inhibitory activity in a CYP 3A4 bioassay to assess their potential use as pesticide synergists. The synergistic activity of dillapiol has been improved 45 fold; analog **31** has an $IC_{50} = 0.2 \mu\text{M}$ compared with dillapiol $IC_{50} = 9.18 \mu\text{M}$. A number of other compounds structurally related to **31** showed similar levels of activity.

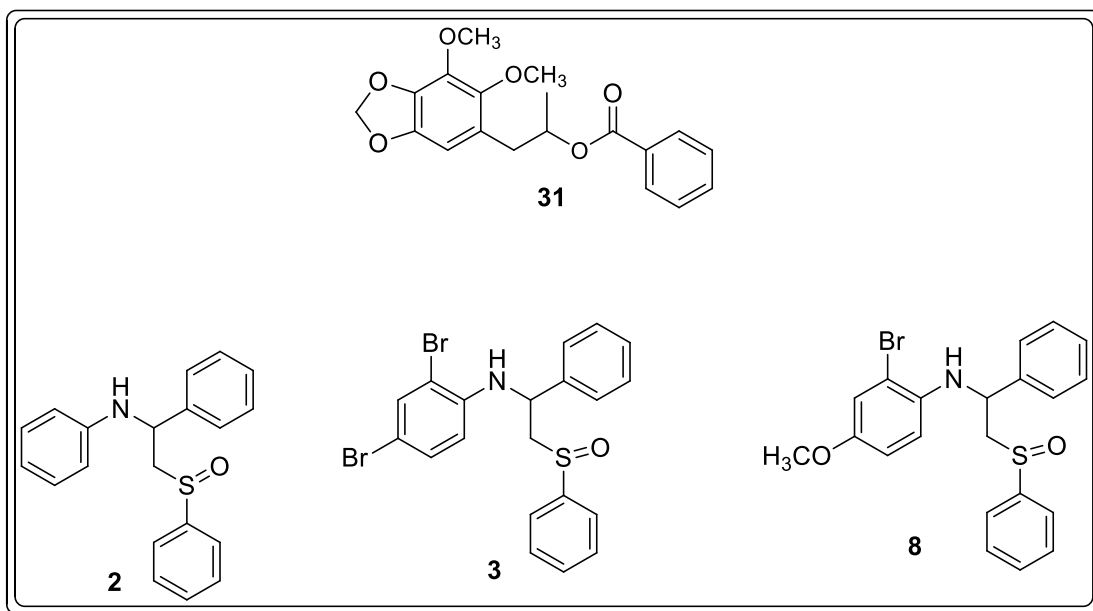
A screening of a compound library identified the amino sulfoxide **3** as a potential lead for the design of a selective connexin blocker with potential application in the treatment of spinal cord injuries. The use of X-ray crystallography permitted the correction of the original structure assigned to **3**. Once the structure was corrected a total of 6 analogs were prepared. Compound **3** has the highest inhibition of GJIC whereas compound **8** and compound **2**, reduced anionic hemi-channel activity. Compound **2** also reduced the cationic activity of the hemi-channels.



1 Abstract

Une méthode validée pour la quantification des six triterpènes pentacycliques (α et β Amyrines, lupeol, l'acide ursolique, betulin et l'acide bétulinique) présents chez *Souroubea* spp a été développée. La quantification de ces triterpènes dans les extraits bruts a été réalisée en utilisant une détection sélective de masse par HPLC-APCI. Les courbes d'étalonnage étaient hautement linéaires ($r^2 > 0,993$) et la récupération des échantillons contenant un étalon interne était supérieure à 94% pour tous les composés. La limite de détection pour l'acide bétulinique était de 0,01 mg dans la colonne et sa limite de quantification était de 0,03 mg. La méthode a été appliquée à 41 extraits bruts de feuilles et de tiges de *Souroubea* spp provenant de deux localisations au Costa Rica. La méthode est adaptée pour le contrôle qualité des matières premières utilisées dans la fabrication de produits naturels de santé. L'utilisation de techniques modernes métabolomiques, UHPLC-QTOF, a permis l'identification de cinq marqueurs qui peuvent potentiellement être utilisés pour distinguer les deux espèces de *Souroubea*. La méthode validée a également été utilisée pour la quantification des triterpènes ci-dessus présents chez treize autres membres de Marcgraviaceae recueillis au Costa Rica. Il a été établi que les acides β -Amyrine et bétulinique pourraient être utilisés en tant que marqueurs pour cette famille de vignes tropicales. Ces mêmes treize extraits de plantes ont été évalués dans des essais biologiques d'inhibition antifongiques et de détection du quorum (QS). *Marcgravia nervosa* était la seule espèce à montrer une activité significative dans les deux essais biologiques. L'essai biologique, réalisé par fractionnement de l'extrait éthanolique brut de *M. nervosa*, a conduit à l'identification de la 2-méthoxynaphthoquinone comme étant le composé bioactif. L'extrait d'éthanol brut des feuilles de *M. nervosa* a montré une inhibition de QS significative, comparable aux extraits de *D. pulcra*, avec des halos respectifs de 21,8 mm et de 15,9 mm. La quinone active a une CMI de 85 μ M contre *Saccharomyces cerevisia* BY4741 (haploïde) et 100 μ M contre *Saccharomyces cerevisiae* BY4743 (diploïde), comparé à la berbérine (témoin positif) avec 600 μ M pour les deux souches. Cette quinone n'est présente dans aucune des douze autres espèces de Marcgraviaceae étudiées. Un total de 57 dérivés semi-synthétiques de dillapiol, safrol et piperonal ont été préparés et leur activité d'inhibition a été testée dans un essai biologique CYP 3A4 afin d'évaluer leur potentielle utilisation comme

synergiques des pesticides. L'activité synergique de dillapiol a été améliorée 45 fois, l'analogue **31** a un IC_{50} de 0,2 μM comparé à dillapiol dont l' IC_{50} est de 9,18 μM . Un certain nombre d'autres composés structurellement liés à **31** ont démontré des niveaux d'activité similaires. À ce jour, il n'a pas été possible de développer un modèle QSAR viable. Un criblage de composés de bibliothèque a identifié l' amino sulfoxide **3** comme potentiel composé de départ pour la conception d'un inhibiteur de connexine, utilisée dans le traitement des lésions de la moelle épinière. L'utilisation des rayons X a permis la correction de la structure d'origine attribuée à **3**. Une fois que la structure a été corrigée, 6 analogues ont été préparés. Le composé **3** a la plus forte inhibition de la jonction des communications intercellulaires, tandis que les composés **2** et **8** ont diminué l'activité anionique de l'hémi-canal. Le composé **2** a également réduit l'activité cationique des hémi-canaux.



1 General Introduction and Literature Review

“Most drugs were discovered rather than developed”¹.

1.1 Natural products as a source of inspiration for chemistry

Throughout the ages nature has provided humankind with its key needs: clothing, food, shelter, tools and medicine. The first records of the use of plants for the treatment of different diseases comes from the Babylonian (ca. 2600 B.C.), ancient Chinese and Egyptian civilizations²⁻⁴. In the beginning mainly whole plant preparations were used. The use of plants and plant derived drugs has evolved through time and by the early 19th century the isolation of active principal from plants was achieved. The discovery of bioactive compounds in plants led to the use of pure compounds as drugs, in their original form as well as leads for modified structures⁵.

Most of the current emphasis in the development of new drugs by the pharmaceutical industry is described as rational design based on the discovery and understanding of cellular mechanisms and disease pathways combined with high throughput screening. It can be divided into two general approaches: 1. Ligand-based and 2. Structure-based, drug design. The use of these approaches has led to a number of important new drugs (**Figure 1-1**) including Gleevec™⁶⁻⁸, Tamoxifen⁹ and Raloxifene¹⁰.

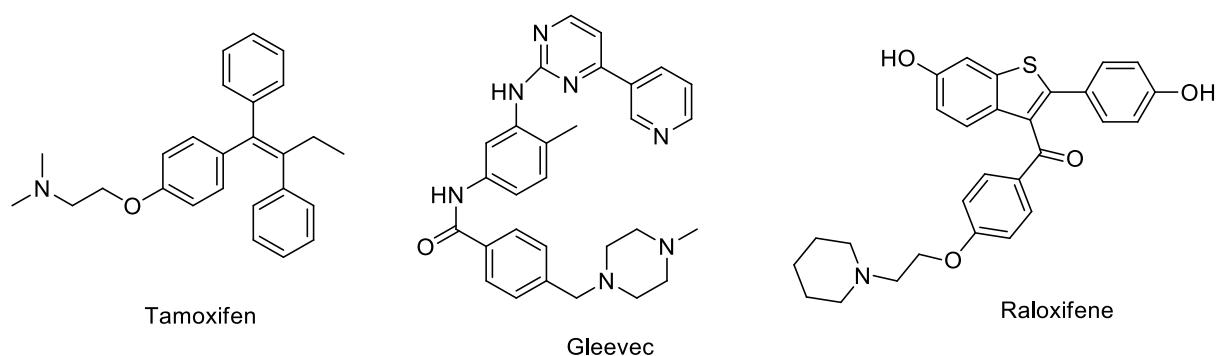


Figure 1-1: Drugs obtained by rational design

Combinatorial libraries containing many thousands of similar compounds were introduced with great fanfare in the early 1990s as alternative to natural products as a source of new lead

structures. A decade later, after investing considerable effort and resources, it became clear that these combinatorial libraries had largely failed as a source of new drugs since many had little structural diversity and often consisted of “non-drug like molecules” based on the simple Lipinski rule^{11,12}. The industry subsequently changed its focus to screen much smaller libraries consisting of small molecules whose properties were much more likely to match the Lipinski rule of 5 and thus be bioavailable. The Lipinski rules, proposed in 1997¹³, constitute one of the simplest ways to assess drug-like properties of a molecule, ADME (adsorption, distribution, metabolism, and excretion). They constitute a quantitative examination of basic molecule descriptors like molecular weight (MW), lipophilicity (log P), polar surface area (PSA), counts of hydrogen bond donors (HBD) and acceptors (HBA), and number of rotatable bonds (RB). Lipinski established the limits for these descriptors in drug molecules as follow: MW < 500, computed log P < 5, HBA < 10, and HBD < 5. His postulate also points out that the violation of any two of these limits could result in poor absorption or permeability¹⁴.

Natural product structures have some of the most desirable characteristics such as high chemical diversity, biochemical specificity, number of chiral centers and high steric complexity¹⁵. Only 10%¹⁵ of natural compounds used as drugs violate one or two of these rules. It is also important to point out that there are many natural compounds with interesting bioactivities that do not fulfill the Lipinski rules. Nature has managed to create high molecular weight molecules with low hydrophobicity and intermolecular H-bond donating potential¹⁶.

Most significant, according to many experts in the field¹⁷, nature has proved to be the best reliable source for new drugs in terms of diversity and specificity¹⁸. Structures found in nature are the result of evolutionary pressure; by this process nature has perfected the molecules in order to fulfill specific goals. Nature uses highly conserved molecules with selected common backbones and these molecules interact with different organisms by diverse pathways. It does this by modifying common structures often via oxidation or reduction reactions, rearrangements of the carbon skeleton, typically via carbocation intermediates and alkylation reactions. As a result of these variations, natural compounds perform very specific tasks. A single plant species often produces a number of similar compounds (analogs) as a defense

mechanism for protection against herbivores or fungal infections. This diversity of similar compounds, which is called phytochemical redundancy, makes it difficult for insects or the fungi to develop resistance to the defense mechanism since resistance to one of the compounds could easily result in increased sensitivity to a related derivative.

Despite the fact that many thousands of natural compounds have been isolated and identified over the past one hundred and fifty years, new and unusual structures with unexpected biological activity continue to be reported. Nature provides an unlimited source of inspiration for chemistry that includes; diverse applications such as antifreeze glycoproteins isolated from spruce budworm¹⁹ and species of marine teleosts²⁰, anticancer compounds isolated from *Halichondria okadae*²¹ and spider silk polymers used to develop bullet-proof vests¹⁷. Observing nature closely, understanding how natural products work, where they come from and studying how they have evolved¹⁷, allows for the development of novel molecules for a great amount of applications, apart from drug development.

Some of the molecules harvested from nature go beyond a synthetic chemist's imagination, and have resulted in unique drugs for very important diseases (**Figure 1-2**). Artemisinin, was isolated from *Artemisia annua*, a plant traditionally used in China to treat malaria, and has become the most effective drug on the market to treat this disease²². Eribulin methysilate is the newest drug approved by the FDA for cancer therapy. It is an analog of the compound Halichondrin B that comes from a marine sponge, *Halichondria okadae*²³. Similarly, vinigrol is a relatively new antihypertensive and platelet aggregation inhibitory agent produced by the fungus, *Virgaria nigra*²⁴.

Therefore, the discovery of new molecules from natural sources provides the opportunity to access novel structures and activities, which inspires the development of new methodologies to synthesize these molecules¹⁷.

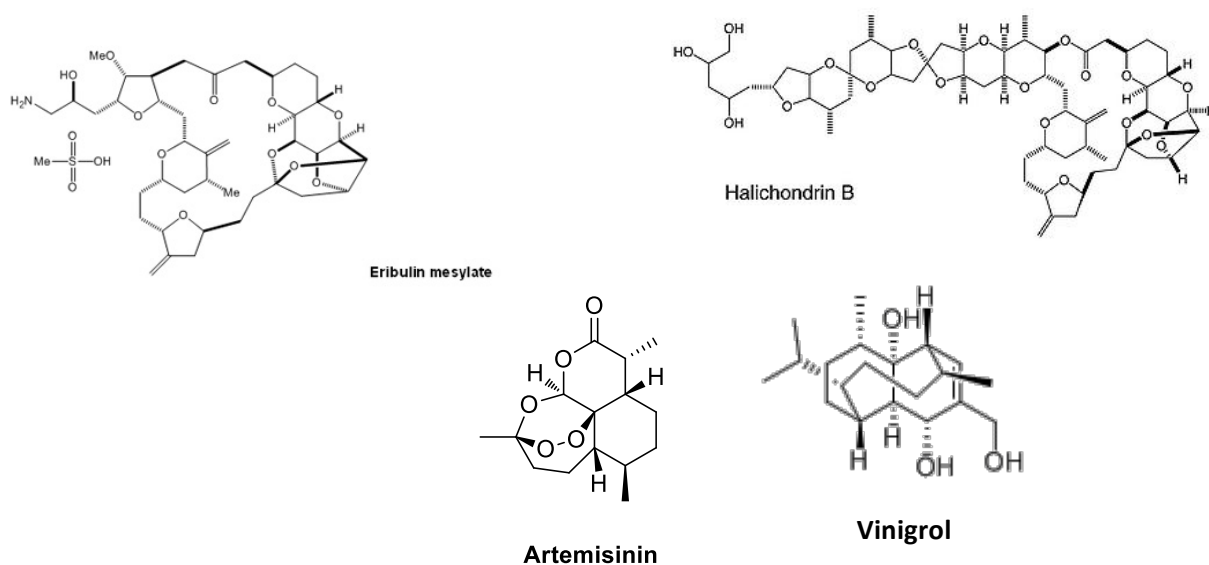


Figure 1-2: Nature as a source of inspiration of unique hit compounds

Furthermore, nature has provided new ways to target the same problem. Many of the bioactive compounds isolated for the treatment of cancer have different modes of action. Vincristine and vinblastine, alkaloids present in *Catharanthus roseus* treat cancer by inhibition of tubulin polymerization²⁵, while podophyllotoxins isolated from *Podophyllum hexandrum* inhibit cell mitosis via a mechanism known as spindle poison²⁶.

This rich source of structural diversity opens new opportunities to the discovery of new pharmacophores. As a result, medicinal chemists can develop new drugs capable of inhibiting illnesses via novel modes of action.

Over 50% of the drugs currently prescribed in the US are either natural products or derivatives of natural products. The chart in **Figure 1-3** shows the situation related to FDA approval of new drugs for the period 1985 -2007. According to an analysis done by Newman and coworkers around 70% of the total “New Chemical Entities” for drugs have a significant relationship with a natural product, being either: a natural product (N), a compound derived from a natural product and is usually a semisynthetic modification (ND), a compound made by total synthesis, but the pharmacophores is/was from a natural product (S*), compounds that mimic natural product (NM).

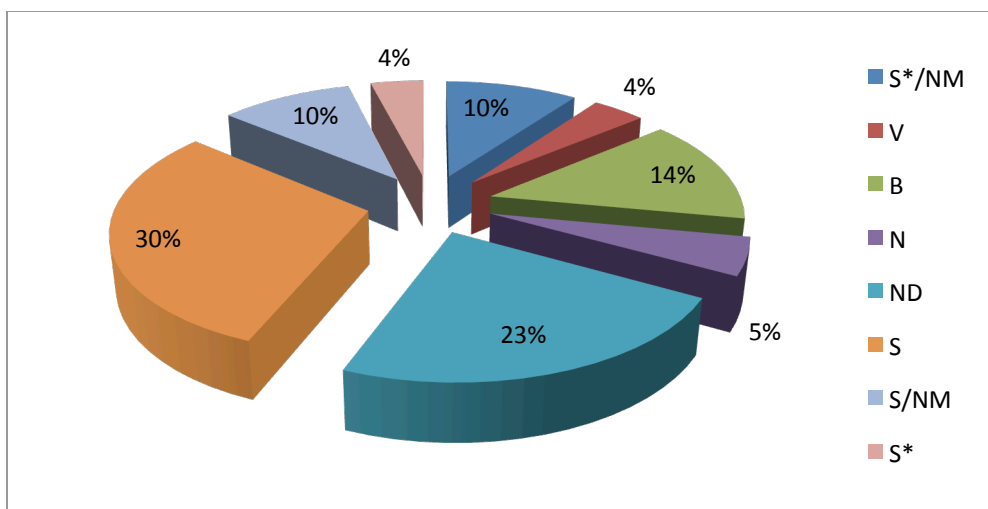


Figure 1-3: All New Chemical Entities, 01/1981-06/2006, by source (N=1184). “B”: Biological, usually a large (>45 residues) peptide or protein either isolated from an organism/cell line or produced by biotechnological means in a surrogate host. “N”: Natural product. “ND”: Derived from a natural product and is usually a semisynthetic modification. “S”: Totally synthetic drug, often found by random screening/ modification of an existing agent. “S*”: Made by total synthesis, but the pharmacophores is/was from a natural product. “V”: Vaccine. “NM”: Natural product mimics. Modified from: Newman *et Al.*, 2003^{27, 28}.

The drug discovery process can be long and costly; Taxol represents one of the best examples for this situation. The compound was first isolated in 1966 from the bark of the Pacific Yew tree, *Taxus brevifolia*. The complete structure was elucidated in 1971. Then, in 1979 the mode of action of the compound was reported and clinical trials were carried out in the early 1980’s. However, the activity against breast and ovarian cancer was not discovered until the early 1990’s^{29,30}. In total, it took 23 years to develop taxol as an approved drug. Nevertheless, it has become a blockbuster drug, generating 1.6 billion dollars in profits for Bristol- Myers in 2000, the year patent protection ended³⁰.

Compounds found in the resin obtained from the root of mayapple, *Podophyllum peltatum* yielded podophyllin and the semi-synthesis of analogs allowed for the development of compounds that are used to treat lung and testicular cancer. The discovery of artemisin from *Artemisia annua* and the synthesis of potent analogs used to treat human malignant cerebral malaria, have helped revive the interest in higher plants as a source of new drugs²⁹.

Nature has provided many important drugs; in the last six years alone, five new plant-derived pharmaceuticals were released on the market and others are being tested in clinical trials⁵. Undoubtedly, the major constraint in the development of new drugs derived from plants is the amount of time required from compound isolation and identification, to finally bringing a product on the market. Nevertheless, the development of new analytical techniques (HPLC-MS, GC-MS and ultra HPLC-MS-QTOF) combined with high-throughput screening, is a promising solution that will allow for the rapid analysis of new plant extracts, and will enable a fast dereplication to identify the unknown components in crude plant extracts.

Ethnobotany and ethnopharmacology are the most widely used approaches for plant selection. It has been shown that they have a high percentage of success in delivering useful plant-derived drugs, in comparison to random bioprospecting³¹. Indeed, a review done in 2001 identified 122 drugs, as plant-derived drugs. Most importantly, 80% of these drugs were used to treat the same illness that was reported by ethnomedicine³². However, natural compounds that have high bioactivities often have several problems such as: low bioavailability, high toxicity, and limited supply. Medicinal chemistry has resolved many of these issues.

1.2 Plant derived drugs and medicinal chemistry

Generally, ethnobotanical studies have resulted in lead compounds that are classified under one of the next three categories: 1. unmodified natural plant products with clinical efficacy suggested by ethnomedicine (e.g. morphine), 2. unmodified natural plant products with therapeutic efficacy remotely suggested by their ethnobotanical use (e.g. vincristine), and finally, 3. modified natural plant products or synthetic compounds derived from natural products used in traditional medicine (e.g. aspirin)³³. **Figure 1-4** shows a typical process for drug discovery from plants. This process has major constraints. First, the dereplication process becomes crucial so as to avoid the isolation of known compounds with known bioactivity in the same field; the most useful tool to overcome this problem is the use of hyphenated analytical techniques such as HPLC-MS-MS or ultra HPLC-MS QTOF combined with comprehensive compound libraries. The second constraint is the structural assignment to complex natural metabolites. This has been resolved by the use of modern NMR techniques such as Nuclear

Overhauser effect spectroscopy (NOESY), homonuclear correlation spectroscopy COSY, etc. Once the compound has been isolated and identified, the last limitation is short supply due to the tedious and low yield isolations; this is one of the biggest limitations in plant-derived drug discovery. Most of the active compounds from plants represent approximately 1% of a crude extract.¹⁵

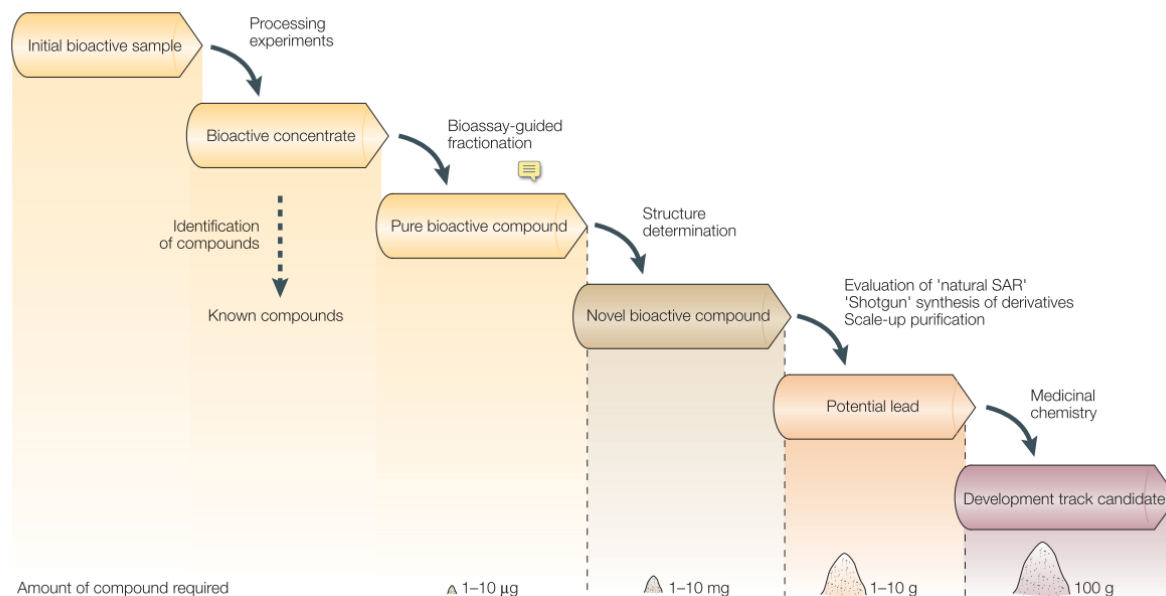


Figure 1-4: Chemical process for natural product discovery¹⁵

Equally important, is to mention that despite nature's success in providing very potent new drugs and new drug scaffolds; the drug discovery process can take as long as 10 years and requires the investment of millions of dollars. Most of this money and time is invested in the development of analogs. In fact, it has been estimated that from 5000 lead compounds only one will ultimately succeed to finally be approved as a drug.³⁴ Consequently, the identification of a good lead becomes critical, since this is the first step in a very long process. **Figure 1-5** shows the scheme for the development of drugs from plants from the point of view of medicinal chemistry.

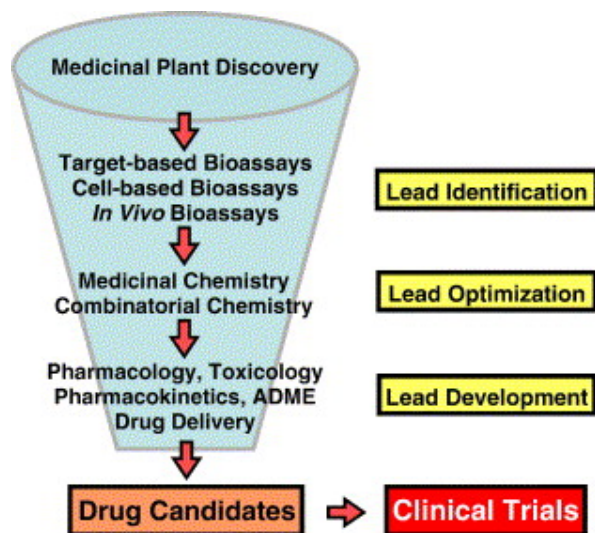


Figure 1-5: Plant drug development from medicinal chemistry perspective³⁴.

A lead, which is a bioactive compound that demonstrated selectivity in the bioassay step of the process, needs to have other desirable characteristics such as: originality, patentability and accessibility, through extraction or synthesis¹. Once the lead has been identified, it will go through a process of molecular modification to tune its physicochemical characteristics so as to make it suitable for ADME (absorption, distribution, metabolism, and excretion). As a result, a preclinical candidate is developed. If the compound does not show toxicity in cells and animal models it becomes a clinical candidate. The final step is to stand clinical trials; after this process a new drug is born¹.

On the other hand, medicinal chemistry has also generated large libraries of synthetic compounds that are evaluated in different bioassays to generate new drugs. Years of work on optimization of lead compounds have generated massive synthetic compound libraries that can be evaluated in high throughput screenings. The current availability of new bioassays opens new opportunities for the discovery of novel natural compounds and new uses for known compounds.

1.3 Natural Health Products

Natural Health products (NHP) is a term coined in Canada that includes any substances that occur naturally and can be found in plants, animals, fungi, algae or micro-organisms that are used to diagnose, treat or prevent disease and are suitable for self-care use (i.e., that have a medicinal indication)^{35,36}. NHPs include: vitamin and mineral supplements, herbal and other plant-based health products, traditional medicines such as traditional Chinese medicines, homeopathic medicines, probiotics and enzymes, and some personal care products like toothpastes that contain natural ingredients³⁵. This definition was introduced for the first time in January 2004 as part of the “*Natural Health Products Regulations*”. The idea behind this regulation is to “ensure that all Canadians have access to natural health products that are safe, effective, and of high quality, while respecting the freedom of choice and philosophical and cultural diversity”³⁶.

In order for a NHP to be sold in Canada it must have a product license, and to get the license for the product good manufacturing practices must be followed and safety and efficacy evidence must be provided. The studies performed in research labs to give a scientific foundation for the traditional use of plants contributes to their safe use and also provides analytical tools for the quality control of starting materials and process control.

The Canadian initiative to regulate this type of product is important, since contrary to popular belief, natural does not always mean safe. For example, substitution of black cohosh (*Actea racemosa*) with Asian species of *Actea* led to adverse reactions in patients. Even correctly registered products may cause adverse effects in certain situations. A common adverse effect is interactions with prescribed drugs. Some of these interactions can be life threatening like the ones observed between St John’s wort (*Hypericum perforatum*) and HIV drugs like indinavir³⁷. However, the use of regulated NHP’s with an NPN number can provide ethical treatments for conditions that they are approved for.

The present research includes different projects that will exemplify many of the aspects involved in the process of drug and NHP discovery and development discussed in this general

introduction. It has been divided in two major sections to facilitate the reading of the document:

Section I: The evaluation of the plant families Marcgraviaceae and Platanaceae as a source of new drug molecules and NHPs

The Marcgraviaceae was targeted as a rare and poorly studied Neotropical family that may be a source of new NHPs and drugs based on triterpene and other natural products. The objectives for this section were:

Objective 1: To evaluate the content of pentacyclic triterpenes in eleven species of the Marcgraviaceae family.

Specific objective 1.1: To develop a validated method for the quantification of pentacyclic triterpenes in crude extracts of Marcgraviaceae species samples. *This objective was originally developed with the genus Souroubea as an NHP quality control tool, but then expanded for application to 11 species of Marcgraviaceae as a chemotaxonomic tool.*

Specific objective 1.2: To apply metabolomics methods to identify botanical material to species and to find marker compounds in *Souroubea* spp. This represents a contribution to NHP identity assessment.

Specific objective 1.3: To isolate and identify the bioactive compound responsible for the quorum sensing inhibitory activity observed in leaf extract of *Marcgravia nervosa*. *This project is an example of natural product lead discovery.*

Section 2: Organic synthesis: Synthesis of insecticide synergists and compounds with activity in connexins.

Objective 2: To develop dillapiol analogs with improved activity (for example at least 20 times better than the lead compound based on IC_{50} values) through semi-synthesis.

Specific objective 2.1: To synthesize analogs of dillapiol changing chemical properties based on Log P and binding affinity to CYP450 3A4.

Specific objective 2.2: To evaluate the synthesized analogs *in vitro* for inhibitory activity of CYP 3A4 enzyme.

Objective 3: To synthesize analogs of compound AF 101 (2,4-dibromo-N-(1-phenyl-2-(phenylsulfinyl)ethyl)aniline) to evaluate bioactivity observed in a connexin bioassay.

Specific objective 3.1: To synthesize analogs of compound AF101 (2,4-dibromo-N-(1-phenyl-2-(phenylsulfinyl)ethyl)aniline) by changing structural features to analyze the characteristics of the compound and their impact in the bioassay.

Hypotheses:

1. Because *M. nervosa* was the only Marcgraviaceae species with significant biofilm inhibition, it was hypothesized that novel phytochemistry may be responsible. It was predicted that bioassay guided isolation and spectroscopic identification would lead to the isolation of a bioactive secondary metabolite different from the triterpenes identified in other species.
2. Because phytochemical diversity is usually somewhat different in each plant species, it is hypothesized that analysis of the metabolome by ultra HPLC-MS QTOF may lead to identification of phytochemicals which are species markers. It is predicted that use of the S= plot statistical technique comparing the metabolome of *S. gilgii* and *S. sympetala* will lead to selection of unique species markers.
3. In the semi-synthesis of dillapiol analogues, it is hypothesized that the CYP3A4 inhibition by dillapiol analogs depends on chemical structure. The chemical structures have lipophilicity (log P) and molecular refractivity (MR) variables that could predict this activity.

Collaborative work was required in order to achieve the objectives and to test the hypotheses that were outlined in this research work. Therefore, while the majority of the research presented in this thesis was conducted by the author, additional data obtained by collaboration with other labs or other members of the research group are included when corresponds, to

enhance and complement the data in order to obtain a better answer to the hypothesis and achieve the stated objectives.

1.4 References

1. Wemuth, C. G. *The practice of medicinal chemistry. A History of Drug Discovery*. Academic Press.(2008).
2. A Pictorial History of Herbs in Medicine and Pharmacy. *HerbalGram* **42**, 33–47 (1998).
3. Cragg, G. M.; Boyd, M. R.; Khanna, R.; Kneller, R.; Mays, T. D.; Mazan, K. D.; Newman, D. J.; Sausville, E. a. International collaboration in drug discovery and development: the NCI experience. *Pure and Applied Chemistry* **71**, 1619–1633 (1999).
4. Sneader, W. *Drug Discovery: A history*. John Wiley & Sons. (2005).
5. Salim, A. A., Chin, Y. & Kinghorn, A. D. Drug Discovery from Plants. *Bioactive Molecules and Medicinal Plants* 1–25 (2008).
6. Häyry, P.; du Toit, D.; Sarwal, M. & Aavik, E.; Hoffrén, A.; Vamvakopoulos, J. Rational drug design: making drugs that make a difference. *Transplantation Proceedings* **34**, 2000–2 (2002).
7. Eck, M. J. & Manley, P. W. The interplay of structural information and functional studies in kinase drug design: insights from BCR-Abl. *Current Opinion in Cell Biology* **21**, 288–95 (2009).
8. Stegmeier, F., Warmuth, M., Sellers, W. R. & Dorsch, M. Targeted cancer therapies in the twenty-first century: lessons from imatinib. *Clinical Pharmacology and Therapeutics* **87**, 543–52 (2010).
9. Jordan, V. C. Tamoxifen (ICI46,474) as a targeted therapy to treat and prevent breast cancer. *British Journal of pharmacology* **147 Suppl** , S269–76 (2006).
10. Micaelo, N. Design and synthesis of new selective estrogen receptor modulators. *Molecular Modeling and simulation Lab*. At <<http://www.simulation.quimica.uminho.pt/?p=119>>. Accessed January, 2013.
11. Lipinski, C. a, Lombardo, F., Dominy, B. W. & Feeney, P. J. Experimental and computational approaches to estimate solubility and permeability in drug discovery and development settings. *Advanced Drug Delivery Reviews* **46**, 3–26 (2001).
12. Zogheib, C. Editorial. *Nature Reviews. Drug discovery* **6**, 853 (2007).
13. Lipinski, C. a. Lead- and drug-like compounds: the rule-of-five revolution. *Drug Discovery Today: Technologies* **1**, 337–341 (2004).
14. Egan, W. J. Predicting ADME properties in Drug Discovery. *Drug design* 165–178 (2010).

15. Koehn, F. E. & Carter, G. T. The evolving role of natural products in drug discovery. *Nature Reviews. Drug Discovery* **4**, 206–20 (2005).
16. Ganesan, A. The impact of natural products upon modern drug discovery. *Current opinion in Chemical Biology* **12**, 306–17 (2008).
17. Hunter, P. Harnessing Nature’s wisdom. Turning to Nature for inspiration and avoiding her follies. *EMBO Reports* **9**, 838–40 (2008).
18. Harvey, a Strategies for discovering drugs from previously unexplored natural products. *Drug Discovery Today* **5**, 294–300 (2000).
19. Graether, Steffen P.; Gagné, S. M. & Spyropoulos, Leo Jia, Zongchao Davies, Peter L.; Sykes, B. D. Spruce Budworm Antifreeze Protein: Changes in Structure and Dynamics at Low Temperature. *Journal of Molecular Biology* **327**, 1155–1168 (2003).
20. Bouvet, V. & Ben, R. N. Antifreeze Glycoproteins. *Cell Biochemistry and Biophysics* **39**, (2003).
21. Andersen, R. J. *et al. Handbook of Marine Natural Products*. (Springer Netherlands: Dordrecht, 2012).
22. O’Neill, P. M. & Posner, G. H. A medicinal chemistry perspective on artemisinin and related endoperoxides. *Journal of Medicinal Chemistry* **47**, 2945–64 (2004).
23. Simmons, T. L., Andrianasolo, E., Mcphail, K., Flatt, P. & Gerwick, W. H. Marine natural products as anticancer drugs Minireview Marine natural products as anticancer drugs. *Molecular Cancer Therapeutics* **4**, 333–342 (2005).
24. Ando, Takeshi; Tsurumi, Yasuhisa; Ohata, Nobutaka; Uchida, Itsuo; Yoshida, Keizo; Okuhara, M. Vinigrol, a novel antihypertensive and platelet aggregation inhibitory agent produced by a fungus, *virgaria nigra*. *The Journal of Antibiotics* **XLI**, 1–6
25. Cragg, G. M. & Newman, D. J. Nature: a vital source of leads for anticancer drug development. *Phytochemistry Reviews* **8**, 313–331 (2009).
26. Bhatia, A., Arora, S., Singh, B., Kaur, G. & Nagpal, A. Anticancer potential of Himalayan plants. *Phytochemistry Reviews* **10**, 309–323 (2010).
27. Newman, D. J. & Cragg, G. M. Natural products as sources of new drugs over the last 25 years. *Journal of Natural Products* **70**, 461–77 (2007).
28. Newman, D. J., Cragg, G. M. & Snader, K. M. Natural products as sources of new drugs over the period 1981-2002. *Journal of Natural Products* **66**, 1022–37 (2003).
29. Phillipson, J. D. Phytochemistry and medicinal plants. *Phytochemistry* **56**, 237–43 (2001).
30. Frank, S. The taxol story. *Florida State University Research in review* **XII**, 13–37 (2002).

31. Farnsworth, N. R., Akerele, O., Bingel, a S., Soejarto, D. D. & Guo, Z. Medicinal plants in therapy. *Bulletin of the World Health Organization* **63**, 965–81 (1985).
32. Fabricant, D. S. & Farnsworth, N. R. The value of plants used in traditional medicine for drug discovery. *Environmental Health Perspectives* **109 Suppl** , 69–75 (2001).
33. Cox, P. A. Ciba Foundation Symposium 185 - Ethnobotany and the Search for New DrugsThe Ethnobotanical Approach to Drug Discovery: Strengths and Limitations. *Ciba Foundation Symposium 185 - Ethnobotany and the Search for New Drugs* 25–41 (1994).
34. Balunas, M. J. & Kinghorn, A D. Drug discovery from medicinal plants. *Life Sciences* **78**, 431–41 (2005).
35. Government of Canada, H. C. Natural Health Products - Drugs and Health Products Regulations - Main Page - Health Canada. (2004).at <<http://www.hc-sc.gc.ca/dhp-mps/prodnatur/index-eng.php>> Accessed February 2013
36. Walji, R. & Boon, H. Natural health product regulations: perceptions and impact. *Trends in Food Science & Technology* **19**, 494–497 (2008).
37. Gilmour, J., Harrison, C., Asadi, L., Cohen, M. H. & Vohra, S. Natural health product-drug interactions: evolving responsibilities to take complementary and alternative medicine into account. *Pediatrics* **128 Suppl** , S155–60 (2011).

2 Phytochemistry of the family Marcgraviaceae

2.1 Introduction

Marcgraviaceae is a small Neotropical family of lianas, epiphytic and hemi-epiphytic shrubs, and rarely small trees that comprises 130 species divided in eight genera¹. The family is distributed from southern Mexico to northern Bolivia and is also native to many islands in the Caribbean, **Table 2.2.1.1** shows a more detailed distribution of the different genera in the family²⁻⁴. Taxa are mostly found in lowland humid tropical forests as well as mountain, and cloud forests². This family has been understudied as there is little information about the phytochemistry, or biological activity. Most significantly, this family is considered of conservation interest because its taxa are rare and tend to occur in habitats that compete with human activity^{2,3}.

Table 2.2.1.1: Distribution of Marcgraviaceae species in the Neotropics².

Genus	Number of species	Location
<i>Marcgravia</i>	65 spp.	Mexico, Mesoamerica, South America, Antilles
<i>Marcgraviastrum</i>	17 spp.	Nicaragua to Peru, Bolivia, and 2 spp. Brazil.
<i>Norantea</i>	2 spp.	Caribbean and Amazonian basin of NE South America
<i>Ruyschia</i> Jacq	9 spp.	Mesoamerica, Andes, Lesser Antilles
<i>Sarcopera</i>	10 spp.	Honduras to N. Bolivia, Guyana Highlands
<i>Schwartzia</i> Vell.	16 spp.	Costa Rica through the Andes south to Bolivia, in the Caribbean basin and 1 sp. in E. Brazil
<i>Souroubea</i>	19 spp.	Mexico to Bolivia (absent in the Antilles)

A review of the published literature has demonstrated that not much is known of the phytochemistry of Marcgraviaceae family. The only published report on secondary metabolites in these plants corresponds to a single report on flavonoid glycosides in the flowers of *Norantea guianensis*⁵.

Our research group has worked in collaboration with an expert group of botanists from Costa Rica for 25 years. As a result of this collaboration, several Marcgraviaceae species were collected in Costa Rica. The main interest behind the project was to generate scientific knowledge to promote the preservation of these taxa. As part of the project, a total of 11 species have been collected from Costa Rica. To have a better understanding of the taxonomic relationship of the plants that have been collected as part of our research, **Figure 2-1** presents a partial phylogenetic tree of Marcgraviaceae based on three chloroplast genes³.

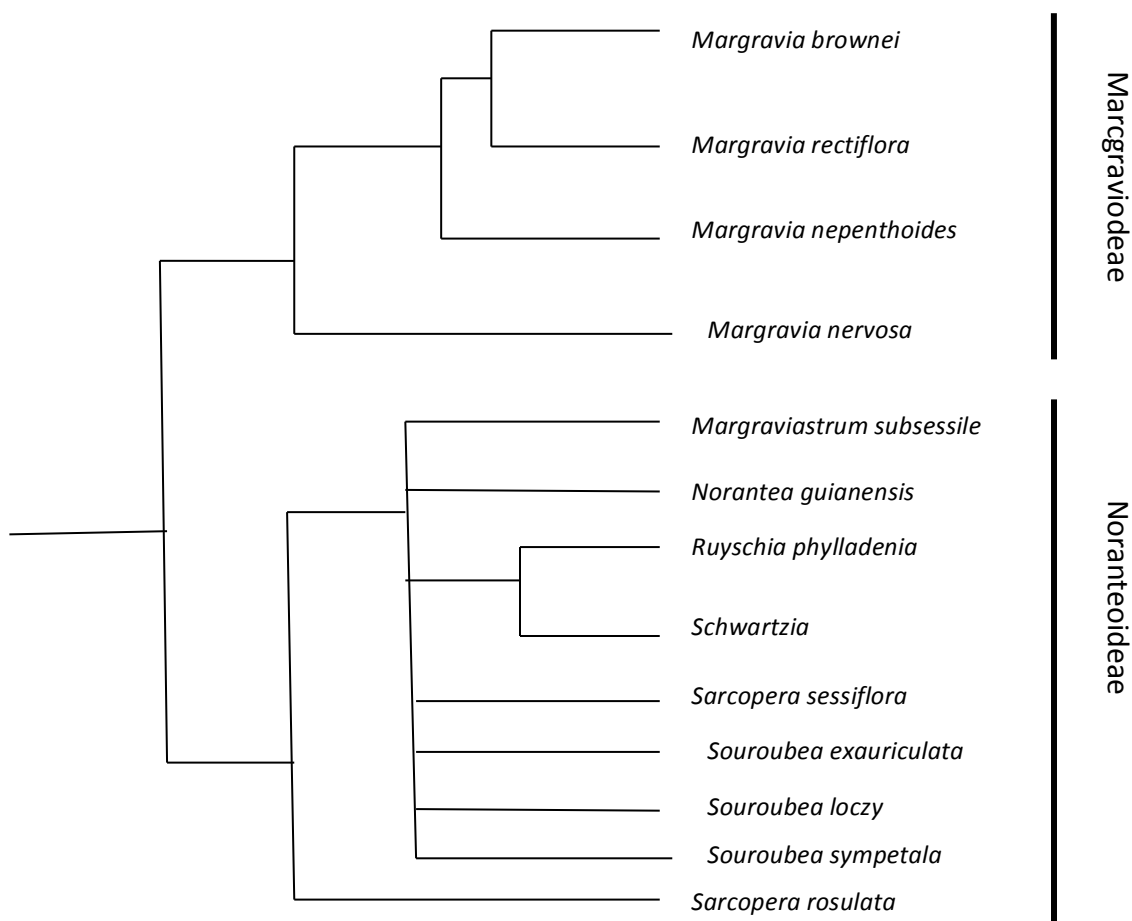


Figure 2-1: Phylogenetic of Marcgraviaceae, modified from Ward, 2002³.

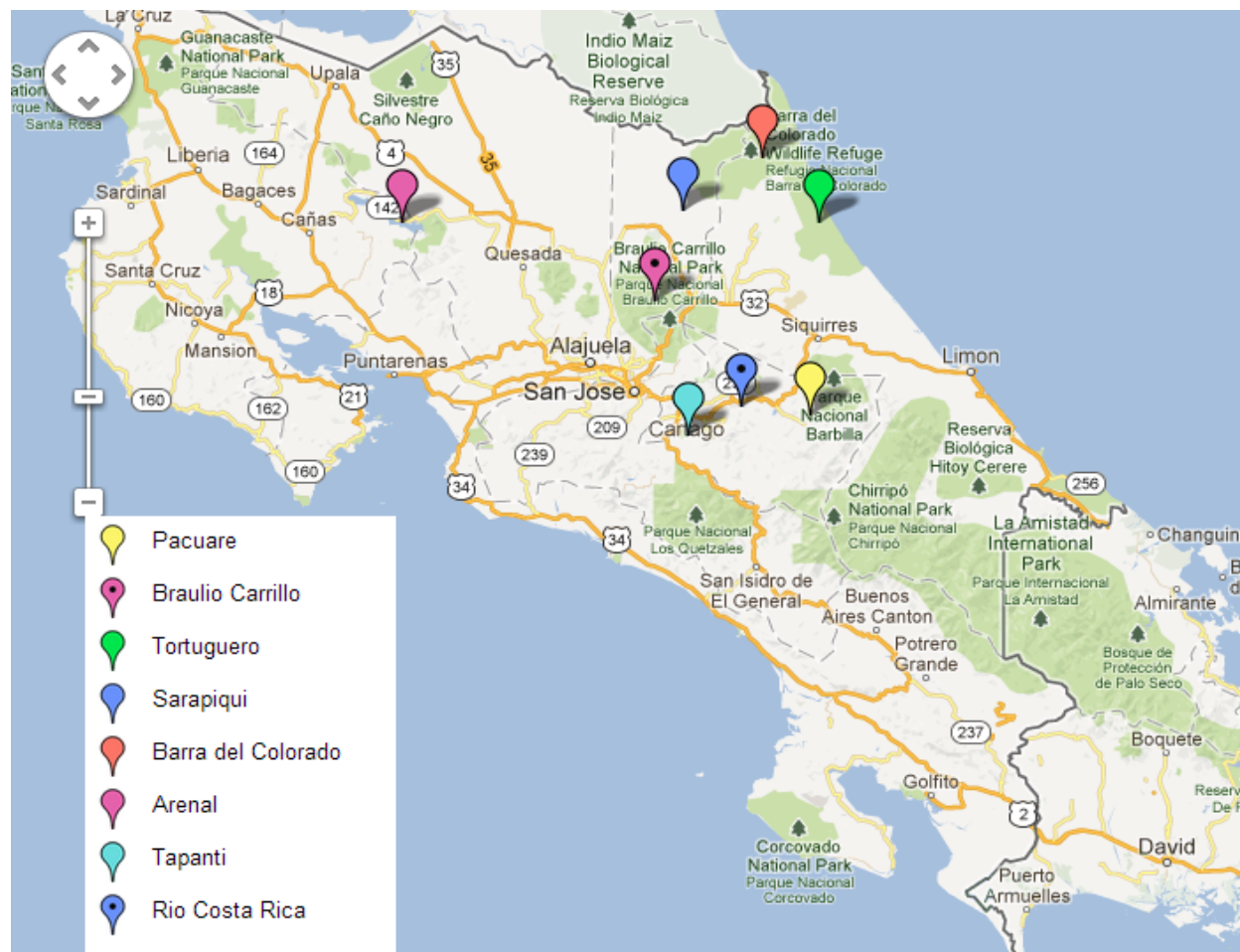
Leaves of *Souroubea sympetala* and *Souroubea gilgii* were collected initially for the purpose of phytochemical investigation. A literature research showed that another member of the Marcgraviaceae family was used by Amazonian healers to treat “susto”⁶, which is a folk description of what the American Psychiatric Association (APA) and the World Health Organization (WHO) have linked to mental disorders, including anxiety^{7,8}.



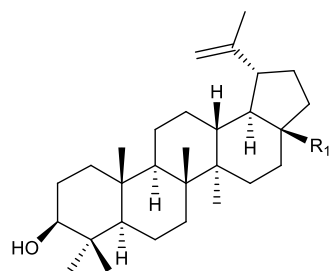
Figure 2-2: A. *Souroubea gilgii* B. *Souroubea sympetala*. Photos belong to Dr. Arnason personal collection.

Because of the Schultes report describing the use of a Marcgraviaceae for the treatment of “susto”, it was decided to test extracts for anxiety in one of the several anti-anxiety paradigms used by psychologists to study anxiety in animal models. Extracts of *S. sympetala* were found to have significant activity in rat behavioral models of anxiety such as the elevated plus maze and fear-potentiated startle paradigm⁹. The bioassay guided fractionation of the plant extract associated this bioactivity with the triterpenes rich fractions containing betulinic acid (**1**), ursolic acid (**5**), α -Amyrin (**3**) and β -Amyrin (**6**)¹⁰. **Figure 2-4** summarizes the compounds discovered by Dr. Evaloni Puniani and Melinda Tiv in different organs of *Souroubea gilgii*. Further analysis of this fraction showed betulinic acid as the main compound responsible for the activity observed in the bioassay¹⁰⁻¹².

Figure 2-3: Geographical distribution for the plant collection in Costa Rica. Map modified from Google maps

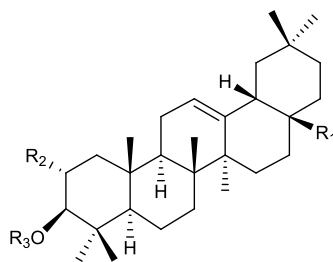


Pentacyclic triterpenes are secondary plant metabolites widely distributed in different plant families. They can be found in several plant organs such as fruit peel, leaves, stems and wood¹³. The bioactivity of pentacyclic triterpenes has been an area of recent interest. Besides the anxiolytic activity described above, betulinic acid and its derivatives have a wide range of bioactivities including antibacterial, anti-inflammatory, anti-HIV and anti-cancer-activity¹⁴. Lupeol, betulin, betulinic acid, oleanolic acid and ursolic acid are considered as novel options for cancer treatment because they are multi-target agents. They can be used for the treatment of the tumour and its environment; they can also help boost the immune system and can be used as preventive treatment¹⁵.



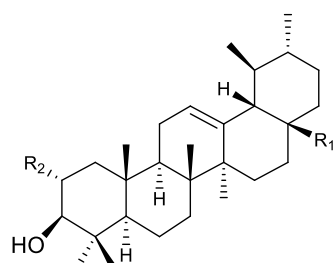
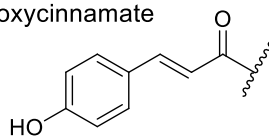
Lupane

1. Betulinic acid, R₁: COOH
2. Lupeol R₁: CH₃
8. Betulonic aldehyde R₁: CHO



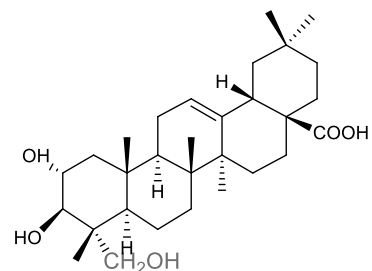
Oleanane

3. β -Amyrin R₁: CH₃ R₂: H
4. R₃: Taraxeryl- trans-4-hydroxycinnamate



Ursane

5. Ursolic acid: R₁: COOH, R₂: OH
6. β -Amyrin: R₁: CH₃, R₂: H
7. Malisnic acid: R₁: COOH, R₂: OH



9. Arjunolic acid

Figure 2-4: Pentacyclic triterpenes identified in *Souroubea sympetala*

The partial phytochemistry of leaves from *Souroubea gilgii* showed the presence of several flavonoids¹⁰. Besides *Souroubea* species, *Marcgravia nepenthoides* has also been collected from Costa Rica and the partial phytochemical characterization of the bark and wood of the plant has been completed. The approach used for this plant was traditional phytochemistry; a total of six known triterpenes were isolated¹⁶, including compounds **1**, **3** and **6**, previously isolated from *Souroubea* spp. The other three triterpenes isolated were: lupeol (**2**), betulonic aldehyde (**8**) from the bark and arjunolic (**9**) acid from the wood.

α -Amyrin and β -Amyrin have been shown to possess anti-depressant activity¹⁷. Furthermore, maslinic acid has a wide range of bioactivities, which include: anti-tumour, anti-HIV, anti-oxidant, and anti-obesity. It inhibits glycogen phosphorylase (GP) an enzyme responsible for glycogen breakdown to produce glucose and related metabolites for energy supply; therefore, it could potentially be used for treatment of type 2 diabetes¹⁸.

The diverse range of bioactivities and low toxicity are characteristics that make plants containing pentacyclic triterpenes a good choice for phytopharmaceutical products (such as Natural Health Products (NHP) in Canada) as well as a good source of lead compounds to develop new drugs for treatment of different conditions¹⁹. A pilot study using HPLC- APCI-MS¹¹ was developed in order to detect the presence of the four triterpenes previously found in *S. sympetala*.

Since the discovery of the anti-anxiety properties of the extracts, considerable effort has been made to commercialize this discovery both with respect to the total extracts and the key active component betulinic acid. Canadian, US and European patents have been issued covering these discoveries²⁰.

Successful work has also been carried out in Costa Rica where plantations of both *S. sympetala* and *S. gilgii* were created so that the supply of this material would no longer be dependent on wild crafting. Finally, all of this work has resulted in the launching of a veterinary NHP called Sin Susto™ in January of 2013 as a treatment for fear and anxiety in pet dogs by Bioniche Life Sciences of Belleville ON. The final commercial product is a 55:45 mixture of *Souroubea* spp. (ground dry leaves and small branches) and ground bark from *Platanus* spp., the latter being used to increase the betulinic acid content of the final product. Potential additional applications of this material either as whole plant material or as ethanol extracts for the treatment of anxiety and the lowering of stress biomarkers in other animals including horses and eventually humans are currently being pursued.

The mechanism of action of both betulinic acid and the crude extracts of the *Souroubea* spp. leaves has also been investigated. Evaluation of the crude ethanolic extracts of *Souroubea gilgii* showed inhibition of rat gamma amino butyric acid-transaminase (GABA-T) activity ($IC_{50} = 0.6$

mg/mL)²¹. However, the main mechanism of action is similar to benzodiazepine anti-anxiety agents. Agonist activity at the post synaptic GABA_A binding site has been demonstrated *in vivo* by Mullally et al²².

In this context, it has become important to investigate the phytochemistry of other Marcgraviaceae species in order to determine not only the chemical components of these species and show how they relate but also to ascertain whether other members of this family could have commercial potential and value.

Key issues in the development of evidence based NHPs to be registered in Canada and elsewhere are:

- 1) The development of identity assurance methods that allows the identification of commercial plant species that distinguishes them from related species.
- 2) The development of quality control procedures to produce a reproducible product that can be compared with clinically tested materials. For NHPs the most important step is the development of a validated method for quantitative determination of the active principles in plant material.

This section of the thesis describes the analysis and characterization of the 13 species collected in Costa Rica. Section **2.2** describes the development of a validated method for the quantification of five pentacyclic triterpenes in *Souroubea sympetala*. To address the quality issues Section **2.3** presents the plant metabolomics work done in two species of *Souroubea*: *S. sympetala* and *S. gilgii* to address identity issues at the genus level. Section **2.4** is the quantification of five pentacyclic triterpenes in 11 species of Marcgraviaceae to address identity issues at the family level and provide a basic contribution to chemosystematics. Finally, Section **2.5** is the bioassay-guided fractionation of *Marcgravia nervosa* as a basic science contribution to phytochemical discovery and potential drug development.

2.2 A validated HPLC-APCI-MS/MS method for the quantification of pentacyclic triterpenes of *Souroubea sympetala*

2.2.1 Introduction

A validated method was developed to quantify five triterpenes in crude extracts of *Souroubea sympetala* (Marcgraviaceae) a plant used for treatment of anxiety. Quantification of the triterpenes in the crude extracts was achieved using HPLC-APCI / mass selective detection. The method focuses on identification of five triterpenes including Betulinic acid, which has been identified as the active principle. The objective for this study was to develop a validated method for the quantification of five pentacyclic triterpenes in crude ethyl acetate extracts of *Souroubea sympetala* (and the phytochemically similar *Souroubea gilgii*).

No validated analytical method is available for the suitable determination of secondary metabolites in *S. sympetala* or any other member of the Marcgraviaceae family. Since these species are now being used in a botanical anxiolytic, quality assurance methods were required. The current method was completely validated and was successfully applied for the analysis of two plant organs of *S. sympetala*.

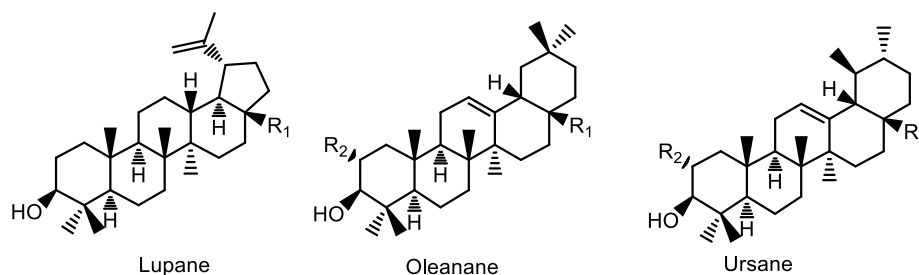
2.2.2 Results and discussion

Method validation for six pentacyclic triterpenes

The present method was optimized and validated to identify and quantify up to five triterpenes known to be present in *Souroubea sympetala*⁹. The optimized separation method could separate the six compounds selected for the analysis allow the incorporation of structurally related compounds for future analysis of related species (**Table 2.2.2.1**). This is an advance on the pilot method for the detection of four triterpenes on *Souroubea sympetala* previously developed in our research group¹¹ which was not validated for quantitative analysis. In order to overcome the detection problems due to the similarity in structures for the triterpenes selected for the analysis betulinic acid (**1**) and ursolic acid (**2**) both produce a mass peak at 455.3 UMAS, and lupeol, α -Amyrin and β -Amyrin produce a peak at 425.4 UMAS), a good separation and

detection system was required. To achieve the best separation of compounds, several gradient programs of a binary system consisting of acetonitrile (+0.05 % formic acid) and water were tested and the linear gradient was the one that provided suitable separation of all compounds (**Figure 2-5 A and B**). The nature of the ionization for each compound allowed the detection of betulinic acid and ursolic acid in the positive mode and lupeol, α -Amyrin and β -Amyrin in the negative mode. Details of the ions selected and detected are provided (**Table 2.2.2.2**). The optimized separation method could separate the six compounds selected for the analysis and also presents some gaps that will allow the incorporation of structurally related compounds for future analysis of related species.

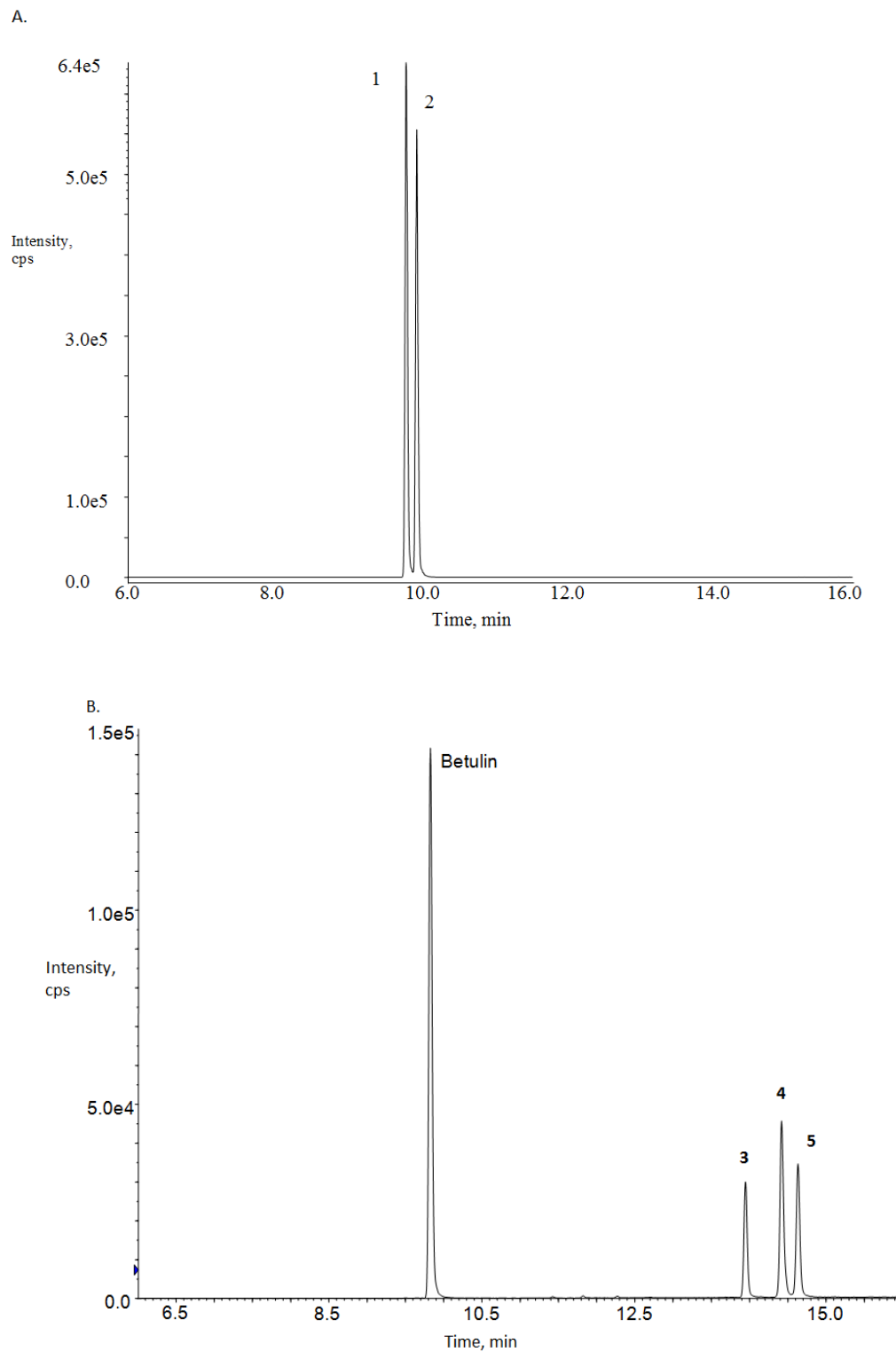
Table 2.2.2.1: Structural family, functional groups and molecular weight of the pentacyclic triterpenes quantified in stem and leaf of *S. sympetala*



Triterpene family	Triterpene	R ₁	R ₂	MW (g/mol)	Rt (min) ^a	Code ^b
Lupane	Lupeol	CH ₃	-	426.70	13.67	3
	Betulinic acid	COOH	-	456.71	9.66	1
Oleanane	β -Amyrin	CH ₃	H	426.70	14.07	4
Ursane	α -Amyrin	CH ₃		426.70	14.25	5
	Ursolic acid	COOH		456.71	9.81	2

a. RT: retention time, b. Code used on the document and chromatograms to refer to the specific compound.

Figure 2-5: HPLC chromatographic separation of selected triterpenes of *S. sympetala*. Positive ionization A (1-2) detection. B Negative ionization (3-5)



The method has also been validated for the quantification of betulin (RT: 9.8 min). Nevertheless, this is not included in further tables since it was not detected in most of the samples. The linear regression of the detector response to amount injected, calculated as average of three runs, showed excellent correlation ($R^2 > 0.997$), for all of the compounds shown in **a**. Code used on the document and chromatograms to refer to the specific compound.

Table 2.2.2.3, within a range of 0.2-25.0 μg for betulinic acid **1** in column, 0.2-10.0 μg of ursolic acid in column, and 1.0-100.0 μg in column for compounds **3**, **4** and **5**.

Table 2.2.2.2: Chromatographic and spectrometric data of pentacyclic triterpenes

Triterpene	Code ^a	Rt (min)	Ion detected
Betulinic acid	1	9.8	$[\text{M}-\text{H}]^+$, 455.3
Ursolic acid	2	10.0	$[\text{M}-\text{H}]^+$, 455.3
Lupeol	3	13.	$[\text{M}+\text{H}-2\text{H}]^+$, 425.4
β -Amyrin	4	14.1	$[\text{M}+\text{H}-2\text{H}]^+$, 425.4
α -Amyrin	5	14.2	$[\text{M}+\text{H}-2\text{H}]^+$, 425.4

a. Code used on the document and chromatograms to refer to the specific compound.

Table 2.2.2.3: Linearity and range of the calibration curve of triterpenes under study

Triterpene	Linearity (R^2)	Range (μg)
1	0.998	0.2-25.0
2*	0.997	0.2-10.0
3	0.993	1.0-100.0
4	0.998	1.0-100.0
5	0.998	1.0-100.0

*quantification based on peak height.

Calibration conditions are: linear, weighting: (1/n equal)

Limits of detection and quantification were determined for each of the compounds evaluated in the analysis, **Table 2.2.2.4**. The values obtained for each of these parameters and the

corresponding analyte showed no significant differences between the plant parts. The recommended extract concentration for quantifiable detection of major metabolites is 250 µg/mL.

Table 2.2.2.4: Limits of detection (LOD, 3:1 signal to noise) and limits of quantification (LOQ, 10:1 signal to noise), of each marker on column (6 x standard deviation) in leaf and stem of *S. sympetala*

Code	LOD (ng)	LOQ (ng)
1	0.01	0.03
2	6.60	21.9
3	610.	2030.
4	363.	1210.
5	300.	998.

Recovery analyses were performed for the five triterpenes analyzed by the developed method. Known quantities of the triterpenes were spiked into either the leaf or stem prior to extraction. A plot relating recovered amount and spiked amounts, the corresponding regression line provides the mean recovery across concentrations (slope), the linearity (R^2) and the approximate content of unspiked sample (y-intercept). **Table 2.2.2.5** shows the values of percentage recovery obtained for the selected triterpenes. All the recoveries observed are good. Based on the results observed for the recoveries the extraction described in the sample preparation is highly recommended. A percentage recovery of 102% for betulinic acid can be explained by the CV, ($CV = \text{standard deviation} / \text{mean} * 100$), observed 1.55% for intraday variation (**Table 2.2.2.5**). These results revealed that the method is highly reproducible.

The accuracy and precision of the method were assessed by calculating the variation in the results for each quantified compound within and in between days. This factor was calculated as a coefficient of variation CV; results for this parameter are shown in **Table 2.2.2.6**. The variation between trials (intraday variation) did not exceed 3.5%. Repeatability of the method was assessed on the basis of compound content, the results obtained are: 1.55%, **1**, 3.46%, **2**,

2.71%, **3**, 2.16%, **4**, and 0.79%, **5**. The interday variation was: 4.96%, **1**, 5.66%, **2**, 10.34%, **3**, 5.11%, **4**, and 5.04%, **5**, this parameter allows assessing the reproducibility of the method.

Table 2.2.2.5: Recovery of selected pentacyclic triterpenes from leaves and stems of *S. sympetala*

Code	% Recovery			Mean ^a	SEM	R ^{2b}
	Level 1	Level 2	Level 3			
1	105.7	98.4	102.7	102.27	2.14	0.996
2	98.8	90.9	95.7	95.11	2.29	0.999
3	96.3	93.6	99.5	96.48	1.69	0.997
4	91.5	96.4	95.8	94.58	1.55	0.990
5	100.2	101.3	97.9	99.77	1.00	0.994

^a As determined from slope of regression analysis injected and recovered quantities.

^b R², R-squared value of linear regression

LOD= 3x S/N, LOQ= 10x SN, S/N= 6x Stdev

Table 2.2.2.6: Intraday and interday variation in quantitative results

Triterpene	Intraday variation (%)	SEM	Interday variation (%)	SEM
1	1.55	0.44	4.96	0.69
2	3.46	0.56	5.66	0.82
3	2.71	0.93	10.34	1.39
4	2.16	0.18	5.11	0.72
5	0.79	0.25	5.04	1.03

Analysis of plant extracts using LC-APCI-MS method

To evaluate and assess the validated method, 21 accessions of leaf and stem of *S. sympetala* were analyzed. **Table 2.2.2.7** summarizes the collection information regarding the samples used in the analysis. **Table 2.2.2.8** shows the variation in content of the five triterpenes analyzed in

the samples evaluated; **Figure 2-65** shows the chromatogram for one of the crude extracts analyzed using the developed method.

Based on the results obtained in the evaluation of the method it is clear that all the selected triterpenes are present in detectable levels in both plant parts of *S. sympetala*. There was a significant variation in the content of this triterpenes according to the plant part. Betulinic acid is mainly present in the stems, accompanied with ursolic acid and β -Amyrin. On the other hand, the leaves have a higher content of α - and β -Amyrin. The evaluation of two different locations allowed monitoring the influence of the different altitudes and humidity levels in the production of triterpenes in these Marcgraviaceae species. **Table 2.2.2.9** shows data regarding climate and altitude for the two collection sites. As shown in

Figure 2-7 **A**, the content of betulinic acid in the stems of *S. sympetala* differs with the collection site. Stems from Tortuguero show a higher production of betulinic acid than the stems from Sarapiquí.

Figure 2-7 B shows the result of the analysis for the leaves; the overall trend of triterpene production is maintained in both species. Leaves from Tortuguero have a lower concentration of Amyrins than the samples collected from Sarapiquí.

Table 2.2.2.7: Collection sites for *Sourobea sympetala* samples included in the study (vouchers are held at JVR herbarium, Universidad nacional, Heredia, Costa Rica)

Code	Sample	Location*	Year collection	of	Plant part	Voucher number
SS-01	SS-B-S2-09	Sarapiqui	2009		Stem	12145
SS-02	SS-B-S4-09	Sarapiqui	2009		Stem	12160
SS-03	SS-B-S3-09	Sarapiqui	2009		Stem	12180
SS-04	SS-B-S2-09	Sarapiqui	2009		Stem	12210
SS-05	SS-B-S1-09	Sarapiqui	2009		Stem	12260
SS-06	SS-B-S1-11	Tirimbina	2009		Stem	12346
SS-07	SS-B-Tr5-09	Barra Colorado	2009		Stem	12356
SS-08	SS-B-Tr4-09	Barra Colorado	2009		Stem	12366
SS-09	SS-B-Tr1-09	Tortuguero	2009		Stem	12436
SS-10	SS-B-Tr3-09	Tortuguero	2009		Stem	12439
SS-11	SS-B-Tr2-09	Tortuguero	2009		Stem	12449
SS-12	SS-L-S4-09	Sarapiqui	2009		Leaf	12320
SS-13	SS-L-S4-09	Sarapiqui	2009		Leaf	12325
SS-14	SS-L-S2-09	Sarapiqui	2009		Leaf	12340
SS-15	SS-L-S5-09	Sarapiqui	2009		Leaf	12343
SS-16	SS-L-S1-11	Sarapiqui	2011		Leaf	13125
SS-17	SS-L-Tr5-09	Tortuguero	2009		Leaf	12381
SS-18	SS-L-Tr2-09	Cano Palma	2009		Leaf	12396
SS-19	SS-L-Tr3-09	Tortuguero	2009		Leaf	12406
SS-20	SS-L-Tr1-11	Tortuguero	2009		Leaf	12416
SS-21	SS-L-Tr2-11	Tortuguero	2009		Leaf	12426

- Locations in Costa Rica

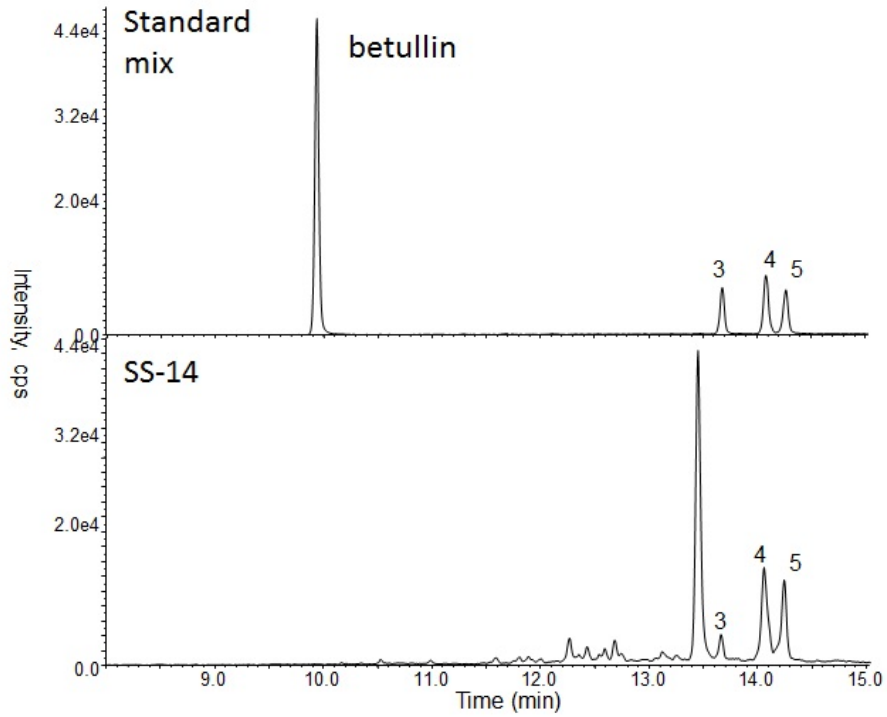
Table 2.2.2.8: Quantification (mg of compound/g of dried plant) of five pentacyclic triterpenes in leaf and stems of representative *S. sympetala* accessions

Location	Plant Part	Sample Code	cpd1	SEM	cpd2	SEM	cpd 3	SEM	cpd 4	SEM	cpd 5	SEM
Sarapiqui	Stem	SS-01	0.82	0.47	0.03	0.02	0.19	0.00	0.24	0.01	0.11	0.00
		SS-02	2.61	1.51	0.27	0.16	0.81	0.02	0.93	0.03	0.19	0.01
		SS-03	2.18	1.26	0.02	0.01	0.48	0.01	0.58	0.04	0.70	0.01
		SS-04	0.12	0.07	0.01	0.00	0.04	0.00	0.03	0.00	0.01	0.00
		SS-05	1.43	0.83	0.03	0.02	1.18	0.03	2.83	0.09	0.13	0.01
		SS-06	0.83	0.48	0.06	0.03	0.09	0.00	0.14	0.01	0.07	0.00
Tortuguero	Leaf	SS-07	2.50	1.44	0.02	0.01	1.36	0.03	1.41	0.03	1.28	0.02
		SS-08	2.91	1.68	0.06	0.04	1.65	0.02	1.37	0.04	1.75	0.02
		SS-09	7.22	4.17	0.10	0.06	1.25	0.02	0.79	0.01	0.07	0.00
		SS-10	3.70	2.14	0.10	0.06	0.74	0.02	0.97	0.03	1.54	0.04
		SS-11	4.92	2.84	0.05	0.03	0.30	0.02	0.45	0.03	0.06	0.00
Sarapiqui	Stem	SS-12	0.11	0.06	0.18	0.10	0.74	0.05	4.71	0.06	7.57	0.09
		SS-13	0.02	0.01	0.11	0.07	1.85	0.07	5.83	0.17	5.31	0.17
		SS-14	0.00	0.00	0.05	0.03	0.58	0.01	2.86	0.07	0.47	0.02
		SS-15	0.04	0.02	0.37	0.22	2.57	0.09	5.54	0.09	8.25	0.07
		SS-16	0.03	0.02	0.37	0.21	3.88	0.17	10.14	0.45	10.94	0.60
Tortuguero	Leaf	SS-17	*	*	*	*	0.71	0.02	5.12	0.09	7.00	0.21
		SS-18	0.01	0.01	0.09	0.05	0.18	0.00	2.17	0.02	0.61	0.01
		SS-29	0.01	0.01	0.45	0.26	1.66	0.06	6.63	0.07	8.12	0.06
		SS-20	0.00	0.00	0.25	0.14	1.15	0.04	3.18	0.02	1.15	0.04
		SS-21	0.00	0.00	0.09	0.05	0.66	0.01	3.38	0.04	4.20	0.10

Results are averages of 3 replicates injected intraday * below limit of detection

Figure 2-6: HPLC chromatographic separation of marker compounds in a crude extract of leaf *S. sympetala*. Negative ionization A (3-5), Positive ionization B (1-2) detection.

A.



B.

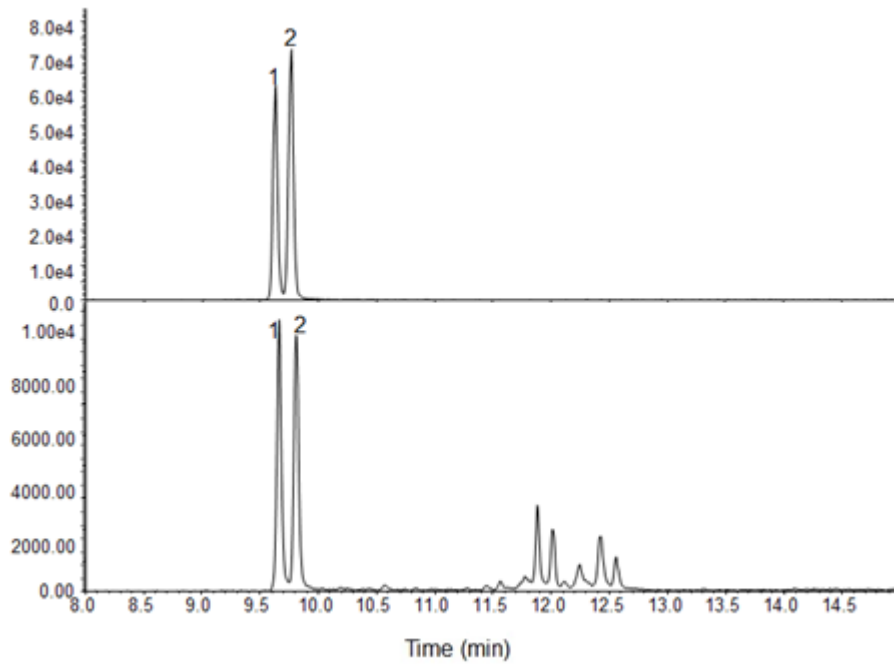
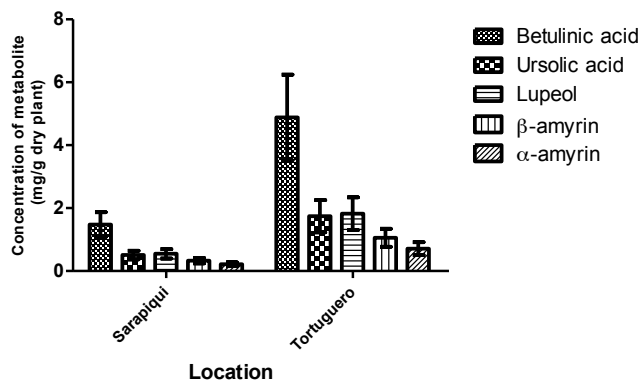


Figure 2-7: Mean content of five triterpenes in A. stems, B. Leaf of *S. sympetala* from two different locations in Costa Rica (n=5)

Content of five triterpenes in stems of *S. sympetala* from two different locations in Costa Rica



Content of five triterpenes in leaf of *S. sympetala* from two different location from Costa Rica

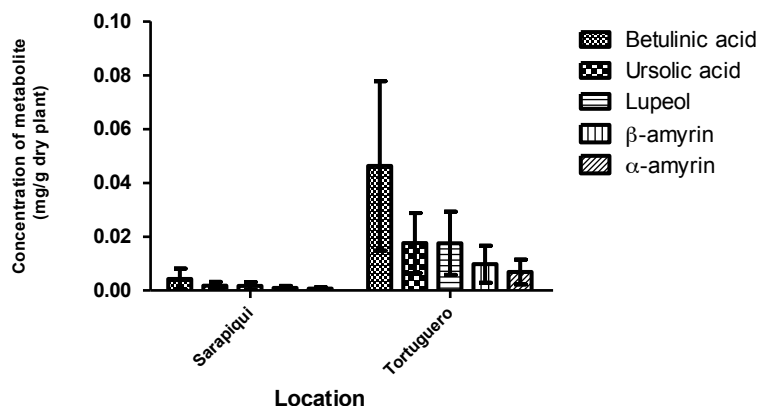


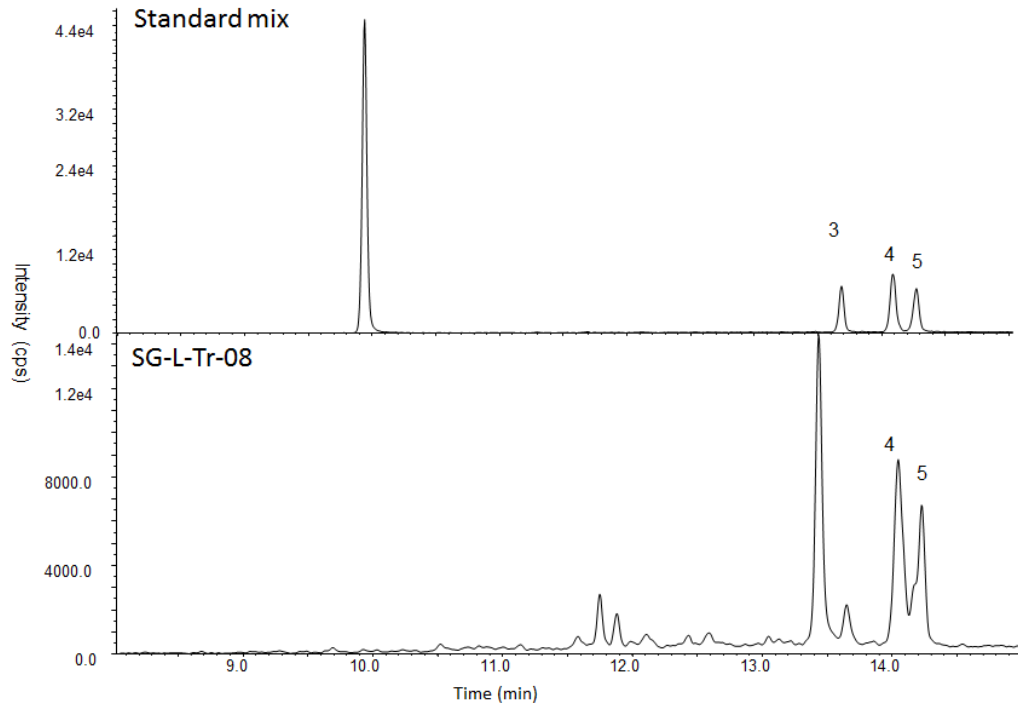
Table 2.2.2.9: Physical description of the two collection sites

Location	Average temp.(°C)	Highest temp. (°C)	Lowest temp (°C)	Altitude (m over sea level)	Annual precipitation (mm)
Totuguero*	26.0	31.0	21.0	20	>5000
Sarapiquí ^o	25.3	30.0	20.2	180-220	3777

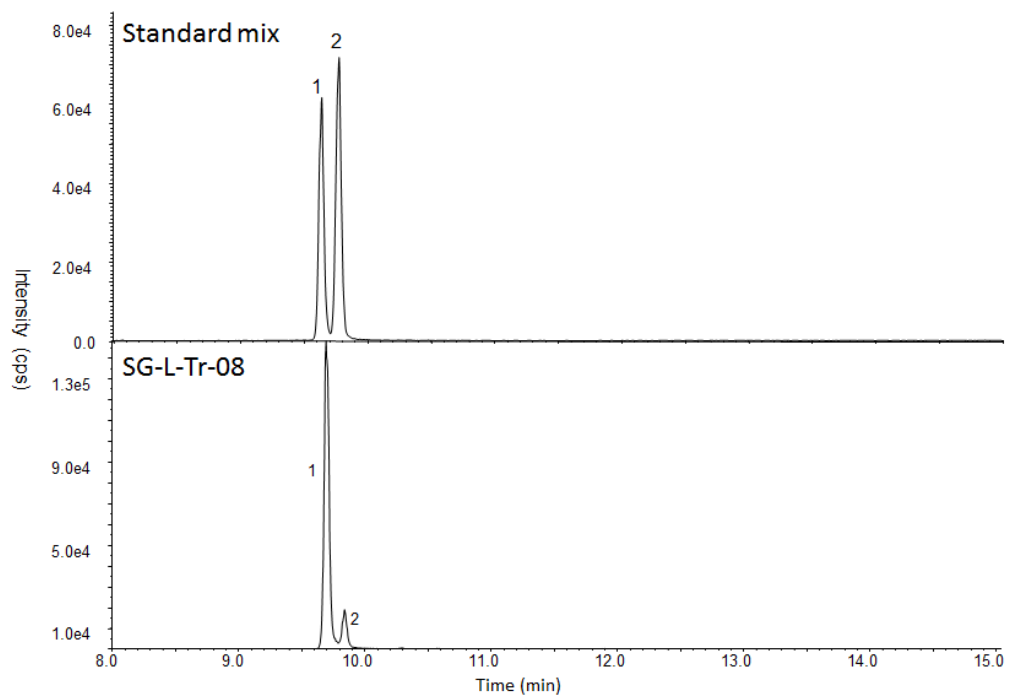
* Tortuguero National park is used as reference for climate²³.^o Tirimbina reserve is used as a reference for Sarapiquí climate, because most of the samples were collected near this location²⁴.

Figure 2-8: HPLC chromatographic separation of marker compounds in a crude extract of leaf *S. gilgii*. Negative ionization A (3-5), Positive ionization B (1-2) detection.

A.



B.



During the analysis of *S. sympetala* samples, some samples of both plant organs from the related species *Souroubea gilgii* were also analyzed, (Table 2.2.2.10) shows details of the collections sites and voucher numbers. It is important to mention that these two species grow in the same locations described for *S. sympetala*. *S. gilgii* shows the presence of the five triterpenes evaluated in the method in similar amounts and in similar metabolic profiles, (Figure 2-9). Both species are comparable in anxiolytic activity and phytochemistry, and could be used as a mixed species product as for Hawthorne, which is a mixture of *Craetagus* spp. However, it may be desirable to differentiate them for regulatory purposes, in a later chapter provide metabolomics methods to distinguish the species.

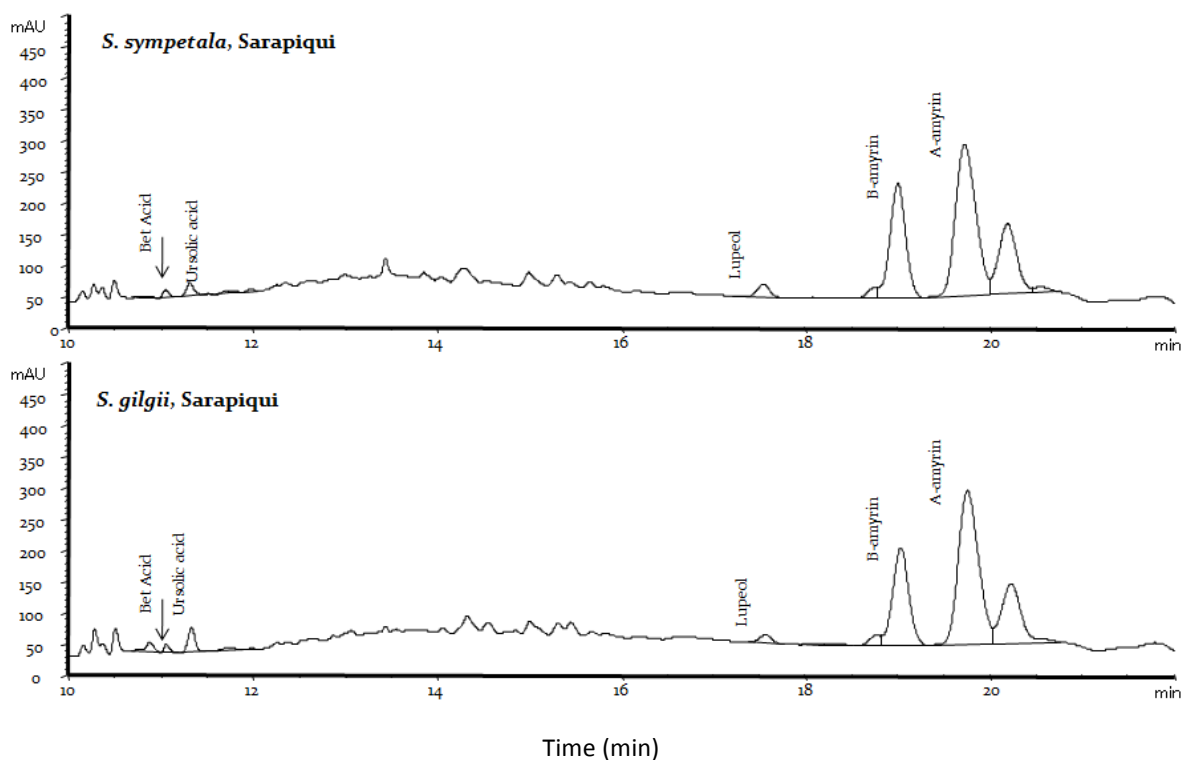
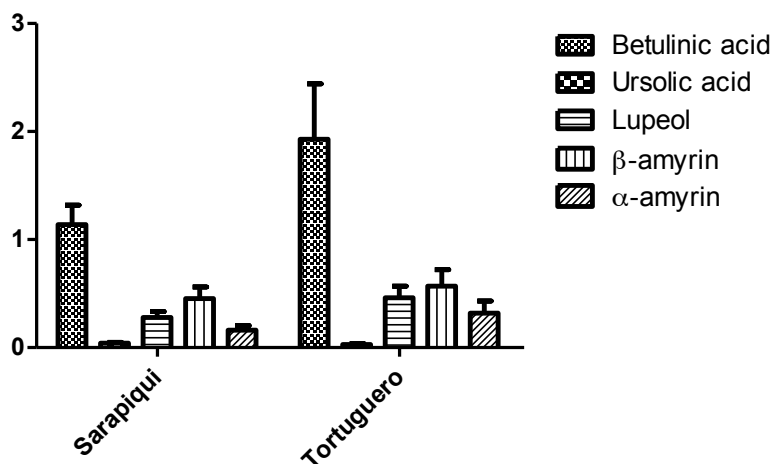


Figure 2-9: HPLC-DAD profiles of leaf extracts of *Souroubea* spp.

The analysis developed for the evaluation of triterpenes in *Souroubea* species has shown interesting trends in the content of betulinic acid, α - Amyrin and β -Amyrin. Comparing the distribution of these triterpenes in the plant samples from the two locations in Costa Rica, one

can conclude that leaves from the two species and the two location present higher content of Amyrins than betulinic acid. Stem samples are richer in betulinic acid. The leaf samples collected in Sarapiquí area have a higher concentration of triterpenes than the leaf samples of *S. gilgii*. The highest concentration of betulinic acid is present in stems of *S. sympetala*, but the content of Amyrins in this plant organ is low **Figure 2-10**.

Content of five triterpenes in s of *S. gilgii* from two different location from Costa Rica



Content of five triterpenes in leaf of *S. gilgii* from two different location from Costa Rica

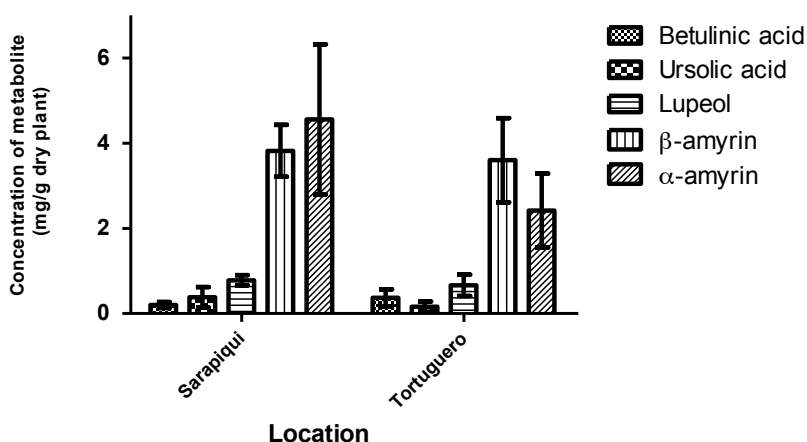


Figure 2-10: Mean content of five pentacyclic triterpenes in stem (A) and leaf (B) of *Souroubea gilgii*

The distribution and occurrence of the five different pentacyclic triterpenes analyzed by the method described seems to be highly influenced by the collection site. This factor is reflected in the error bars of the corresponding graphs. There is high variability among the samples because they were collected from different areas among the locations. A rigorous quality control method for plant material used for commercial production processes becomes really important to assure the activity of the NHP. Further studies regarding influence of location and season of collection seems to be imperative to have better control over starting materials and final quality of the marketed product.

The comparison of the content of betulinic acid content in **Figure 2-11** shows that the highest concentration of betulinic acid can be obtained from *S. sympetala* stems from Tortuguero. Nevertheless, the easiest plant organ to harvest will be the *S. gilgii* leaf from Tortuguero, which has the highest content of betulinic acid.

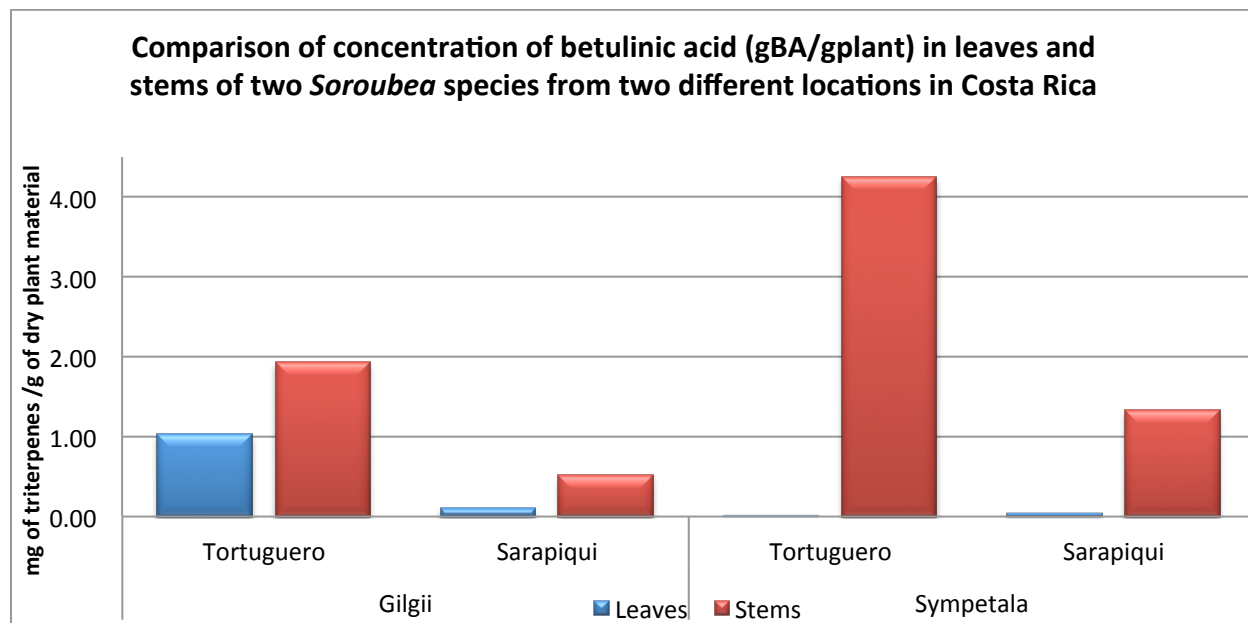


Figure 2-11: Content of betulinic acid in two species of *Souroubea* from two locations from Costa Rica

Table 2.2.2.10: Mean and SEM (mg of compound/g of dried plant) of five pentacyclic triterpenes in leaf and stems of representative *S. gilgii* accessions

Location	Plant Part	Sample Code	cpd1	SEM	cpd 2	SEM	cpd 3	SEM	cpd 4	SEM	cpd 5	SEM
Sarapiqui	Stem	SG-1	0.58	0.33	0.03	0.02	0.28	0.00	0.52	0.01	0.12	0.00
		SG-2	0.85	0.49	0.08	0.05	0.10	0.00	0.15	0.01	0.06	0.00
		SG-3	0.70	0.40	0.04	0.02	0.36	0.01	0.95	0.03	0.02	0.00
		SG-4	1.42	0.82	0.03	0.02	0.38	0.01	0.50	0.01	0.19	0.00
		SG-5	1.15	0.66	0.06	0.03	0.08	0.00	0.10	0.00	0.13	0.00
Tortuguero	Stem	SG-6	1.26	0.73	0.02	0.01	0.16	0.00	0.20	0.01	0.23	0.01
		SG-7	3.09	1.78	*	*	0.26	0.01	0.42	0.01	0.02	0.00
		SG-8	1.13	0.65	0.04	0.02	0.52	0.01	0.44	0.00	0.49	0.00
		SG-9	2.04	1.18	0.01	0.00	0.73	0.01	0.75	0.01	0.80	0.02
		SG-10	4.38	2.53	0.05	0.03	0.83	0.01	0.94	0.01	0.53	0.02
		SG-11	0.84	0.49	0.03	0.02	0.09	0.00	0.09	0.01	0.02	0.00
		SG-12	0.74	0.43	0.03	0.02	0.66	0.01	1.14	0.02	0.14	0.01
Sarapiqui	Leaf	SG-13	0.05	0.03	0.30	0.18	0.34	0.01	2.37	0.06	0.92	0.01
		SG-14	0.09	0.05	0.01	0.01	0.96	0.04	4.07	0.05	3.45	0.16
		SG-15	0.18	0.10	0.34	0.19	1.05	0.03	4.74	0.04	11.95	0.12
		SG-16	0.21	0.12	1.56	0.90	1.02	0.03	6.15	0.08	7.87	0.15
		SG-17	0.01	0.01	0.01	0.01	0.88	0.05	3.57	0.07	3.38	0.06
Tortuguero	Leaf	SG-18	0.10	0.06	0.02	0.01	0.54	0.01	3.80	0.06	2.27	0.10
		SG-19	0.21	0.12	0.02	0.01	0.51	0.02	3.90	0.08	0.48	0.03
		SG-20	0.01	0.00	0.19	0.11	0.26	0.00	2.01	0.03	2.39	0.06
		SG-21	0.20	0.12	0.70	0.41	0.81	0.06	4.92	0.36	14.49	0.56
		SG-22	1.25	0.72	0.03	0.02	1.71	0.08	6.66	0.15	4.75	0.09

* below limits of detection

Table 2.2.2.11: Collection sites for *Souroubea gilgii* samples included in the study (vouchers are held at JVR herbarium, Universidad nacional, Heredia, Costa Rica)

Code	Sample	Location*	Year collection	of	Plant part	Voucher number
SG-1	SG-S-HO-10	Horquetas	2010		Stem	12877
SG-2	SG-S-SA-10	Sarapiqui	2010		Stem	12878
SG-3	SG-S-SA1-09	Sarapiqui	2009		Stem	12841
SG-4	SG-S-SA-11	Sarapiqui	2011		Stem	13125
SG-5	SG-S-TI-11	Tirimbina	2011		Stem	13128
SG-6	SG-S-CP11-10	Cano Palma	2010		Stem	12874
SG-7	SG-S-Tr3-09	Tortuguero	2009		Stem	12362
SG-8	SG-S-Tr4-09	Tortuguero	2009		Stem	12363
SG-9	SG-S-Tr1-10	Tortuguero	2010		Stem	12873
SG-10	SG-S-CP1-09	Cano Palma	2009		Stem	12365
SG-11	SG-S-TR-10	Tortuguero	2010		Stem	12872
SG-12	SG-S-TR-0111	Tortuguero	2011		Leaf	13141
SG-13	SG-L-HO-0111	Horquetas	2011		Leaf	13137
SG-14	SG-L-T1-09	Tirimbina	2009		Leaf	12367
SG-15	SG-L-SA-0111	Sarapiqui	2011		Leaf	13096
SG-16	SG-L-SA-0111	Sarapiqui	2011		Leaf	13098
SG-17	SG-L-TI-0111	Tirimbina	2011		Leaf	13099
SG-18	SG-L-Tr-10	Tortuguero	2010		Leaf	12878
SG-19	SG-L-CP4-10	Cano Palma	2010		Leaf	12882
SG-20	SG-L-Tr-10	Tortuguero	2010		Leaf	12884
SG-21	SG-L-Tr4-09	Tortuguero	2009		Leaf	12370
SG-22	SG-L-Tr-08	Tortuguero	2008		Leaf	11973

- Locations in Costa Rica

2.2.3 Experimental

Materials

Extraction and HPLC grade solvents were purchased from Fisher Scientific (Ottawa, ON, Canada). Betulinic acid, ursolic acid, lupeol, α -Amyrin and β -Amyrin (95% purity) standards were purchased from Extra-synthase (Lyon, France).

Plant collection

Leaves and stems of *Souroubea sympetala* and *Souroubea gilgii* were collected during the dry season (dry season in Costa Rica goes from beginning of November until the end of April) of 2009 and 2011 from wild plants growing in Tortuguero, (Limon) and Sarapiquí, (Heredia) Costa Rica. The samples were collected and identified by botanists from the herbarium Juvenal Rodriguez, Universidad Nacional of Costa Rica, where vouchers have been deposited. (See **Table 2.2.2.7** for voucher numbers *S. sympetala* collection and

Table 2.2.2.11 for *S. gilgii*).

Sample preparation

Plant material was dried at 35 °C in a plant drier for 2 hr and ground to 0.2 mesh in a Willey mill. Ground material (2.0 g) was placed in cellulose thimbles and extracted in a soxhlet system using 250 mL ethyl acetate (1:125, w: v). The soxhlet system was set up to perform six cycles per hr. for two hrs. The extracts were concentrated under reduced pressure using a Yamato Rotary Evaporator RE50 (Yamato Scientific, Japan) at 40 °C, lyophilized (Super Modulo, Thermo Electron, USA) and extraction yields were recorded. In total, 21 botanical accessions were extracted, corresponding to two different locations and two plant organs, leaf and stem. The extracts were stored at 4 °C in amber HPLC vials.

HPLC-APCI-MS analysis

HPLC-MS analyses were carried out on a 3200 QTRAP (ABSciex, Concord, ON, Canada) hyphenated with a 1200 series HPLC system (Agilent Technologies, Santa Clara CA, USA). HPLC system consisted of a high performance auto sampler, a binary pump, a column thermostat, and an online degasser. The HPLC was connected in tandem with an LC-MS/MS system

consisting of a turbo V source and mass analyzer, operated in Q1M1 mode. The separations were performed at 1 mL/ min on a Kinetex C18 column, particle size 2.6 micron, particle diameter 100 Å, 100 x 2.1 mm ID (Phenomemex, Torrence, CA, USA). Column thermostat was maintained at 45 °C. A linear gradient of 30-100 % acetonitrile in water was applied. The column was then washed with 100 % acetonitrile 5 column volumes, returned to the initial conditions in 0.1 min and re-equilibrated for 5 min before the next injection, resulting in a total running time of 30 min. One mL of each extract dissolved in 100 % methanol at 250 µg/ mL was injected in triplicate through the auto-sampler. The MS detection was performed in positive ionization mode for lupeol, α- and β-Amyrin and negative mode for betulinic acid and ursolic acid (**Table 2.2.2.2**).

Compound quantification

Betulinic acid, lupeol, α- Amyrin and β-Amyrin were quantified based on area under the peak, while ursolic acid was quantified based on peak height. Calibration curves were generated by injecting pure standards.

Method validation

The HPLC-APCI-MS/MS method was validated following ICH guidelines in terms of precision, accuracy, and linearity (ICH., 2005).

Accuracy: The accuracy of the method was evaluated by spike recovery experiment. Recovery experiments were undertaken at three concentration levels for each of the metabolites evaluated. Spiked and unspiked samples were extracted following the procedure described above. The experiment was carried out in triplicates and coefficients of variation were determined accordingly.

Linearity and range: Calibration curves for each of the triterpenes evaluated by the method were prepared using five concentration levels, linear regressions were performed and R² values obtained for each triterpene.

Sensitivity: LOD and LOQ. The limits of detection (LOD) defined as a 3:1 peak to noise ratio and limits of quantification (LOQ) defined as a 10:1 peak to noise ratio, were determined for the five triterpenes by analysis of serial dilutions of the standards.

Ruggedness: Inter/intraday variation. The repeatability of the method was evaluated by performing the triplicate analysis of the five samples.

Analysis of representative accessions: The developed and validated method was used to analyze and quantify the five selected triterpenes in plant samples of *S. sympetala*. All samples were processed as described in the sample preparation section and the analysis run under the conditions developed for the validated method.

Statistical Analysis

All the statistical analyses were performed using Graph Pad Prism software.

2.2.4 References

1. Giraldo-Canas, Diego. A new genus of the Neotropical family Marcgraviaceae (Ericales) and circumscription of the Norantea Complex un nuevo género de la familia neotropical marcgraviaceae (ericales) y. *Flora* **29**, 203–217 (2007).
2. Dressler, S. Neotropical Marcgraviaceae. *neotropikey* at <<http://www.kew.org/science/tropamerica/neotropikey/families/Marcgraviaceae.htm>> Accessed February 2013
3. Ward, N. M. & Price, R. A. Phylogenetic Relationships of Marcgraviaceae : Insights from Three Chloroplast Genes. *Systematic Botany* **27**, 149–160 (2002).
4. Lens, F.; Dressler, S.; Vinckier, S.; Janssens, S.; Dessein, S.; van Evelghem, L.; Smets, E. Palynological variation in balsaminoid ericales. I. Marcgraviaceae. *Annals of botany* **96**, 1047–60 (2005).
5. Saleh, Nabil A.M.; Tower, G. H. N. Flavonol glycosides of norantea guianensis flowers. *Phytochemistry* **13**, 2012 (1974).
6. Schultes, Richard Evans, and Raffauf, R. F. *The Healing Forest: Medicinal and Toxic Plants of the Northwest Amazonia*. (Dioscorides Press: Portland, OR, 1990).

7. Bourbonnais-Spear, N.; Awad, R.; Merali, Z.; Maquin, P.; Cal, V.; Arnason, J. Ethnopharmacological investigation of plants used to treat susto, a folk illness. *Journal of ethnopharmacology* **109**, 380–7 (2007).
8. World Health Organization *The ICD-10 Classification of Mental and Behavioral Disorders*. (World Health Organization: Geneva, 1993).
9. Puniani, E. Novel natural product base anti-anxiety therapy and natural insecticides. PhD Thesis. Ottawa University (2004). At: <https://www.ruor.uottawa.ca/en/handle/10393/29155> Accessed: December 2013.
11. Mullally, M.a, Kramp, K.a, Saleem, A, Rojas, M.O, Vindas, P.S, Garcia, M.b, Alvarez, L.P, Durst, T., Trudeau, V.L., Arnason, J. T. Characterization and Quantification of triterpenes in the neotropical medicinal plant *Souroubea sympetala* (Marcgraviaceae) by HPLC-APCI-MS. Natural Product Communications. *Natural Product Communications* **3**, 1885–1888 (2008).
12. Cayer, C. In vivo behavioral characterization of anxiolytic botanicals. Master Thesis. Ottawa University (2011). At http://www.ruor.uottawa.ca/en/bitstream/handle/10393/20473/Cayer_Christian_2011_thesis.pdf?sequence=3 Accessed December 2013.
13. Jäger, S., Trojan, H., Kopp, T., Laszczyk, M. N. & Scheffler, A. Pentacyclic triterpene distribution in various plants - rich sources for a new group of multi-potent plant extracts. *Molecules (Basel, Switzerland)* **14**, 2016–31 (2009).
14. Yogeewari, P. & Sriram, D. Betulinic acid and its derivatives: a review on their biological properties. *Current Medicinal Chemistry* **12**, 657–66 (2005).
15. Laszczyk, M. N. Pentacyclic triterpenes of the lupane, oleanane and ursane group as tools in cancer therapy. *Planta medica* **75**, 1549–60 (2009).
16. Tiv, M. Triterpenoids Isolation from *Marcgravia nepenthoides*: Bark and Wood. Report Summer 2010 BPS 4902 Presented to Dr . John T. (2010).
17. Aragão, G.F.; Carneiro, L.M.; Junior, P.F.; Vieira, L.C.; Bandeira, P.N.; Lemos, T.L.G.; Viana, G.S. A possible mechanism for anxiolytic and antidepressant effects of alpha- and beta-Amyrin from *Protium heptaphyllum* (Aubl.) March. *Pharmacology, biochemistry, and behavior* **85**, 827–34 (2006).
18. Wen, X.; Zhang, P.; Liu, J.; Zhang, L.; Wu, X.; Ni, P.; Sun, H. Pentacyclic triterpenes. Part 2: Synthesis and biological evaluation of maslinic acid derivatives as glycogen phosphorylase inhibitors. *Bioorganic & Medicinal Chemistry Letters* **16**, 722–6 (2006).
19. Laszczyk, M. Pentacyclic tuterpenes of the lupane, oleanane and ursane group as tools in cancer therapy. *Planta Med.* **75**, 1549–1560 (2009).

20. Durst, Tony; Merali, Zulfiqar; Sanchez-Vindas, Pablo E.; Poveda Alvarez, L. J. Anxiolytic Marcgraviaceae compositions containing betulinic acid, betulinic acid derivatives and methods. Us Patent EP1476031A1 (2009).
21. Awad, R; Levac, D. & Cybulska, P; Merali, Z; Trudeau, V L; Arnason, J. T. Effects of traditionally used anxiolytic botanicals on enzymes of the gamma-aminobutyric acid (GABA) system. *Canadian Journal of Physiology and Pharmacology* **85**, 933–42 (2007).
22. Mullally, M. Anxiety-Reducing Tropical Plants. PhD thesis. Ottawa University (2011).
23. Conservancy, S. turtle <http://www.conserveturtles.org/volunteer-research-programs.php?page=tortnp>. (2011).at <<http://www.conserveturtles.org/volunteer-research-programs.php?page=tortnp>> Accessed February 2013
24. Reserve, T. biological <http://www.tirimbina.org/>. (2010).at <<http://www.tirimbina.org/what-is-tirimbina/physical-description.html>> Accessed February 2013
25. International conference on harmonisation of technical requirements for registration of pharmaceuticals for human use ich harmonised tripartite guideline: validation of a nalytical p rocedures.(2005).at <http://www.ich.org/fileadmin/Public_Web_Site/ICH_Products/Guidelines/Quality/Q2_R1/Step4/Q2_R1__Guideline.pdf> Accessed February 2013

2.3 Untargeted metabolomic analysis of *Souroubea sympetala* and *Souroubea gilgii*, by UPLC-QTOF

2.3.1 Introduction

Metabolomics is a relatively new field developed from metabolic profiling¹. Advances in GC-MS analysis expanded analysis from a few targeted compounds to the analysis of a large number of compounds in human urine and breath samples² and this marked the beginning of metabolomic analysis in medicine. In botanical sciences, plant metabolomics is a field of study pioneered by researchers from The Max Planck Institute in the early 1990's³. It has been defined as "a comprehensive analysis in which all the metabolites of a biological system are identified and quantified"⁴. At the time at which the definition of the term was introduced, it was expected that the analysis would allow access to the complete metabolome of a biological system. Therefore it should avoid exclusion of any metabolite. In order to achieve this, much attention should be drawn to sample collection, preparation, extraction techniques and the use of suitable and sensitive analytical techniques⁴. Today, it is appreciated that this is almost an impossible task, considering the fact that around 100,000 secondary metabolites have been isolated and just half of these compounds have been completely characterized⁵. Furthermore, these secondary metabolites include a vast chemical diversity. For example, alkaloids are the secondary metabolites most studied and around 12,000 different structures have been identified just for this particular group⁵, which makes chromatographic separation of closely structural related compounds a challenging step in the analysis.

The complexity of the field and the lack of understanding of many of the biosynthetic pathways that give rise to this colossal number of structures make the original task set for metabolomics challenging. As a consequence, five classifications of metabolomics have emerged: 1. Targeted analysis: relates to the quantitative determination of a limited number of key compounds, 2. Metabolite profiling: refers to the analysis of a specific pathway or metabolite group, 3. Metabolomics: is the exhaustive determination of metabolites in an extract from an organism, 4. Finger printing: for which the goal is to generate a profile of an extract in which peak identification is not essential⁶. The final classification corresponds to the untargeted

metabolomics where the aim of this approach is to collect as much information as possible about the metabolites present in a particular biological system, considering all the information present in the different data sets⁷.

In order to gather a suitable set of data to work in any of the metabolomic areas some aspects must be fulfilled: as much as possible, the analysis should be efficient and unbiased, the best separation of analytes should be achieved, a good detection method must be used, and once the data is available, multivariate analysis should be performed on the data set and identification and quantification of the metabolites should be performed if needed⁸. Essentially all metabolomics approaches give a “metabolic snapshot” of a specific biological system in a particular time-point. This is an important aspect when drawing conclusions about the data analyzed⁸.

Plant collection plays a crucial role in the outcome of the metabolomic analysis. The biological variation associated with plant collection is much more significant than any variation caused by the analytical technique used in the analysis⁸. This could be a key aspect in obtaining results with biological significance or deciding to do more experiments. Samples should be collected from the most similar environments possible. Sample preservation after collection and extraction procedures are defined by the metabolomic approach selected for the analysis^{4,8}. Several different approaches exist and they have been described in several papers.

A wide number of analytical techniques are used to profile small molecules in biological systems, all of them based on MS or NMR detection. The use of these two techniques is based on the fact that they can provide a good amount of spectroscopic and structural information on a wide variety of molecules with analytical precision⁹. The most commonly used chromatographic systems include gas chromatography (GC), liquid chromatography (LC), ultra performance liquid chromatography (UPLC) and capillary electrophoresis (CE). Each of the techniques mentioned have their own advantages and limitations. Sensitivity is one of the most important limitations that varies with the technique, **Figure 2-12**.

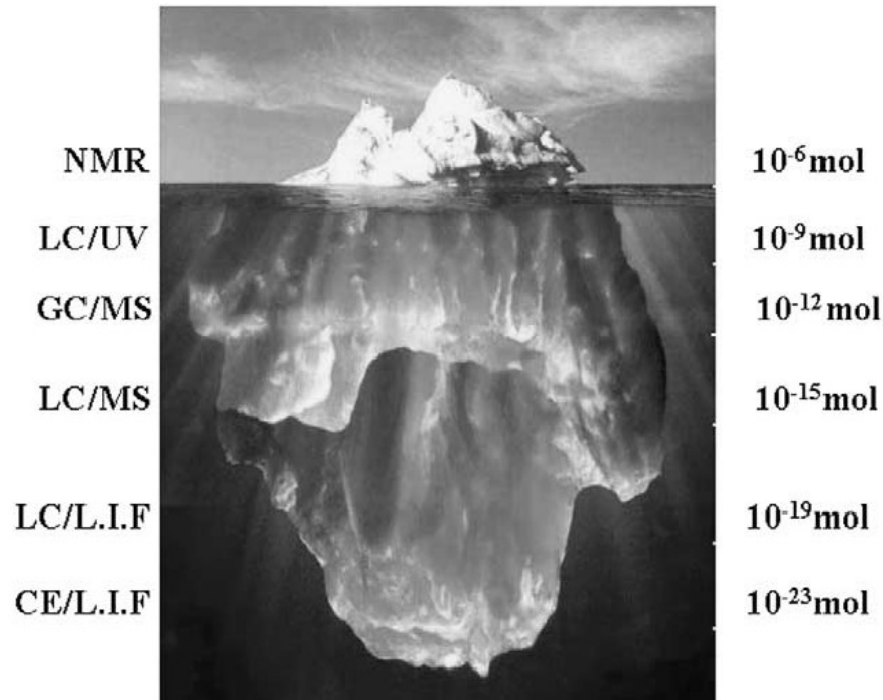


Figure 2-12: Comparison of relative sensitivities of various analytical techniques used in metabolomic experiments³. L.I.F (Laser induced fluorescence)

Gas chromatographic analysis requires chemical derivatization, slowing the preparation of samples that are analyzed. LC on the other hand does not usually require derivatization of the sample previous to injection. NMR allows the analysis of a whole sample in a single measurement with a high robustness, but it has the limitation of sensitivity. NMR detection can achieve micromolar levels in a normal set up and nanomolar levels using cryoprobes, while MS can detect concentrations as low as picomolar⁹.

Despite the selected analytical technique, metabolomic analyses generate complex multivariate data sets that require the use of chemometric and bioinformatics methods to be interpreted. Some of the methods used for interpretation of data in metabolomics are: principal component analysis (PCA) an unsupervised method, and as part of the supervised methods partial least square (PLS), orthogonal partial least square (OPLS), and these can be combined with discriminant analysis (DA)^{3,9}.

Metabolomics has a broad range of applications from generation of basic knowledge, elucidation of metabolic pathways and biosynthetic routes⁵, analysis of adulteration in foods and natural products^{6,10} to search for biomarkers in plants¹¹.

During the development of the validated method for the analysis of *Souroubea* spp. it was noticed that the two plant species evaluated: *S. gilgii* and *S. sympetala* have similar metabolic profiles. This result was seen using different analytical techniques: LC-MS, LC-QTRAP and LC-DAD **Figure 2-13**.

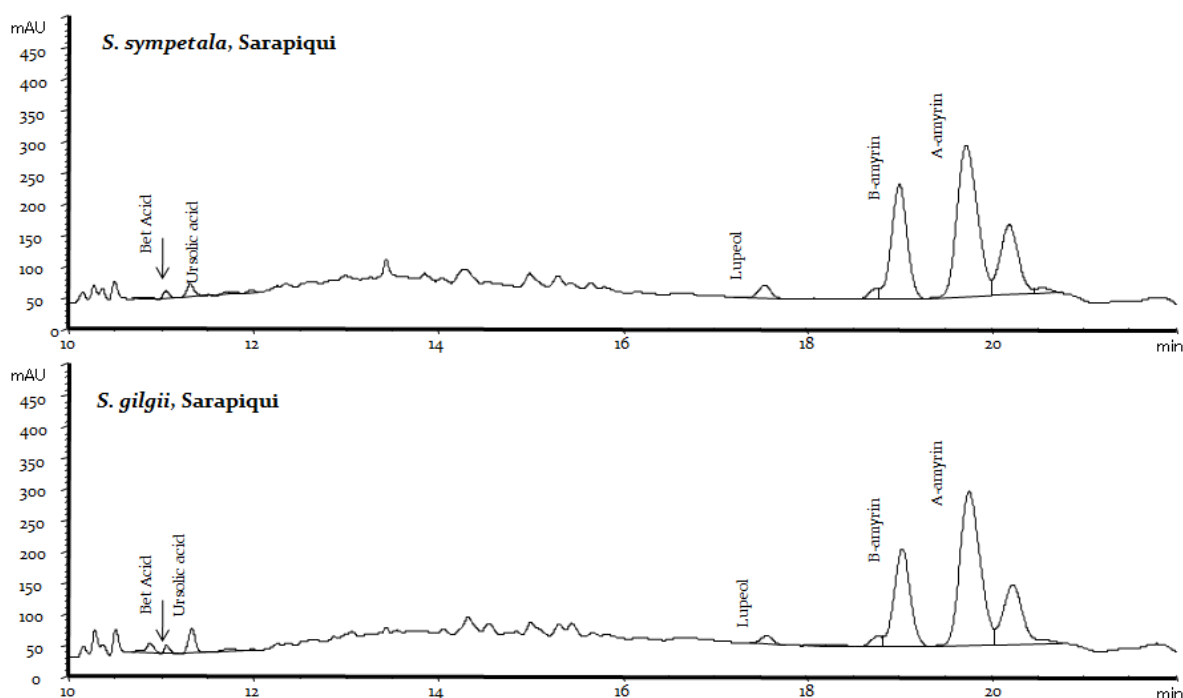


Figure 2-13: LC-DAD profile of crude leaf extracts of *Souroubea* spp.

Based on these observations and considering the fact that these plants will be used in the development of a veterinary NHP, it was considered necessary to find a way to distinguish between them. *Souroubea sympetala* and *Souroubea gilgii* are two different species of the genus, and based on other results in chemosystematics, it is known that different species usually produce some different metabolites. Consequently, the objective of the present study was to use metabolomic analysis to find a marker that could distinguish the two species.

2.3.2 Results and discussion

As mentioned in the introduction, the purpose of untargeted metabolomics is to describe the metabolome of a living biological system in a certain moment in time, under specific environmental constraints¹². Taking this under consideration this methodology was selected to try to identify a marker that would allow the discrimination between the two *Souroubea* spp. The multivariate analysis was used to identify the putative markers in the species.

All samples were prepared following the same protocol of extraction to avoid inclusion of variability in the analysis in this step, nevertheless, samples were collected in different times and different years (**Table 2.3.2.1**) and they come from different locations and environments from Costa Rica. The season of collection remained the same, as all the samples were collected during the dry season (November-April). It is important to state that the plant is a rare vine and it was difficult to have a more standardized method of collection.

In order to evaluate the influence of the collection site on the metabolite production two distinct areas were included: Sarapiquí, located in Heredia province and Tortuguero, located in Limon province.

Figure 2-14: Geographical distribution of the plant collection for *Souroubea* spp. Map modified from Google maps.

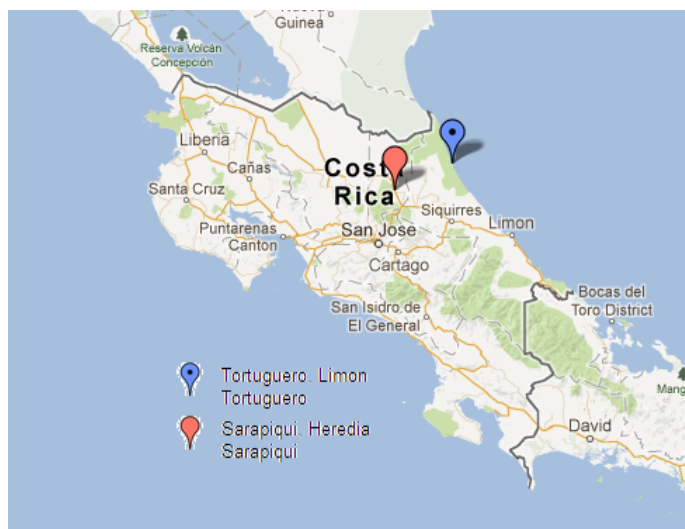


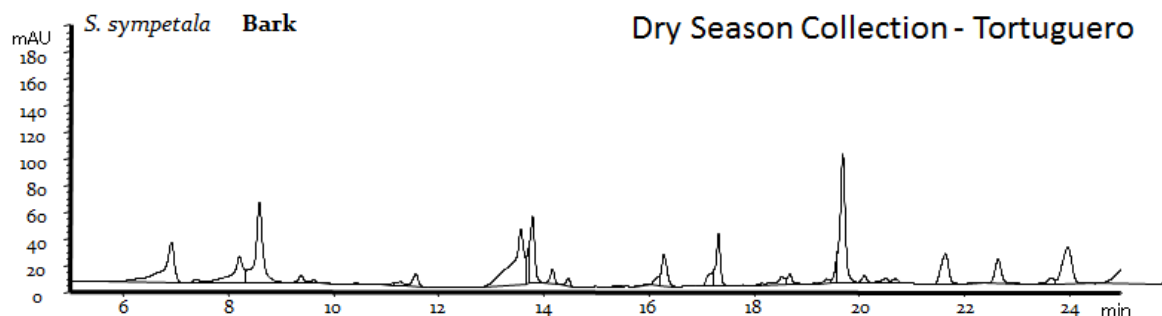
Table 2.3.2.1: Sample information for sample collection of *Souroubea* spp.

species	Sample code	Collection site	Voucher number	Year of collection	
<i>S. sympetala</i>	SS-Sa01	Sarapiqui	13099	2009	
	SS- Sa02	Sarapiqui	12367	2011	
	SS- Sa03	Sarapiqui	12325	2009	
	SS- Sa03	Sarapiqui	12841	2009	
	SS- Sa03	Sarapiqui	13098	2009	
	SS- Sa04	Sarapiqui	13099	2009	
	SS-Tr01	Tortuguero	12362	2011	
	SS-Tr02	Tortuguero	12370	2011	
	SS-Tr03	Tortuguero	11973	2009	
	SS-Tr04	Tortuguero	12362	2009	
	SS-Tr05	Tortuguero	12363	2011	
	SS-Tr06	Tortuguero	12874	2004	
	<i>S. gilgii</i>	SG-Sa01	Sarapiqui	12320	2011
		SG-Sa02	Sarapiqui	13125	2009
SG-Sa03		Sarapiqui	12343	2009	
SG-Sa04		Sarapiqui	12340	2009	
SG-Sa05		Sarapiqui	12325	2011	
SG-Sa06		Sarapiqui	12260	2011	
SG-Tr01		Tortuguero	12370	2009	
SG-Tr02		Tortuguero	12365	2009	
SG-Tr03		Tortuguero	12381	2008	
SG-Tr04		Tortuguero	12396	2009	
SG-Tr05		Tortuguero	12363	2009	
SG-Tr06		Tortuguero	12884	2010	

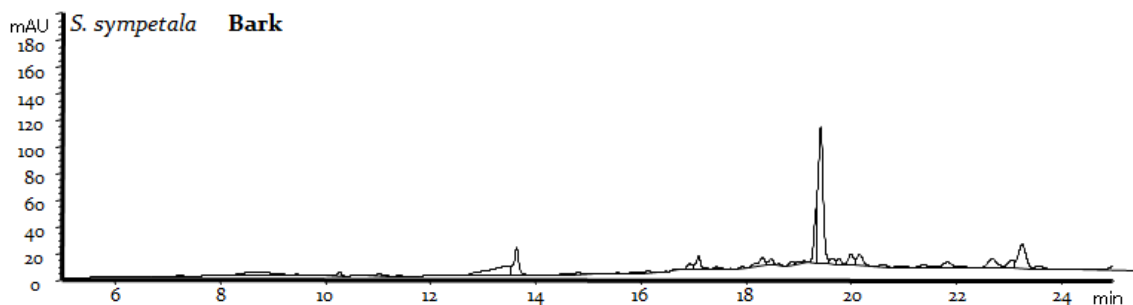
Samples were run in a hyphenated system consisting in UHPLC-MS-QTOF (Quadrupole Time of Flight). The use of MS-QTOF as the detection method provides high resolution in the mass spectra and high sensitivity for profiling of intact ions generated from metabolites by ESI (Electrospray ionization)¹³. The combination of the TOF and the quadrupole also allows the detection of metabolites in low concentrations.

Pentacyclic triterpenes are present in both species as major components and there is a difference in their concentration between the two species, as discussed in section 2.1. The concentration of secondary metabolites has a high dependency on environmental factors making the use of concentration variation of these metabolites as a discriminating variable between the two species inappropriate. It has also been observed that there is a high impact on

the metabolic profile of samples collected in the two different seasons in Costa Rica (**Figure 2-15**). This figure depicts a bark sample and it was chosen to illustrate this fact since the bark extracts are less complex in terms of secondary metabolite content, and it becomes easy to see the changes that are described above.



Rainy Season Collection - Tortuguero



23

Figure 2-15: Variation of the production of metabolites in *S. sympetala* according with the collection season, using HPLC-DAD as analytical method

The metabolomic approach selected for this experiment was the use of OPLS-DA¹⁴ multivariate analysis. After samples were run in the UHPLC-MS QTOF systems, the data were analyzed using MarkerLynx software (Waters). Samples were run in positive and negative mode, but only the negative mode signal was used in the analysis of the data because a manual exploration of the data revealed that this signal had more information about each of the samples. This is a normal procedure since the use of both signals will create a vast amount of data and also will include some redundancy of compounds that can be ionized in both polarities. Again ESI becomes a

better choice for this procedure, ESI has offers a greater coverage of polar metabolites without excluding non-polar species such as sterols and phospholipids¹³.

Data obtained from the UHPLC-MSQTOF is first scaled and transformed. MakerLynx does this via a Pareto scaling, and after this process is done the second step requires depurating the data: removal of outliers, samples that can affect the final model or suspicious samples that can be removed after investigation¹⁴. The OPLS-DA analysis of the metabolome of the botanical samples is shown in **Figure 2-16**. Samples were clustered into group A which corresponds to *S. gilgii* samples and group B to *S. sympetala* samples. There were also three samples identified as outliers. Both the hybrids and the outliers were removed from the discriminant analysis since it is necessary to have distinct species groups with less metabolic “noise” in order to find species biomarkers. Once a biomarker is tentatively identified, it can be assessed in all samples.

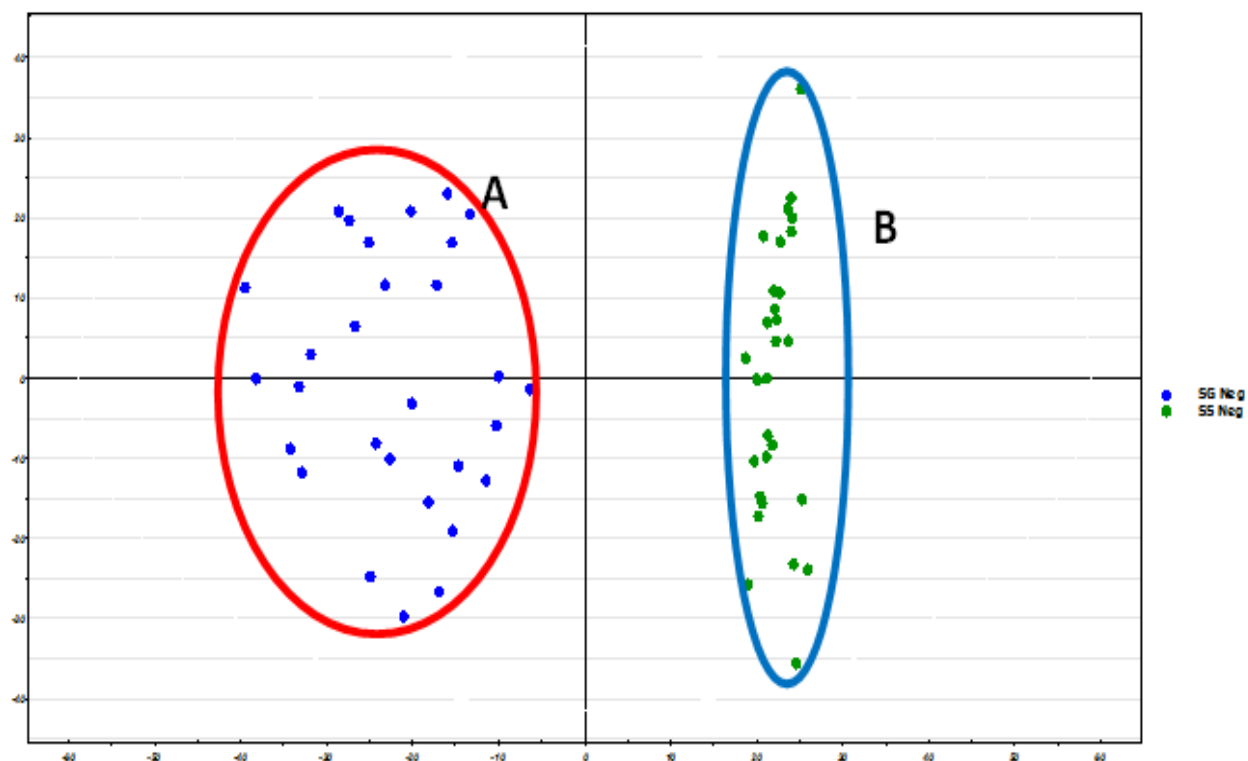


Figure 2-16: OPLS-DA score plot of twenty-four samples of *Souroubea* spp. samples. Group A corresponds to *S. gilgii* samples (SG Neg), group B to *S. sympetala* samples (SS Neg). The first component is plotted on the x- axis and the second component on the y-axis.

The samples used for the analysis included two species, and two distinct locations. This result and the fact that the other two clusters observed in the plot also represent samples from different locations permits me to conclude that location is not a factor in the separation seen for the two clusters and that the two species can be separated based on the metabolic profile. Variations related to plant homeostasis are commonplace, factors like local environment, developmental differences, and many others can affect the metabolic profile so in order to draw conclusions from the data, sample collection data becomes meaningful, and allows us to draw conclusions with biological significance.⁸

After the removal of the samples identified as outliers a new OPLS-DA analysis was performed (**Figure 2-17**). The resulting score plot presented two simple clusters with a mean separation of 40.4 units in the first component (x-axis) The analysis of the variation in the second component (y-axis) allows observation of some of the variation within the groups, which were 55 units for the *S. gilgii* samples and 71 units for the *S. sympetala*.

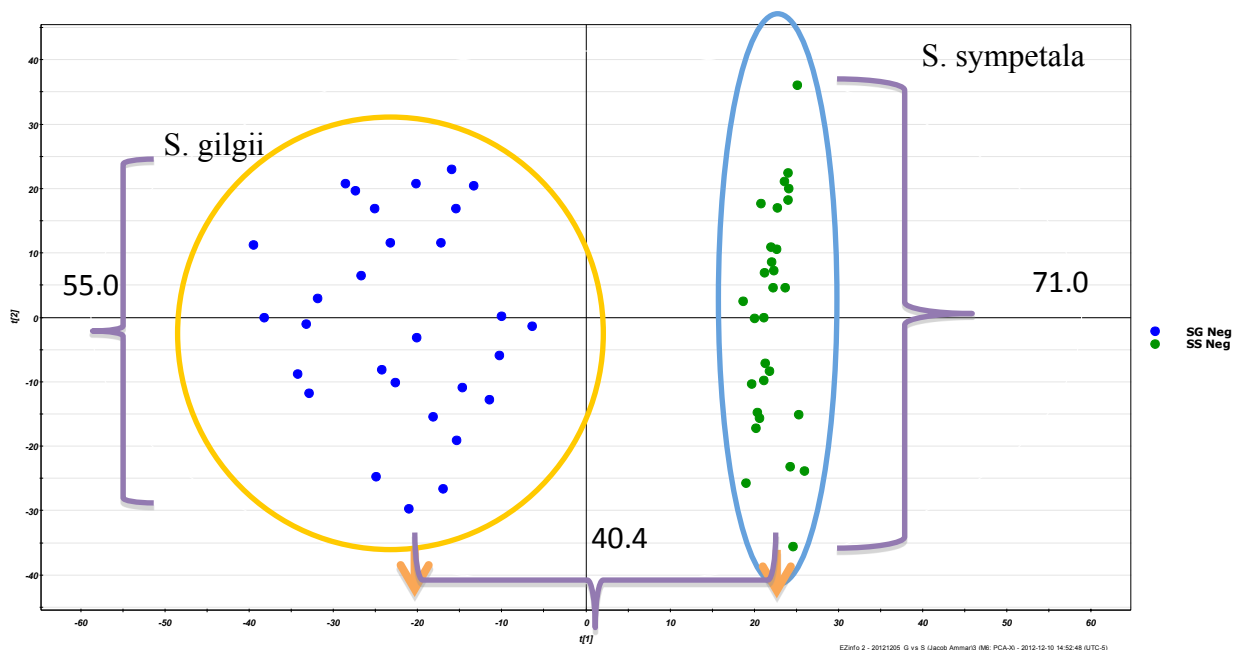


Figure 2-17: OPLS-DA score plot of samples of *Souroubea* spp. with outliers removed.

Figure 2-17 represents the Score plot of components from the OPLS-DA model that illustrates unambiguous inter-group separation. A three dimensional plot using the first three components

(Figure 2-18) confirms this intergroup separation. Once the OPLS-DA showed the separation between the groups the corresponding S-plot was obtained by discriminant analysis (**Figure 2-19**). This tool helps in the identification of putative biomarkers. This plots gives the loading from the OPLS-DA analysis, where P (corr) represents the reliability in the (“y” axis) and the p[1] represents the magnitude of each variable in “x”axis. A good biomarker must have a high magnitude and high reliability. The only plant that showed metabolites bearing these two characteristics was *S. gilgii*, and a total of five possible markers were identified from the discriminant analysis (**Table 2.3.2.2, Figure 2-19**). *S. sympetala* does not have reliable biomarkers absent in *S. gilgii*. The metabolite labeled as SGN1 represents the most interesting one in our study, since this metabolite has the highest magnitude and the highest reliability out of the five putative makers identified for *S. gilgii*. The distribution and statistical significance of this metabolite can be seen in (**Figure 2-20**), showing that metabolite SGN1 is present in all *S.gilgii* samples and absent in all *S. sympetala* samples.

The masses obtained and the elemental compositions obtained from the QTOF-MS analysis were searched using different public databases including: Metlin, NIC, and PubMed. Scifinder was also consulted in the process but no hits for the data available were found. This result and the lack of phytochemical studies on these plants make us believe these masses and elemental compositions could correspond to new compounds. Identification of these compounds and, in particular SGN1, could lead to the identification of a marker in *Souroubea gilgii* that can be used in the quality assurance process for the manufacturing of the NHP.

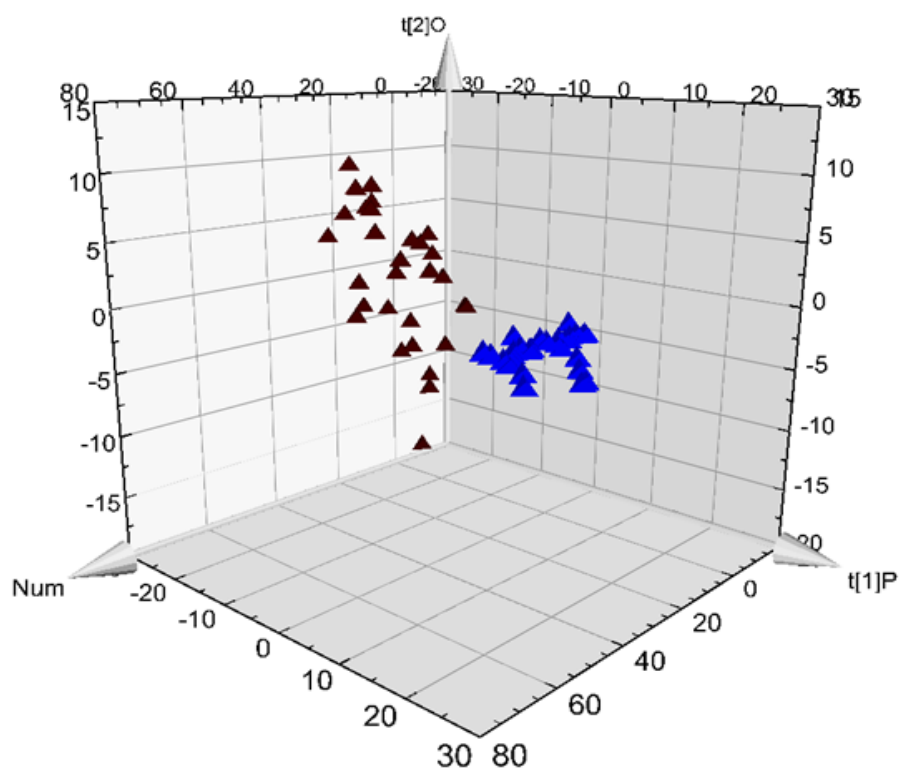


Figure 2-18: Score plot of the OPLS-DA scores for the two clusters corresponding to two *Souroubea* species

Table 2.3.2.2: Putative markers found in *S. gilgii*

Code	Rt (min)	Neutral Mass	Mol Formula
SG1N	3.03	386.2390	C ₂₄ H ₃₄ O ₄
SG2N	5.24	296.2365	C ₁₄ H ₂₈ N ₆ O
SG3N	2.70	372.2226	C ₂₂ H ₂₈ O ₅
SG5N	3.13	950.6811	C ₆₅ H ₉₀ O ₅
SG10N	6.94	383.2083	C ₂₄ H ₃₂ O ₄
SG17N	6.58	356.1672	C ₁₉ H ₂₀ N ₂ O ₃ S

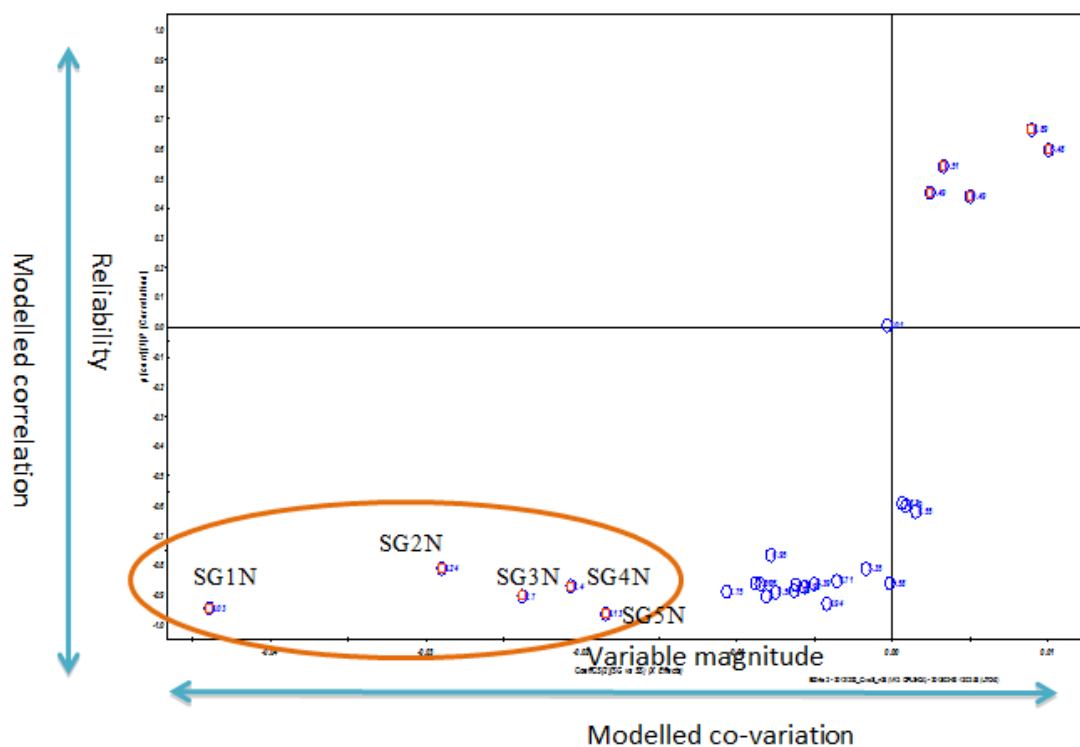


Figure 2-19: S-plot for the corresponding OPLS-DA loadings calculated for the *Souroubea* spp. Samples. S-plot shows correlation p (corr) of variables of the discriminating component of OPLS-DA model plotted against covariance

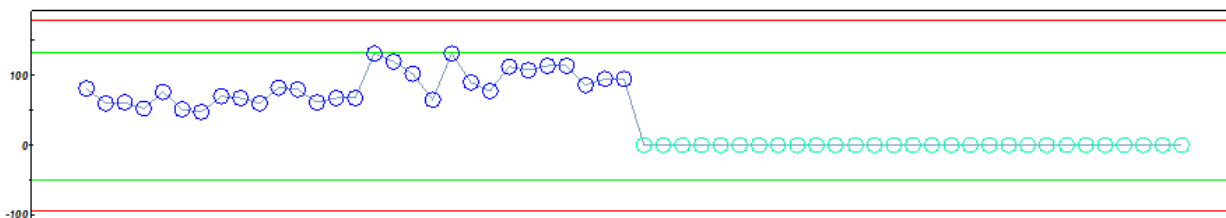


Figure 2-20: Distribution of metabolite SGN1 in *Souroubea* spp. samples. Blue dots are *S. gilgii* and aquamarine dots are *S. sympetala*

2.3.3 Experimental

Plant collection

Leaves of *Souroubea sympetala* and *Souroubea gilgii* were collected during the dry season (November to April) of 2004 to 2011 from wild plants growing in Tortuguero, (Limon) and Sarapiquí, (Heredia) Costa Rica. The samples were collected and identified by botanists from the herbarium Juvenal Rodríguez, Universidad Nacional of Costa Rica, where vouchers have been deposited. (See **Table 2.3.2.1** for voucher numbers).

Sample preparation:

Plants used in this part of the research were collected, extracted and prepared as described in **Section 1.1**.

UPLC-QTOF analysis:

UPLC conditions: Acquity BEH C18 1.7 μ m 2.1 x 100mm column connected with a VanGuard Pre-column 2.1 x 5 mm. Mobile phase A, water + 0.1% formic acid, B-acetonitrile + 0.1% formic acid (FisherOptima LC-MS). Flow rate 0.5 mL/min. Column temperature, 50 °C, sample temperature 10 °C. Mobile phase composition, 0-1 min 5% A isocratic, 1-6 min linear gradient 5-50% B, 6-8 min 50-95% B, 8.01-10 min 5% A isocratic (total run time 10 min).

Sample injection conditions:

A 1 μ L injection was followed by a strong wash 200 μ L (90% acetonitrile + 10% water) and weak wash 600 μ L (10% acetonitrile + 90% water). QTOF analysis conditions were: MassLynx software, MS ESI+ mode, lock mass Leucine Enkephalin 12C 556.2615, source temperature 120 °C, desolvation temperature 400 °C, Cone gas (N₂) flow 50 L/hr, desolvation gas (N₂) flow 1195 L/hr. MS conditions, mass range 100-1500 Da, F1 CE, 6V, F2 CER 10-30V, Cone voltage 20 V, Scan time 1 sec. Calibration, 50-1000 Da.

Statistical analysis:

Prior to statistical analyses the data were Pareto scaled which is the recommended method for LC-MS data since both medium and small features in the data are important. One independent multivariate analysis method was used for the analysis of the samples OPLS-DA (Orthogonal Partial Least Squares Discriminant Analysis). The statistical analysis was performed by

MarkerLynx (version 8.03)(Waters Corp.,USA). The observed results for putative markers were searched in public compound libraries: NIC, Metlin, Chemsp, Pubchem and Scifinder.

2.3.4 Future work

The analysis presented in this part of the research represents the first successful attempt for the finding a marker to distinguish *Souroubea gilgii* and *Souroubea sympetala*. The application of principal component analysis and other analytical tools for the evaluation of the same set of samples failed in the search and identification of possible markers. Nevertheless, to have a conclusive result, the putative markers found following the analysis described, must be isolated and purified in order to perform a complete structural elucidation. A practical methodology to achieve this is to identify from the set of samples evaluated, which plant contains the highest concentration of the metabolite, re-collect the sample and make a larger crude extraction. The fractionation of the crude can be done by classical column chromatography guided by UHPLC-MS to achieve the isolation of the targeted mass.

Plantations of *S. gilgii* and *S. sympetala* are being established in Costa Rica for the manufacturing of the “Sin susto” product and samples from these plantations can be used to find a marker for the plants since these are grown in similar conditions. It is expected they will show less variation among the samples.

Once these are identified they can be used to create an internal library and more plant samples of the two species must be collected and extracted. The crude extracts would be analyzed using the UHPLC-QTOF system in order to search for the identified marker. At this stage a model can be generated and cross-validated in order to classify future samples.

2.3.5 References

1. Maloney, V. Plant Metabolomics. *BioTech Journal* **2**, 92–99 (2004).
2. Pauling, L., Robinson, a B., Teranishi, R. & Cary, P. Quantitative analysis of urine vapor and breath by gas-liquid partition chromatography. *Proceedings of the National Academy of Sciences of the United States of America* **68**, 2374–6 (1971).

3. Sumner, L. W., Mendes, P. & Dixon, R. A Plant metabolomics: large-scale phytochemistry in the functional genomics era. *Phytochemistry* **62**, 817–836 (2003).
4. Fiehn, O. Metabolomics--the link between genotypes and phenotypes. *Plant Molecular Biology* **48**, 155–71 (2002).
5. Oksman-Caldentey, K.-M. & Inzé, D. Plant cell factories in the post-genomic era: new ways to produce designer secondary metabolites. *Trends in Plant Science* **9**, 433–40 (2004).
6. Steward, Derek; Shepherd, Louise V.T.; Hall, Robert D.; Fraser, P. D. Crops and tasty nutritious food: How can metabolomics help? *Annual Plant Reviews, Biology of Plant Metabolomics* 181–217 (2011).
7. De Vos, R. C. H.; Moco, Sofia, L., Arjen, K., Joost, J. B., Bino, R.J., Hall, R. D. Untargeted large-scale plant metabolomics using liquid chromatography coupled to mass spectrometry. *Nature Protocols* **2**, 778–91 (2007).
8. Hall, R. D. Plant metabolomics: from holistic hope, to hype, to hot topic. *The New phytologist* **169**, 453–68 (2006).
9. Lindon, J. C. & Nicholson, J. K. Spectroscopic and statistical techniques for information recovery in metabonomics and metabolomics. *Annual review of analytical chemistry (Palo Alto, Calif.)* **1**, 45–69 (2008).
10. Heyman, H. M. & Meyer, J. J. M. NMR-based metabolomics as a quality control tool for herbal products. *South African Journal of Botany* **82**, 21–32 (2012).
11. Li, Y., Wang, Y., Su, L., Li, L. & Zhang, Y. Exploring potential chemical markers by metabolomics method for studying the processing mechanism of traditional Chinese medicine using RPLC-Q-TOF/MS: a case study of Radix Aconiti. *Chemistry Central Journal* **7**, 36 (2013).
12. Jankevics, A., Merlo, M., de Vries, M., Vonk, R. J., Takano, E., Breitling, R. Separating the wheat from the chaff: a prioritisation pipeline for the analysis of metabolomics datasets. *Metabolomics : Official Journal of the Metabolomic Society* **8**, 29–36 (2012).
13. Allwood, J. W. & Goodacre, R. An introduction to liquid chromatography-mass spectrometry instrumentation applied in plant metabolomic analyses. *Phytochemical analysis : PCA* **21**, 33–47 (2010).
14. Wiklund, S. Multivariate Data Analysis for Omics. (2008).at <[http://www.metabolomics.se/Courses/MVA/MVA in Omics_Handouts_Exercises_Solutions_Thu-Fri.pdf](http://www.metabolomics.se/Courses/MVA/MVA%20in%20Omics_Handouts_Exercises_Solutions_Thu-Fri.pdf)> Accessed march 2013

2.4 Characterization of Marcgraviaceae species from Costa Rica

2.4.1 Introduction

WHO has long recognized the importance of traditional medicine. It also has acknowledged the great risk associated with the use of herbal preparations without proper control of these products¹. As a consequence it has established important guidelines in order to unify the criteria for the use and validation of traditional knowledge in plant use. These guidelines are stated in "General Guidelines for Methodologies on Research and Evaluation of Traditional Medicine World Health Organization". According to this document the first stage in quality control of herbal medicines is the botanical identification and verification of the plant used².

The effectiveness and the quality of a natural health product relies on the concentration of the active ingredients in the plants, which are affected by many factors such as: climate, cultivation conditions, harvest time, drying, storage, extraction procedure which may cause a large variability in active ingredients¹. Another problem is adulteration with less expensive similar species or even other plant material. All these issues make quality assessment and control of natural products a challenging task. The biggest risk behind this is the patient's health. There have been several reports of adverse effects of natural products³.

A plant extract typically consists of many metabolites; some of them are present in very low concentrations. Even though some of these metabolites are found in low concentration they could play an important role in the bioactivity of the extracts either as the active ingredient or a synergist in the mixture. Due to the complexity of a herbal extract, several analytical chromatography techniques have been used for its characterization and plant identification^{1,4-6}. Among them are: Thin Layer Chromatography (TLC), High Performance Liquid Chromatography (HPLC), Ultra High Performance Liquid Chromatography (UHPLC), Gas Chromatography (GC), and Capillary Electrophoresis (CE). Each of them has their advantages and disadvantages¹.

The idea behind the analysis is to develop a suitable system consisting in the combination of a chromatographic technique and a detection system that will allow the separation and detection of individual components and to develop a characteristic profile for the sample called fingerprinting (**Figure 2-21**). The advantage of fingerprinting is that it becomes a high

throughput technique that allows fast classification and characterization of samples⁷. It has been used successfully in the classification of economically important species like *Ginseng radix*⁸.

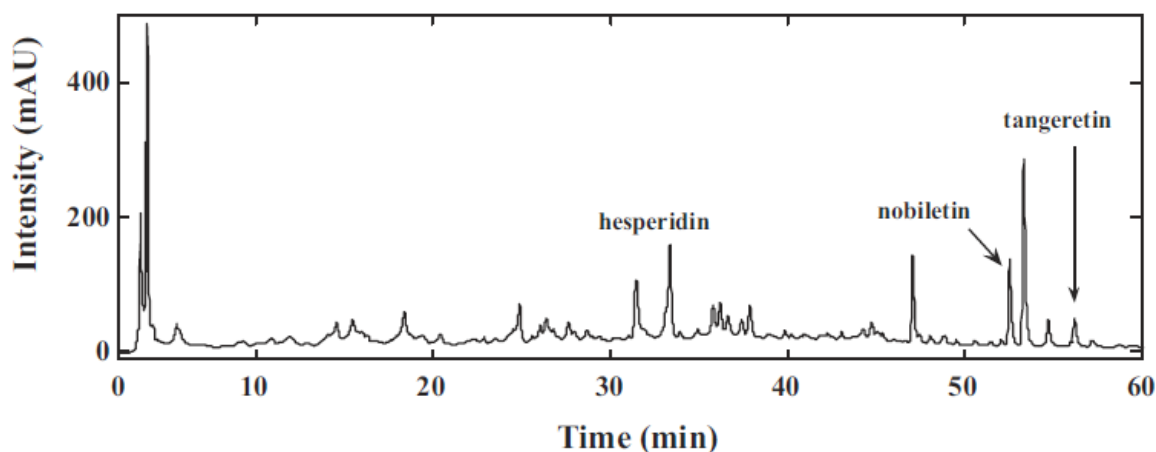


Figure 2-21: Example of a characteristic HPLC-UV herbal fingerprint of pericarpium *Citrus reticulatae* with some identified marker compounds

As mentioned before, Marcgraviaceae is a rare Neotropical family of vines. The two *Souroubea* plants studied by our research group belong to the Marcgraviaceae family. The evaluation of the crude extracts in animal models of these two plants showed their bioactivity as anti-anxiolytics⁹. This bioactivity was linked to the occurrence of pentacyclic triterpenes^{9,10}. These occurrence of pentacyclic triterpenes has also been observed in other Marcgraviaceae members studied in our group such as *Marcgravia nepenthoides*¹¹. Pentacyclic triterpenes could be used as biomarkers for the family members, since they have the potential of becoming starting materials in the development of new Natural Health Products.

2.4.2 Results and discussion

A. Fingerprinting for plant identification

Samples corresponding to thirteen different species belonging to the Marcgraviaceae family present in Costa Rica were collected in different areas in the country **Table 2.4.2.1**. Samples were extracted by dynamic maceration using 80% ethanol to generate a whole extract and to

have as much of each metabolite as possible present in the extract. Yields of extraction for the different plants are summarized in **(Table 2.4.2.1)**.

There have been few phytochemical analyses of the Marcgraviaceae family, besides the ones developed in our research group by: Dr. Puniani¹², and Melinda Tiv¹¹. The presence of the triterpenes among the members of the Marcgraviaceae makes this family a possible source for the development of new NHPs, because of the bioactivities associated with these type of secondary metabolites and the findings of the antianxiety properties for some of the member in the family: *Souroubea gilgii* and *Souroubea sympetala*⁹. Fingerprints of the available species **Table 2.4.2.1** were developed in order to analyze the presence of the triterpenes in these thirteen species and to establish a possible differentiation method through herbal fingerprinting.

Generally speaking, different chromatographic techniques can be used to obtain a relatively complete picture of a herbal extract; this is what is called a fingerprint and is used to represent what is called phyto-equivalence¹³. In the manufacturing of herbal products variation between batches of herbal material is allowed to some extent. Nevertheless, the manufacturer must provide proof that the material used in the process is "not significantly different" / "essentially the same"; fingerprinting can be used for this purpose. The profile chromatogram should have some characteristics in order to be used for this purpose¹⁴.

The development of a proper herbal fingerprinting to identify the plant will require a large collection of samples, from different locations and seasons. All this is done to evaluate the natural normal variation of the metabolites present in a particular plant extract. The present work shows the first attempt for the development of fingerprints to differentiate between different species of the Marcgraviaceae family.

The analytical technique selected for the development of the profiles was UHPLC-DAD. Samples were run in a modified method derived from the validated method discussed in Section 2.1, and six standards were incorporated to the analysis to help in the dereplication process of the samples **(Figure 2-22)**.

Table 2.4.2.1: Meta data for the Marcgraviaceae plant collection

Species Name	Codes	Voucher number	Origin	Yield of extraction %	Date Collected
<i>Macgraviastrum subsessili</i>	MS	13130	Rio Costa Rica, Cartago	13.90	March 2011
<i>Sarcopera rosulata</i>	MSR	13142	Tapanti, Costa Rica	7.90	March 2011
<i>Marcgravia nepenthoides</i>	MN	13145	Tortuguero, Limón	1.74	April 2011
<i>Marcgravia mexicana</i>		13150	Tortuguero; Cerro Coronel, Limón	9.46	March 2011
<i>Marcgravia globulosomarginata</i>	MSch	13152	Tapanti, Cartago	7.99	April 2012
<i>Sarcopera sessiflora</i>	MSS	13154	Lago Arenal, Alajuela	3.47	March 2012
<i>Marcgravia nervosa</i>		13157	Pacuare, Limon	5.87	April 2012
<i>Marcgravia brownei</i>	MB	13159	Tirimbina, Virgen de Sarapiquí, Heredia	10.17	March 2012
<i>Schwartzia tarrazensis</i>	ST	13160	San Marcos de Tarrazú, Cartago	10.01	March 2012
<i>Sourobea loczyi</i>	SL	13228	Monumento Nacional Guayabo, Turrialba, Cartago.	7.52	March 2012
<i>Schwartzia costaricensis</i>	SC	13298	Tapanti, Cartago	19.24	March 2011
<i>Sourobea sympetala</i>	SS	13300	Tortuguero, Limón	12.89	March 2010
<i>Sourobea gilgii</i>	SG	13321	Tortuguero, Limón	11.36	March 2010

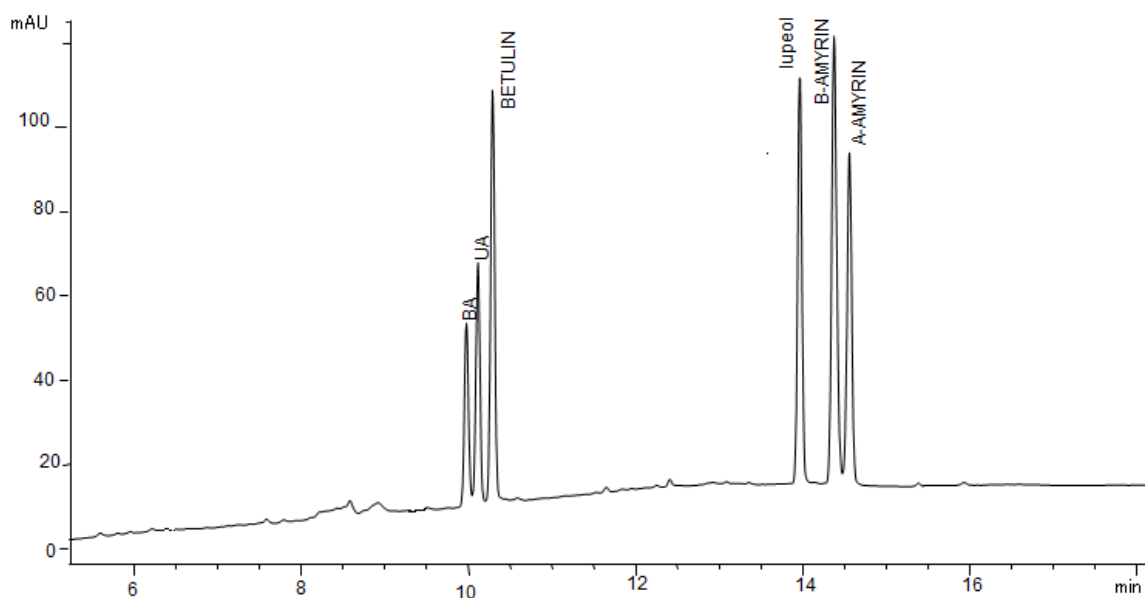


Figure 2-22: Standard mix of six pentacyclic triterpenes used in the development of fingerprints of Marcgraviaceae members. The extracts were separated on a Kinetex C18 column using a linear gradient of 30-100% acetonitrile in water

Code	Compound	Number	Retention time (min)
BA	Betulinic acid	1	10.0
UA	Ursolic acid	2	10.2
Betulin	Betulin	3	10.5
Lupeol	Lupeol	4	13.8
β-Amyrin	B-Amyrin	5	14.2
α-Amyrin	α-Amyrin	6	14.3

The selected UV wavelength was 210 nm since this is the wavelength that provides the best detection for the metabolites present in the extracts. Different sample concentrations were tested and 20.0 mg/mL was the best concentration to obtain the maximum information of the targeted triterpene metabolome. The chromatograms obtained showed a considerable variation of the metabolites present in the different species (**Figure 2-23A-H**).

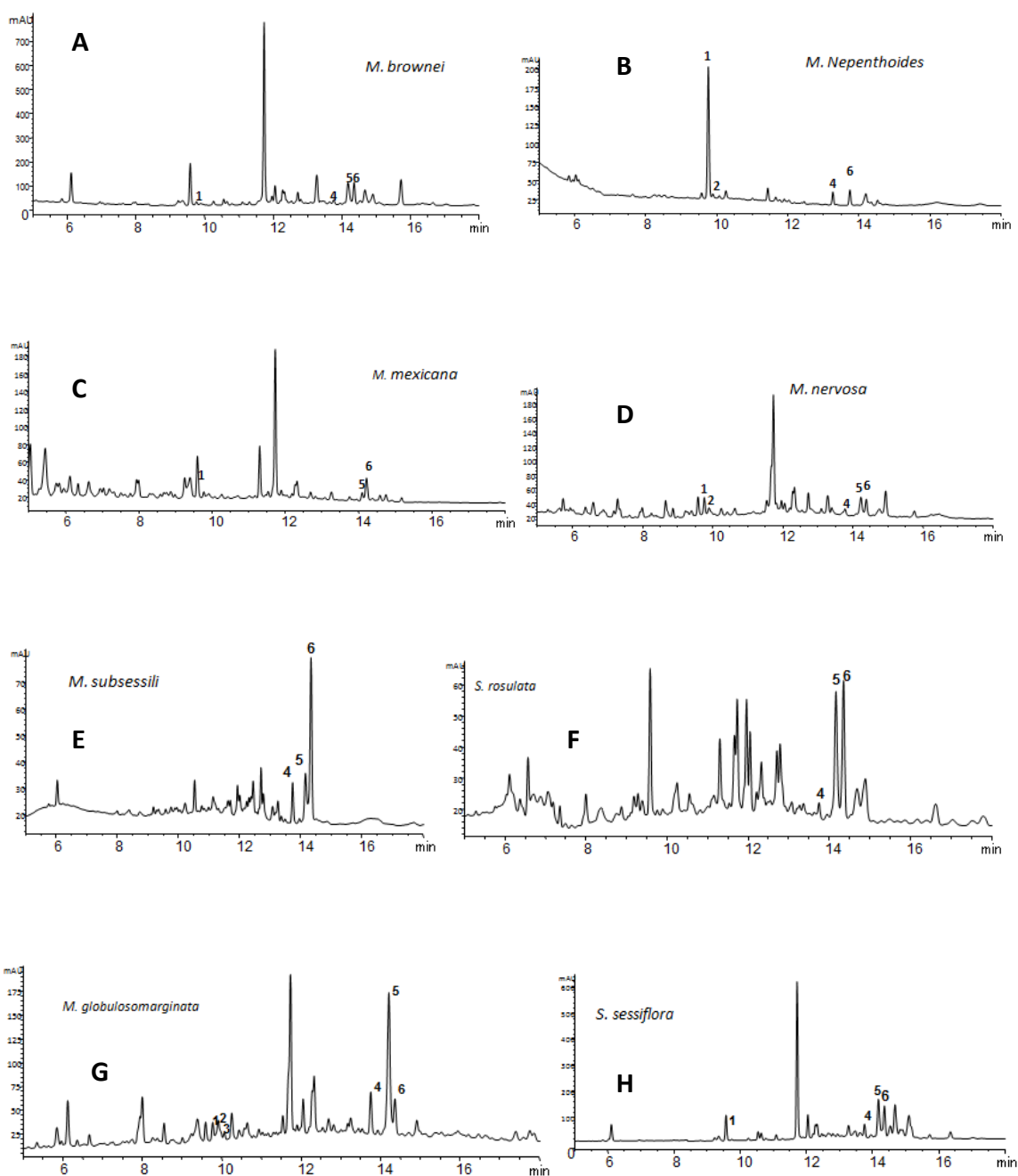


Figure 2-23: Fingerprints of eight different Marcgraviaceae species, the numbers correspond to the standards of the corresponding triterpenes (**Table 2.2.2.1**).

The observed variation is also present among members of the same genera **Figure 2-24** and (**Figure 2-25**). This makes them suitable for one of the requirements for the use of this

technique as a discriminatory tool to distinguish among herbal extracts, the chromatogram has to be unique¹⁴.

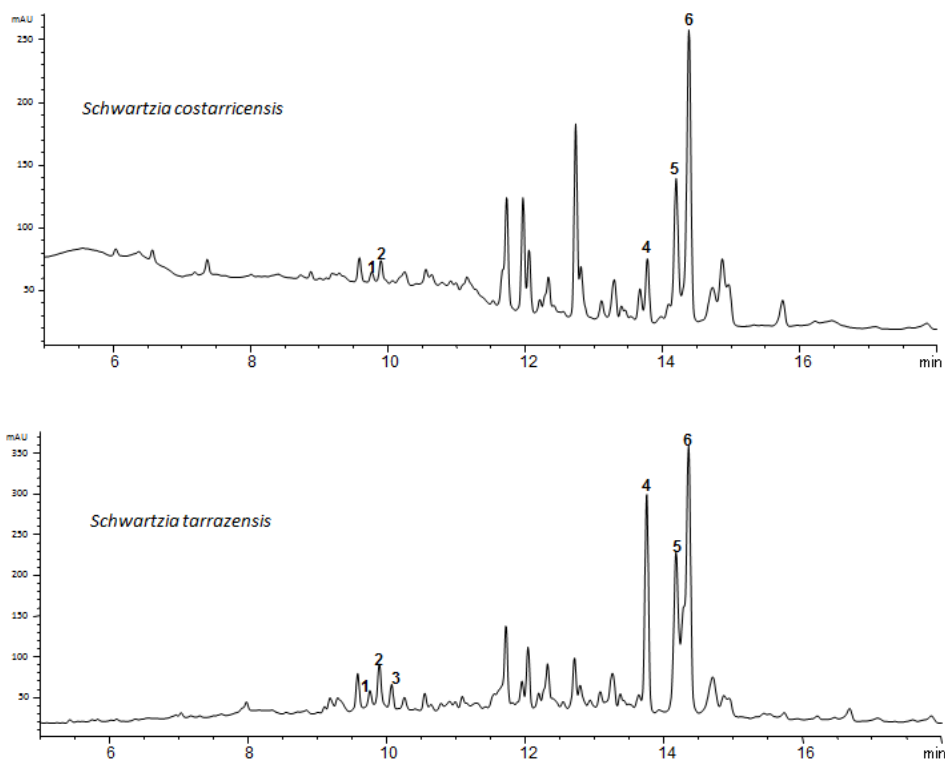


Figure 2-24: Comparison of the metabolic profiles of two species of *Schwartzia* from Costa Rica

As part of the Marcgraviaceae collection, one sample was identified only with a code and not the scientific name. This sample was extracted and analyzed following the same protocol described in the Experimental Section. Comparison of the metabolic profile of this sample and the existing profiles for the other Marcgraviaceae members allowed the identification of the sample as *Marcgravia globulosomarginata* (**Figure 2-26**). When the code was revealed, the sample was indeed a botanically identified *M. globulosomarginata*. This illustrated the value and applicability of the fingerprinting for identifying unknown specimens.

In the case of samples that present more variation among them, statistical methods like Principal Component Analysis (PCA) can be used to develop a model for the classification of the samples¹ once the chromatographic profiles of different samples has been acquired.

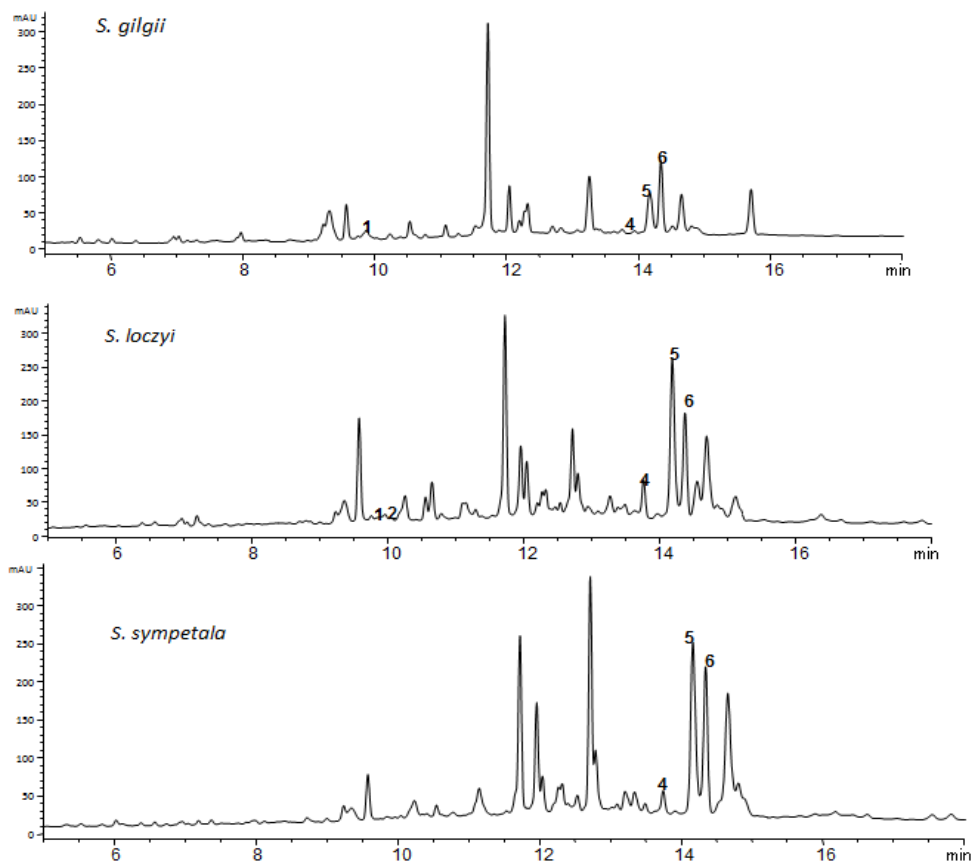


Figure 2-25: Comparison of the metabolic profiles of three species of *Souroubea* from Costa Rica

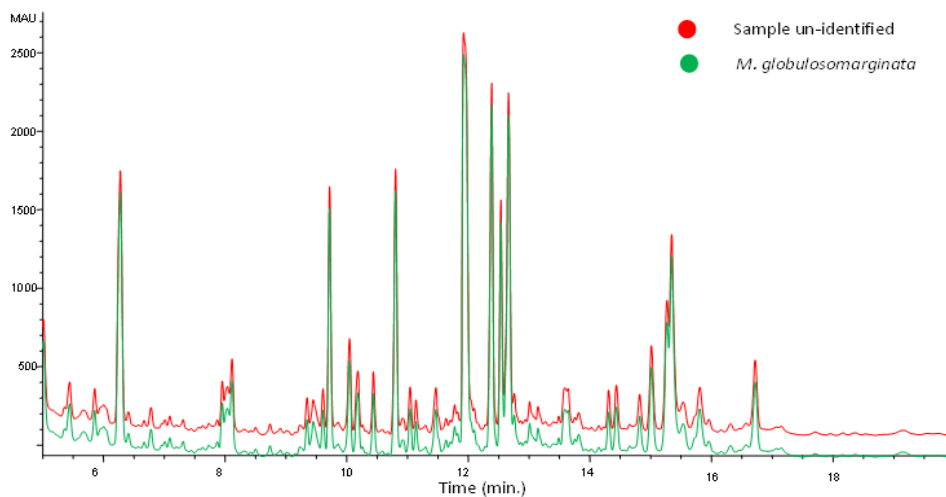
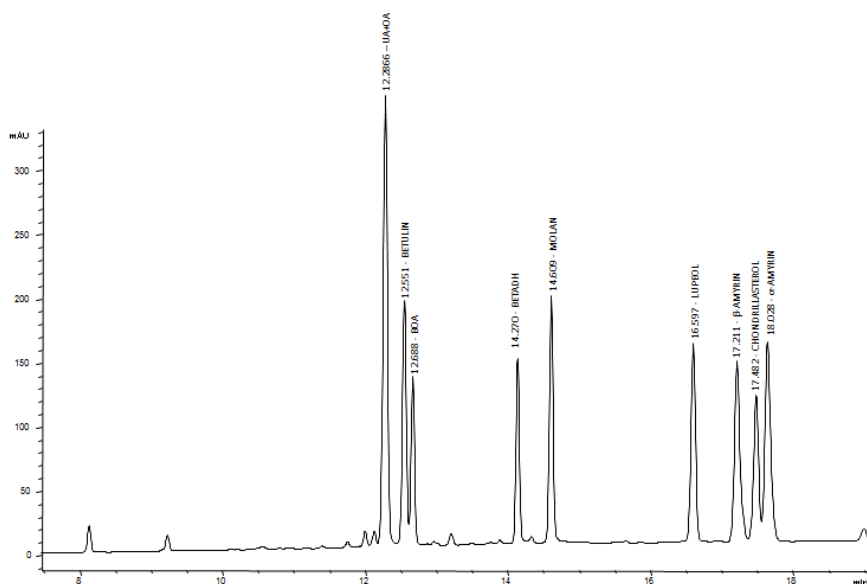


Figure 2-26: Comparison of the metabolic profile of two samples: red un-identified sample, and green: *M. globulosomarginata*

The method developed has good separation between most of the standards used to allow peak integration for quantification. For those peaks where complete baseline separation is not achieved, quantification can be done by peak height. This large separation between some compounds allows the future incorporation of more standards into the method as shown in **(Figure 2-27)** where betulonic acid, betulin aldehyde, methyl oleanate and chondrillasterol have been added. With more known compounds, this method can be used to facilitate the dereplication process in order to target unknown compounds in the samples analyzed.



Code	Compound	Retention time (min)
UA +OA	Ursolic acid+ oleanolic acid	12.29
Betulin	Betulin	12.55
BOA	Betulonic acid	12.69
BETADH	Betulin aldehyde	14.27
MOLAN	Methyl oleanate	14.61
Lupeol	Lupeol	15.60
β-Amyrin	β-Amyrin	17.21
chondrillasterol	Chondrillasterol	17.48

Figure 2-27: Standard mix chromatogram with the incorporation of four new standards

B. Untargetted Metabolomic Analysis

The analysis of the samples in the UHPLC-QTOF-MS system is an untargetted analysis of a much larger sample (up to a thousand compounds) of the metabolome of the plants. The analysis showed the possibility of finding markers to distinguish between the samples that are closely related. OPLS-DA score plot depicts the samples that cluster together based on the similarity of the metabolites produced by the plant (**Figure 2-28**). As shown in the plot, species like *S. souroubea* and *S.gilgii* are highly related in terms of metabolite production, the other plants that cluster are *M. subsessile* and *S. brasiliensis*, *M. Mexicana* and *M. nervosa* and finally *M. polyantha* and *M. nepenthoides*.

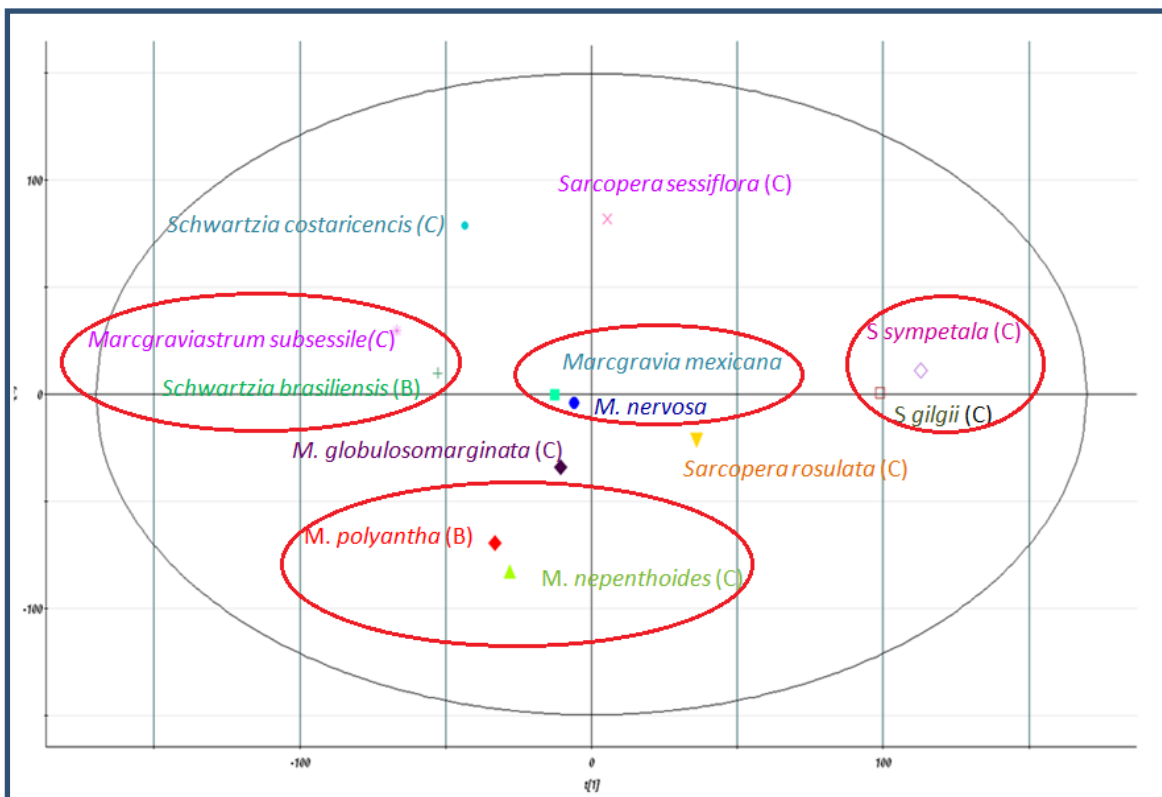


Figure 2-28: OPLS-DA score plot for the Marcgraviaceae samples the circles indicate species pairs that were similar and submitted for S plot identification of unique phytochemical markers Table 2.4.2.2:

The analyses of the corresponding S-plots (**Figure 2-29**) for each of the species pairs that cluster together based on metabolites produced allows evaluation of the compounds that could be used as putative markers for each species. Section 1.2 explains in detail the process of finding markers in plants using OPLS-DA analysis for *Souroubea sympetala* and *Souroubea gilgii*. Metabolites with an arrow represent the possible markers for the species. These metabolites have high magnitude and high reliability¹⁵.

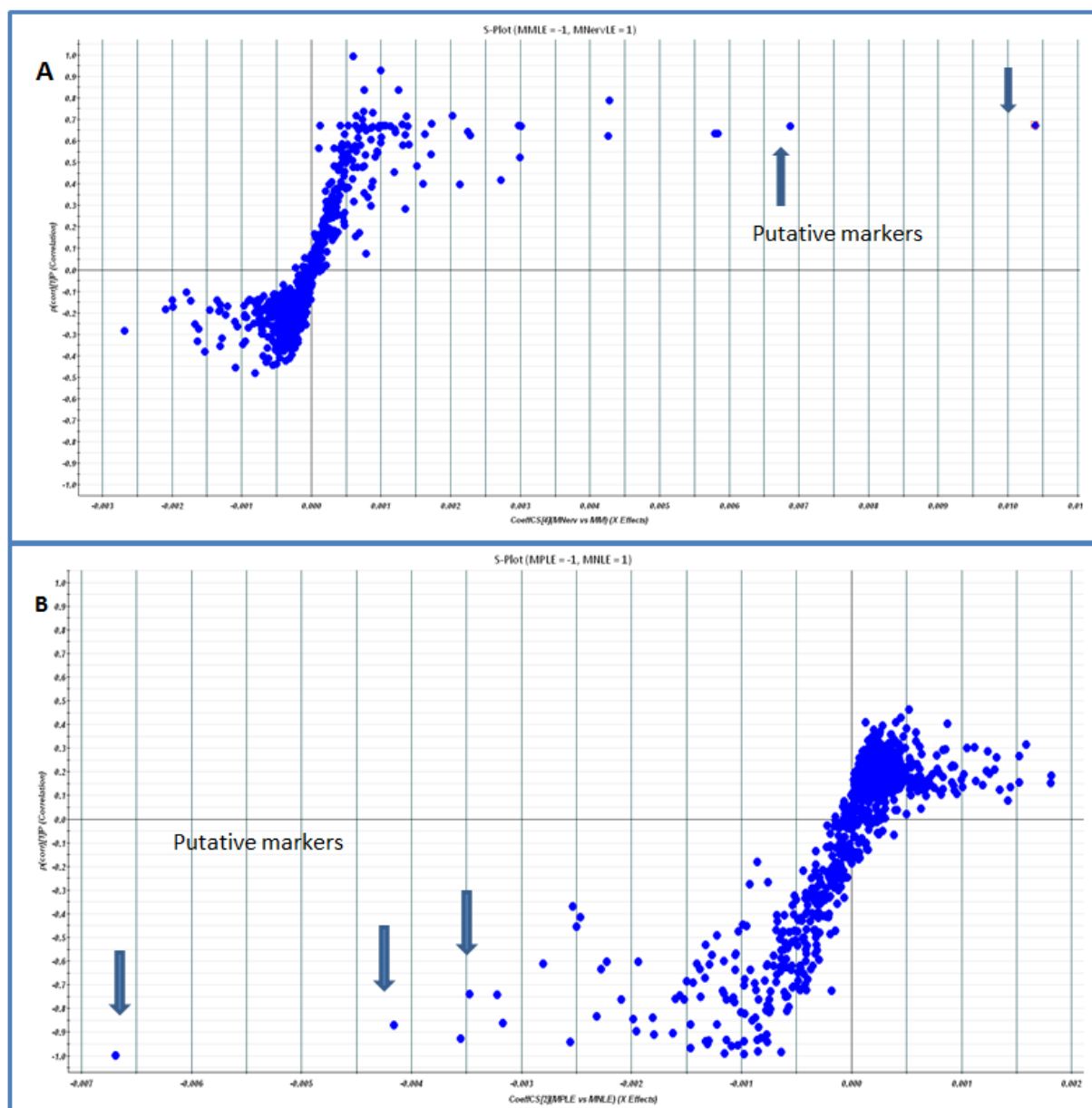


Figure 2-29: S-plots for Marcgraviaceae species that cluster together in the OPLS-DA score plot.

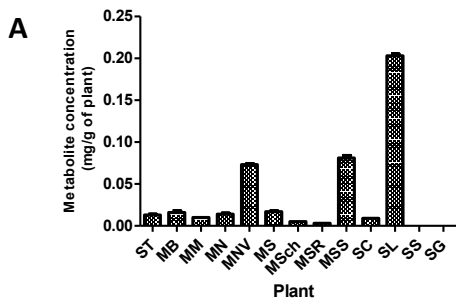
A. *M. nervosa* (left) and *M. Mexicana* (right), **B.** *M. Nepenthoides* (left) and *M. polianta* (right) arrows indicate the putative markers found in the analysis.

C. Quantification of pentacyclic triterpenes in Marcgraviaceae species.

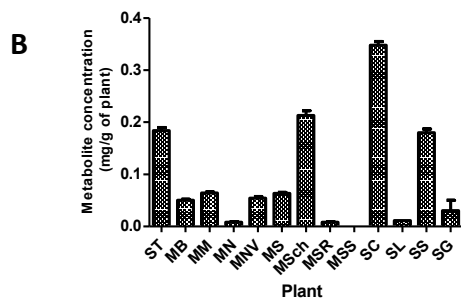
The idea behind finger printing is to have access to as much information of a targeted metabolome as possible (triterpenes in this case), in high throughput analysis, in order to use information to classify samples. This is also used as a tool to discriminate between samples of different origin or biological status^{7,16}. The extraction process of the samples plays a very important role since it becomes the first selective step in the analysis, defining the type of metabolites present according with their solubility and polarity. The extraction using 80% ethanol was used considering the broad spectrum of metabolites that could be present in the samples, rather than just the target triterpenes.

In order to evaluate the occurrence of the pentacyclic triterpenes in the different genera, the crude extracts were evaluated using the validated method described in Section 1.1. **Figure 2-30 A-F** presents the results. In the graphs the concentration of the different triterpenes varies along all the plants evaluated. The analysis demonstrates that not all the triterpenes evaluated are present in all the genera, ursolic acid is absent in *Sarcoopera sessiliflora*, betulin is absent in *Souroubea gilgii* and *S. sympetala*, lupeol is not present in *Marcgravia globulosomarginata* and α Amyrin is absent in *Marcgravia nepenthoides*. Amongst the triterpenes evaluated, betulinic acid and β -Amyrin are the two triterpenes present in all the genera evaluated. These results indicate that the same biosynthetic pathway is expressed in all of the Marcgraviaceae family and that betulinic acid and β -Amyrin could serve as biomarkers for the family.

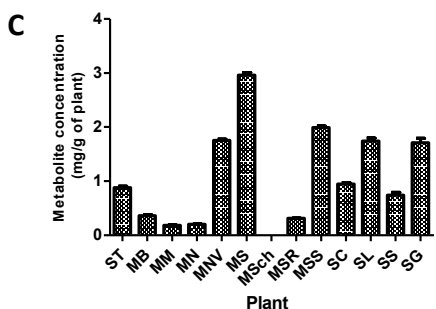
Content of betulin in thirteen Marcgraviaceae species from Costa Rica



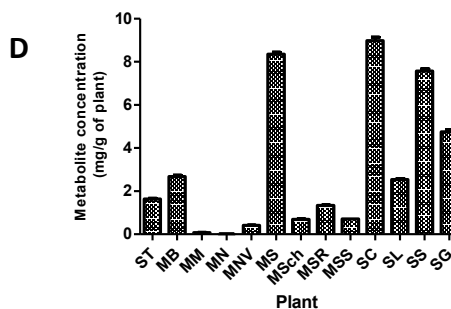
Content of ursolic acid in thirteen Marcgraviaceae species from Costa Rica



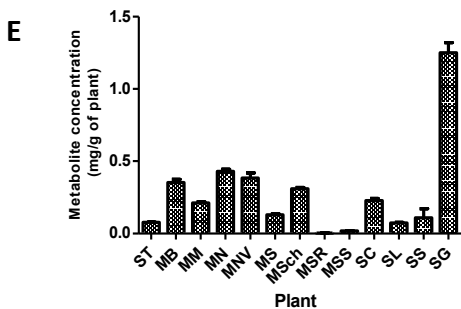
Content of lupeol in thirteen Marcgraviaceae species from Costa Rica



Content of α -amyrin in thirteen Marcgraviaceae species from Costa Rica



Betulinic acid content in thirteen Marcgraviaceae species from Costa Rica



Content of β -amyrin in thirteen Marcgraviaceae species from Costa Rica

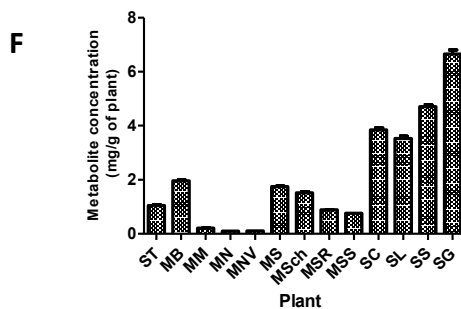


Figure 2-30: Content of pentacyclic triterpenes in leaf extracts of eleven genera of Marcgraviaceae: A. Betulin, B. Ursolic acid, C. Lupeol, D. α -Amyrin, E. Betulinic acid, F. β -Amyrin, Betulinic acid and the Amyrins have been linked to the bioactivity observed in *Souroubea* extracts^{9,12}.

Legend for the graphs: *Macgraviastrum subsessili*: **MS**, *Sarcopera rosulata*: **MSR**, *Marcgravia nepenthoides*: **MN**, *Marcgravia mexicana*: **MM**, *Marcgravia globulosomarginata*: **MSch**, *Sarcopera sessiflora*: **MSS**, *Marcgravia nervosa*: **MNV**, *Marcgravia brownei*: **MB**, *Schwartzia tarrazensis*: **ST**, *Souroubea loczyi*: **SL**, *Schwartzia costaricensis*: **SC**, *Souroubea sympetala*: **SS**, *Souroubea gilgii*: **SG**

Figure 2-31 compares the mean (standard error) content of these three triterpenes along the thirteen samples analyzed, the highest content of α -Amyrin corresponds to *Schwartzia costaricensis* (8.98mg/g), the highest concentration of betulinic acid (1.25mg/g) and β -Amyrin (6.66 mg/g) are present in *S. gilgii*.

Content of three pentacyclic triterpenes in thirteen Marcgraviaceae species from Costa Rica

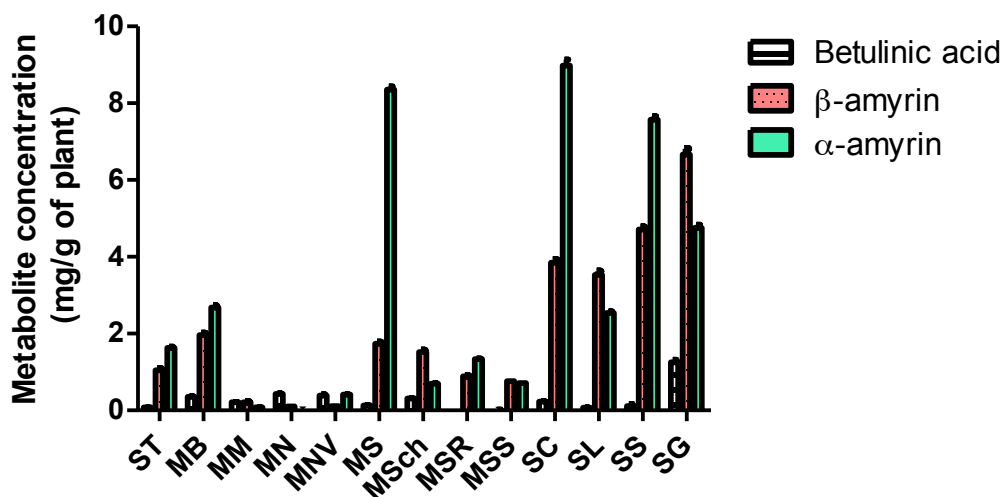


Figure 2-31: Comparison of mean content of betulinic acid, β -Amyrin and α - Amyrin in thirteen species of Marcgraviaceae

2.4.3 Experimental

Materials

Extraction and HPLC grade solvents were purchased from Fisher Scientific (Ottawa, ON, Canada). Betulinic acid, ursolic acid, lupeol, α -Amyrin and β -Amyrin (95% purity) standards were purchased from Extra-synthese (Lyon, France).

Plant collection

Leaves of different Marcgraviaceae plants were collected during the dry season from wild plants in different sites in Costa Rica. The samples were collected and identified by botanists from the Herbarium Juvenal Rodriguez, Universidad Nacional of Costa Rica, where vouchers have been deposited (**Table 2.4.2.1**).

Extraction

Plant material was dried at 35 °C in a plant drier for 2hr and ground to 0.2 mesh in a Willey mill. Ground materials (**Table 2.4.2.1**) were extracted using 80% ethanol, by dynamic maceration overnight, at room temperature. The extracts obtained were concentrated under reduced pressure using a Yamato Rotary Evaporator RE50 (Yamato Scientific, Japan) at 40 °C, lyophilized (Super Modulo, Thermo Electron, USA) and extraction yields were recorded. In total, 3 botanical accessions were extracted, corresponding to two different locations. The extracts were stored at 4 °C in amber HPLC vials.

Evaluation of pentacyclic triterpenes in Marcgraviaceae species

Samples were prepared for triterpenes quantification using the same procedure described in Section 2.1 and were analyzed using the same validated method.

Fingerprinting for plant identification

For the acquisition of the herbal fingerprints a hyphenated HPLC-DAD was used. The analysis was performed in leaf extracts of the different Marcgraviaceae species collected. HPLC-DAD analyses were carried out on a 1100 series HPLC system (Agilent Technologies, Santa Clara CA, USA). HPLC system consisted of a high performance auto-sampler, a quaternary pump, a column thermostat, an online degasser and a diode-array detector (DAD). The separations were performed at 0.4 mL/min on a Kinetex C18 column, particle size 2.6 micron, particle diameter 100A, 100 x 2.1 mm ID (Phenomenex, Torrence, CA, USA). Column thermostat was maintained at 55°C. A linear gradient of 30-100% acetonitrile in water was applied. The column was then washed with 100% acetonitrile 5 column volumes, returned to the initial conditions in 3 min and re-equilibrated for 5 min before the next injection. The diode-array detector was set at 210 nm.

Metabolomic analysis

The metabolomic analysis was done using the same procedures and methodology described in Section 2.3.3

Data Analysis and statistical analysis

The statistical analysis for the triterpene quantification was done using Graph Pad Prism software. The statistical analysis was performed for the metabolomic section was done using MarkerLynx (version 8.03)(Waters Corp.,USA).

2.4.4 Conclusions and future work

The study carried out in this part of the research highlights the importance of the use of chemotaxonomy and metabolomics in the study of plants for which ethnobotanical knowledge is not available. Although there are no use reports, the similarity of the phytochemistry of these species to *Souroubea*, which has a known use and pharmacology in anxiety, suggests they have similar properties. This pilot study of a limited plant collection set also illustrates the efficiency of the method in order to evaluate the prospective use of a plant family, without investing a lot of time in samples collections and preparation. A larger scale collection and further study of these plants will be useful.

Although the qualitative differences in phytochemistry represented in the profiles are reasonably sound, In order to validate the range of concentration of markers in species of the family, more samples should be collected for statistical analysis. The sample collection should reflect seasonal variation and geographical variation

The evaluation of the other Marcgraviaceae members using different analytical techniques and chemometrics, showed the value of this family as a potential source for new NHPs. Recent experiments by Chris Cayer have shown that amyirin synergizes the anti-anxiety activity of betulinic acid. Therefore extracts that have large amounts of Amyrins when combined with sycamore bark that is rich in betulinic acid should be effective for this purpose. The study described above indicates that four of the species including the *S. sympetala* and *S. gilgii* currently used in commercial “Sin Susto” meet this requirement. Two others, *Macgraviastrum*

subsessili and *Schwartzia costaricensis* show amyrin content comparable to the currently used *Souroubea* species and could be considered potential components of an anti-anxiety treatment.

2.4.5 References

1. Tistaert, C., Dejaegher, B. & Vander Heyden, Y. Chromatographic separation techniques and data handling methods for herbal fingerprints: a review. *Analytica chimica acta* **690**, 148–61 (2011).
2. WHO-Geneva *General Guidelines for Methodologies on Research and Evaluation of Traditional Medicine* World Health Organization. (2000).
3. Government of Canada. *IT ' S YOUR HEALTH: Adulteration of Natural health products*. Available at: <http://www.hc-sc.gc.ca/hl-vs/iyh-vsv/med/nat-prod-adulter-eng.php> (2011). Accessed December 2013.
4. Azarowych, N. A. J. L. Use of fingerprinting and marker compounds for identification and standardization of botanical drugs : strategies for applying pharmaceutical hplc analysis to herbal products. **32**, 497–512 (1998).
5. Bobzin, S. C., Yang, S. & Kasten, T. P. LC-NMR: a new tool to expedite the dereplication and identification of natural products. *Journal of Industrial Microbiology & Biotechnology* **25**, 342–345 (2000).
6. Cieśła, Ł. Biological Fingerprinting of Herbal Samples by Means of Liquid Chromatography. *Chromatography Research International* **2012**, 1–9 (2012).
7. Fiehn, O. Metabolomics--the link between genotypes and phenotypes. *Plant Molecular Biology* **48**, 155–71 (2002).
8. Chuang, Wu-Chang; Wu, Hsin-Kai; Sheu, Shuenn-Jyi; Chiou, Shiow-Hua; Chang, Hsien-Chang; Chen, Y.-C. A comparative study on commercial samples of Ginseng radix. *Planta Med.* **61**, 459–465 (1995).
9. Mullally, M. Anxiety-Reducing Tropical Plants. PhD thesis. (2011).at <<http://www.ruor.uottawa.ca/en/handle/10393/20379>> Accessed February 2013
10. Puniani, T. E. Novel natural product based anti-anxiety therapy and natural insecticides. PhD. Thesis. at <https://www.ruor.uottawa.ca/en/handle/10393/29155> (2003).
11. Tiv, M. Triterpenoids Isolation from *Marcgravia nepenthoides*: Bark and Wood. Report Summer 2010 BPS 4902 Presented to Dr . John T . (2010).
12. Puniani, E. Novel natural product base anti-anxiety therapy and natural insecticides. <https://www.ruor.uottawa.ca/en/handle/10393/29155> (2004).

13. Liang, Y.-Z., Xie, P. & Chan, K. Quality control of herbal medicines. *Journal of chromatography. B, Analytical technologies in the biomedical and life sciences* **812**, 53–70 (2004).
14. Therapeutic Goods Administration. *Guidance on equivalence of herbal extracts in Complementary Medicines*. 1–16 (2011).
15. Wiklund, S. Multivariate Data Analysis for Omics. (2008).at
<<http://www.metabolomics.se/Courses/MVA/MVA> in
Omics_Handouts_Exercises_Solutions_Thu-Fri.pdf>Accessed February 2013
16. Ellis, D. I., Dunn, W. B., Griffin, J. L., Allwood, J. W. & Goodacre, R. Metabolic fingerprinting as a diagnostic tool. *Pharmacogenomics* **8**, 1243–66 (2007).

2.5 Bioassay guided isolation of a bacterial quorum sensing inhibitor from *Marcgravia nervosa* (Marcgraviaceae) from Costa Rica

2.5.1 Introduction

Marcgravia is a neotropical genus of vines with over forty well described species¹, distributed mainly in evergreen and semi evergreen tropical forests¹. The genus is represented by eight species in Costa Rica² including *Marcgravia nervosa* Triana & Planch. (syn. *Marcgravia membranacea* Standl)³(**Figure 2-32**). This is an undergrowth species found in lowland forest on both Atlantic and Pacific slope. It grows along riverbanks and in lower parts of cloud forest such as Braulio Carrillo.

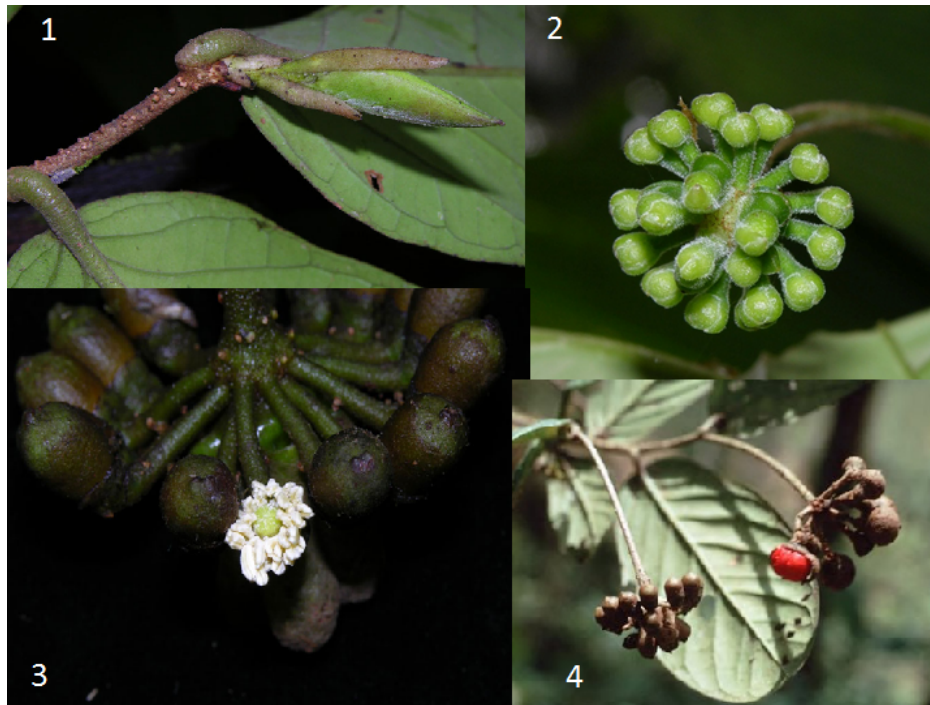


Figure 2-32: Leaf and flower of *M. nervosa* 1-3

(http://sloth.ots.ac.cr/local/florula/list_bigimg.phtml?img_name=marcgravia_nervosa_2472_07.jpg&key_species_code=LS001298&name=nervosa&genu=Marcgravia) 4. (Tropicos.org. Missouri Botanical Garden. 19 Feb 2013 <http://www.tropicos.org/Image/64651>)

In another part of this thesis, the first comprehensive phytochemical investigation of members of the Marcgraviaceae family native to Costa Rica is described. In this short chapter, the discovery of bacterial quorum sensing inhibition and anti-fungal activity is described for extracts of *M. nervosa*. Bioassay-guided fractionation of the crude leaf extract of *M. nervosa* led to identification of its active principle. This work was carried out jointly with Chieu Anh Ta, a Ph.D. student in the Arnason group, who carried out the bioassays.

The proper growth of bacterial colony depends on the secretion of extracellular factors. The presence of these factors allows colonies to perform vital functions, such as nutrient acquisition, and protection from the environment and competitors and will help them establish an enemy-free space⁴. Recently, there has been a growing awareness about the social behaviour of microorganisms. Microorganisms communicate in order to achieve multicellular behaviours such as: dispersal, foraging, biofilm formation, "chemical warfare" and quorum sensing. It has also been clearly stated that this behavior plays a key role in bacterial virulence⁵. Biofilms are communities of microorganisms that unfold on surfaces of natural and artificial environments. The communities are embedded in a matrix of polysaccharide, proteins and nucleic acids⁶. They develop via a cycle explained in **Figure 2-33**⁷. Within these biofilms, bacteria are protected from antibacterial chemicals (including natural antibiotics), environmental bacteriophages, and phagocytic amoebae. These are the reasons why they are relevant in the clinical environments, chronic biofilm infections resist antibiotic therapy and become resistant to clearance mechanisms like antibodies and phagocytes^{4,8}. One of the major problems in the treatment of infectious diseases is the development of biofilms since this makes the bacteria antibiotic resistant. This is particularly prevalent in opportunistic pathogens like *Pseudomonas aeruginosa*; this organism is involved in many nosocomial infections such as urinary tract infections, respiratory system infections, dermatitis, chronic wounds, soft-tissue infections, and a variety of systemic infections, particularly in patients with severe burns and in cancer and AIDS patients who are immunocompromised. It is also linked to the development of chronic lung infections of patients who suffer cystic fibrosis⁹. The formation of this biofilm is initiated by Quorum Sensing (QS).

Quorum Sensing is a cell-to-cell signalling process⁶, in this mode small diffusible signalling molecules are released and accumulate¹⁰. The concentration of the signalling molecule has to reach a threshold concentration to trigger genes expression for coding of extracellular factors, like virulence, secondary metabolite production, motility and swarming, conjugation, biofilm formation and growth inhibition^{4,11}. It is important to establish that QS is a special category of diffusion sensing where the threshold concentration of a signalling molecule can only be achieved by more than one cell¹¹.

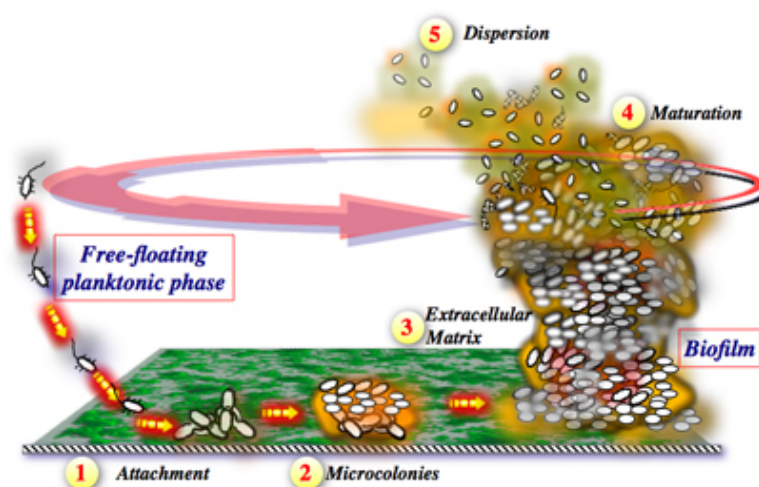


Figure 2-33: Essential steps in biofilm formation¹

The current understanding of QS makes this a target for drug discovery, since disruption of QS in certain pathogens could diminish signalling-dependent virulence. This approach diminishes the possibility of development of resistant mutants. The main idea is to control virulence with small molecules that will function as narrow range signalling antagonist, by doing this the host's immune system will eradicate the biofilm^{12,13}. Such compounds are called antipathogenic drugs.

In addition to bacterial infections, WHO has identified fungal infections as a serious cause of disease worldwide^{14,15}. One of the major challenges in the area of bacterial infection is the fact that these microorganisms have developed resistance to many antibiotics available in the market today. The discovery of new active compounds to treat systemic opportunistic fungal infections is a major challenge in this area, some of the standards used in this research area are:

fungicidal (but toxic) or safer compounds (but fungistatics)¹⁶. The economic impact of fungal infections is not limited to human diseases; they have an important impact on agriculture as well. Fungi are the main destroyers of foodstuff and grains during storage, by production of micotoxins. More than 25 % of the world cereals are contaminated with known micotoxins and more than 300 fungal metabolites are reported to be toxic to animals and humans, producing health problems such as cancer, nephrotoxicity, hepatotoxicity, reproductive disorders and immunosuppression¹⁷. There is a growing need for the development of new antifungal compounds with low toxicity and low environmental impact. Plant extracts and plant metabolites represent an attractive potential for the discovery of new antifungal that can serve as templates for further medicinal chemistry modifications¹⁷.

2.5.2 Results and Discussion

Crude ethanolic extracts of leaf of eleven Marcgraviaceae species were prepared and tested in two available bioassays: 1. Quorum Sensing inhibition, 2. Antifungal activity. Out of the eleven species shown in (Table 1.4.1) evaluated in the screening, *M. nervosa* leaf extract was the only one active in these bioassays.

Table 2.5.2.1: Marcgraviaceae species evaluated in the bioassays

Plant	Quorum sensing inhibition	Antifungal activity
<i>Macgraviastrum subsessili</i>	-	-
<i>Sarcopera rosulata</i>	-	-
<i>Marcgravia nepenthoides</i>	-	-
<i>Marcgravia mexicana</i>	-	-
<i>Marcgravia globulosomarginata</i>	-	-
<i>Sarcopera sessiflora</i>	-	-
<i>Marcgravia Nervosa</i>	+	+
<i>Marcgravia brownei</i>	-	-
<i>Schwartzia tarrazensis</i>	-	-
<i>Sourobea loczyi</i>	-	-
<i>Schwartzia costaricensis</i>	-	-
<i>Sourobea sympetala</i>	-	-
<i>Sourobea gilgii</i>	-	-

Once the activity of the crude extract was established, a second, larger scale extraction of *M. nervosa* leaf was carried out. Thus, 42.87 g of dry leaf were extracted using three different solvents to obtain three different fractions based on polarity as shown in **Figure 2-34**.

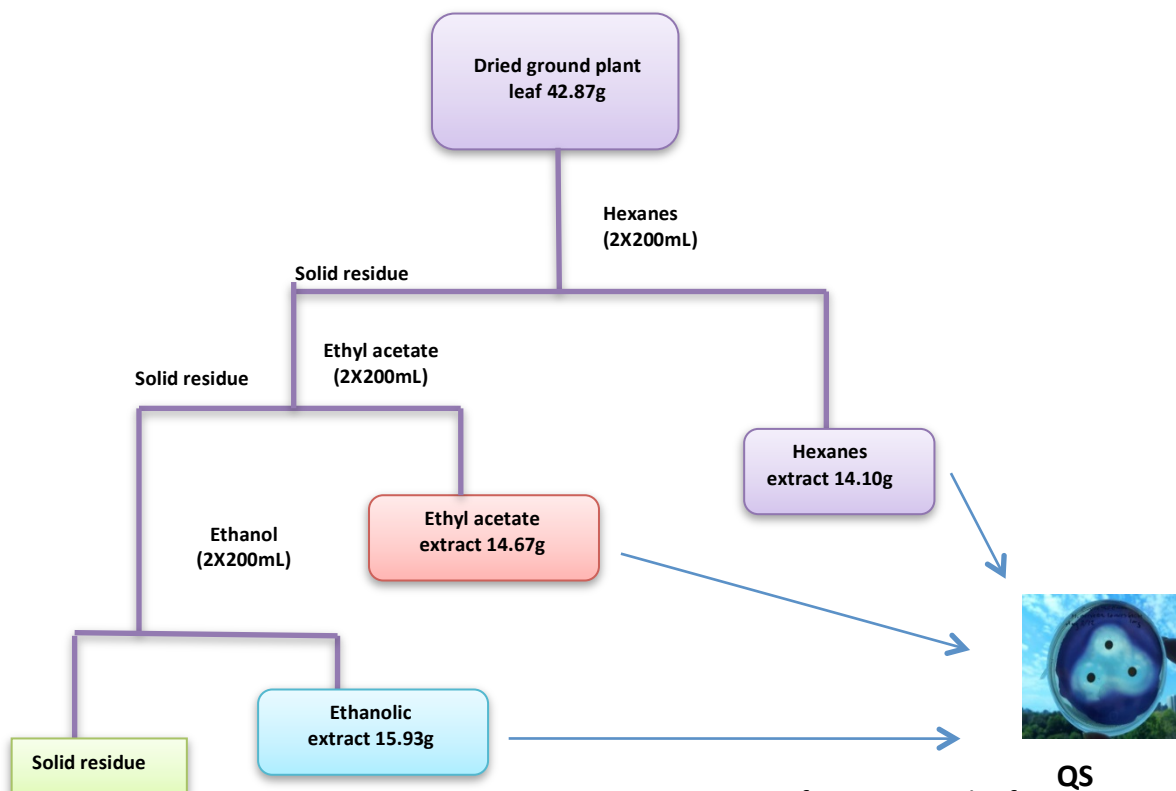


Figure 2-34: Fractionation of *M. nervosa* leaf

The dried extracts obtained after fractionation were sent for bioassay evaluation in order to identify the bioactive fraction. **Figure 2-35** and **Figure 2-36** show the results obtained for the different fractions. Three fractions were active with the ethanolic fraction having the highest bioactivity with an inhibition halo of 26.67 mm compared with the crude ethanolic extract with an inhibition halo of 21.78 mm. The other extracts, especially the ethyl acetate soluble material also showed inhibition. This result indicated that a somewhat polar compound soluble in a variety of solvents was the active principle in both the antifungal and Quorum Sensing assay. The ^1H NMR spectra of the three extracts (ethanolic, hexanes and ethyl acetate) showed the presence of the same metabolite that featured a prominent O-CH₃ group in the 3.9 ppm range and two low field aromatic multiplets. The key difference among the extracts was the

concentration of this compound with the highest concentration residing in the ethanolic extract.

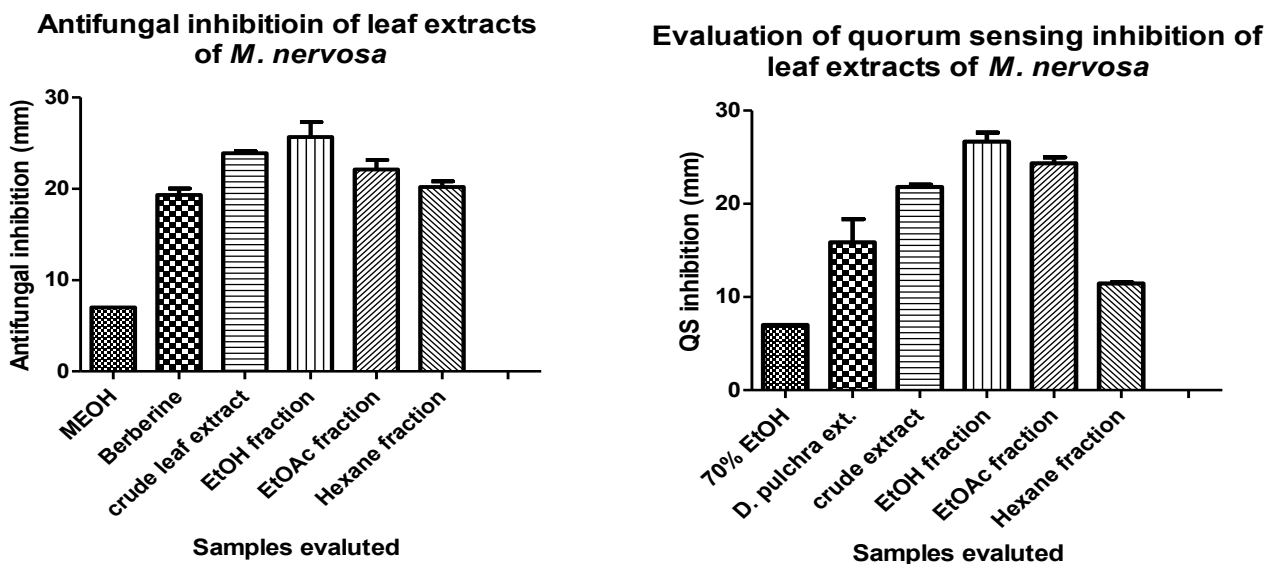


Figure 2-35: Effect of leaf extracts of *Marcgravia nervosa* in the anti-Quorum sensing and antifungal bioassay at a maximum concentration of (1mg /disc), tested in disc diffusion assay in *C. violaceum* and anti- fungal activity in *S. cerevisiae*. Each value is the mean \pm SEM (n=3) in each group

Silica gel column chromatography techniques were next applied to the most active extract (ethanolic) to isolate and identify the metabolite. The crude ethanolic extract (2.56g) was placed in 160g of silica gel and the column was eluted with solvent volumes of 300mL going from 100% hexanes to 100% ethyl acetate, with increments of 5% (ethyl acetate) until 60% hexanes and thereafter increments of 10% until 100% ethyl acetate. Finally the column was flushed using a mixture of ethyl acetate: methanol (8:2). A total of 299 eluates were collected. These were combined into a final number of 18 based on their analytical TLCs. The bioactive compound was collected in fractions corresponding to elution with 85%-90% hexanes. This combined fraction was again evaluated using the same bioassays to confirm its activity. The NMR analysis of this fraction also showed that the bioactive component had co-eluted with

betulinic acid. A second column was performed on this fraction to obtain a pure sample of the active metabolite. ^1H and ^{13}C spectra of the isolated metabolite were obtained. The simplicity of the spectra enabled us to readily identify this compound as 2-methoxy-1,4-naphthoquinone, **1**. 2-Methoxy-1,4-naphthoquinone was first isolated from *Impatiens balsamina*^{18–20} a plant widely used in Traditional Chinese Medicine²¹. A comparison of the NMR properties of the isolated compound **1** and those reported in the literature is shown in **Table 2.5.2.2**. The yield of the active metabolite in *M. nervosa* was 3.5% based on dry leaf material. This represents a remarkably high concentration for a secondary metabolite. Extraction of the leaves of the same plant collected in a different season and a second sample collected at a very different collection site showed somewhat lower but still very substantial levels of **1** in a qualitative analysis performed using LC-DAD system at 280 nm.

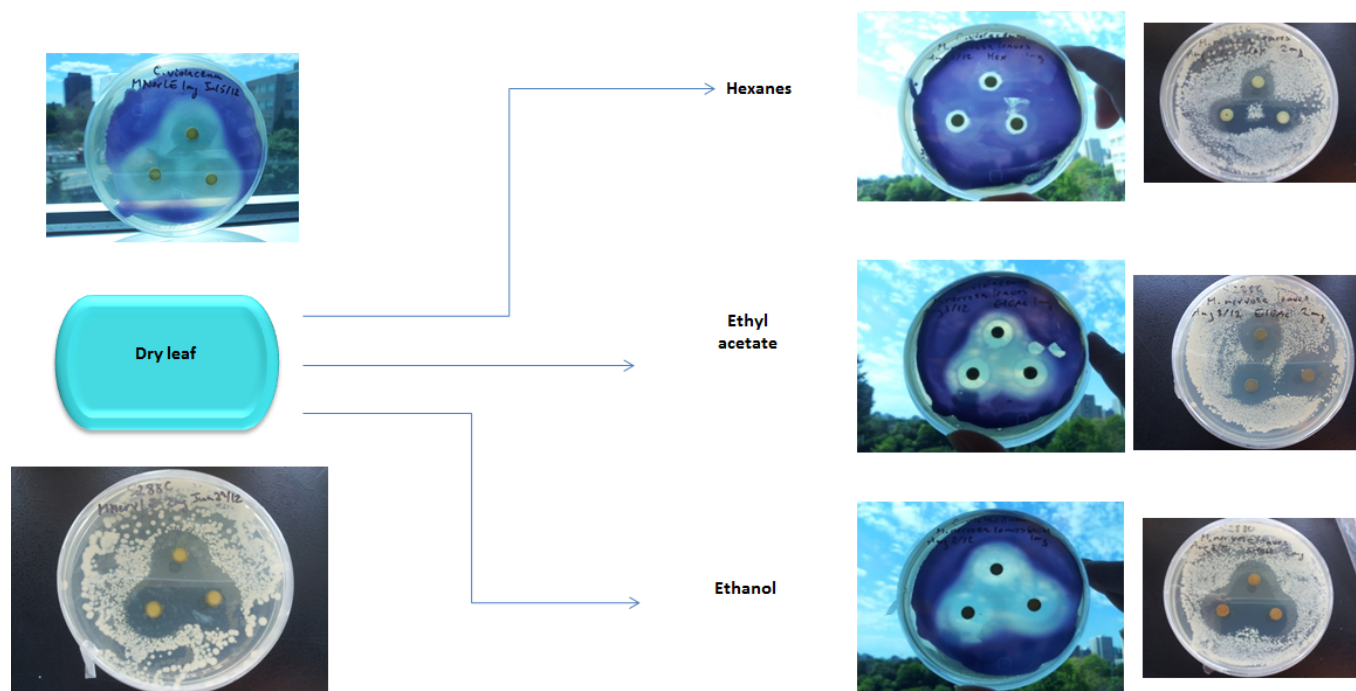


Figure 2-36: Quorum sensing and antifungal activity of *M. nervosa* extracts, (1mg/disc) Photographs by Chieu Ahn Ta.

Figure 2-37: ^1H NMR, spectrum of 2-methoxy-1,4-naphthoquinone isolated from *M. nervosa* (400 MHz, CDCl_3)

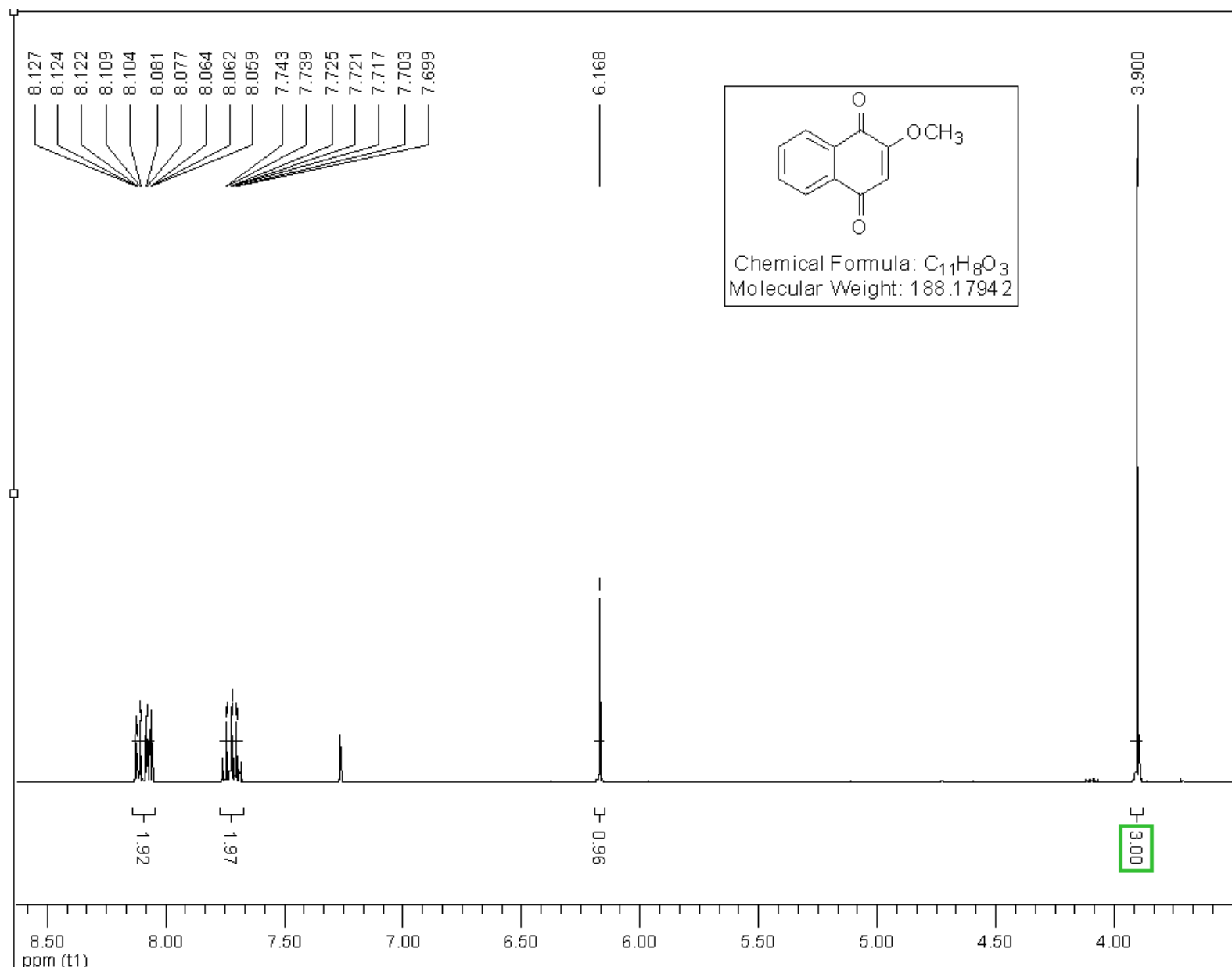


Figure 2-38: ^{13}C NMR, spectrum of 2-methoxy-1,4-naphthoquinone isolated from *M. nervosa* (100 MHz, CDCl_3)

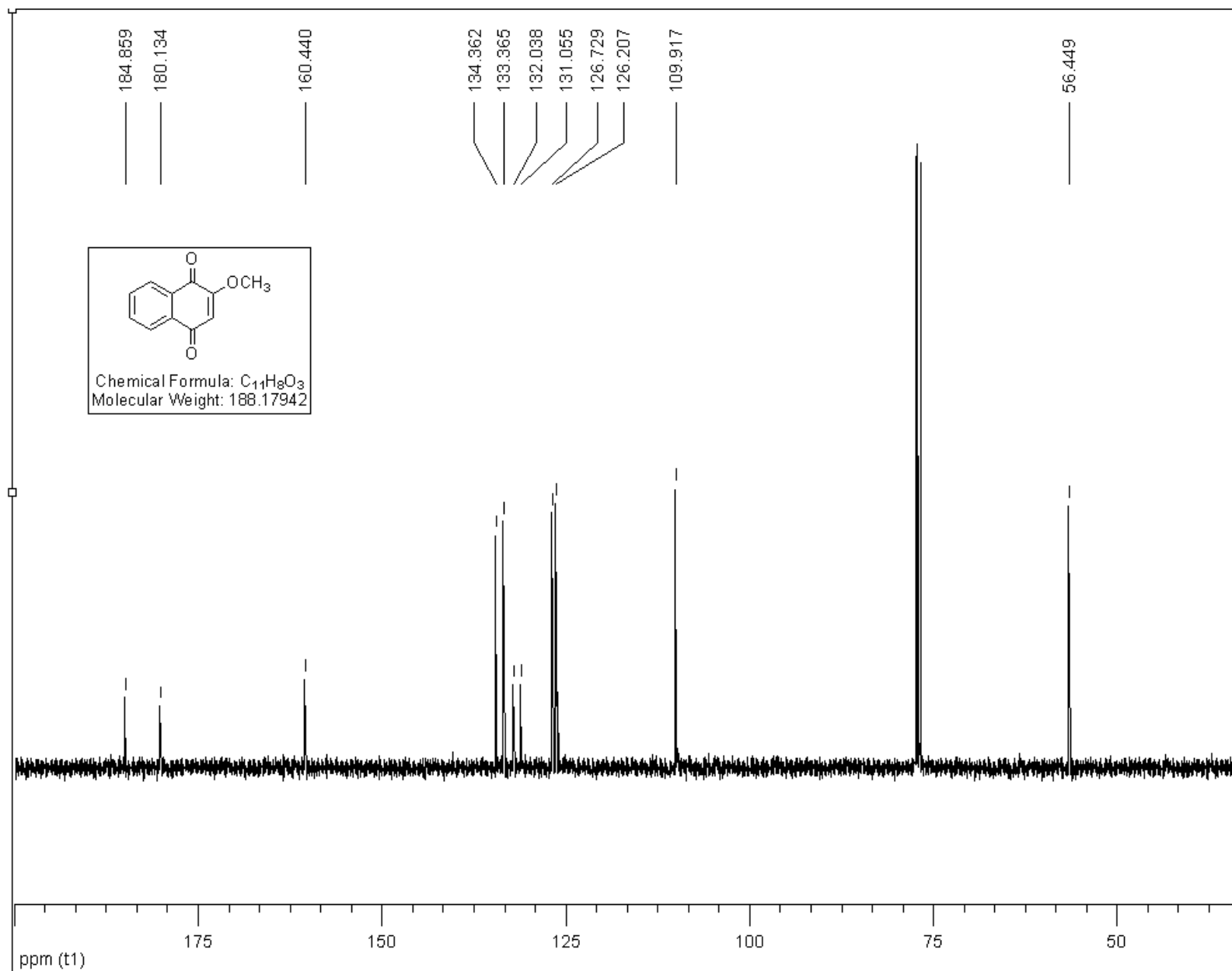
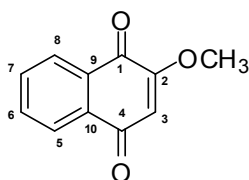


Table 2.5.2.2: Proton (^1H) and carbon ^{13}C data for bioactive compound isolated from *M. nervosa*. Comparison with data published for 4-methoxy-1,4-naphthoquinone, **1**.

^{13}C	δ (reported) (600MHz, CDCl_3)	δ (found) (100 MHz, CDCl_3)	^1H	δ (reported) (600MHz, CDCl_3)	δ (found) (400MHz, CDCl_3)
1	180.1	180.1	1		
2	160.4	160.4	2		
3	109.9	109.9	3	6.19s, 1H	6.16s, 1H
4	184.9	184.9	4		
5	126.7	126.7	5	8.13dd(1.2,7.2) 1H	8.09 m, 2H*
6	134.4	134.4	6	7.76td (1.2,7.2), 1H	7.72 m, 2H ∞
7	133.4	133.4	7	7.73 td (1.2,7.2), 1H	∞
8	126.2	126.2	8	8.10 td (1.2,7.2), 1H	*
9	131.0	131.1	9		
10	132.0	132.0	10		
11			11	3.92s, 3H	3.90s, 3H

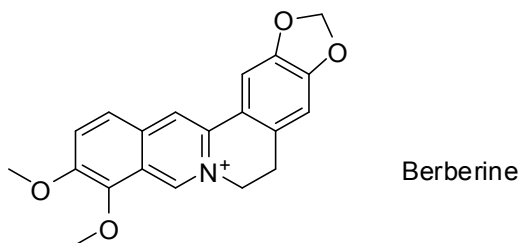


2-methoxynaphthalene-1,4-dione, **1**

Quinones are naturally occurring compounds known for their antibacterial and anti-fungal activity²². The antibacterial activity of this naphthoquinone against several bacterial strains as *Staphylococcus aureus*, *Bacillus cereus*, *Aeromonas salmonicida* and fungi like *Fusarium oxysporum* has been reported²⁰. More recently it showed promising activity in the treatment of multi-antibiotic resistant strains of a bacterium responsible for stomach ulcers, *Helicobacter*

*pylori*²³. The activity observed for the compound has been rationalized to occur via oxidative stress.

The minimal inhibitory antifungal concentration determined for the pure 2-methoxy-1,4-naphthoquinone, **1**, was also evaluated by PhD candidate Chieu Ahn Ta. The MIC for **1** is 85 μM against *Saccharomyces cerevisiae* BY4741 (haploid) and 100 μM against *Saccharomyces cerevisiae* BY4743 (diploid). The MIC for berberine (positive control) against the same strains is 600 μM for both. Berberine is a plant alkaloid isolated from different plants like *Hydrastis canadensis* (goldenseal), *Coptis chinensis* (Coptis or goldenthread), *Berberis aquifolium* (Oregon grape), *Berberis vulgaris* (barberry), and *Berberis aristata* (tree turmeric)²⁴. It is used clinically for the treatment of bacterial diarrhea caused by *E. coli* and *V. cholera*, intestinal parasites and ocular trachoma infections, among others²⁵. The quinone **1** found in the *M. nervosa* extract shows at least a fivefold increase in activity compared to berberine in the bioassay carried out.

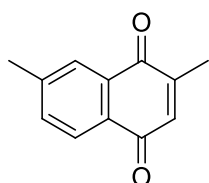


The positive control used for the QS assay is *Delisia pulchra* extracts. *D. pulchra* is a benthic marine macroalgae that produces brominated furanones which act as quorum sensing inhibitors by mimicking the native prokaryotic N-acyl-L-homoserine lactones (AHL signal).²⁶ The crude leaf ethanolic extract from *M. nervosa* showed a significant inhibition of QS compared to *D. pulchra* extracts. The crude *M. nervosa* extract has a stronger inhibition of the QS with a halo of 21.8mm than *D. pulchra* extracts with a halo of 15.9mm.

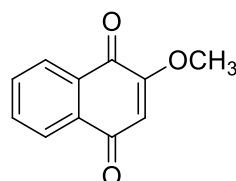
Quinones are widely present in nature and have a broad spectrum of bioactivities²⁷. A comparison of the antifungal activity of chimaphilin **10**, a naphthoquinone previously isolated in our research group, shows that 2-methoxy-1,4-naphthoquinone (MNQ) is more active²⁸. The activity found for 2-methoxy-1,4-naphthoquinone (MNQ) is higher by more than a factor of about 30 than chimaphillin with a MIC of 0.0016 mg/mL (0.09 μM) for *S. cerevisiae* (haploid) and 0.0019 mg/mL (0.1 μM) *S. cerevisiae* (diploid). In contrast chimaphilin has a MIC of 0.05 mg/mL

(0.3) μM against *S. cerevisiae*. The molecular weights for these two naphthoquinone are very similar (188 g/mol vs. 186 g/mol).

A comparison with the standard antifungal agent berberine, in the inhibition halo assay, shows that the antifungal activity of MNQ is higher than berberine (600 μM) vs. 85 μM - 100 μM for MNQ.



10. 2,7-Dimethyl-1,4-naphthalenedione
Chimaphilin



2-Methoxy-1,4-naphthalenedione

In addition to the bioactive naphthoquinone **1**, this study resulted in the isolation and structure elucidation of four known triterpenes typically also found in the other Marcgraviaceae species (**2-5**) **Figure 2-39**. The concentration of these compounds in *M. nervosa* leaves is similar to that found in the other Marcgraviaceae species investigated (see graphs for the quantification of pentacyclic triterpenes in **section 2.3**).

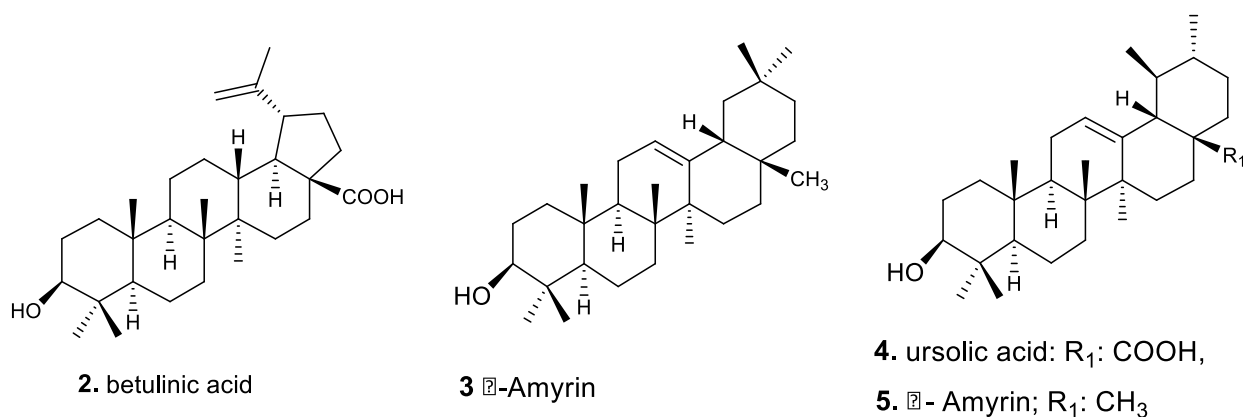


Figure 2-39: Triterpenoid metabolites from *M. nervosa* leaf extract

The Marcgraviaceae species studied in our research group are characterized by the presence of pentacyclic triterpenes as shown in section 1.2 of this dissertation. These compounds are considered biomarker compounds for this plant family. The finding of the quinone **1** in *Marcgravia nervosa* is the first report of the isolation of such a metabolite in in this family. Based on these observations the authenticity of the sample used in the analysis was questioned. In order to corroborate the identity of the plant collected, our collaborators from the Juvenal Rodriguez Herbarium at Universidad Nacional were requested to revisit the first location where the plant was collected. The authenticity of that plant identity was verified and a second sample was collected for analysis. Additionally, another collection was made in Braulio Carrillo National Park. (Refer to map in the general introduction of this section to see the collection sites (**Table 2.5.2.3**). As shown in the NMR analysis of the crude ethanolic extracts of the three samples, prepared at the same concentration (20mg/mL) and ran under the same conditions can be superimposed (**Figure 2-41**).

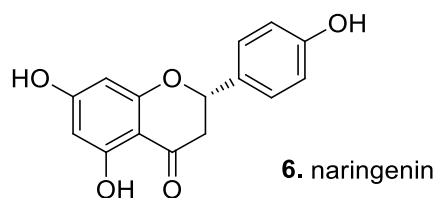
Table 2.5.2.3: Meta data for the plant collection of *M. nervosa*

Sample	Collection site	Voucher number	Season of collection
MN-L-RP-12	Rio Pacuare	13157	Dry
MN-L-RP-1202	Rio Pacuare	13157	Rainy
MN-L-BC-12	Braulio Carrillo	13489	Rainy

The three crude extracts were also injected in an UPLC-MS system (**Figure 2-42**); profiles obtained for the samples were the same. The difference in the content of the naphthoquinone between the two samples collected from Pacuare can be explained in terms of the seasonal variation of the sample, since the first and second samples were collected during the dry and rainy seasons, respectively. The sample from Braulio Carrillo also has the lower concentration of the naphthoquinone. The Braulio Carrillo collection site is a considered a cloud forest and experiences high levels of precipitation. It is also at a higher altitude compared with the Rio Pacuare location.

The other eleven genera of Marcgraviaceae available (**Table 2.4.2.1**) were analyzed using LC-DAD-MS to look for the presence of the naphthoquinone *M. nervosa* leaf was the only sample containing the naphthoquinone.

A phytochemical investigation previously done in our lab by Dr. Puniani²⁹ showed the presence of other types of secondary metabolites in the leaf of *Souroubea gilgii* besides than triterpenes, like naringenin **6**. Although both **1** and the flavonoids are highly oxygenated aromatics and have considerable similarity, they are form by different biogenetic pathways³⁰. Thus far we have no evidence concerning the presence of flavonoids in *M. nervosa*. The finding of the occurrence of this new secondary metabolite in *M. nervosa* and the absence of this one in the other species evaluated could be the result of evolutionary pressure for this particular plant. Secondary metabolites can be unique to a specific specie or genera, and they originate in the plants as a strategy for survival and to overcome the threats in their specific environment³¹. The environments where *M. nervosa* has been collected are of high humidity and temperature, for both the Pacuare and Braulio Carrillo sites, making of this the perfect climate for the development of pathogenic microorganisms. The evolution of a biosynthetic pathway of a compound like the naphthoquinone with a broad spectrum of antimicrobial activity provides a selective advantage for these plants to survive in this climate.



The content of pentacyclic triterpenes in *M. nervosa* and the other Marcgraviaceae species was evaluated using the validated method described in section 1.1; betulinic acid and ursolic acid are present in higher concentration than the amyryns. β -Amyrin is present in a higher concentration than α -Amyrin, lupeol, the precursor to betulinic acid is absent (**Figure 2-40**).

The analysis of the proton NMR spectra obtained for the other fractions collected from the columns also shows the presence of glycerol esters or ethyl (the result of storing in ethanol) esters of fatty acids. These esters and the naphthoquinone are the major components of the leaf extract. This observation was also confirmed by UPLC-MS analysis. Interestingly and

somewhat surprisingly, investigation of the crude ethanol extracts obtained from *M. nervosa* branches did not show the presence of the naphthoquinone metabolite.

Content of five triterpenes in leaf of *M. nervosa* from Pacuare, Costa Rica

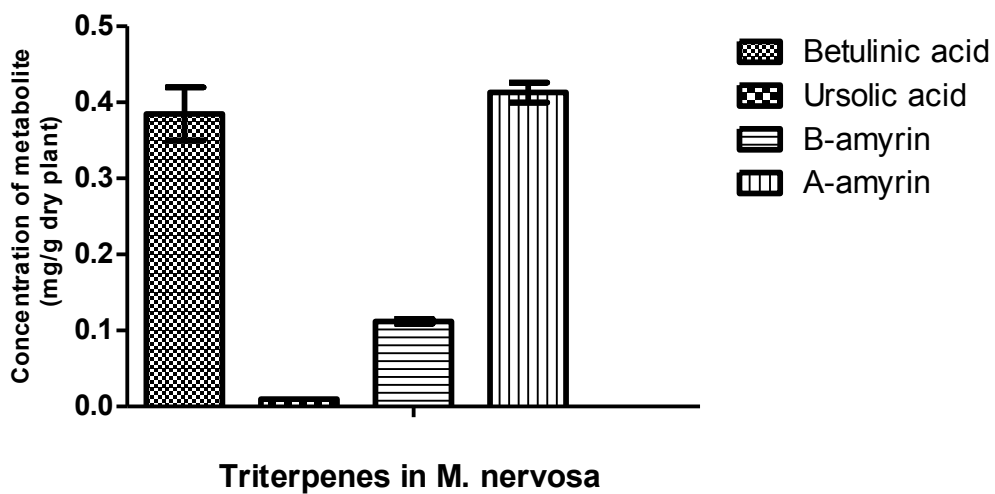


Figure 2-40: Mean content of pentacyclic triterpenes in ethanolic leaf extracts of *M. nervosa*

Figure 2-41: NMR analysis of crude extracts of three different plant collections of *M. nervosa*, at two locations in Costa Rica.

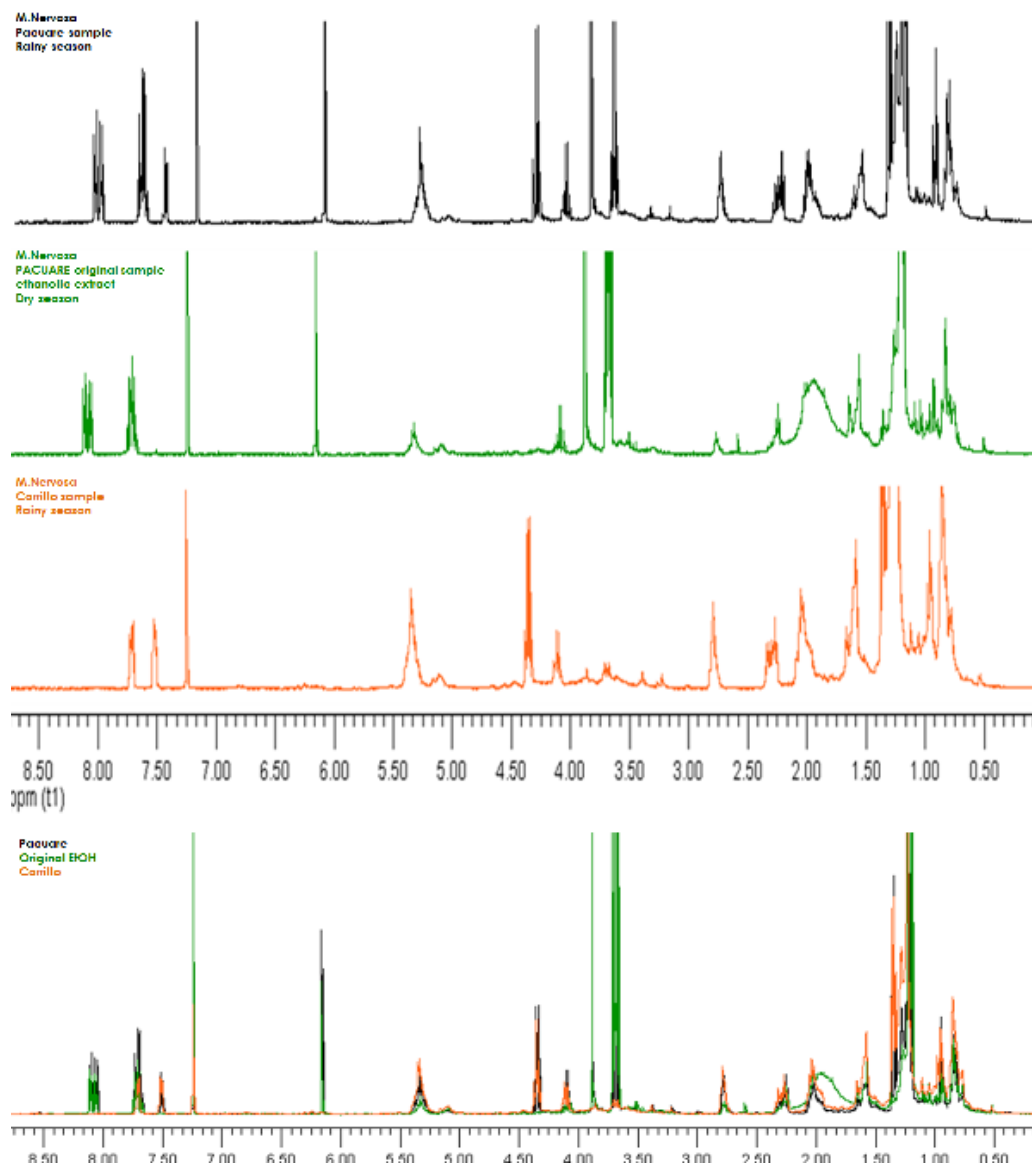
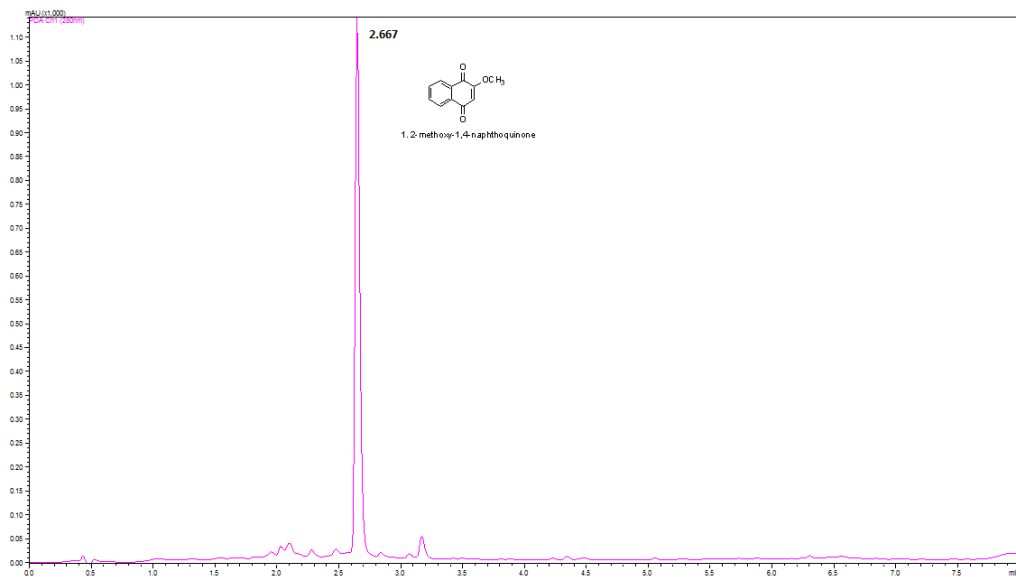
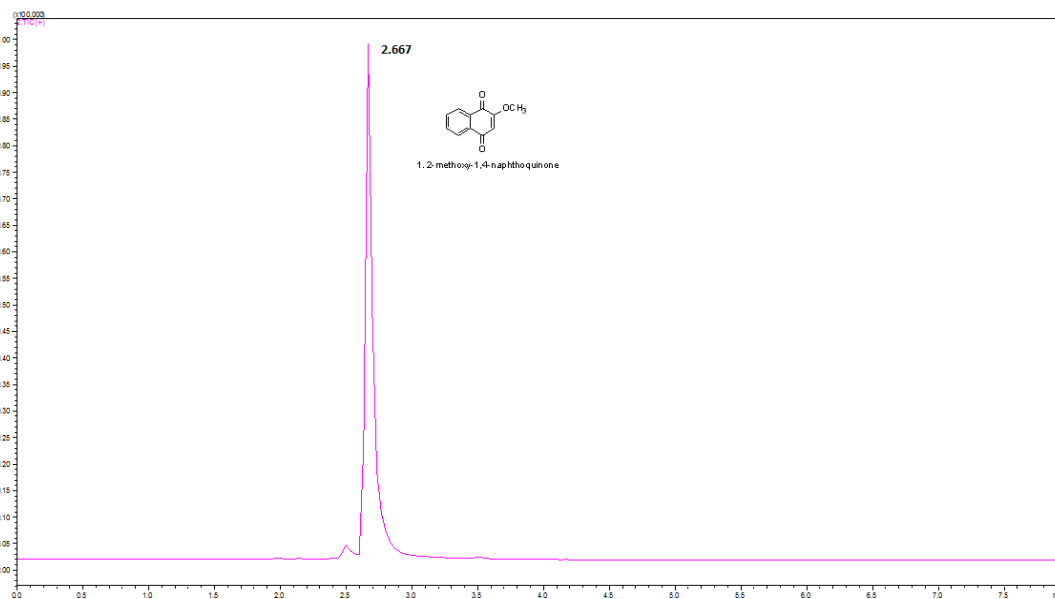


Figure 2-42: UPLC-DAD-MS data of the ethanolic extract of *M. nervosa* leaf from Rio Pacuare, dry season

a. UV signal at 280nm



b. Selected ion 189 [M+H]



2.5.3 Experimental Section.

General procedures

NMR spectra were recorded on a Bruker Avance 400 spectrometer in CDCl₃. Open column chromatography was carried out on silica gel 60 (70-230 mesh, Merck). TLC analyses were performed on silica gel 60 F254 plates (Merck), and visualization of the plates was carried out using a Hanessian stain.

Materials

Extraction and HPLC grade solvents were purchased from Fisher Scientific (Ottawa, ON, Canada). Betulinic acid, ursolic acid, lupeol, α -Amyrin and β -Amyrin (95% purity) standards were purchased from Extra-synthase (Lyon, France) or were purified by preparative HPLC.

Plant collection

Leaves of *Marcgravia nervosa* were collected during the dry season and rainy season of 2012 from Rio Pacuare, Costa Rica and from the cloud forest area of Braulio Carrillo. The samples were collected and identified by Marco Otarola and Pablo Sanchez at the Herbarium Juvenal Rodriguez, Universidad Nacional of Costa Rica, where vouchers have been deposited. (**Table 2.5.2.3**).

Extraction and isolation

Plant material was dried at 35 °C in a plant drier for 2hr and ground to 0.2 mesh in a Willey mill. Ground materials (see **Table 2.5.3.1**) were extracted using ethanol 90%, by dynamic maceration overnight, at room temperature. For the isolation of the pure naphthoquinone, the ground leaf material was placed in an Erlenmeyer and extracted following the procedure described in **Figure 2-34**. The extracts obtained were concentrated under reduced pressure using a Yamato Rotary Evaporator RE50 (Yamato Scientific, Japan) at 40 °C, lyophilized (Super Modulo, Thermo Electron, USA) and extraction yields were recorded. In total, 3 botanical accessions were extracted, corresponding to two different locations. The extracts were stored at 4 °C in amber HPLC vials.

For isolation purposes, 2.6 g of the ethanolic extract were chromatographed on 160 g silica gel column and separated into 5 fractions (MNE-C1-MNE-C5), using a solvent system from 100% hexanes to 100% ethyl acetate with increments of 25 %, the column was flushed with 10% methanol (Table 2.5.3.2).

Table 2.5.3.1: Percentage yield of extraction for different *M. nervosa* collection using ethanol: water (9:1)

Sample	Dry material (g)	% Yield of extraction
MN-L-RP-1301	42.87	9.9*
MN-L-RP-1302	39.57	5.4
MN-L-BC-1301	43.61	5.9

* This sample was extracted differently; it is described in scheme 1.4.1: hexanes extract 2.2%, ethyl acetate 2.02, ethanol 5.7%

Table 2.5.3.2: Column chromatography of ethanolic partition of *M. nervosa* leaf (MNE). Crude extract applied in column 14.67g.

Fraction code	Solvent system	Yield (g)
MNE-C1.1	100% hexanes	0.0
MNE-C1.2	75% Hexanes	0.9
MNE-C1.3	50% Hexanes	4.3
MNE-C1.4	100% ethyl acetate	2.2
MNE-C1.5	10% methanol	2.1

The highest concentration and activity was detected in fraction MNE-C1.3. This fraction was rechromatographed on silica gel column to yield compound **1** as a pure compound in 35 mg/g dry plant.

HPLC-DAD-MS analysis

The identification of compound was carried out on a Shimadzu UPLC-MS system (Mandel scientific company Inc, Guelph, Ontario) which consisted of LC30AD pumps, a CTO20A column oven, a SIL-30AC auto sampler and a LCMS-2020 mass spectrometer with an electrospray-ionization source. Briefly, the separation of the quinone compounds was carried out on a phenomenex Kinetex™ C18 column (100 x 2.1mm, 2.6µm particle size, phenomenex, Mississauga, Ontario) with a gradient elution method. The initial solvent was 95% solvent A (0.1% formic acid) and 5% solvent B (ACN), the ratio then changed to 95: 5 in 6 min. The column was then washed with 95% B for 1 min and changed back to the initial condition. The flow was set at 0.6 mL/min with a column temperature at 55°C.

Peak identifications were undertaken by co-chromatographic comparison of the retention time and mass data with purified compounds (by Ana Carballo). Qualitative data was obtained, since no quantification was performed.

Quantification of pentacyclic triterpenes was done using methodology describe in section 1.1

Bioassays evaluation (This work was done in collaboration with PhD candidate Chieu Anh Ta, from Biology Department, all the bioassay work and results is part of her PhD research)

Quorum sensing (QS) bioassay

A modified disk diffusion assay described by Adonizio *et al.* [2006] was used to determine whether the plant extracts could interfere with the QS of *C. violaceum*. *C. violaceum* produces a purple pigment, violacein, which is under QS control [2006]. The inhibition of violacein production will indicate the disruption of QS. Briefly, sterile paper disks (Oxoid, Basingstoke, Hants, UK) loaded each with 1 mg of extract were placed onto TGY agar plates (BD, Sparks, MD, USA) inoculated 100 µl of overnight cultures then incubated without agitation for 24 hr at 30°C (incubator: Precision Automatic CO₂ Incubator). QS Inhibition was indicated by a colourless

opaque halo around the disc and growth inhibition by a clear halo. Plates were examined under a dissecting microscope to confirm whether the extract has anti-QS and/or antibacterial activity. Two positive controls were used: *Delisea pulchra* extract (provided by B. Baker from University of South Florida) and N-decanoyl-L-homoserine lactone (C10-HSL) (Cayman Chemical, Ann Arbor, MI, USA). Each sample was tested in triplicate.

Antifungal disc diffusion assay:

Saccharomyces cerevisiae S288C was used for the initial screening of the plant extracts for antifungal activity, performed in a triplicate. Plant extracts were prepared to a final concentration of 40mg/mL, using HPLC grade methanol as a solvent. Berberine was used as an antifungal positive control and HPLC grade methanol was used as a negative control.

S. cerevisiae was inoculated into Sabouraud's broth medium and grown to an optical density of 600 nm (OD₆₀₀) of ~1.0 and diluted 1:100. Aliquots (100 μ L) of the diluted broth culture were spread over the surface of Sabouraud's agar plates. Paper discs (7.0 mm diameter) were impregnated with crude extract (2 mg/disc), berberine (1mg/disc) or HPLC methanol and allowed to air-dry. All treatments were subsequently incubated in the dark for 48 hr at 30 °C. Inhibition zones from active extracts were then measured. Plates were stored at 4°C. Active extracts were then tested for antifungal activity on *C. neoformans* and *C. albicans* D10, using the same method described above.

Statistical Analysis

All the statistical analyses were performed using Graph Pad Prism software.

2.5.4 Conclusion and future work

The present study has identified a new structure capable of inhibiting the formation of biofilms. This is not the first report of this kind of activity associated with quinone type compounds. It was reported previously in the evaluation of TCM actives as potential Quorum sensing inhibitors (QSis). That study found that the anthroquinone emodin,**7**, inhibits biofilm formation at 20 μ M when tested on *P. aeruginosa* and *S. maltophilia*³². Nevertheless, there are not many

QSiS of non-bacterial origin available beyond the halogenated furanones **8** and **9** from the red alga *Delisea pulchra*³³.

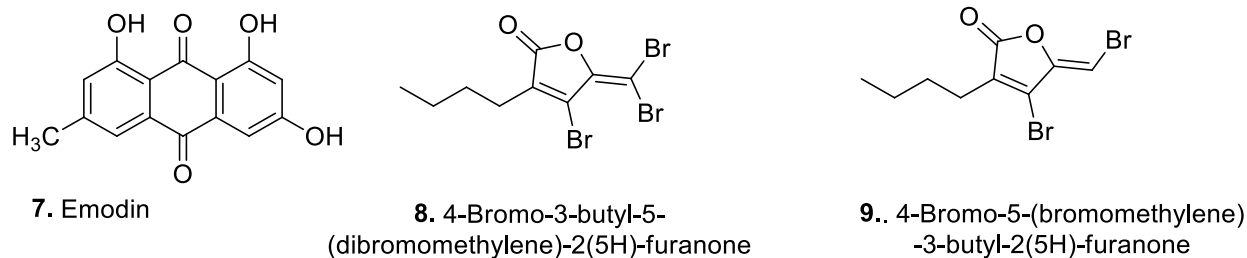


Figure 2-43: Halogenated furanones in *D. pulchra*³⁴

Patients that suffer from cystic fibrosis become very sensitive to bacterial lung infections. They are treated with many antibiotics over a long period of time that often results in the generation of resistant pathogens. When these pathogens form biofilms, lung transplant becomes the only remaining treatment³⁵. It has been shown that the combination of QSiS compound with antibiotics increases the effectiveness of the treatment, making the discovery of new structures and sources of such compounds very important.

Based on the findings from this bioassay-guided fractionation of the extracts of the leaves of *M. nervosa* we suggest that further evaluation of quinones as potential QSiS be carried out. A wide diversity of quinone structures is available from different plant extracts or commercial sources.

The discovery of an antifungal and QSi inhibitor in *M. nervosa* illustrates once more the potential use of natural products as source of new lead structures. It also demonstrates that the availability of new bioassay protocols and techniques can provide new applications of known compounds.

2.5.5 References

1. Missouri Botanical Garden. Tropicos.org. at <<<http://www.tropicos.org/Name/40013713>>> Accessed March 2013
2. Rica, U. de C. Costa Rica Biodiversity Portal. at <<http://crbio.cr/portalCRBio/species/browse/resource/7/taxon/388919/>> Accessed March 2013

3. The plant list. *version1* (2010).at <<http://www.theplantlist.org>> Accessed March 2013
4. Popat, Roman Cruz, Shanika a Messina, Marco Williams, Paul West, Stuart a Diggle, S. P. Quorum-sensing and cheating in bacterial biofilms. *Proceedings. Biological sciences / The Royal Society* **279**, 4765–71 (2012).
5. West, S. a, Griffin, A. S., Gardner, A. & Diggle, S. P. Social evolution theory for microorganisms. *Nature reviews. Microbiology* **4**, 597–607 (2006).
6. Annous, B. a, Fratamico, P. M. & Smith, J. L. Quorum sensing in Biofilms: why bacteria behave the way they do. *Journal of Food Science* **74**, R24–37 (2009).
7. Biofilms, L. G. of Annual Report. *Activity Reports 2006 - Institut Pasteur* (2006).At <<http://www.pasteur.fr/recherche/RAR/RAR2006/Ggb-en.html>> Accessed March 2013
8. Donlan, R. M. & Costerton, J. W. Biofilms : Survival Mechanisms of Clinically Relevant Microorganisms Biofilms : Survival Mechanisms of Clinically Relevant Microorganisms. *Clinical Microbiology Reviews* **15**, (2002).
9. Yang, Liang Rybtke, Morten Theil Jakobsen, Tim Holm Hentzer, M., Bjarnsholt, Thomas Givskov, M. & Tolker-Nielsen, T. Computer-aided identification of recognized drugs as *Pseudomonas aeruginosa* quorum-sensing inhibitors. *Antimicrobial Agents and Chemotherapy* **53**, 2432–43 (2009).
10. Cady, Nathaniel C. McKean, K. A., Behnke, Jason Kubec, R. & Mosier, Aaron P. Kasper, Stephen H, Burz, David S. Musah, R. A. Inhibition of biofilm formation, quorum sensing and infection in *Pseudomonas aeruginosa* by natural products-inspired organosulfur compounds. *PLoS One* **7**, e38492 (2012).
11. Williams, P., Winzer, K., Chan, W. C. & Cámara, M. Look who's talking: communication and quorum sensing in the bacterial world. *Philosophical Transactions of the Royal Society of London. Series B, Biological Sciences* **362**, 1119–34 (2007).
12. Von Bodman, S. B., Willey, J. M. & Diggle, S. P. Cell-cell communication in bacteria: united we stand. *Journal of Bacteriology* **190**, 4377–91 (2008).
13. Palmer, R. J. & Stoodley, P. Biofilms 2007: broadened horizons and new emphases. *Journal of Bacteriology* **189**, 7948–60 (2007).
14. WHO *World Health Report Life in the 21st century A vision for all Report of the Director-General.* (1998).
15. Navarro García, V.M.; Gonzalez, A. & Fuentes, M.; Aviles, M.; Rios, M.Y.; Zepeda, G.; Rojas, M. G. Antifungal activities of nine traditional Mexican medicinal plants. *Journal of Ethnopharmacology* **87**, 85–88 (2003).
16. Fostel, J. & Lartey, P. Emerging novel antifungal agents. *Drug Discovery Today* **5**, 25–32 (2000).

17. Satish, S., Mohana, D. C., Raghavendra, M. P. & Raveesha, K. A. Antifungal activity of some plant extracts against important seed borne pathogens of *Aspergillus* sp . *Journal of Agricultural Technology* 109–119 (2007).
18. Panichayupakaranant, P., Noguchi, H. & De-eknamkul, W. Naphthoquinones and coumarins from *Impatiens balsamina*. *Phytochemistry* **40**, 1141–1143 (1995).
19. Panichayupakaranant, P. Naphthoquinone Formation in Cell Cultures of *Impatiens balsamina*. *Pharmaceutical Biology* **39**, 293–296 (2001).
20. Summerhurst, D. K., Koval, S. F., Ficker, C., Myron, L. & Bernards, M. A. Isolation of an Antimicrobial Compound from *Impatiens balsamina* L . using Bioassay-Guided fractionation. **680**, 676–680 (2001).
21. Ding, Zhi-Shan; Jiang, Fu-Sheng; Chen, Ni-Pi; Lv, Gui-Yuan Zhu, C.-G. Isolation and identification of an anti-tumor component from leaves of *Impatiens balsamina*. *Molecules (Basel, Switzerland)* **13**, 220–9 (2008).
22. Savoia, D. Plant-Derived Antimicrobial Compounds. *Future Microbiology* **8**, 979–990 (2012).
23. Wang, Yuan-Chuen; Li, W.-Y., Wu, Deng-Chyang; Wang, J.-J. & Wu, Cheng-Hsun; Liao, Jyun-Ji; Lin, C.-K. In Vitro Activity of 2-methoxy-1,4-naphthoquinone and Stigmasta-7,22-diene-3 β -ol from *Impatiens balsamina* L. against Multiple Antibiotic-Resistant *Helicobacter pylori*. *Evidence-based Complementary and Alternative Medicine*. **2011**, 704721 (2011).
24. Birdsall, T. C. & Kelly, G. S. Berberine : Therapeutic Potential of an Alkaloid Found in Several Medicinal Plants Berberine. *Alternative Medicine Review* **2**, 94–103 (1997).
25. Thorne Research, I. Monograph: Berberine. *Alternative Medicine Review* **5**, 175–177 (2000).
26. Rasmussen, T B.; Manefield, M. & Andersen, J B.; Eberl, L.; Anthoni, U.; Christophersen, C.; Steinberg, P.; Kjelleberg, S.; Givskov, M. How *Delisea pulchra* furanones affect quorum sensing and swarming motility in *Serratia liquefaciens* MG1. *Microbiology (Reading, England)* **146 Pt 12**, 3237–44 (2000).
27. *Anthraquinones in plants: source, safety and applications in gastrointestinal health*. 153 (Nottingham, University press: 2008).
28. Galván, Imelda J.; Mir-Rashed; Nadereh Jessulat; Matthew Atanya; Monica Golshani; Ashkan; Durst, Tony; Petit, Philippe; Amiguet, V. T. ; B. T. & Summerbell Richard; Cruz Isabel; Arnason, John T.; Smith, M. L. Antifungal and antioxidant activities of the phytomedicine pipsissewa, *Chimaphila umbellata*. *Phytochemistry* **69**, 738–46 (2008).
29. Puniani, T. E. Novel natural product based anti-anxiety therapy and natural insecticides. PhD. Thesis. At <https://www.ruor.uottawa.ca/en/handle/10393/29155> (2003).
30. Dewik, P. . *Medicinal Natural Products: a Biosynthetic Approach*. (John Wiley & Sons, Ltd.: 2002).

31. Kennedy, D. O. & Wightman, E. L. Herbal Extracts and Phytochemicals : Plant Secondary Metabolites and the Enhancement of Human Brain Function 1. *Advances in Nutrition* 32–50 (2011).
32. Ding, X. *et al.* Screening for novel quorum-sensing inhibitors to interfere with the formation of *Pseudomonas aeruginosa* biofilm. *Journal of Medical Microbiology* **60**, 1827–34 (2011).
33. Manefield, M.; de Nys, R.; Kumar, N., Read, R.; Givskov, M.; Steinberg, P. & Kjelleberg, S. Evidence that halogenated furanones from *Delisea pulchra* inhibit acylated homoserine lactone (AHL)-mediated gene expression by displacing the AHL signal from its receptor protein. *Microbiology (Reading, England)* **145 (Pt 2)**, 283–91 (1999).
34. Nys, R De Steinberg, P. D.; Willemsen, P. . & Dworjanyn, S. A.; Gabelish, C. L.; King, R. J. Biofouling : The Journal of Bioadhesion and Biofilm Research Broad spectrum effects of secondary metabolites from the red alga *Delisea pulchra* in antifouling assays. *Biofouling* 37–41 (2009).
35. Jolivet, B. Synthesis of some furanone derivatives : Putative quorum sensing or chitinase inhibitors. At http://edoc.unibas.ch/332/1/DissB_7339.pdf (2005).

3 Section II: Organic synthesis

3.1 Synthesis of Dillapiol analogs as potential synergists for pesticides

3.1.1 Introduction

A pesticide is “any substance or mixture of substances intended for preventing, destroying or controlling any pest, including vectors of human or animal disease, unwanted species of plants or animals causing harm during or interfering with the production processing, storage, transport or marketing of food, agricultural commodities, wood and wood products or animal feedstuffs, or substances which may be administered to animals for the control of insects, arachnids or other pests in or on their bodies”¹.

It was estimated that the consumption of pesticides in the European Union countries in 2009 was approximately 140,000 tons for agricultural purposes² alone. This number becomes even higher in tropical countries where the humidity and warmth of these regions and lack of winter interruption of life cycles, exacerbates the incidence of pathogens, weeds and insect pests in general³, making the pesticides consumption even higher.

These tropical countries play an important role in the world food supply, since the climate in the tropics allows these countries to harvest up to three crops a year⁴. The development of agriculture is highly influenced by the increasing food demand. It is expected that the world population will increase to 7.5 billion people by 2020⁵. Due to environmental effects and health concerns, many synthetic carbamate, organophosphate, and organophthalide pesticides have been withdrawn from the market and many others are under evaluation⁶. It is for these reasons that the search for alternative solutions to pest control becomes very important. Botanical pesticides can be an interesting option to substitute synthetic pesticides, in organic agriculture. They may also provide leads for development of new products with a lower impact on human health and the environment^{2,3}.

Pest control in agriculture with plant extracts can be traced to ancient China, Egypt, Greece and India⁷. At the beginning of 1940, before the development and use of synthetic pesticides plant products were the major tools in pest control by farmers⁸. In recent years, there has been a

return to the use of natural products for pest control in organic agriculture and home and garden use where human contact is more prevalent. One of the major limitations for use of these products is lower efficacy and greatly reduced lifetime compared to synthetics, which have been optimized for these traits. Another problem is the high cost of some of them such as pyrethrins⁸. Currently there are two major registered botanical products used for insect control: pyrethrum, and essential oils. Other commercial plant products used are: ryania, rotenone, nicotine, sabadilla, neem, garlic oil and Capsicum oleoresin⁷(**Table 3.1.1.1**).

Plants constitute a good source of active secondary metabolites with potential use as pesticides. Plants are organisms that rely on allelochemicals as a defence against herbivores, weeds and phytopathogens⁹. The evolution of these active secondary metabolites has helped plants survive in different habitats and compete in areas such as tropical forests.

Table 3.1.1.1: Major botanical products use for pest control

Botanical product	Plant source/ product
Pyrethrum	<i>Tanacetum cinerariaefolium</i>
Neem tree ¹	<i>Azadirachta indica</i>
Essential oils	<i>rosemary (Rosmarinus officinale)</i> <i>and eucalyptus (Eucalyptus globus); eugenol from clove oil (Syzygium aromaticum); thymol from garden thyme (Thymus vulgaris)</i>
Rotenone ²	tropical legumes <i>Derris, Lonchocarpus, and Tephrosia</i>

¹ experimental use in Canada, ² recently delisted in US and Canada

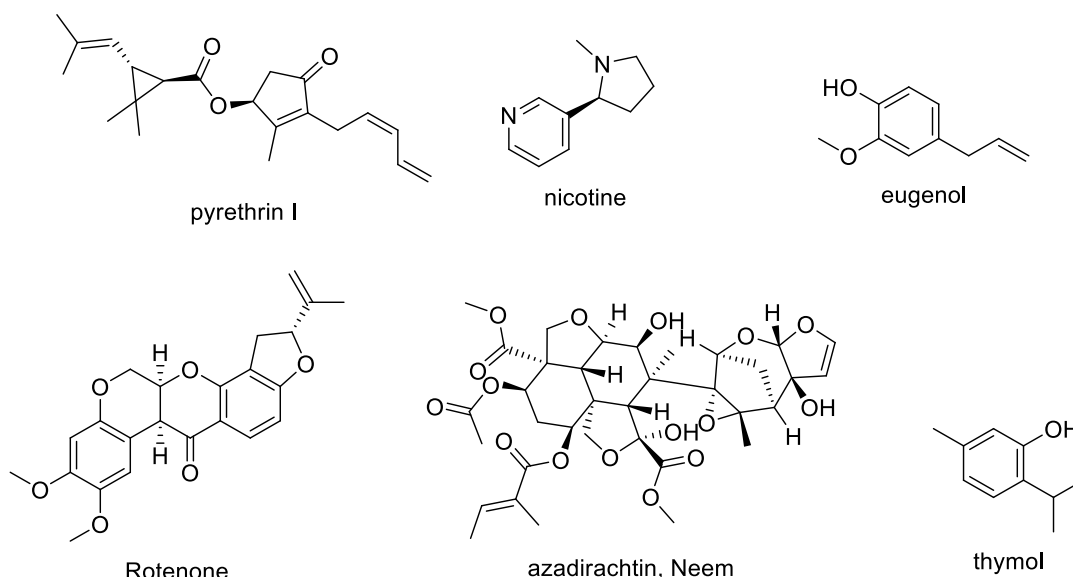


Figure 3-1 : Active metabolites in some of the commonly used botanical pesticides

Other potential sources of biopesticides under development but not yet registered are the seeds of tropical *Annona* species⁷, and the piperamides present in *Piper* species, members of the Piperaceae Family¹⁰.

The Piperaceae is a large pantropical family of flowering plants, constituted of approximately 2000 species, divided into four major genera: *Piper*, *Peperomia*, *Sarchorhachis*, and *Ottonia*.¹¹ *Piper* and *Peperomia* are the most representative members of the family, with 700 and 600 species, respectively¹².

The phytochemistry of *Piper* has been extensively studied in African and Asian species, providing around six hundred secondary metabolites with different bioactivities. According to the review by Virinder et al. in 1997¹³, 351 compounds have been isolated from *Piper* spp., which can be classified as follows: 145 alkaloids/amides, 47 lignans, 70 neolignans and 89 terpenes. Co-evolutionary pressure seems to have played an important role in the diversity of bioactive secondary metabolites present in the *Piper* members. A bioassay-guided fractionation of *Piper* extracts resulted in the isolation of compounds with deterrent activity to leafcutting ants. These ants are one of the dominant herbivores in tropical forest, and the presence of these compounds in *Piper* makes it one of the most abundant species in the understory¹⁴.

Piper species have been traditionally used as pesticides. *P. guineense* is used in African as molluscicides and *P. rotundistipulum* is used in the Amazon region as an insecticide. A study

conducted previously by our research group on *Piper* species from Costa Rica demonstrated that they have similar pesticide activity as those reported for *Piper* plants native to Asia and Africa¹⁵. Most of the pesticide activity associated with *Piper* species is related to the presence of piperamides^{10,16,17}. Nevertheless, the genus has other active compounds such as phenylpropanoids, they include the following compounds: apiol, dillapiol, myristicin, eugenol, and safrol, and dimers of phenylpropanoids, such as the lignans sesamin, cubebin, yangambin or diaeudesmin¹⁵ and terpenes such as β -pinene, β -caryophyllene, bicyclogermacrene, α -pinene, germacrene B and δ -3-carene^{18,19}.

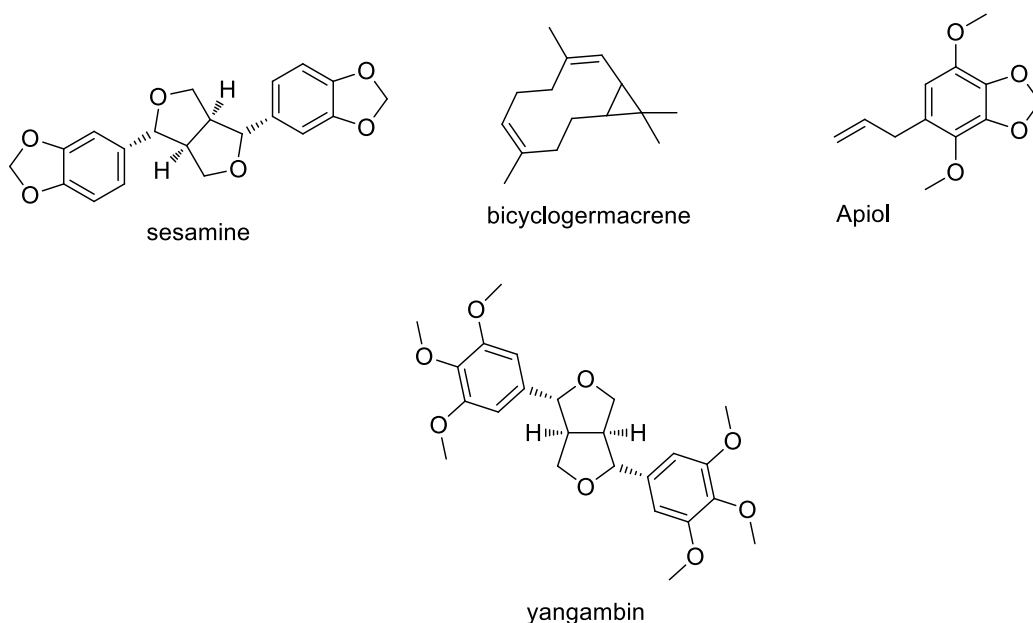


Figure 3-2: Other bioactive secondary metabolites present in *Piper* species

Piper aduncum L. is a tropical shrub native to Central America and widespread in South and Central America (**Figure 3-3**). This species was introduced to Asia and the Pacific islands in the mid-1930's and it has become an invasive species competing with native flora^{20,21}. This plant is used in traditional medicine for the treatment of stomach-aches, trachoma, leishmaniasis and is also used as an insect repellent^{22,23}.

The evaluation of the essential oil of *P. aduncum* L. has provided interesting results. It has activity against important health pests as the malaria mosquito, *Anopheles* spp. and the vector of dengue and yellow fever, *Aedes aegypti*²⁴, as well as important agricultural pests as the European corn borer¹⁵. The analysis of the essential oil from leaves and fruits of *P. aduncum* L.

has shown the presence of dillapiol **1** as a major component with the concentration in the range of 37 to 75%^{18,25–29}.

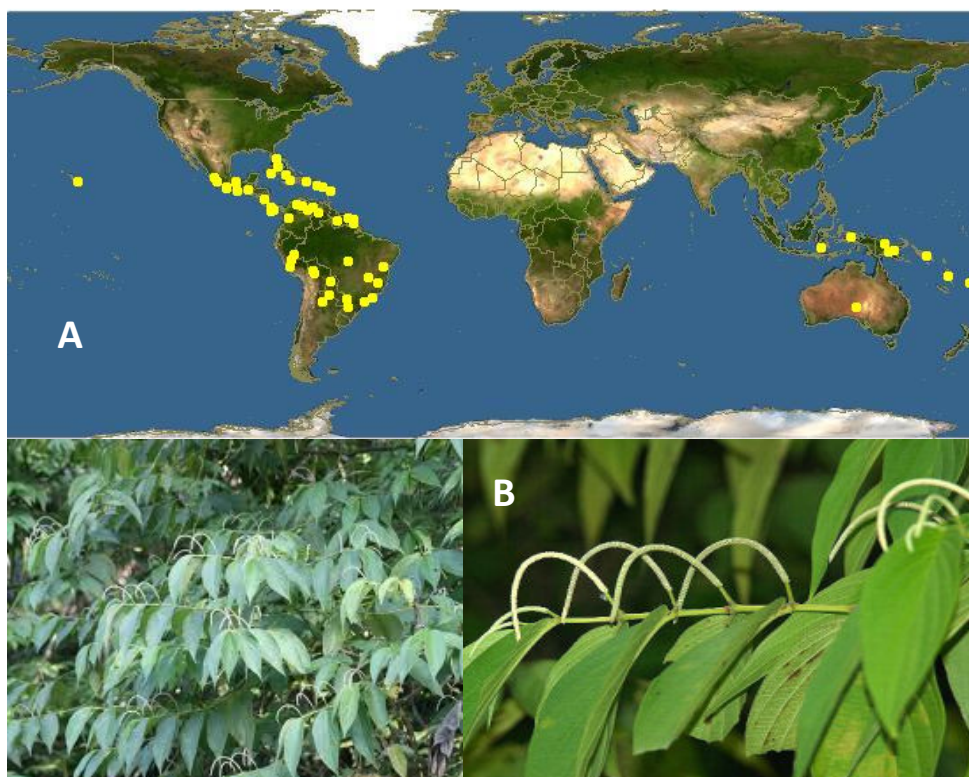
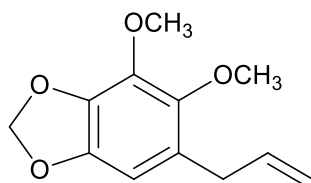


Figure 3-3: A. geographical distribution of *Piper aduncum* L., B. Leaves and fruit of *Piper aduncum* L. Modified from: <http://www.discoverlife.org/mp/20q?search=Piper+aduncum>

The composition of the essential oil varies with plants from Brazil, Cuba and Costa Rica having the highest content of dillapiol³⁰. A study of the Costa Rican plants reported a 61% concentration of dillapiol in the essential oil obtained from the leaves and fruits of the plant²⁵. Due to the high concentration of this metabolite in *P. aduncum* L., researchers deemed this plant as a possible commercial source for dillapiol²⁷.



1. Dillapiol

Dillapiol is a methylenedioxyphenyl (MDP) compound that acts as synergist in combination with certain pesticides³¹. A pesticide synergist is a non-toxic compound that is added to insecticides to increase their effects against insect pests³². These compounds do not have pesticide activity by themselves but they act in combination (or together) with an active compound to increase the overall effect. These synergists can be classified with respect to their chemical structure according to Casida³³: N-alkyl compounds, O-(2-propynyl) esters and ethers, organophosphates and carbamates and finally methylenedioxyphenyl compounds, which represent one of the most important classes of synergists³³. This group includes a series of natural occurring compounds such as: sesamin **2**, sesamol **3**, safrole **4** and its synthetic derivate piperonyl butoxide **5** (Figure 3-4).

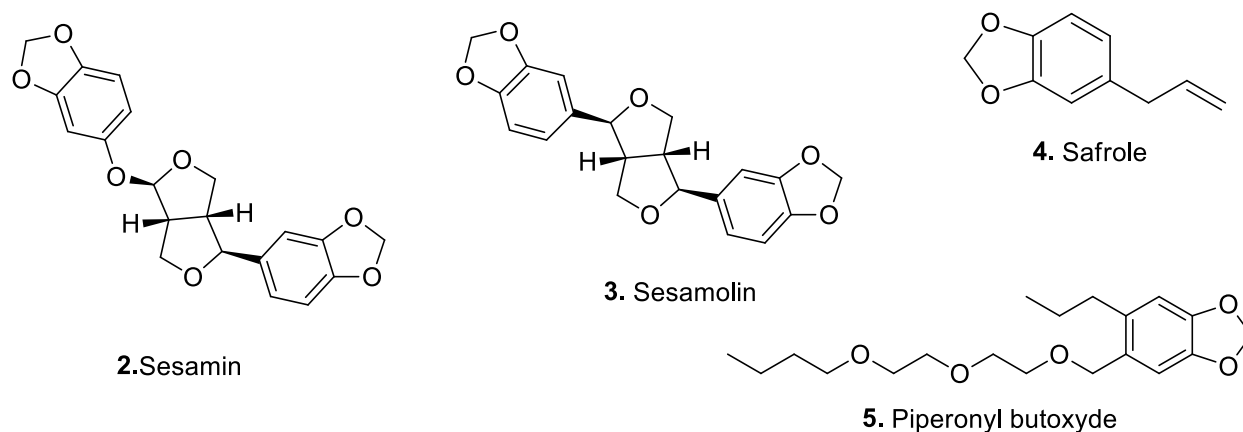
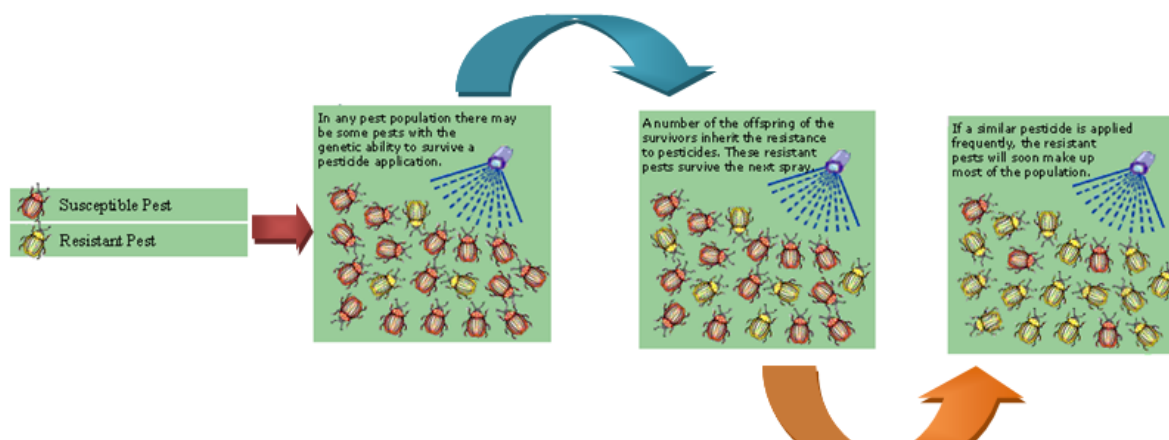


Figure 3-4: Methylenedioxyphenyl compounds used as pesticide synergists

Pesticide synergists play an important role since insects can develop pesticide resistance quite quickly. This resistance is linked to recurrent selection. When insect populations are exposed to pesticides, some of the individuals in the population may have the metabolic machinery needed to metabolize the insecticide, which allows them to survive. Through a recurrent selection

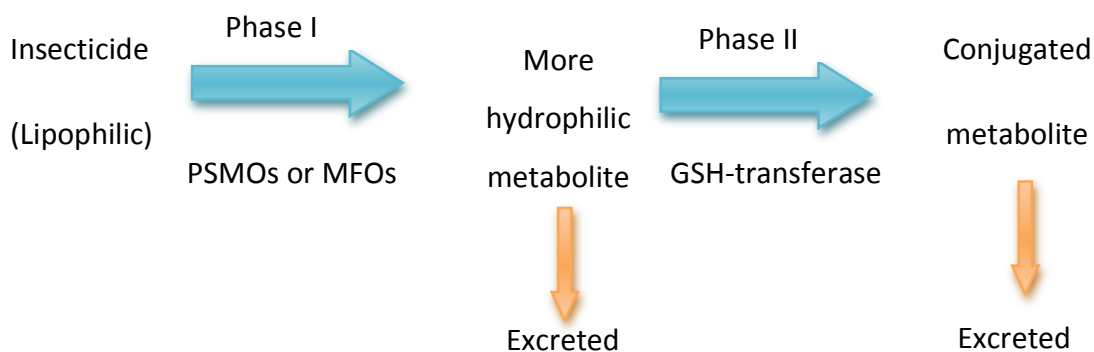


process the population exposed many times to the same insecticide evolves higher resistance (**Figure 3-5**). This involves the selection of resistant individuals in the population that reproduce and pass on the genetic changes needed for this resistance. In extreme situations, farmers may apply higher doses of pesticide leading to greater resistance and more environmental contamination.

Figure 3-5: Schematic representation of pesticide resistance development in insect populations. This phenomenon is known as the “pesticide treadmill”. Modified from: http://www.agf.gov.bc.ca/pesticides/a_4.htm

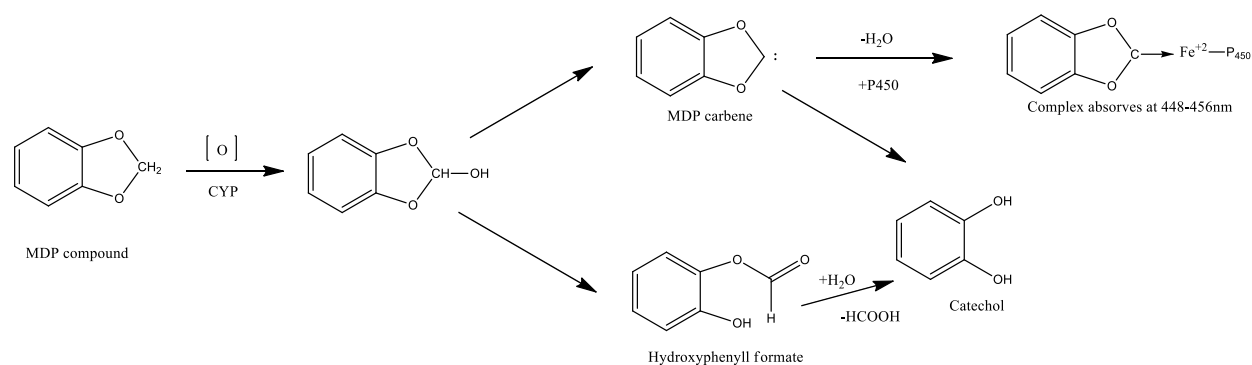
The detoxification of insecticides, as with other lipophilic xenobiotics, involves the fast conversion of compounds to more polar, excretable products via a series of enzymatic reactions called: phase I and phase II metabolism (**Scheme 3.1**).

Phase I metabolism is carried out by the mixed function oxidases, also called the cytochrome P-450 dependent poly-substrate monooxygenases (PSMOs). P-450 enzymes provide one of the most important detoxification pathways and they are present in all living systems examined³⁴. The selection for higher rates of metabolism of toxic compounds via this system is a major cause of the development of pesticide resistance in insects³³. Compounds containing a methylene dioxyphenol (MDP) moiety are inhibitors. It has been established that MDP compounds act by inhibiting CYP-450 enzymes^{33,35}, and as a consequence, the pesticide can no longer be metabolized and remains in the insect's hemolymph for a longer period of time. The mixture of pesticides with the MDP compounds enhances the activity of the pesticide.



Scheme 3.1: General detoxification pathways for most insecticides³²

CYPs oxidize MDP compounds to catechols, which are stable compounds that can bind to the heme group causing inhibition of oxidation of the substrate. Depending on the hydrophobic and electronic characteristics of the MDP some metabolite intermediates (MI) can be formed. These MI adducts are stable when the heme group is in the ferrous form in the oxidized state. These MI complexes can be displaced by lipophilic compounds, thereby restoring the activity of the CYP MDPs with electron donating groups on the aromatic ring and aliphatic side chains tend to form stable MI adducts, on the other hand, MDPs with electron withdrawing groups on the aromatic ring, promote the formation of CO₂ and the corresponding catechol³⁶ **Scheme 3.2.**



Scheme 3.2: Oxidations of MDP compounds by CYP-450 enzymes.

Adapted from Murray, 2008³⁶

The main objective for this section of the thesis was the development of analogs using the lead MDP compound dillapiol to improve its inhibitory activity in the CYP 3A4 bioassay and evaluate the features needed for the molecule to be highly active. In order to achieve this goal analogs of dillapiol were synthesized and tested in the CYP 3A4 bioassay. Modifications at positions: 4, 5 and 6 were evaluated using the essential oil of from *P. aduncum* fruit as starting material. Additional compounds were prepared from sesamol, safrol and piperonal, all of which are naturally occurring compounds containing the methylenedioxyphenyl structure motif.

3.1.2 Results and discussion

The insecticide synergistic activity of dillapiol was first reported by Gulati and Parmar in 1969³⁷. Subsequently it has shown to be a potent synergist in combination with many different pesticides including pyrethrines and DDT^{38,39}. Piperonyl butoxide is currently the most widely

used synergists for pyrethrines. Other compounds such as the sulfoxide **A** and the diester **B**^{40,41} have been patented as synergists for use to enhance pyrethrin activity **Figure 3-6**. These compounds are manufactured from safrole. They belong to the methylenedioxyphenyl (MDP) family of compounds and their bioactivity is linked to the presence of the benzo-1,3-dioxole group, as explained in the Introductory part of this section.

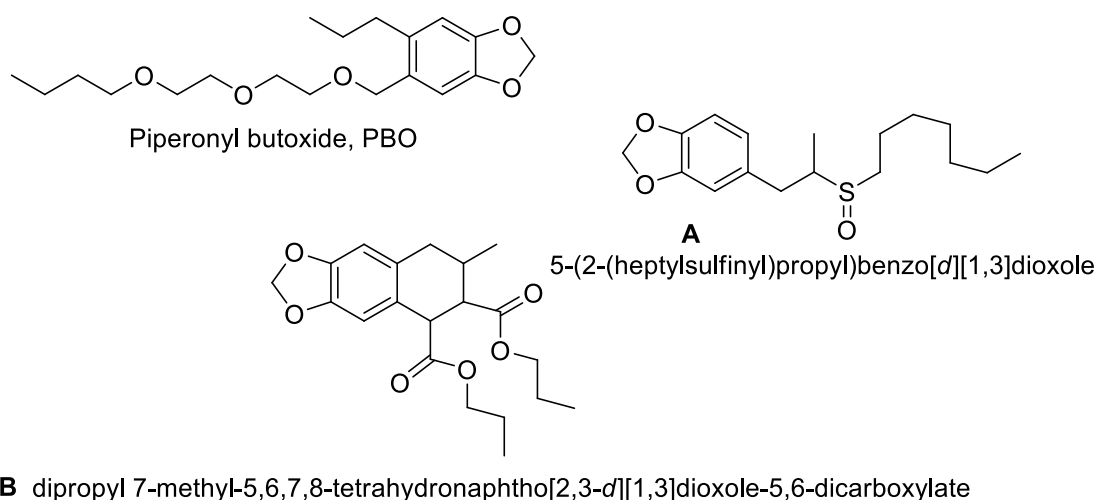
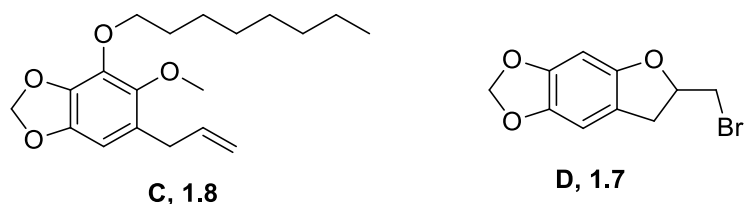


Figure 3-6: Safrole analogs used as pyrethrines synergists

In 1997, Sherry Majerus, a Master student in our research group worked on the development of a novel synthetic pathway for the preparation of dillapiol and of several analogs⁴². These dillapiol analogs showed interesting activities as: chemosensitizers to drug-resistant tumor cells, and also showed synergistic activity towards the insecticide α -T. Dillapiol itself had the highest synergistic activity with a factor of 1.8, followed by compound **C** and **D**. The activity observed by Majerus was linked to the Log P value.



In 2000, another member of the research group Master student Jason Budzinsky, performed an *in vitro* evaluation of human cytochrome P450 3A4 inhibition by herbal extracts and pure herbal derived compounds⁴³, in his study he found that dillapiol **1** was the most potent inhibitor of the

enzyme among the 40 herbal products tested⁴³. This result suggests an explanation of the synergist effect observed for dillapiol and its analogs as inhibitor of insect CYP enzymes. The inhibition of the CYP enzymes blocks the metabolism of other xenobiotic compounds present in the organism, therefore the exposure time to the compound is increased and the overall toxicity is enhanced. The bioassay used by Budzinsky used 7-benzyloxy resorufin **E** as the enzyme substrate, the bioassay used in the present research uses a different substrate at the one used by Budzinsky.



E, 7-benzyloxy resorufin

The previous results obtained in our research group suggested that dillapiol analogs could be developed for use as pesticide synergist. Such compounds might have low toxicity; certainly dillapiol is considered a safe compound. Piperonyl butoxide has been linked to long and short term toxicological effects, like cancer⁴⁴, inhibition of lymphocyte response⁴⁵, neurological damage⁴⁶, among others. Despite these facts the EPA (Environmental Protection Agency of The United States) allows its commercial use⁴⁷, but much criticism has been made of the data used for the evaluation of this product⁴⁴. A more suitable synergist with less human risk and environmental impact has to be developed prior to PBO being removed from the market is highly desirable.

The main goal of this part of the research was to produce dillapiol analogs, and to use a newer version of the human CYP 3A4 bioassay to determine potential activity in this class of enzyme, with a follow up in more challenging insect bioassay. Eventually, the objective was to develop a SAR relationship, which would allow us to understand the different characteristics in the molecules that determine the desired activity. In the end such an understanding could be used to develop new and more potent synergist for both drugs and insecticides. A unit of BASF via Dr. Steve Sims funded this project initially. It received additional funding from NSERC in the

from a matching CRD grant. The development of bioassays and *in vivo* analysis has been done in collaboration with Dr. Ian Scott and PhD student Suqi Liu.

In order to analyze the data obtained, two molecular descriptors were used: Log P, which is defined by **Equation 2.2.1**, and MR (Molecular Refractivity), which is defined by **Equation 2.2.2**.

$$\log_{10} P \quad \text{Equation 2.2.1}$$

Where, P is the partition coefficient = $\left(\frac{[solute]_{octanol}}{[solute]_{water}}\right)$, and gives the ratio of concentration between octanol: water. This descriptor is related to the hydrophobicity of the molecule, the higher the value of this descriptor the less soluble the molecule is in water.

MR, is one of the most successful descriptors used in the design of QSAR models, which is why it was incorporated in this research. It is defined by the Lorentz-Lorentz **Equation 2.2.2**, and it has a strong correlation with molecular polarizability⁴⁸.

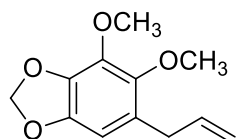
$$MR = \left(\frac{n^2-1}{n^2+2}\right) \left(\frac{MW}{d}\right) \quad \text{Equation 2.2.2}$$

Where n = refractive index, MW = molecular weight, d = density, units: mol/mL

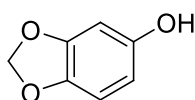
Polar functional groups increase MR, but decrease log P. Therefore, some authors suggest that MR is a measure of non-lipophilic interactions, while log P is a measure of lipophilic interactions⁴⁹.

Synthesis of MDP analogs

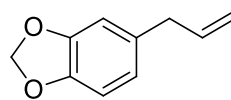
The starting materials used in this project were dillapiol, sesamol, safrol and piperonal.



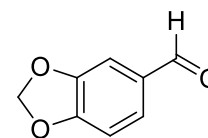
dillapiol



sessamol



safrole



piperonal

The latter three compounds were sourced commercially. Dillapiol was obtained by steam distillation of plant material; mainly fruit, of *P. aduncum* growing in different areas in Costa Rica. The yields obtained via this procedure are presented in **Table 3.1.2.1**. The data obtained from the extraction of the essential oil shows that the content of the oil in fruits is higher than the content in leaves. The NMR analysis of the oil obtained also showed a higher content of dillapiol in the essential oil from the fruits. The concentration of dillapiol in the essential oil varied considerably depending on the collection site. In some cases the content was as low as 37% in others higher than 95%. The latter material (**Figure 3.7**), was sufficiently pure for subsequent chemical transformations. Other samples required purification by column chromatography. Plant material collected from the Sarapiquí region gave oil with the highest dillapiol content.

The GC-MS of a specific sample collected from Braulio Carrillo, Limon (leaf) Costa Rica, confirmed the results observed by NMR analysis. The concentration of dillapiol in this sample is 36.8% being the major component in the mixture, a total of 20 different compounds were also detected in the analysis (**Appendix 1A**) for the complete report on the sample analysis. All the compounds identified have been previously reported by Ciccio and co-workers²⁵. For the synthesis of the analogs the essential oil was purified by flash chromatography.

Table 3.1.2.1: Yield of extraction for fresh *P. aduncum* tissues, all samples were collected during dry season 2011

Collection site	Yield of essential oil%
Arenal Lake, Alajuela	1.1
Atenas, Alajuela	1.2
Braulio Carrillo, Limon	0.8

Braulio Carrillo, Heredia	0.7
Rio Costa Rica, Cartago	0.5
Braulio Carrillo, Limon (leaf)	0.4
Braulio Carrillo, Limon (stems)	0.01

All of the analogs that are described below were prepared from four different starting materials shown above. The goal of this part of the research was to develop a small focused library of compounds and evaluate their inhibitory activity towards CYP3A4. **Figure 3-7** shows the methylenedioxyphenyl core with the corresponding IUPAC numeration. Almost all of the structure modifications focused on position **4**, **5** and **6**. This stage of the work does not include optimization of reaction yields. Once a highly active compound is identified this aspect will be addressed.

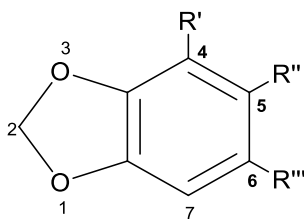


Figure 3-7: IUPAC numbering system for the benzo-1,3- dioxole group.

Dillapiol 2
400MHz, CDCl3

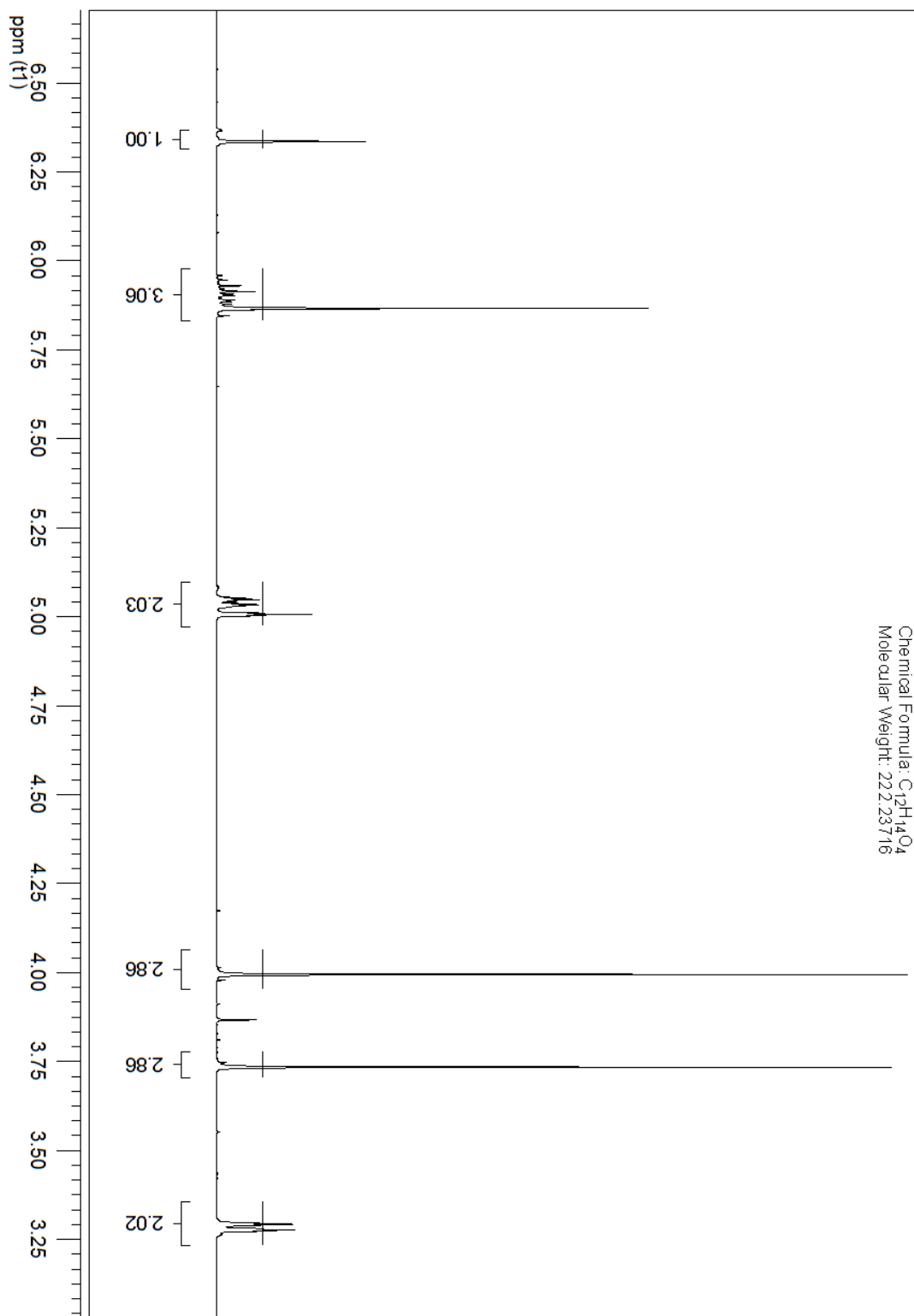
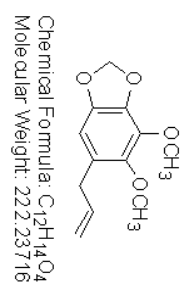


Figure 3.8: ¹H-NMR spectrum of "crude" essential oil-mainly dillapiol 400MHz, CDCl₃

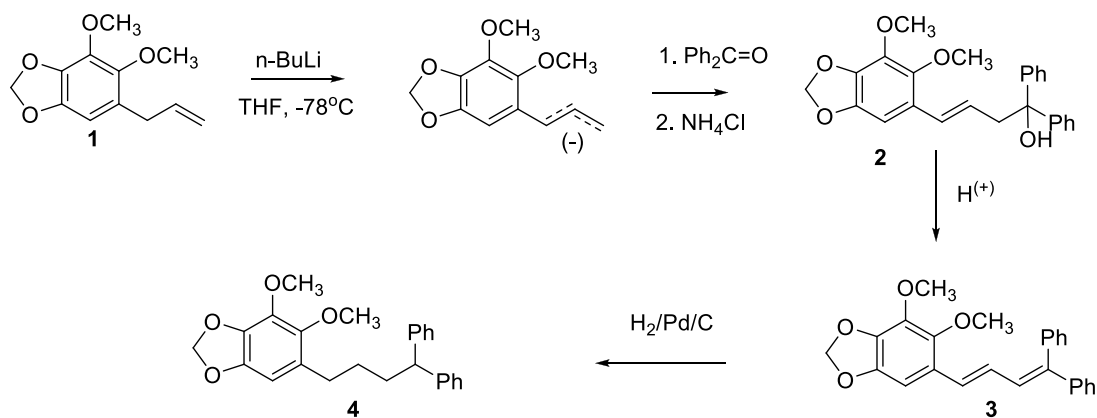
Dillapiol analogs

The first set of analogs was synthesized using dillapiol obtained by purification of the crude essential oil obtained by steam distillation from *P. aduncum* fruits by flash chromatography as described in the experimental section. The hydrodistillation of the fruit of *P. aduncum* provided oil slightly heavier than water, which was deposited at the bottom of the water column in the Dean-Stark apparatus.

A total of 31 analogs of dillapiol were synthesized. Structural modifications focused on reactions involving the double bond in the C6 side chain.

C-C Bond Forming Reactions

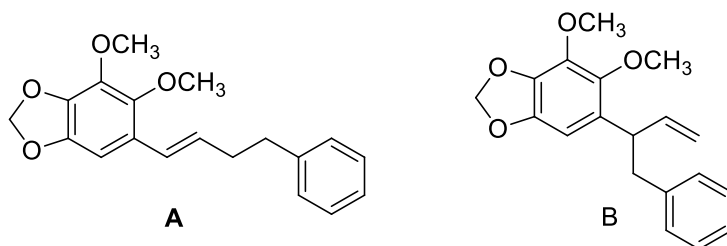
Compound **2** compound was previously reported by Majerus⁴² and shown by the earlier bio-assays to be a rather potent P450 inhibitor. It was decided to re synthesize this compound using the procedure described in Majerus' thesis. Access to **2** would enable us to verify the P450 inhibition via the new bio-assay and also allow us to prepare of several related compound readily derived from **2** and determine whether the activity is specific to **2** or a more general property of all of these compounds. Treatment of dillapiol with n-butyllithium removes one of the acidic benzylic protons generating an allyl carbanion, which is stabilized by resonance. As previously reported by Majerus, the α -condensation product was not observed and compound **2** was obtained with 33% yield. The spectroscopic data of **2** matched that reported by Majerus⁴². (**Scheme 3.3**)



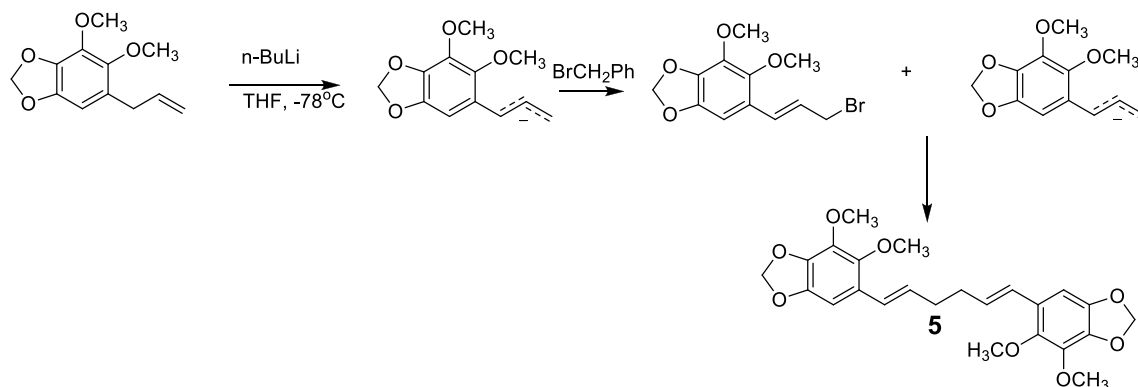
Scheme 3.3: Synthesis of dillapiol analogs **2**, **3** and **4**.

Treatment of compound **2** with *p*-toluenesulfonic acid (PTSA) afforded diene **3** as a yellowish powder in 81% yield. The ¹H-NMR spectrum showed the three alkene hydrogens as a three nuclei spin system at 6.97(d, *J*= 15.6Hz) 6.91 (d, *J*=11.0Hz) and 6.73 (dd, *J*=15.6 and 11.0 Hz). The 15.6 MHz coupling constant signifies the *trans* configuration. The other resonances were as expected. (See experimental Section) Compound **3** was hydrogenated using hydrogen and Pd/C to obtain compound **4** in a 96% yield as clear oil. The proton NMR showed the loss of the alkene hydrogen atoms and the appearance and high field multiplets due to the CH₂ groups; the methine benzylic hydrogen appears at 3.89 ppm as triplet (*J* = 7.85 Hz).

We expected that generation of the allyl anion from dillapiol followed by addition of benzyl bromide would lead to alkylation either at the α or γ position. Thus dillapiol was treated with *n*-BuLi at -78°C, for 1 h followed by addition of benzyl bromide. The expected product from this reaction was either A or B.

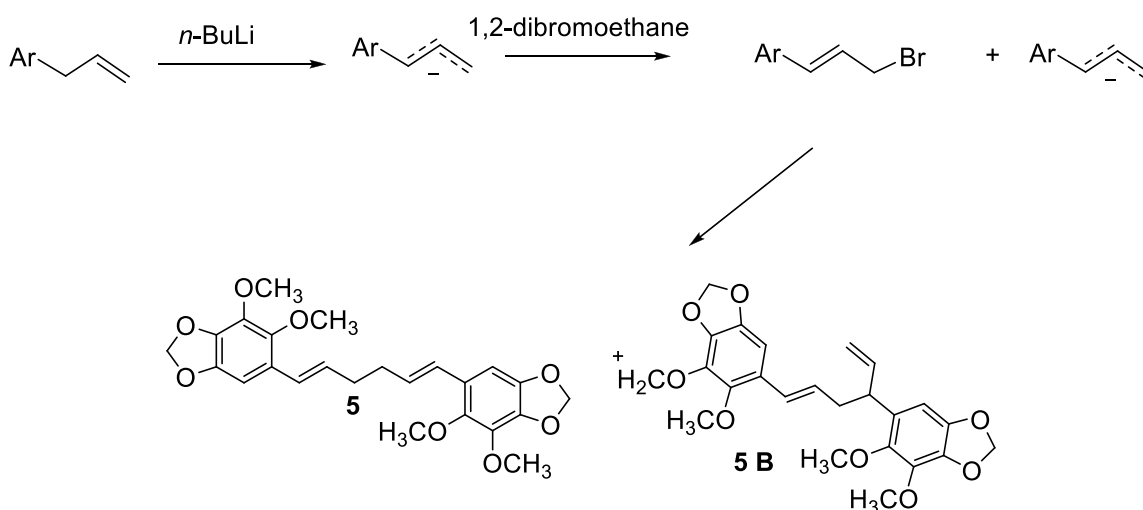


The major product obtained in 28% yield as white solid after purification via several chromatography columns was assigned structure **5** according to the ¹H-NMR spectra analysis. The ¹H NMR spectrum indicated a symmetrical dimeric structure of dillapiol. The formation of this compound can be rationalized via the mechanism presented in **Scheme 3.4**.

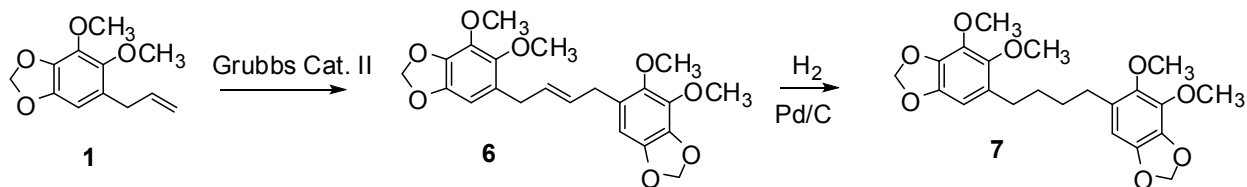


Scheme 3.4: Proposed mechanism for the formation of compound 5.

To support the proposed mechanism, dillapiol was treated with $n\text{-BuLi}$ at -78°C , to form the allylic anion. 1,2-Dibromoethane (0.5eq.), a known positive bromine reagent, was added to the reaction mixture. The main product of this reaction was the dimer. The function of 1,2-dibromoethane was to convert the anion into an allylic bromide which then reacts with the remaining anion to form the dimer. The main product isolated in this reaction was the symmetrical dimer **5**. The $^1\text{H-NMR}$ of the crude product indicated also the presence of small amount of unsymmetrical dimer **5B**.



The next strategy used for the formation of new C-C bonds was olefin metathesis using Grubbs catalyst second generation. Compound **6** was obtained in 57% as off white crystals from the treatment of dillapiol with Grubbs II catalyst (**Scheme 3.5**). Analysis of the proton spectra showed the characteristic signals of the MDP nucleus and the corresponding signals for hydrogen atoms on the double bond. The ^{13}C spectrum confirmed the structure showing only 11 signals as required by the symmetrical structure. Hydrogenation of **6** gave **7**. The most significant change in the proton NMR is the loss of signals at 5.57 ppm due to the alkene hydrogens and appearance of a peak the at 1.58 and 2.55 as a multiplets corresponding to the two CH_2 groups.



Scheme 3.5: Synthesis of compound **6** and **7**.

Compound **2**
CDCl₃, 400MHz

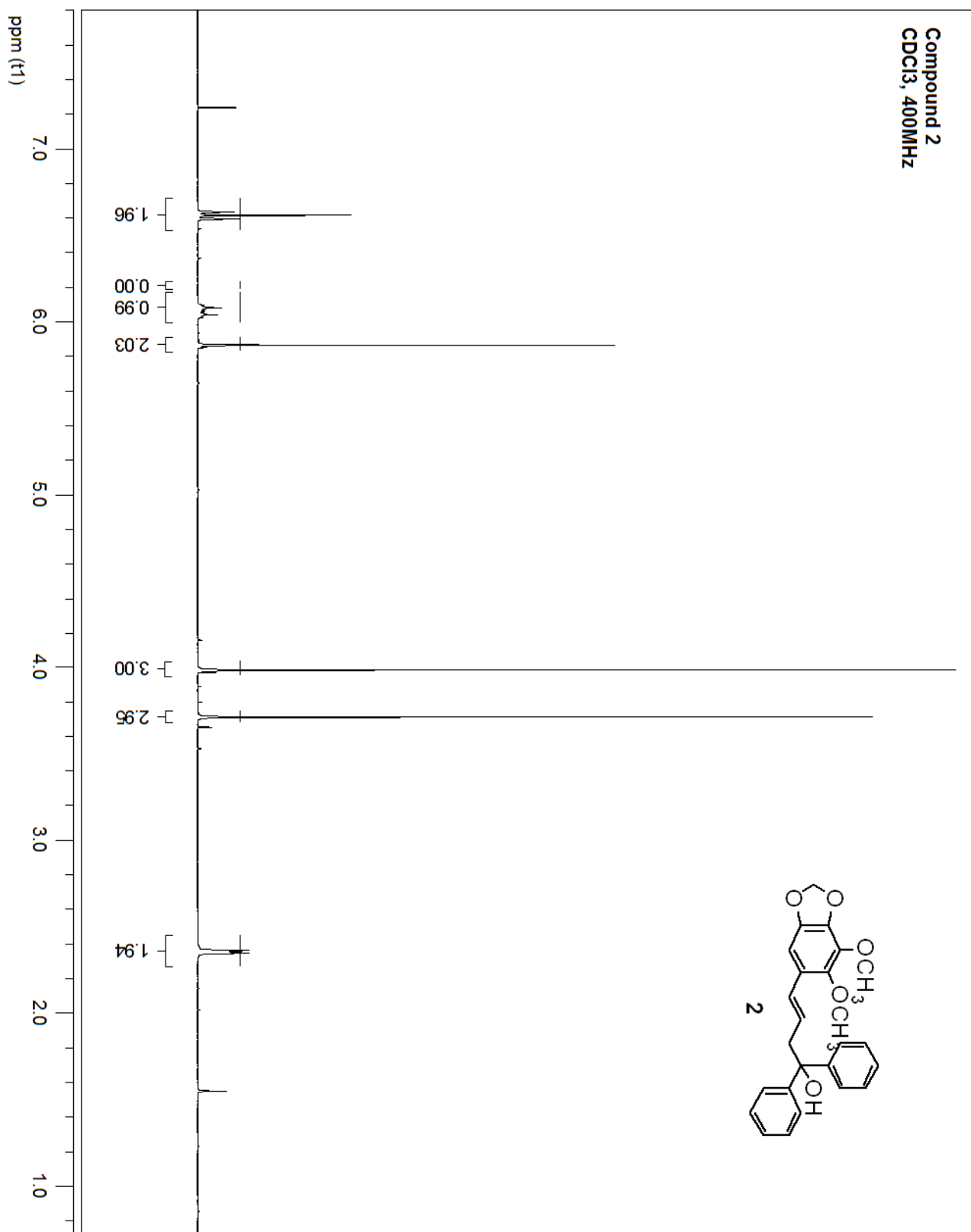
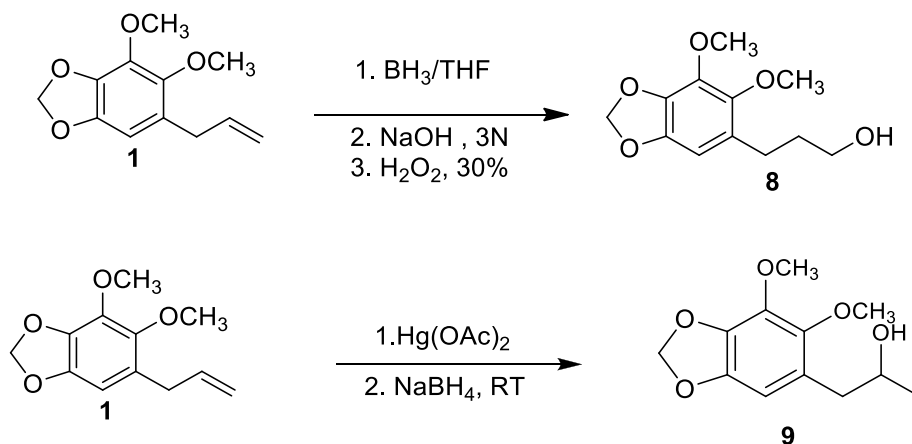


Figure 3.9: 300 MHz ¹H-NMR Spectrum of compound **2** in CDCl₃

Synthesis of esters and ethers

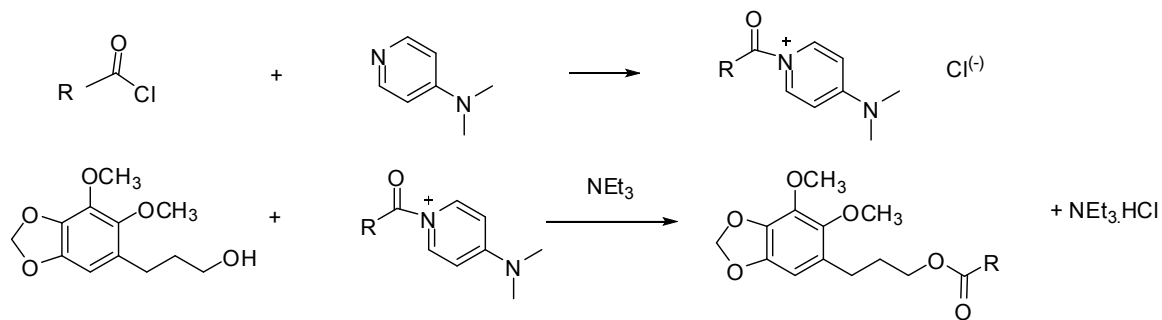
Hydroboration of dillapiol

As anticipated, hydroboration of dillapiol gave the **8** (anti-Markownikov addition) as the major product. A small amount of the isomeric alcohol **9** was also formed. The latter isomer was best obtained via the oxymercuration-demercuration route developed by Majerus. The spectral data for both **8** and **9** corresponded to that reported by Majerus⁴².

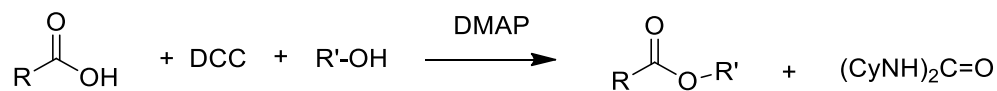


Scheme 3.6: Synthesis of alcohols **8** and **9**

Compounds **8** and **9** were used in the synthesis of ethers and esters. Esters were prepared either by direct acylation with available acid chlorides (**Scheme 3.7** and **Table 3.1.2.2**) or by in situ activation of a carboxylic acid using DCC followed by acyl transfer to either **8** or **9** (Steglich Esterification), (**Scheme 3.8** and **Table 3.1.2.2**). The direct acylation with acid chlorides was catalyzed by DMAP.



Scheme 3.7: Esterification via acyl chloride intermediates



Scheme 3.8: Steglich Esterification.

The esters synthesized were chosen to reflect mainly differences in size and substitution patterns adjacent to the ester carbonyl group. Some of the initial choices also reflected the availability of starting materials in our laboratory.

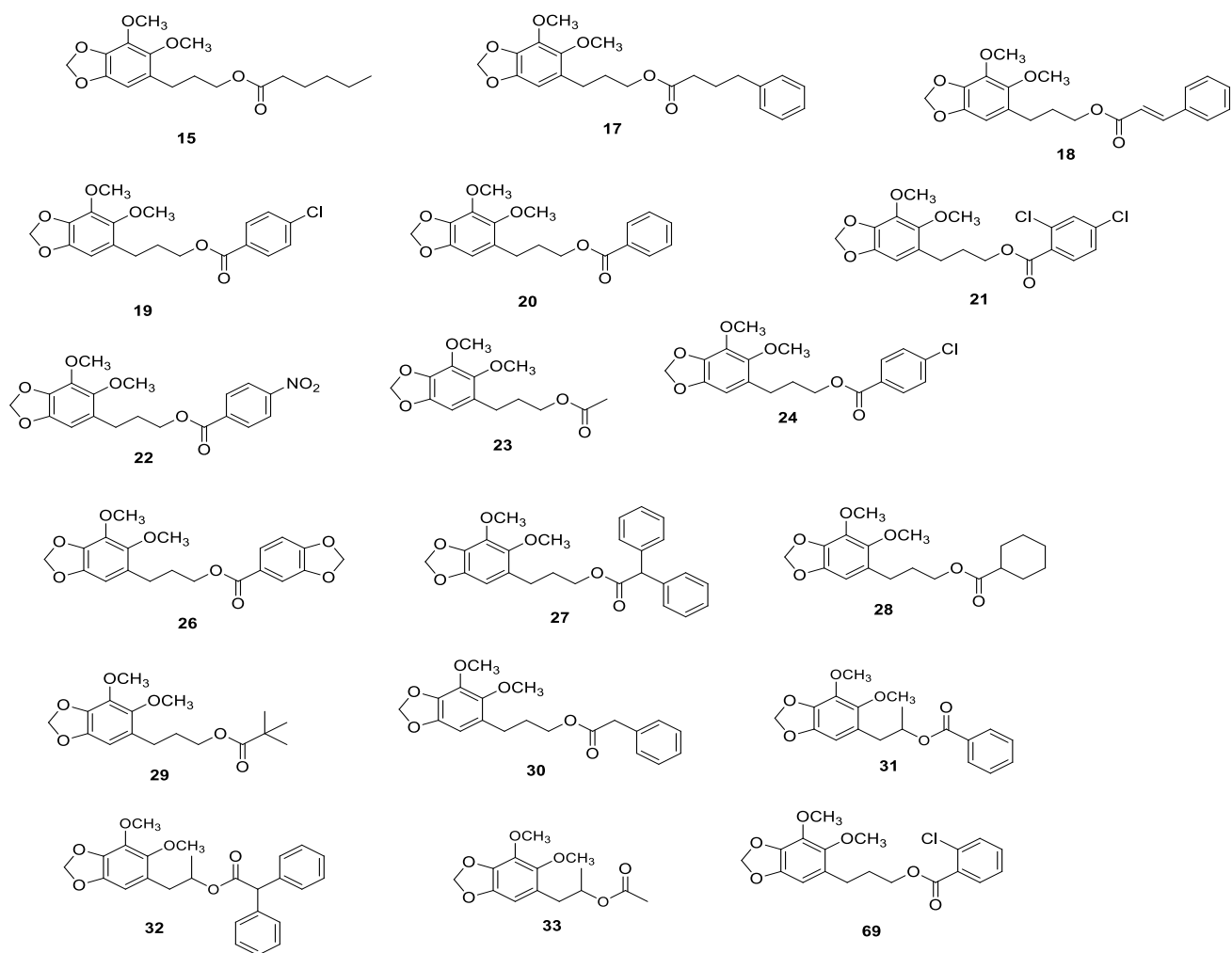


Figure 3-10: Dillapiol esters synthesized by the two methods described in **Scheme 3.7** and **3.8**

These compounds were characterized by both proton and carbon NMR and by HRMS when appropriate. The ^1H NMR of the esters derived from compound **8** showed a typical triplet

around 4.38 ppm corresponding to the methylene group of the ester bond. This signal was used as a diagnostic signal to determine the product formation in the crude mixtures (**Figure 3.11**).

Table 3.1.2.2: Reaction yields for the ester analogs of dillapiol

Compound Number	Yield %	Method used
15	53	Direct acylation
17	76	Steglich Esterification
18	91	Steglich Esterification
19	66	Steglich Esterification
20	33	Direct acylation
21	51	Steglich Esterification
22	66	Direct acylation
23	91	Direct acylation
25	59	Steglich Esterification
26	85	Steglich Esterification
27	65	Direct acylation
28	75	Direct acylation
29	60	Direct acylation
30	70	Direct acylation
31	83	Direct acylation
32	93	Direct acylation
69	48	Direct acylation

Esters derived from compound **9** presented a more interesting set of spin systems due to the newly creates chiral center α to the ester oxygen. The remaining H together with the adjacent CH_2 group generates an ABX system **Figure 3-12 A** in which the AB portion has a chemical shift centered near 2.9 ppm and that of the X part is found near 5.3 ppm.

Compound 22
400MHz, CDCl₃

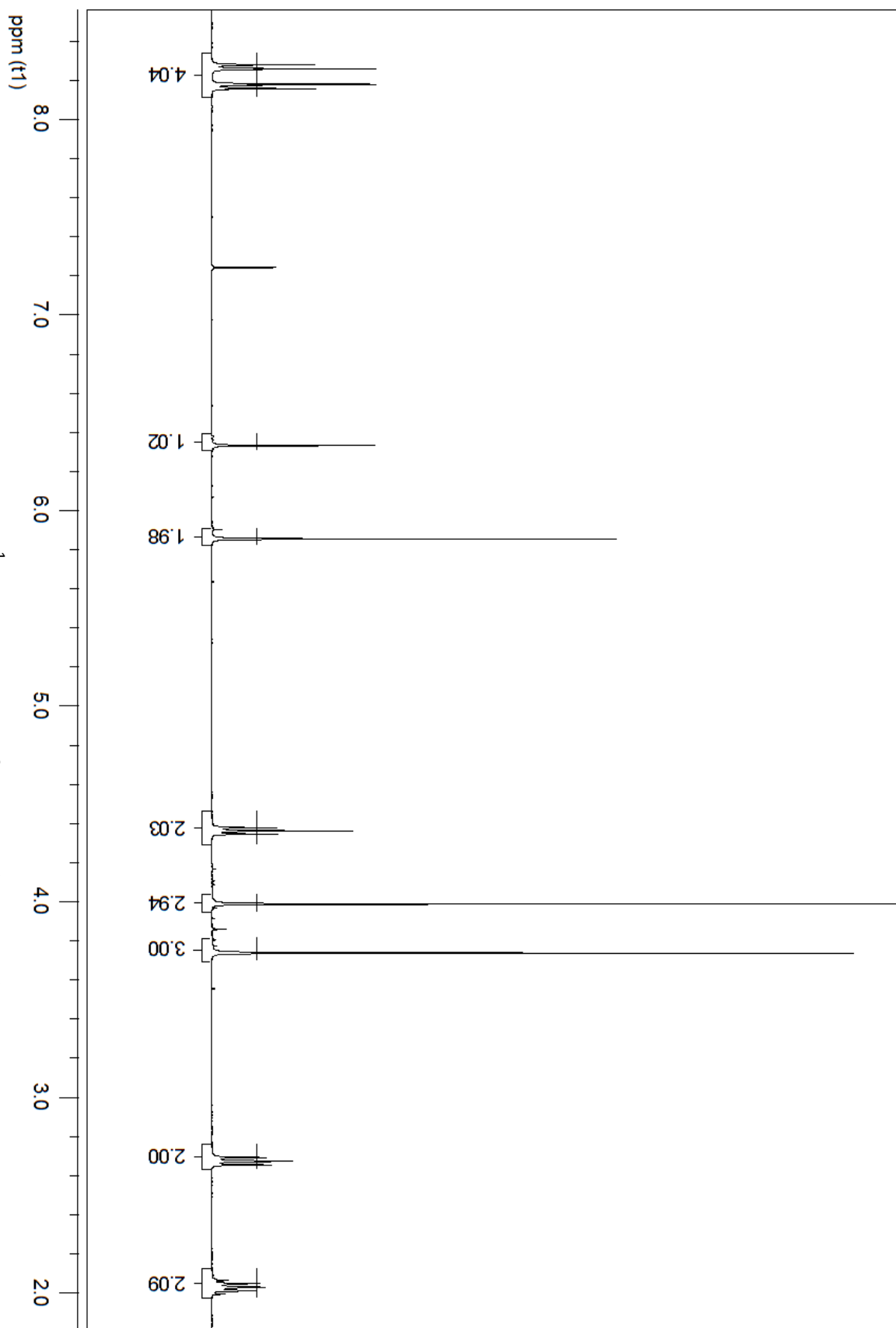
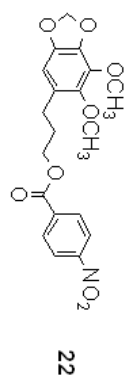


Figure 3.11: 400 MHz ¹H-NMR Spectrum of compound 22 in CDCl₃

Interestingly in these derivatives the methylene hydrogens of the of the benzo-1,3- dioxole group are also diastereotopic and have slightly different chemical shifts and thus appear as an AB quartet. (**Figure 3-12B**).

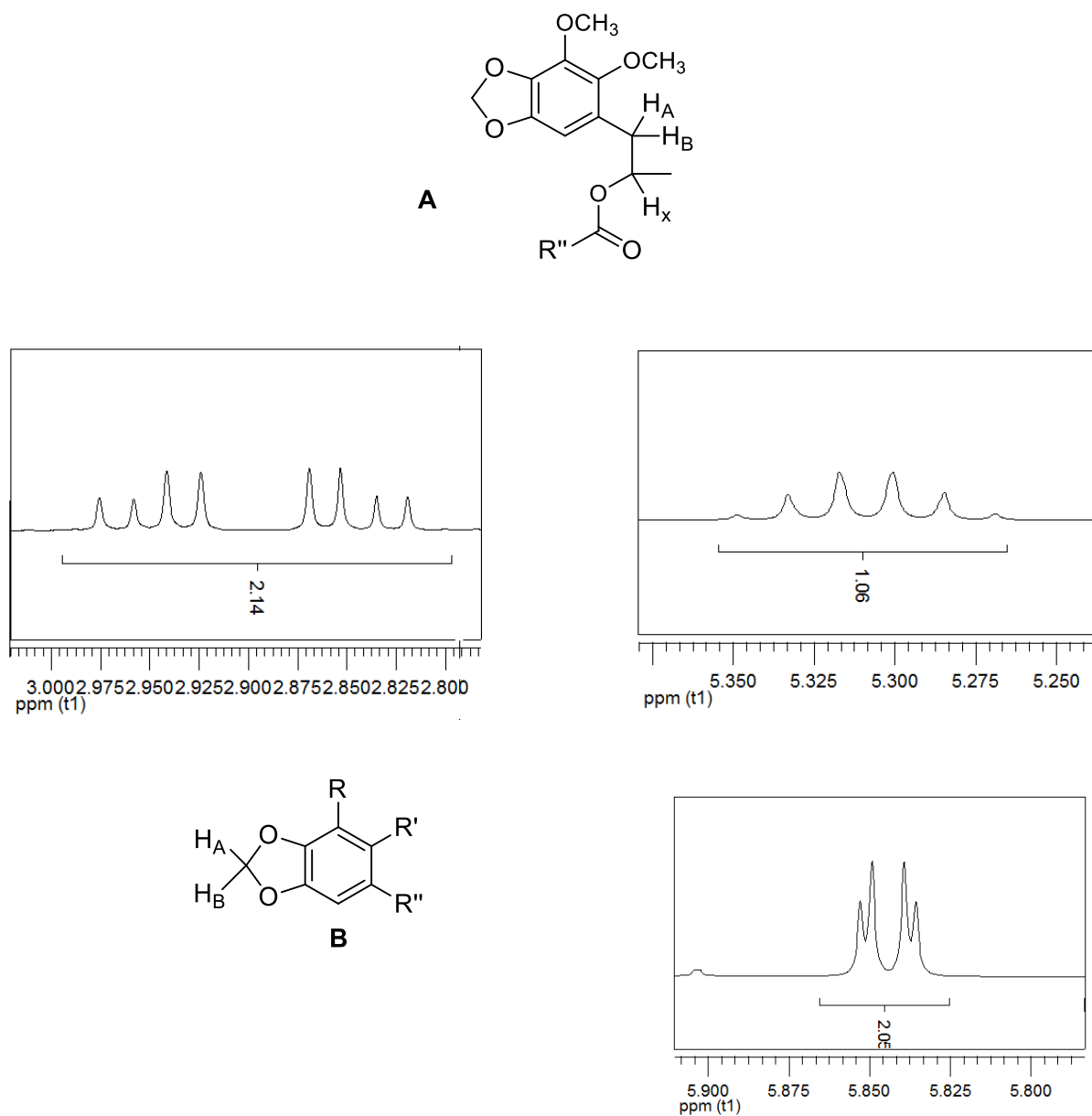
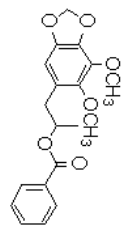


Figure 3-12: A ABX system in dillapiol analogs **B**, AB systems of the benzo-1,3- dioxole group

Compound 30
400MHz, CDCl₃



30

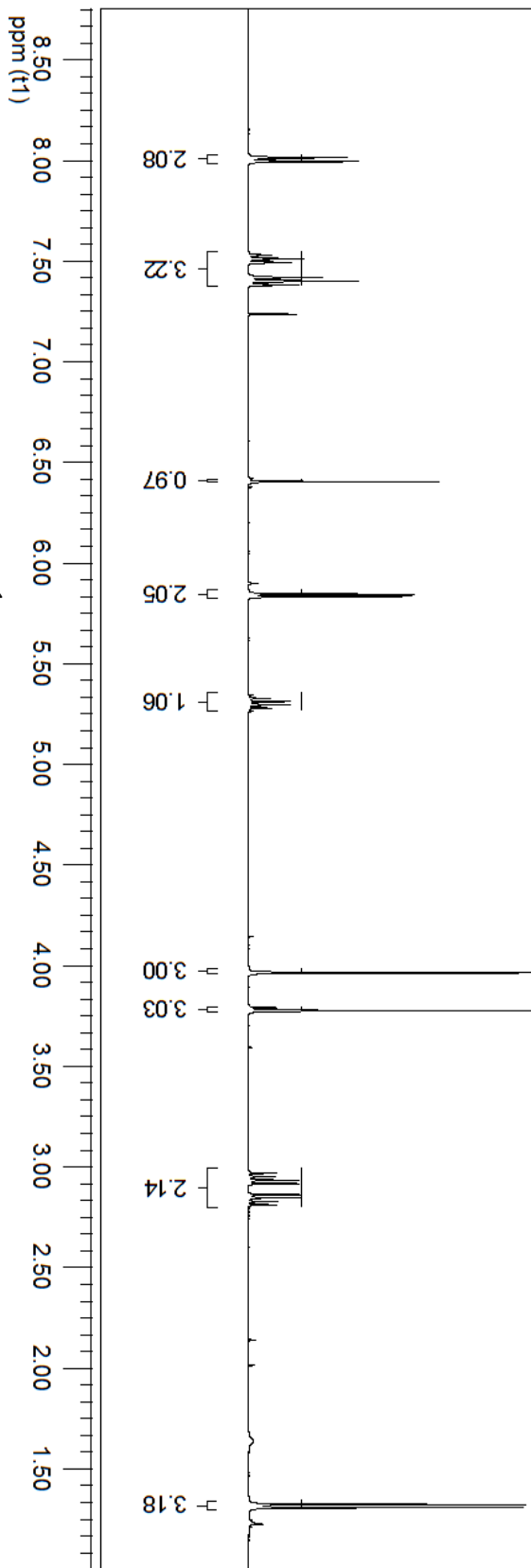
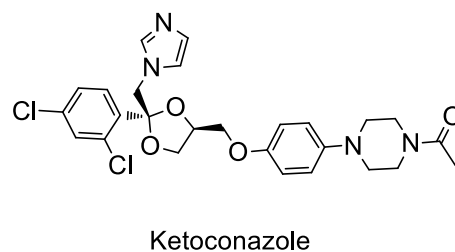
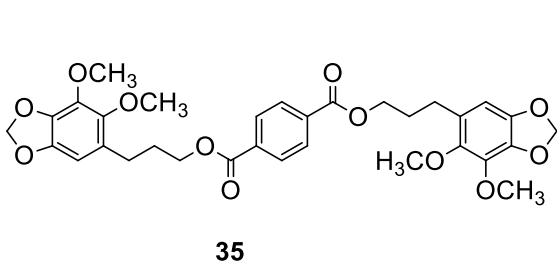


Figure 3.13: 400 MHz ¹H-NMR Spectrum of compound 30 in CDCl₃

The positive control in our CYP3A4 bioassay was ketokonazole. Since this is a rather large molecule it is reasonable to assume that the enzyme active site can readily accommodate large molecules. Thus it was decided to prepare the diester **35** by reacting terephthaloyl dichloride with the alcohol **8**. The yield of **35**, as a white powder was 35%. The spectroscopic properties of this symmetrical compound were as expected **Figure 3.14** and **Figure 3.15**. An attempt to prepare an analog of **35** starting with 1,3-benzene dicarboxylic acid was not successful. Surprisingly, compound **35** did not show significantly better bioactivity than the benzoic acid ester, $IC_{50} = 1.6 \mu\text{M}$ and $2.1 \mu\text{M}$, respectively.



Two ether analogs were synthesized from dillapiol by the Williamson ether synthesis procedure. Reaction of the alcohol, **8**, with benzyl bromide and *p*-benzyl bromide yielded the ethers **14** **Figure 3.16** and **16** **Figure 3.17** in fair yield. **Scheme 3.9**. The carbon-13 and proton spectra clearly supported the structure assignments.

Compound 35
400MHz, CDCl₃

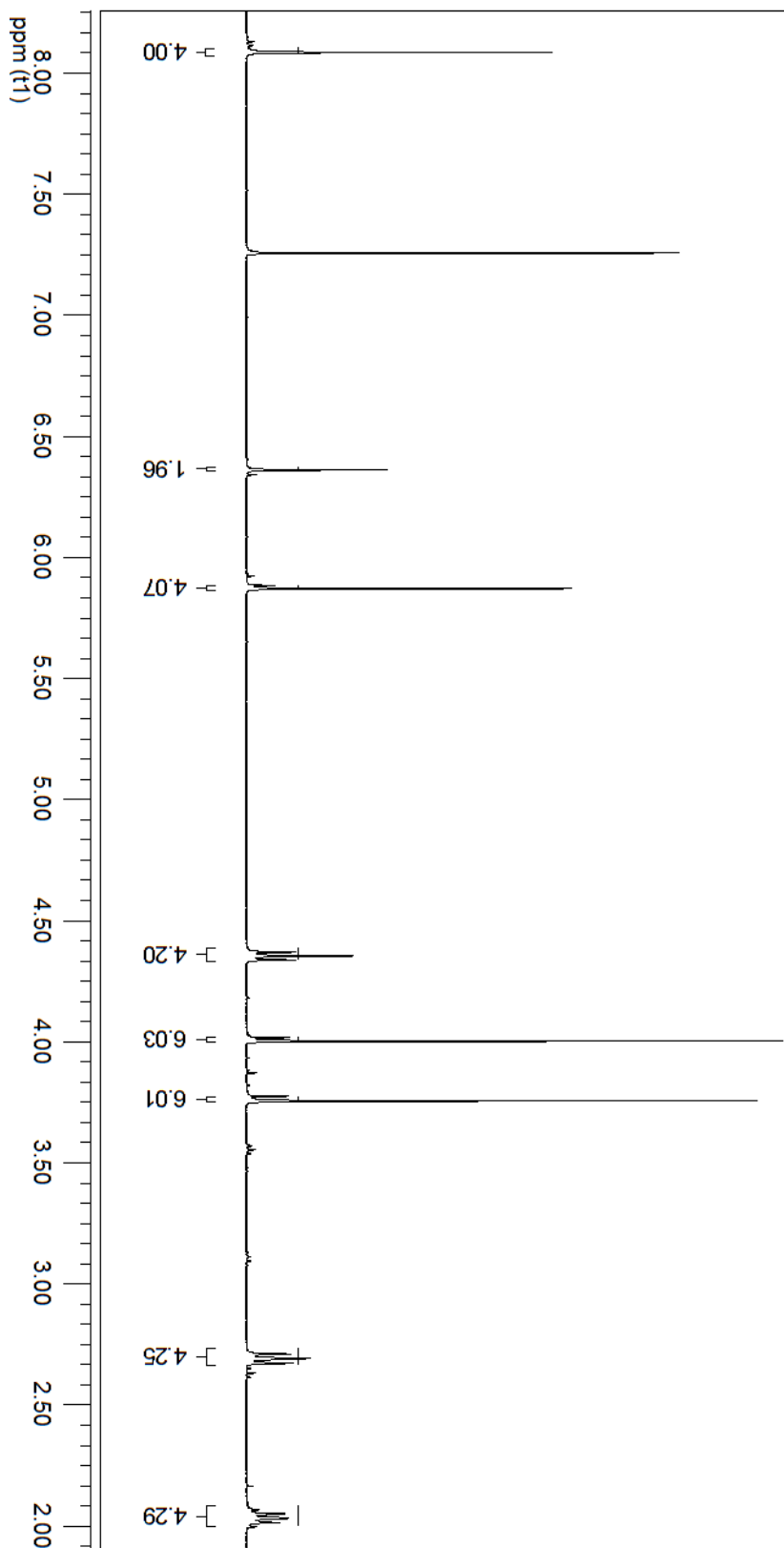
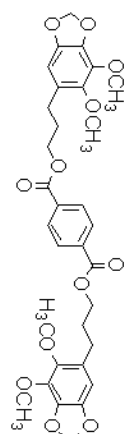


Figure 3.14: 400 MHz ¹H-NMR Spectrum of compound 35 in CDCl₃

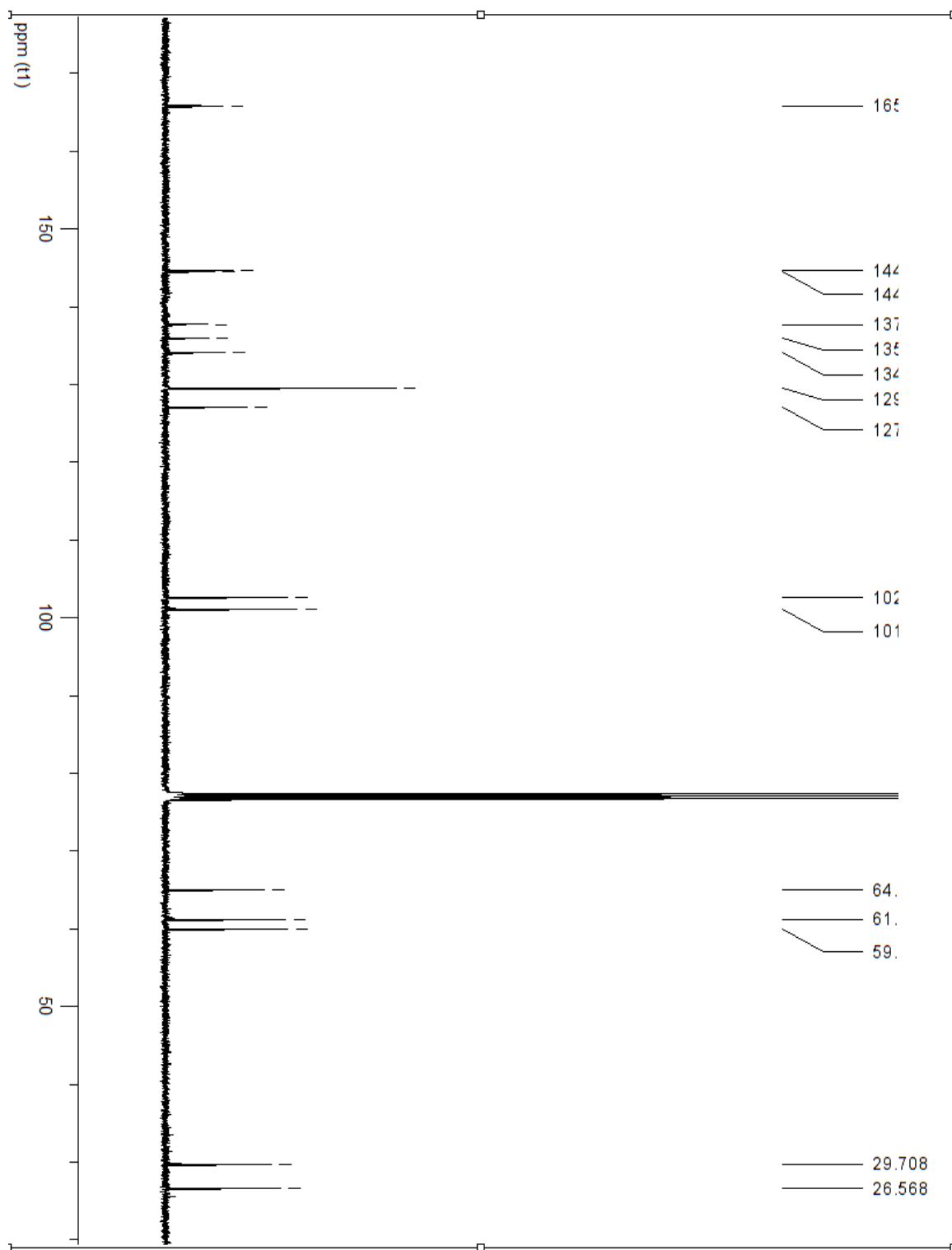


Figure 3.15: 100 MHz ^{13}C -NMR Spectrum of compound **35** in CDCl_3

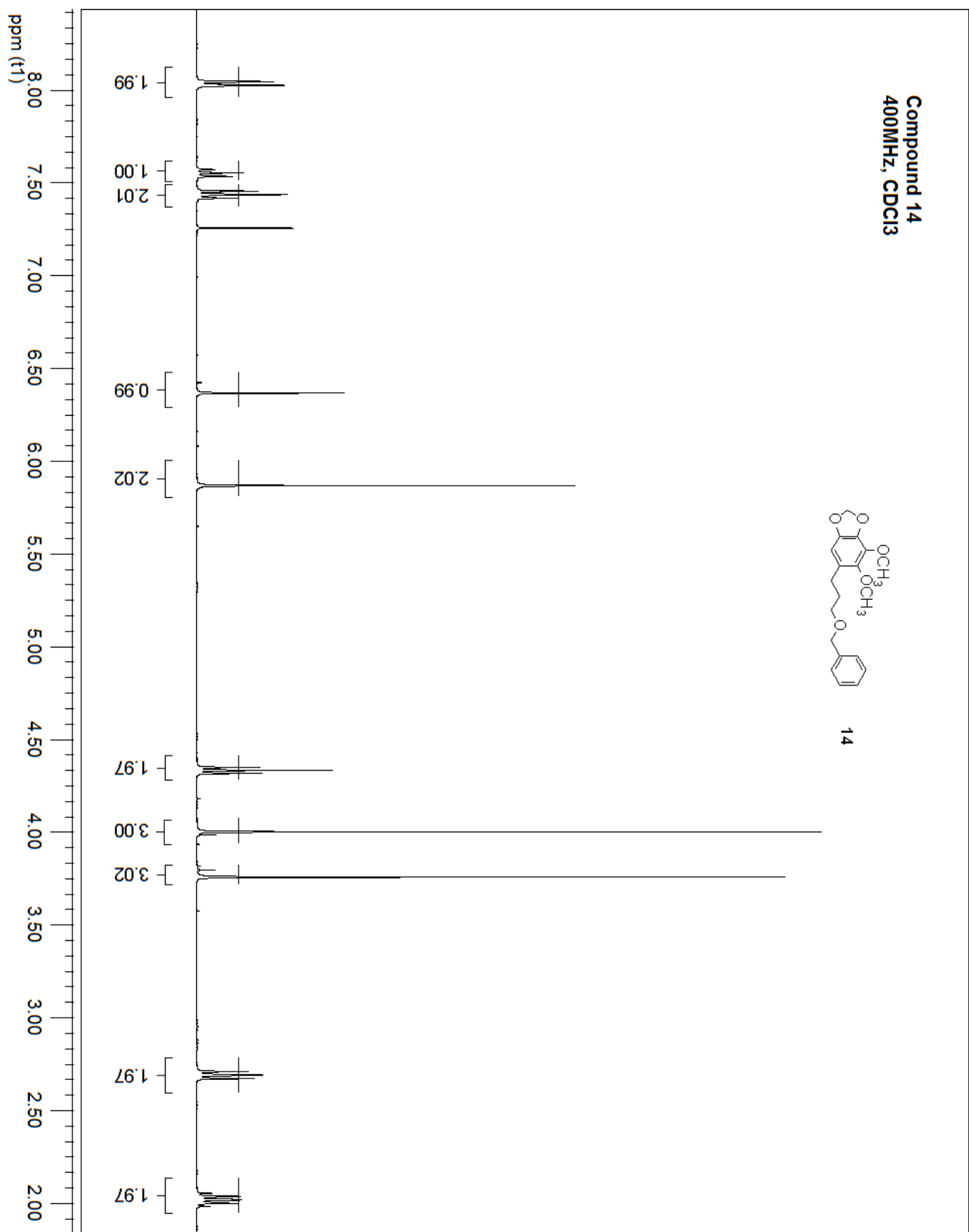
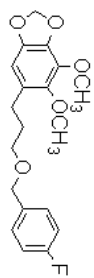


Figure 3.16: 400 MHz ^1H -NMR Spectrum of compound **14** in CDCl₃

Compound 16
CDCl₃, 400MHz



16

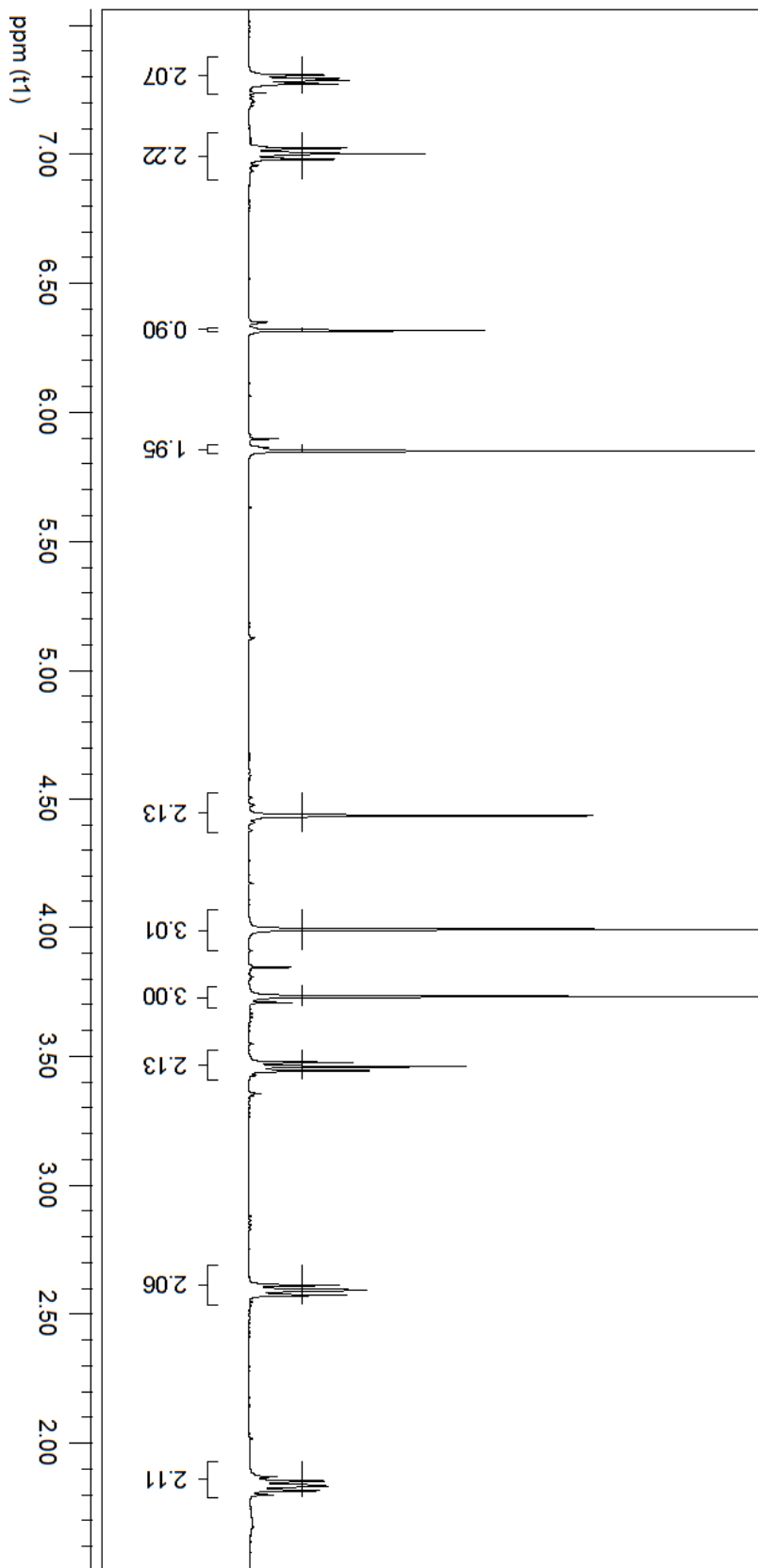
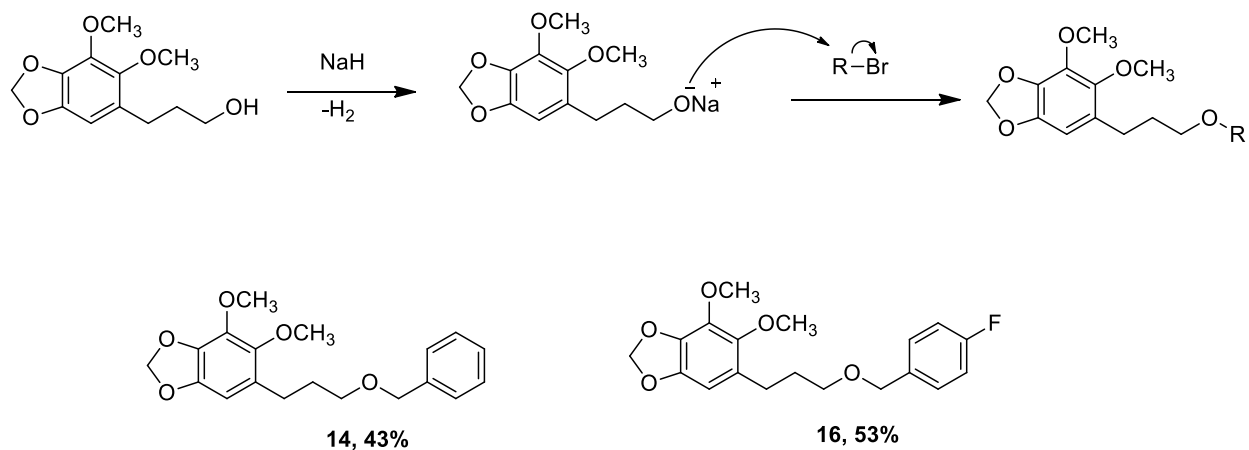


Figure 3.17: 400 MHz ¹H-NMR Spectrum of compound 16 in CDCl₃



Scheme 3.9: Synthesis of dillapiol derived ethers

Dillapiol was also used in the synthesis of two furan derivatives, **33** and **34**. The method used to synthesize these compounds is described by Majerus (**Scheme 3.10**). The spectroscopic data obtained for compound **34** matched that reported ⁶. The use of excess bromine resulted in electrophilic addition at the remaining position open in the aromatic ring of **34** to give **33** as an off-white solid in 46% yield. The ¹H-NMR of **33** showed a pattern similar to **34** with the exception that the remaining aromatic hydrogen signal of **34** was missing. Specifically the ¹H NMR of **33** showed a set of doublets of doublets at 3.13 and 3.30 corresponding to the CH₂ in the furan ring and a ddd at 3.57 for two hydrogen atoms due to the α hydrogen to the bromine atom. The multiplet at 5.05 corresponds to the one hydrogen atom on the chiral center in the furan ring **Figure 3.18**. The structure was confirmed by ¹³C spectrum and HRMS.

Compound **33**
400MHz, CDCl₃

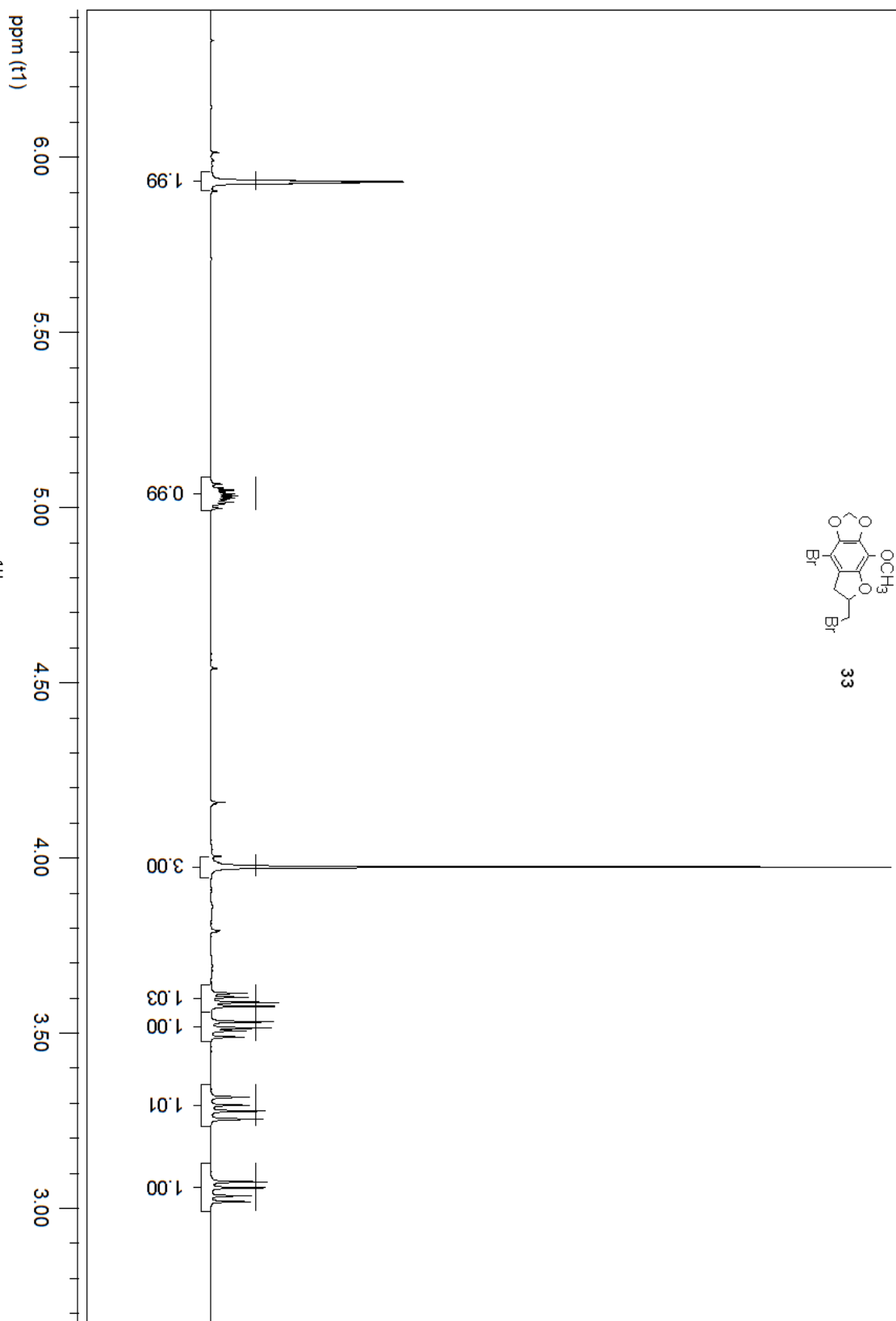
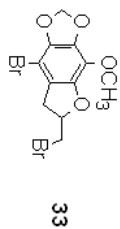
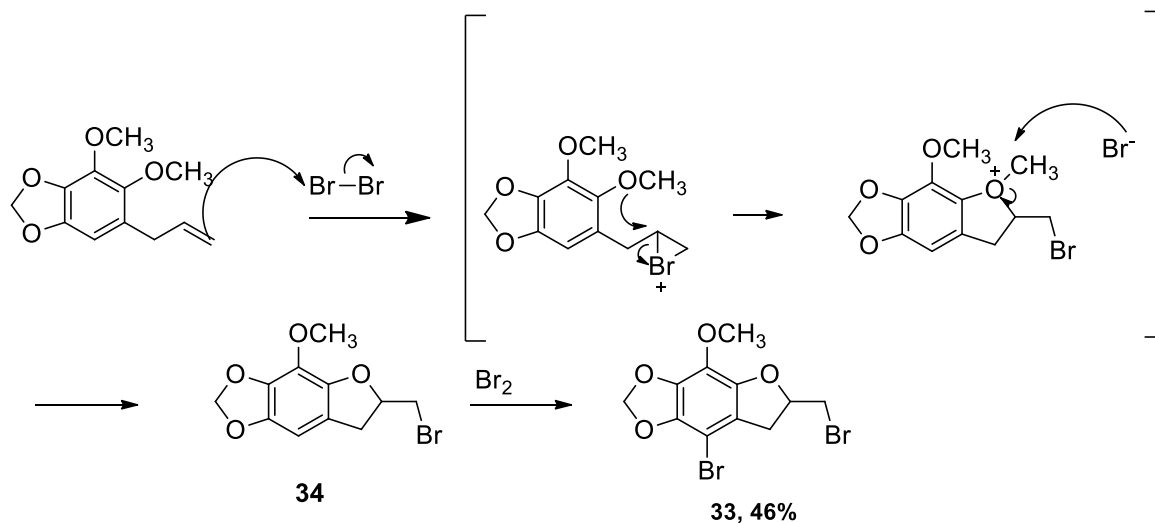
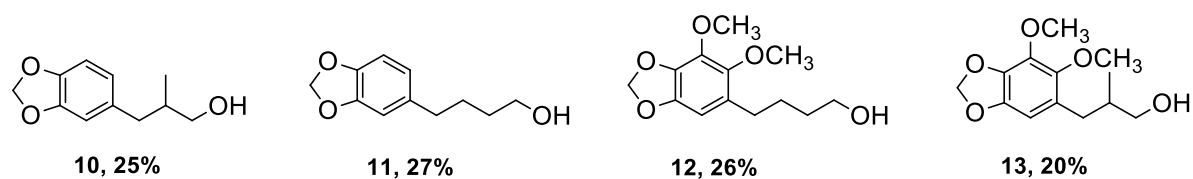


Figure 3.18: 400 MHz ¹H-NMR Spectrum of compound **33** in CDCl₃

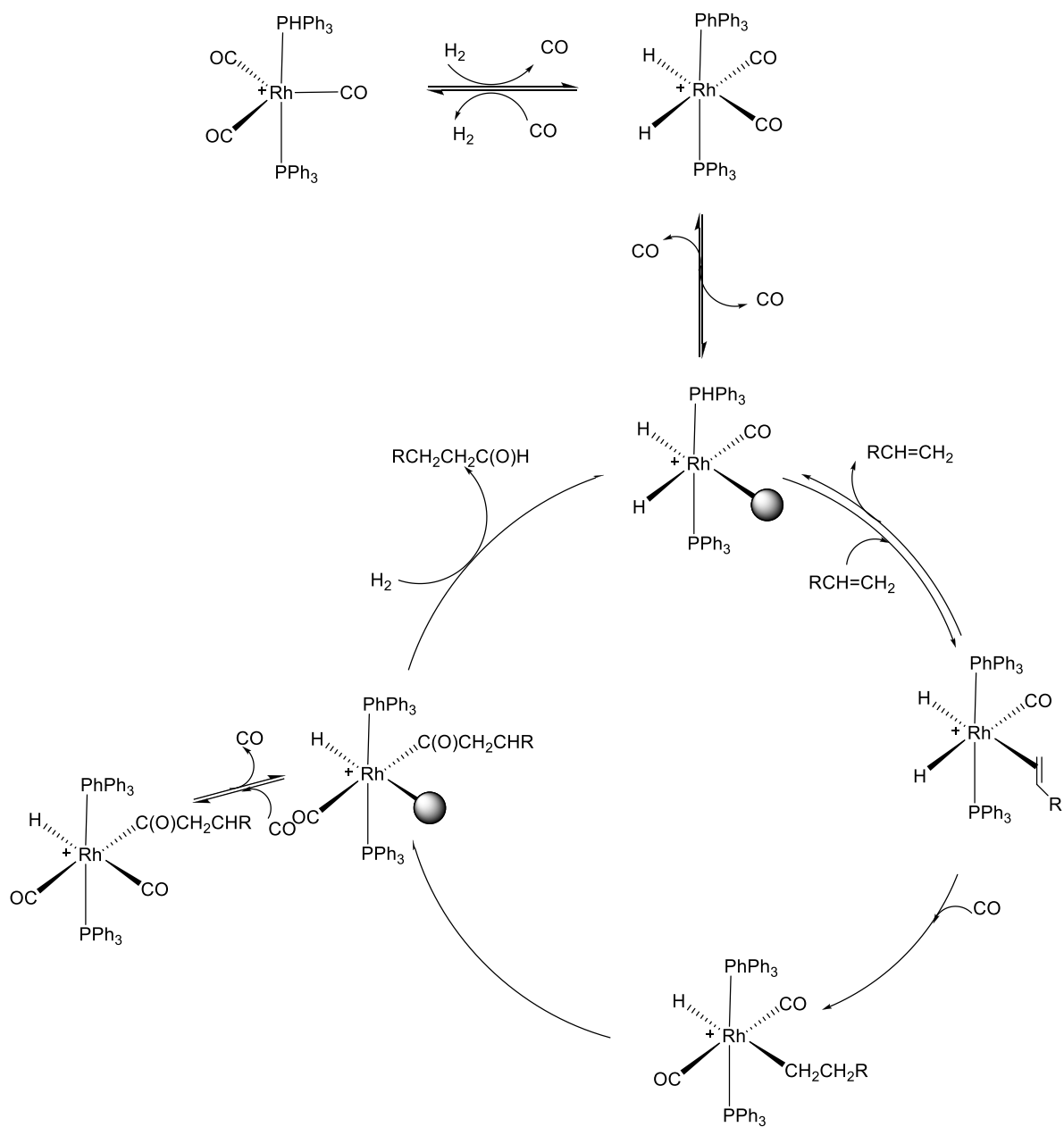


Scheme 3.10: Synthesis of dillapiol analogs **33** and **34**

Hydroformylation of dillapiol using carbon monoxide and Rh catalyst at 500 psi and post treatment of the corresponding aldehydes with hydrogen provided alcohols **12** and **13** (**Scheme 3.12**). The hydroformylation procedure was carried on both dillapiol and safrole by Prof. Vasopollo (Lecce, Italy) who spent several months at the University of Ottawa. The isomers obtained in each case were separated by us via flash chromatography to give the alcohols **10** and **11** from safrol and **12** and **13** from dillapiol.



Scheme 3.11: Dillapiol and Safrole analogs obtained by hydroformylation

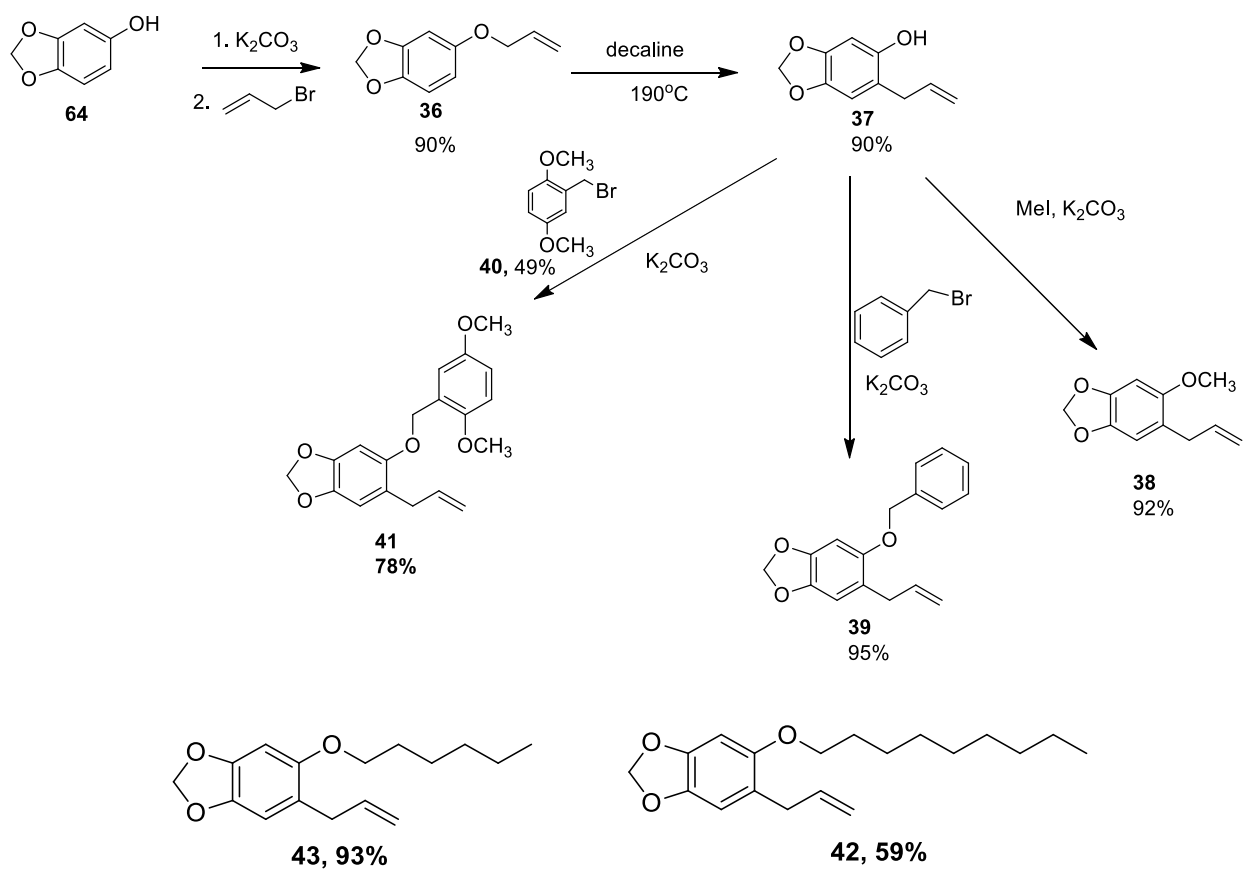


Scheme 3.12: General mechanism for hydroformylation of terminal alkenes according to Rosales and co-workers⁵⁰.

Sesamol analogs

Treatment of sesamol **64** with allyl bromide provided intermediate **36**. This compound when heated to 180-190 °C underwent a Claisen rearrangement as the allyl group migrates with high regioselectivity to the less hindered position to afford compound **37**. All the spectra obtained for this set of compounds match the previously reported spectra by Majerus⁴².

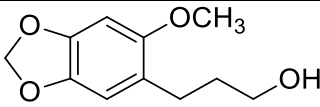
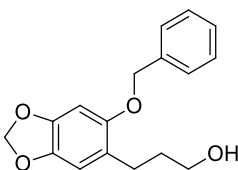
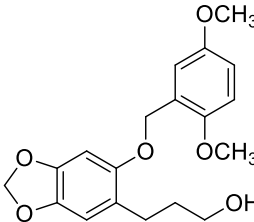
Alkylation of the phenol **37** with methyl iodide afforded the methyl ether **38**. Similarly reaction with benzyl bromide or 2-(bromomethyl)-1,4-dimethoxybenzene (**40**) gave **39** and **41**, respectively (**Scheme 3.13**). Two additional analogs, **42** and **43**, were synthesized by the same procedure.



Scheme 3.13: Synthesis of allyl intermediates from sesamol

The three ethers that were most potent in inhibiting CYP3A4 were treated with borane dimethyl sulphide complex to obtain the corresponding terminal alcohols via anti-Markovnikov addition to the double bond (**Table 3.1.2.3**). $^1\text{H-NMR}$ and ^{13}C were used for the structural characterization of the compound; all showed the signals corresponding to backbone structure compound **37** and the changes expected for each of the different ether residues.

Table 3.1.2.3: Reaction yields of sesamol alcohol analogs

Compound code	Structure	% Yield
45		67
46		68
47		71

A total of eight different esters from the above mentioned alcohols were prepared; using the two synthetic methods described for the dillapiol esters.

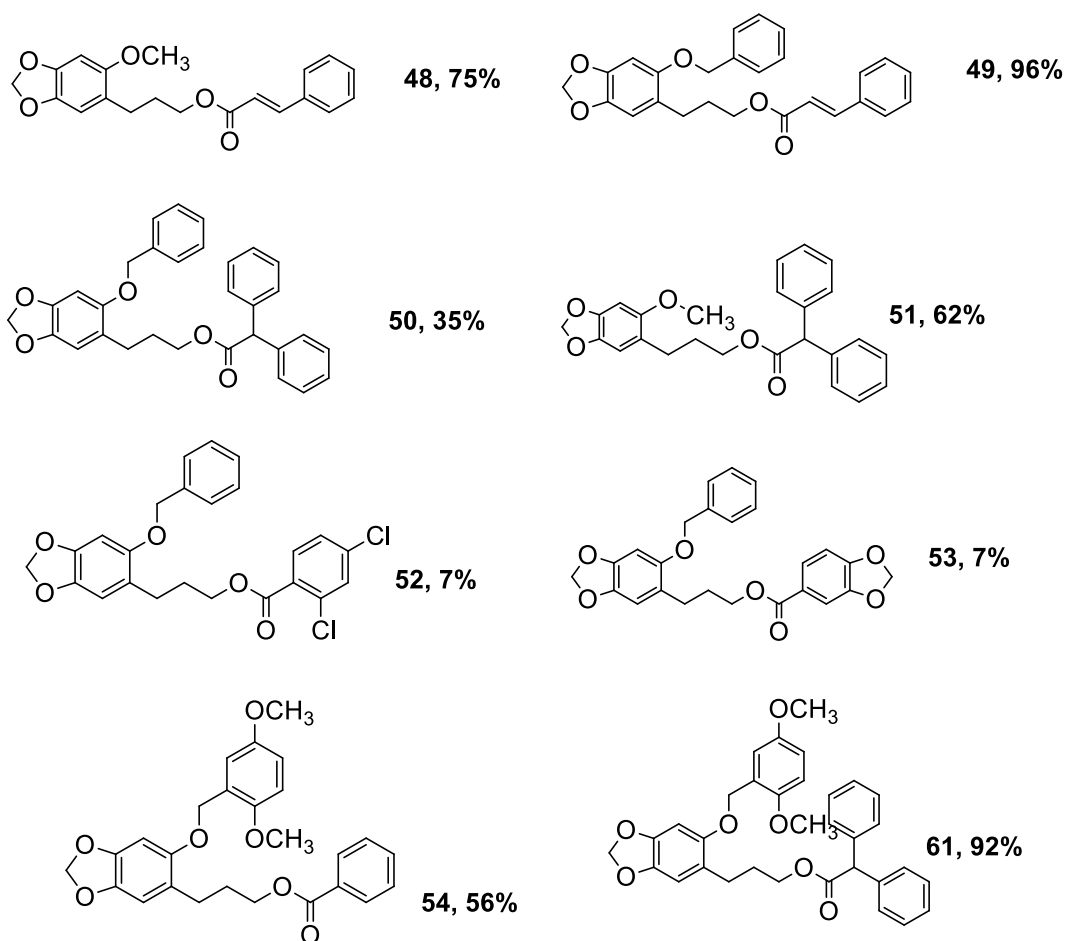
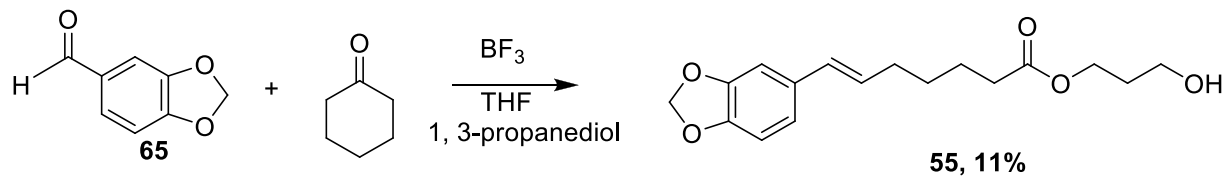


Figure 3-19: Esters of the corresponding sesamol alcohols in **Table 3.1.2.3**

1.2.1.2 Piperonal Analogs

Piperonal **65** was used as a parent compound to afford analogs without additional substituents on the benzo-1,3-dioxole group. Boron trifluoride-catalyzes the reaction of piperonal and cyclohexanone, with subsequent addition of 1,3-propanediol, gave the ester **55** in 11% yield as previously described by Strunz and co-workers⁵¹. This type of ring cleavage based on intermolecular Aldol Condensation, was first observed by Nagumo and co-workers⁵². As reported by this group the ring cleavage occurs via a three step mechanism that involves: a) intermolecular aldol condensation, b) acetalization, c) a Grob-type fragmentation of the acetal formed from the initial aldol product⁵¹⁻⁵³. The analysis of the ¹H-NMR obtained for compound **55** matches the data previously reported by Strunz and co-workers⁵¹.



Scheme 3.14: Synthesis of piperonal analog **55**

Ester **55** was used as a precursor for all subsequent analogs. Treatment of **55** with KOH promoted its saponification; the salt obtained was treated with HCl, 10%, to afford **56**, 53% as pink powder. The spectral analysis of the $^1\text{H-NMR}$ of compound **56** showed high field signals at 1.50, 1.69, 2.18, 3.38 ppm accounting for the three methylene groups in the molecule. Signals at 6.05 and 6.30 ppm correspond to the hydrogen atoms on the double bond and the coupling constant value of 16 Hz confirmed the assignment of the E configuration around this double bond. The rest of the characteristic signals for the presence of MDP nucleus are also present (**Figure 3.20**).

Compound **56**
CDCl₃, 400 MHz

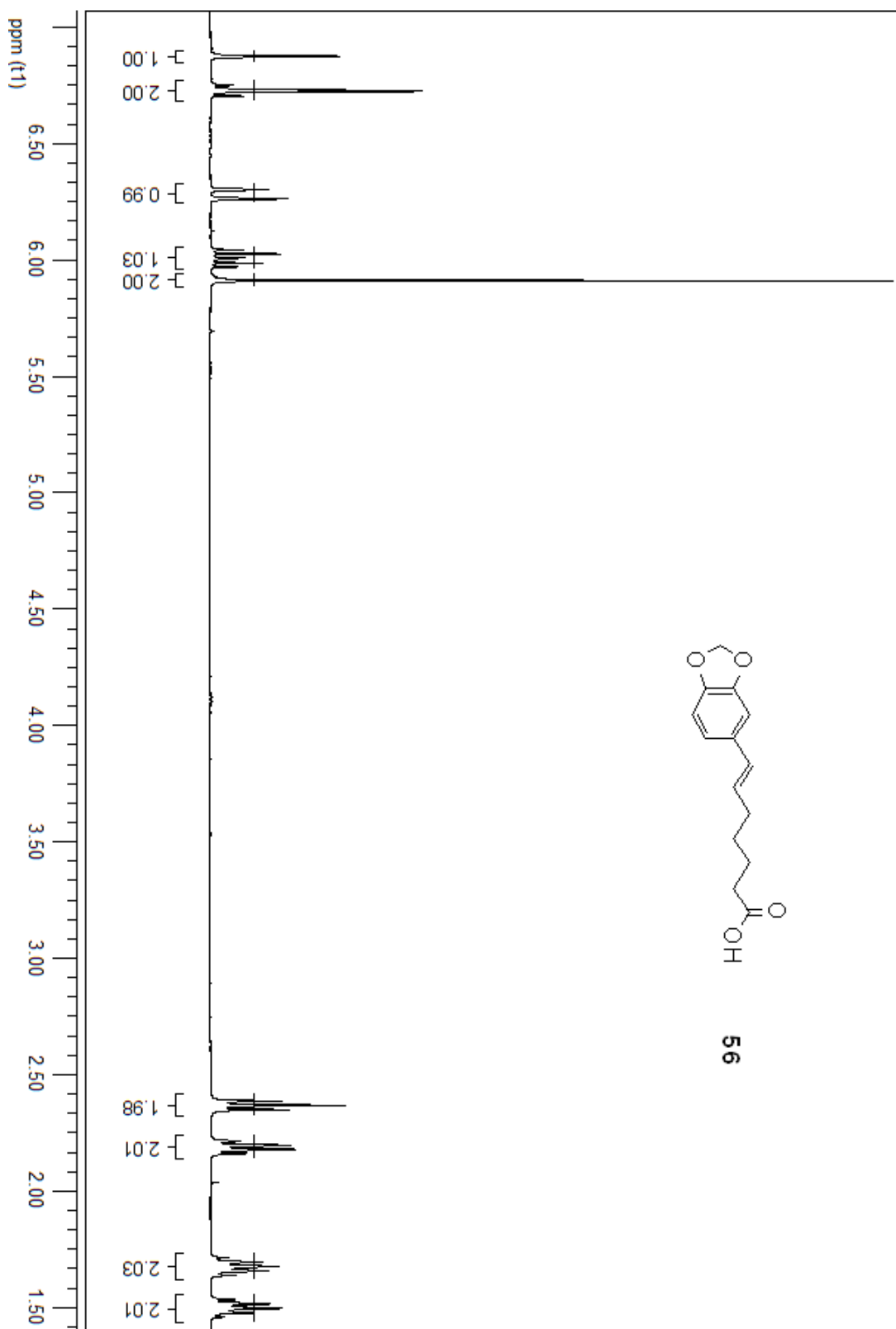
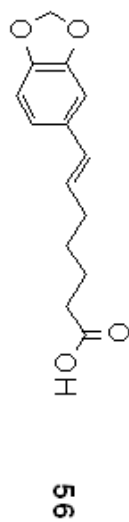
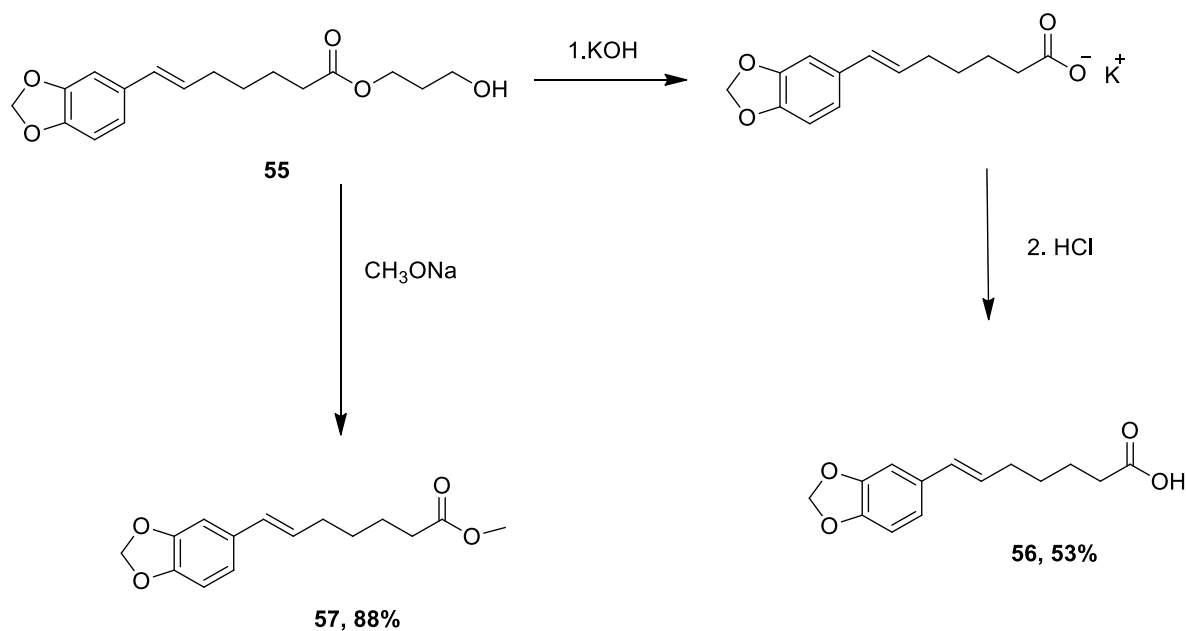


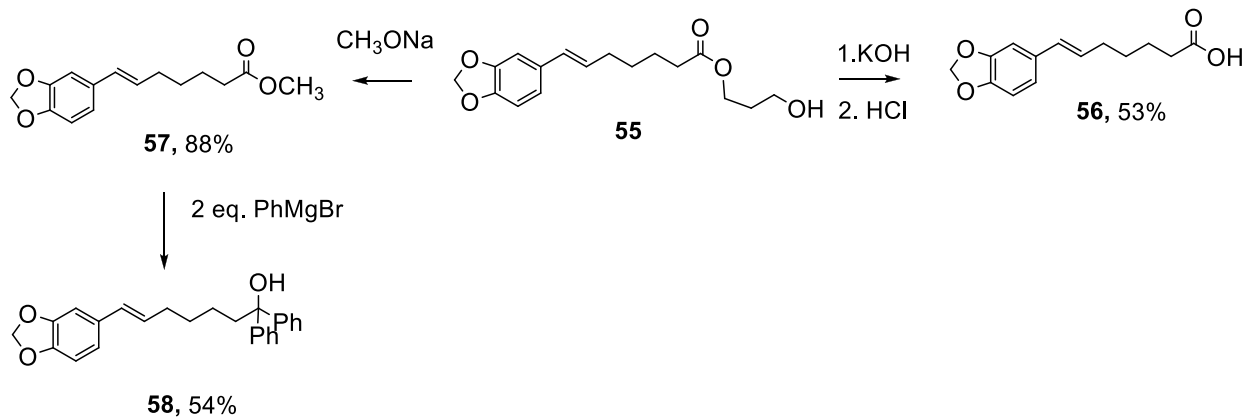
Figure 3.20: 400 MHz ¹H-NMR Spectrum of compound **56** in CDCl₃



Scheme 3.15: Synthesis of piperonal analogs **56** and **57**

Trans-esterification of compound **56** in the presence of sodium methoxide and methanol afforded ester **57**, in 88%, as a yellow oil. The analysis of the spectra showed the loss of the low field signals at 4.16 ppm and 3.62 ppm corresponding to the two methylene groups first adjacent to the ester bond and the later next to the hydroxyl group. Ester **57** showed the presence of a singlet at 3.62 ppm corresponding to the terminal methyl ester group.

Finally, ester **57** was dissolved in dry diethyl ether and treated with phenylmagnesium bromide for the synthesis of compound **58**, 54%, as a yellow oil (**Scheme 3.16**). The analysis of the ¹H-NMR spectra showed signals at 7.23, 7.31 and 7.42 ppm accounting for the 10 hydrogen atoms of the two newly introduced aromatic rings.



Scheme 3.16: Synthesis of compound **58**

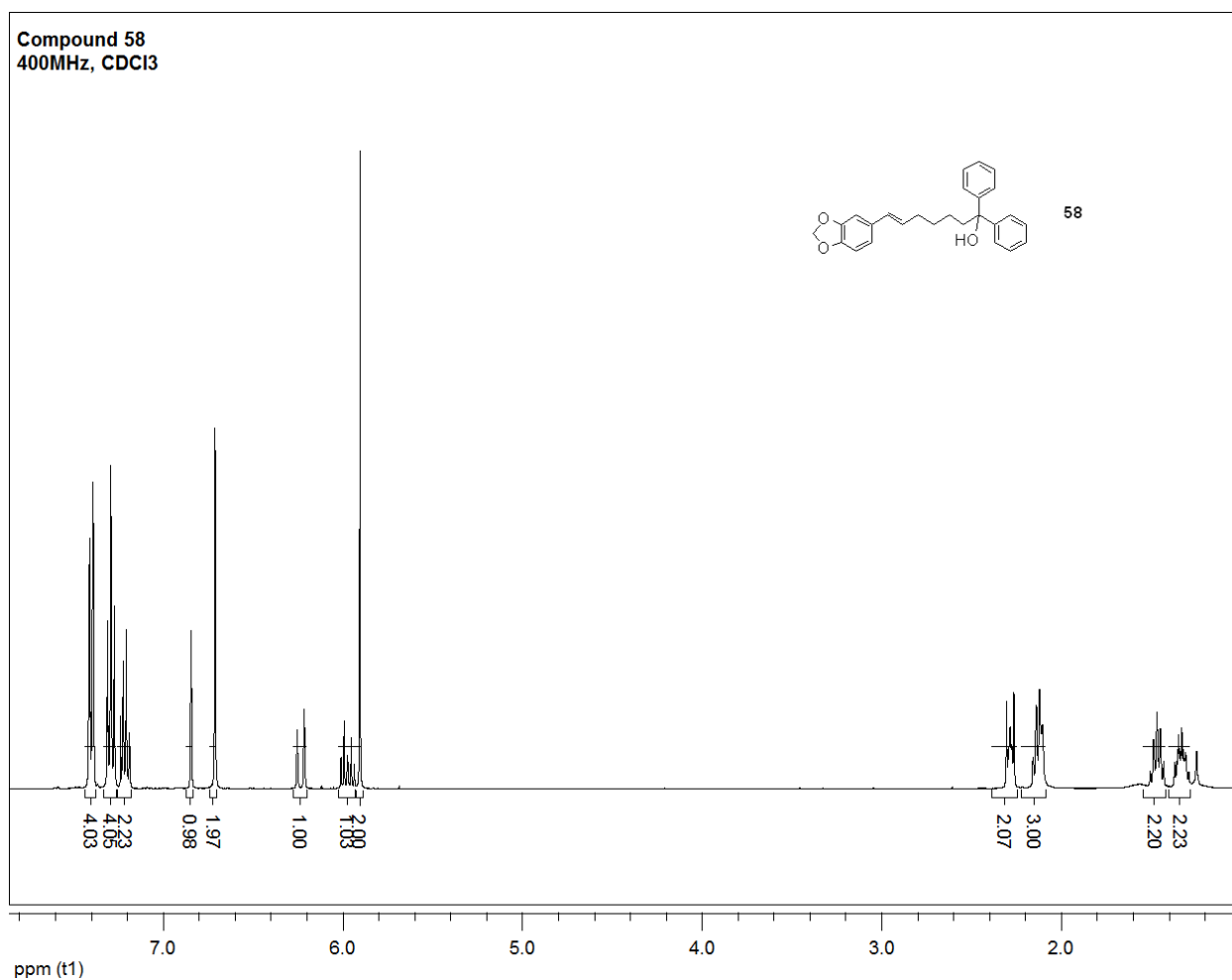
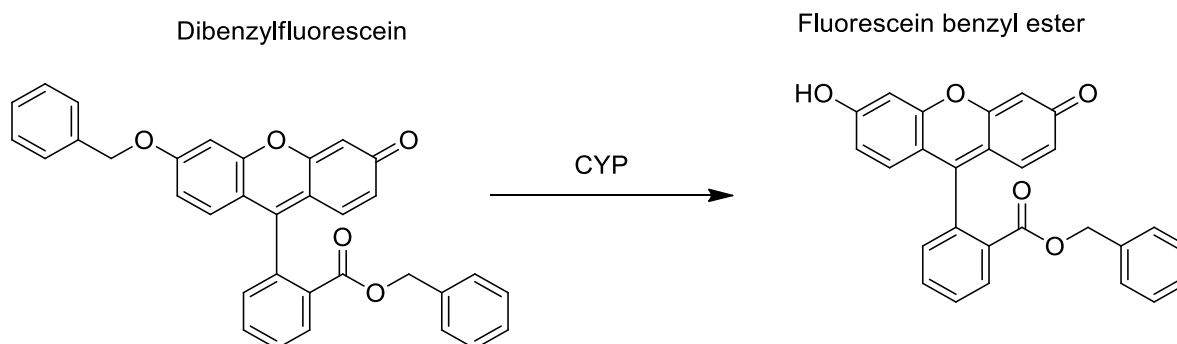


Figure 3-21: 400 MHz ¹H-NMR Spectrum of compound **58** in CDCl₃

Evaluation of MDP analogs as CYP3A4 inhibitors

The library of compounds whose synthesis was described in the previous section was evaluated with respect to their ability to inhibit CYP3A4. These experiments were carried out by Suqi Liu a PhD student in the Dr. Arnason group, as part of her Ph.D. research. The enzyme 3A4 is one of the most important enzymes in the CYP metabolism, this enzyme metabolizes around 30% of the clinically used drugs⁵⁴. The discovery of an inhibitor for this enzyme that can be used in insects will block the metabolism of the pesticide active molecule increasing the exposition time of the insect to the active principle, making it more potent.

CYP6 genes are present in insects as one of the most numerous clades and they are related with human CYP 3 and CYP 5 families. It has been established that these enzymes are involved in the development of pesticide resistance and they tend to be expressed in insect species that have evolved to become resistant to some pesticides⁵⁵. The protocol used for rapid screening uses dibenzylfluorescein (DBF) as substrate for the enzyme, cleavage of the benzyl group on the fluorescein moiety releases a fluorescent species, fluorescein benzyl ester (**Scheme 3.17**).

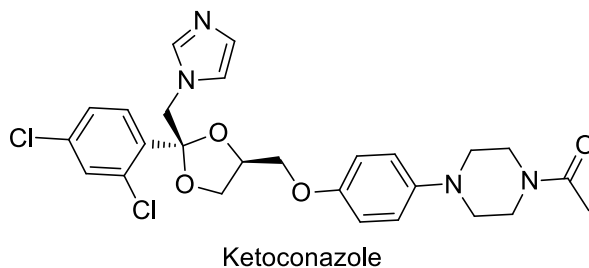


Scheme 3.17: Formation of fluorescein benzyl ester by CYP metabolism⁵⁶.

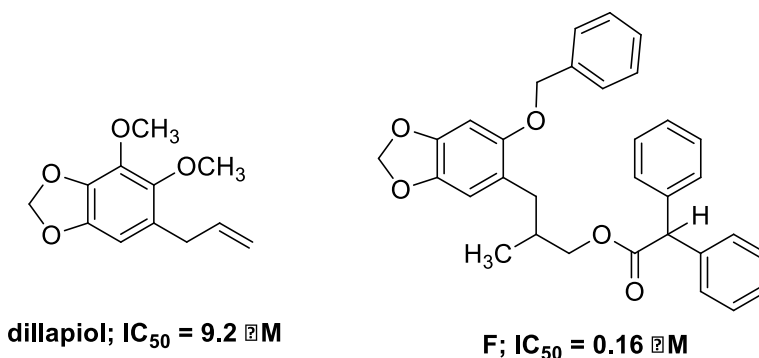
The presence of an inhibitory substrate in the media will block the metabolism of DBF and therefore no fluorescence will be produced⁵⁷.

Previous work done in the Arnason laboratory by Budzinski and co-workers, identified dillapiol as a potent inhibitor of 3A4 enzyme, compared with ketoconazole, the positive control used in the assay⁴³. Dillapiol itself was used as the positive control in current bioassays; its IC₅₀ value for inhibition of CYP3A4 was determined as 9.2 μ M. Additionally, the inhibitory power of each

compound relative to dillapiol equal to 1.0 was calculated. Thus all compounds that inhibit CYP3A4 more strongly than dillapiol have a relative inhibition number greater than 1.



At this stage, despite the fact that we have prepared and bio-assayed close to fifty derivatives whose IC_{50} values range from more than 50 to less than 0.25 μ M, a range of more than 200 fold, we are not yet able to develop a satisfactory QSAR model. Attempts to relate the inhibition to a combination of MR and LogP do not satisfactorily account for the changes in activity perhaps due to the heterogeneity of the compounds used. Additional modelling using Gaussian methods are underway by collaborators. The lack of a predictive model at present makes it very difficult to design molecules with a high degree of confidence. Nevertheless, we have sufficient qualitative indications of structural features, which enabled us to predict that the molecule F recently prepared by Ms. Jackiewicz, a senior undergraduate in our group would strongly, inhibit CYP3A4. Indeed, to our delight, this compound is the most potent of all the compounds prepared by us thus far with an IC_{50} value of 0.02 μ M and a potency of 58 relative to dillapiol.

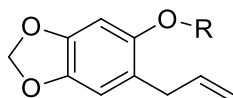


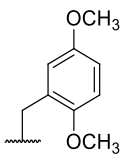
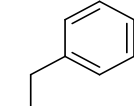
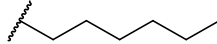
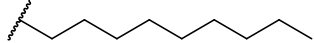
The following discussion focuses on trends we observed with various subsets of compounds. It should be recognized that there may be obvious “missing” structures in each subset. Due to time constraints it was not possible to prepare the additional compounds that might have resulted in result in a clearer picture. Perhaps as a result of this analysis, another student may take up this challenge. In some of the other discussions of various subgroups, the calculated MR and LogP values are included to show their potential importance and limitations in explaining the inhibition of CYP3A4 by these molecules.

Ethers derived from 6-Allyl sesamol

This group of compounds comprises five ethers resulting from the alkylation of the phenolic OH group in 6-allyl sesamol (**Table 3.1.2.4**). With the exception of compound **41** the ability to inhibit CYP3A4 increases as the Log P increases. The exception to this trend is compound **41 a** compound with a very high Log P indicating that it has low solubility in water. Since the bioassay is carried out in a mainly aqueous media it may not be reliable for compounds with very low water solubility. The activity of this set of compounds does not correlate with the MR.

Table 3.1.2.4: IC₅₀ values for 5-alkoxy-6-allyl sesamol derivatives arranged in order if increasing log P



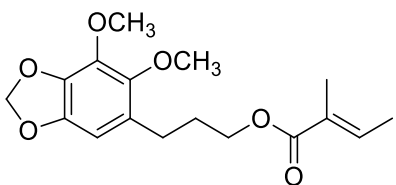
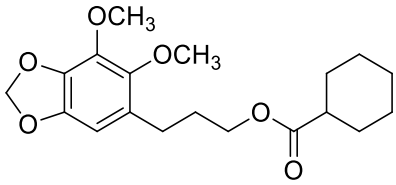
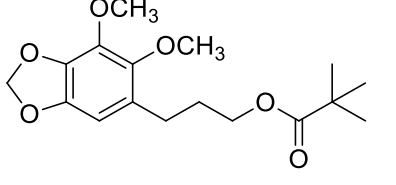
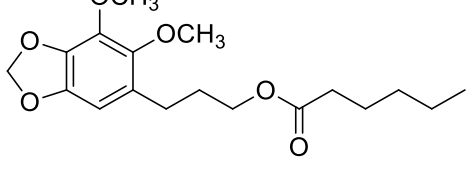
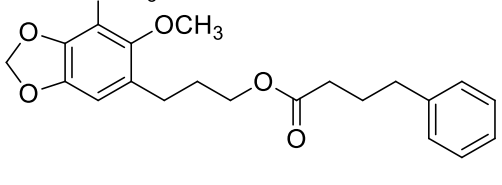
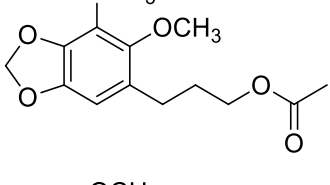
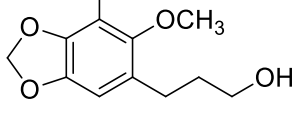
R=	Code	Log P	MR (cm ³ /mol)	IC ₅₀ μM
H	36	2.48	50.41	>28
CH ₃	37	2.74	55.85	>16
	40	4.22	94.85	2.15
	38	4.47	80.47	1.44
	42	4.82	79.05	1.93
	41	6.07	92.84	>50
Dillapiol	1	2.61	63.1	9.18

Esters derived from dillapiol

A. Alkyl esters

This set of compounds consists of six compounds in addition to the parent alcohol. These compounds are arranged in **Table 3.1.2.5** in order of decreasing inhibitory power. The acetate **23**, is the least active with an $IC_{50} = 9.2 \mu\text{M}$, essentially the same as dillapiol and nearly twice as potent as the parent alcohol **8**. Based on Log P the 4-phenyl butanoate ester **17** should have been the strongest inhibitor; it is the second least potent one. Three of the derivatives have almost identical Log P values but differ in their activity by a factor of about 2. As seen in the table there is no correspondence between the activities observed for the set of compound and their MR values. Analysis of the structures of these compounds indicates that substitution α to the carbonyl carbon increases the desired activity. The change from hexyl to cyclohexyl has no effect on Log P but decreases the IC_{50} from 4.1 to 1.9 μM . The *t*-butyl ester **28** also has a lower IC_{50} than the hexyl ester.

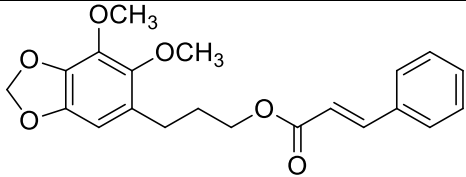
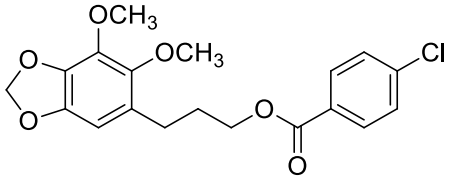
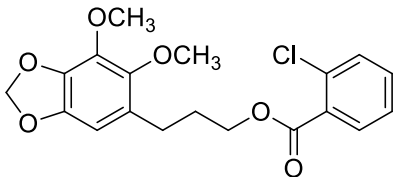
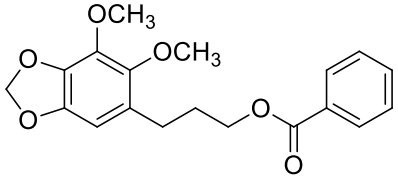
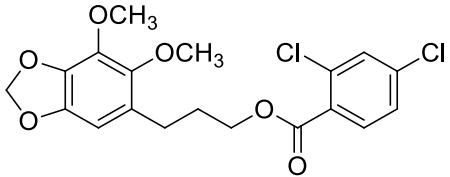
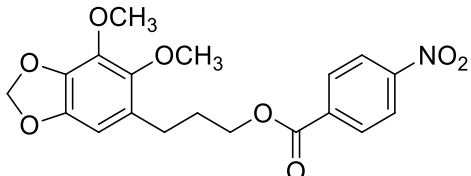
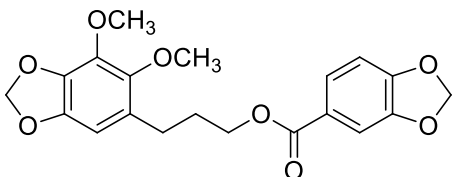
Table 3.1.2.5: IC₅₀ values for alkyl esters from dillapiol arranged in order of increasing IC₅₀

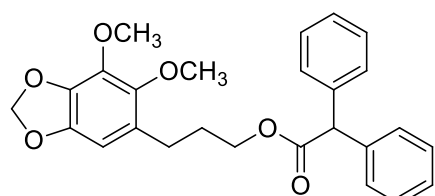
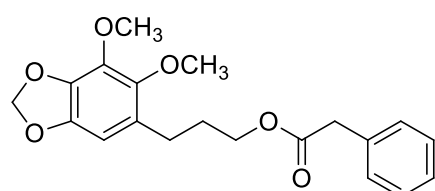
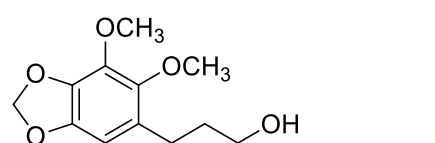
Compound	Code	Log P	MR (cm ³ /mol)	IC ₅₀ (μM)
	68	3.3	89.0	1.6
	27	3.9	95.0	1.9
	28	3.8	88.0	2.8
	15	3.82	92.3	3.3
	17	4.59	107.4	4.1
	23	1.9	73.8	9.2
	8	1.7	64.4	16

B. Benzylic and aromatic esters

A set of 10 aromatic and benzylic esters of the alcohol **8** were evaluated (**Table 3.1.2.6**). Based on the conclusion concerning structural parameters mentioned in the above paragraph, we expected these compounds to be relatively potent CYP3A4 inhibitors. In this set of compounds the diphenyl acetic acid ester **26** has an IC_{50} value of 0.4 μ M, making it 25 and 40 times more potent than dillapiol or the parent alcohol, respectively. All the other esters are more active than dillapiol, but a correlation with structural changes or Log P or MR is not obvious. For example the IC_{50} of the parent benzoate ester **20** is 2.1 μ M. Addition of chlorine at the *para* position **19** increases the activity to 1.6 μ M, addition of a second chlorine to give the *ortho, para* dichloro compound **21** results in slightly higher activity (IC_{50} = 1.4 μ M) but activity is lost when a single chlorine is placed in the *ortho*, position **69** (IC_{50} = 5.3 μ M). Finally, the low activity of the *para* nitro was unexpected. The strong inhibition observed for the diphenyl acetate **26** agreed with the hypothesis drawn from previous results by Budzinsky⁵⁸ that large substituents at C6 of the dillapiol ring will increase the inhibition of CYP3A4. The conclusion drawn in the previous paragraph also supports this observation. Based on this result a number of other diphenyl acetates were prepared and evaluated.

Table 3.1.2.6: IC₅₀ values for benzylic and aromatic esters from dillapiol arranged in order of increasing IC₅₀

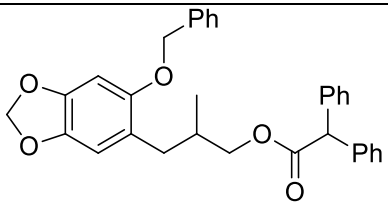
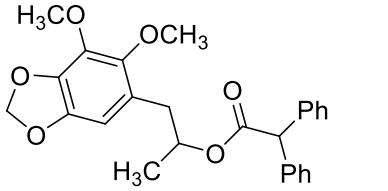
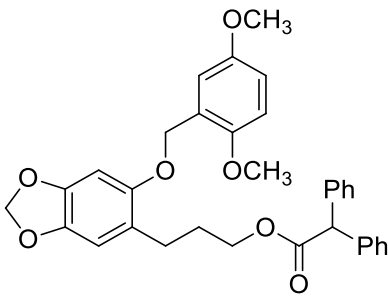
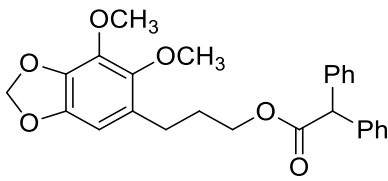
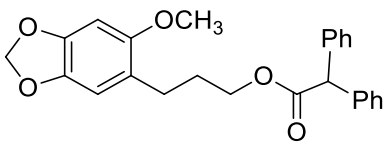
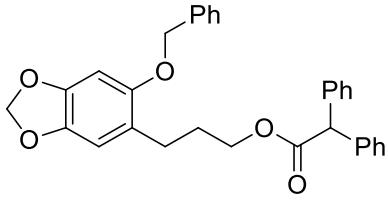
Compound	Code	Log P	MR (cm ³ /mol)	IC ₅₀ (μM)
	18	4.2	104.7	2.4
	19	4.4	98.5	1.6
	69	4.4	98.5	5.3
	20	3.8	93.9	2.1
	21	4.9	103.1	1.4
	22	3.4	NC	>13
	25	3.6	102.1	2.6

	26	5.5	122.8	0.4
	29	3.8	98.2	0.7
	8	1.7	64.4	16

Comparison of the diphenyl acetates

All of the compounds in this set are potent inhibitors of CYP3A4 with compound **31** having an $IC_{50} = 0.2 \mu\text{M}$, that is 46 times more potent than dillapiol. Derivative **G**, prepared by V. Jackiewicz, has an $IC_{50} = 0.16 \mu\text{M}$. It has an additional methyl group β , while **31** has a methyl group α to the alkyl oxygen suggesting that substitution in this part of the molecule leads to greater CYP3A4 inhibition. One might suggest that replacement of the above mentioned methyl group by a larger substituent while maintaining the other part of the molecule intact would lead to even more potent compounds.

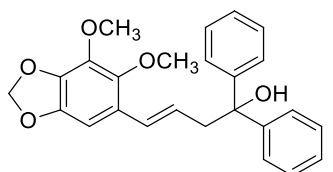
Table 3.1.2.7: IC₅₀ values for benzylic and aromatic esters from dillapiol arranged in order of increasing IC₅₀

Compound	Code	IC ₅₀ (μM)	Activity relative to dillapiol=1
	F	0.2	46
	31	0.16	46
	53	0.22	42
	26	0.4	21
	70	0.5	20
	50	0.6	14
dillapiol	1	9.2	1

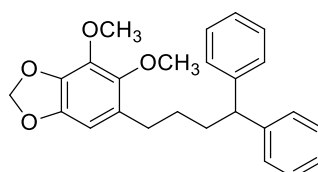
The IC₅₀ data for the dillapiol derived esters will be used for the development of a QSAR model by Professor Cesar Compadre at University of Arkansas. As mentioned earlier we are concerned that the bioassay for compounds with Log P values > 5.0 may be inaccurate due to the insolubility of such compounds in the mainly aqueous medium required for the bio-assay. The complete set of molecules and IC₅₀ values for all the compounds synthesized for this project can be accessed in **Appendix 3.A**.

Miscellaneous compounds with potent activity

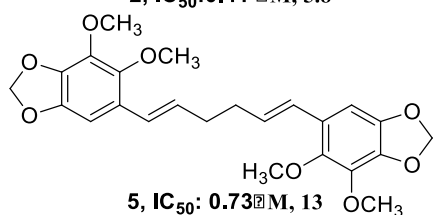
The activity of the benzophenone adduct **2** initially prepared by Majerus was determined in the new bioassay and shown to be about 20 times more potent than dillapiol. This level of activity is consistent with that observed for the diphenyl acetates, since both have similar shapes. The saturated analog **3** which again has a similar shape is equally active. Compounds **5** and **6** which also have large substituents in at position 6 of the dillapiol molecule also show relatively high levels of CYP3A4 inhibition.



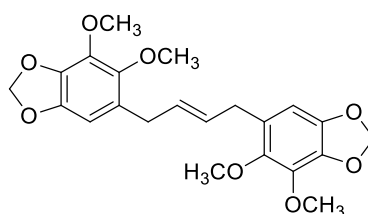
2, IC₅₀:0.41 μM, 5.8



3, IC₅₀:0.39 μM, 6.5



5, IC₅₀: 0.73 μM, 13

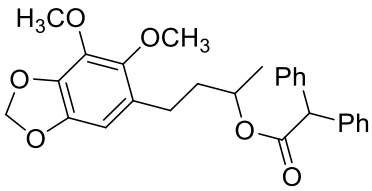
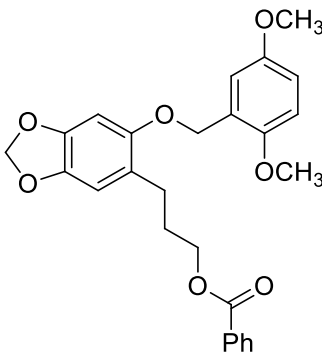
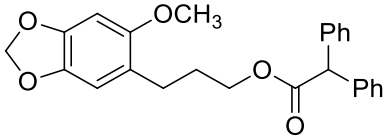
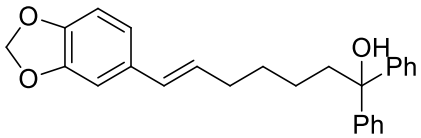


6, IC₅₀:1.18 μM, 1.1

In summary, substitutions at position 4 in the benzo-1,3- dioxole do not seem to play an important role in the bioactivity therefore, the synergist does not need to have a substituent at this position. The presence of bulky substituents as ethers at position 5 of the MDP core increases the activity of the substrate. In the ester family, bulky substituents α to both the ester carbonyl and alkoxy carbon increase the bioactivity of the compounds. The two descriptors, Log P and MR must likely be used in combination and possible include additional parameters in

order to predict the bioactivity of the molecules. Generally, based on the results obtained at this point, molecules with high MR and high Log P have shown better activity. (Table 3.1.2.8) summarizes the best analogs developed as part of this project.

Table 3.1.2.8: IC₅₀ values for the best analogs developed

Compound	Code	Log P	MR (cm ³ /mol)	IC ₅₀ (μM)	Times better*
	31	5.8	127.5	0.2	46
	53	5.4	125.6	0.36	26
	70	5.6	115.0	0.47	20
	59	6.6	118	0.54	17
dillapiol	1	2.61	63.1	9.2	1

* Using dillapiol activity equal to 1

***In vivo* Bioassays**

The results of this part of the research belong to the PhD Candidate Suqi Liu and are presented here just to evaluate the activity of the compounds designed.

A set of five compounds were selected to be tested in an “*in vivo*” model (**Figure 3.23**). The number under the structures represents how many times the compound is more potent than dillapiol in the *in vivo* bioassay. The bioassay using Colorado potato beetle (*L. decemlineata*), showed that the *in vitro* screening can be used in the prediction of the relative bioactivity of the compounds but also showed that the bioactivity of dillapiol remains better than any of the analogs tested (**Figure 3.22 A and B**). Figure A depicts the results for the topical application of the selected analogs, in which compound AF45 and AF46 have the highest activity. However it is not higher than the one observed for dillapiol (**Figure 3.23**). Graphic B shows the results of the ingested bioassay of the same analogs, in this case there is better correspondence between the results observed in the *in vitro* analysis and the *in vivo* analysis. The analogs developed have better activity when ingested by the insect than by topic application. The ingested bioassay also allows assessment of repellent activity, but none of the analogs evaluated have this activity. A new set of *in vivo* test is been currently run. As part of this new test a few more compounds have been included. The new compounds included belong to the C-C set of compounds prepared. It is important to note that these compounds would not be susceptible to break down by insect esterases. The presence of esterases has proven to be involved in the development of pesticide resistance towards pesticides like pyrethrines⁵⁹.

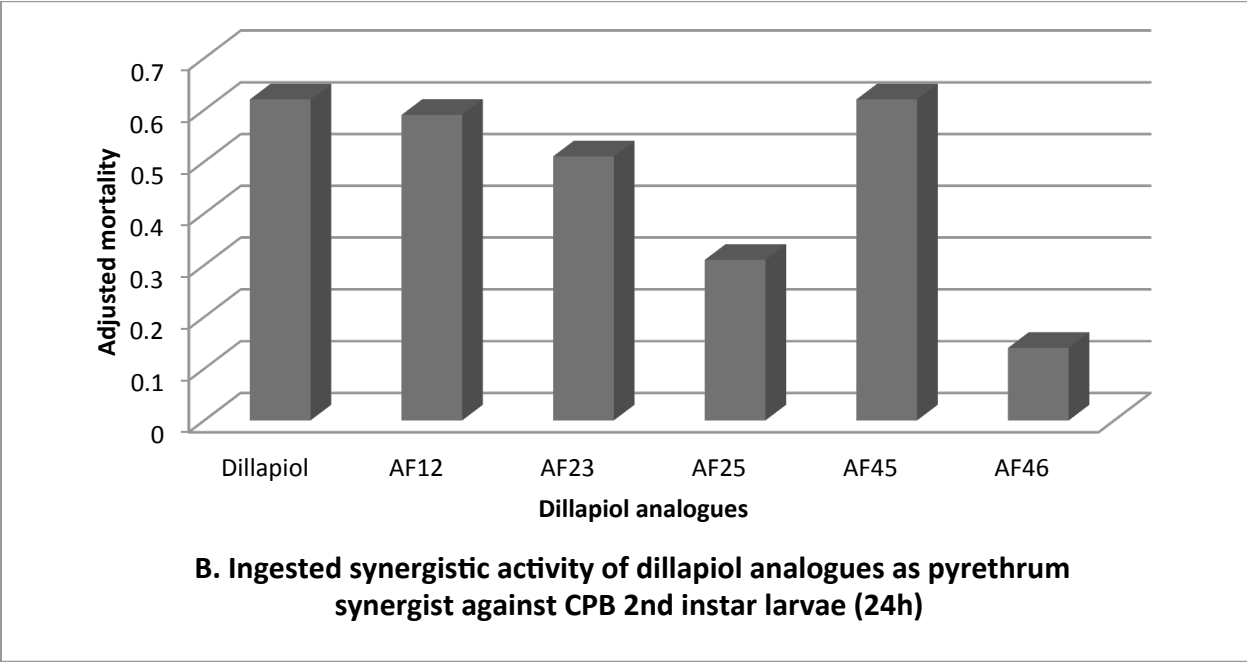
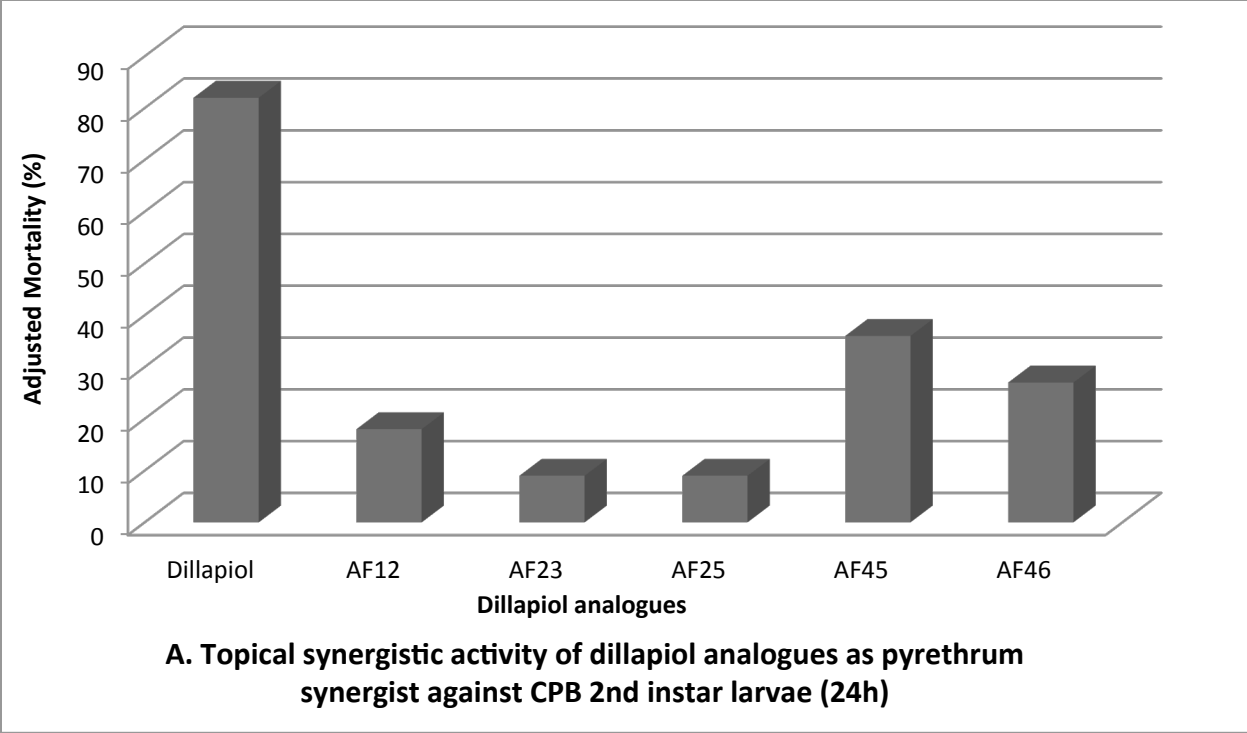


Figure 3-22: Results for the *in vivo* bioassays A. Topical application of selected analogs, B. Ingested application of selected analogs. Graphs presented belong to Suqi Liu, Ph.D. student at Dr. Arnason’s lab.

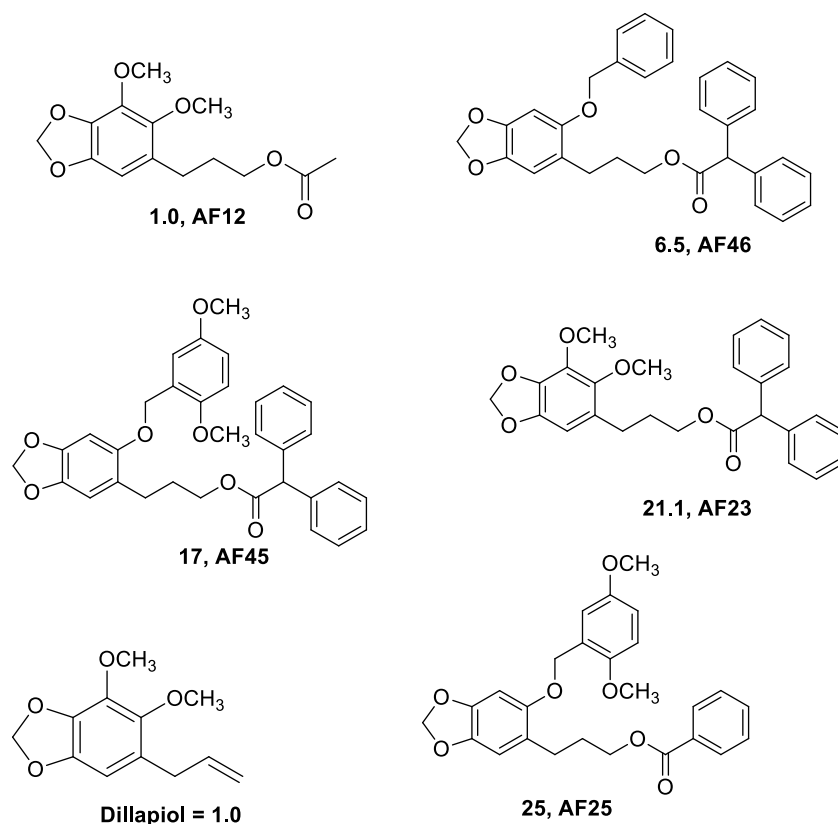


Figure 3-23: Selected MDP analogs for *in vivo* model using Colorado Potato Beetle (*L. decemlineata*). Number next to the code represent the increment in potency compared to dillapiol.

Conclusions

We have produced more than fifty MDR compounds derived by simple manipulations of mainly dillapiol and sesamol. The compounds showing the strongest inhibition are those with large substituents at C5 and C6 of the MDR ring system with the best inhibitors having IC₅₀ values ranging from 0.16 to 0.2 μ M for CYP3A4 inhibition being more than 50 times more potent than dillapiol. Disappointingly, this increase level of *in vitro* activity has thus far not been translated into *in vivo* synergistic activity either via topical application or ingestion. One potential reason for this is that all compounds tested *in vivo* were esters. These may be sensitive to insect esterase activity, which would result in the formation of the relatively inactive alcohol **8** and a carboxylic acid. The testing of non-ester derivatives should shed light on this hypothesis and force further synthetic effort away from esters perhaps towards the related ethers.

A panel of four compounds and dillapiol (**Figure 3-24**) will be sent to Dr Huyun Lee at the Sudbury Regional Cancer Research Institute for potential synergism of anti-cancer compounds, by the same inhibition of CYP 450 metabolism.

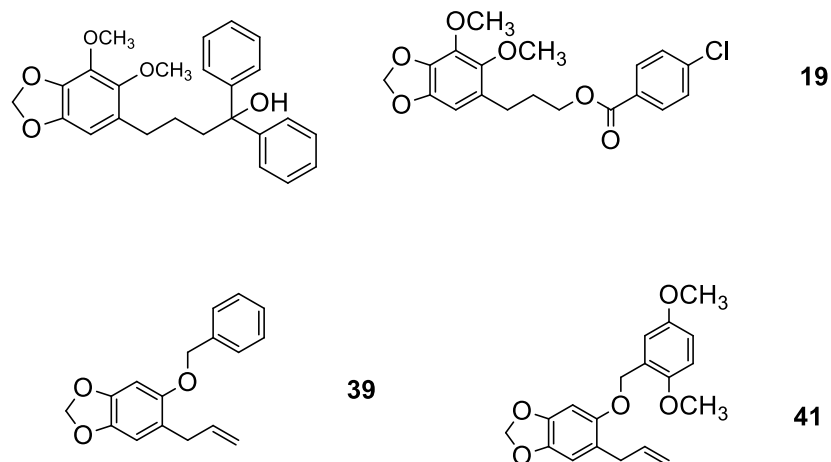


Figure 3-24: Compounds that will be evaluated for anti-cancer activity

3.1.3 Experimental

General procedure

The ^1H and ^{13}C NMR spectra were obtained from either a Bruker Advance 300 or 400 MHz spectrometer. The samples were run in spectroscopic grade deuterated chloroform. Chemical shifts are in parts per million relative to tetramethyl silane. The multiplicities of the NMR signals are reported as s, singlet; d, doublet; dd, doublet of doublets; ddd, doublet of doublet of doublets; dt, doublet of triplets; t, triplet; q, quartet; and m for multiplet. Mass spectrum analysis and high-resolution mass spectra were performed by the analytical services available at University of Ottawa.

Reactions were monitored by thin layer chromatography (TLC) using silica gel on alumina sheets, 60 F₂₅₄. Individual compounds were visualized either by ultraviolet light or by staining. The stain that was used was a 5% solution of ammonium molybdate in 10% aqueous H₂SO₄. Reactions were monitored by TLC using aluminum-backed TLC plates (EMD Chemicals, TLC Silica

gel 60 F₂₅₄), which were visualized by UV light (254 nm) then permanently stained with Hanessian's stain.

All reactions were performed under a nitrogen atmosphere unless otherwise stated. The glassware, that was used or moisture sensitive reactions, was dried overnight in an oven. "Drying refers to removing the water from the organic mixture with anhydrous magnesium sulfate if is not stated. "Concentrated" refers to the removal of the solvent by roto-evaporation. Purification by preparative HPLC was performed using a reverse phase C18 prep-HPLC column (10 µm particle size, 21.2 x 250 mm).

Mass spectrometry (MS), using either electron impact (EI) or chemical ionization (CI), was performed on a V. G. Micromass 7070 HS mass spectrometer with electron beam energy of 70 eV (for EI). High-resolution mass spectrometry (HRMS) was performed on a Kratos Concept-11A mass spectrometer with an electron beam of 70 eV or a JEOL double focusing magnetic sector mass spectrometer JMS-AX505H. All spectral analyses were performed at facilities located at the University of Ottawa.

Steam Distillation

Plant collection:

Different plant organs of *Piper aduncum* were collected during the dry season (November to April) and rainy season (May to October) from wild plants growing in different locations in Costa Rica. The samples were collected and identified by botanist from the herbarium Juvenal Rodriguez, Universidad Nacional of Costa Rica (**Table 3.1.3.1** for voucher numbers).

Table 3.1.3.1: Voucher number for *P. aduncum* sample collection

Collection site	Year of collection	Voucher number
Arenal Lake, Alajuela	2010	13513
Atenas, Alajuela	2010	13515
Braulio Carrillo, Limon	2010	13517
Rio Costa Rica, Cartago	2010	13518

Essential oil extraction:

Fresh plant material was submitted to steam distillation with a Clevenger-type apparatus **Figure 3.25**. The obtained mixture of water and oil was further extracted with hexanes; the combined organic layers were dried over MgSO₄. Yields of extraction were provided in **Table 3.1.2.1**.

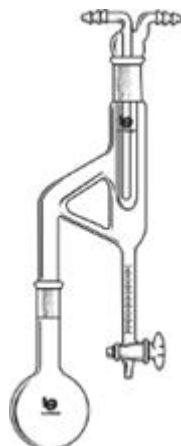
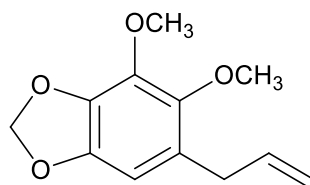


Figure 3-25: Clevenger apparatus - volatile Oil Distilling Apparatus (Heavier than Water)

The crude oil was purified by flash chromatography packed with silica gel (1.0g crude oil: 60g silica) eluting with hexanes: ethyl ether (9:1) to afford dillapiol 95-98% as a clear oil. The purity of the obtained oil was evaluated by NMR analysis and GC-MS, conditions for GC-MS analysis are provided in **Appendix 2.1**. The obtained ¹H-NMR spectrum matches the one reported in literature⁴².

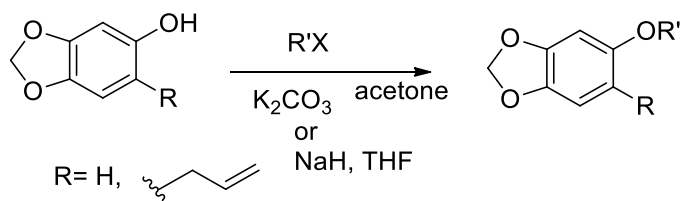


1. Dillapiol

$^1\text{N NMR}$ (400 MHz; CDCl_3): δ ppm 3.31 (td, $J = 6.55, 1.29$ Hz, 2H), 3.76 (s, 3H), 4.02 (s, 3H), 5.03 (t, $J = 1.47$ Hz, 1H), 5.08-5.04 (m, 1H), 5.92 (m, 3H), 6.35 (s, 1H)

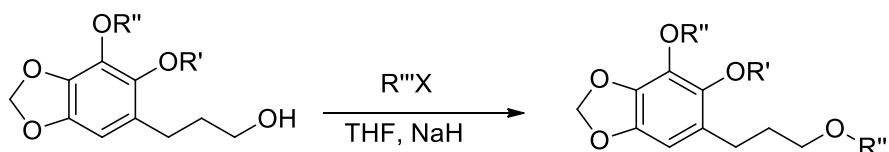
General procedures for synthesis:

1. Alkylation of methylenedioxy phenols



Potassium carbonate (2.0 molar equivalents) was added to the methylenedioxy phenol (1.0 molar equivalent) dissolved in dry acetone. The mixture was stirred for 10 min at room temperature and then the alkyl halide (1.5 molar equivalents) was added. The reaction mixture was refluxed and monitored by TLC until completion. After cooling the mixture to room temperature the solvent was removed *in vacuo*. The remaining potassium carbonate was dissolved in water and the aqueous phase was extracted with ethyl acetate (3 X 40 mL). The combined organic extracts were dried over magnesium sulfate, filtered and concentrated to provide the desired phenoxy ether.

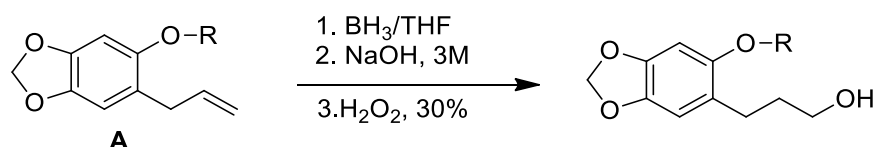
2. Synthesis of ethers



NaH (1.2 molar equivalents) was added to the methylenedioxy phenol (1.0 molar equivalent) dissolved in dry THF under nitrogen atmosphere. Once the NaH was used up, the resulting

reaction mixture was cooled to 0°C and the alkyl halide (1.1 molar equivalents) dissolved in dry THF are added. The ice bath is removed and the reaction was left to warm up to RT 15 min. The reaction mixture was quenched using saturated NH₄Cl solution (5 mL) and the aqueous phase was extracted with DCM (3 X 10 mL). The organic phase was dried over MgSO₄, filtered and concentrated in vacuo. The crude residue was purified by flash chromatography using different solvents systems consisting in hexane: ethyl acetate, to give the desired ether.

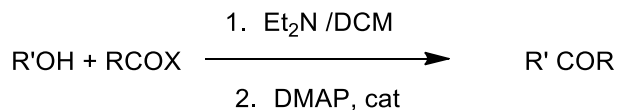
3. Hydroboration



Borane/THF complex (1.5 molar equivalents) was added to a cooled (0°C) solution of compound **A** (1.0 molar equivalent) in dry THF. The resulting reaction mixture was allowed to warm to RT and stirred overnight. After this time the reaction was quenched with 10 mL of sodium hydroxide (3 M), then 10 mL of H₂O₂ (30%) was added. The resulting mixture was extracted with ethyl acetate (3 X 20mL). The organic extracts were combined and dried over magnesium sulfate, MgSO₄, filtered and evaporated to dryness. Purification of the alcohol was achieved by flash chromatography (8:2, hexanes: ethyl acetate).

4. Synthesis of esters:

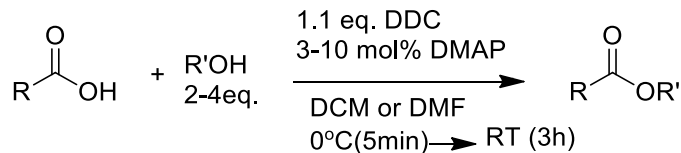
A. From acyl chlorides



Et₂N (1.5 molar equivalents) and a catalytic amount of DMAP was added to the alcohol R'OH (1 molar equivalent) dissolved in dry DCM (5 mL/equivalent of ROH). The resulting solution was stirred at 0°C for 5 min after which time the RCOX (1.5 molar equiv.) was added dropwise. The reaction mixture was refluxed for 12 h, cooled to RT and quenched with brine (1 mL) and distilled water (1mL). The aqueous phase was extracted with DCM (3 X 10 mL). The organic

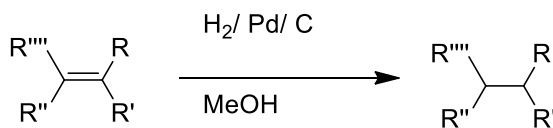
phase was dried over MgSO_4 , filtered and concentrated in vacuo. The crude residue was purified by flash chromatography (8:2/hexane: ethyl acetate) to give the desired ester.

B. Steglich Esterification



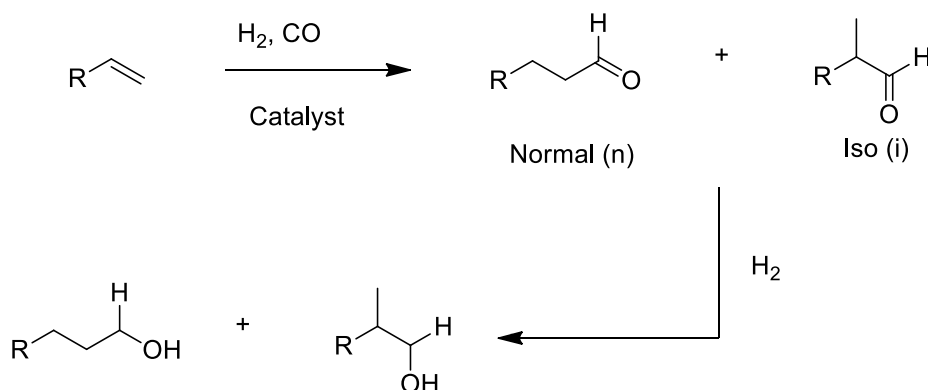
DMAP (10 mol %) and alcohol ($\text{R}'\text{OH}$, typically obtained in the hydroboration process, 1.5 molar equivalents) was dissolved in dry DCM containing the 1.5 equiv. of acid. DCC (1.7 molar equivalents) dissolved in dry DCM was added to the above solution at 0° C. The resulting mixture was stirred at 0°C for 5 min, warmed up to RT and left to react for 3 hr. The crude reaction mixture was filtered to remove the DCU formed in the reaction. The filtrate was taken up in DCM, and if necessary filtered again to remove any remaining DCU. The DCM solution was washed twice with 0.5 N HCl and with saturated NaHCO_3 solution. The organic phase was dried over MgSO_4 , and evaporated to dryness. Purification by flash chromatography (8:2, hexanes: ethyl acetate) afforded the corresponding ester.

5. Hydrogenation



A catalytic amount of Pd/C was added to a solution of alkene (1.0 molar equivalent) dissolved in methanol in an appropriated round bottom flask fitted with a rubber septum. A balloon containing hydrogen was attached via syringe. The reaction mixture was stirred for 72 h then filtered through a Pasteur pipette filled with celite, silica and sand. The filtered solution was dried under vacuum to obtain the desired alkane.

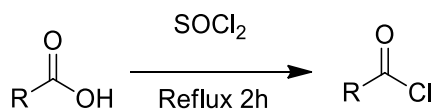
6. Hydroformylation



All the hydroformylation reactions were conducted in a 45 mL stainless steel autoclave equipped with a magnetic stirring bar. The reactor was charged with an appropriate amount of the substrate (1.0 molar equivalent), catalyst: HRh(CO)(PPh₃)₂: Ph₂PCH₂CH₂CH₂CH₂PPh₂ (dppb) (1:1, 0.05 mM), and toluene to achieve a concentration of 0.15 M of the corresponding substrate. After flushing 3 times with carbon monoxide, the reactor was pressurized with 1000 psi of syn-gas (CO: 500 psig, H₂: 500 psig). The reactor mixture was stirred at 60°C, overnight then cooled to room temperature, filtered and concentrated under vacuum. The products were purified by flash chromatography⁶⁰.

7. Acyl chlorides

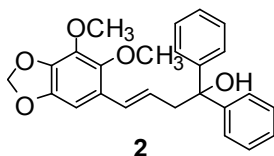
All the acyl chlorides used in this project were freshly prepared using the following method:



Acid (1.0 g) was dissolved in SOCl₂ (10 mL). The mixture was refluxed for 2 hr, after which time the reaction mixture was left to cool down to R.T. Any remaining SOCl₂ was removed under high vacuum to give the required acyl chloride, obtained as the only product. The acid chlorides were used as obtained.

Synthesis of specific compounds:

(E)-4-(6,7-Dimethoxybenzo[d][1,3]dioxol-5-yl)-1,1-diphenylbut-3-en-1-ol (2)

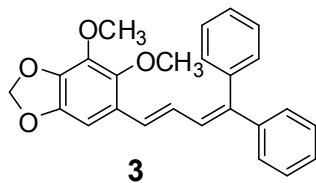


n-BuLi (1.25 mL, 2.0M) was added dropwise to a cooled (-78°C) solution of dillapiol **1** (0.4 g, 1.8 mmol) in dry THF (10 mL) The reaction mixture was stirred for 30 min, allowed to warm up to 0°C and kept at 0°C for another 30 min. After this time the reaction mixture was cooled to -78°C for 5 minutes and then benzophenone (0.43 g, 1.3 mmol) was added. The resulting mixture was stirred for 5 minutes then quenched with saturated NH₄Cl solution (3 mL) and extracted with Et₂O (3 X 20 mL). The organic phase was dried over MgSO₄, filtered and concentrated in vacuo. The crude was purified by Flash chromatography (8:2, hexanes: ethyl acetate) to provide compound **2** as a white powder (598mg, 82%). The spectra obtained matches the one previously reported⁴².

¹H-NMR (300 MHz; CDCl₃): δ ppm 1.60 (s, 2H), 2.60 (s, 1H), 3.24 (d, *J* = 7.3 Hz, 2H), 3.69 (s, 3H), 4.01 (s, 3H), 5.89 (s, 3H), 6.49 (s, 1H), 6.78 (d, *J* = 16.0 Hz, 1H), 7.28-7.25 (m, 2H), 7.34 (t, *J* = 7.5 Hz, 4H), 7.49 (d, *J* = 7.6 Hz, 4H).

¹³C NMR (100MHz; CDCl₃): δ 46.2, 60.0, 61.5, 77.4, 98.6, 101.3, 124.0, 124.2, 126.1, 126.9, 128.2, 129.2, 137.1, 137.5, 144.5, 145.0 146.6

(E)-6-(4,4-Diphenylbuta-1,3-dienyl)-4,5-dimethoxybenzo[d][1,3]dioxole (3)



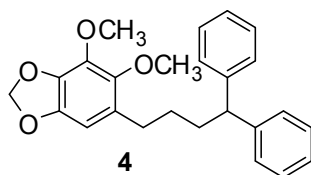
A solution of **2** (250mg, 0.62mmol) in toluene (1 mL) containing a catalytic amount of *p*-toluensulfonic acid (PTSA) was heated to boiling using a heating gun. The reaction mixture was allowed to cool and toluene was removed using roto-evaporation. The residue was purified by

flash chromatography (9:1, hexanes: ethyl acetate) to give compound **3** as a yellowish powder (93mg, 81%).

$^1\text{H NMR}$ (400 MHz; CDCl_3): δ 3.77 (s, 3H), 4.01 (s, 3H), 5.88 (s, 2H), 6.51 (s, 1H), 6.73 (dd, $J = 15.6, 11.0$ Hz, 1H), 6.91 (d, $J = 11.1$ Hz, 1H), 6.97 (d, $J = 15.6$ Hz, 1H), 7.44-7.23 (m, 10H).

$^{13}\text{C NMR}$ (100MHz; CDCl_3): 145.1, 145.0, 142.5, 142.3, 139.9, 137.6, 137.2, 130.6, 128.8, 128.3, 128.2, 127.9, 127.6, 127.5, 127.4, 126.6, 124.6, 101.3, 98.2, 61.7, 60.1

6-(4,4-Diphenylbutyl)-4,5-dimethoxybenzo[d][1,3]dioxole (**4**)

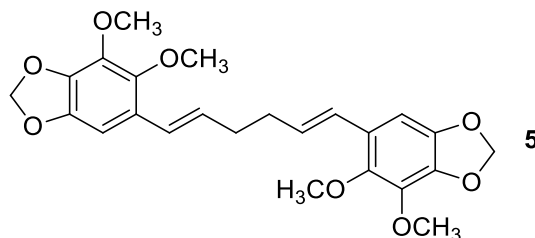


Compound **4** was obtained following general procedure **5**, starting with 44.7 mg (45mg, (0.116mmol) of **3** in 2 mL of methanol (2 mL) containing a catalytic amount of Pd/C. The crude was purified by flash chromatography (8:2, hexanes: ethyl acetate) to yield compound **4** as clear oil (108mg, 96%).

$^1\text{H NMR}$ (400 MHz, CDCl_3): δ ppm 1.53-1.44 (m, 2H), 2.11-2.02 (m, 2H), 2.52 (t, $J = 7.7$ Hz, 2H), 3.65 (s, 3H), 3.89 (t, $J = 7.9$ Hz, 1H), 3.97 (s, 3H), 5.84 (s, 2H), 6.25 (s, 1H), 7.26-7.11 (m, 10H)

$^{13}\text{C NMR}$ (100MHz; CDCl_3): 146.6, 145.0, 144.4, 129.2, 128.3, 1283, 128.2, 128.2, 126.9, 126.1, 124.1, 123.9, 101.3, 98.5, 61.5, 60.1, 46.2

(E)-4,5-Dimethoxy-6-(4-phenylbut-1-enyl)benzo[d][1,3]dioxole (**5**)



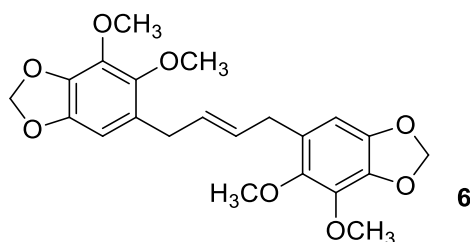
Compound **5** was prepared using the same procedure described for the preparation of compound **1**. Using the following amounts of reagents dillapiol (250mg, 1.12 mmol) to which

benzyl bromide (222mg, 1.2mmol) was added. The crude was purified by Flash chromatography (8:2, hexanes: ethyl acetate) to obtain compound **5** was obtained as a clear oil (134mg, 28%)

¹H NMR (400 MHz, CDCl₃): δ ppm 2.39-2.36 (m, 4H), 3.73 (s, 6H), 4.00 (s, 6H), 5.88 (s, 4H), 6.12-6.03 (m, 2H), 6.63 (s, 2H), 6.63 (d, J = 16.0Hz, 2H)

¹³C NMR (100MHz; CDCl₃): 145.1, 144.1, 137.5, 136.6, 129.6, 124.7, 124.2, 101.2, 98.4, 61.5, 60.1, 33.2

(E)-1,4-bis(6,7-Dimethoxybenzo[d][1,3]dioxol-5-yl)but-2-ene, (**6**)

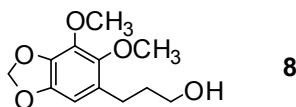


Grubbs II catalyst (30 mg, 0.135 mmol) was added to a solution of dillapiol **1** (200 mg, 0.9 mmol) dissolved in dry DCM. The mixture was kept under nitrogen and refluxed for 72h. The crude residue was purified by flash chromatography (9:1, hexane: ethyl acetate) to give compound 636 mg (57%) of **6** as a thick clear oil.

¹H NMR (400 MHz, CDCl₃): δ ppm 3.26 (dd, J = 3.6, 1.4 Hz, 4H), 3.73 (s, 6H), 4.01 (s, 6H), 5.57 (ddd, J = 5.0, 3.5, 1.33 Hz, 2H), 5.88 (s, 4H), 6.34 (s, 2H)

¹³C NMR: 144.6, 144.2, 137.6, 135.8, 130.1, 126.8, 102.7, 101.1, 61.3, 59.9, 32.6

3-(6,7-Dimethoxybenzo[d][1,3]dioxol-5-yl)propan-1-ol (**8**)

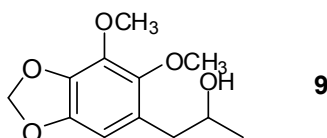


Compound **8** was synthesized following general procedure **3** using 3.37 mL (3.37 mmol) of borane dimethyl sulphide complex and (0.5 g, 2.25 mmol) of dillapiol in 10 mL of CH₂Cl₂.

Purification by flash chromatography (6:4, Hexanes: ethyl acetate) afforded **8** as a clear oil (380 mg, 71%). The spectrum matched the previous reported¹.

¹H NMR (400 MHz, CDCl₃): δ ppm 1.72-1.64 (m, 2H), 2.51 (t, *J* = 7.4Hz 2H), 3.48 (t, *J* = 6.3 Hz, 2H), 3.66 (s, 3H), 3.91 (s, 3H), 5.77 (s, 2H), 6.25 (s, 1H)

1-(6,7-Dimethoxybenzo[d][1,3]dioxol-5-yl)propan-2-ol (**9**)



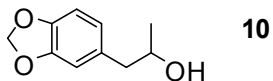
Alcohol **7** was obtained as a minor product from the reaction described for **8**. Purification of the crude residue by flash chromatography (6:4, hexanes: ethyl acetate) provided **9** as a yellow oil (150mg, 28%)

Alternate route for the synthesis of (**9**)

Dillapiol **1** (1.0 g, 4.5 mmol) in THF (15 mL) was added over a period of 20 min was added to a vigorously stirred suspension of mercuric acetate (1.43 g, 4.5 mmol) in THF: water (3:1, 24 mL) at 0 °C. The reaction mixture was allowed to warm up to RT and stirred for 1 h and then treated with an alkaline solution of NaBH₄ (3.6 g KOH/13mL H₂O + 1.0 g NaBH₄). This mixture was stirred for 1h. The liberated mercury was filtered and the filtrate was extracted with CHCl₃ (3 X 30mL). The combined organic extracts were dried over MgSO₄ filtered and evaporated to dryness under vacuum. Purification by flash chromatography (8:2, hexanes: ethyl acetate) afforded compound **9** as a yellowish liquid (0.8 g, 71%). The spectral data for this compound are in accordance with those reported in the literature⁴².

¹H NMR (400 MHz, CDCl₃): δ ppm 1.19 (d, *J* = 6.2 Hz, 3H), 2.13 (d, *J* = 3.1 Hz, 1H), 2.61 (dd, *J* = 13.6, *J* = 7.9 Hz), 2.68 (dd, *J* = 13.6, *J* = 4.3, 1H) 3.76 (s, 3H), 3.95-3.99 (m, 1H), 4.00 (s, 3H), 5.87 (s, 2H), 6.34 (s, 1H)

3-(Benzo[d][1,3]dioxol-5-yl)-2-methylpropan-1-ol (10)

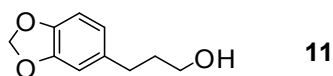


Compound **10** was obtained as the byproduct product in 25% yield in the hydroboration of Safrole (500mg) following general procedure **6**. Purification by flash chromatography (7:3, hexanes: ethyl acetate) afforded **10** as a clear oil (151 mg, 25%).

¹H NMR (400 MHz, CDCl₃): δ ppm 0.86 (d, *J* = 6.76 Hz, 3H), 1.92-1.77 (m, 1H), 2.29 (dd, *J* = 13.57, 8.13 Hz, 2H), 2.64 (dd, *J* = 13.55, 6.23 Hz, 1H), 3.43 (ddd, *J* = 23.37, 10.56, 6.00 Hz, 2H), 5.87 (s, 2H), 6.58 (dd, *J* = 7.87, 1.68 Hz, 1H), 6.64 (d, *J* = 1.55 Hz, 1H), 6.7 (d, *J* = 7.9 Hz, 1H)

¹³C NMR (100MHz; CDCl₃): 147.2, 145.4, 134.2, 121.7, 109.2, 107.8, 100.5, 67.2, 39.1, 37.6, 16.1

4-(Benzo[d][1,3]dioxol-5-yl)butan-1-ol (11)

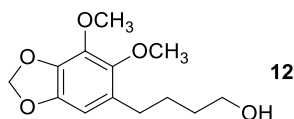


Compound **11** was synthesized from 500 mg of Safrole following general procedure **6**. Purification by flash chromatography (7:3, hexanes: ethyl acetate) afforded **11** as a yellowish oil (159 mg, 27%).

¹H NMR (400 MHz, CDCl₃): δ ppm 1.70-1.52 (m, 4H), 1.95 (s, 1H), 2.55 (t, *J* = 7.36 Hz, 2H), 3.62 (t, *J* = 6.36 Hz, 2H), 5.89 (s, 2H), 6.72-6.60 (m, 3H)

¹³C NMR (100MHz; CDCl₃): 147.3, 145.4, 136.1, 120.9, 108.7, 107.9, 100.6, 62.5, 35.2, 32.0, 27.6

4-(6,7-Dimethoxybenzo[d][1,3]dioxol-5-yl)butan-1-ol (12)

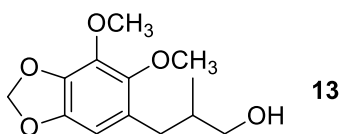


Compound **12** was synthesized following general procedure **6**. Using the following amounts for the corresponding reagents dillapiol (500 mg, 2.3 mmol). Purification by flash chromatography (8:2, hexanes: ethyl acetate) afforded **12** as a brown oil (150 mg, 26%).

¹H NMR (400 MHz, CDCl₃): δ ppm 1.59 (dd sext., *J* = 8.67, 4.60, 2.99 Hz, 4H), 1.67 (s, 1H), 2.56-2.50 (m, 2H), 3.63 (ddd, *J* = 6.19, 3.65, 1.39 Hz, 2H), 3.73 (s, 3H), 3.99 (s, 3H), 5.85 (s, 2H), 6.04-6.04 (m, 1H), 6.32 (s, 1H)

¹³C NMR (100MHz; CDCl₃): 144.5, 144.3, 137.6, 135.6, 128.3, 102.5, 101.0, 62.8, 61.2, 59.9, 32.3, 29.4, 27.1

3-(6,7-Dimethoxybenzo[d][1,3]dioxol-5-yl)-2-methylpropan-1-ol (**13**)

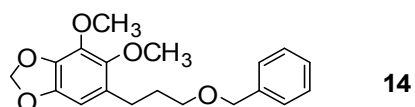


Compound **13** was synthesized following general procedure **6** and is a co-product of the synthesis of compound **12**. Using the following amounts of reagents: dillapiol (500 mg, 2.3 mmol). Purification by flash chromatography (8:2, Hexanes: Ethyl Acetate) afforded **13** as a pale yellow oil (116 mg, 20%).

¹H NMR (400 MHz, CDCl₃): δ ppm 0.95 (d, *J* = 6.86 Hz, 3H), 2.45 (dd, *J* = 13.44, 6.29 Hz, 1H), 2.60 (dd, *J* = 13.4, 7.7 Hz, 1H), 3.36 (dq, *J* = 11.2, 5.1 Hz, 1H), 3.77 (s, 3H), 4.02 (s, 3H), 5.89 (s, 2H), 6.32 (s, 1H)

¹³C NMR (100MHz; CDCl₃): 144.7, 144.4, 137.4, 135.8, 126.1, 103.3, 101.1, 66.3, 61.4, 59.9, 37.2, 32.8, 16.9

6-(3-(Benzyloxy)propyl)-4,5-dimethoxybenzo[d][1,3]dioxole (**14**)



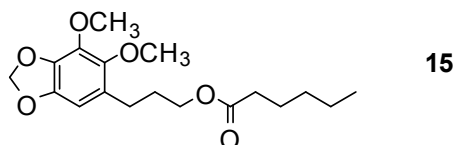
NaH (27 mg, 1.5 molar equiv.) was added to alcohol **8** (100 mg, 0.416mmol) dissolved in dry THF (3 mL). The resulting solution was stirred at 0°C for 10 min after which time benzylbromide (93mg, 0.541mmol) was added dropwise. The reaction mixture was refluxed for 12 hours,

cooled to RT and quenched using saturated NH_4Cl solution (5 mL). The aqueous phase was extracted with DCM (3 X 10 mL). The organic phase was dried over MgSO_4 , filtered and concentrated *in vacuo*. The crude residue was purified by flash chromatography (9:1, hexane: ethyl acetate) to give compound **14** as a pale yellow oil (60mg, 43%).

$^1\text{H NMR}$ (400 MHz, CDCl_3): δ ppm 2.03 (dd, $J = 8.9, 6.5$ Hz, 2H), 2.72-2.68 (m, 2H), 3.76 (s, 3H), 4.01 (s, 3H), 4.34 (t, $J = 6.4$ Hz, 2H), 5.87 (s, 2H), 6.37 (s, 1H), 7.48-7.41 (m, 2H), 7.58-7.53 (m, 1H), 8.05-8.03 (m, 2H)

$^{13}\text{C NMR}$ (100MHz; CDCl_3): 166.6, 144.6, 144.5, 137.7, 135.9, 132.8, 130.5, 129.6, 128.3, 127.2, 102.6, 101.1, 64.5, 61.2, 59.9, 29.8, 26.6

3-(6,7-Dimethoxybenzo[d][1,3]dioxol-5-yl)propyl hexanoate (**15**)

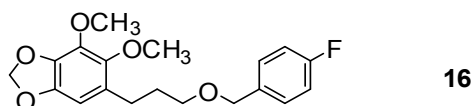


Compound **15** was synthesized following general procedure **4A** from 100 mg of alcohol **8** (in dry DCM (5 mL) and hexanoyl chloride (0.1 mg, 0.624 mmol). The crude residue was purified by flash chromatography (8:2, hexane: ethyl acetate) to give compound **15** as a clear oil (75 mg, 53%).

$^1\text{H NMR}$ (400 MHz, CDCl_3): δ ppm 0.90 (t, $J = 7.0$ Hz, 3H), 1.34-1.29 (m, 4H), 1.67-1.59 (m, 2H), 1.91-1.83 (m, 2H), 2.30 (t, $J = 7.6$ Hz, 2H), 2.59 (dd, $J = 8.5, 6.9$ Hz, 2H), 3.76 (s, 3H), 4.01 (s, 3H), 4.08 (t, $J = 6.6$ Hz, 2H), 6.33 (s, 1H), 5.88 (s, 2H)

$^{13}\text{C NMR}$ (100MHz; CDCl_3): 173.9, 144.5, 144.4, 137.6, 135.8, 127.2, 102.5, 101.1, 61.1, 59.9, 56.5, 34.3, 31.3, 29.7, 26.4, 24.7, 22.3, 13.9

6-(3-((4-fluorobenzyl)oxy)propyl)-4,5-dimethoxybenzo[d][1,3]dioxole (**16**)



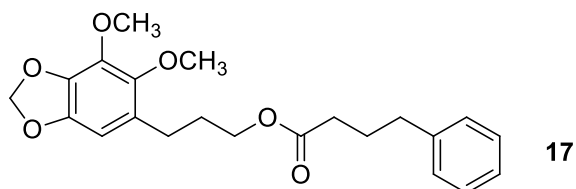
Compound **16** was synthesized following the same procedure used for compound **14** starting with 100 mg, (0.416 mmol) of following amounts for the corresponding reagents alcohol **8**

dissolved in dry THF (5 mL), NaH (27 mg), and *p*-flourobenzylbromide (118 mg, 0.624 mmol). The crude product was purified by flash chromatography (8:2, hexane: ethyl acetate) to give compound **16** as a yellow oil (78 mg, 53%)

¹H NMR (400 MHz, CDCl₃): δ ppm 1.90-1.78 (m, 2H), 2.62-2.58 (m, 2H), 3.47 (t, *J* = 6.4 Hz, 2H), 3.74 (s, 3H), 4.00 (s, 3H), 4.44 (s, 2H), 5.85 (s, 2H), 6.32 (s, 1H), 7.05-6.97 (m, 2H), 7.29 (dd, *J* = 8.4, 5.6 Hz, 2H)

¹³C NMR (100MHz; CDCl₃): 163.5, 160.9, 144.5, 144.3, 129.4, 129.3, 127.9, 115.3, 115.1, 102.6, 101.1, 72.1, 69.7, 61.2, 59.9, 30.7, 26.5

3-(6,7-Dimethoxybenzo[d][1,3]dioxol-5-yl)propyl 4-phenylbutanoate (**17**)

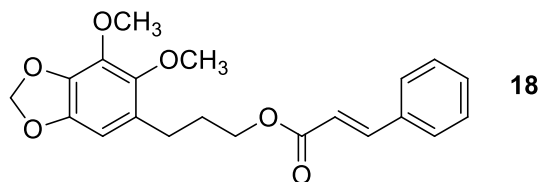


Compound **17** was synthesized following general procedure **4B**. Starting with 4-phenylbutanoic acid (103 mg, 0.624 mmol) dissolved in dry DCM (3 mL). To this was added DMAP in catalytic amount, then 100 mg of alcohol **8** (0.416 mmol) dissolved in dry DCM (1 mL). Finally, DCC (146 mg, 0.707 mmol) soluble in dry DCM (1 mL) was added. Purification by flash chromatography (8:2, hexanes: ethyl acetate) afforded **17** as a yellow oil (122 mg, 76%).

¹H NMR (400 MHz, CDCl₃): δ ppm 1.86 (qd, *J* = 9.2, 6.5 Hz, 2H), 2.00-1.91 (m, 2H), 2.32 (t, *J* = 7.5 Hz, 2H), 2.61-2.55 (m, 2H), 2.67-2.62 (m, 2H), 3.73 (s, 3H), 3.99 (s, 3H), 4.07 (t, *J* = 6.6 Hz, 2H), 5.85 (s, 2H), 6.32 (s, 1H), 7.20-7.14 (m, 3H), 7.28-7.24 (m, 2H)

¹³C NMR (100MHz; CDCl₃): 173.6, 144.6, 144.4, 141.4, 137.7, 135.9, 128.5, 128.4, 128.4, 127.2, 125.9, 102.5, 101.1, 63.9, 61.2, 59.9, 35.2, 33.7, 29.7, 26.6, 26.4

3-(6,7-Dimethoxybenzo[d][1,3]dioxol-5-yl)propyl cinnamate (18)

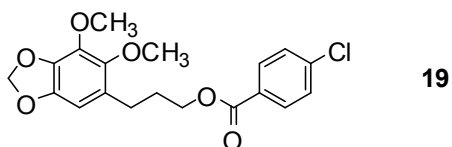


Compound **18** was synthesized following general procedure **4B**. Using the following amounts for the corresponding reagents alcohol **8** (100 mg, 0.416 mmol) to which Cinnamic acid (92 mg, 0.624 mmol) was added. The crude was purified by flash column (8:2, hexanes: ethyl acetate) to obtain compound **18** as a white powder (140 mg, 91%)

¹H NMR (400 MHz, CDCl₃): δ ppm 2.01-1.86 (m, 2H), 2.65-2.60 (m, 2H), 3.77 (s, 3H), 4.00 (s, 3H), 4.22 (t, *J* = 6.5 Hz, 2H), 5.85 (s, 2H), 6.36 (s, 1H), 6.44 (d, *J* = 16.0 Hz, 1H), 7.37 (td, *J* = 6.4, 2.3 Hz, 3H), 7.54-7.50 (m, 2H), 7.67 (d, *J* = 16.0 Hz, 1H)

¹³C NMR (100MHz; CDCl₃): 167.0, 144.7, 144.6, 144.5, 137.7, 135.9, 134.5, 130.3, 128.9, 128.2, 128.1, 128.1, 127.2, 118.2, 102.6, 101.1, 64.1, 61.2, 59.9, 29.8, 26.5

3-(6,7-Dimethoxybenzo[d][1,3]dioxol-5-yl)propyl 4-chlorobenzoate (19)

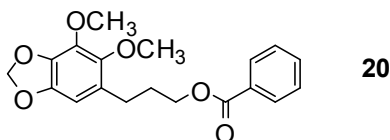


Reaction of alcohol **8** (100 mg, 0.416 mmol) in dry DCM (3mL), DMAP (5.08 mg, 0.0416 mmol) with 4-chlorobenzoic acid (97.76 mg, 0.624 mmol), and DCC (85.83 mg, 0.000416 mmol) gave 103 mg (65%) of **19** as white crystals after purification via flash chromatography (8:2, hexanes: ethyl acetate).

¹H NMR (400 MHz, CDCl₃): δ ppm 2.00 (tt, *J* = 13.1, 6.5 Hz, 2H), 2.68-2.64 (m, 2H), 3.74 (s, 3H), 3.98 (s, 3H), 4.31 (t, *J* = 6.4 Hz, 2H), 5.85 (s, 2H), 6.33 (s, 1H), 7.41-7.36 (m, 2H), 7.95-7.92 (m, 2H)

¹³C NMR (100MHz; CDCl₃): 165.7, 144.6, 144.4, 139.3, 138.8, 137.7, 135.9, 130.9, 128.9, 128.7, 127.1, 102.5, 101.1, 64.7, 61.2, 59.9, 29.7, 26.6

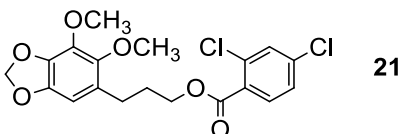
3-(6,7-Dimethoxybenzo[d][1,3]dioxol-5-yl)propyl benzoate (20)



Compound **20** was obtained in 33 % yield as a white crystals following general procedure **4A** starting with 250 mg of alcohol **8**, 0.18 mL benzoylchloride and 0.23 mL of Et₂NH. The crude product was purified by preparative HPLC using C18 column and a solvent system consisting in 85:15 ACN:H₂O. The spectra obtained was compared with the one previously reported⁴².

¹H NMR (400 MHz, CDCl₃): δ ppm 2.08-1.95 (m, 2H), 2.70 (dd, *J* = 8.3, 6.9 Hz, 2H), 3.76 (s, 3H), 4.01 (s, 3H), 4.34 (t, *J* = 6.4 Hz, 2H), 5.87 (s, 2H), 6.37 (s, 1H), 7.47-7.41 (m, 2H), 7.58-7.53 (m, 1H), 8.05-8.03 (m, 2H)

3-(6,7-Dimethoxybenzo[d][1,3]dioxol-5-yl)propyl 2,4-dichlorobenzoate (21)

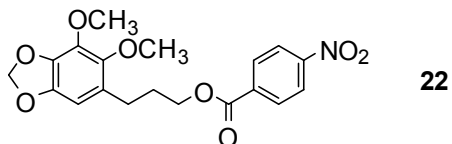


Compound **21** was obtained in 51% yield as white crystals after flash chromatography (8:2, hexanes: ethyl acetate from alcohol **8** (250 mg, 1.04 mmol) and 2,4-dichlorobenzoic acid (119.2 mg, 0.624 mmol) via procedure **4B**.

¹H NMR (400 MHz, CDCl₃): δ ppm 2.01 (qd, *J* = 8.9, 6.4 Hz, 2H), 2.68 (dd, *J* = 8.3, 6.9 Hz, 2H), 3.76 (s, 3H), 4.01 (s, 3H), 4.34 (t, *J* = 6.4 Hz, 2H), 5.88 (s, 2H), 6.35 (s, 1H), 7.30 (dd, *J* = 8.4, 2.1 Hz, 1H), 7.48 (d, *J* = 2.0 Hz, 1H), 7.79 (d, *J* = 8.4 Hz, 1H)

¹³C NMR (100MHz; CDCl₃): 164.9, 144.6, 144.5, 138.2, 137.7, 135.9, 134.9, 132.6, 131.0, 128.6, 126.9, 102.6, 101.1, 65.6, 61.2, 59.9, 29.7, 26.6

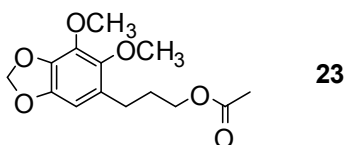
3-(6,7-Dimethoxybenzo[d][1,3]dioxol-5-yl)propyl 4-nitrobenzoate (22)



Compound **22** was obtained in 66 % yield as a pink powder after chromatography (8:2 hexanes: ethyl acetate) following procedure **4A**. Starting with 100 mg (0.416 mmol) of alcohol **8** (100 mg, 0.416 μ -nitro benzoyl chloride (116 mg, 0.624 mmol) and Et₂NH (0.09 mL, 0.624 mmol).

¹H NMR (400 MHz, CDCl₃): δ ppm 2.11-1.99 (m, 2H), 2.70-2.66 (m, 2H), 3.74 (s, 3H), 3.99 (s, 3H), 4.37 (t, J = 6.5 Hz, 2H), 5.86 (s, 2H), 6.34 (s, 1H), 8.19-8.15 (m, 2H), 8.28-8.26 (m, 2H)

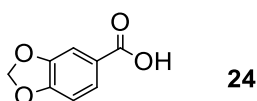
3-(6,7-Dimethoxybenzo[d][1,3]dioxol-5-yl)propyl acetate (23)



Esterification of alcohol **8** (100 mg, 0.416 mmol) with acetic anhydride (0.1 mL, 0.924 mmol) and Et₂NH (0.15 mL, 1.05 mmol) following procedure 4A afforded 107 mg (93%) of compound **23** after purification via flash chromatography (8:2, hexanes: ethyl acetate). The spectra obtained matches the reported in literature⁴².

¹H NMR (400 MHz, CDCl₃): δ ppm 1.93-1.82 (m, 2H), 2.06 (s, 3H), 2.61-2.55 (m, 2H), 3.76 (s, 3H), 4.01 (s, 3H), 4.08 (t, J = 6.6 Hz, 2H), 5.88 (s, 2H), 6.33 (s, 1H)

Benzo[d][1,3]dioxole-5-carboxylic acid (piperonylic acid) (24)



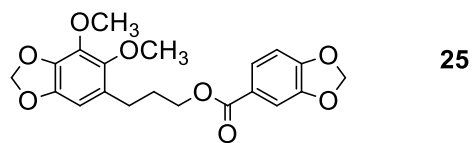
Piperonal (5.0 g, 33.33 mmol) and 125 mL of water were placed in a 500mL RBF, fitted with an efficient mechanical stirrer. The flask was placed on a heating mantle, heated to 70-80°C and stirred started. A solution of KMnO₄ and water was allowed to flow into the emulsion of

piperonal and water over a period of 40-45 min. The stirring and heating were continued for another hour, at the end of which the KMnO_4 was reduced.

Enough 10% KOH solution was added to make the solution alkaline. The solution was filtered while hot and MnO_2 is washed with 2 X 100 mL of cooled. At this point any unreacted piperonal that separates was filtered. The resulting solution was acidified with HCl until no further precipitate was formed. The acid is filtered and washed until is Cl^- free and then dried⁶¹. To obtain compound **24** as a white powder (4.95 g, 89%). The spectroscopic data was compared with that reported in literature.

¹H NMR (400 MHz, CDCl_3): δ ppm 6.08 (s, 2H), 6.96 (d, $J = 8.1$ Hz, 1H), 7.32 (d, $J = 1.5$ Hz, 1H), 7.51 (dd, $J = 8.1, 1.7$ Hz, 1H), 9.77 (s, 1H)

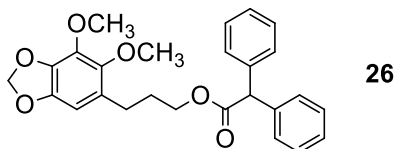
3-(6,7-Dimethoxybenzo[d][1,3]dioxol-5-yl)propyl benzo[d][1,3]dioxole-5-carboxylate (**25**)



Esterification of alcohol **8** (100 mg, 0.416 mmol), dry DCM (3 mL) with piperonylic acid **24** (98 mg, 0.624 mmol), DCC (86 mg, 0.000416 mmol) and DMAP (5 mg, 0.0416 mmol) in dry DCM afforded compound **25** as a clear oil (95 mg, 59%) after flash chromatography using 8:2 hexanes-ethyl acetate. The spectra was compared with the data previously reported⁴².

¹H NMR (400 MHz, CDCl_3): δ ppm 1.89-1.76 (m, 2H), 2.53-2.47 (m, 2H), 3.58 (s, 3H), 3.82 (s, 3H), 4.11 (t, $J = 6.40$ Hz, 2H), 5.69 (s, 2H), 5.84 (s, 2H), 6.18 (s, 1H), 6.65 (d, $J = 8.18$ Hz, 1H), 7.26 (d, $J = 1.49$ Hz, 1H), 7.46 (dd, $J = 8.18, 1.57$ Hz, 1H)

3-(6,7-Dimethoxybenzo[d][1,3]dioxol-5-yl)propyl 2,2-diphenylacetate (26)



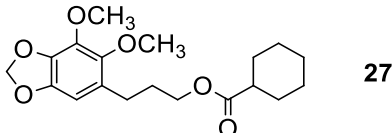
Alcohol **8** (1.5 g, 6.22 mmol), dry DCM (5mL), DMAP (190 mg, 1.56 mmol), diphenylacetyl chloride (2.2 g, 9.33 mmol) and Et₂NH (5 mL, 12.44 mmol) in dry DCM gave 2.3 g (85%) of **26** as a white powder after chromatography using 8:2, hexanes: ethyl acetate as eluent.

¹H NMR (400 MHz, CDCl₃): δ ppm 1.84 (qd, *J* = 9.2, 6.5 Hz, 2H), 2.51-2.45 (m, 2H), 3.67 (s, 3H), 3.98 (s, 3H), 4.14 (t, *J* = 6.5, 2H), 5.02 (s, 1H), 5.85 (s, 2H), 6.17 (s, 1H), 7.33-7.22 (m, 10H)

¹³C NMR (100MHz; CDCl₃): 172.4, 144.4, 144.4, 138.7, 137.6, 135.8, 128.6, 128.5, 128.4, 127.5, 127.2, 126.9, 126.5, 102.6, 101.0, 64.6, 61.1, 59.9, 57.2, 29.6, 26.3

HRMS: Cal. For C₂₆H₂₆O₆ Exact Mass: 434.1729, obtained: 434.1732

3-(6,7-Dimethoxybenzo[d][1,3]dioxol-5-yl)propyl cyclohexanecarboxylate (27)



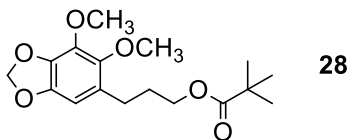
Compound **27** was prepared in 65% yield as a white powder via procedure **4A** using alcohol **8** (100 mg, 0.416 mmol), DMAP (12.7 mg, 0.104 mmol), cyclohexanecarbonyl chloride (73.6 mg, 0.5 mmol), and Et₂NH (0.145 mL, 1.04 mmol) in dry DCM. The product was purified by flash chromatography (8:2, hexanes: ethyl acetate).

¹H NMR (400 MHz, CDCl₃): δ ppm 1.52-1.16 (m, 5H), 1.68-1.63 (m, 1H), 1.95-1.77 (m, 6H), 2.29 (tt, *J* = 11.2, 3.7 Hz, 1H), 2.58 (dd, *J* = 8.6, 6.8 Hz, 2H), 3.75 (s, 3H), 4.01 (s, 3H), 4.07 (t, *J* = 6.5 Hz, 2H), 5.87 (s, 2H), 6.32 (s, 1H)

¹³C NMR (100MHz; CDCl₃): 176.1, 144.5, 144.4, 137.6, 135.8, 127.2, 102.5, 101.0, 63.6, 61.2, 59.9, 43.2, 29.8, 29.2, 26.4, 25.8, 25.4

HRMS: Cal. C₁₉H₂₆O₆ Exact Mass: 350.1729, obtained: 350.17171

3-(6,7-Dimethoxybenzo[d][1,3]dioxol-5-yl)propyl pivalate (28)



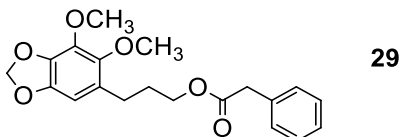
Esterification of alcohol **8** (100 mg, 0.416 mmol), with pivaloyl chloride (61 mg, 0.5 mmol) in dry DCM (5mL) catalyzed by DMAP (12.7 mg, 0.104 mmol), and Et₂NH (0.145 mL, 1.04mmol) afforded ester **28** in 75 % yield as a white powder.

¹H NMR (300 MHz, CDCl₃) δ ppm 1.20 (s, 9H), 1.91-1.80 (m, 2H), 2.58 (dd, *J* = 8.6, 6.8 Hz, 2H), 3.75 (s, 3H), 4.00 (s, 3H), 4.06 (t, *J* = 6.4 Hz, 2H), 5.87 (s, 2H), 6.32 (s, 1H)

¹³C NMR (100MHz; CDCl₃): 26.4, 27.2, 29.8, 38.7, 59.8, 61.1, 63.7, 101.0, 102.5, 127.2, 135.8, 137.6, 144.3, 144.4, 178.5

HRMS: Cal. For C₁₇H₂₄O₆: 324.1573, obtained: 324.15532

3-(6,7-Dimethoxybenzo[d][1,3]dioxol-5-yl)propyl 2-phenylacetate (29)



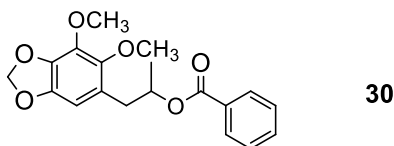
Ester **29** was obtained as a white powder in 60 % yield following procedure **4A** starting with alcohol **8** (100 mg, 0.416 mmol), (5 mL), DMAP (12.7 mg, 0.104 mmol), 2-phenylacetyl chloride (77 mg, 0.5 mmol), and Et₂NH (0.145 mL, 1.04 mmol). The reaction was carried out in dry DCM.

¹H NMR: (400 MHz, CDCl₃): δ ppm 1.91-1.80 (m, 2H), 2.57-2.51 (m, 2H), 3.63 (s, 2H), 4.01 (s, 3H), 4.10 (t, *J* = 6.5 Hz, 2H), 5.88 (s, 2H), 6.25 (s, 1H), 7.33-7.28 (m, 5H)

¹³C NMR (100MHz; CDCl₃): 171.6, 144.5, 144.4, 137.6, 135.8, 134.1, 129.3, 129.2, 128.5, 127.0, 102.5, 101.0, 64.3, 61.1, 59.9, 41.5, 29.6, 26.3

HRMS: Cal. For C₂₀H₂₂O₆ Exact Mass: 358.1416, obtained: 358.1432

1-(6,7-Dimethoxybenzo[d][1,3]dioxol-5-yl)propan-2-yl benzoate (30)

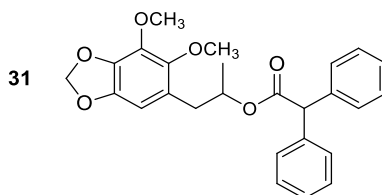


Alcohol **9** (100 mg, 0.416 mmol) in dry DCM 5 mL was reacted with), benzoyl chloride (0.106 mL, 1.04 mmol), catalyzed by dry DCM (5 mL), DMAP (13 mg, 0.104 mmol and Et₂N (0.145 mL, 1.04 mmol). The yield benzoate ester **30**, as a white powder 100 mg (70%).

¹H NMR (400 MHz, CDCl₃): δ ppm 1.32 (d, *J* = 6.3 Hz, 3H), 2.84 (dd, *J* = 13.6, 6.3 Hz, 1H), 2.95 (dd, *J* = 13.6, 7.0 Hz, 1H), 3.78 (s, 3H), 3.97 (s, 3H), 5.43-5.27 (m, 1H), 5.84 (dd, *J* = 5.4, 1.5 Hz, 2H), 6.41 (s, 1H), 7.5-7.4 (m, 3H), 8.01 (td, *J* = 8.5, 1.6 Hz, 2H)

¹³C NMR (100MHz; CDCl₃): 166.1, 145.1, 144.4, 137.6, 136.4, 132.7, 130.8, 129.5, 128.3, 123.5, 103.6, 101.2, 71.9, 61.2, 59.9, 36.1, 19.7

1-(6,7-Dimethoxybenzo[d][1,3]dioxol-5-yl)propan-2-yl 2,2-diphenylacetate (31)



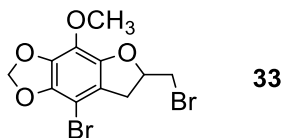
Reaction of diphenylacetyl chloride (116 mg, 0.5 mmol,) with alcohol **9** 100 mg, 0.416 mmol) in dry DCM catalyzed by DMAP (12.7 mg, 0.104 mmol and Et₂NH (0.145 mL, 1.04 mmol) yielded 150.3 mg, (83%) of the diphenyl ester **31** as a white powder.

¹H NMR 400 MHz, CDCl₃): δ ppm 1.32 (d, *J* = 6.3 Hz, 3H), 2.71 (dd, *J* = 13.7, 5.6 Hz, 1H), 2.77 (dd, *J* = 13.8, 7.6 Hz, 1H), 3.78 (s, 3H), 3.97 (s, 3H), 4.95(s, 1H), 5.23-5.15 (m, 1H), 5.84 (dd, *J* = 5.4, 1.5 Hz, 2H), 6.41 (s, 1H), 7.32-7.17 (m, 10H)

¹³C NMR (100MHz; CDCl₃): 171.9, 144.9, 144.3, 138.8, 138.8, 137.5, 136.3, 128.7, 128.5, 128.5, 128.4, 127.1, 127.0, 123.4, 103.5, 101.1, 72.0, 61.1, 59.9, 57.3, 35.9, 19.7

HRMS: calc. C₂₆H₂₆O₆: 434.1729, obtained: 434.17462

6-(Bromomethyl)-4-methoxy-6,7-dihydro-[1,3]dioxolo[4,5-f]benzofuran (33)

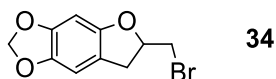


Bromine (0.1 mL, 1.8 mmol) was added over a period of time of 5 min to a cooled (-20 to -30 °C) mixture of *t*-butylamine (0.23 mL, 2.16 mmol) and dry toluene (9 mL). The reaction was then cooled to -78 °C at which time dillapiol (200 mg, 0.9 mmol) dissolved in toluene 5 mL was added. The resulting solution was allowed to warm up to RT and left to react for 6 hr, diluted with hexanes (50 mL) and washed with water (4 X 50 mL). The organic phase was dried over MgSO₄, filtered and evaporated to dryness. Purification of the residue by flash chromatography (8:2, Hexanes: ethyl acetate) gave product **33** as a yellowish oil (106 mg, 46%)

¹H NMR (400 MHz, CDCl₃) δ ppm 3.07 (dd, *J* = 15.91, 6.75 Hz 1H), 3.30 (dd, *J* = 15.9, 9.3 Hz, 1H), 3.53 (dd, *J* = 10.4, 7.1 Hz, 1H), 3.61 (dd, *J* = 10.42, 4.54 Hz, 1H), 4.02-3.96 (m, 3H), 5.09-5.02 (m, 1H), 5.99-5.92 (m, 2H)

HRMS: calc. for C₁₁H₁₀Br₂O₄. Exact Mass: 363.8946, obtained: 363.89678

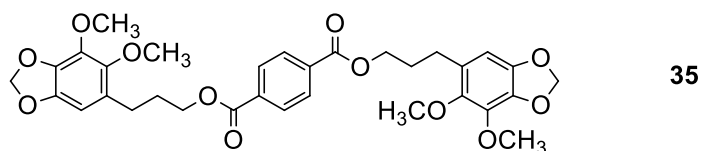
6-(Bromomethyl)-6,7-dihydro-[1,3]dioxolo[4,5-f]benzofuran (34)



Compound **34** was prepared from dillapiol using the same procedure as compound **33**, except that the amount of bromine used was 1.0 molar equivalent. The yield of **34**, a clear oil, was 26 %. The NMR spectra matched those reported before⁴².

¹³C NMR (100MHz; CDCl₃): 34.5, 34.6, 82.0, 93.2, 101.2, 105.0, 116.3, 141.8, 147.8, 147.3, 153.5

Bis(3-(6,7-Dimethoxybenzo[d][1,3]dioxol-5-yl)propyl) terephthalate (35)

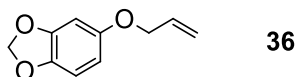


Alcohol **8** (350 mg, 1.46 mmol) was added to a (0°C) solution of terephthaloyl chloride in toluene containing Et₃N (0.1 mL, 2.2 mmol). The resulting reaction mixture was kept at RT and monitored by TLC until reaction was completed. NaHCO₃, (5 mL, 5%) and 5 ml of distilled water were added. The aqueous layer was extracted with ethyl acetate (3 X 30 mL). The combined organic layer were dried over MgSO₄ and evaporated under vacuum. Purification of the crude residue by flash chromatography (8:2, hexanes: ethyl acetate) gave the diester **35** as a white powder (80 mg, 35%).

¹H NMR (400 MHz, CDCl₃) δ ppm 2.08-2.01(m, 4H), 2.72-2.67 (m, 4H), 3.76 (s, 6H), 4.01 (s, 6H), 4.36 (t, *J* = 6.4 Hz, 4H), 5.88 (s, 4H), 6.36 (s, 2H), 8.09 (s, 4H)

¹³C NMR (100MHz; CDCl₃): 165.8, 144.6, 144.5, 137.7, 135.9, 134.1, 129.5, 127.0, 102.6, 101.1, 64.9, 61.2, 59.9, 29.7, 26.6

5-(Allyloxy)benzo[d][1,3]dioxole (36**)**

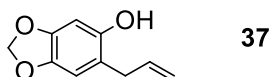


Alkylation of safrole (2.0 g, 14.48 mmol) was carried out with allyl bromide (2.3 g, 18.82 mmol) in dry acetone (15 mL) to which was added 2.6 g of potassium. The ether **36** was obtained as orange oil (2.34 g, 90%). The spectroscopy data corresponds to those reported in literature⁴².

¹H NMR (400 MHz, CDCl₃): δ ppm 4.37 (d, 2H, *J*=5.3 Hz), 5.25 (dd, 1H, *J*=10.6 Hz, *J*=1.2 Hz), 5.39 (dd, 1H, *J*=17.3 Hz, *J*=1.4 Hz), 5.96 (s, 2H), 6.07-5.98 (m, 1H), 6.31 (dd, 1H, *J*=8.5 Hz, *J*=2.5 Hz), 6.53 (d, 1H, *J*=2.6 Hz), 6.69 (d, 1H, *J*=8.5 Hz)

¹³C NMR (100MHz, CDCl₃): δ ppm 69.8, 93.3, 101.1, 106.1, 107.9, 117.6, 133.4, 141.7, 148.2, 154.1

6-Allylbenzo[d][1,3]dioxol-5-ol (37**)**

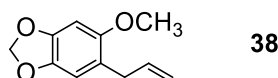


Compound **36** (2.30g, 13.5mmol) was dissolved in decalin (50 mL). The solution was heated to 190°C for 8 hr using an oil bath. The cooled mixture was diluted with ethyl acetate and washed with NaOH (1 N, 3 X 50mL). The alkaline extract was acidified with concentrated HCl and the aqueous phase extract with ethyl acetate (3 X 40mL). The combined organic extracts were dried

over magnesium sulfate, filtered and concentrated *in vacuo*. The crude residue was purified by flash chromatography (9:1, hexanes: ethyl acetate) to provide **37** (2.2 g, 90%) as colorless needles. The spectroscopy data for the obtained compound corresponds to that reported in previous literature⁴².

¹H NMR (400 MHz, CDCl₃): δ ppm 3.29 (td, $J = 6.2, 1.5$ Hz, 2H), 4.74 (s, 1H), 5.11 (qd, $J = 5.1, 1.7$ Hz, 1H), 5.17-5.13 (m, 1H), 5.86 (s, 2H), 6.00-5.89 (m, 1H), 6.41 (s, 1H), 6.56 (s, 1H)

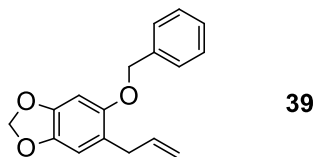
5-Allyl-6-methoxybenzo[d][1,3]dioxole (**38**)



Methylation of 500 mg (2.8 mmol) of the phenol **37** dry acetone (5mL), containing 582 mg, (4.2 mmol) of potassium and 20.26 mL (4.2 mmol) of methyl iodide afforded 485 (92%) mg of **38** as a light colorless oil after chromatography. The spectra corresponds to the one reported in literature⁶².

¹H NMR (400 MHz, CDCl₃): δ ppm 3.29 (d, 2H, $J=5.3$ Hz), 3.75 (s, 3H), 5.01 (dd, 1H, $J=10.6$ Hz, $J=1.2$ Hz), 5.18 (dd, 1H, $J=17.3$ Hz, $J=1.4$ Hz), 5.87 (s, 2H), 5.98-5.89 (m, 3H), 6.51 (s, 1H), 6.65 (s, 1H)

5-Allyl-6-(benzyloxy)benzo[d][1,3]dioxole (**39**)

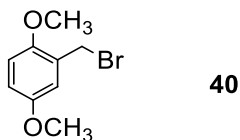


Reaction of **37** (500 mg, 2.8 mmol) in 3 ml of dry THF with NaH (100.8 mg, 4.2 mmol) followed by benzyl bromide (0.44 mL, 3.64 mmol) gave 715mg (95%) of the benzyl ether **39** as off white needles. Compound has been synthesized before⁶³.

¹H NMR (400 MHz, CDCl₃): δ ppm 3.35 (td, $J = 6.6, 1.3$ Hz, 2H), 5.00 (s, 2H), 5.05-4.99 (m, 2H), 5.89 (s, 2H), 5.98-5.88 (m, 1H), 6.57 (s, 1H), 6.67 (s, 1H), 7.42-7.30 (m, 5H)

¹³C NMR (100MHz; CDCl₃): 151.0, 146.2, 141.4, 137.3, 137.2, 128.5, 127.9, 127.3, 121.5, 115.4, 109.689, 101.0, 96.5, 71.5, 34.2

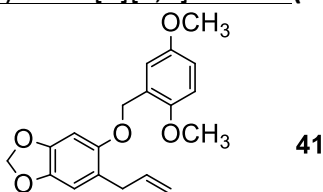
2-(Bromomethyl)-1,4-dimethoxybenzene (40)



To a solution of (2,5-dimethoxyphenyl)methanol (1.0g, 6.0 mmol) in THF 50mL was added PPh_3 (3.4 g, 13 mmol) and then CBr_4 (3.01 g, 9.08 mmol). The mixture was stirred at R.T. for 3h then diluted with saturated aqueous NaHCO_3 , extracted with ethyl acetate (3 X 50 mL) and washed with brine (1 X 20mL). The organic layer was dried over MgSO_4 and concentrated in vacuo. The residue was purified by flash chromatography (8:2, hexanes: ethyl acetate) to yield the bromide **41** (678 mg, 49%) as a white needles. The spectroscopy data for the obtained compound corresponds to that reported in previous literature⁶⁴.

$^1\text{H NMR}$ (400 MHz, CDCl_3): δ ppm 6.90-6.79 (m, 3H), 4.52 (s, 2H), 3.84 (s, 3H), 3.75 (s, 3H)

5-Allyl-6-(2,5-dimethoxybenzyl)oxy)benzo[d][1,3]dioxole (41)

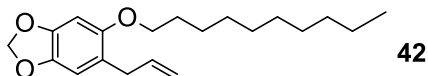


Alkylation of the phenol **37** (100 mg, 0.56 mmol) with the bromide **40** (194 mg, 0.84 mmol) in dry acetone (3 mL) to which had been added K_2CO_3 (116 mg, 0.84mmol) gave **41** as white crystals (143 mg, 78%) after flash chromatography (8:2, hexanes: ethyl acetate).

$^1\text{H NMR}$ (400 MHz, CDCl_3): δ ppm 3.29 (d, 2H), 3.75 (s, 3H), 3.80 (s, 3H), 4.98 (m, 2H), 5.04 (m, 2H), 5.87 (s, 2H), 5.93 (m, 1H), 6.51 (s, 1H), 6.65 (s, 1H), 6.79 (m, 2H), 7.06 (d, 1H, $J=2.5$ Hz)

$^{13}\text{C NMR}$ (100MHz; CDCl_3): 153.7, 151.1, 150.7, 146.234, 141.2, 137.3, 126.9, 121.4, 115.3, 114.1, 113.0, 111.1, 109.6, 100.9, 96.6, 66.3, 55.9, 55.7, 34.3

5-Allyl-6-(decyloxy)benzo[d][1,3]dioxole (42)

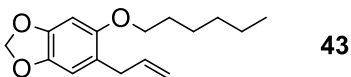


The phenol **37** (100 mg, 0.56 mmol), was alkylated by refluxing it for 2 h in dry acetone (3 mL), with K_2CO_3 (100 mg, 0.72 mmol) and 1-bromodecane (159 mg, 0.72 mmol). Flash chromatography (8:2, hexanes: ethyl acetate) gave pure **42** as yellowish liquid (87 mg, 59%).

1H NMR(400 MHz, $CDCl_3$): δ 0.86 (t, $J = 6.7$ Hz, 3H), 1.35-1.20 (m, 12H), 1.47-1.37 (m, 2H), 1.73 (td, $J = 14.4, 6.5$ Hz, 2H), 3.28 (td, $J = 6.7, 1.22$ Hz, 2H), 3.85 (t, $J = 6.5$ Hz, 2H), 5.07-4.96 (m, 2H), 5.86 (s, 2H), 5.95-5.86 (m, 1H), 6.48 (s, 1H), 6.63-6.62 (m, 1H)

^{13}C NMR (100MHz; $CDCl_3$): 151.5, 146.2, 140.8, 137.4, 121.1, 115.2, 109.5, 100.9, 95.9, 69.4, 34.2, 31.9, 29.5, 29.6, 29.4, 29.4, 29.3, 26.1, 22.7, 14.1

5-Allyl-6-(hexyloxy)benzo[d][1,3]dioxole (43)

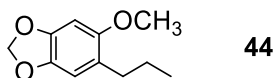


Following the procedure for **42**, compound **37** (100 mg, 0.48 mmol), anhydrous acetone (3 mL), K_2CO_3 (100 mg, 0.72 mmol), 1-bromohexane (165 mg, 0.72 mmol) was converted in 93% yield into **43**, as a yellowish oil.

1H NMR (400 MHz, $CDCl_3$): δ ppm 0.94-0.86 (m, 2H), 1.36-1.30 (m, 4H), 1.44 (ddd, $J = 13.2, 8.7, 4.46$ Hz, 2H), 1.80-1.71 (m, 2H), 3.28 (d, $J = 6.6$ Hz, 2H), 3.86 (t, $J = 6.4$ Hz, 2H), 5.08-4.98 (m, 2H), 5.86 (s, 2H), 5.99-5.88 (m, 1H), 6.49 (s, 1H), 6.63 (s, 1H)

^{13}C NMR (100MHz; $CDCl_3$): 151.5, 146.2, 140.8, 137.4, 121.1, 115.2, 109.6, 100.9, 95.9, 69.4, 34.2, 31.6, 29.4, 25.8, 22.6, 14.0

5-Methoxy-6-propylbenzo[d][1,3]dioxole (44)

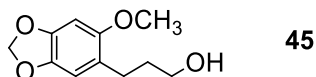


Hydrogenation of 248 mg, (1.29 mmol) of compound **38** in MeOH (3 mL) afforded **44** as clear oil (233 mg, 93%).

¹H NMR (400 MHz, CDCl₃): δ ppm 0.91 (t, J=7.4 Hz, 3H), 1.56-1.50 (m, 2H), 2.45 (t, J=7.8, 2H), 3.74 (s, 3H), 5.87 (s, 2H), 6.50 (s, 1H), 6.63 (s, 1H)

¹³C NMR (100MHz; CDCl₃): 152.2, 145.8, 140.7, 123.5, 109.7, 100.8, 94.8, 56.5, 32.0, 23.4, 13.9

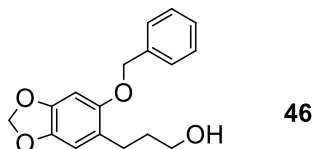
3-(6-Methoxybenzo[d][1,3]dioxol-5-yl)propan-1-ol (45)



Hydoboration of 200 mg, (1.04 mmol) of **38** with 1.56 mL of borane dimethyl sulphide complex (1.56 mL, 1.56 mmol) in CH₂Cl₂ (10 mL) at 0 °C gave after purification by flash chromatography (8:2, hexanes: ethyl acetate) 148 mg (67%) of **45** as white needles.

¹H NMR (400 MHz, CDCl₃): δ ppm 1.55 (qt, 2H, J=6.5 Hz), 2.38 (t, 2H, J=7.3 Hz), 3.37 (t, 2H, J=6.4 Hz), 3.54 (s, 3H), 5.87 (s, 2H), 6.51 (s, 1H), 6.65 (s, 1H)

3-(6-(Benzyloxy)benzo[d][1,3]dioxol-5-yl)propan-1-ol (46)

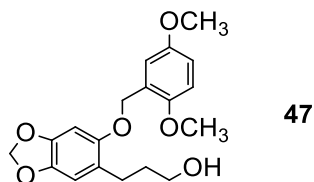


Compound **46** was obtained in 68% yield after purification as white crystals starting with 200 mg (0,79 mmol) of **39** and mmol borane dimethyl sulphide complex in 10 mL of CH₂Cl₂ at (0°C).

¹H NMR (400 MHz, CDCl₃): δ ppm 1.70-1.70 (m, 1H), 1.85-1.75 (m, 2H), 2.68 (t, J = 7.2 Hz, 2H), 3.56 (t, J = 6.2 Hz, 2H), 5.00 (s, 2H), 5.89 (s, 2H), 6.58 (s, 1H), 6.66 (s, 1H), 7.43-7.33 (m, 5H)

¹³C NMR (100MHz; CDCl₃): 25.8, 33.3, 61.6, 71.7, 96.3, 101.0, 109.8, 122.8, 127.4, 128.1, 128.7, 136.9, 141.5, 146.1, 151.2

3-(6-((2,5-Dimethoxybenzyl)oxy)benzo[d][1,3]dioxol-5-yl)propan-1-ol (47)

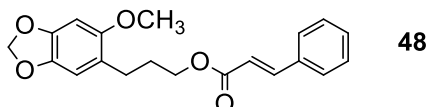


Hydroboration of the alkene **41** (61 mg, 0.18 mmol) in CH₂Cl₂ (10 mL) with borane dimethyl sulphide complex (1.18 mL, 1.18 mmol) at cooled (0°C) solution of compound afforded **47** as yellow liquid (44 mg, 71%) after purification by flash chromatography (8:2, Hexanes: ethyl acetate)

¹H NMR (400 MHz, CDCl₃): δ ppm 1.84-1.73 (m, 2H), 2.69 (t, *J* = 7.2 Hz, 2H), 3.57 (t, *J* = 6.1 Hz, 2H), 3.77 (s, 3H), 3.82 (s, 3H), 5.01 (s, 2H), 5.88 (s, 2H), 6.63 (d, *J* = 15.4 Hz, 2H), 6.82 (d, *J* = 2.6 Hz, 2H), 7.04 (d, *J* = 1.9 Hz, 1H)

¹³C NMR(100MHz; CDCl₃): 153.7, 151.345, 150.9, 146.133, 141.4, 126.4, 122.8, 114.6, 113.3, 111.3, 109.7, 100.9, 96.6, 66.8, 61.6, 55.9, 55.7, 33.4, 25.9

3-(6-Methoxybenzo[d][1,3]dioxol-5-yl)propyl cinnamate (48)

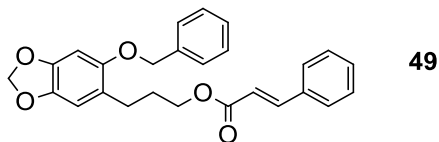


Acylation of **45** (100 mg, 0.48 mmol) with cinnamoyl chloride (106 mg, 0.71 mmol) and DMAP (9 mg, 0.071) in dry DCM (2 mL), yielded 122mg (75%) **48** as a white powder.

¹H NMR (400 MHz, CDCl₃): δ ppm 2.03-1.90 (m, 2H), 2.69-2.63 (m, 2H), 3.75 (s, 3H), 4.21 (t, *J* = 6.6 Hz, 2H), 5.87 (s, 2H), 6.45 (d, *J* = 16.0 Hz, 1H), 6.51 (s, 1H), 6.66 (s, 1H), 7.41-7.36 (m, 3H), 7.56-7.51 (m, 2H), 7.68 (d, *J* = 16.0 Hz, 1H)

¹³C NMR (100MHz; CDCl₃): 167.1, 152.3, 146.2, 144.6, 140.8, 134.5, 130.2, 128.9, 128.1, 121.8, 118.3, 109.8, 100.9, 94.7, 64.2, 56.3, 29.1, 26.6

3-(6-(Benzyloxy)benzo[d][1,3]dioxol-5-yl)propyl cinnamate (49)

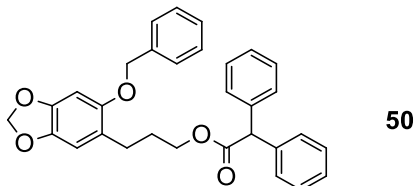


Compound **46** (100 mg, 0.35 mmol) in dry DCM (2 mL) containing DMAP (4 mg, 0.035 mmol) was reacted with cinnamoyl chloride (77 mg, 0.524 mmol) to obtain compound 139 mg (96%) of **49** as a white powder (139 mg, 96%).

¹H NMR (400 MHz, CDCl₃): δ ppm 2.04-1.96 (m, 2H), 2.77-2.71 (m, 2H), 4.23 (t, *J* = 6.48 Hz, 2H), 5.02 (s, 2H), 5.89 (s, 2H), 6.43 (d, *J* = 16.02 Hz, 1H), 6.59 (s, 1H), 6.70 (s, 1H), 7.55-7.27 (m, 10H), 7.67 (d, *J* = 16.03 Hz, 1H)

¹³C NMR (100MHz; CDCl₃): 167.1, 151.3, 146.2, 145.9, 144.6, 141.2, 137.3, 130.2, 128.9, 128.6, 128.1, 127.8, 127.1, 122.4, 118.2, 109.8, 100.9, 96.3, 71.2, 64.2, 29.2, 26.8

3-(6-(Benzyloxy)benzo[d][1,3]dioxol-5-yl)propyl 2,2-diphenylacetate (50)



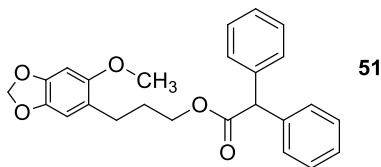
Compound **51** was synthesized via procedure **4B** by adding 121mg diphenylacetyl chloride (0.52mmol) dissolved in DCM to 100 mg (0.35 mmol) of **47**, DMAP (10 mg, 0.1 mmol) and Et₂N (121 mg, 0.52 mmol), in 2 ML of dry DCM. Purification of the crude by preparative HPLC H₂O: ACN (85%) afforded compound **51** as a white powder (52 mg, 35%).

¹H NMR (400 MHz, CDCl₃): δ ppm 1.92-1.81 (m, 2H), 2.57-2.51 (m, 2H), 4.12 (t, *J* = 6.5 Hz, 2H), 4.94 (s, 2H), 4.99 (s, 1H), 5.86 (s, 2H), 6.47 (s, 1H), 6.51 (s, 1H), 7.40-7.24 (m, 15H)

¹³C NMR (100MHz; CDCl₃): 172.5, 151.2, 146.2, 141.0, 138.8, 137.3, 129.1, 128.6, 128.6, 128.5, 127.9, 127.7, 127.4, 127.4, 127.2, 127.1, 122.2, 109.9, 100.9, 96.2, 71.1, 64.8, 57.2, 28.9, 26.7

HRMS calc. C₃₁H₂₈O₅: 480.1937, obtained: 480.19419

3-(6-(Benzyloxy)benzo[d][1,3]dioxol-5-yl)propyl benzoate (51)



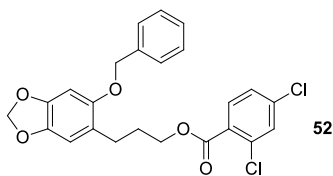
Reaction of **45** (100 mg, 0.35 mmol) with 120 mg (0.52 mmol) of diphenylacetyl chloride in dry DCM catalyzed by 10 mg (0.1 mmol) of DMAP, gave **51** which was purified by Column chromatography (hexanes: ethyl acetate, 8:2) afforded compound **51** as a white powder (87 mg, 62%).

¹H NMR (400 MHz, CDCl₃): δ ppm 1.88-1.81 (m, 2H), 2.52-2.47 (m, 2H), 3.68 (s, 3H), 4.13 (t, *J* = 6.5 Hz, 2H), 5.02 (s, 1H), 5.86-5.86 (m, 2H), 6.46 (d, *J* = 1.0 Hz, 2H), 7.34-7.23 (m, 10H)

¹³C NMR (100MHz; CDCl₃): 172.5, 152.2, 146.2, 140.6, 138.7, 128.6, 128.5, 127.2, 121.5, 109.8, 100.9, 94.6, 64.7, 57.2, 56.2, 28.9, 26.5

HRMS Calc. for C₂₅H₂₄O₅ 404.1624, obtained: 404.1635

3-(6-(benzyloxy)benzo[1,3]dioxol-5-yl)propyl 2,4-dichlorobenzoate (52)

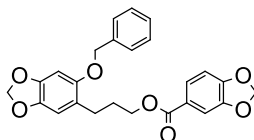


Compound **52** was synthesized following general procedure **4B**. Using the following amounts of reagents: compound **46** (100mg, 0.35mmol), anhydrous DCM (2mL), DMAP (10mg, 0.1mmol) 2,4-dichlorobenzoyl chloride (0.07mL, 0.524mmol). Purification of the crude by preparative HPLC H₂O: ACN (85%) afforded compound **52** as a white powder (11mg, 7%).

¹H NMR (400 MHz, CDCl₃): δ ppm 2.02 (tt, *J* = 13.1, 6.5 Hz, 2H), 2.76-2.71 (m, 2H), 4.31 (t, *J* = 6.4 Hz, 2H), 4.98 (s, 2H), 5.87 (s, 2H), 6.55 (s, 1H), 6.65 (s, 1H), 7.22 (dd, *J* = 8.4, 2.05 Hz, 1H), 7.40-7.27 (m, 5H), 7.44 (d, *J* = 2.0 Hz, 1H), 7.70 (d, *J* = 8.4 Hz, 1H)

¹³C NMR (100MHz; CDCl₃): 164.7, 151.1, 146.1, 141.0, 137.9, 136.9, 134.7, 132.3, 130.8, 128.4, 128.4, 127.7, 126.9, 126.8, 122.0, 109.6, 100.8, 96.1, 71.1, 65.2

3-(6-(Benzyloxy)benzo[d][1,3]dioxol-5-yl)propyl benzo[d][1,3]dioxole-5-carboxylate (53)



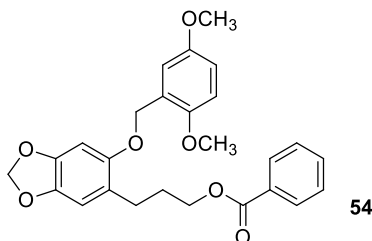
53

Compound **53** was obtained by coupling the alcohol **46** (100 mg, 0.35 mmol) with the acid compound **24** (87 mg, 0.5 mmol) in anhydrous DCM (2 mL). The coupling reaction was catalyzed by DMAP (4.3 mg, 0.0349 mmol) and DCC (44.04 mg, 0.349 mmol), Purification of the crude product by preparative HPLC H₂O: ACN (85%) afforded compound **53** as a white powder (10 mg, 7%).

¹H NMR (400 MHz, CDCl₃): δ ppm 2.08-1.96 (m, 2H), 2.76-2.71 (m, 2H), 4.28 (t, *J* = 6.4 Hz, 2H), 4.99 (s, 2H), 5.88 (s, 2H), 6.03 (s, 2H), 6.56 (s, 1H), 6.67 (s, 1H), 6.80 (d, *J* = 8.2 Hz, 1H), 7.42-7.27 (m, 5H), 7.43 (d, *J* = 1.6 Hz, 1H), 7.61 (dd, *J* = 8.2, 1.66 Hz, 1H)

¹³C NMR (100MHz; CDCl₃): 151.5, 151.3, 147.6, 146.2, 141.2, 137.2, 128.6, 127.8, 127.1, 125.3, 124.5, 122.4, 109.8, 109.5, 107.9, 101.7, 100.9, 96.3, 71.2, 64.6, 29.2, 26.9

3-(6-((2,5-Dimethoxybenzyl)oxy)benzo[d][1,3]dioxol-5-yl)propyl benzoate (54)



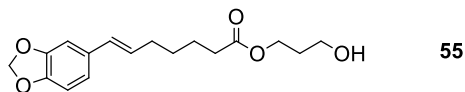
54

Acylation of alcohol **47** (24 mg, 0.1 mmol) with benzoyl chloride (14.61 mg, 0.1 mmol) in anhydrous DCM (5 mL) containing DMAP (12.7 mg, 0.104mmol), Et₂N (0.015 mL, 0.1 mmol) afforded compound **54** as a white powder (25 mg, 56%).

¹H NMR (400 MHz, CDCl₃): δ ppm 2.01 (qt, 2H, *J*=6.6 Hz), 2.76 (t, 2H, *J*=7.2 Hz), 3.71 (s, 3H), 3.78 (s, 3H), 4.31 (t, 2H, *J*=6.5 Hz), 4.99 (s, 2H), 5.85 (s, 2H), 6.58 (s, 1H), 6.65 (s, 1H), 6.78 (m, 2H), 7.04 (s, 1H), 7.39 (t, 2H, *J*=7.9 Hz), 7.51 (t, 1H, *J*=7.4 Hz), 7.98 (d, 2H, *J*=7.1 Hz)

HRMS: calc. C₂₆H₂₆O₇: 450.1679, obtained: 450.16783

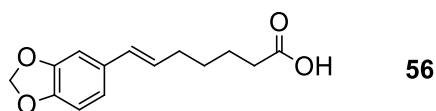
(E)-3-Hydroxypropyl 7-(benzo[d][1,3]dioxol-5-yl)hept-6-enoate (55)



Piperonal (891 mg, 5.94 mmol) was dissolved in dry THF and cooled in an ice bath and BF_3OEt_2 (5.3 mL, 42 mmol) was added. The reaction mixture was stirred for 10 min. After this time cyclohexanone (0.61 mL, 5.94 mmol) was added dropwise. The reaction mixture was removed from the ice bath and let to warm up to RT and stirred overnight. 1,3-Propanediol (2.21 mL, 5.15 mmol) was added dropwise to the resulting dark red colored solution. The mixture was allowed to react overnight to react. The reaction was quenched with NaHCO_3 (10 mL) and the aqueous phase was extracted with ethyl ether (2 X 100mL). The combined organic phase was washed with saturated NaHCO_3 (2 X 50mL), and dried over MgSO_4 . The solvent was removed under vacuum. The crude product was purified by Flash chromatography (8:2, hexanes: ethyl acetate). Compound **55** was obtained as an orange liquid (198 mg, 11%). The spectroscopy data for the obtained compound corresponds to that reported in previous literature⁵¹

$^1\text{H NMR}$ δ ppm (400 MHz, CDCl_3): 1.42 (m, 2H), 1.62 (m, 2H), 1.81 (qt, 2H, $J=6.4$ Hz), 2.13 (q, 2H, $J=7.2$ Hz), 2.28 (t, 2H, $J=7.6$ Hz), 3.62 (t, 2H, $J=6.0$ Hz), 4.16 (t, 2H, $J=6.4$ Hz), 5.85 (s, 2H), 5.96 (m, 1H), 6.21 (d, 1H, $J=15.6$ Hz), 6.67 (m, 1H), 6.69 (m, 1H), 6.83 (s, 1H)

(E)-7-(benzo[d][1,3]dioxol-5-yl)hept-6-enoic acid (56)



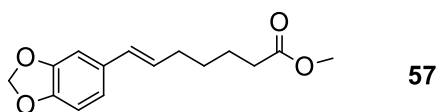
Compound **56** (169 mg, 0.55 mmol) was dissolved in H_2O : MeOH (1:3), to this KOH was added (93 mg, 1.69 mmol). The resulting reaction mixture was refluxed for 1h, cooled to R.T., diluted with water (10 mL) and extracted with DCM (2 X 10 mL). The aqueous phase was acidified with HCl (10%) and then extracted using ethyl acetate (3 X 10 mL). The combined organic phase was washed with saturated NaHCO_3 (2 X 50 mL), and dried over MgSO_4 . The solvent was removed

under vacuum. The crude product was purified by Flash chromatography (8:2, hexanes: ethyl acetate). Compound **56** was obtained as a yellowish liquid (73mg, 53%).

¹H NMR (400 MHz, CDCl₃): δ ppm 1.50 (m, 2H), 1.69 (m, 2H), 2.18 (q, 2H, J=7.2 Hz), 2.38 (t, 2H, J=7.2 Hz), 5.96 (s, 2H), 6.05 (m, 1H), 6.30 (d, 1H, J=16 Hz), 6.72 (m, 2H), 6.87 (s, 1H)

¹³C NMR (100MHz; CDCl₃): 179.6, 147.9, 146.6, 132.3, 129.8, 128.5, 120.3, 108.2, 105.4, 100.9, 33.8, 32.5, 28.8, 24.2

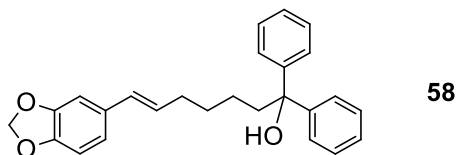
(E)-Methyl 7-(benzo[d][1,3]dioxol-5-yl)hept-6-enoate (**57**)



Freshly distilled methanol (5mL) was placed in a RBF equipped with a condenser and under nitrogen atmosphere; NaOCH₃ (30 mg, 1.3 mmol) was added. Compound **56** (130 mg, 0.42 mmol) was dissolved in MeOH and added dropwise. The reaction mixture was refluxed for 3h. After this time, the reaction was left to cool to R.T. and water was added (5mL). The aqueous phase was extracted using ethyl acetate (3 X 30 mL). The combined organic phase was washed with saturated NaHCO₃ (2 X 50 mL), and dried over MgSO₄. The solvent was removed under vacuum. The crude product was purified by flash chromatography (8:2, hexanes: ethyl acetate). Compound **57** was obtained as a yellow liquid (49 mg, 44%).

¹H NMR (400 MHz, CDCl₃): δ ppm 1.50 (m, 2H), 1.69 (m, 2H), 2.18 (q, 2H, J=8.0 Hz), 2.38 (t, 2H, J=7.4 Hz), 3.62 (s, 3H), 5.96 (s, 2H), 6.05 (m, 1H), 6.30 (d, 1H, J=15.8 Hz), 6.72 (m, 2H), 6.87 (s, 1H)

(E)-7-(benzo[d][1,3]dioxol-5-yl)-1,1-diphenylhept-6-en-1-ol (58)



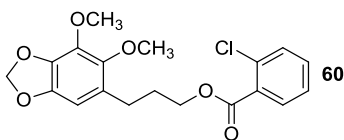
Compound **58** dissolved in anhydrous THF (1mL) was added to a 0 °C solution of PhMgBr (0.1 mL, 0.34 mmol) in 5 mL of anhydrous THF. The mixture was stirred for 1 hour at that temperature. The ice bath was removed and reaction was left to reach R.T. After 2 h stirring at room temperature the mixture was quenched with 2 mL of HCl (1N) aqueous solution. The aqueous phase was extracted using ethyl acetate (3 X 30 mL). The combined organic phase was washed with saturated NaHCO₃ (2 X 50 mL), and dried over MgSO₄. The solvent was removed under vacuum. The crude product was purified by flash chromatography (8:2, hexanes: ethyl acetate). Compound **58** was obtained as a yellow liquid (30 mg, 52%).

¹H NMR (400 MHz, CDCl₃): **δ ppm** 1.50 (m, 2H), 1.69 (qt, 2H, J=7.3 Hz), 2.18 (q, 2H, J=7.0 Hz), 2.38 (m, 2H), 5.96 (s, 2H), 6.05 (m, 1H), 6.30 (d, 1H, J=15.8 Hz), 6.72 (m, 2H), 6.87 (s, 1H), 7.23 (m, 2H), 7.31 (t, J=7.9 Hz, 4H), 7.42 (d, 4H, J=7.1 Hz)

¹³C NMR (100MHz; CDCl₃): 147.9, 147.1, 146.6, 132.4, 129.5, 129.1, 128.2, 128.2, 126.9, 126.8, 126.0, 120.2, 108.2, 105.4, 100.9, 41.8, 32.7, 29.8, 23.3

HRMS: C₂₆H₂₆O₃: 386.1882, obtained: 386.18813

3-(6,7-dimethoxybenzo[d][1,3]dioxol-5-yl)propyl 2-chlorobenzoate (60)



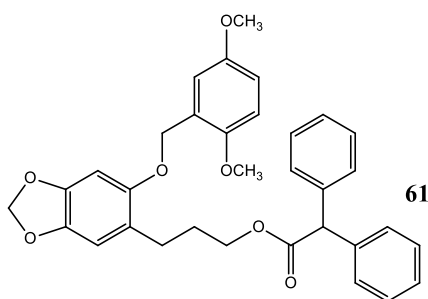
Compound **60** was synthesized following general procedure **4B**. Using the following amounts for the corresponding reagents alcohol **8** (100 mg, 0.416 mmol), dry DCM (3 mL), DMAP (5.08 mg, 0.0416 mmol), 2-chlorobenzoic acid (98 mg, 0.624 mmol), DCC (85.83 mg, 0.000416 mmol)

soluble in dry DCM was added. The crude was purified by Flash chromatography (8:2, hexanes: ethyl acetate) to obtain compound **60** as an orange oil (75.0 mg, 48%)

¹H NMR (400 MHz, CDCl₃): δ ppm 2.05-1.95 (m, 2H), 2.70-2.65 (m, 2H), 3.74 (s, 3H), 3.98 (s, 3H), 4.33 (t, *J* = 6.42 Hz, 2H), 5.85 (s, 2H), 6.34 (s, 1H), 7.31-7.26 (m, 1H), 7.44-7.36(m, 2H), 7.79 (dd, *J* = 7.71, 1.60 Hz, 1H)

165.8, 144.5, 144.5, 137.7, 135.9, 133.6, 132.5, 131.4, 131.1, 130.4, 127.1, 126.6, 102.6, 101.1, 65.1, 61.2, 59.9, 29.7, 26.6

3-(6-methoxybenzo[d][1,3]dioxol-5-yl)propyl benzoate (**61**)



Compound **61** was synthesized using procedure **4A** and the following amount of reagents: Compound **47** (85 mg, 0.4093 mmol) was dissolved in CH₂Cl₂ (5 mL) and triethylamine (0.685 mL, 0.607 mmol) DMAP (2 mg), benzoyl chloride (85.25 mg, 0.61 mmol) to yield compound **61** (118.3 mg, 92.0%) as a clear oil.

¹H NMR (400 MHz, CDCl₃): δ ppm 1.96-1.85 (m, 2H), 2.59-2.54 (m, 2H), 3.71 (s, 3H), 3.78 (s, 3H), 4.14 (t, *J* = 6.5 Hz, 2H), 4.97 (s, 2H), 5.01 (s, 1H), 5.85 (s, 2H), 6.46 (s, 1H), 6.56 (s, 1H), 6.79 (d, *J* = 2.4 Hz, 2H), 7.02-7.00 (m, 1H), 7.31-7.23 (m, 10H)

¹³C NMR (100MHz; CDCl₃): 172.5, 153.6, 151.3, 150.7, 146.2, 140.9, 138.7, 128.6, 128.5, 127.2, 126.7, 122.0, 114.1, 112.9, 111.0, 109.7, 100.9, 96.2, 66.1, 64.7, 57.1, 55.8, 55.6, 28.8, 26.7

HRMS: Calc. C₃₃H₃₂O₇: 540.2148, obtained: 540.2190

Bioassays

This part of the work is done in collaboration with Suqi Liu, PhD. Candidate at Dr. Arnason's group

1. A CYP 3A4 assay was used for fast screening the active compounds

Enzyme inhibition assays are conducted with a cloned CYP3A4 isozyme. The method described by Foster and co-workers⁵⁷ was used for this isozyme. Assays were performed in clear-bottom, opaque-welled microtiter plates. Wells are designated as either "Control," "Blank," "Test," or "Test-Blank." Control wells consist of ddH₂O and NADPH (β -nicotinamide adenine dinucleotide phosphate) solution; blank wells consist of ddH₂O and buffer solution; test wells consist of the derivatives of dillapiol at a particular concentration and NADPH solution; and test-blank wells consist of the corresponding derivative compounds and buffer solution. Enzyme solution will be added to all wells. A Millipore Cytofluor 4000 Fluorescence Measurement System set to 485-nm excitation filter (20-nm bandwidth) will be used to analyze each plate. Percent inhibition calculations were based on differences in fluorescence at a single time point between the control/blank wells and test/test blank wells. All assays were performed under gold fluorescent lighting.

2. Bioassay with Colorado Potato Beetle (*L. decemlineata*):

Potato leaves were collected from greenhouse-grown plants and cut into 4 cm diameter discs. In the topical method, the larvae were transferred to the leaf disc and a dose of 1 μ l or 5 μ l of the different solutions was applied using a micro-applicator on the dorsal thoracic region of the 2nd or 4th instar larvae respectively. The treated as well as control larvae were held under the same condition and mortality was recorded at 24 and 48h. For the ingestion method, each leaf disc was dipped into the different solutions for 3 seconds. All leaf discs were held in the fume hood for 20 min to ensure adequate drying before transferring the disc to a petri dish. CPB larvae were placed on each leaf disc and the petri dishes were put into a holding chamber. Mortality was assessed at 24 and 48h.

3.1.4 References

1. FAO *International Code of Conduct on the Distribution and Use of Pesticides (Revised Version)* At <http://www.fao.org/docrep/005/y4544e/y4544e00.htm>. Accessed December 2013.
2. Sifakis, S., Mparmpas, M., Soldin, O. P. & Tsatsakis, A. Pesticide Exposure and Health Related Issues in Male and Female Reproductive System. *Pesticides - Formulations, Effects, Fate* (2011).
3. Okello, J. J. & Swinton, S. M. International Food Safety Standards and the Use of Pesticides in Fresh Export Vegetable Production in Developing Countries : Implications for Farmer Health and the Environment. *Pesticides - Formulations, Effects, Fate* (2011).
4. Ecobichon, D. J. Pesticide use in developing countries. *Toxicology* **160**, 27–33 (2001).
5. Ntalli, N. G. & Menkissoglu-spirodi, U. Pesticides of Botanical Origin : A Promising Tool in Plant Protection. *Pesticides - Formulations, Effects, Fate* (2011).
6. European, C. “ *our food has become greener* ”. At http://ec.europa.eu/food/plant/plant_protection_products/eu_policy/docs/factsheet_pesticides_en.pdf (2009). Accessed december 2013
7. Isman, M. B. Botanical insecticides, deterrents, and repellents in modern agriculture and an increasingly regulated world. *Annual review of Entomology* **51**, 45–66 (2006).
8. Isman, M. B. Botanical insecticides : for richer , for poorer. *Pest Manag Sci* **11**, 8–11 (2008).
9. Lewis, W. M. J. evolutionary interpretations of allelochemical interactions in phytoplankton algae. *The American Naturalist* **127**, 184–194 (1986).
10. Scott, I. M. Analysis of Piperaceae germplasm by HPLC and LCMS: a method for isolating and identifying unsaturated amides from Piper spp extracts. *Journal of Agricultural and Food Chemistry* **53**, 1907–13 (2005).
11. Kato, M. J. & Furlan, M. Chemistry and evolution of the Piperaceae. *Pure and Applied Chemistry* **79**, 529–538 (2007).
12. Dos Santos, P. R., De Limas Moreira, D., Guimarães, E. F. & Kaplan, M. a Essential oil analysis of 10 Piperaceae species from the Brazilian Atlantic forest. *Phytochemistry* **58**, 547–51 (2001).
13. Virinder S. Parmar,* Subhash C. Jain, Kirpal S. Bisht, Rajni Jain, Poonam Taneja, Amitabh Jha, OM D. Tyagi, Ashok K. Prasad, Jesper Wengel, t C. E. O. and P. M. B. phytochemistry of the genus piper. *Phytochemistry* **46**, 597–673 (1997).
14. Dyer, L. A., Richards, J. & Dodson Isolation, Synthesis, and Evolutionary Ecology of Piper amides. *Piper: A Model Genus for Studies of Phytochemistry, Ecology, and Evolution* 117–139 (2004).

15. C, B. Bernard, H.G. Krishnamurty, D. Chauret, I. & Durst, B.J.R. Philogene, j P. Sanchez-Vindas, C. Hasbun, L. Poveda, L. San Roman, and J. T. A. Insecticidal defenses of Piperaceae from the neotropics. *Journal of Chemical Ecology*, **21**, 803–814 (1995).
16. Puniani, E. Novel natural product based anti-anxiety therapy and natural insecticides. (2004).
17. Scott, I. M. *et al.* Botanical insecticides for controlling agricultural pests: piperamides and the Colorado Potato Beetle *Leptinotarsa decemlineata* say (Coleoptera: Chrysomelidae). *Archives of insect biochemistry and physiology* **54**, 212–25 (2003).
18. Assis, A. *et al.* Essential oils composition of four Piper species from Brazil. *Journal of Essential Oil Research* 1–7 (2013).doi:10.1080/10412905.2013.767755
19. Oyedeji, O. a, Adeniyi, B. a, Ajayi, O. & König, W. a Essential oil composition of Piper guineense and its antimicrobial activity. Another chemotype from Nigeria. *Phytotherapy research : PTR* **19**, 362–4 (2005).
20. De Almeida, R. R. P., Souto, R. N. P., Bastos, C. N., Da Silva, M. H. L. & Maia, J. G. S. Chemical variation in Piper aduncum and biological properties of its dillapiole-rich essential oil. *Chemistry & biodiversity* **6**, 1427–34 (2009).
21. Islands, S. The invasive shrub Piper aduncum in Papua New Guinea : a review. **22**, 202–213 (2010).
22. Martínez, J., Rosa, P. T. V, Ming, L. C., Marques, M. O. M. & Angela, M. Extraction of volatile oil from *Piper aduncum* L. with supercritical carbon dioxide. At: <http://www.isasf.net/fileadmin/files/Docs/Versailles/Papers/N10.pdf>. Accessed December 2013.
23. Potzernheim, M. C. L., Bizzo, H. R., Silva, J. P. & Vieira, R. F. Chemical characterization of essential oil constituents of four populations of *Piper aduncum* L. from Distrito Federal, Brazil. *Biochemical Systematics and Ecology* **42**, 25–31 (2012).
24. Rafael, M. S., Hereira-Rojas, W. J., Roper, J. J., Nunomura, S. M. & Tadei, W. P. Potential control of Aedes aegypti (Diptera: Culicidae) with *Piper aduncum* L. (Piperaceae) extracts demonstrated by chromosomal biomarkers and toxic effects on interphase nuclei. *Genetics and molecular research : GMR* **7**, 772–81 (2008).
25. Ciccio, Jose F.; Ballesteros, C. M. Constituyentes Volátiles de las hojas y espigas de piper aduncum (Piperaceae) de Costa Rica. *Rev. Biol. Tropical* **2**, 783–790 (1997).
26. Vila, R., Tomi, Felix Mundina, Marisa Santana, Ana I. Solis, Pablo N. Lopez Arce, Jose B. Balderrama Iclina, J. L. & Iglesias, Jose Gupta, Mahabir P. Casanova, Joseph Cañigueral, S. Unusual composition of the essential oils from the leaves of Piper aduncum. *Flavour and Fragrance Journal* **20**, 67–69 (2005).
27. Taylor, P. Essential Oils of Piper peltata (L .) Miq . and Piper aduncum L . from Cuba. *Journal of essential oil research* **16**, 3–6 (2004).

28. Maia, Â. G. S. Constituents of the essential oil of *Piper aduncum* L. growing wild in the Amazon region. *Flavour and Fragrance Journal* **13**, 269–272 (1998).
29. Guerrini, A. *et al.* Bioactivities of *Piper aduncum* L. and *Piper obliquum* Ruiz & Pavon (Piperaceae) essential oils from Eastern Ecuador. *Environmental Toxicology and Pharmacology* **27**, 39–48 (2009).
30. De Almeida, R. R. P., Souto, R. N. P., Bastos, C. N., Da Silva, M. H. L. & Maia, J. G. S. Chemical variation in *Piper aduncum* and biological properties of its dillapiole-rich essential oil. *Chemistry & Biodiversity* **6**, 1427–34 (2009).
31. Yu, S J, Terriere, L. C. Bimodal Effect of Methylenedioxyphenyl on Detoxifying Enzymes in the. *Pesticide Biochemistry and Physiology* **4**, 160–169 (1973).
32. Taylor, P., Bernard, C. B. & Philogène, B. J. R. Journal of Toxicology and Environmental Health : Current Issues Insecticide synergists : Role , importance , and perspectives. *Journal of Toxicology and Environmental Health* **38**, 199–223 (1993).
33. Casida, J. E. Mixed-function oxidase involvement in the biochemistry of insecticide synergists. *Journal of Agricultural and Food Chemistry* **18**, 753–72 (1970).
34. Scott, J. G. & Wen, Z. Cytochromes P450 of insects: the tip of the iceberg. *Pest management science* **57**, 958–67 (2001).
35. Sun, Yun-Pei, Johnson, E. R. Synergistic and antagonistic actions of insecticide-synergist combinations and their mode of action. *Agricultural and food chemistry* **8**, 261–266 (1960).
36. Murray, M. Modulation of Cytochromes P450 by phytochemicals. *Cytochromes P450 : role in the metabolism and toxicity of drugs and other xenobiotics*. RCS Publishing. First Ed. (2008).
37. Gulati, K. C., Parmar, B. S. Indian Patent 119536.
38. Belzile, A.-S. Dillapiol Derivatives as Synergists: Structure–Activity Relationship Analysis. *Pesticide Biochemistry and Physiology* **66**, 33–40 (2000).
39. Mukerjee, K. New Methylenedioxyphenyl synergists for pyrethrins. *J. Agric. Food Chem.* **27**, 1209–1211 (1979).
40. Tomar, S. S., Maheshwari, M. L. & Mukerjee, S. K. Synthesis and synergistic activity of dillapiole based pyrethrum synergists. *Journal of Agricultural and Food Chemistry* **27**, 547–550 (1979).
41. Synerholm, M. E. Safrole-sulfoxide and sulfone insecticide and pyrethrin synergist. Patent US2486445.(1946).
42. Majerus, S. L. A novel synthesis of dillapiol and its derivatives and their role as chemosensitizers and insecticide synergists. Master Thesis. Ottawa University. 133 (1997).

43. Budzinski, J. W., Foster, B. C., Vandenhoeck, S. & Arnason, J. T. An in vitro evaluation of human cytochrome P450 3A4 inhibition by selected commercial herbal extracts and tinctures. *Phytomedicine* **7**, 273–282 (2000).
44. Factsheet, W. Chemical WATCH Factsheet. At: <http://www.beyondpesticides.org/pesticides/factsheets/Glyphosate.pdf> . Accessed December 2013.
45. Diel, F. Pyrethroids and piperonyl-butoxide affect human T-lymphocytes in vitro. *Toxicology Letters* **107**, 65–74 (1999).
46. Kakko, I., Toimela, T. & Tähti, H. Piperonyl butoxide potentiates the synaptosome ATPase inhibiting effect of pyrethrin. *Chemosphere* **40**, 301–5 (2000).
47. EPA Reregistration Eligibility Decision for Piperonyl Butoxide (PBO). (2006).At: http://www.epa.gov/oppsrrd1/REDs/piperonyl_red.pdf. Accessed December 2013.
48. Pacák, P. Molar refractivity and interactions in solutions I . Molar refractivity of some monovalent ions in aqueous and dimethyl sulfoxide solutions. *Chem. papers* **43**, 489–500 (1989).
49. Computer aided molecular design. At <http://www.chemcomp.com/> (2013).Accessed December 2013.
50. Rosales, M., Durán, J. a., González, Á., Pacheco, I. & Sánchez-Delgado, R. a. Kinetics and mechanisms of homogeneous catalytic reactions. *Journal of Molecular Catalysis A: Chemical* **270**, 250–256 (2007).
51. Strunz, G. M. & Finlay, H. Concise , Efficient New Synthesis of Pipericide , an Insecticidal Unsaturated Amide from Piper nigrum , and Related Compounds. *Tetrahedron* **50**, 11113–11122 (1994).
52. Nagumo, Shinji; Matsukuma, Aki, Suemune, Hiroshi; Sakai, K. Novel Ring Cleavage Based on Intermolecular Aldol Condensation. *Tetrahedron* **49**, 10501–10510 (1993).
53. Strunz, G. M. & Finlay, H. Synthesis of sarmentosine, an amide alkaloid from Piper sarmentosum. *Phytochemistry* **39**, 731–733 (1995).
54. Zanger, U. M. & Schwab, M. Cytochrome P450 enzymes in drug metabolism: Regulation of gene expression, enzyme activities, and impact of genetic variation. *Pharmacology & Therapeutics* **138**, 103–141 (2013).
55. Feyereisen, R. Evolution of insect P450. *Biochemical Society Transactions* **34**, 1252–5 (2006).
56. Salminen, K. A. Simple , Direct , and Informative Method for the Assessment of CYP2C19 Enzyme Inactivation Kinetics ABSTRACT : *Drug Metabolism and Disposition* **39**, 412–418 (2011).

57. Foster, B. C. Comparative study of hop-containing products on human cytochrome p450-mediated metabolism. *Journal of Agricultural and Food Chemistry* **57**, 5100–5 (2009).
58. Budzinski, J. W. CYP3A4 Bioassay results. Non-published data. (2000).
59. Achaleke, J., Martin, T., Ghogomu, R. T., Vaissayre, M. & Brévault, T. Esterase-mediated resistance to pyrethroids in field populations of *Helicoverpa armigera* (Lepidoptera: Noctuidae) from Central Africa. *Pest Management Science* **65**, 1147–54 (2009).
60. Pittman, C. U. & Honnick, W. D. Rhodium-catalyzed hydroformylation of allyl alcohol. A potential route to 1,4-butanediol. *J.O.C.* **886**, 2132–2139 (1980).
61. Shriner, S. R. L. & Kleiderer, E. C. Piperonylic acid. *Organic Syntheses Coll. Vol2.* **2**, 538 (1943).
62. Tanimori, S., Watanabe, K. & Kiriata, M. Synthesis of cinnamyl-sesamol derivatives. *Research on Chemical Intermediates* **35**, 909–917 (2009).
63. Approach, N. & Synthesis, H. A new approach to the synthesis of isoflavones 2'-hydroxyisoflavones and alternative synthesis of (+-) pterocarpin. *Agri. Biol.Chem.* **31**, 1490–1498 (1967).
64. Tang, Y., Wei, Z., Zhong, W. & Liu, X. Diiron Complexes with Pendant Phenol Group(s) as Mimics of the Diiron Subunit of [FeFe]-Hydrogenase: Synthesis, Characterisation, and Electrochemical Investigation. *Eur. Jic.* **2011**, 1112–1120 (2011).

4.1 Towards the design of Cx30, Cx36 and Cx43 blockers as potential spinal cord injury treatments

4.1.1 Introduction

Cellular communication is a vital component in any living organism as it is essential for tissue, organ and organismal development. The existence of this cell to cell communication is the basis for development and homeostasis of tissues and multicellular organisms¹.

The connexins are a family of integral membrane proteins that oligomerize into clusters of intercellular channels that connect the cytoplasm of neighbouring cells therefore, allowing the communication between them; this is also called gap junctions²⁻⁴. This communication is mediated by the intercellular transfer of various ions and molecules bearing a size less than 1.0 kDa, such as nutrients, secondary messengers (such as inositol-1,4,5-triphosphate (IP-3), metabolites, cations and anions^{5,6}.

Six connexin subunits can assemble to form a hemi-channel or connexon in the plasma membrane that can dock to another hemi-channel in the plasma membrane of an adjacent cell, in order to assemble a complete gap junctional channel (**Figure 4-1**).

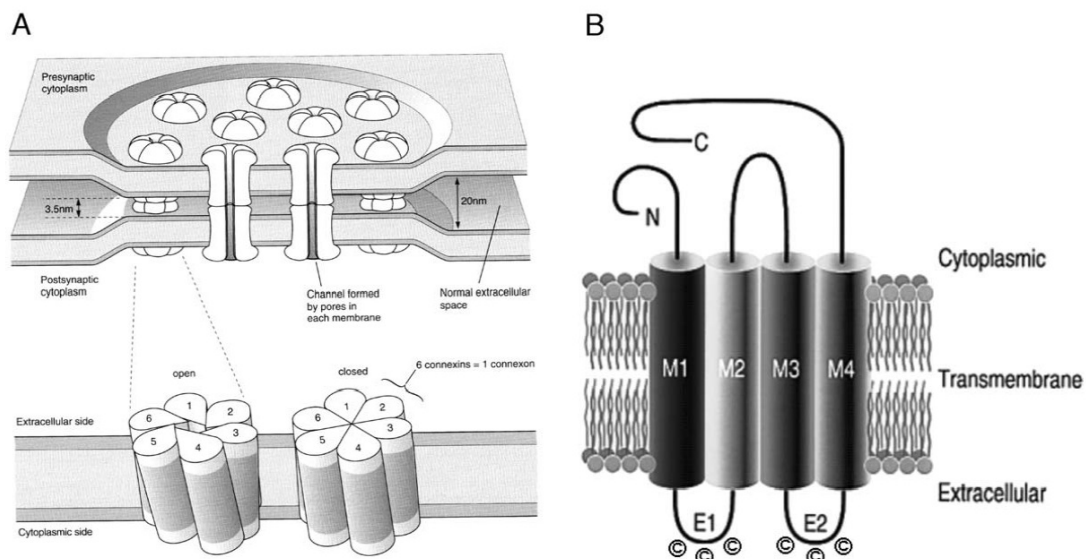


Figure 4-1: A. schematic representation of the gap junction **B.** Topological model of a connexin. Figure from ref ⁶.

The size of the molecules and ions that can be transferred via these channels is limited by the pore size; the size of a gap-junction pore is around 1.0–1.5 nm in diameter³. There are 21 genes in humans that code for different connexins⁷. Connexins are present in different cells in the body and have different physiological characteristics where the properties of the resulting hemi-channel are determined by the combination of connexins that forms the ensemble. Connexons can dock with an identical connexon in the adjacent cell to form a homotypic intercellular channel or to a different connexon to form a heterotypic channel⁴.

The most commonly used nomenclature system identifies each connexin (Cx) by its species of origin and predicted molecular mass: for example, mCx34 refers to a mouse connexin with a predicted mass of 34 kD². They may also be divided into three groups: α , β , and γ , according to their extent of sequence identity and length of the cytoplasmic loop. Connexins in a gap junction can be abbreviated as Gj and a number corresponding to the order of discovery, so Gj α 1 refers to the mCx34, the first connexin discovered in mouse in the α group⁶.

This communication between cells is thought to have an influence in several functions such as: regulation of growth, cell differentiation, and developmental signalling². If the hemi-channels do not dock they remain as hemi-channels and they have similar transporting properties as the ones observed for the gap-junction channels³. The gap-junction, channels and hemi-channels play diverse roles in the tissues where they are present (**Table 4.1.1.1**). Research done by knocking out some of the genes involved in the expression of connexins has shown that this interferes with the gap-junction and hemi-channel formation and these modifications have resulted in several diseases. These findings make connexins an interesting target for the development of new drugs⁸.

The central nervous system (CNS) has 11 different connexins and is highly coupled through the Gap-junction network. Cx26, 30, 32, 36, 37, 40, 43 and 45 are well expressed in the brain with a unique expression pattern for each one during differentiation⁸. In a healthy CNS they play an important role in electrochemical and metabolic coupling by mediating intercellular transfer of various ions and molecules, hemi-channels remain closed in order to avoid dissolution of ionic gradients and leakage of cytoplasmic constituents; nevertheless, the physiological changes

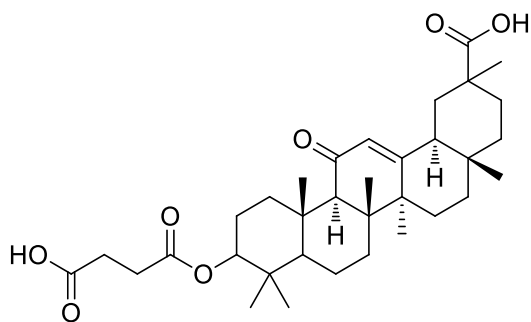
caused by anoxia conditions and ischemia provokes the opening of these hemi-channels. This opening translates into cell swelling and cell death⁵.

After injury (such as stroke, spinal cord injury, and excitotoxic injury) certain connexins are protective whereas others contribute to the injury. Hemi-channels have a much larger opening (~10 Å), than a Gap-junction, allowing the efflux of small cytosolic compounds like ATP and glutamate. Once these are released they will act as transmitters and if the hemi-channels remain open for long periods of time this could jeopardize cellular survival⁹. Cx43 has been linked to the release of ATP by hemi-channels and a high concentration of ATP induces acute inflammatory responses¹⁰. Tissue swelling, especially in the vertebral canal, can reduce tissue perfusion and cause secondary ischemia. The delayed loss of tissue affects functional recovery in spinal cord injured patients, and no effective treatment options currently exist⁹.

Table 4.1.1.1: Roles played by hemi-channels, connexins and Gap-junction in different organs, adapted from *Kar et al. 2012*⁸.

	Organ	Role
Connexin	Brain, inner ear, kidney, liver	Cell death
	Bone, brain, inner ear, heart, ovary, lung, liver	Differentiation
	Brain, bone, heart, lens, ovary, testis, liver	Proliferation, survival
Gap junction channels	Brain, inner ear, heart, kidney, lens, lung, liver	Ionic conduction
	Brain, lens, liver	Metabolic coupling
	Inner ear, ovary, lung, liver	2 nd messenger diffusion
Hemi-channels	Heart	Injury protection
	Brain, heart	preconditioning
	Bone, brain, kidney, ovary, lung, liver	Extracellular cell signalling
	Bone, ovary	Mechanical stimulation, response

Two very different compounds, carbenoxolone **IA** and octanol are known to be capable of inhibiting Gap junction intercellular communication (GJIC). The treatment of ischemic events in pups with carbenoxolone after intrauterine hypoxia–ischemia decreases neuronal damage, similar results have been observed for octanol⁸.



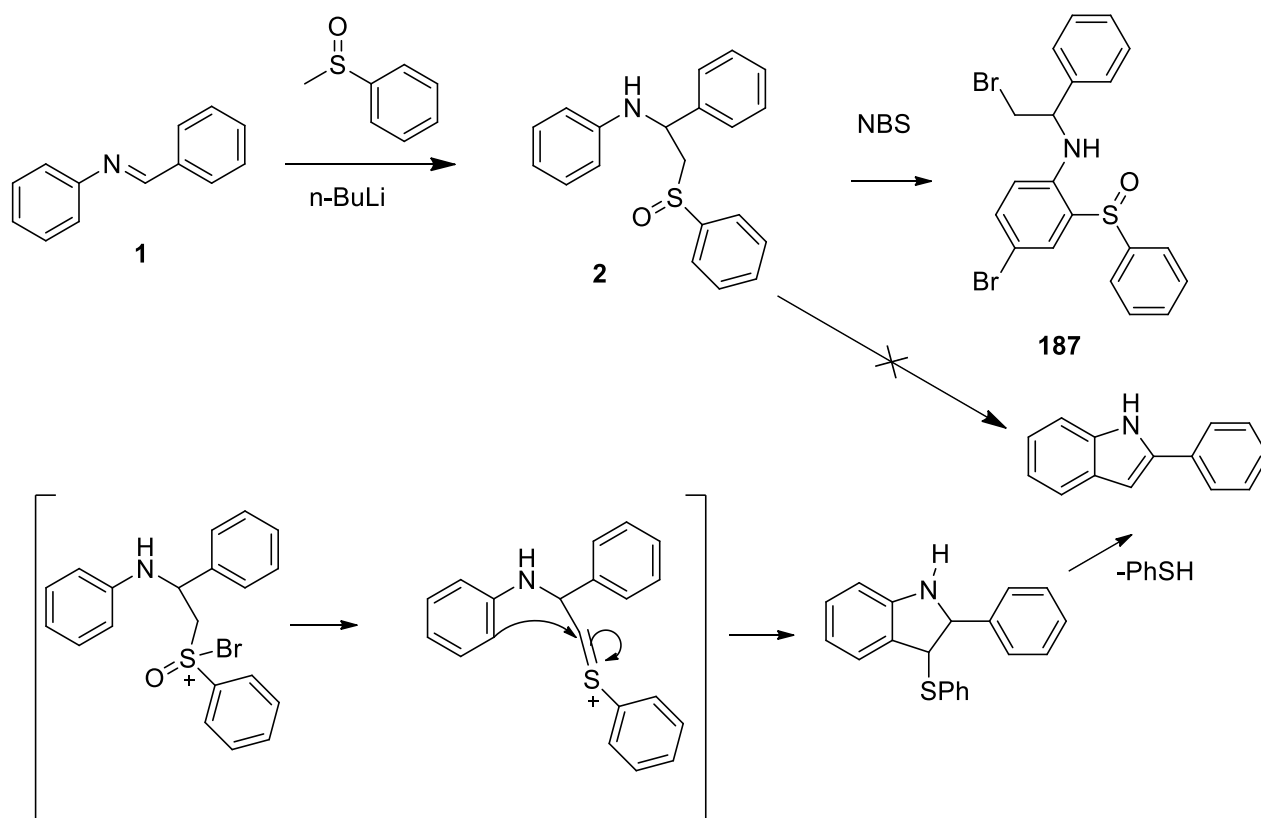
Carbenoxolone IA

In the design of new and better drugs for ischemia, the major challenge is to design structures that can pass through the gap-junction and the hemi-channels to be capable of modulating cellular function. Identification of these molecules will contribute to the development of effective therapeutic means to treat diseases caused by defective or overactive gap-junction or hemi-channel functions⁸. It may also help reduce damage caused by injuries such as spinal cord injuries.

The objective of the work presented in this section was the discovery and development of a small molecule that targets the inhibition of specific connexins: Cx30, Cx36 and Cx43. All the bioassays presented in this section were undertaken by MSc. student Matthew Cook at Dr. Stephanie Bennett's laboratory, Faculty of Medicine at Ottawa University.

4.1.2 Results and Discussion

In 2004, Martin Charron, a Master student in Dr. Durst's research group was interested in discovering new synthetic methods for the formation of indole¹¹. In order to achieve this, a new synthetic path was proposed (**Scheme 4.1**).



Scheme 4.1: Synthesis of compound **187**

However, the formation of the indole ring was not observed and another compound was obtained instead. The structure he assigned to this compound is depicted in Scheme 2.2.2.1. This compound was purified and kept in Dr. Durst's library of compounds with the code number **187** until the summer of 2011 when MSc. student Matthew Cooke at Dr. Stephanie Bennett's research group requested compounds from the existing library for testing in a new bioassay that targets inhibition of connexins from CNS.

Image **A** in **Figure 4-2** shows that compound **187** decreases gap-junction activity; this can be analyzed through the amount of calcein **13** that is present in the image. As seen in the image, the amount of calcein passing through the gap-junction is higher when the vehicle (DMSO) is used than in the presence of compound **187**.

Calcein is a fluorescent "tracer" that is membrane impermeable but passes through gap junctions. Fluorescent dyes are commonly used to assess which molecules or ions are passing through gap junctions. In this bioassay, the amount of calcein that spreads to neighbouring cells is quantified and used as a measurement of gap junction function. The fact that compound **187**

reduced the amount of calcein that passed through, led Matthew Cooke and Dr. Bennett to conclude that the compound has an inhibitory effect on connexins. This finding is very important because most of the drugs that are used to inhibit connexin function (such as carbenoxolone) are non-specific since they inhibit all connexins to the same degree¹². This makes bioactive compounds like carboxolone, un-suitable for therapeutic uses. The ideal drug should inhibit specifically a type of connexin that is expressed in the CNS like Cx30, Cx32, Cx36 and Cx43. These connexins are found in neurons, astrocytes, and the neural stem cells of the adult brain. After injury (such as stroke, spinal cord injury, excitotoxic injury) certain connexins are protective and others contribute to the injury⁸. The discovery of a small molecule that targets CNS connexins could lead to its use as a drug to promote neurogenesis, since connexins play an important role in the regulation of stem cell differentiation and proliferation in many tissues, including the CNS. For example, Cx30 and Cx43 are known to regulate the proliferation of immature neural progenitors in the adult brain, whereas an increase in Cx32 expression is related to differentiation to oligodendrocytes. Furthermore, Cx36 is related to differentiation of stem cells to neurons. Therefore, it would be extremely useful to have connexin-specific compounds that we could administer to selectively regulate these events so as to promote neurogenesis and repair damaged tissue^{8,13}.

Image B in **Figure 4-2** evaluates the Connexin hemichannel (single membrane channel) and the Gap junctional intercellular communication (GJIC). Hemi-channels are normally closed to promote homeostasis, but they can open as a consequence of an injury, providing a channel from the cell to the extra cellular space. In this assay, cells were incubated in a solution with Lucifer yellow **14**, which is a fluorescent compound that passes through connexin channels. The cells were then washed and viewed under a microscope to see how many cells took up Lucifer yellow from the extracellular space through the hemi-channels. Cells with higher intake of Lucifer yellow have greater hemichannel activity. The results observed for compound **187** show that this compound does not affect the opening of the hemi-channels but instead it displays a specific activity solely on GJIC.

As part of this assay, glass beads are used to provoke mechanical opening stimulation of the hemi-channels and carboxolone is used as a positive control. Taken together, these data

suggest that compound **187** reduces connexin-mediated intercellular channel function but not single membrane channels in non-junctional membranes¹³.

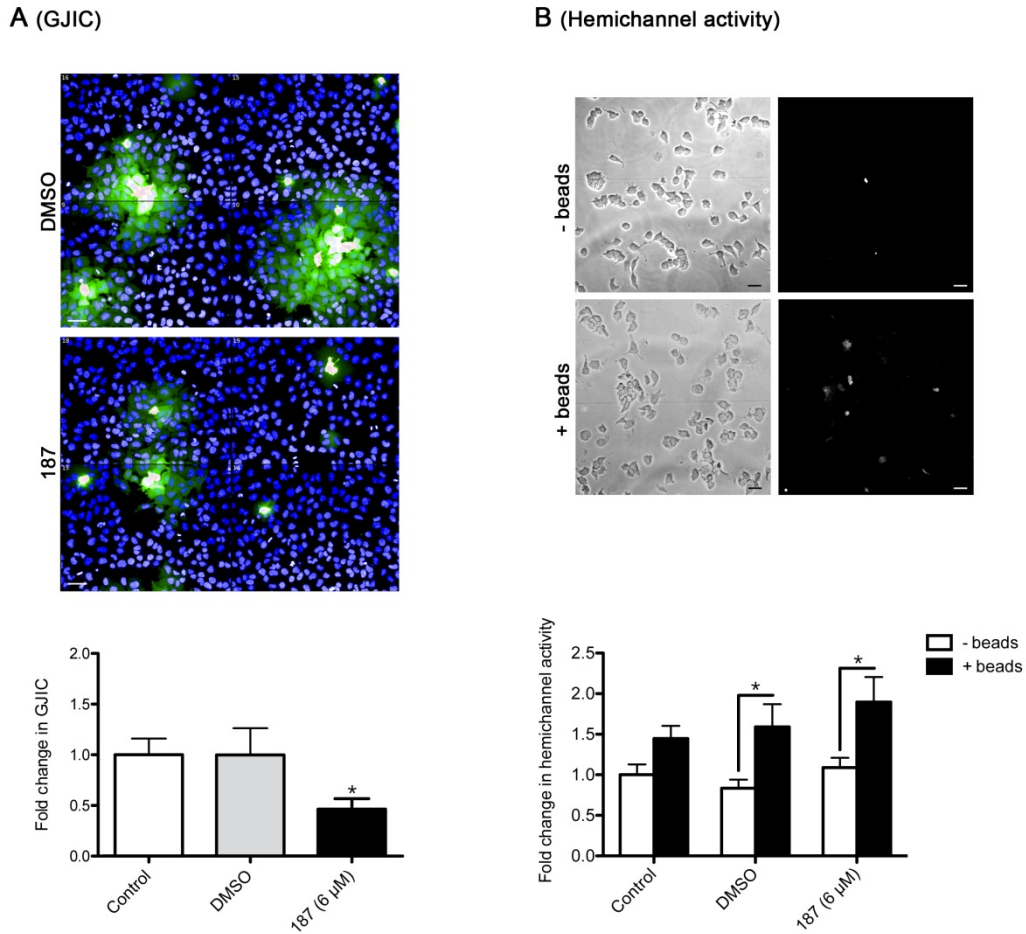
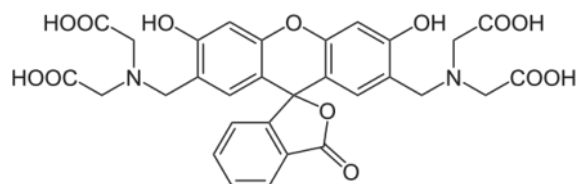
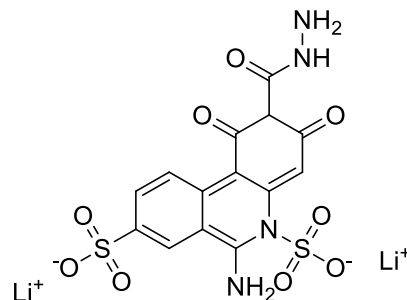


Figure 4-2: Effect of compound **187** on connexin channel function in NT2/D1 cells. (A) The parachute assay was used to assess gap junctional intercellular communication (GJIC). (B) Connexin hemichannel (single membrane channel) function was assessed by measuring the number of cells capable of spontaneous uptake of Lucifer yellow through hemi-channels in a low calcium medium. The image belongs to Mathew Cook's MSc. thesis research¹³.



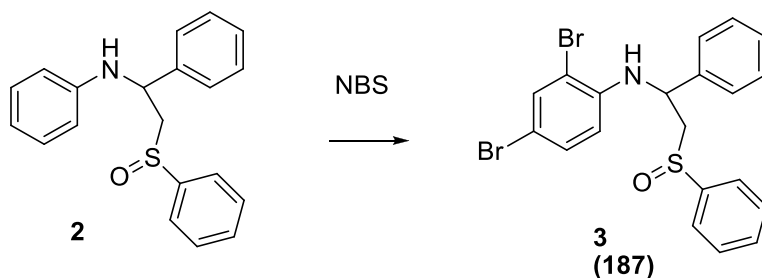
13, calcein



14, Lucifer yellow

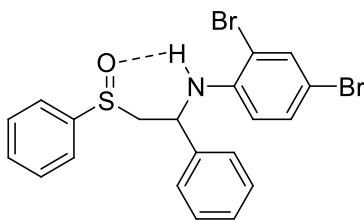
Based on this result, it was decided to go back and follow the synthesis procedure used by Charron to prepare additional amounts of compound **187**. The synthesis pathway is a three step synthesis as depicted in Scheme 4.2. Following the procedure described by Charron, a compound was obtained whose ^1H NMR spectra matched the one available from his records. The formation of the proposed structure would imply a rearrangement proposed by Charron in his notebook but never observed or reported before. The NMR spectroscopic properties of this material were in reasonable agreement with the proposed structure. It should be noted that this compound was obtained as a single diastereomer after recrystallization from hexanes:ethyl acetate, as evidenced by the ^1H and ^{13}C NMR. Since the yield of **2** is very high, the addition of the α -lithio sulfuxide to the benzalaniline must be highly stereoselective.

Once the activity of **187** was discovered it was decided to prepare analogs by replacing the aliphatic bromide with nucleophiles such as thiophenolate or cyanide. Surprisingly heating of this compound with PhSNa on NaCN gave no reaction. This led us to question the Charron structure assignment. In the end an X-ray structure determination (**Figure 4-4**) showed that this compound arose simply from a double aromatic electrophilic bromination at the *ortho* and *para* positions of the amine substituted aromatic ring.



Both the proton and carbon NMR spectra were consistent with the “real” structure **3**. In particular the proton NMR showed the required ABX pattern due to the CH-CH₂ unit in the compound Figure 4.3.

The x-ray structure showed a surprising feature. One would anticipate that **187** would exist in a conformation that allows intramolecular hydrogen bonding between the NH and the polarized S=O bond, forming a six member ring. Clearly such a conformation is not preferred in the crystal form.



Intramolecular hydrogen bond

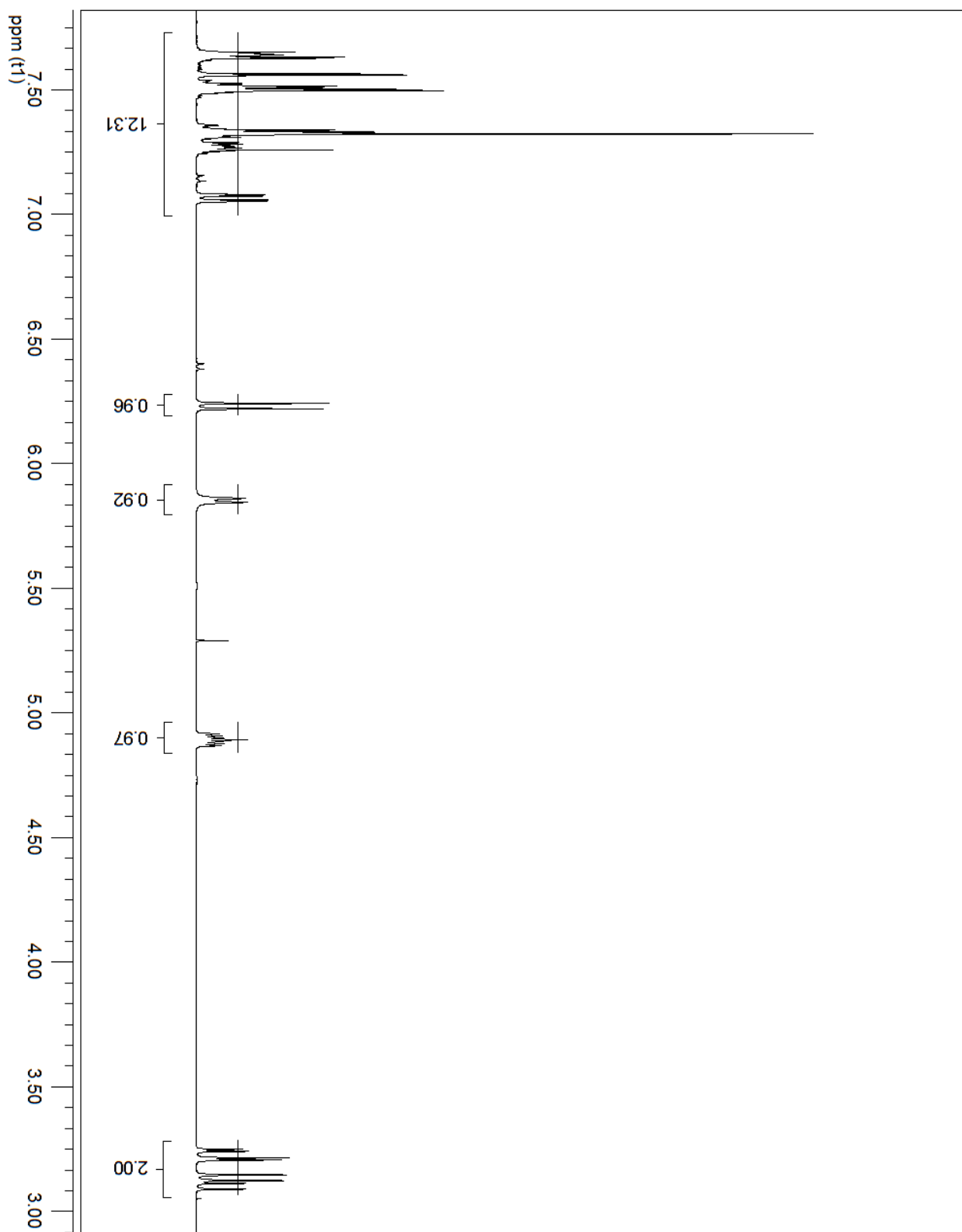


Figure 4.3: 400 MHz $^1\text{H-NMR}$ Spectrum of compound **3** in CDCl_3

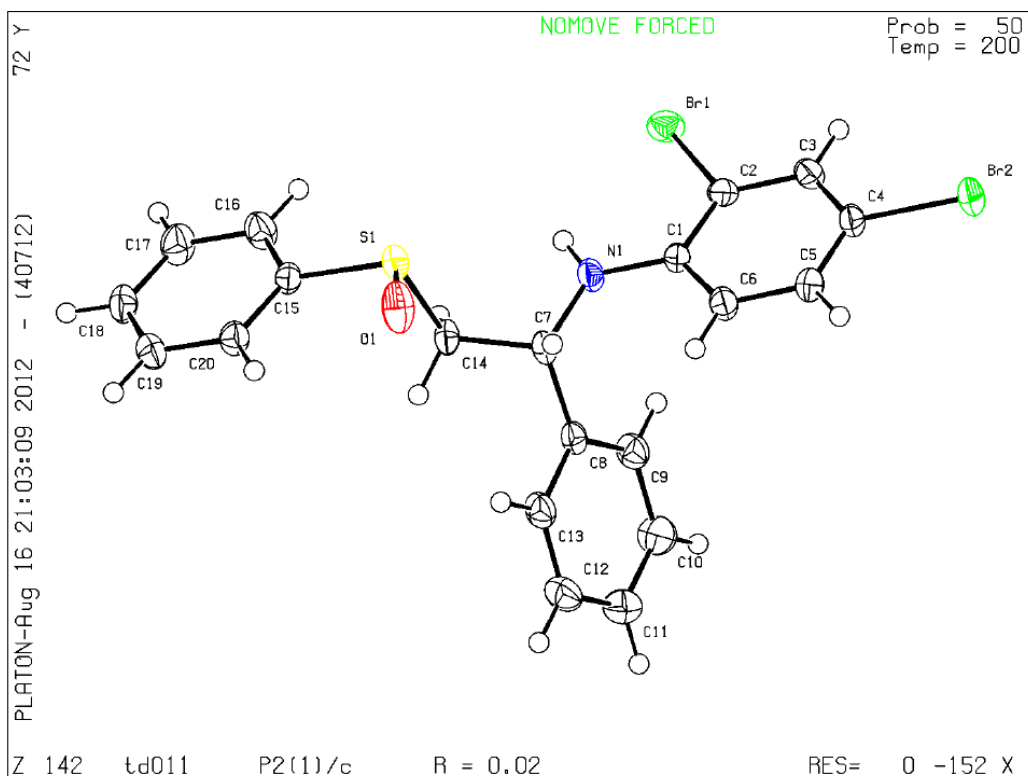
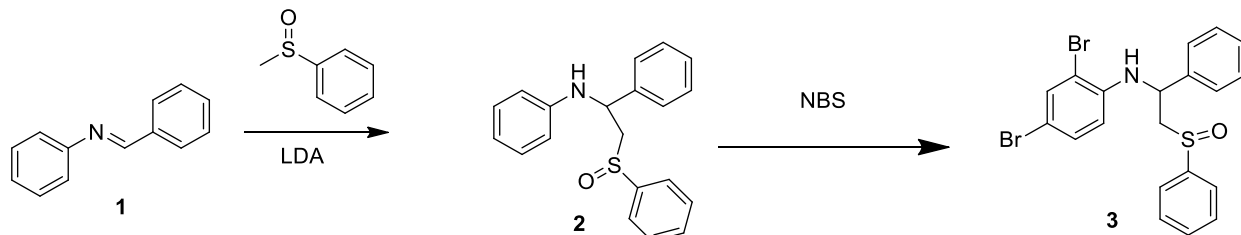


Figure 4-4: The correct structure for compound **3** (187) according to the x-ray analysis.
Appendix 4A



Scheme 4.2: Synthesis of analog **3**

The first reaction used in the synthesis of these compounds was the condensation of aniline with benzaldehyde to produce imine **1**. Compound **3** is obtained via **Scheme 4.2** treatment of methyl phenyl sulfoxide with LDA, generates a carbanion which adds to the polarized C=N bond

to generate, **2**. Finally, treatment of compound **2** with excess NBS results in two nucleophilic aromatic substitutions to form compound **3** in 97% yield as white crystals Figure 4.3-**Figure 4-5**.

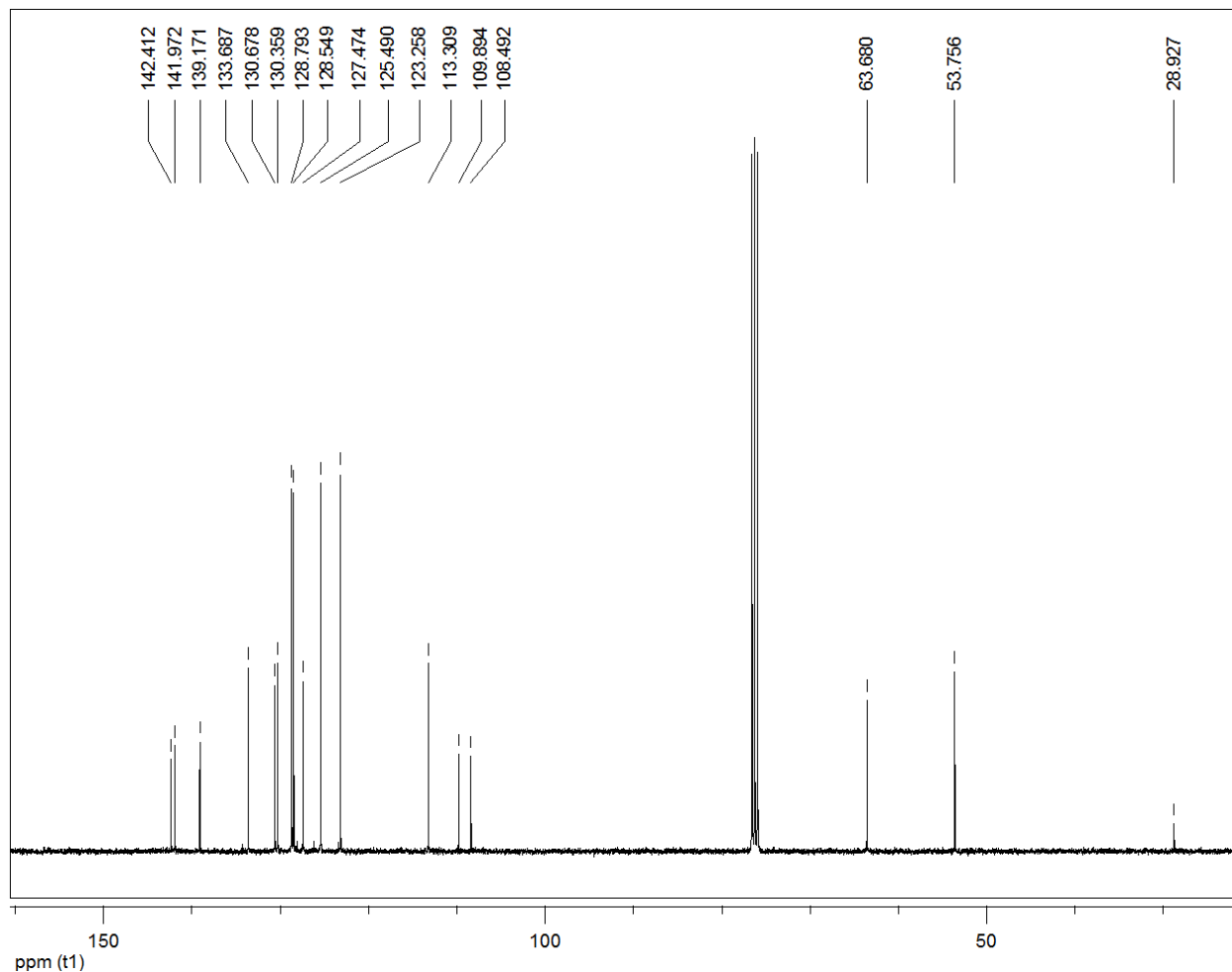
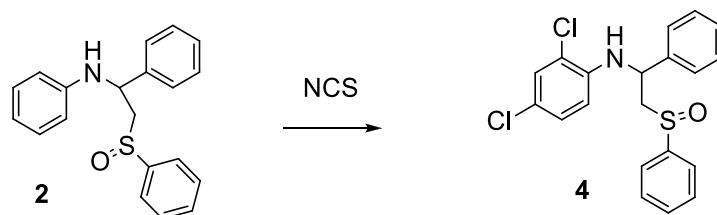


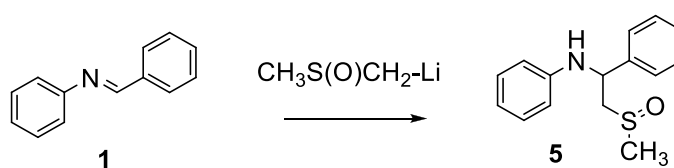
Figure 4-5: 100 MHz ^{13}C -NMR Spectrum of compound **3** in CDCl_3

Once the structure for compound **3** was established, analog compounds were prepared following the same pathway in order to evaluate the effect of electron withdrawing groups and electron donating groups on the observed activity. Other analogs were also synthesized to establish the basic features needed in the molecule to maintain the activity.

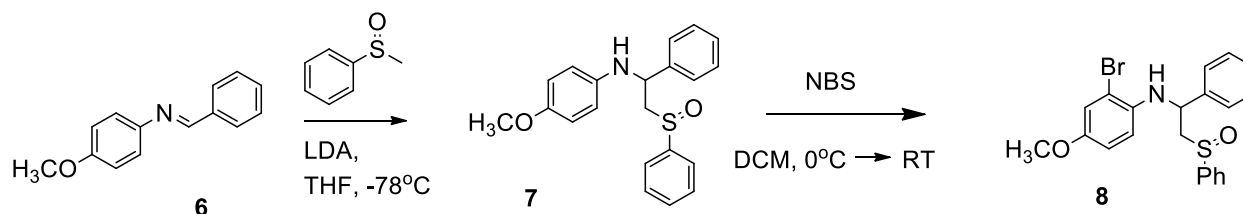
The dichloro analog **4** was obtained by the treatment of compound **2** with NCS. The NMR of **4** was very similar to **3**.



Compound **5** was obtained as a white powder in 82 % yield by addition of $\text{CH}_3\text{S}(\text{O})\text{CH}_2\text{-Li}$ to benzalaniline, **1**. The ^1H NMR of **5** showed the expected 3H methyl group singlet and the ABX pattern in addition to the required aromatic protons.



Two other amino sulfoxide analogs were prepared and evaluated. Addition of the lithio salt of phenyl methyl sulfoxide to *p*-methoxybenzaldehyde, **6**, gave the adduct **7** in 50% yield as an off white solid. Its spectroscopic properties were in agreement with the assigned structure. Bromination of this compound with NBS in DCM afforded the expected ortho-bromo-*p*-methoxyaniline **8**.



Scheme 4.3: Synthesis of compounds **7** and **8**.

Evaluation of the compounds synthesized thus far, in the two bioassays described above provided the results depicted in **Figure 4.6** and fully described in **Appendix 5A**. Removing the bromine atoms from the aniline ring in **3**, greatly reduced the GJIC activity, but compound **2** shows activity in the hemi-channels transport bioassay. Surprisingly, the dichloro derivative **4**

shows no statistically significant results. Replacement of the S(O)Ph with S(O)Me, compound **5**, resulted in an inactive material in the three bioassays. Whether this is due to a decrease in LogP in going from **3** to **5** or the replacement of the aromatic ring by a methyl group is open to speculation. Compound **3** has the highest inhibition of GJIC, whereas compound **8** and compound **2**, reduced anionic hemi-channel activity. Compound **2** also reduced the cationic activity of the hemi-channels. These results demonstrate that a compound could be tuned to specifically inhibit one of the connexins. As discussed before, each connexin plays a different role and controls the transportation of different molecules and ions through the hemi-channels. Incorporation of the methoxy group at the *para* position increased the specificity of the molecule, which in turn selectively decreased the anionic activity of the hemi-channels (**Figure 4-6**). While the current results are intriguing and show the potential for not only activity but also selectivity it is too early to speculate which structural features are important.

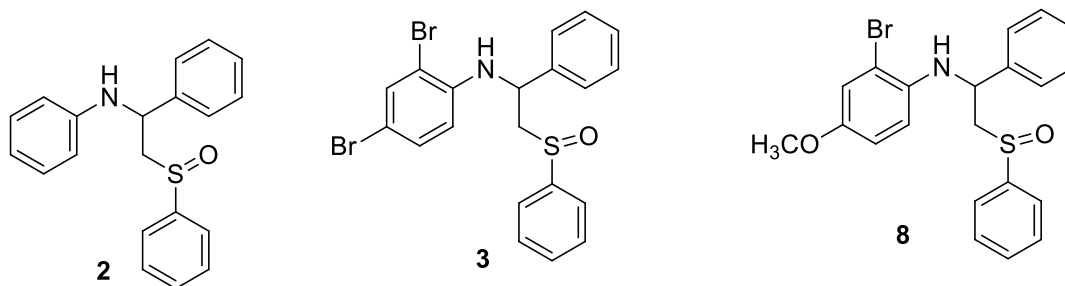
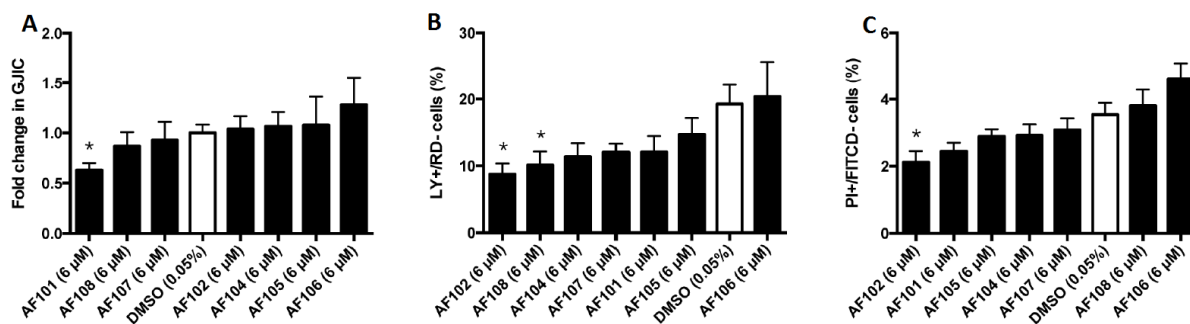
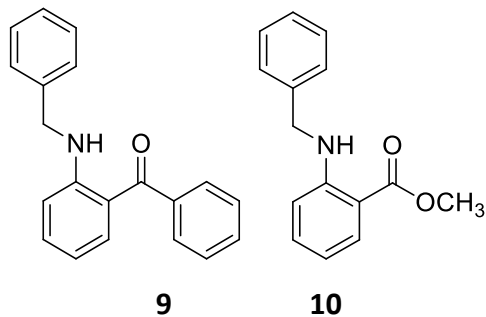


Figure 4-6 contains additional entries for anthranilic acid derivatives **9** and **10**. These compounds were prepared as analogs of the original (incorrect) **187** structure. Neither of these compounds showed activity in the three bioassays.



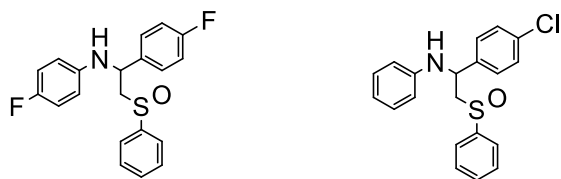
Legend for compounds: AF101= compound **3**, AF102= **2**, AF104= **5**, AF105= **9**, AF106=**10**, AF107=**4**, AF108=**8**

Figure 4-6: Bioassay result summary, **A**. Change in gap junctional intercellular communication, **B** Anionic activity in hemi-channels, **C** Cationic activity in hemi-channels.

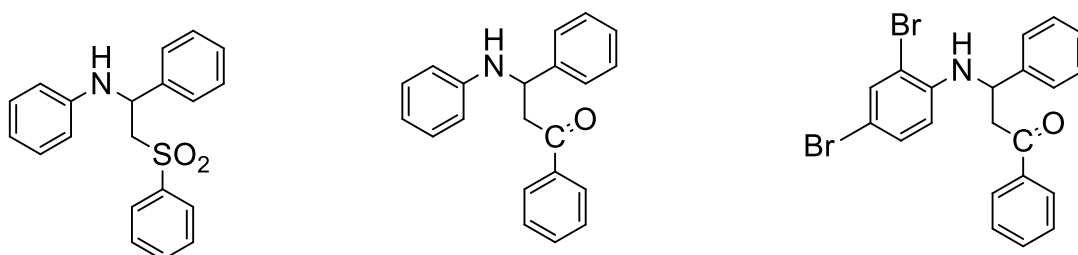
* Compounds with significant results, complete results **Appendix 5A**.

4.1.3 Conclusions and further work

One of the major constraints on this project was the synthesis of the imines as these compounds decompose quickly during purification. These compounds decompose in the presence of acidic conditions like the silica gel in the columns. Recrystallization was the most useful technique to purify these compounds. Several attempts were made to synthesize other imines with different substitution patterns but the resulting compounds were not solids so it became difficult to purify them. In addition, reactions of these crude products with LDA would provide several byproducts, making purification even more challenging. Subsequently, we were able to prepare crystalline samples of imines that led to two additional amino sulfoxides.



Also, the parent sulfoxide **2** was oxidized to the corresponding sulfone. Finally, two amino ketone analogs have been prepared.



These compounds were recently prepared by another member of our research group, and will be evaluated in the above bio-assays. The results should enable us to recognize the key structural features necessary for activity and selectivity and propose further structure modifications with enhanced desired activity. All of the above have chiral centres and thus exist as enantiomers. If this project continues, it will be important to prepare several of the active derivatives in enantiomerically pure form to determine if one of the two show greater activity-selectivity.

This has been a project of serendipity and twists coupled with some frustrations. The serendipity was that Martin Charron saved and labeled **sample 187** despite the fact that it did not give him the expected result, coupled with the fact that Matt Cooke chose to bioassay this compound and found that it had potentially useful bioactivity. The twist came when it was realized that the Charron structure assignment was incorrect. Considerable frustration was experienced with the synthesis of analogs since it was very difficult to purify the intermediate imines.

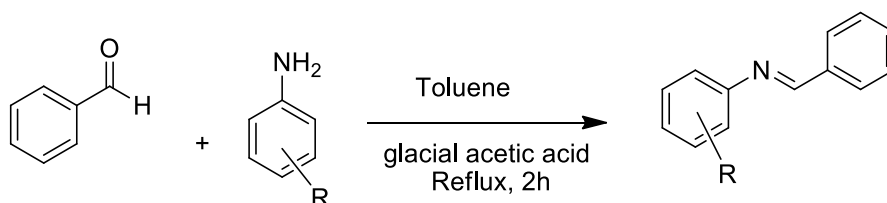
Additionally, the assays are difficult and time consuming; often no feedback was obtained for more than one month. At this stage as is described above, we have several additional compounds including two new amino sulfoxides, one amino sulfone and two amino ketones undergoing bio-assays. The project therefore continues hopefully with pleasant surprises.

4.1.4 Experimental

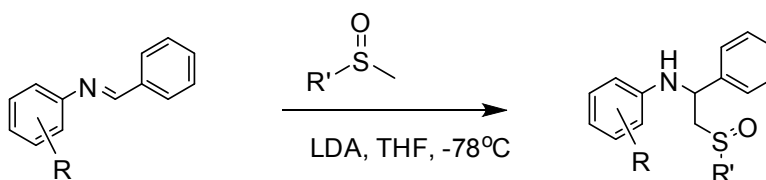
General procedures for compound purification and characterization is the same as described in section 2.1.3

General procedures:

Imine synthesis. Imines were prepared using published procedures following procedure reported by Niazi and co-workers (IJPPS 2, 108–112 (2010))¹⁴ and purified by recrystallization prior to use.

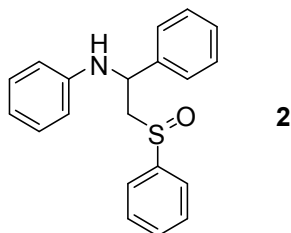


1. LDA induced coupling



Lithium diisopropylamide (LDA) (2.0 molar equivalents) was added dropwise under N₂ to a -78 °C solution of the corresponding sulfoxide (2.0 molar equivalents) in 10 mL of THF cooled to -78 °C. The resulting mixture was kept for 15 min under these conditions after this time then allowed to warm to RT and the imine (1.0 molar equivalent) was added. The progress of the reaction was monitored by TLC. Workup involved quenching with 10% aqueous NH₄Cl followed by extraction with CH₂Cl₂ (2 x 20 mL). The combined extracts were washed with water, dried (MgSO₄) and then evaporated to dryness. The product was purified by recrystallization from Hexanes: ethyl acetate.

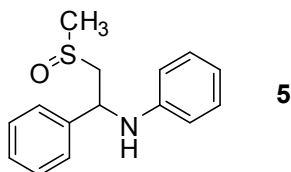
N-(1-phenyl-2-(phenylsulfinyl)ethyl)aniline (2)



Compound **2** was obtained following general procedure **2**, using: methylphenyl sulfoxide (2.0 g, 14.3 mmol) in anhydrous THF (10 mL), LDA (7.9 mL, 14.3 mmol) benzalaniline (2.0 g, 11 mmol) in anhydrous THF (2 mL). The crude product was purified by recrystallization from ethanol giving compound **2** as an off-white powder with a quantitative yield. The obtained spectrum matches the one reported in literature¹⁵.

¹H NMR (400 MHz, CDCl₃) δ ppm 3.10 (dd, *J* = 13.8, 9.3 Hz, 1H), 3.21 (dd, *J* = 13.7, 3.27 Hz, 1H), 4.87 (ddd, *J* = 9.4, 6.3, 3.23 Hz, 1H), 5.83 (d, *J* = 6.2 Hz, 1H), 6.21 (d, *J* = 8.8 Hz, 1H), 7.05 (dd, *J* = 8.7, 2.3 Hz, 1H), 7.34-7.04 (m, 5H), 7.53-7.47 (m, 3H), 7.64-7.60 (m, 2H), 7.55 (d, *J* = 2.3 Hz, 1H)

N-(2-(Methylsulfinyl)-1-phenylethyl)aniline (5)

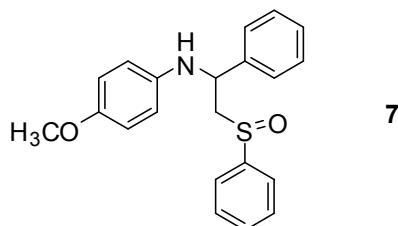


Compound **5** was obtained following general procedure **2**, using dimethyl sulfoxide (0.1 mL, 1.25 mmol) in anhydrous THF (10 mL), LDA (2.0 mL, 2.5 mmol), benzalaniline (200 mg, 0.622 mmol) in anhydrous THF (5 mL). The crude was purified by recrystallization from ethyl acetate: hexanes (2:1), to obtain compound **5** as an off-white powder (132.1 mg, 82%).

¹H NMR (400 MHz, CDCl₃) δ ppm 7.53-7.18 (m, 5H), 7.08 (ddd, *J* = 10.6, 5.83, 2.6 Hz, 2H), 6.6 (ddd, *J* = 42.2, 13.7, 6.2 Hz, 3H), 5.06 (ddd, *J* = 8.5, 2.0, 1.0 Hz, 1H), 4.89 (dd, *J* = 9.2, 5.4 Hz, 1H), 3.24-3.14 (m, 1H), 3.05-2.89 (m, 1H), 2.59 (s, 1H)

¹³C NMR (100 MHz, CDCl₃) 146.6, 141.8, 129.2, 129.2, 129.1, 129.1, 128.1, 126.4, 126.2, 118.2, 114.1, 113.8, 61.7, 56.150, 39.6

4-Methoxy-*N*-(1-phenyl-2-(phenylsulfinyl)ethyl)aniline (**7**)

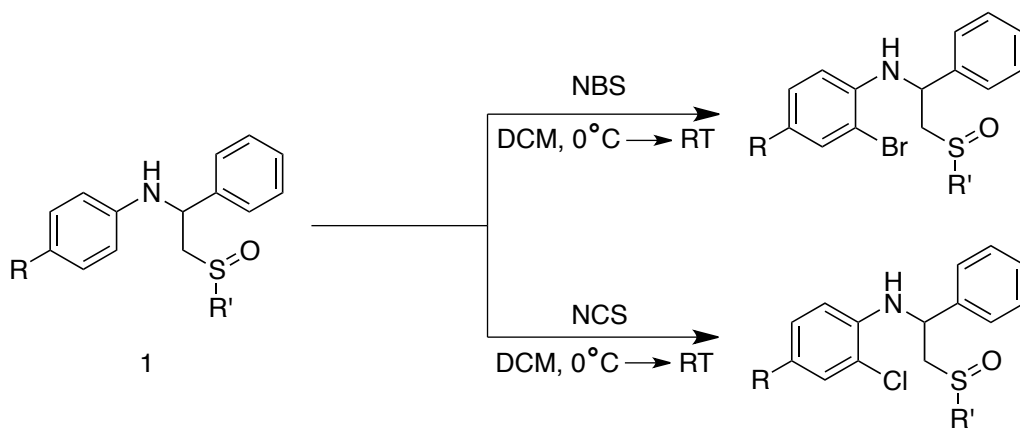


Compound **7** was obtained following general procedure **2**, using the following reagent amounts: methylphenyl sulfoxide (774 mg, 5.51 mmol) in anhydrous THF (10 mL), LDA (12.3 mL, 22.08 mmol) and *N*-benzylidene-4-methoxyaniline (2.0 g, 11 mmol) in anhydrous THF (2 mL). The crude was purified by recrystallization from ethanol, to obtain compound **7** as a off-white powder (957 mg, 50%)

$^1\text{H NMR}$ (400 MHz, CDCl_3) δ ppm 7.66-7.19 (m, 11H), 6.72-6.66 (m, 2H), 6.52 (t, $J = 6.4$ Hz, 2H), 4.77 (t, $J = 6.4$ Hz, 1H), 3.69 (s, 3H), 3.14 (d, $J = 6.3$ Hz, 2H)

$^{13}\text{C NMR}$ (100 MHz, CDCl_3) 131.2, 129.4, 129.0, 127.8, 126.4, 124.0, 115.5, 114.7, 64.1, 55.7, 55.4.

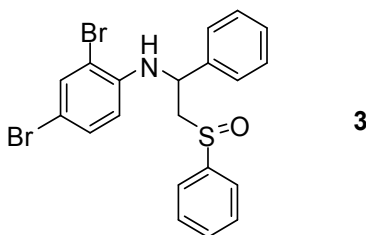
2. Halogenation- General Procedure.



Aminosulfoxide **A** (1.0 molar equivalent) was dissolved in 5 mL of anhydrous DCM at 0°C, and a catalytic amount PTSA was added followed dropwise addition of solution of NBS or NCS dissolved in DCM. The resulting solution was stirred at 0°C for 15 min after this time the ice bath was removed and the reaction mixture was left to warm up to RT. The resulting solution was diluted with water, NaHCO_3 (2 mL, 5%) was added. The aqueous phase was extracted twice with DCM (2 X 10 mL) and the combined organic

layers were dried over MgSO_4 , filtered and solvent evaporated *in vacuo*. The resulting solid was recrystallized from a CH_2Cl_2 : hexanes mixture.

2,4-dibromo-N-(1-phenyl-2-(phenylsulfinyl)ethyl)aniline (3)



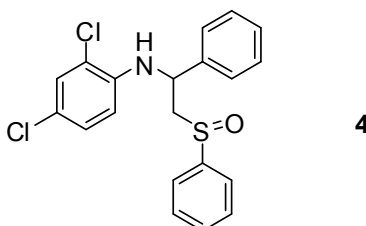
Reaction of 100 mg (0.31 mmol) of compound **2** in 5 mL of anhydrous DCM with 111 mg, (0.60 mmol) of NBS in anhydrous DCM (2 mL), and a catalytic amount of PTSA gave after recrystallization from ethanol 138 mg, (0.29 mmol) of compound **3** as white crystals, 94% yield.

^1H NMR (400 MHz, CDCl_3) δ ppm 3.12 (dd, $J = 13.7, 9.3$ Hz, 1H), 3.22 (dd, $J = 13.7, 3.3$ Hz, 1H), 4.89 (d, $J = 8.3$ Hz, 1H), 5.85 (s, broad, 1H), 6.22 (d, $J = 8.9$ Hz, 1H), 7.06 (dd, $J = 8.7, 2.3$ Hz, 1H), 7.64-7.23 (m, 10H)

^{13}C NMR (100 MHz, CDCl_3) 142.4, 141.9, 139.1, 133.7, 130.7, 130.4, 128.8, 128.5, 127.5, 125.5, 123.3, 113.3, 109.9, 108.5, 63.7, 53.8, 28.9

HRMS calc. for $\text{C}_{20}\text{H}_{17}\text{Br}_2\text{NOS}$, 476.9398 obtained: 476.94151

2,4-Dichloro-N-(1-phenyl-2-(phenylsulfinyl)ethyl)aniline (4)



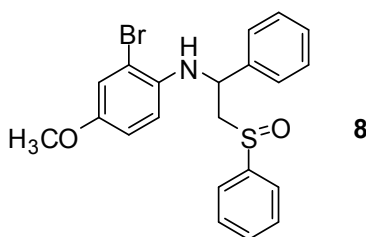
Compound **4** was obtained as white crystals in 21% yield after purification by preparative HPLC (ACN: MeOH, 10% starting 200 mg, (0.622 mmol) of **2** dissolved in 5 mL of anhydrous DCM and (166.2 mg (1.24 mmol) NCS in 10 mL of anhydrous DCM containing a catalytic amount of PTSA.

¹H NMR (400 MHz, *CDCl*₃) δ ppm 3.10 (dd, *J* = 13.8, 9.4 Hz, 1H), 3.21 (dd, *J* = 13.7, 3.3 Hz, 1H), 4.88 (ddd, *J* = 9.5, 6.4, 3.3 Hz, 1H), 5.79 (d, *J* = 6.4 Hz, 1H), 6.28 (d, *J* = 8.8 Hz, 1H), 6.89 (dd, *J* = 8.8, 2.3 Hz, 1H), 7.35-7.24 (m, 7H), 7.63-7.48 (m, 5H)

¹³C NMR (100 MHz, *CDCl*₃) 143.1, 141.2, 140.0, 131.3, 129.5, 129.2, 128.8, 128.1, 127.6, 126.1, 123.9, 122.2, 120.1, 113.4, 64.3, 54.3

HRMS calc. for C₂₀H₁₇Cl₂NOS 389.0408 obtained: 389.03855

2-Bromo-4-methoxy-*N*-(1-phenyl-2-(phenylsulfinyl)ethyl)aniline (8)



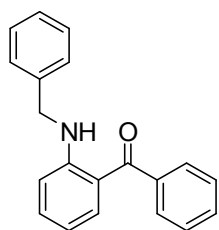
Compound **8** was obtained following general procedure **3**, using compound **7** (212 mg, 0.65 mmol) in anhydrous DCM (5 mL), NBS (231.39 mg, 1.3 mmol) in anhydrous DCM (2 mL), and a catalytic amount of PTSA. The crude was purified by recrystallization from ethanol, to obtain compound **8** as white crystals (19.3 mg, 9%).

¹H NMR (400 MHz, *CDCl*₃) δ ppm 3.12 (d, *J* = 6.3 Hz, 2H), 3.68 (s, 3H), 4.75 (t, *J* = 6.4 Hz, 1H), 6.50 (d, *J* = 8.9 Hz, 2H), 6.67 (d, *J* = 9.0 Hz, 1H), 7.34-7.21 (m, 6H), 7.50-7.47 (m, 3H), 7.61-7.59 (m, 2H)

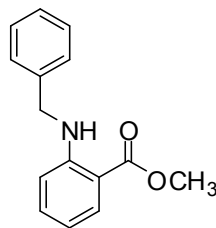
¹³C NMR (100 MHz, *CDCl*₃) 152.2, 143.6, 140.7, 137.8, 131.2, 129.4, 129.1, 127.9, 126.2, 123.9, 118.2, 114.3, 114.1, 110.7, 65.4, 55.9, 54.6

HRMS calc. for C₂₁H₂₀BrNO₂S 429.0398 obtained: 429.0428

(2-(Benzylamino)phenyl)(phenyl)methanone (9) and methyl 2-(benzylamino)benzoate (10)



9



10

These compounds were prepared following literature procedures. The spectroscopic properties of the compounds obtained matched those reported for **9**¹⁶ and **10**¹⁶.

4.1.5 References:

1. Klotz, L.-O. & Giehl, K. Special Issue: cell-cell communication in development and disease. *Archives of Biochemistry and Biophysics* **524**, 1 (2012).
2. Goodenough, D. A., Goliger, J. A. & Paul, D. L. Connexins, connexons and intercellular communications. *Annual Reviews* **65**, 475–502 (1996).
3. Bennett, M. V. L., Contreras, J. E., Bukauskas, F. F. & Sáez, J. C. New roles for astrocytes: gap junction hemichannels have something to communicate. *Trends in Neurosciences* **26**, 610–7 (2003).
4. Goodenough, D.; Paul, D. L. Gap junctions. *Cold Spring Harbor Perspect. in Biology*; **1**:a002576 (2009). At: <http://cshperspectives.cshlp.org/content/1/1/a002576.full.pdf+html>. Accessed December 2013.
5. Goncharenko, K. Changes in Gap Junction Expression and Function Following Ischemic Injury of Spinal Cord White Matter. Master Thesis. University of Toronto. (2011).
6. Söhl, G. & Willecke, K. Gap junctions and the connexin protein family. *Cardiovascular Research* **62**, 228–32 (2004).
7. Dbouk, H., Mroue, R. M., El-Sabban, M. E. & Talhouk, R. S. Connexins: a myriad of functions extending beyond assembly of gap junction channels. *Cell Communication and Signalling*. **7**, 4 (2009).
8. Kar, R., Batra, N., Riquelme, M.; Jiang, J. X. Biological role of connexin intercellular channels and hemichannels. *Archives of Biochemistry and Biophysics* **524**, 2–15 (2012).
9. Huang, C. Critical role of connexin 43 in secondary expansion of traumatic spinal cord injury. *The Journal of Neuroscience*. **32**, 3333–8 (2012).

10. Garré, J. M. FGF-1 induces ATP release from spinal astrocytes in culture and opens pannexin and connexin hemichannels. *Proceedings of the National Academy of Sciences of the United States of America* **107**, 22659–64 (2010).
11. Charron, M. Not published data(2004).
12. Connors, B. W. Tales of a dirty drug: carbenoxolone, gap junctions, and seizures. *Epilepsy Currents (American Epilepsy Society)* **12**, 66–8 (2012).
13. Cooke, M. Connexin biosay results, personal communication. (2012).
14. Niazi, S., Javali, C., Paramesh, M. & Shivaraja, S. Study of influence of linkers and substitutions on antimicrobial activity of some Schiff bases. *International Journal of Pharmacy and Pharmaceutical Sciences* **2**, 108–112 (2010).
15. Pyne, Stephen G., Dikic, B. Diastereoselective additions of (R)-(+)- methyl p- tolyl sulfoxide anion to imines. *Journal of Organic Chemistry*. **55**, 1932–1936 (1990).
16. Kirincich, S. J. Benzhydrylquinazolinediones: novel cytosolic phospholipase A2alpha inhibitors with improved physicochemical properties. *Bioorganic & Medicinal Chemistry* **17**, 4383–405 (2009).

Claims to Original Research

1. Development of a validated method for the quantification of five pentacyclic triterpenes in *Souroubea* spp from Costa Rica.
2. Use of metabolomics techniques for the identification of putative markers to distinguish between *Souroubea* spp.
3. Development of fingerprinting using HPLC-DAD as a technique for the differentiation between Marcgraviaceae species.
4. Quantification of the content of six pentacyclic triterpenes in thirteen species of Marcgraviaceae.
5. The evaluation of the antifungal and Quorum sensing inhibition activity of thirteen Marcgraviaceae species.
6. The isolation and identification of 2-methoxynaphthoquinone as the bioactive compound responsible for the antifungal and Quorum sensing inhibition activity observed for *Marcgravia nervosa*.
7. Evaluation of the occurrence of the 2-methoxynaphthoquinone in thirteen species of the Marcgraviaceae family.

8. The synthesis of a more than 60 new dillapiol, safrol, piperonal and sesamol analogs and the evaluation of their potential use as pesticide synergists via determination of their inhibition of P450 3A4.

9. Correction of an amino sulfoxide structure which was shown to block connexins in the bioassay developed by Dr. Steffany Bennet lab and subsequent synthesis of six analogs some of which showed selectivity towards specific connexins.

Patent

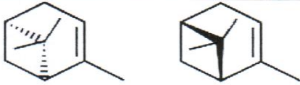
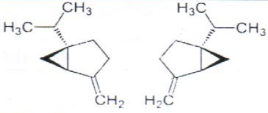

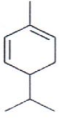
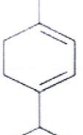
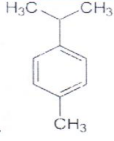
Patent filing for the use of *Platanus* spp. Bark and *Sourobea sympetala* material for the anti-anxiety activity is in process.

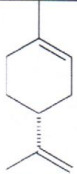
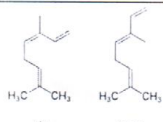
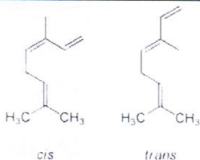
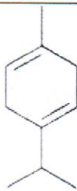
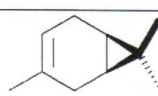

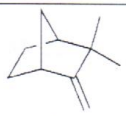
Appendix


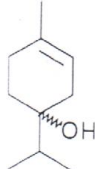
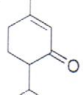
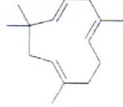
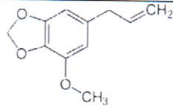
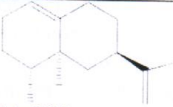
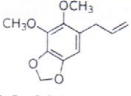
1A GC-analysis of *Piper aduncum*



Essential Oil Analysis

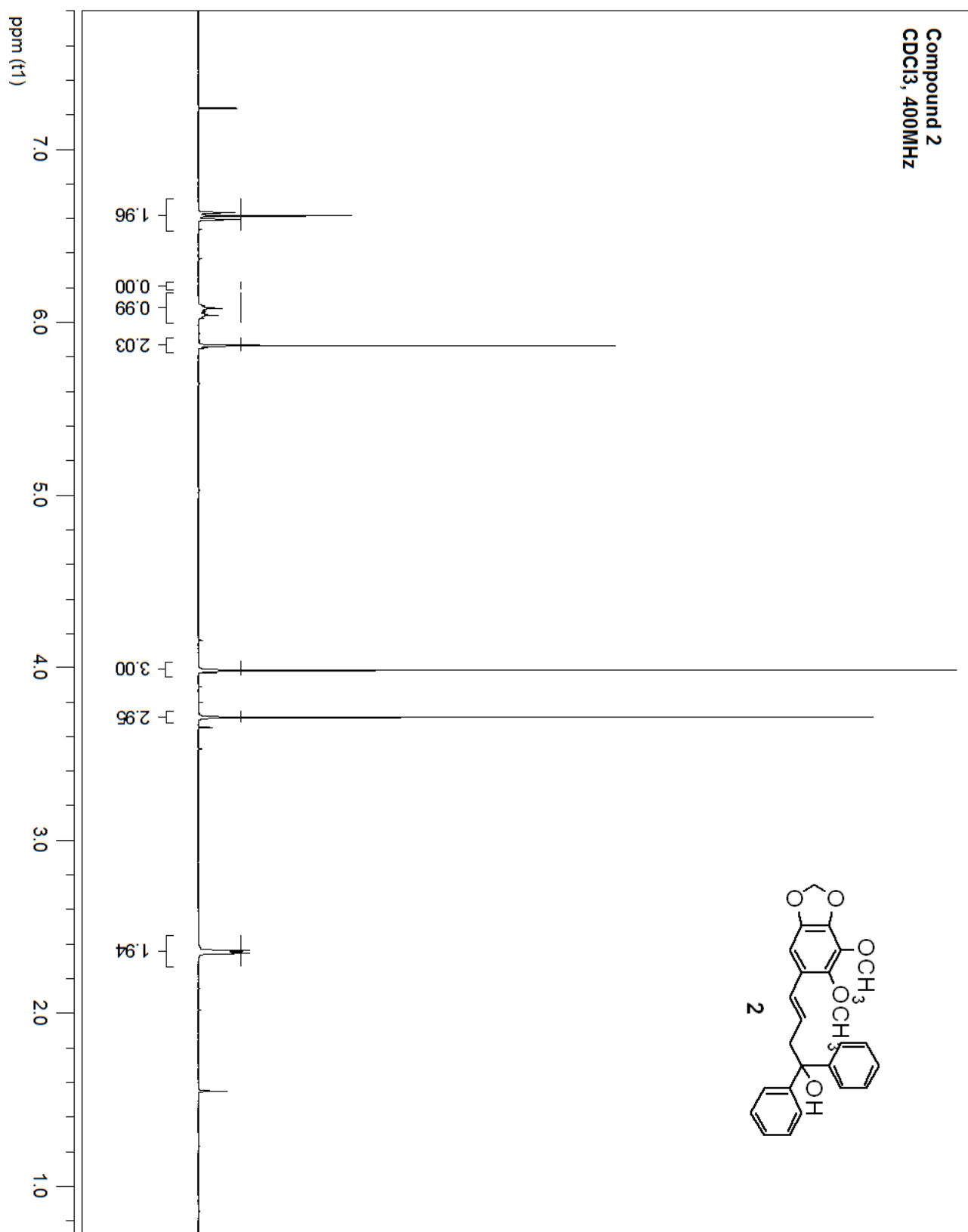
GC: Retention Times	Dill Oil	% total	
5.718	α -pinene	2.227	 (+)- α -pinene (-)- α -pinene MR 136
6.339	-sabinene	1.878	 Mr 136
6.503	β -myrcene	1.067	 Mr 136
6.711	α -phellandrene	2.591	 Mr136
6.883	α -terpinene	2.957	 Mr 136
6.983	Para cymene	0.801	 Mr 134

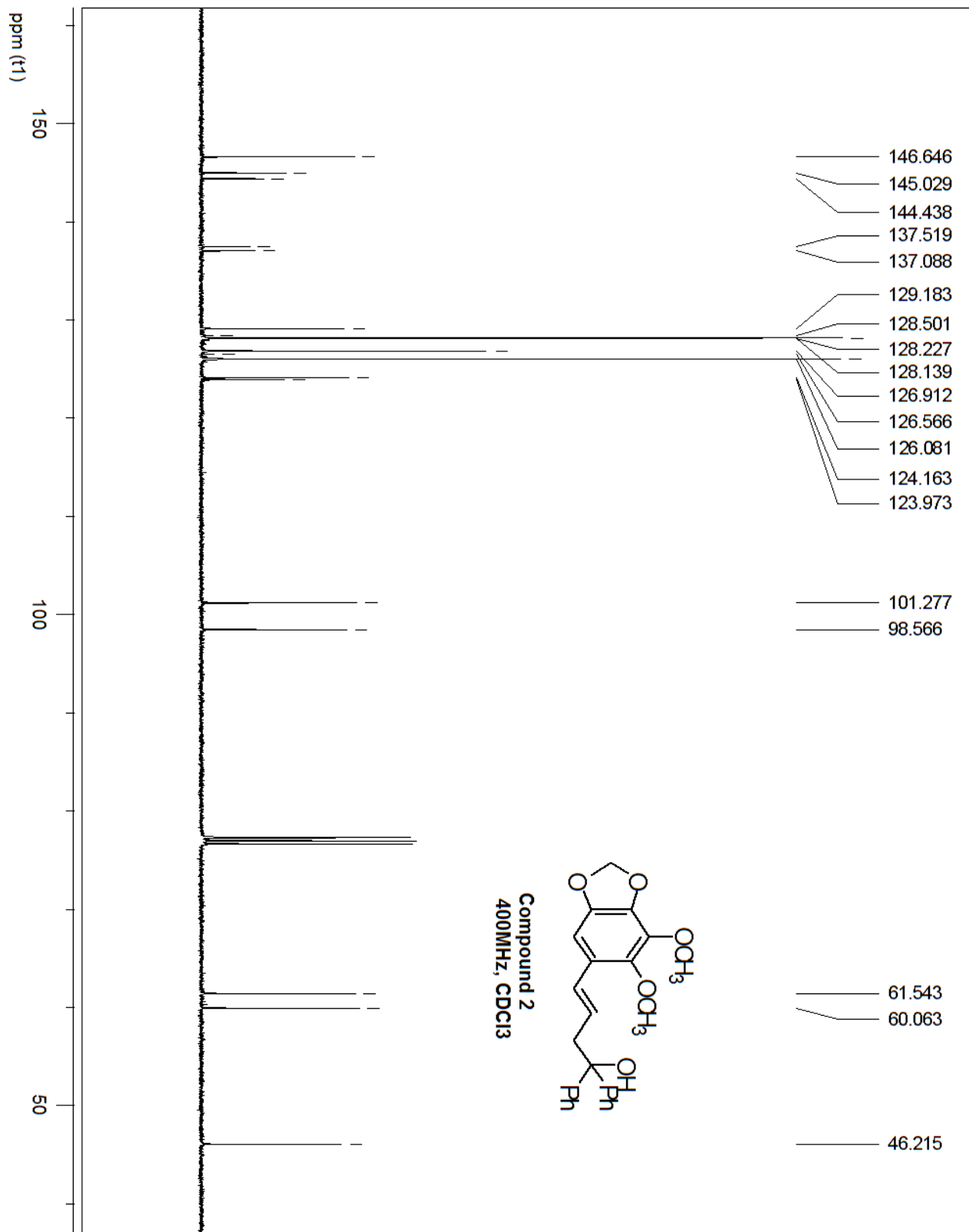
7.05	Limonene/ β -phellandrene	5.223	 Mr 136
7.136	Cis-ocimene	1.161	 Mr 136
7.279	β -ocimene		 Mr 136
7.444	γ -terpinene	5.630	 Mr 136
7.57		Not counted	
7.84	δ -3-carene	2.945	 Mr 136
7.952	linalool	2.913	 Mr 154
8.274	Camphene/sabinene hydrate?	0.876	 Mr 136

8.6	camphor	Not counted	 Mr 152
8.979	Terpinene-4-ol	11.932	 Mr 154
9.902	pipertone	17.917	 Mr 152
12.13	- α -humulene	Not counted	 Mr 204
12.4	- β -cubebene	Not counted	
12.734	myristicin	1.743	 Mr 192
12.78	valencene	Not counted	 Mr 204
13.724	Dillapiole	36.838	 Mr 222

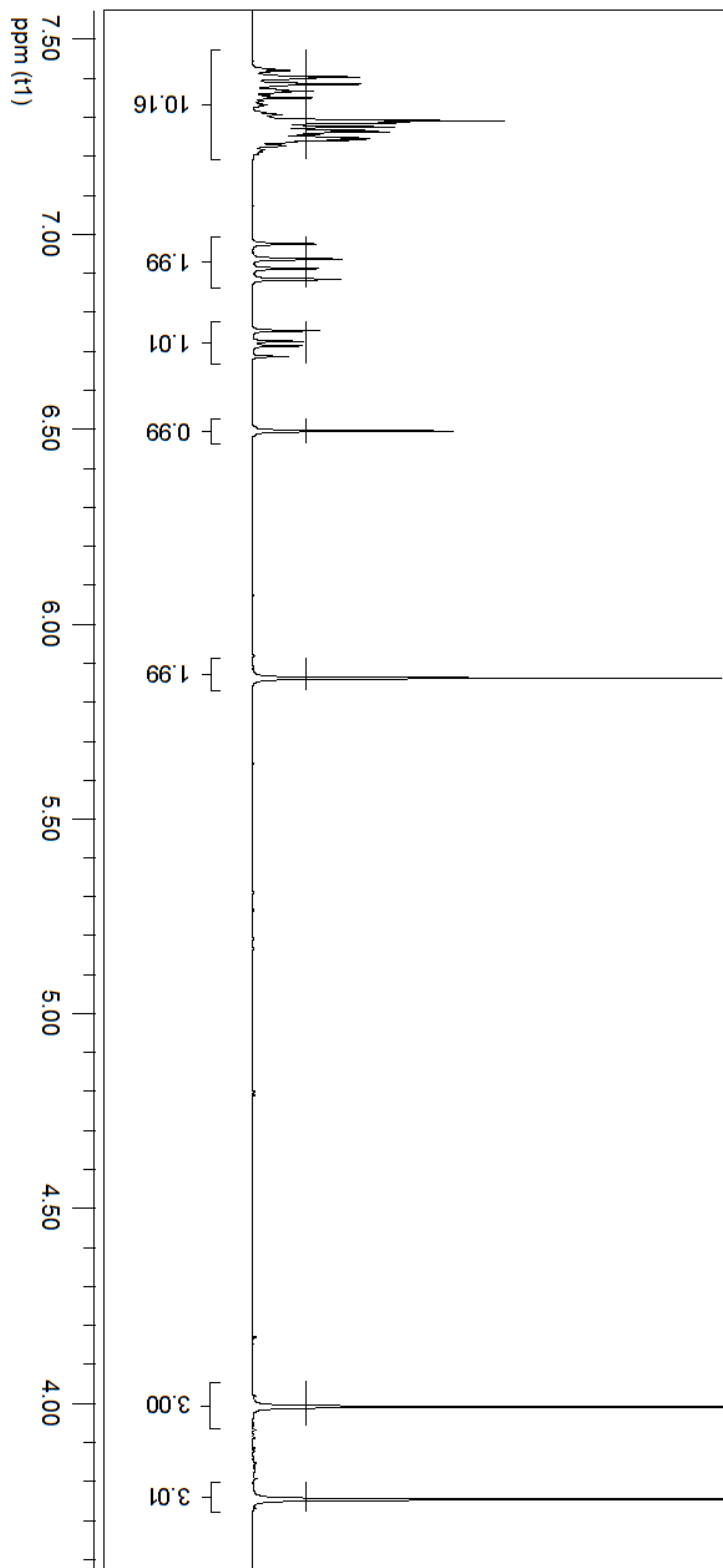
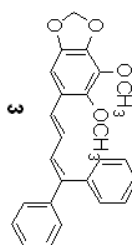
There is a consistent error in designating the magnetic field strength employed for ^{13}C -NMR in the Appendix. The designation should be 100 MHz and not 400 MHz.

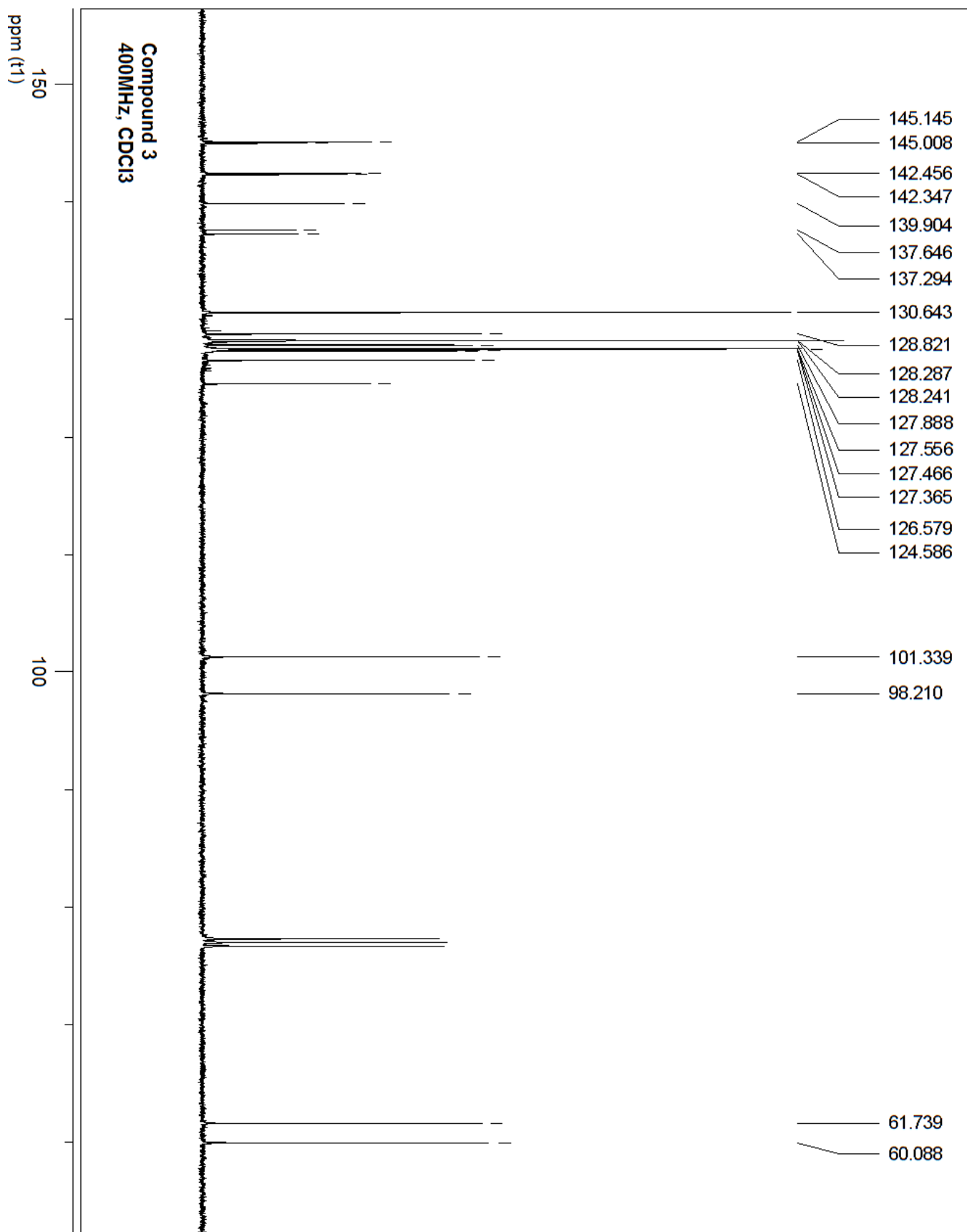
2A. Spectroscopic data for synergist analogs



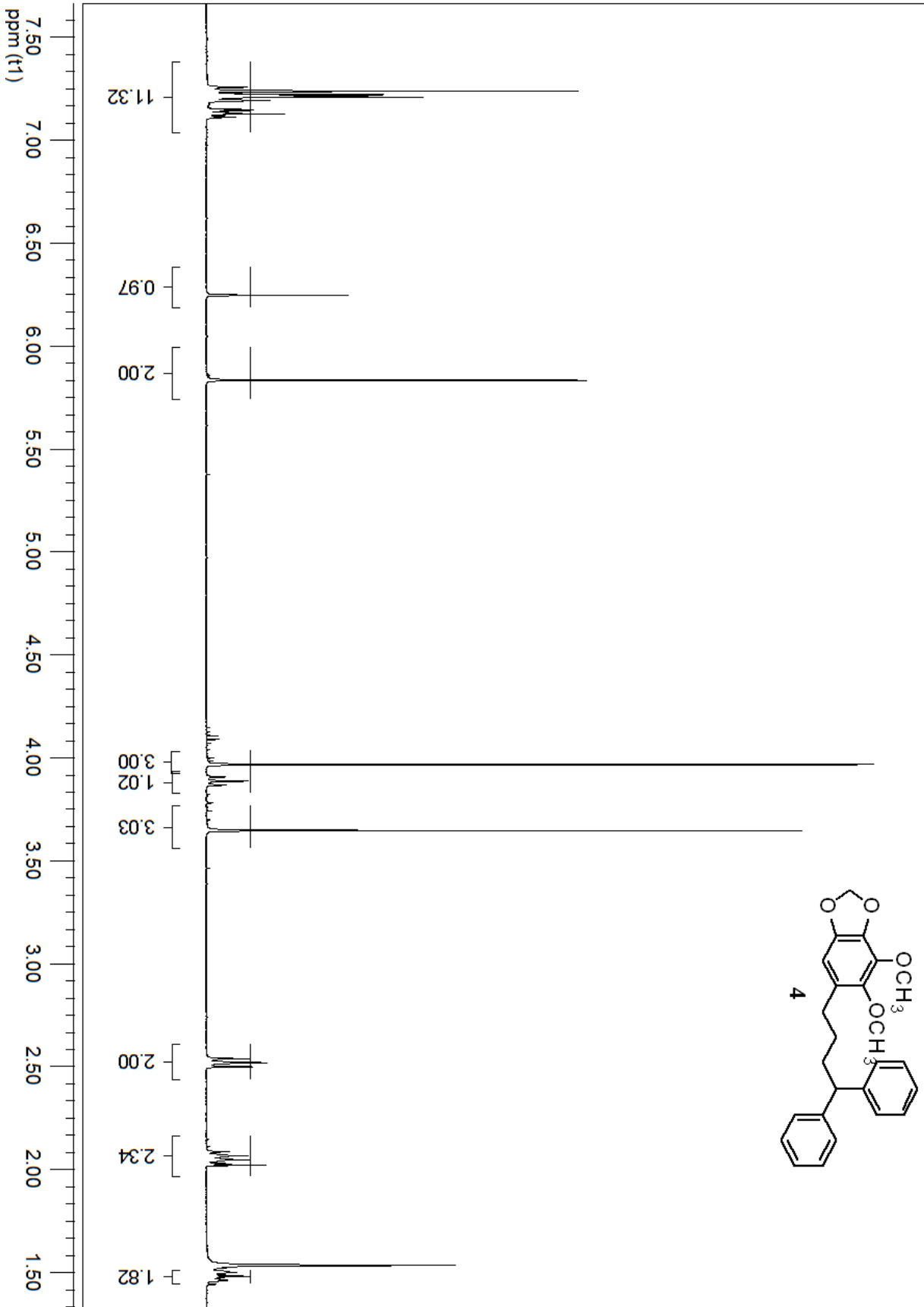


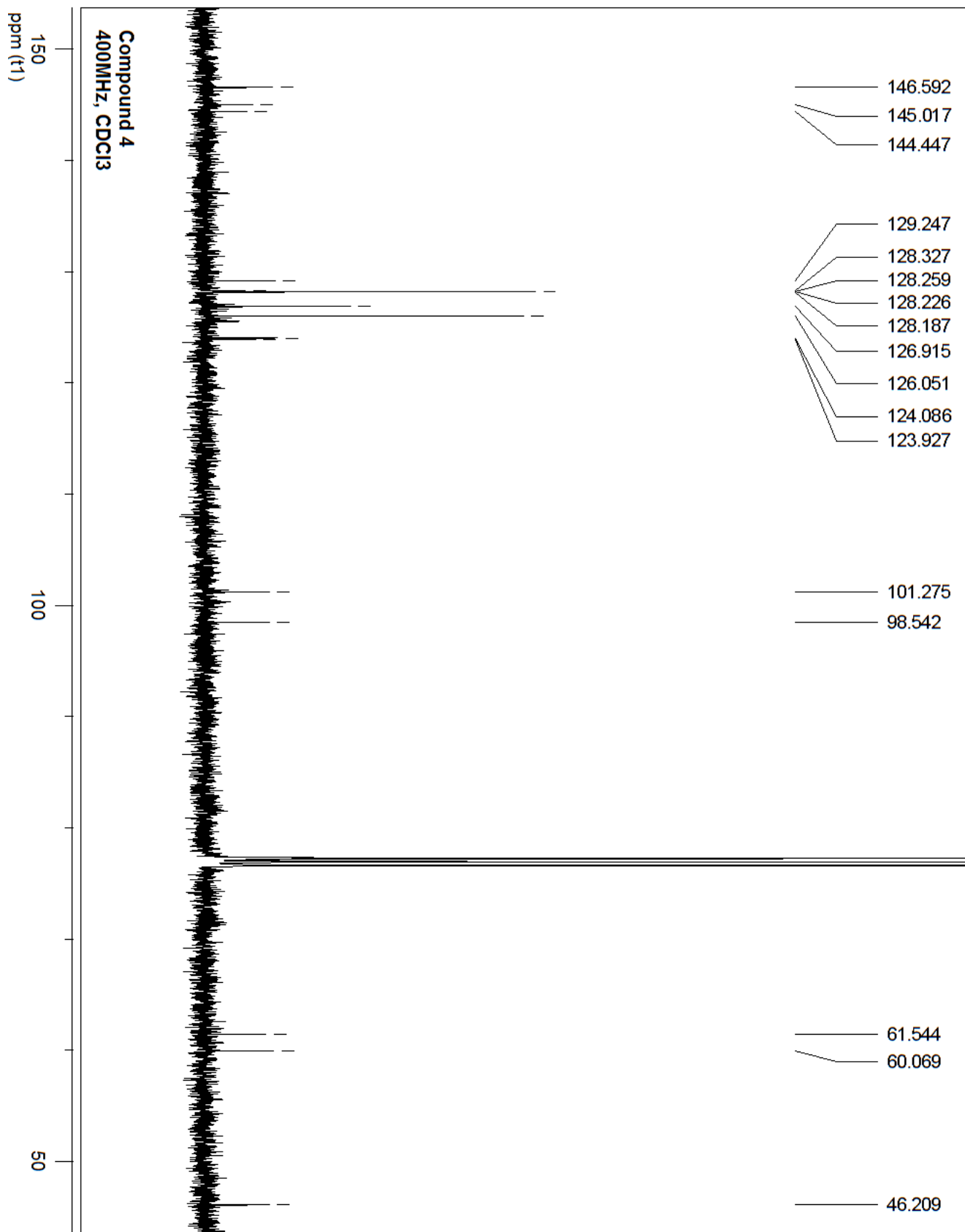
Compound 3
400 MHz, CDCl₃



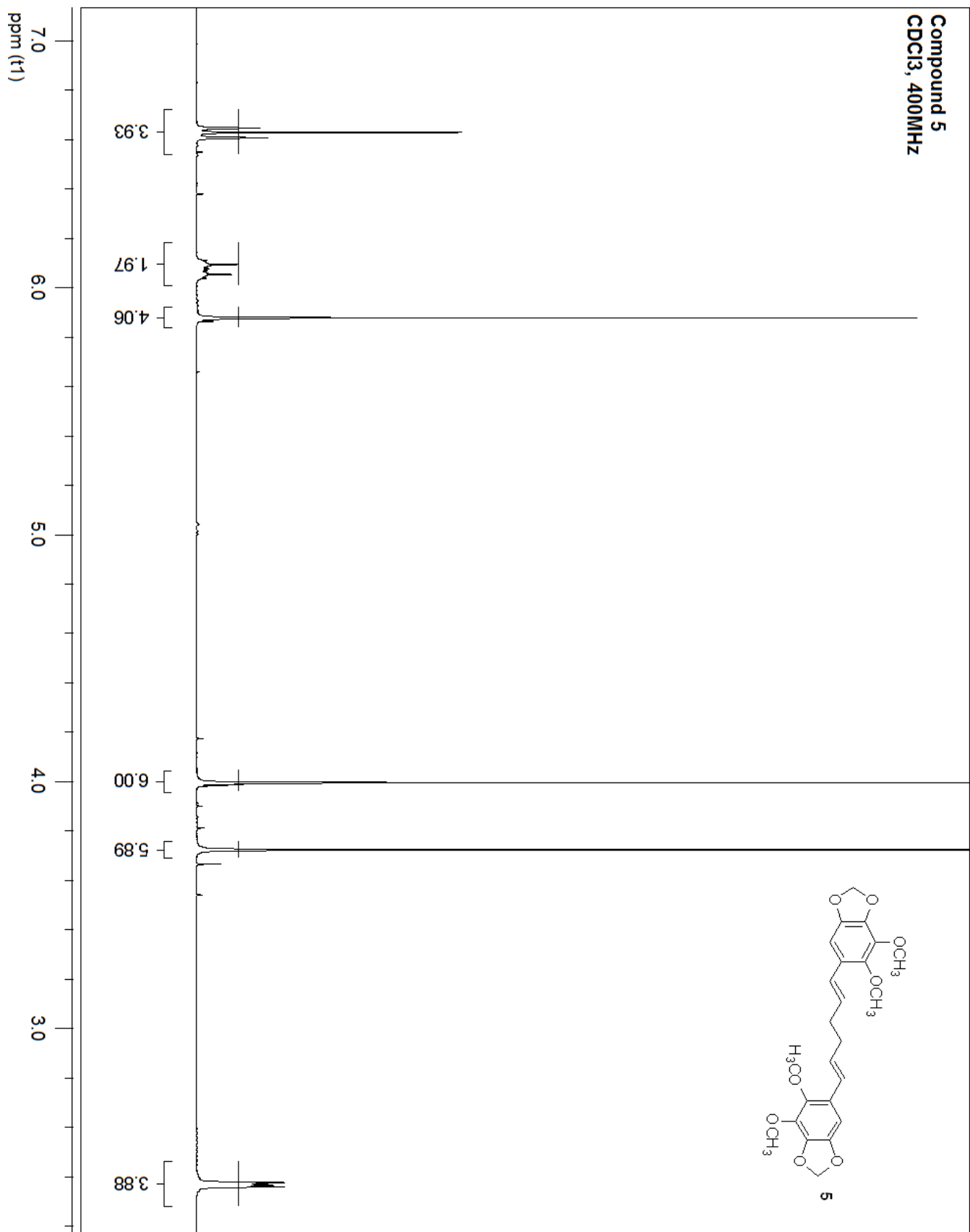
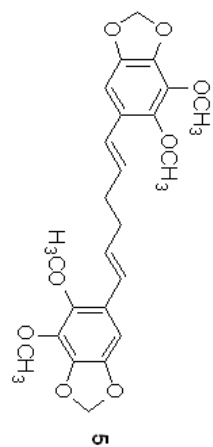


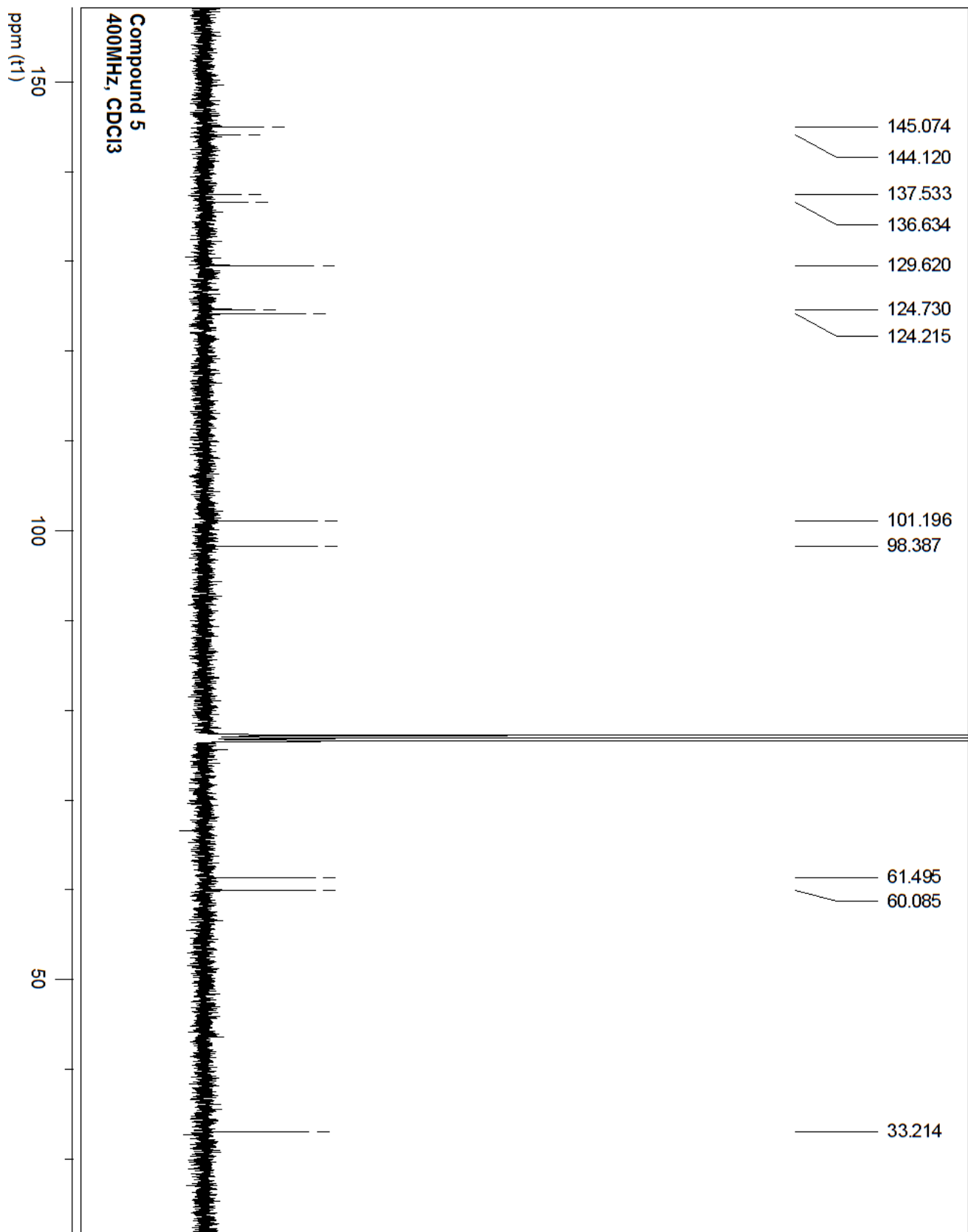
Compound 4
CDCl₃, 400MHz



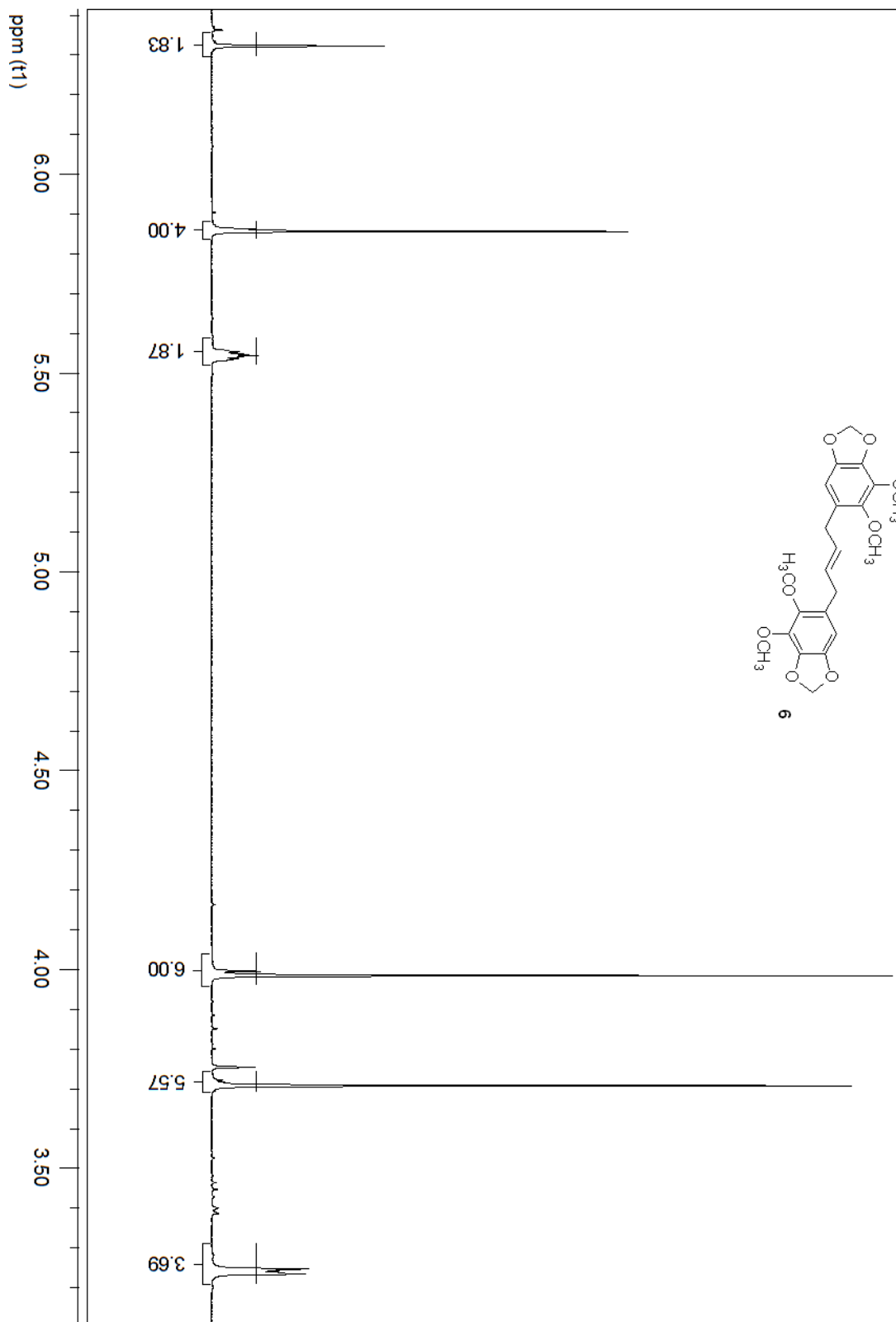
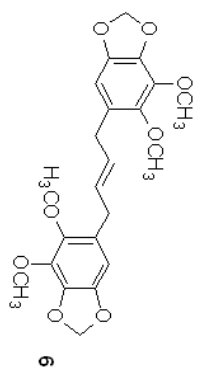


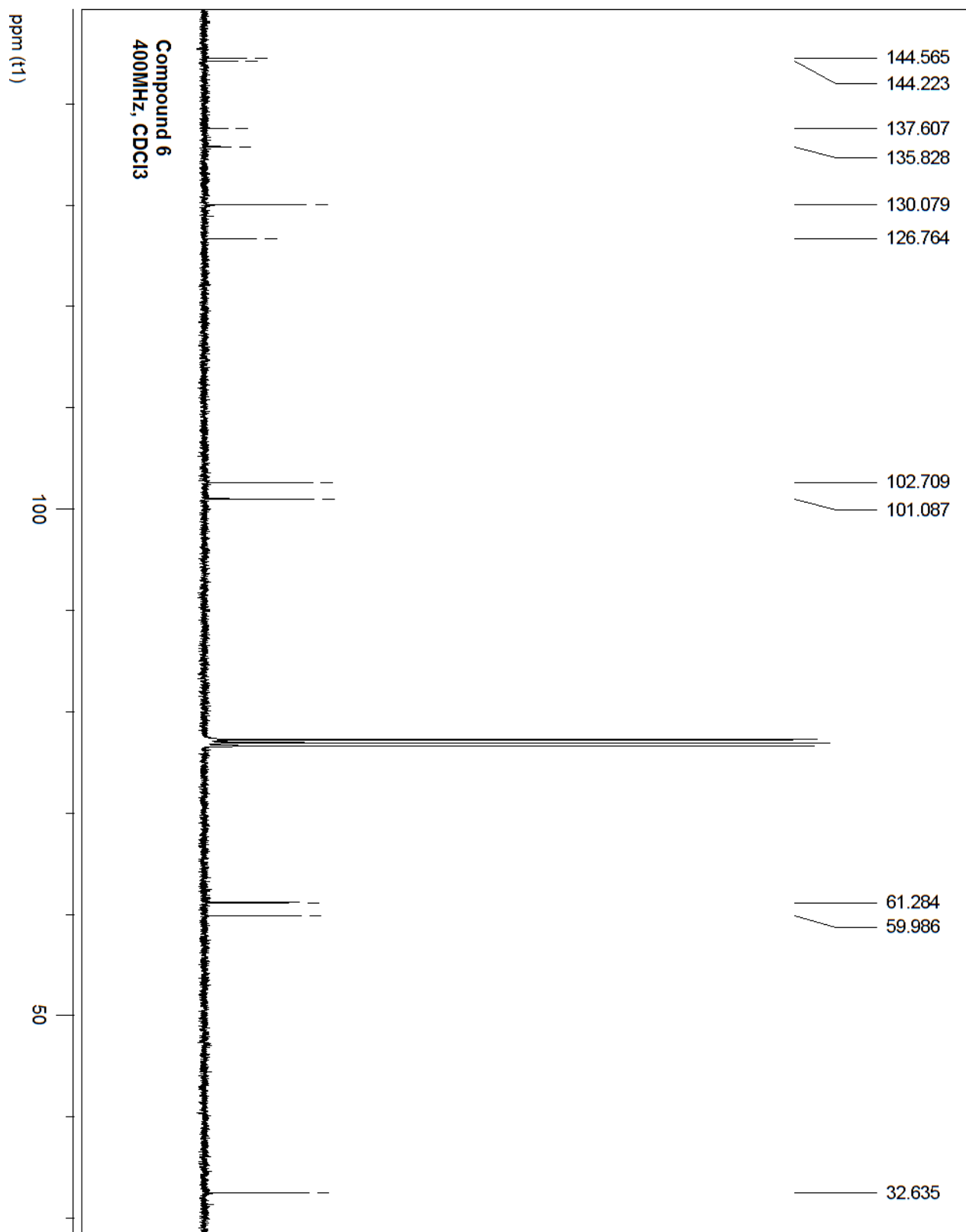
Compound 5
CDCl₃, 400MHz



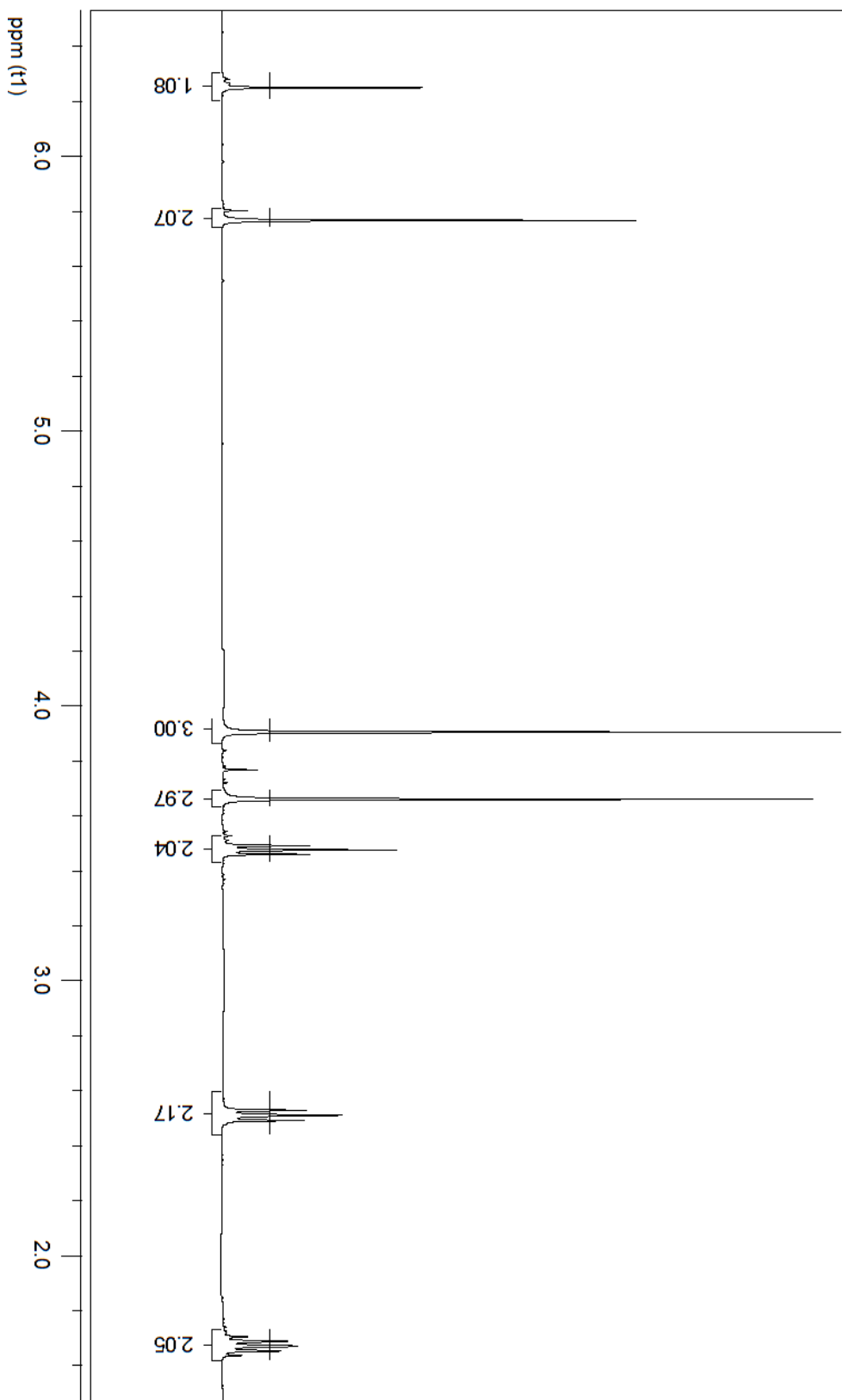
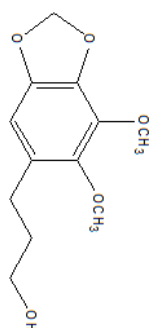


Compound 6
400MHz, CDCl3

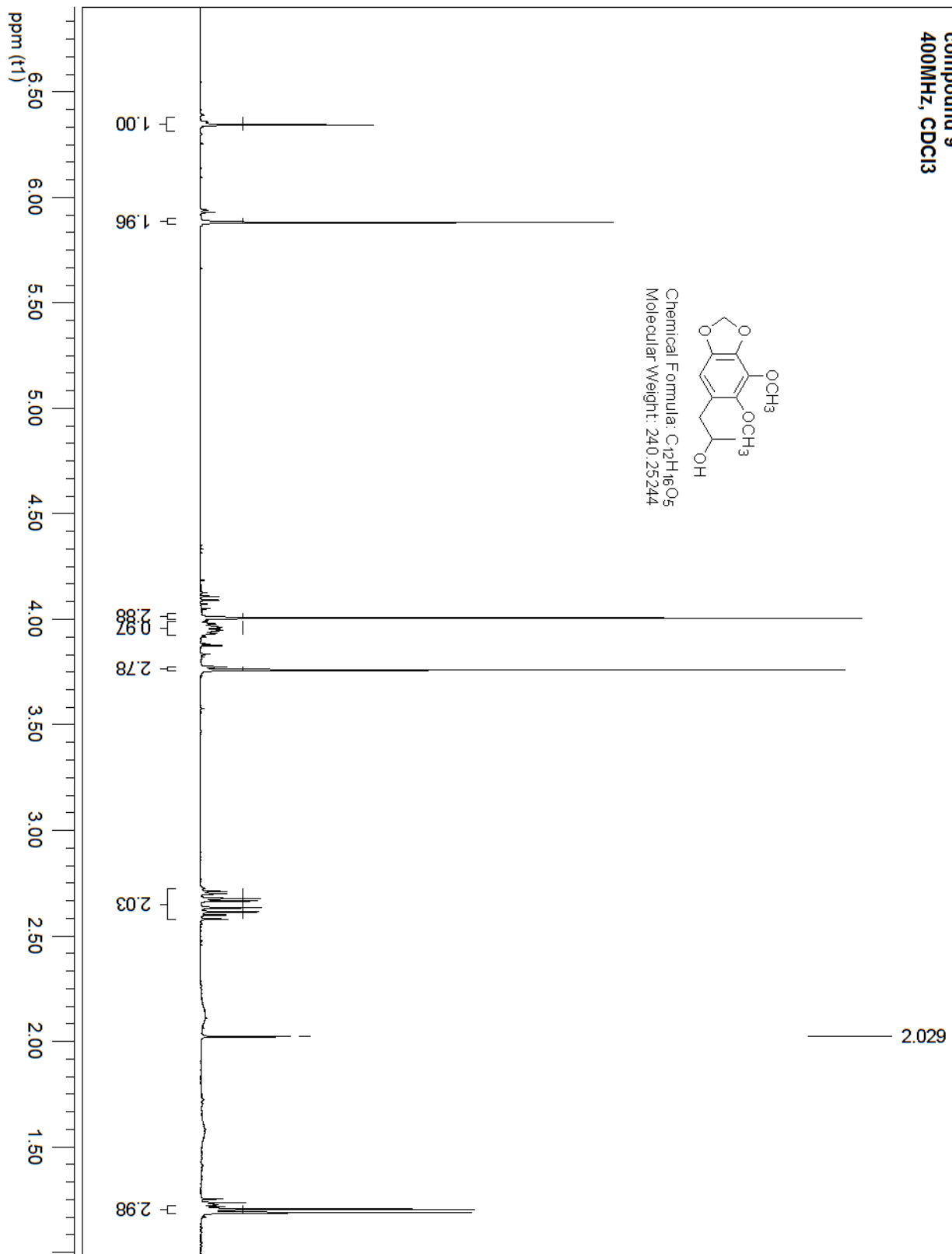
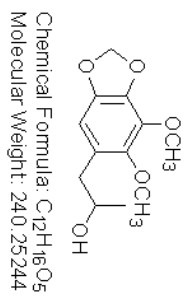




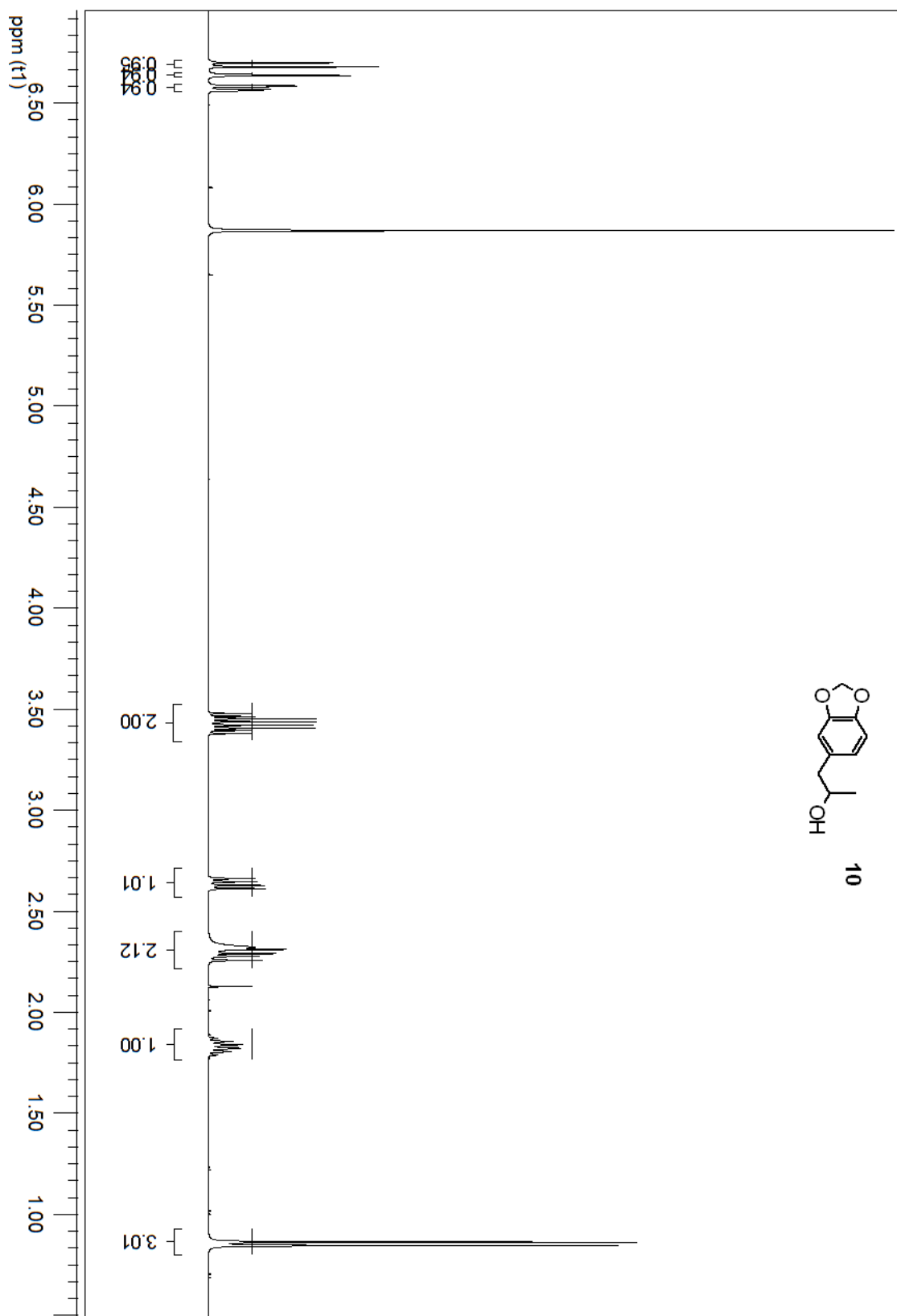
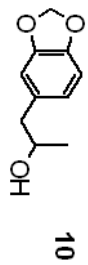
Compound 8
400MHz, CDCl3

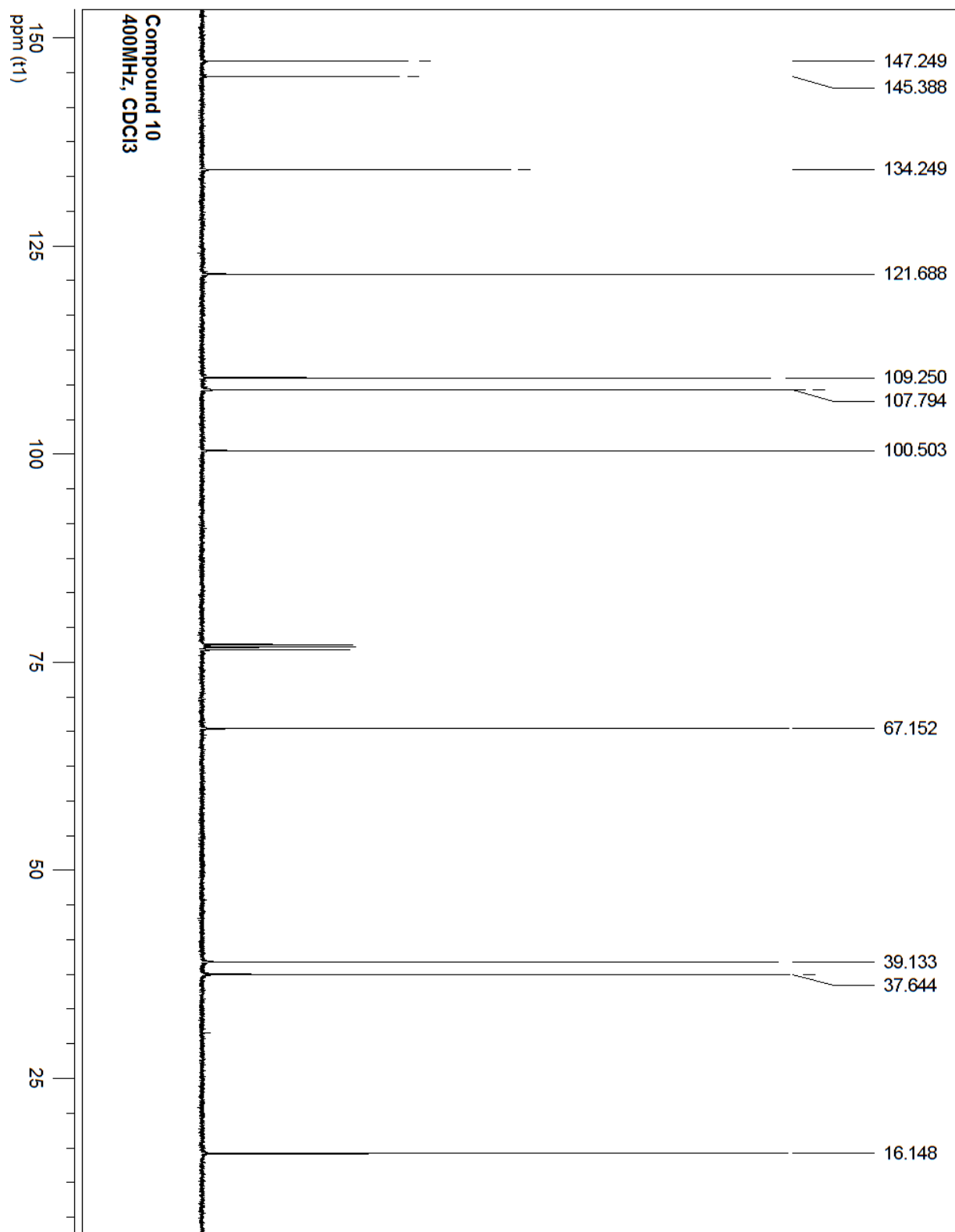


compound 9
400MHz, CDCl3

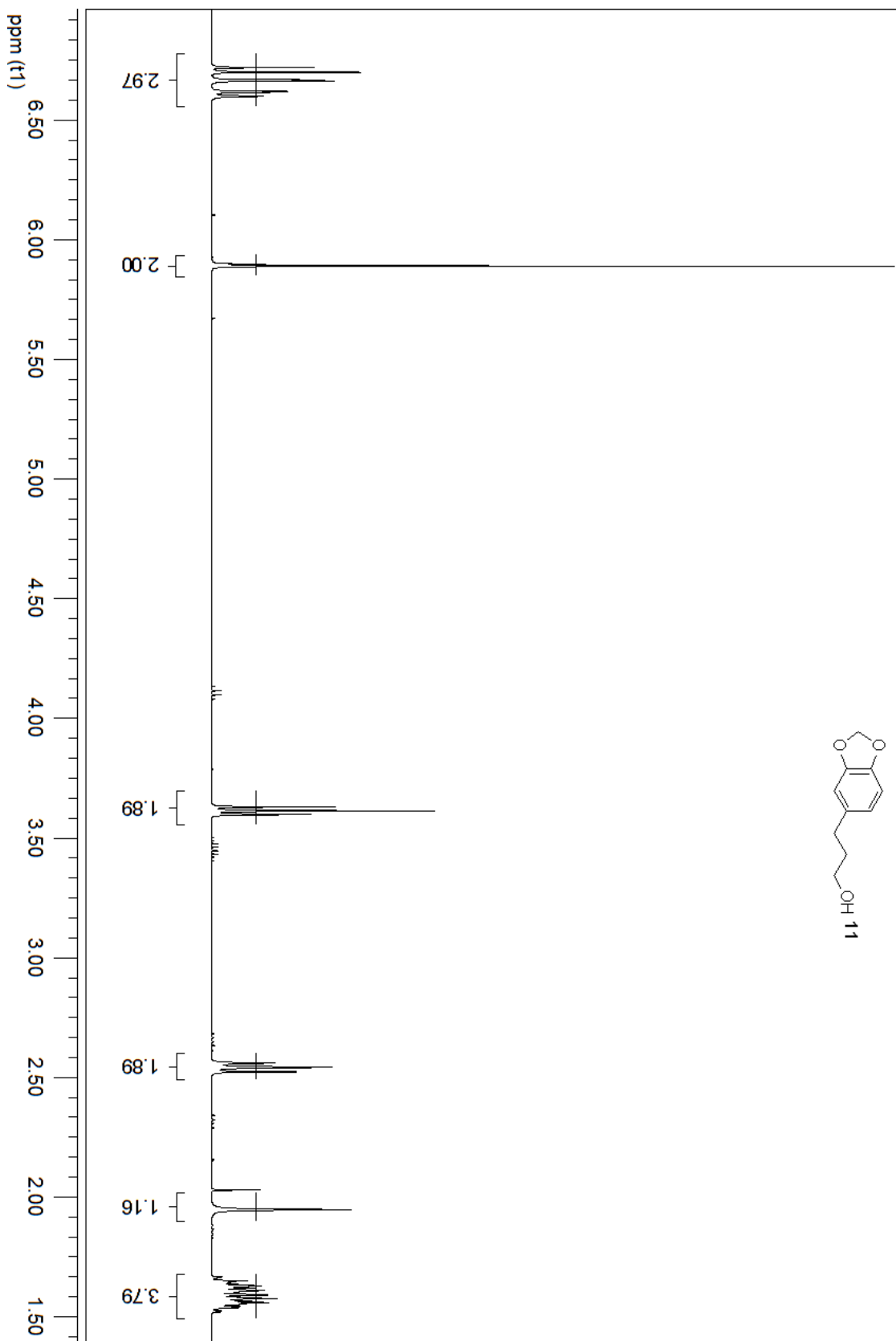
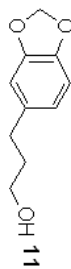


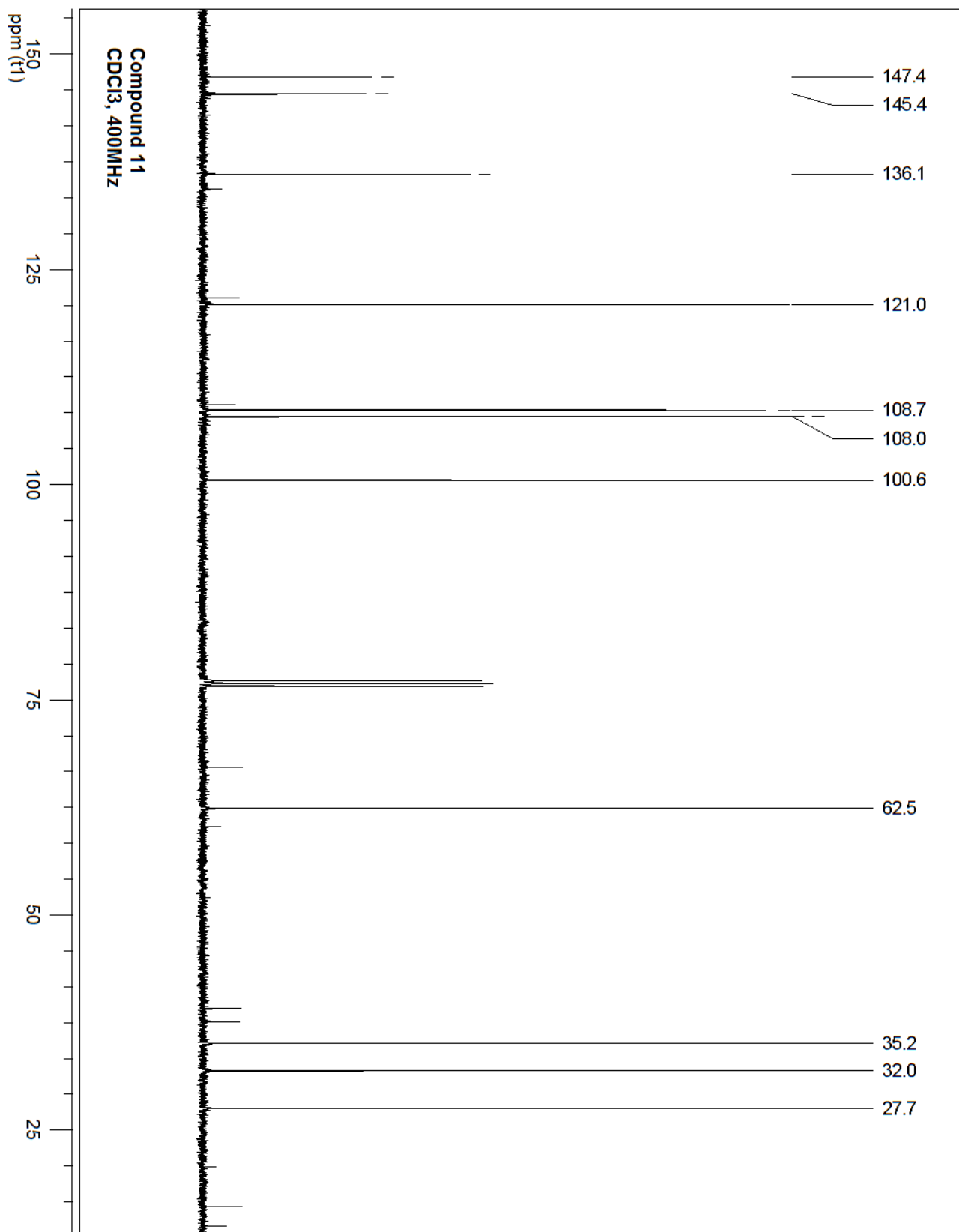
Compound 10
CDCl₃, 400MHz



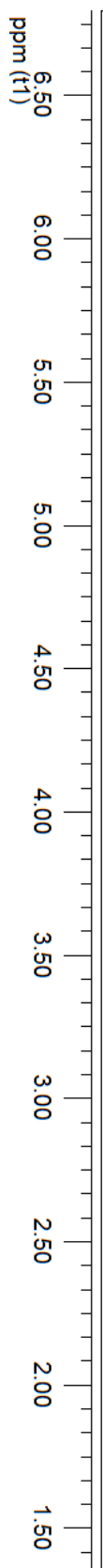
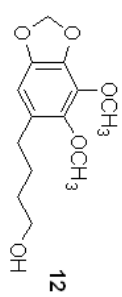


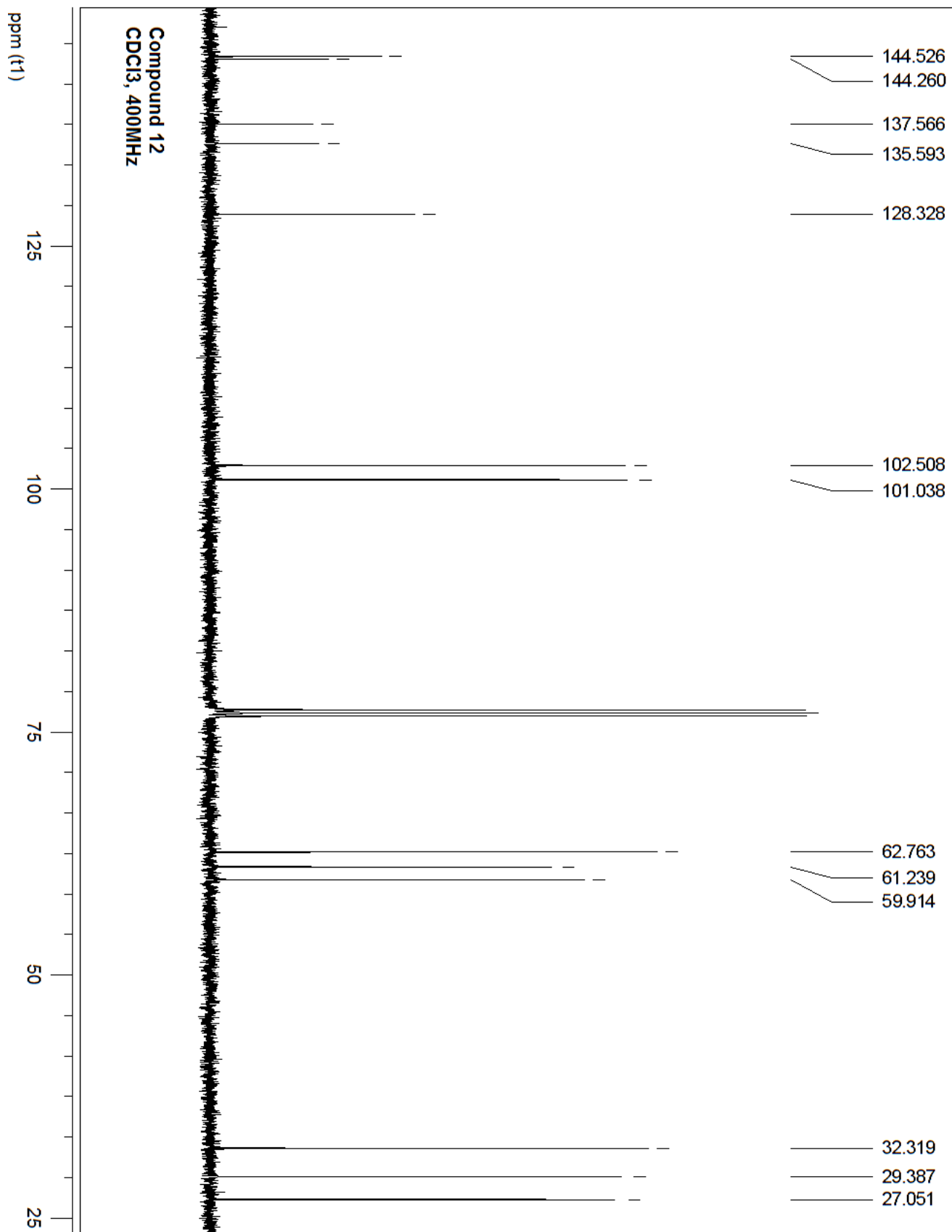
Compound 11
CDCl₃, 400MHz.



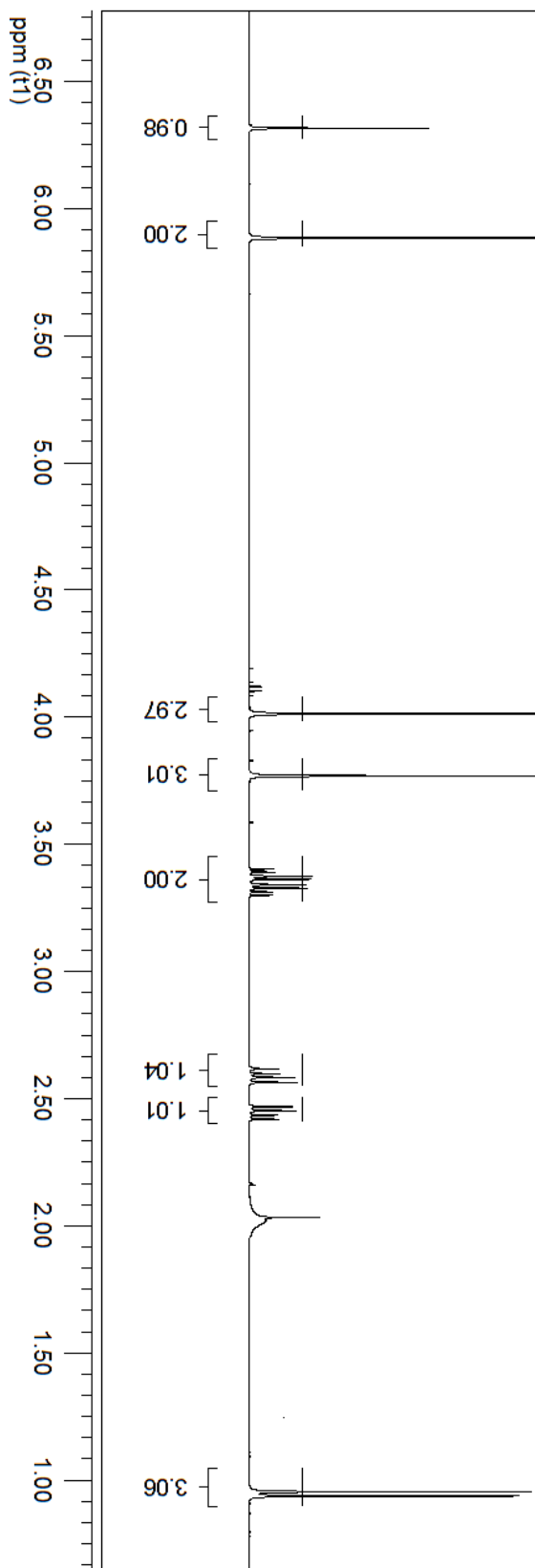
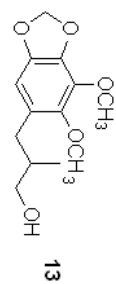


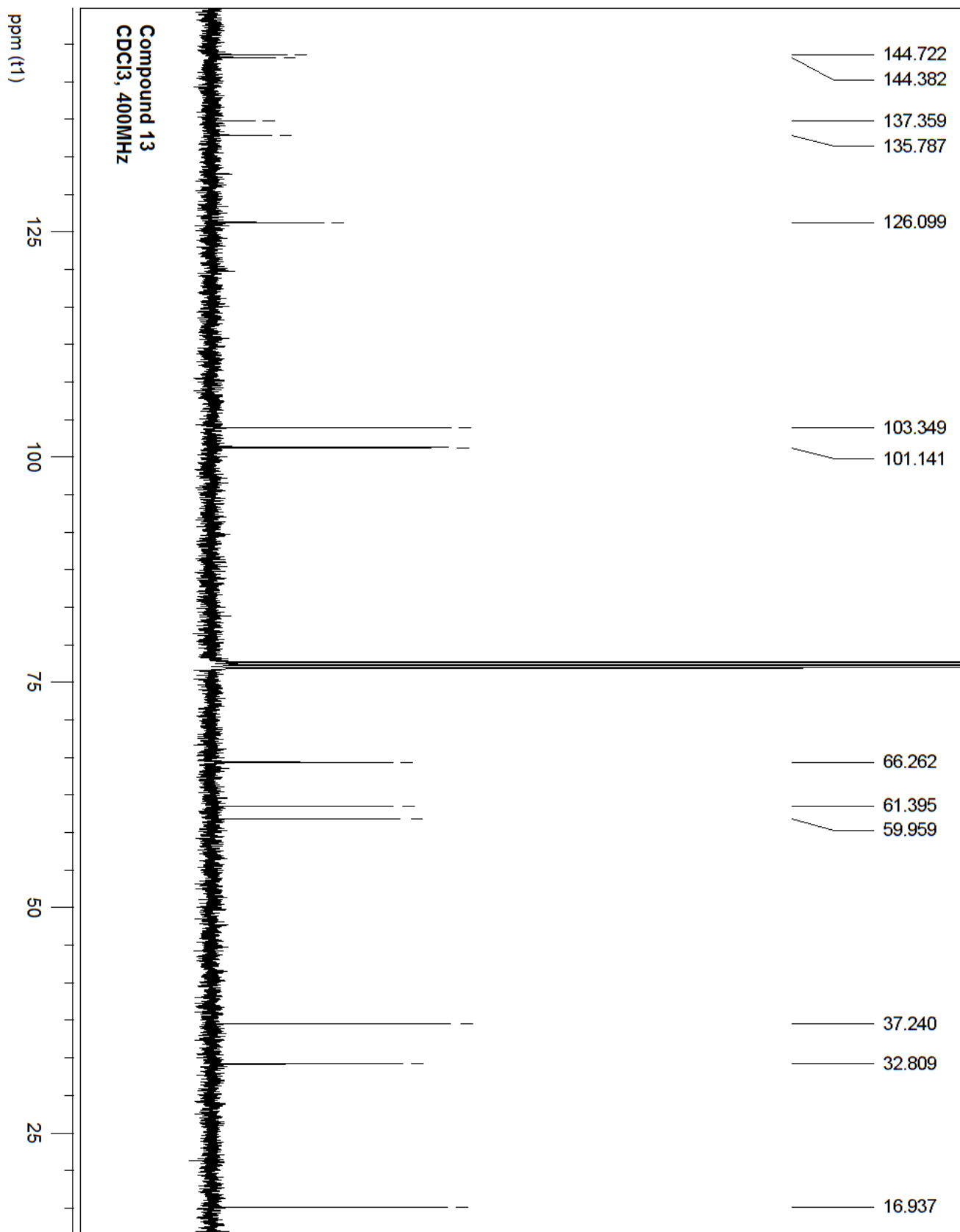
Compound 12
CDCl₃, 400MHz



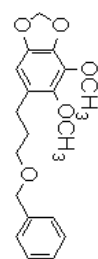


Compound 13
CDCl₃, 400MHz

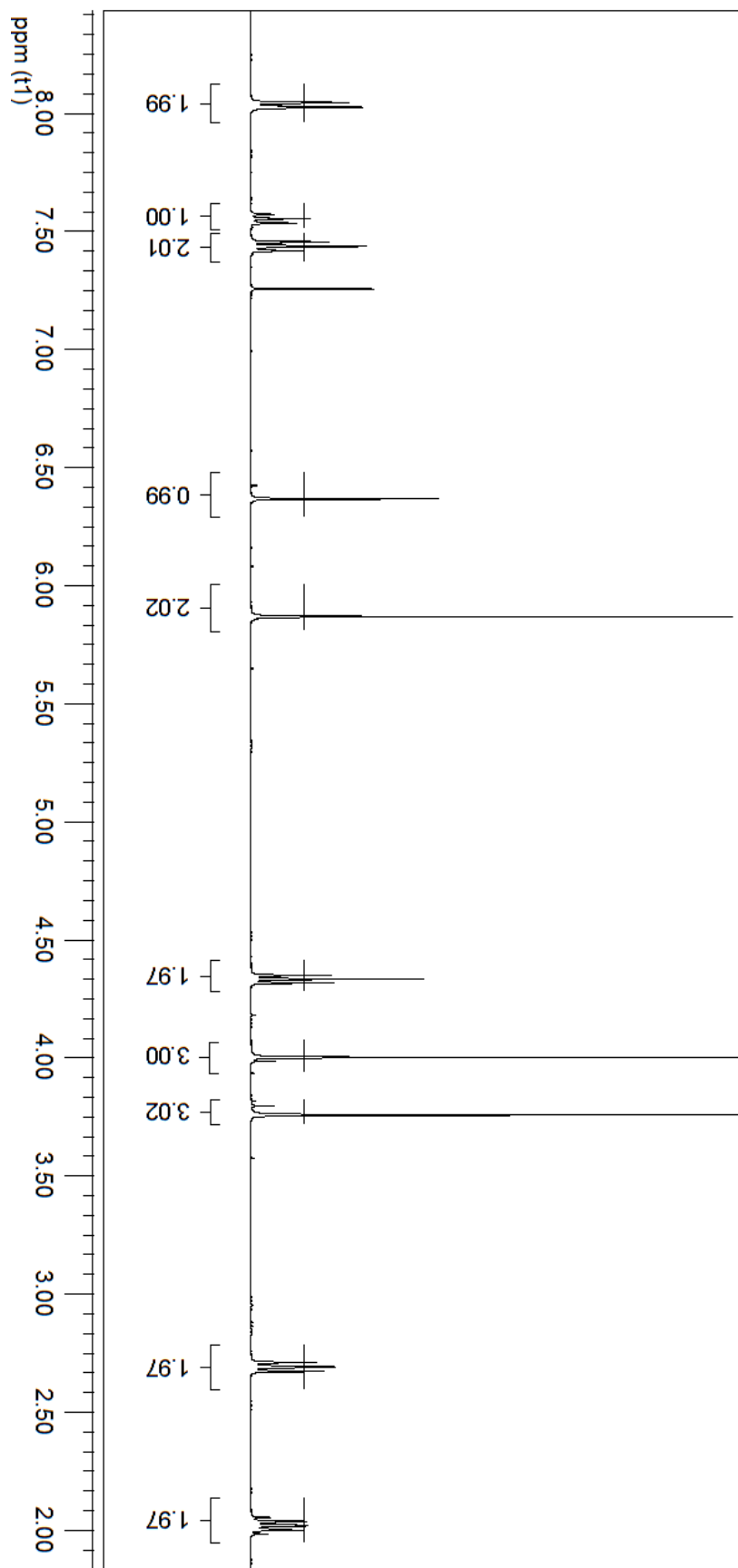


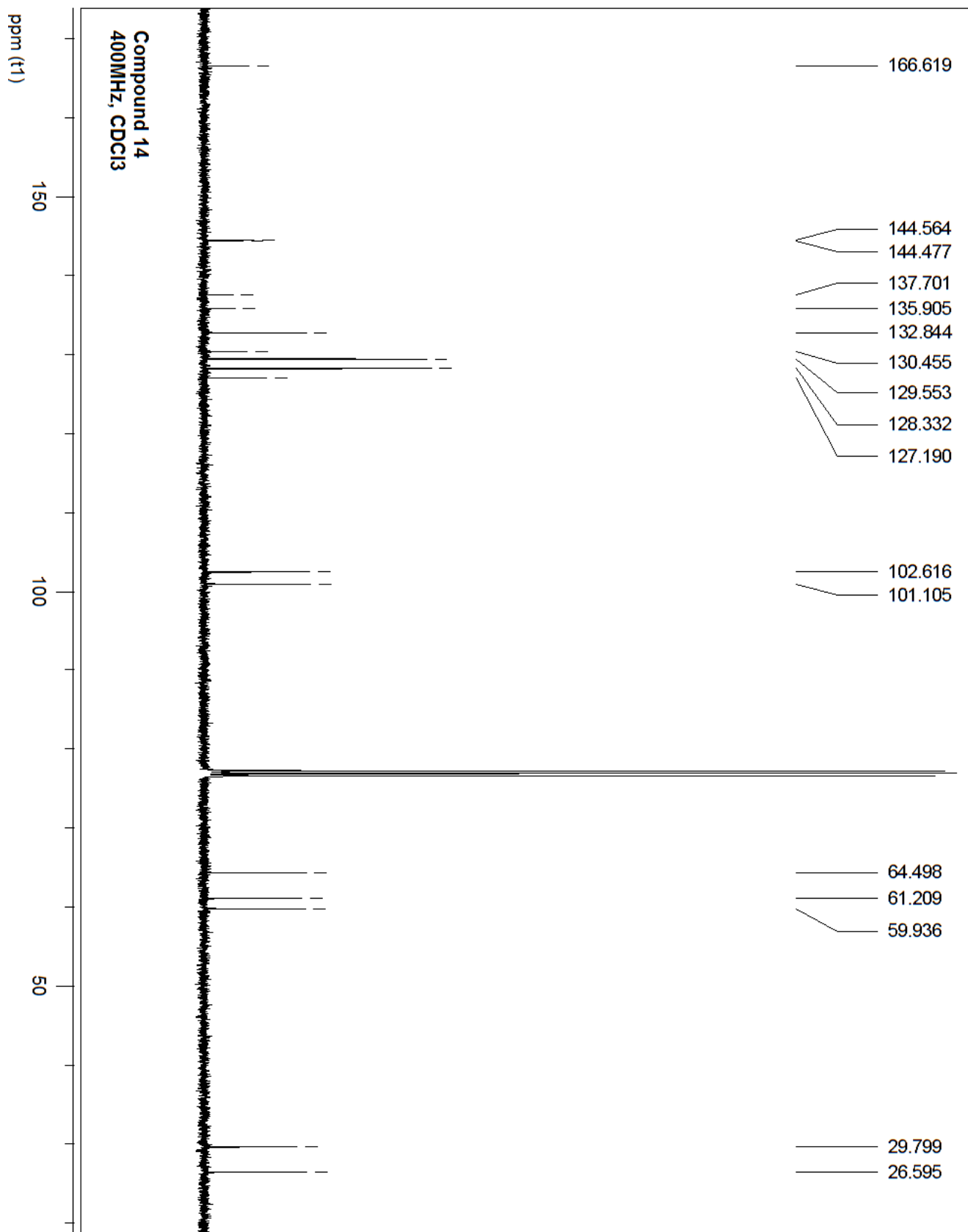


Compound 14
400MHz, CDCl3

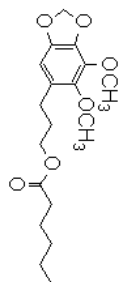


14

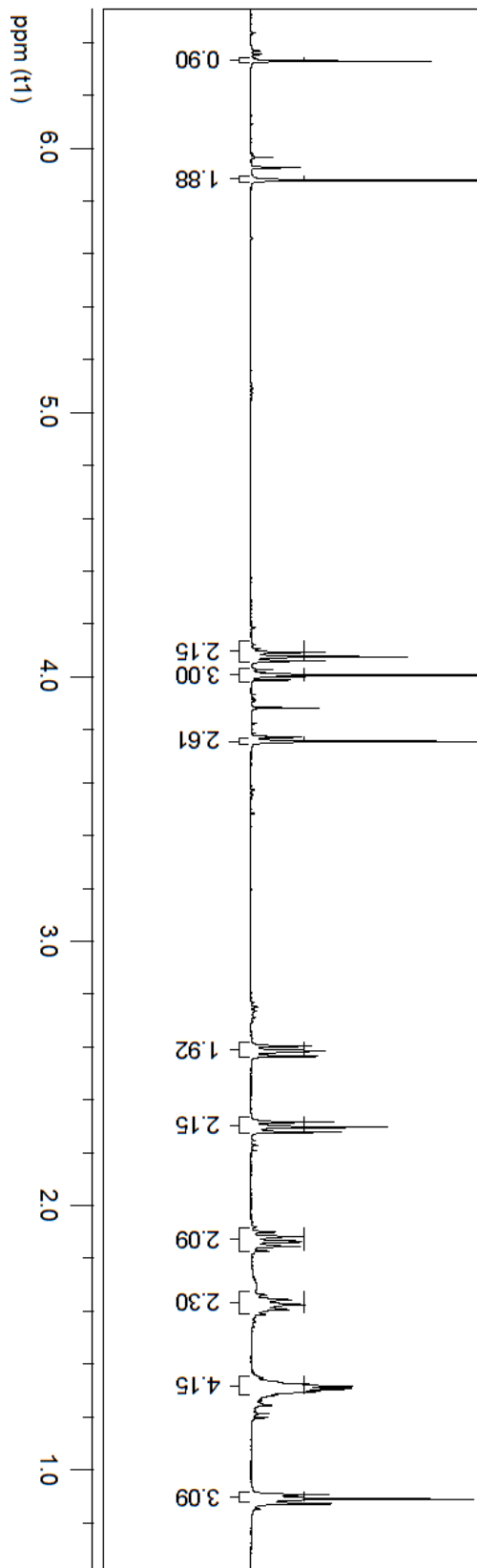


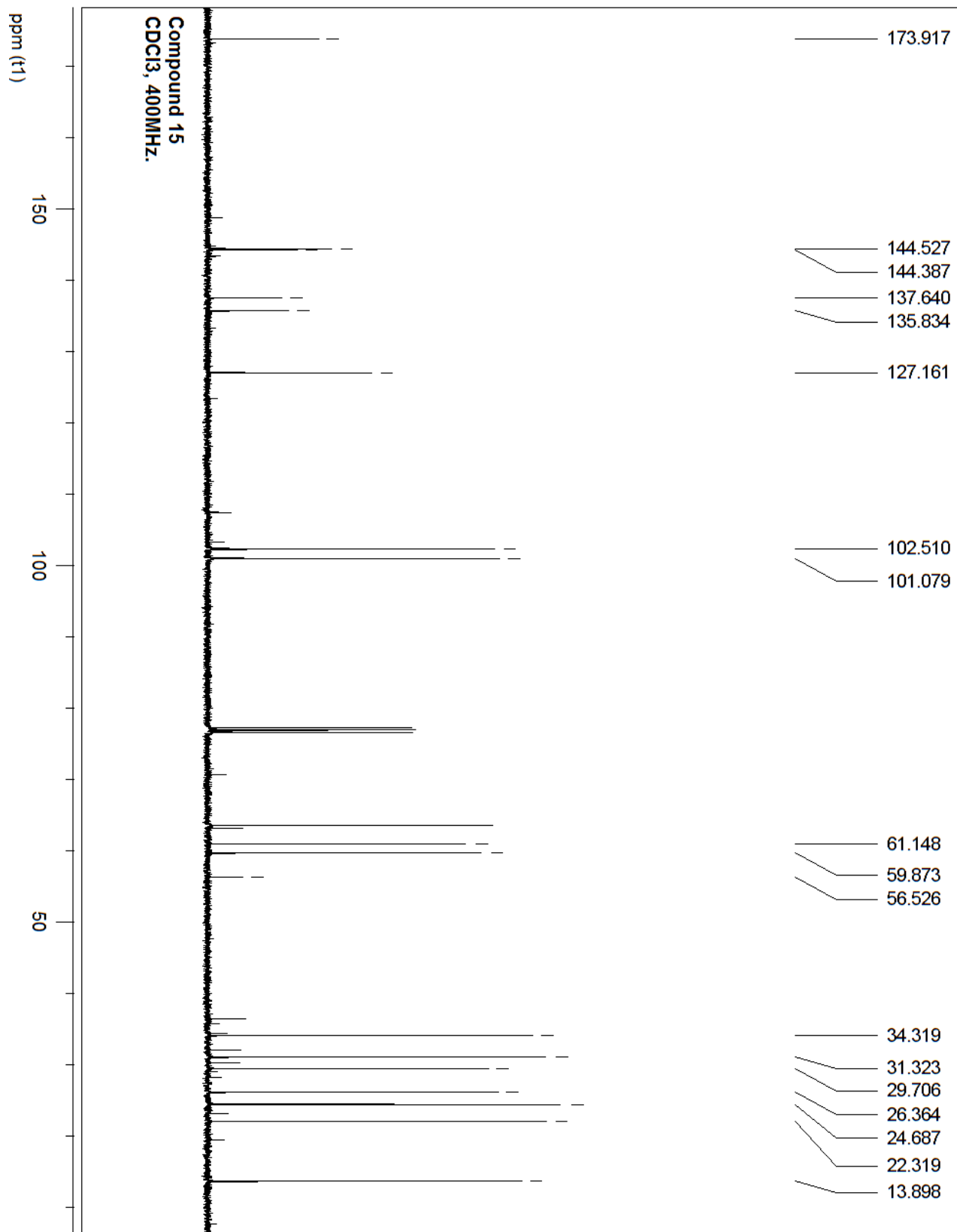


Compound 15
400MHz, CDCl3

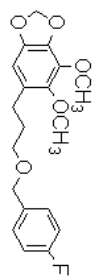


15

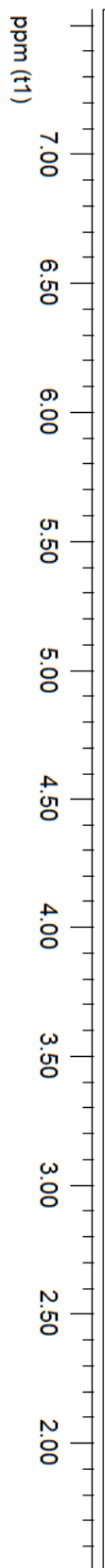


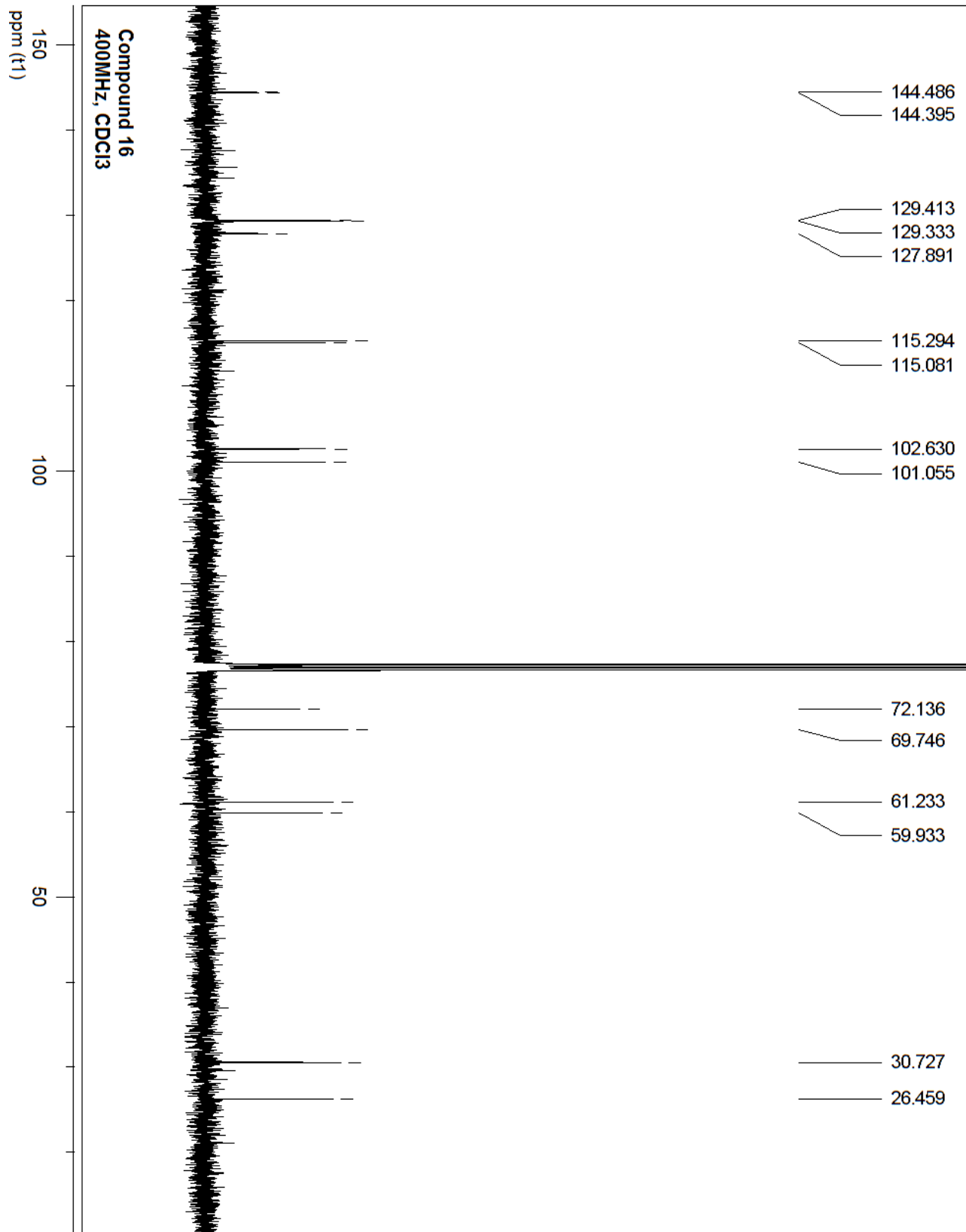


Compound 16
CDCl₃, 400MHz

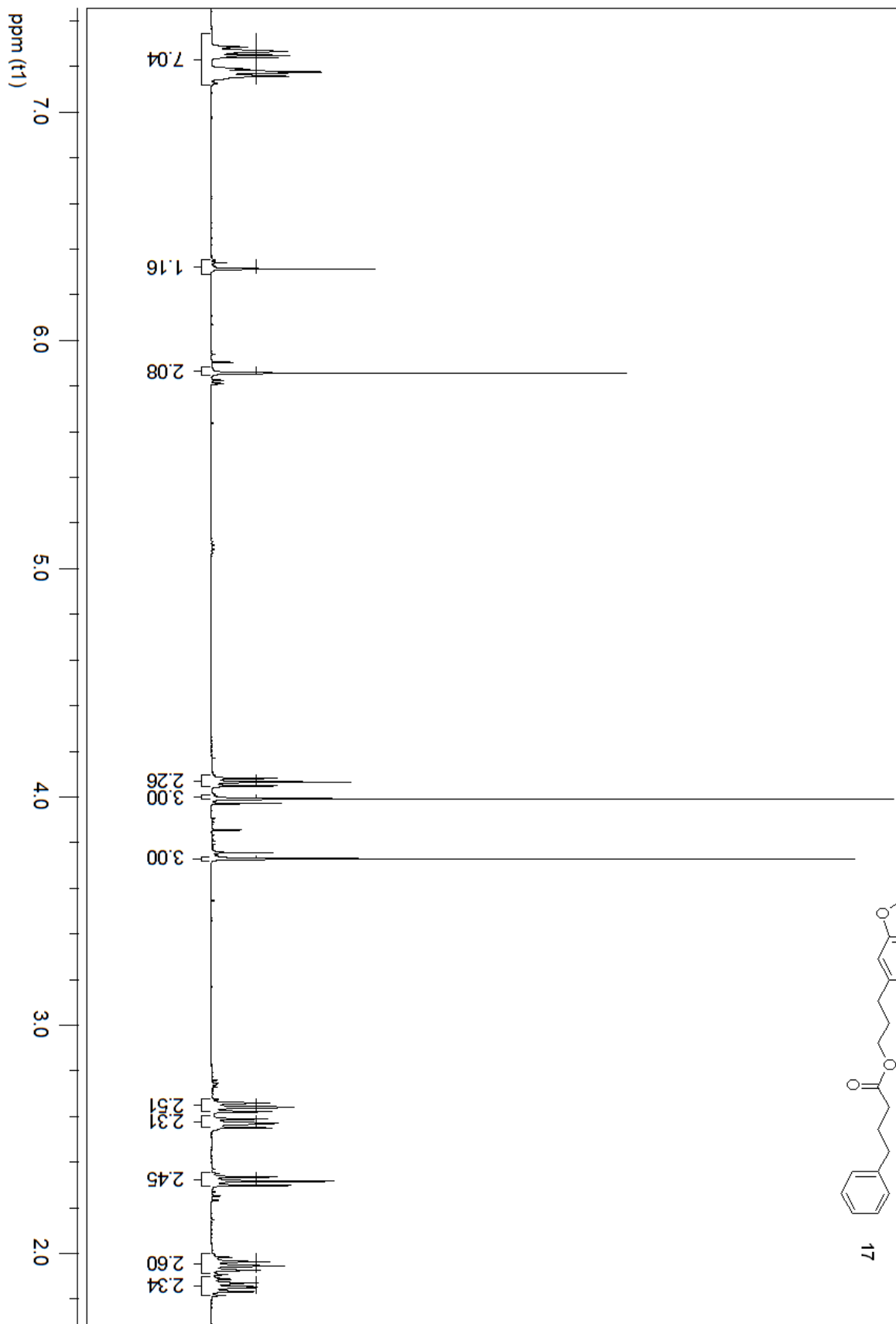
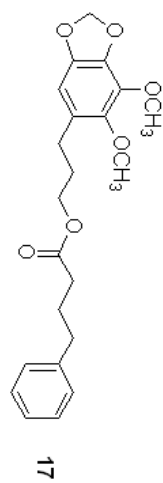


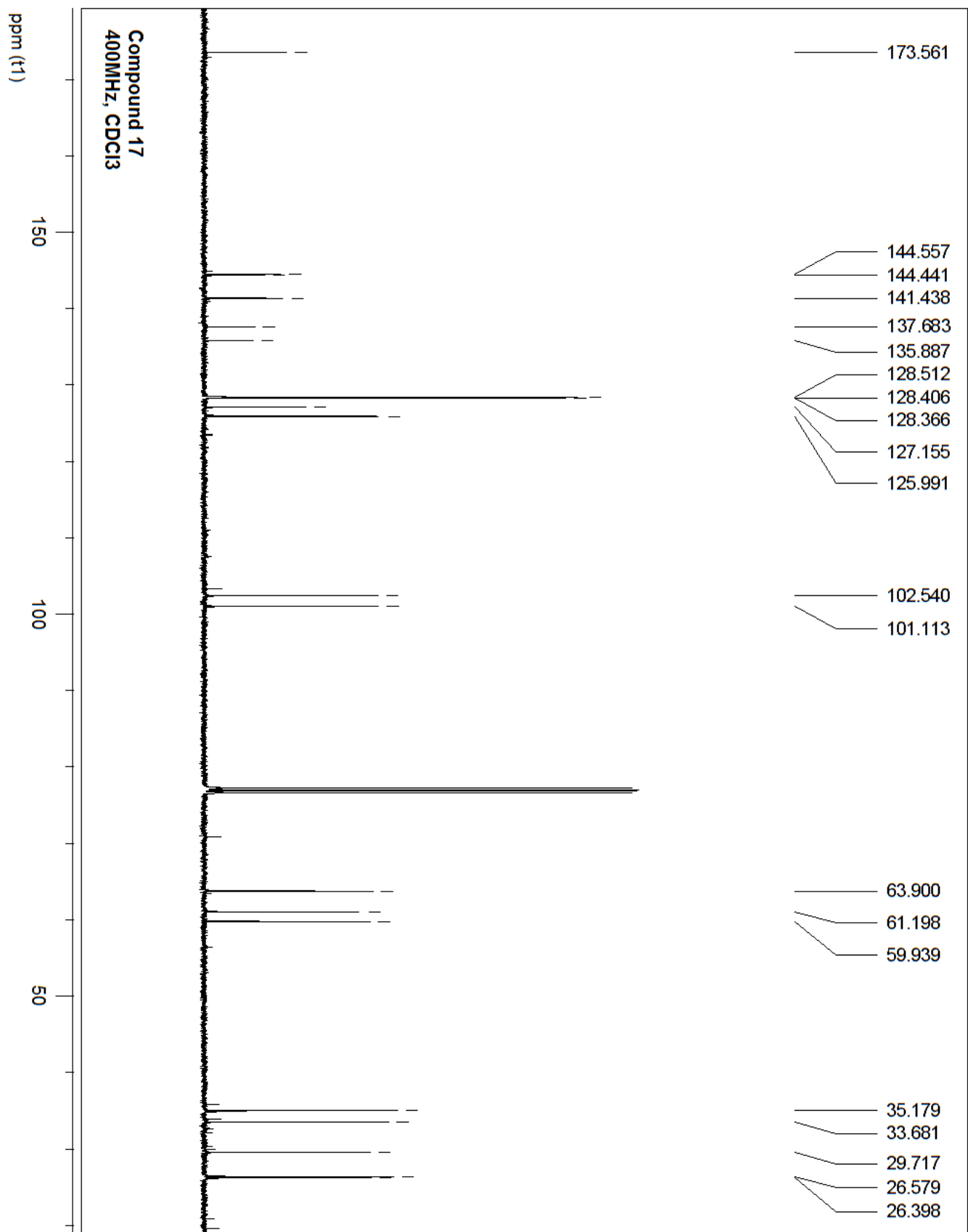
16



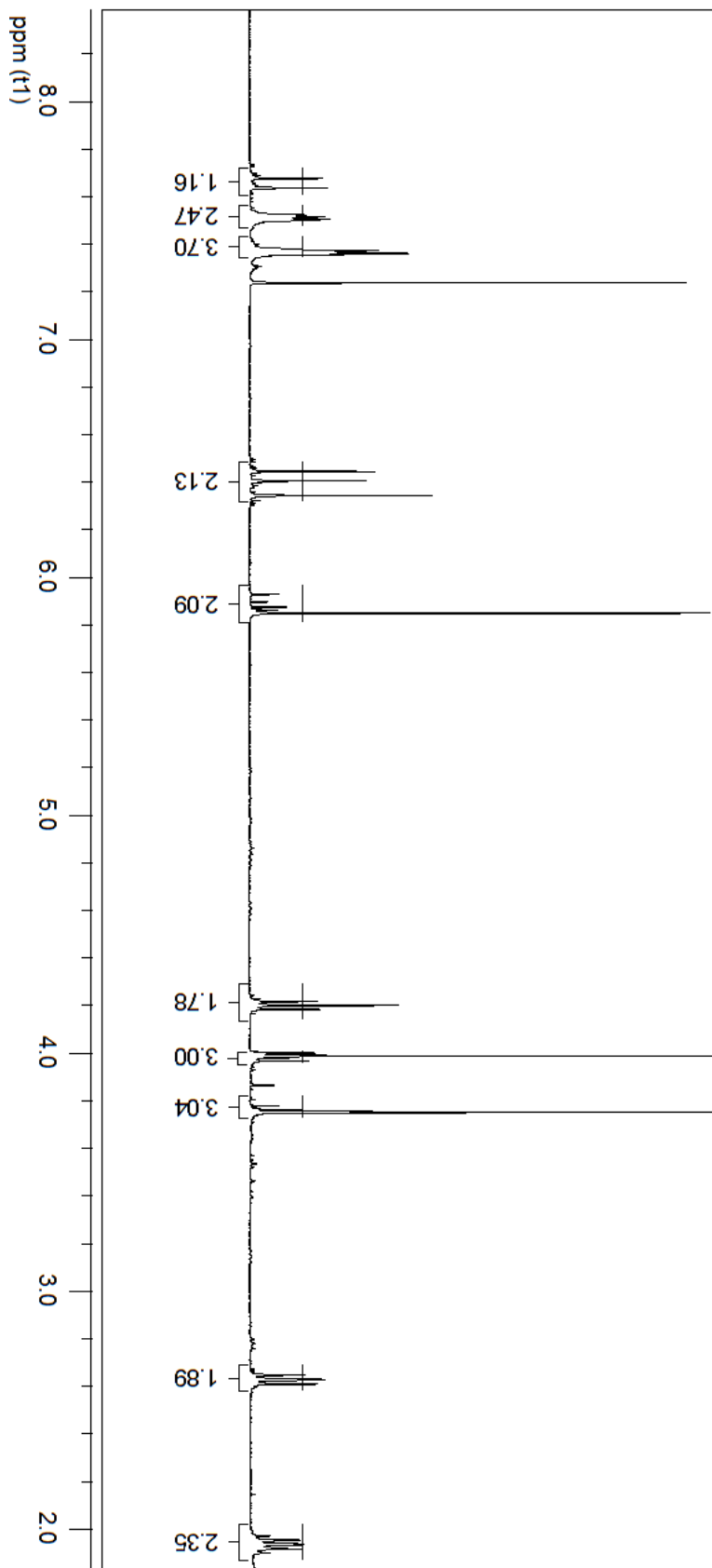
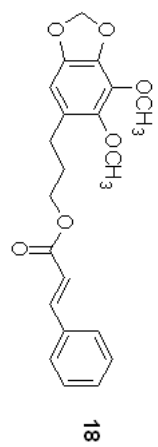


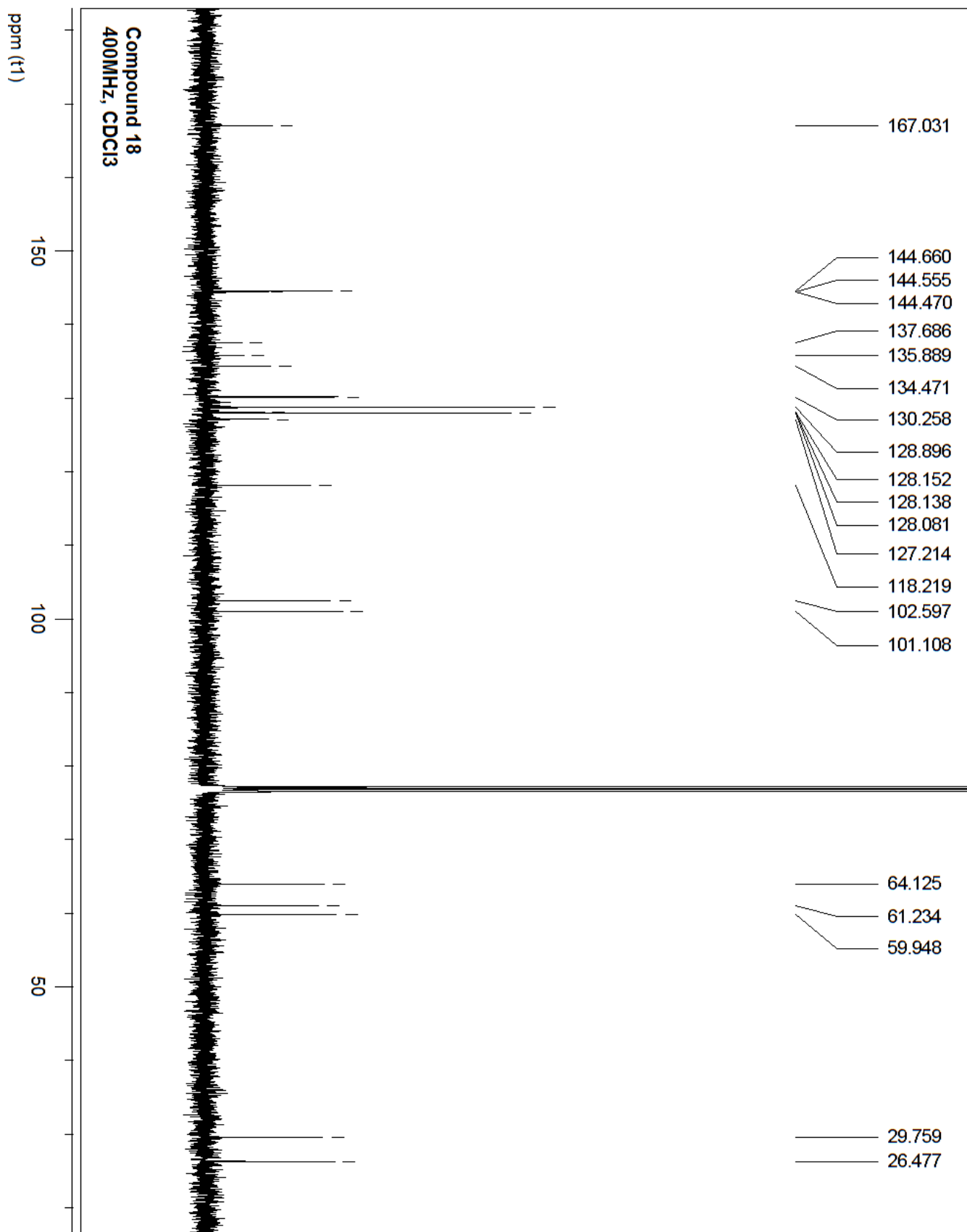
Compound 17
400MHz, CDCl3



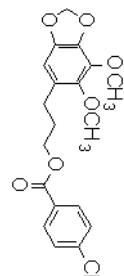


Compound 18
400MHz, CDCl₃

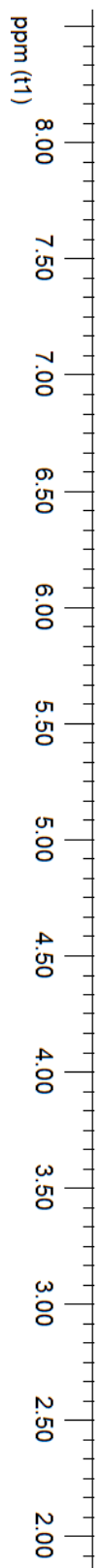


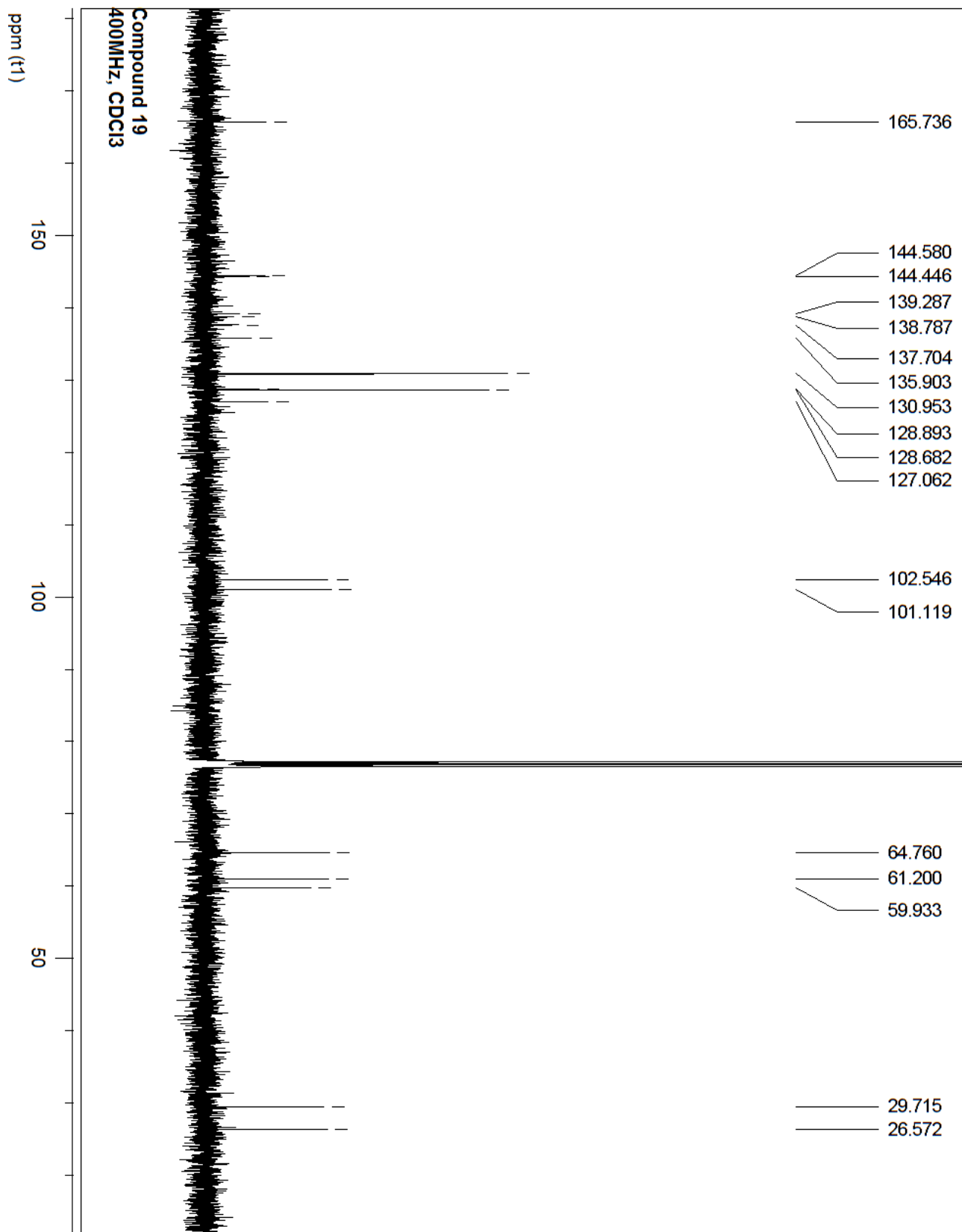


Compound 19
CDCl₃, 400 MHz

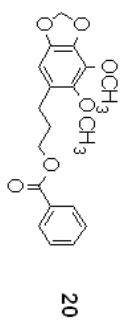


19

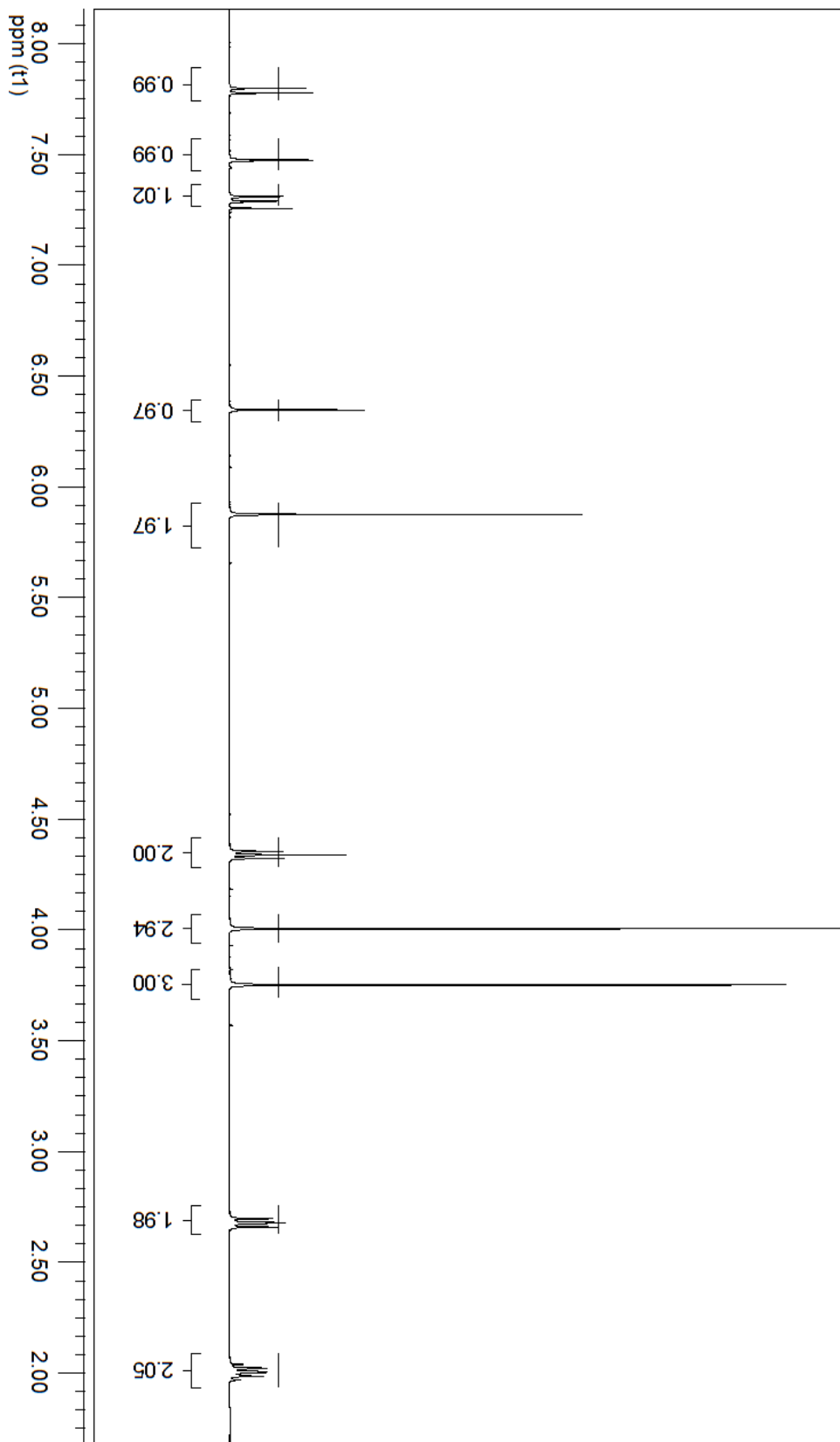
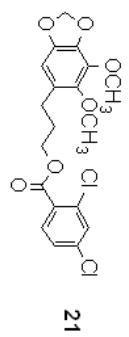




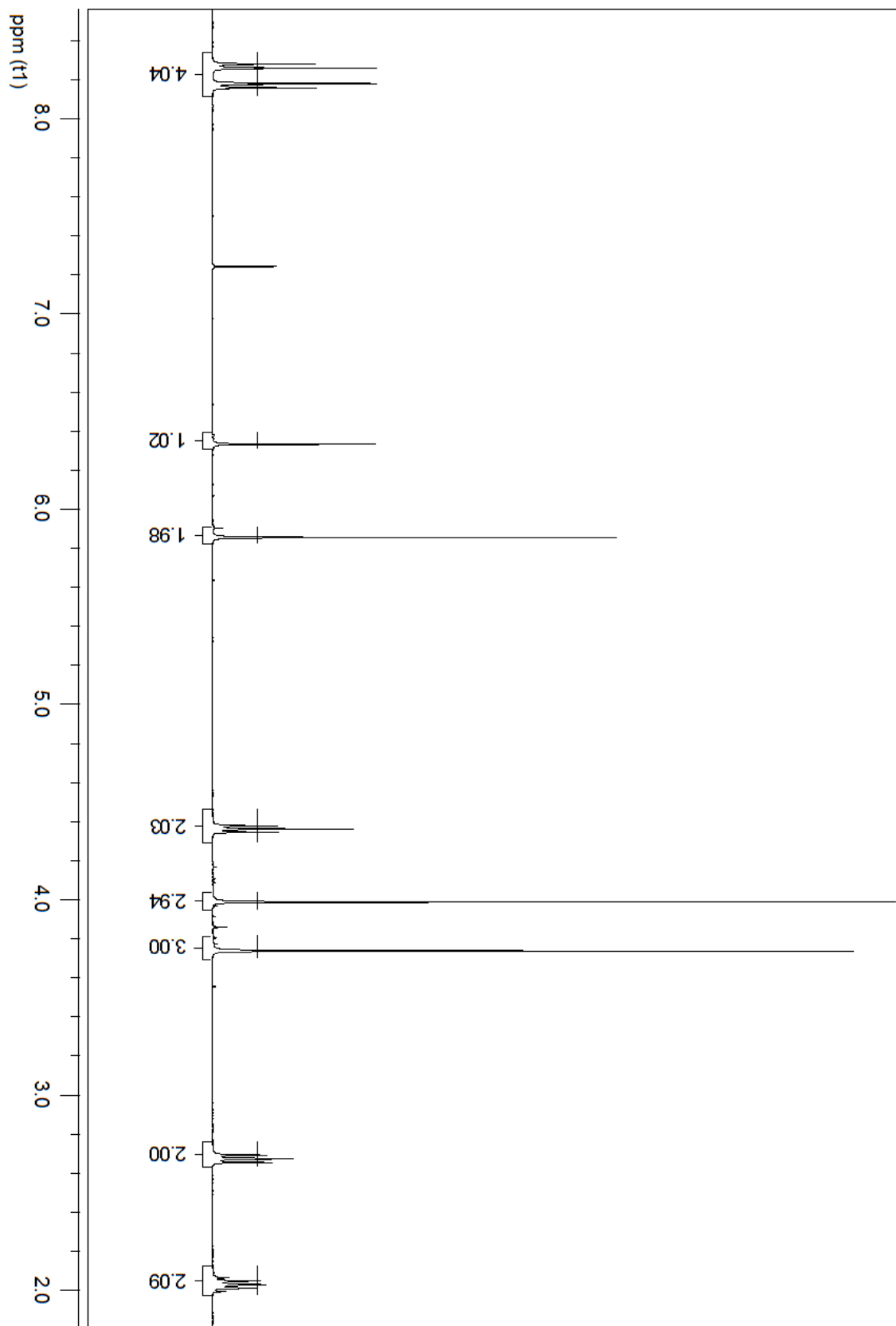
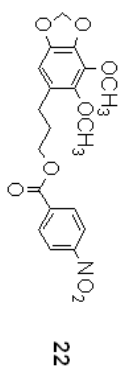
Compound 20
400MHz, CDCl3



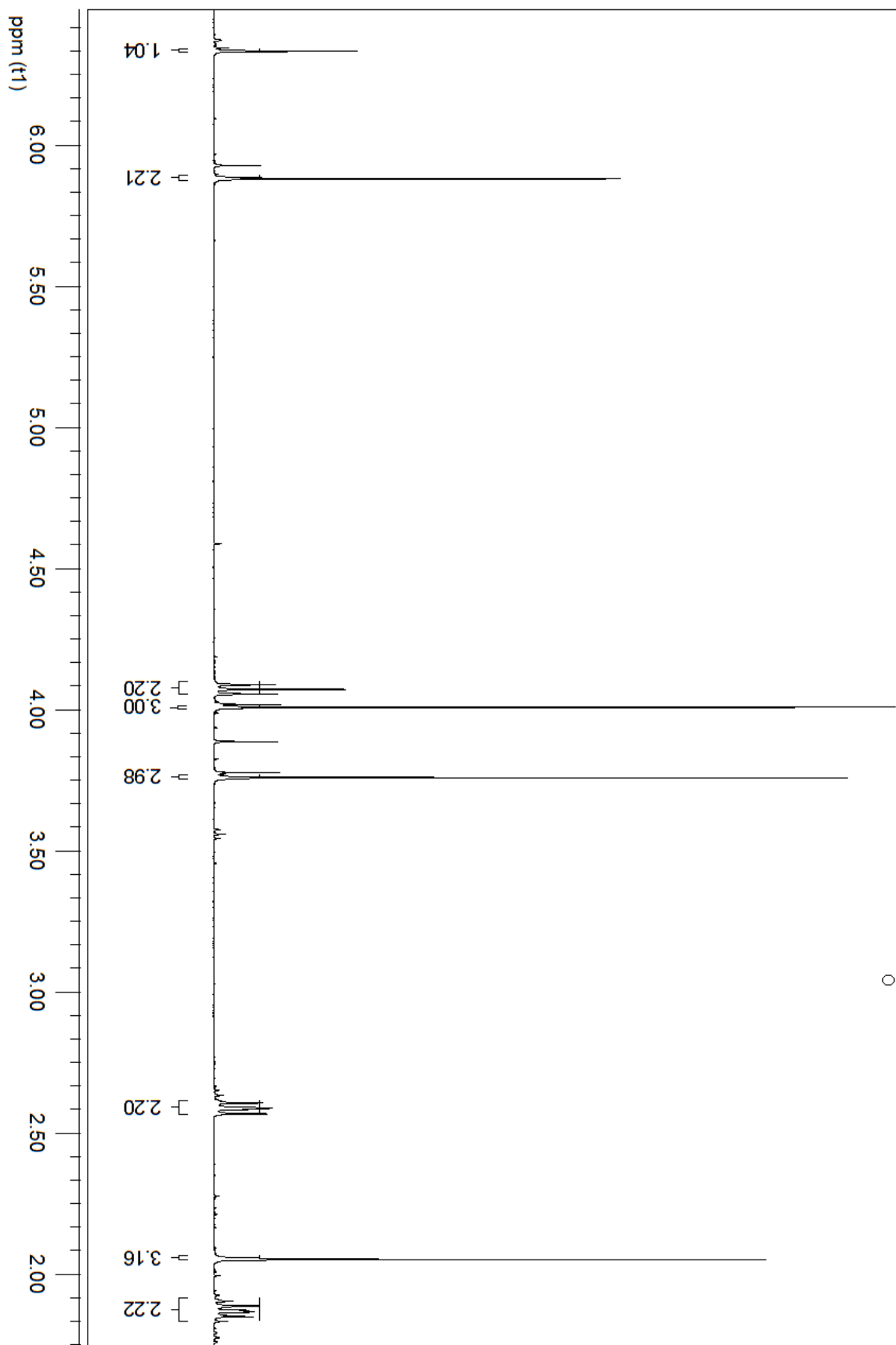
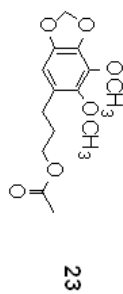
Compound 21
CDCl₃, 400MHz



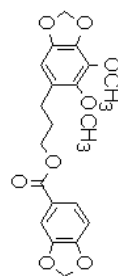
Compound 22
400MHz, CDCl3



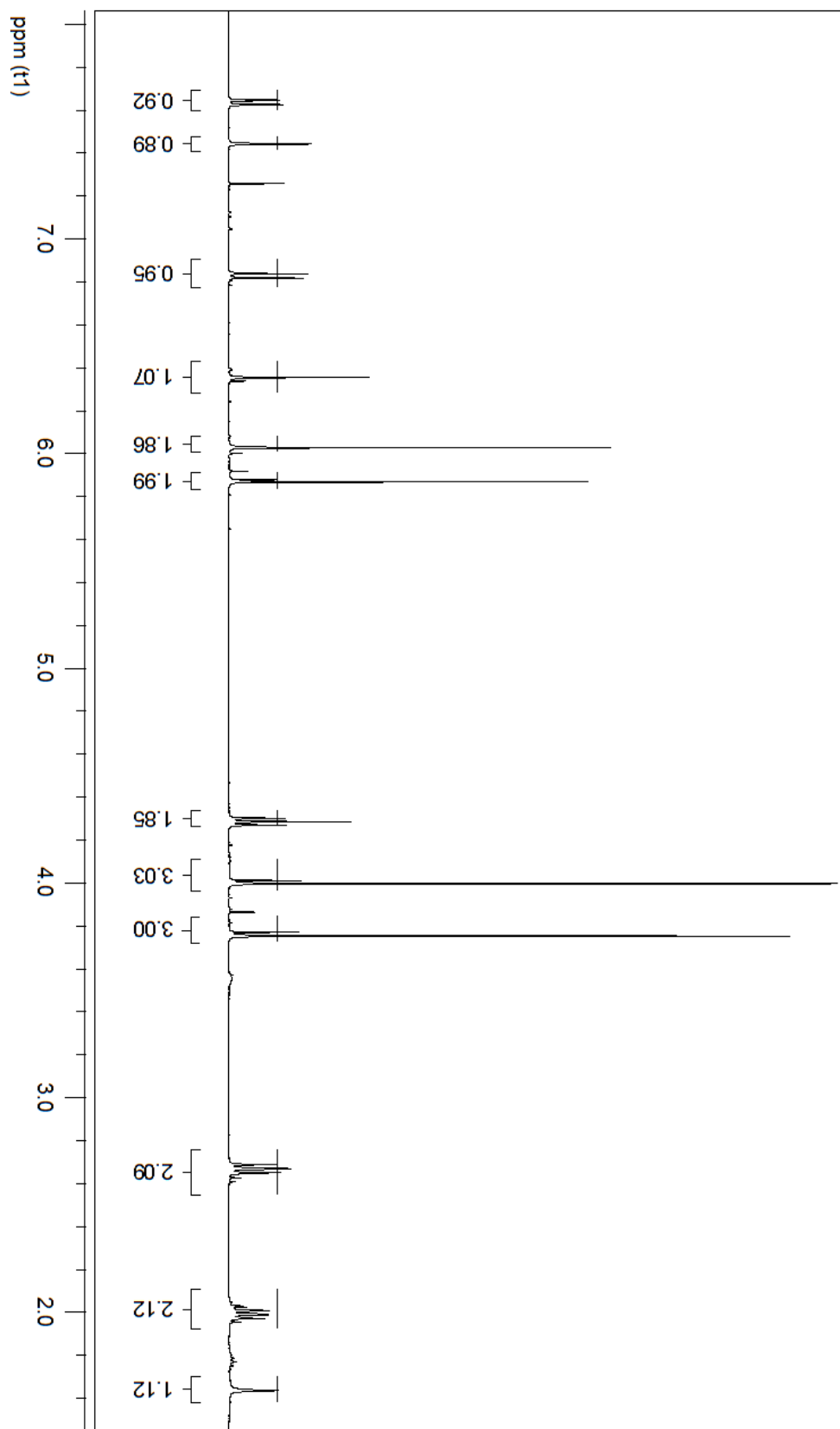
Compound 23
400MHz, CDCl₃



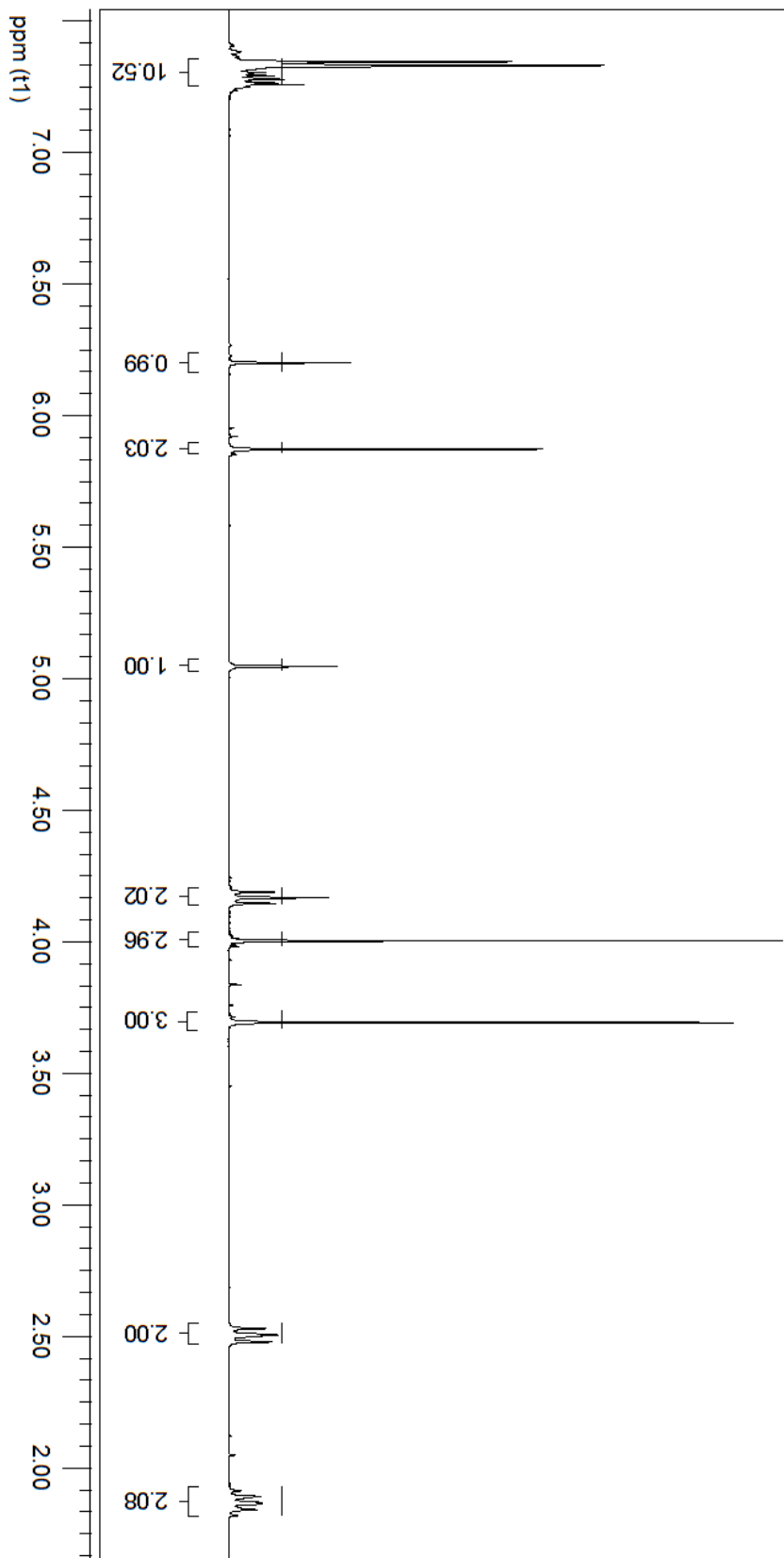
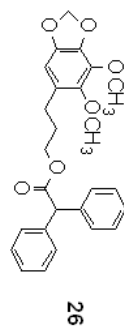
Compound 25
400MHz, CDCl3

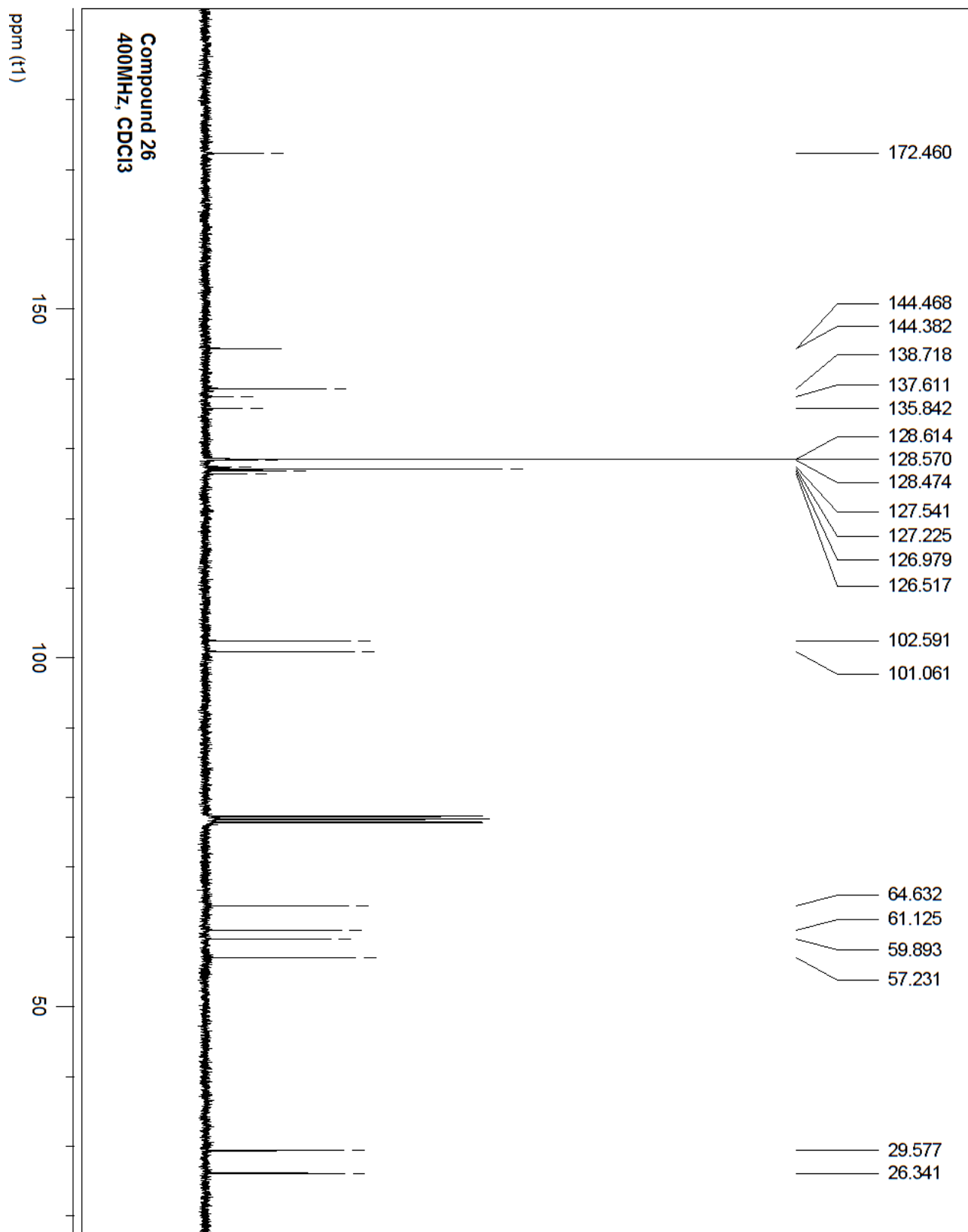


25

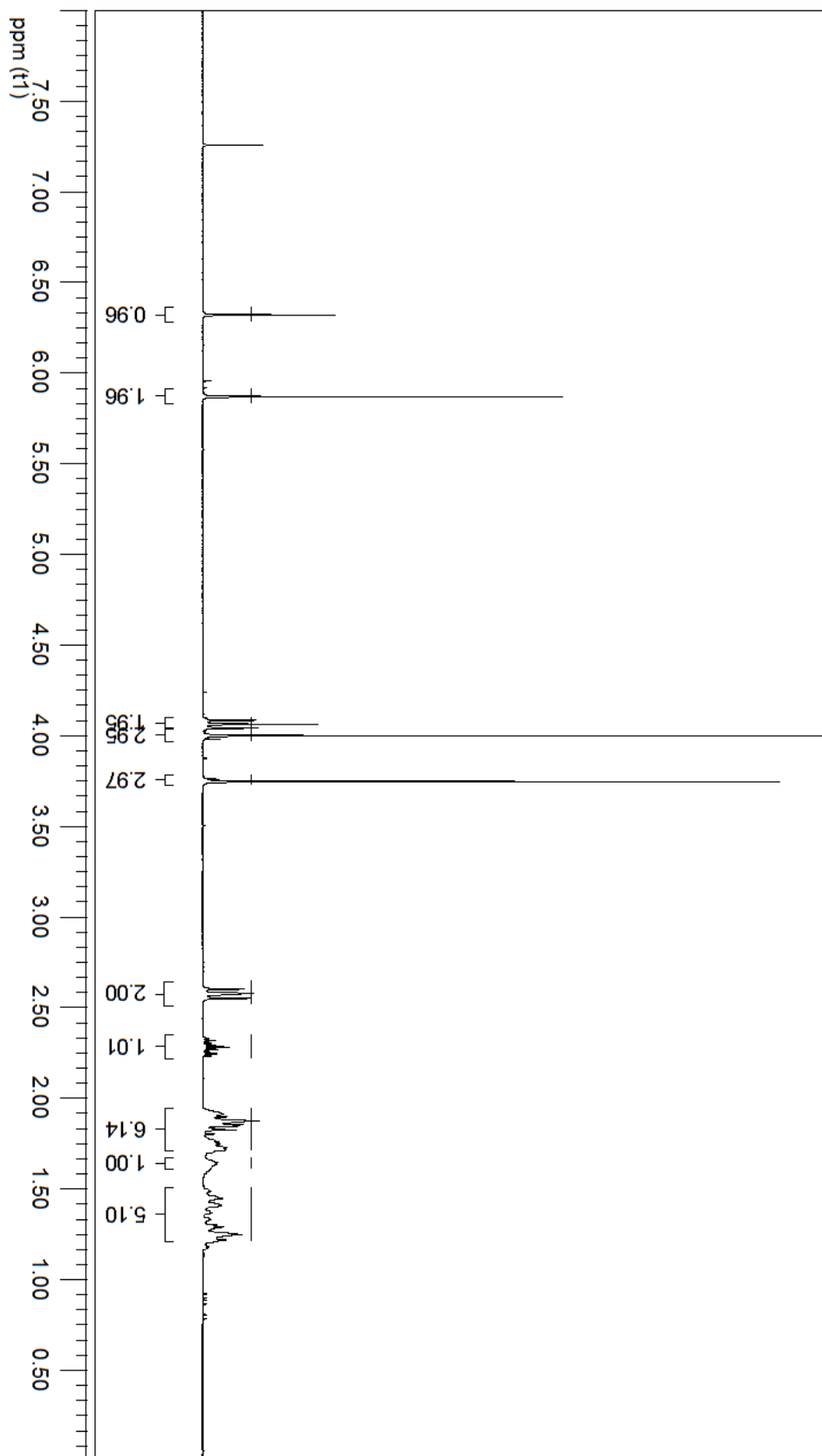
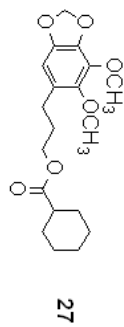


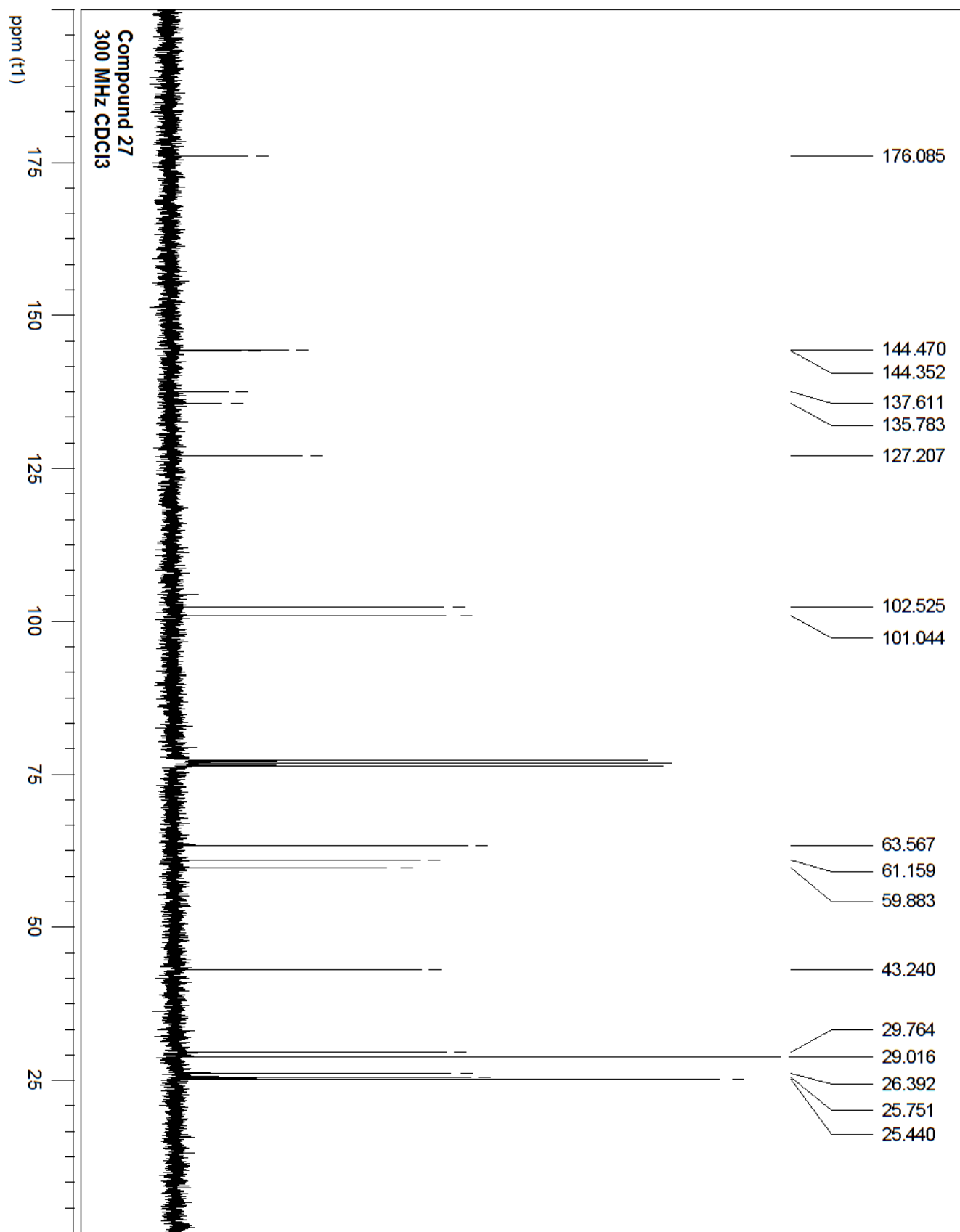
Compound 26
CDCl₃, 400MHz



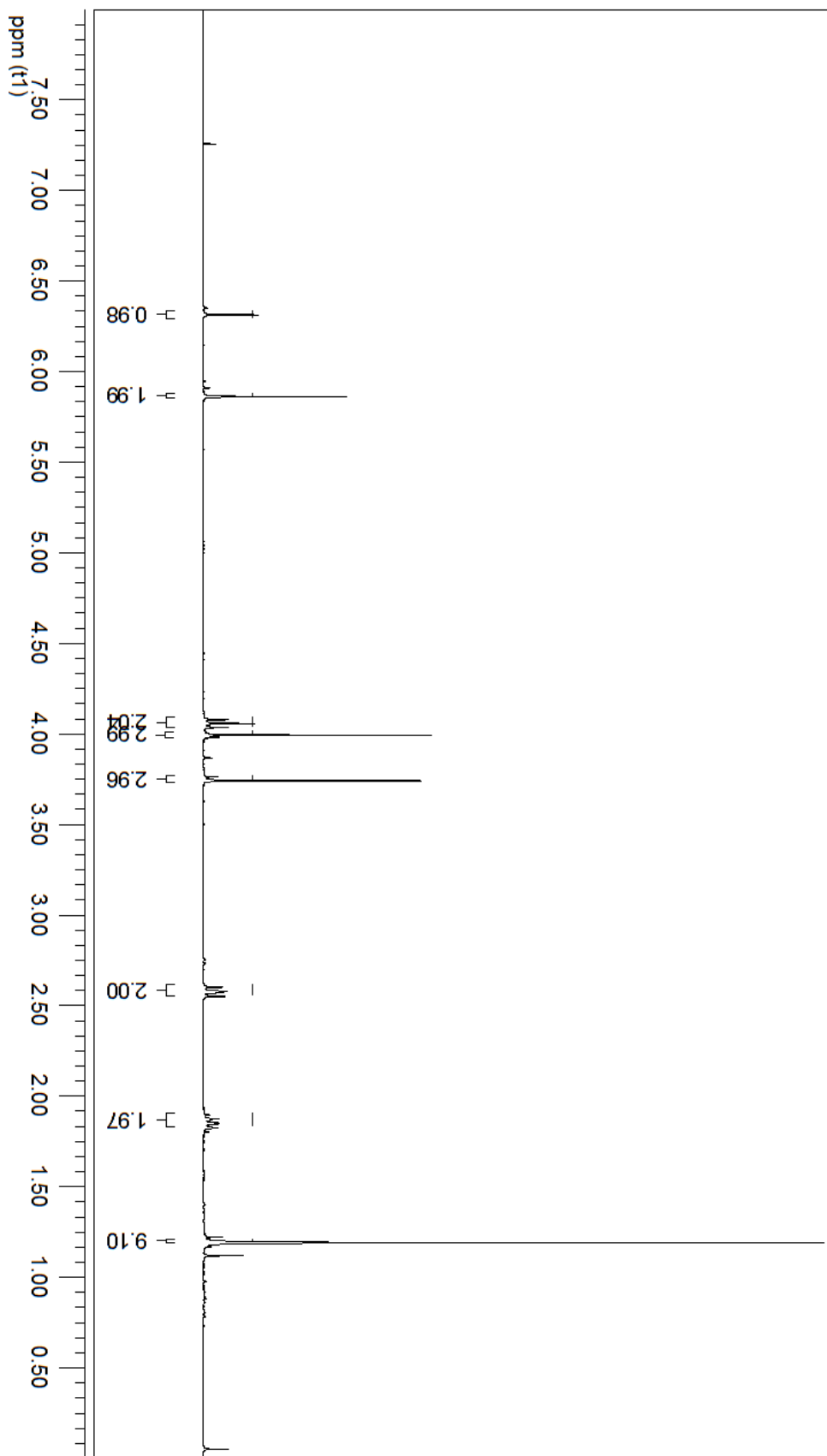
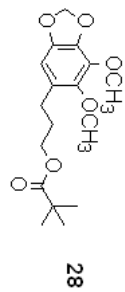


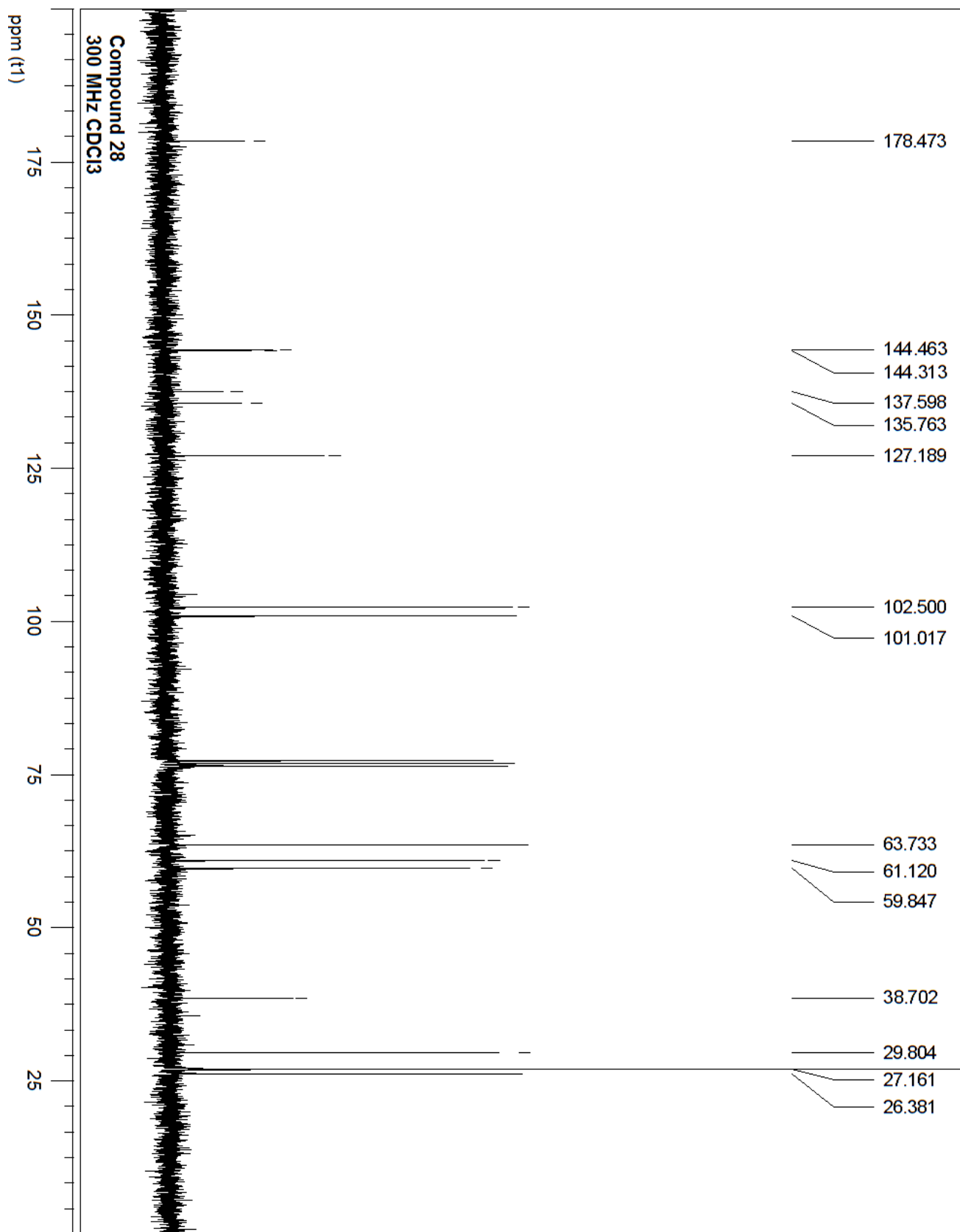
Compound 27
300 MHz CDCl₃



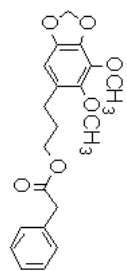


Compound 28
300 MHz CDCl₃

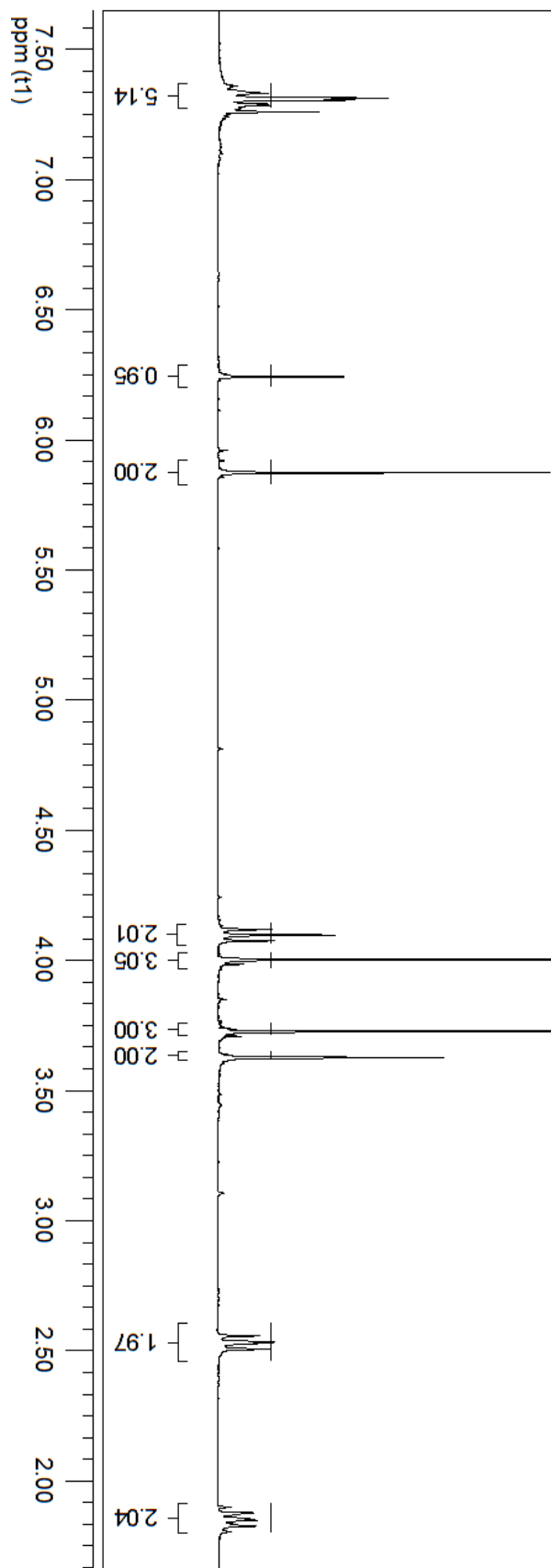


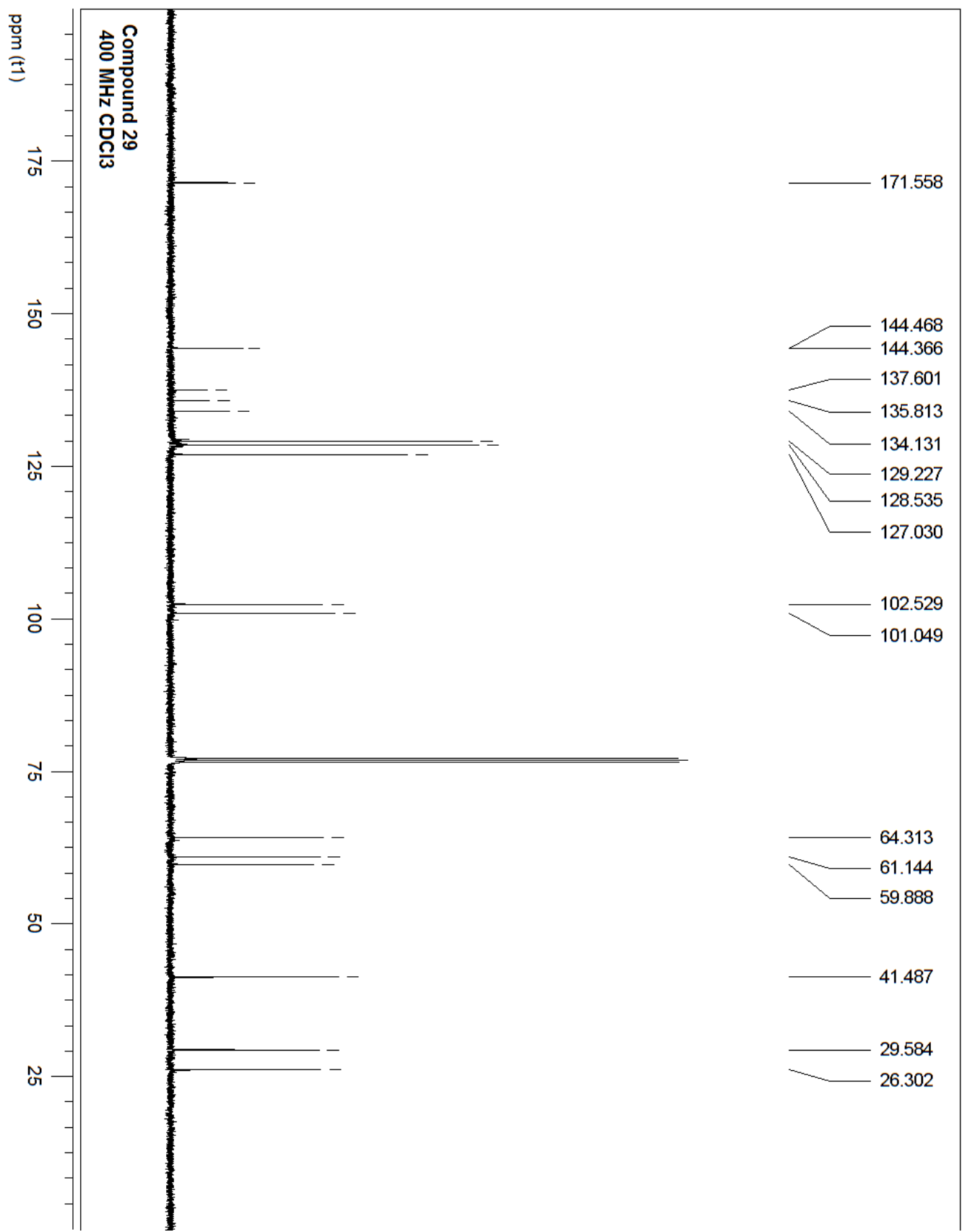


Compound 29
300 MHz CDCl₃

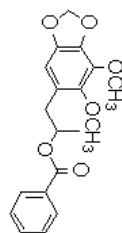


29

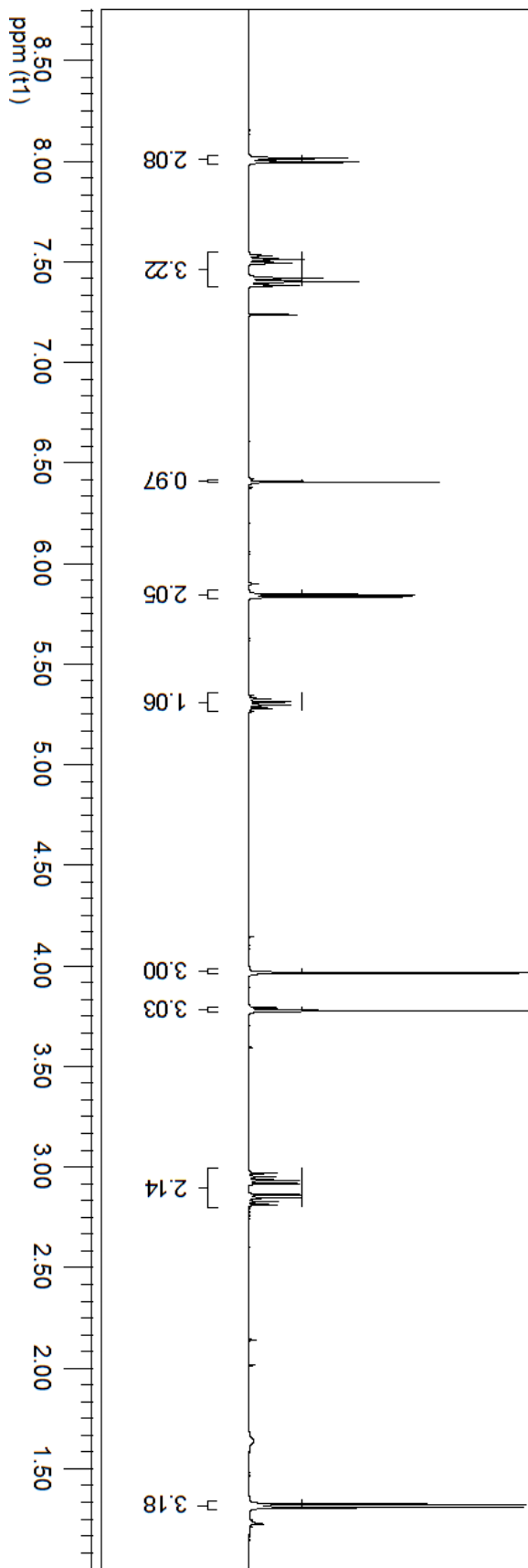


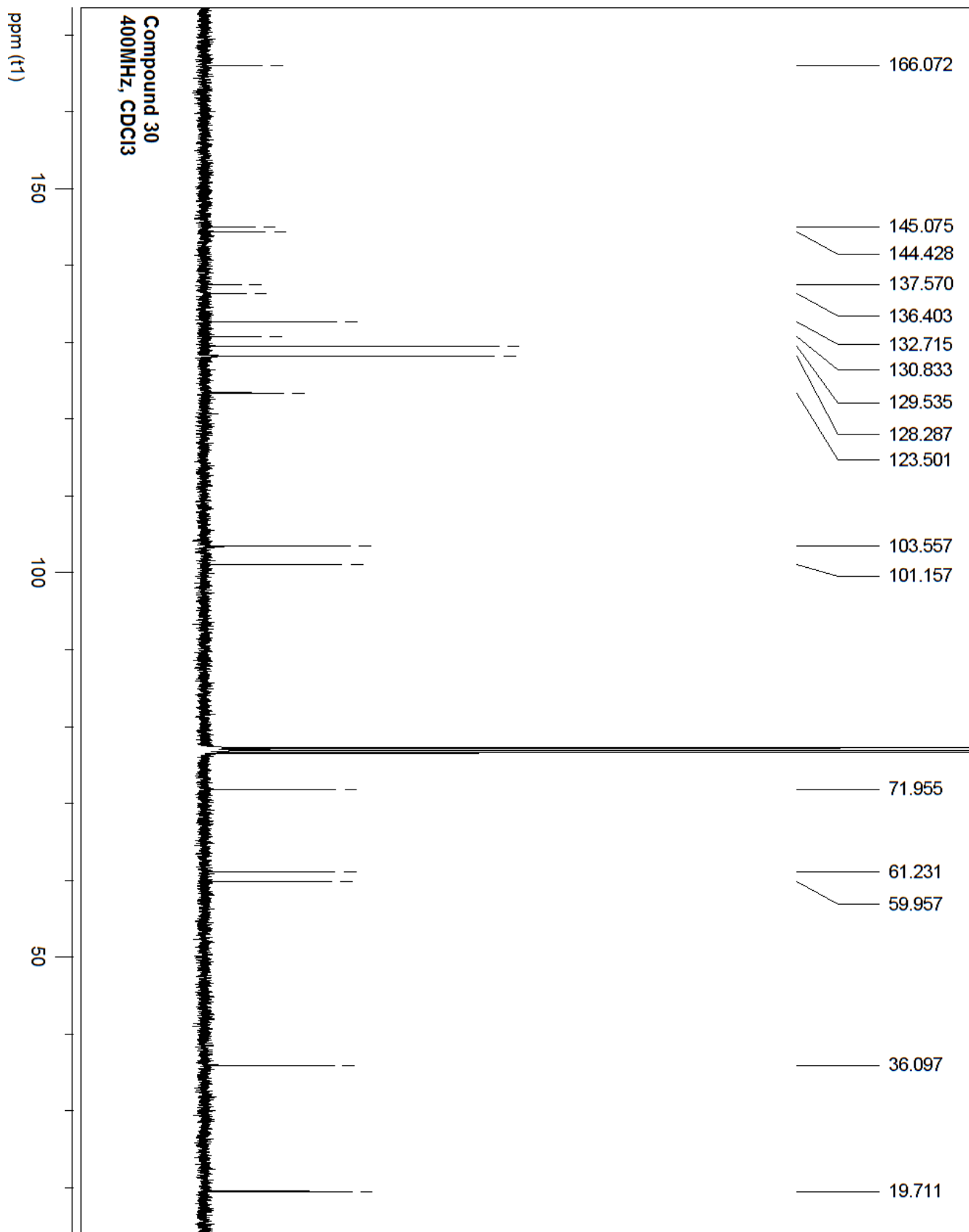


Compound 30
400MHz, CDCl3

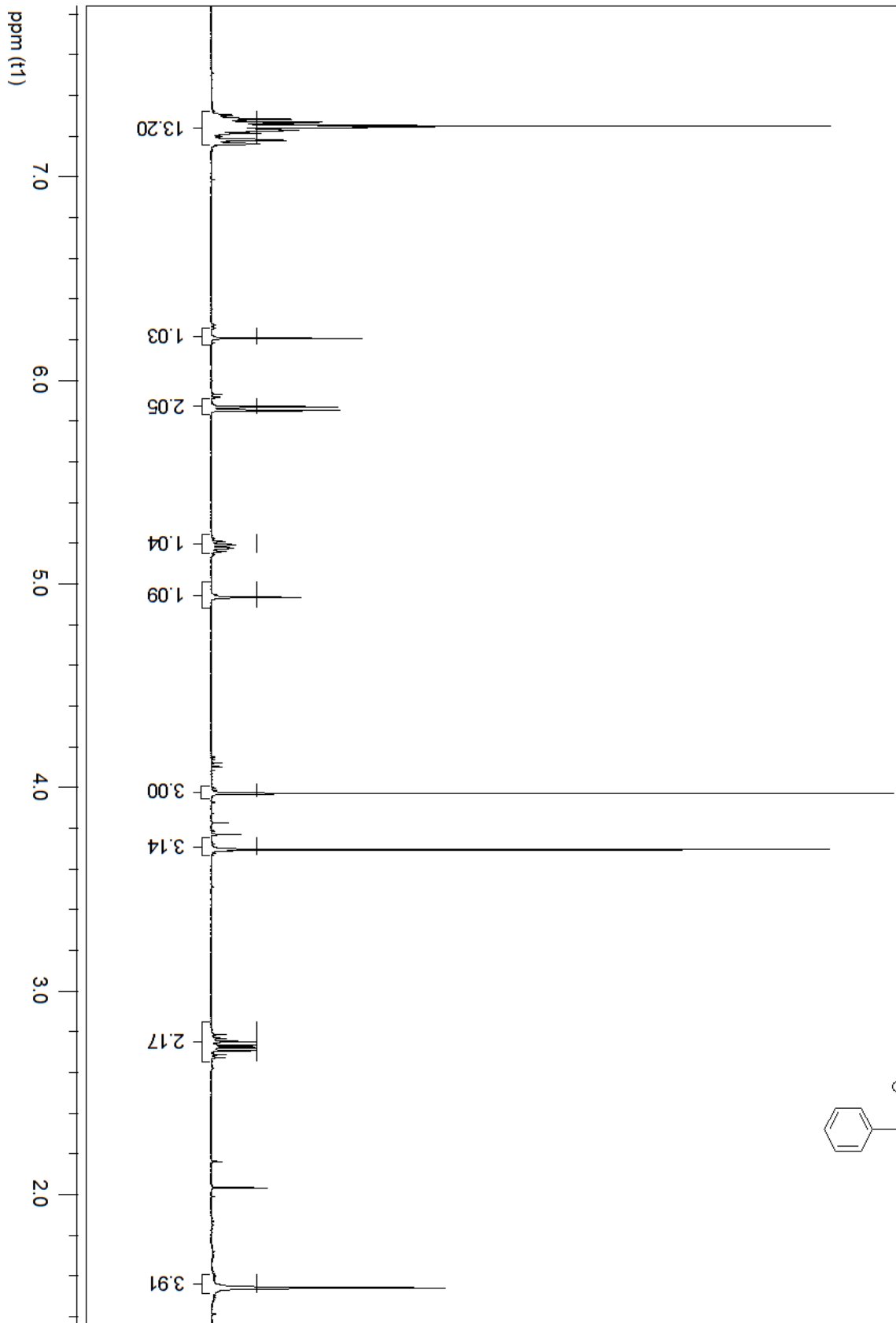
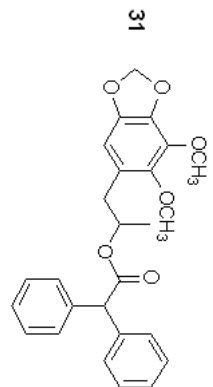


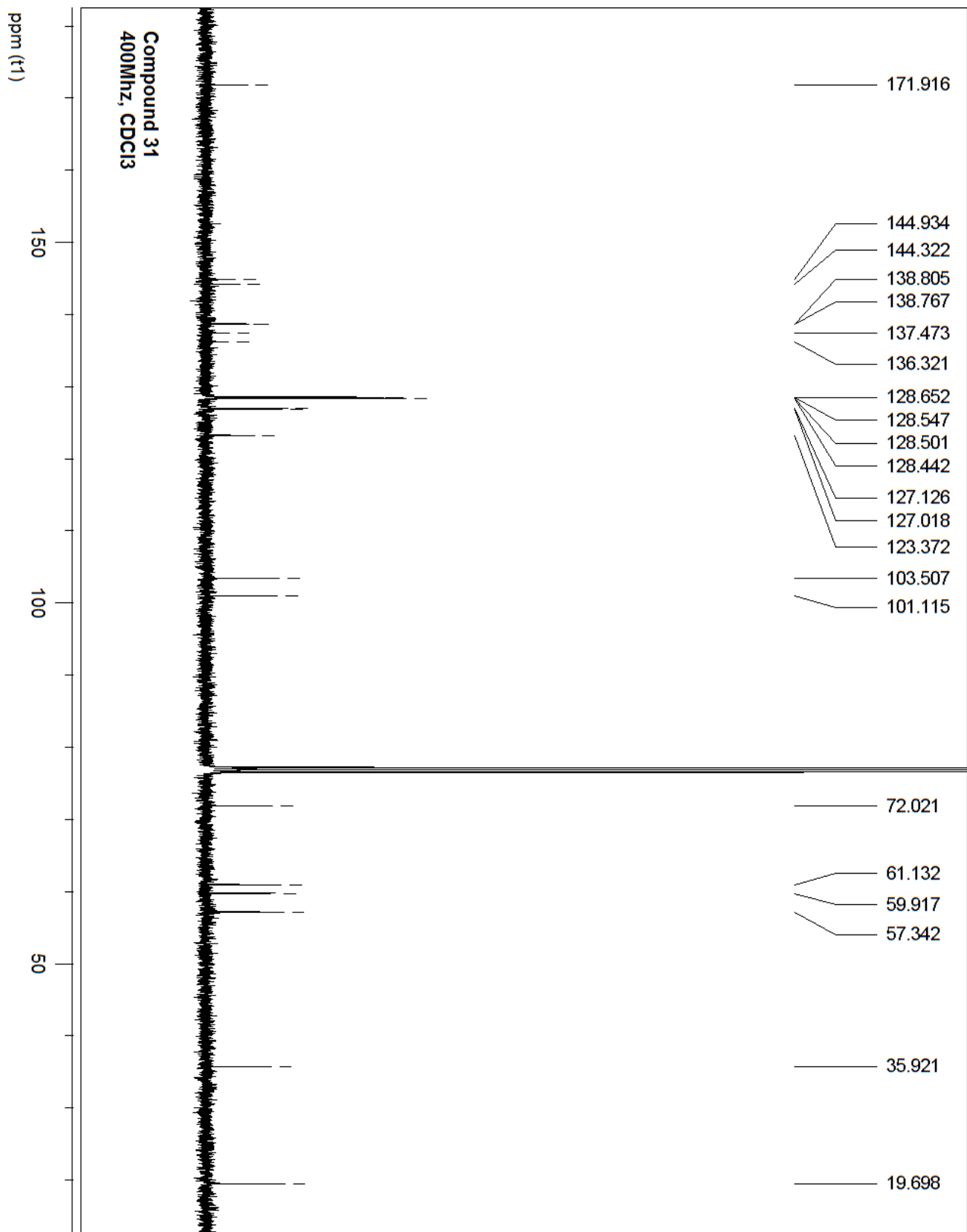
30



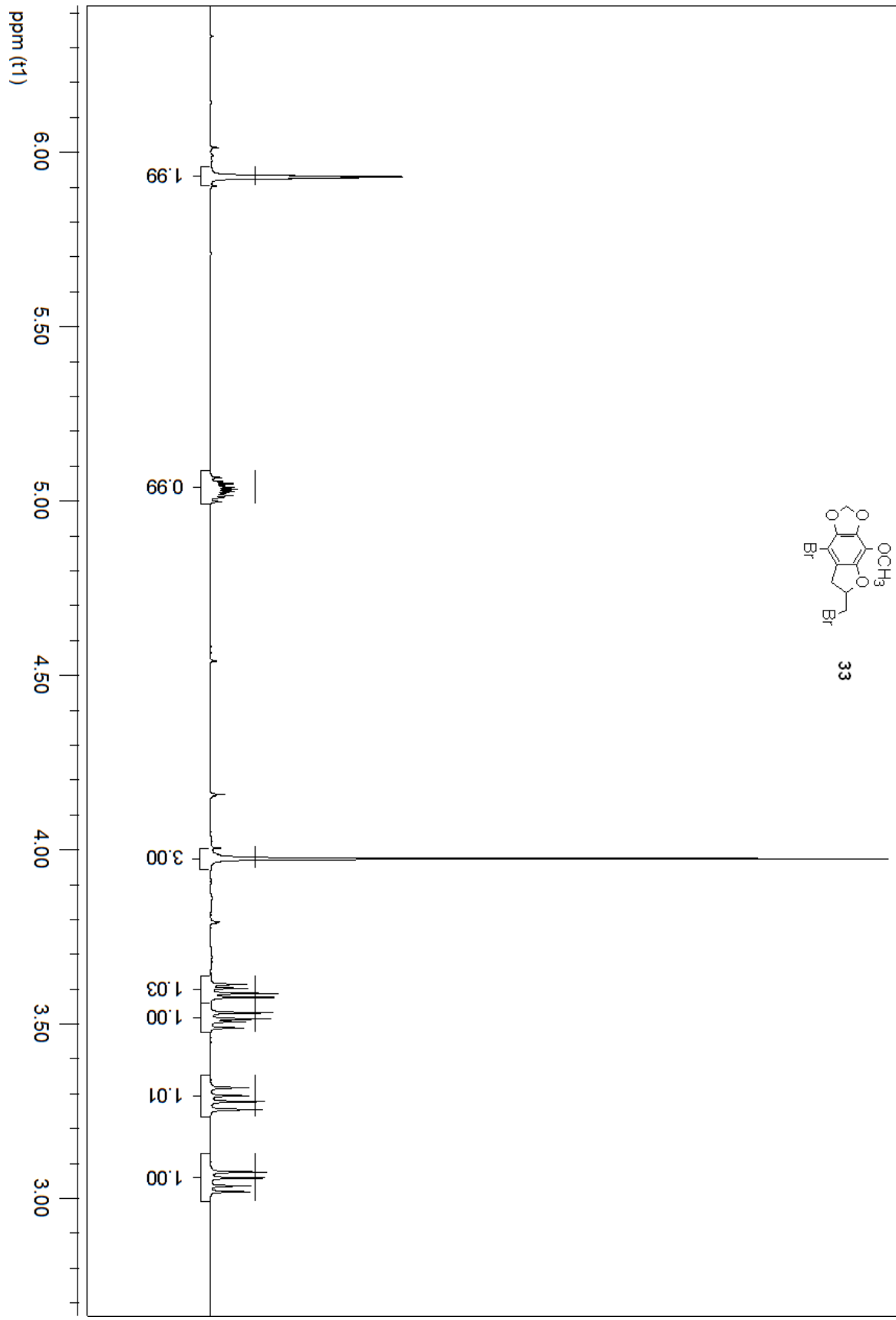
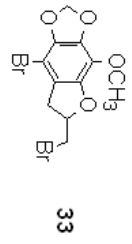


Compound 31
400MHz, CDCl3

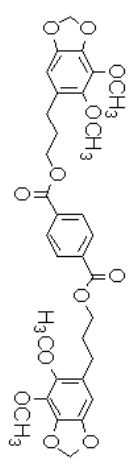




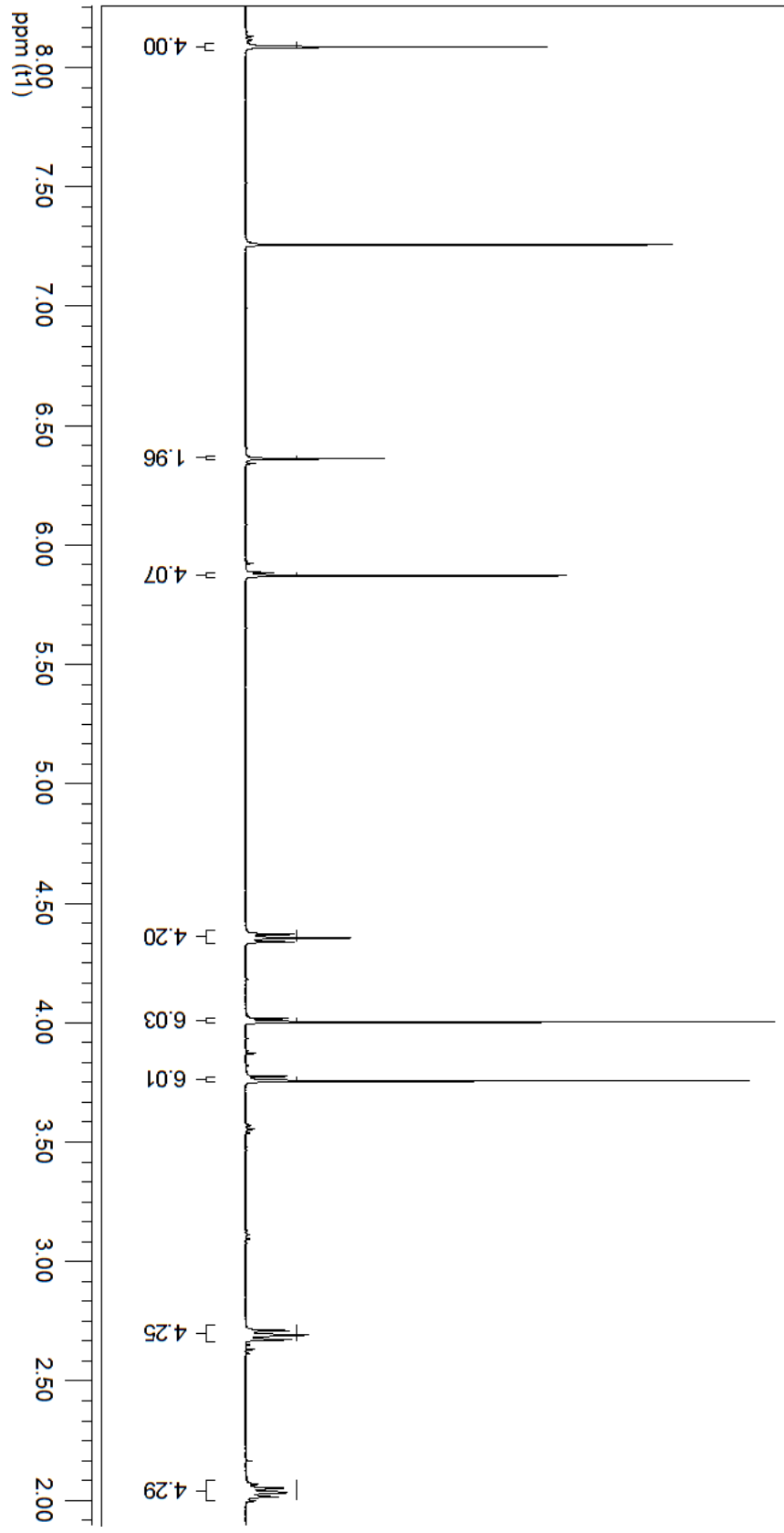
Compound 33
400MHz, CDCl3

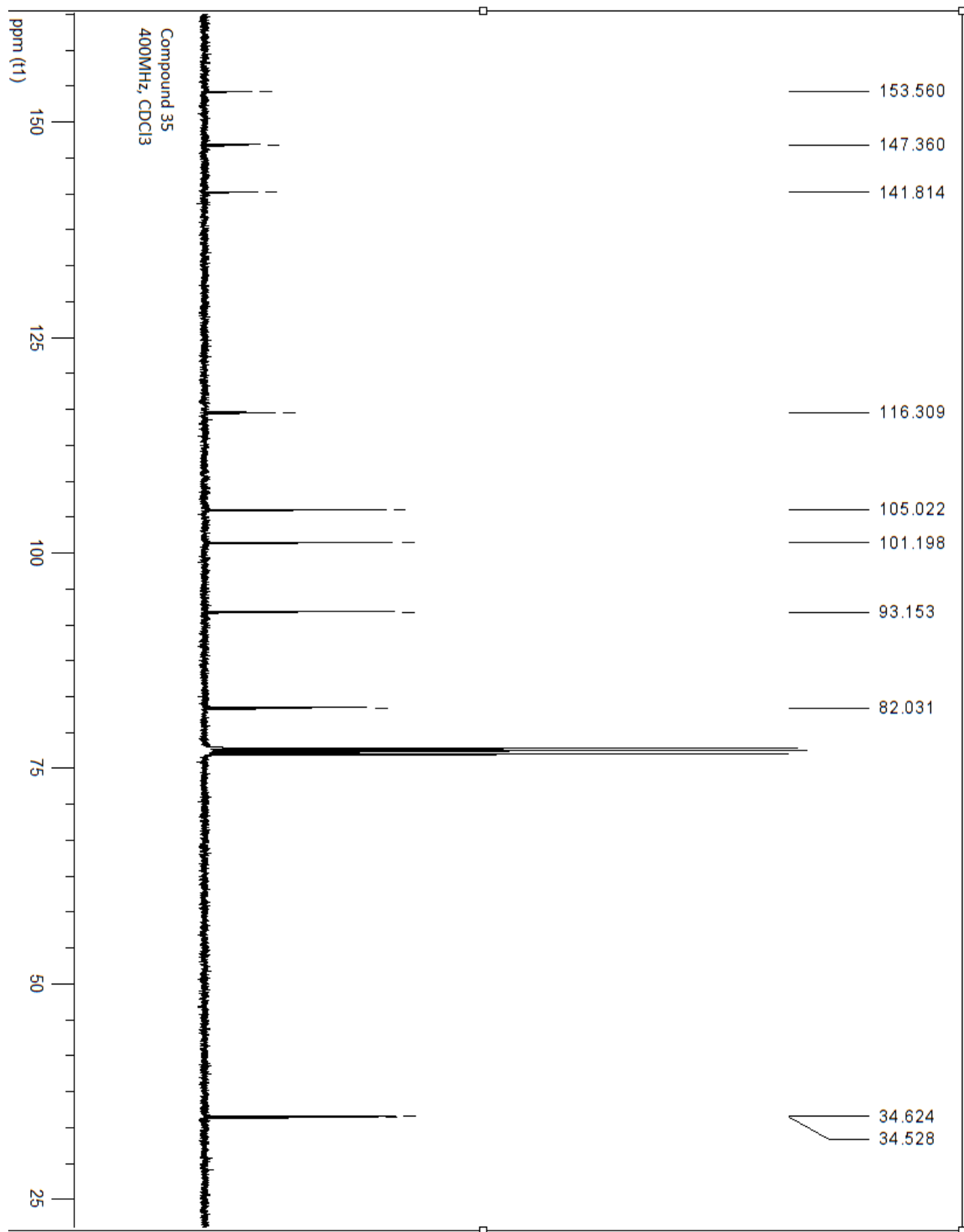


Compound 35
400MHz, CDCl3

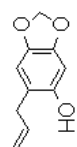


35

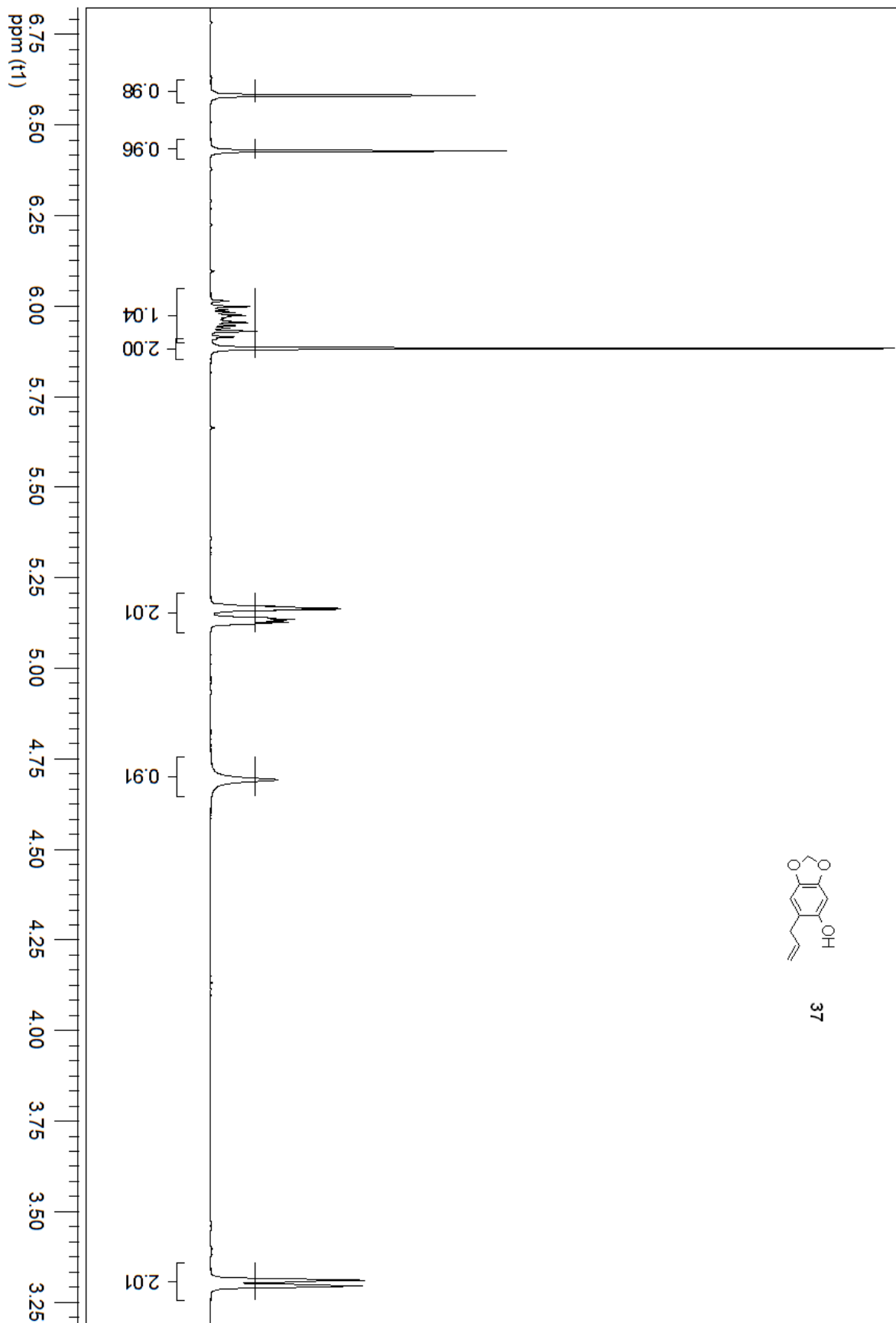




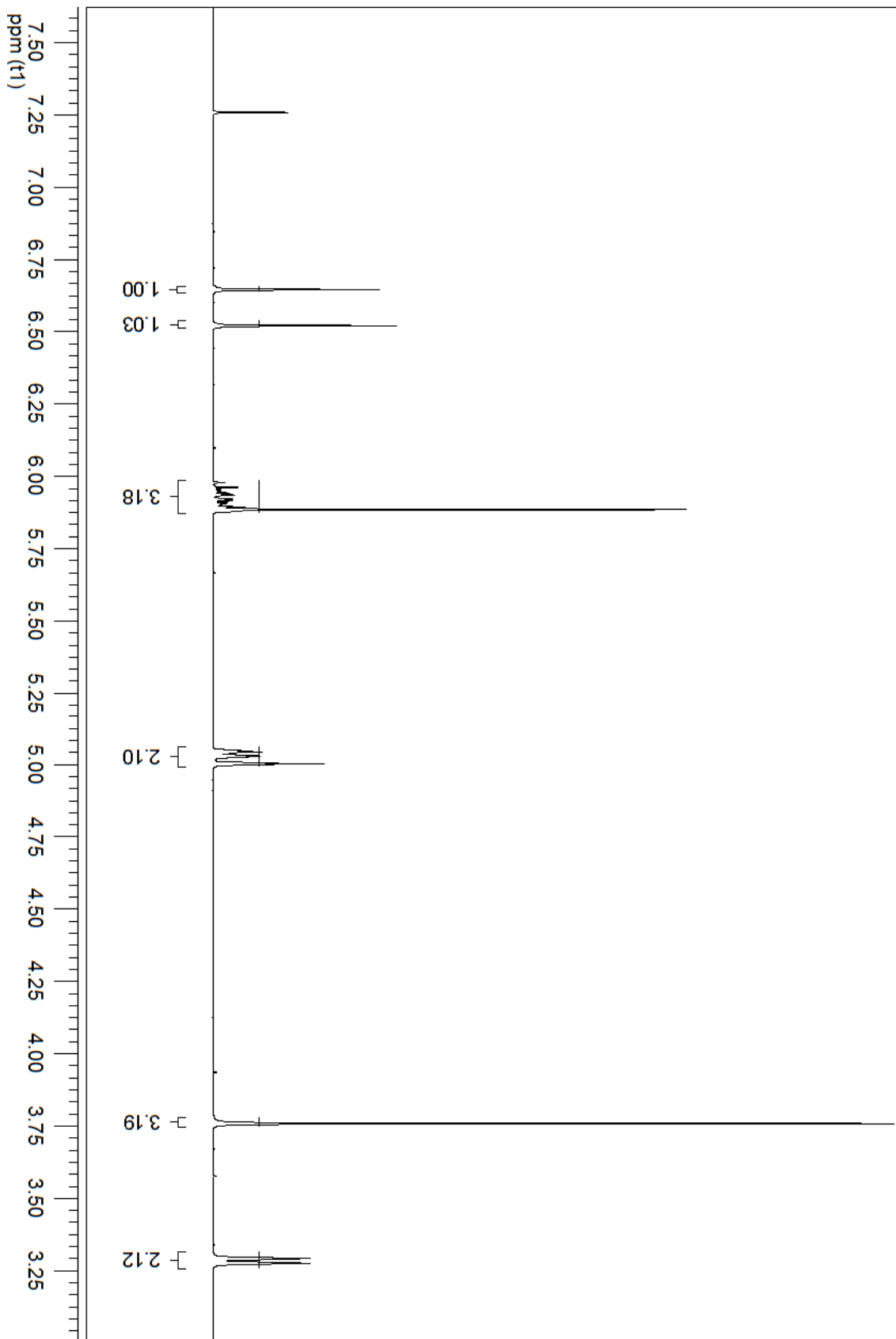
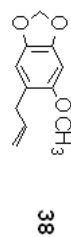
Compound 37
400MHz, CDCl3



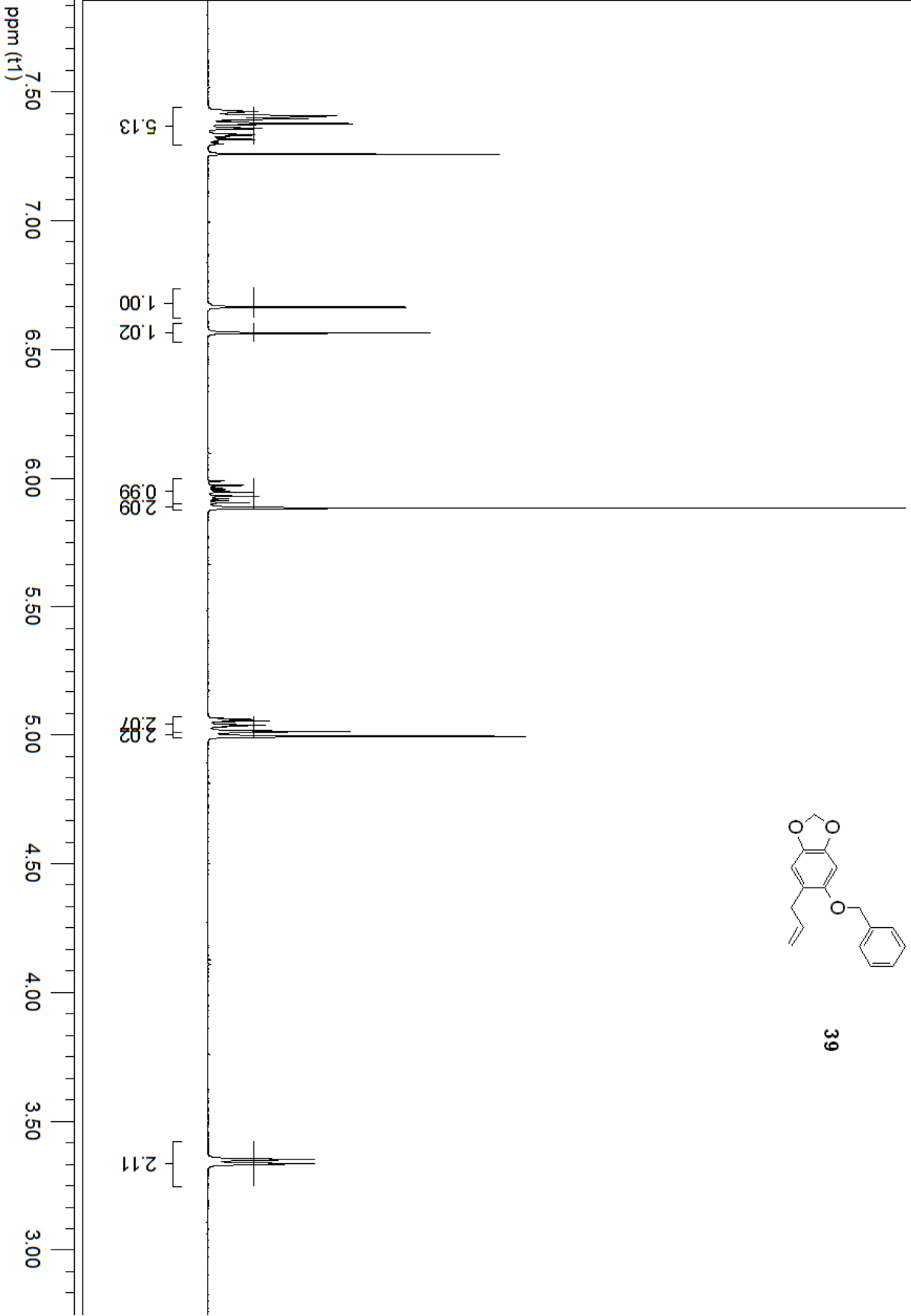
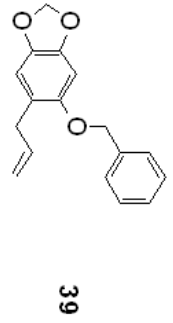
37

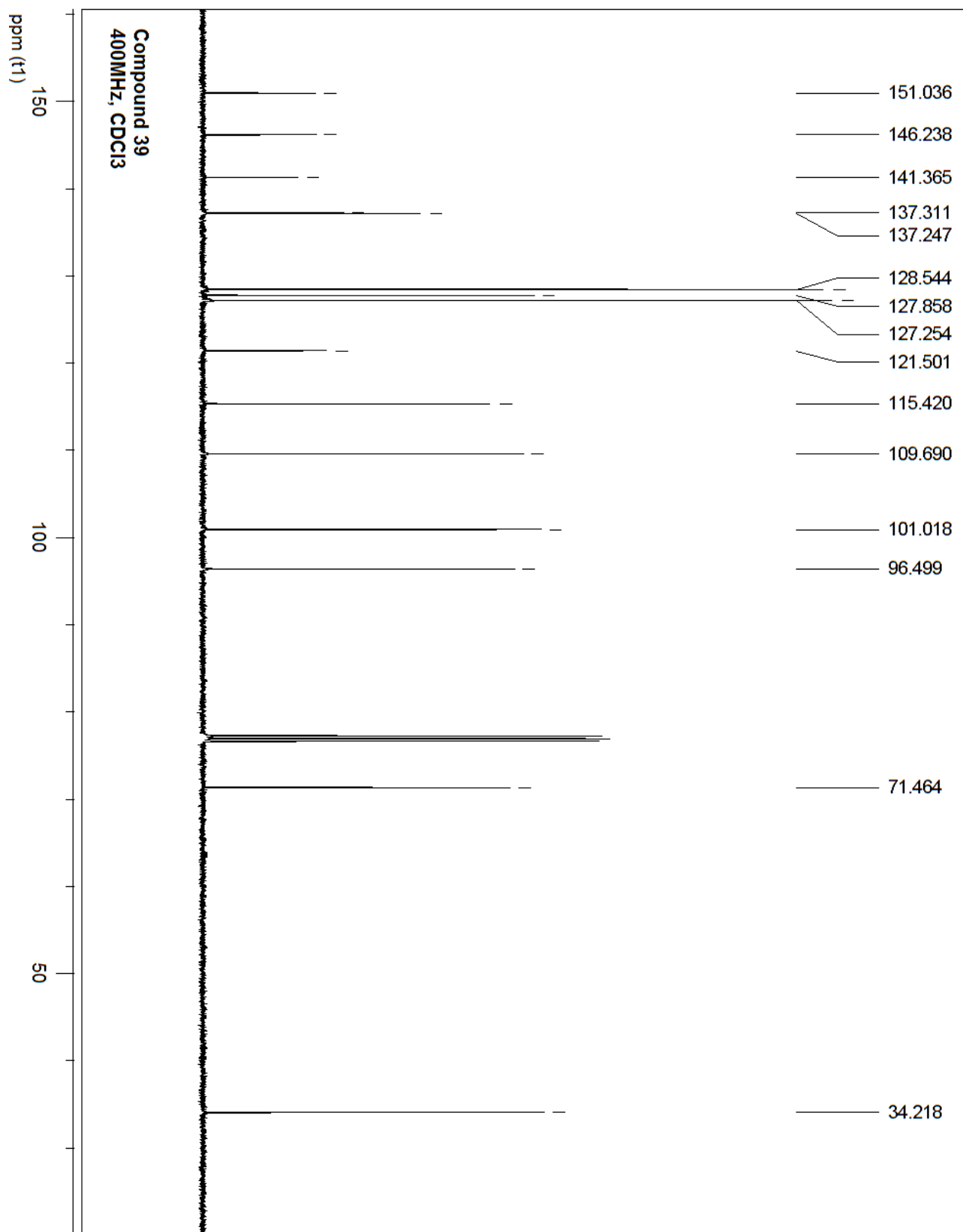


Compound 38
CDCl₃, 400MHz

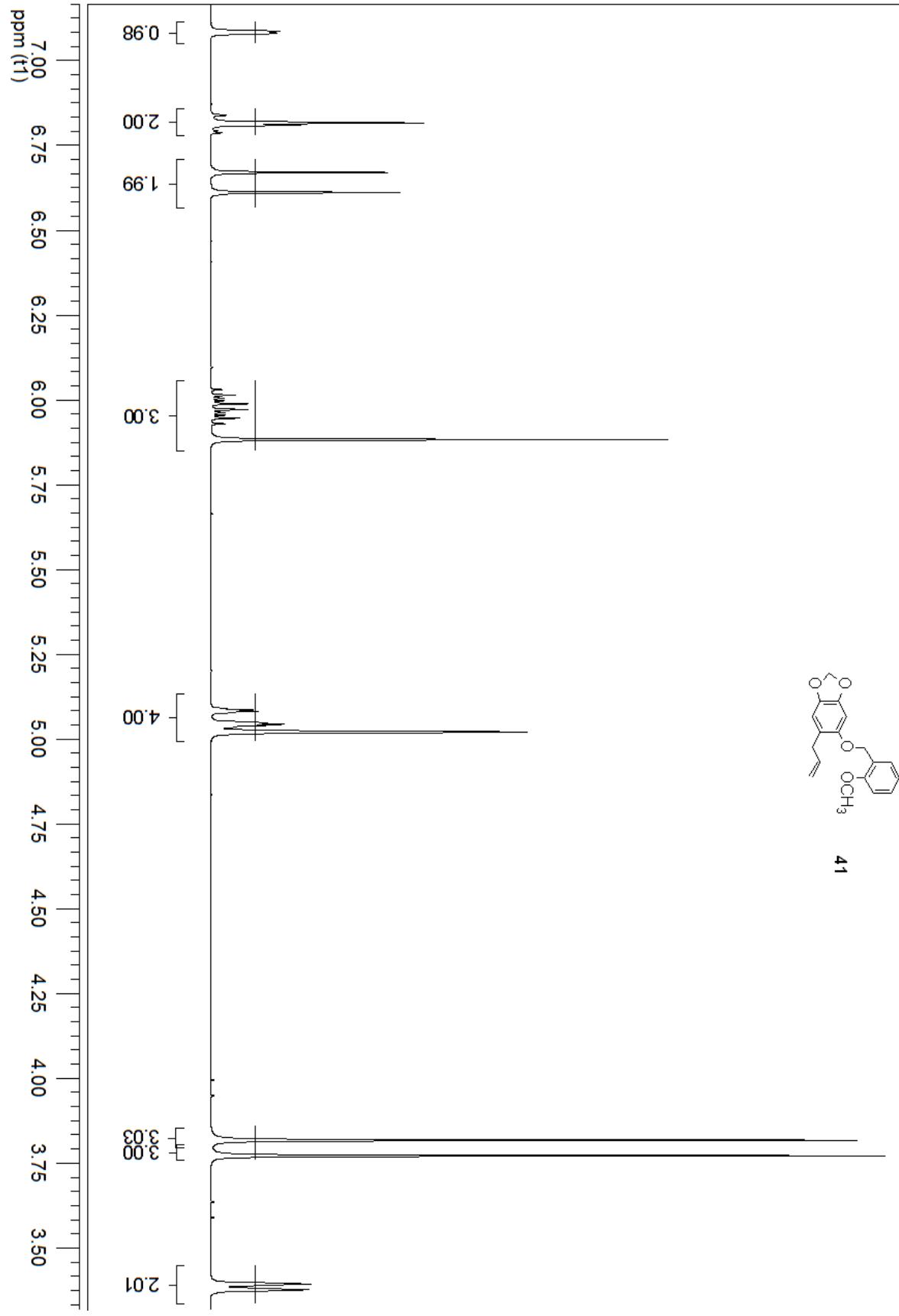
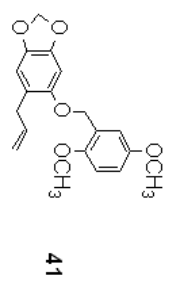


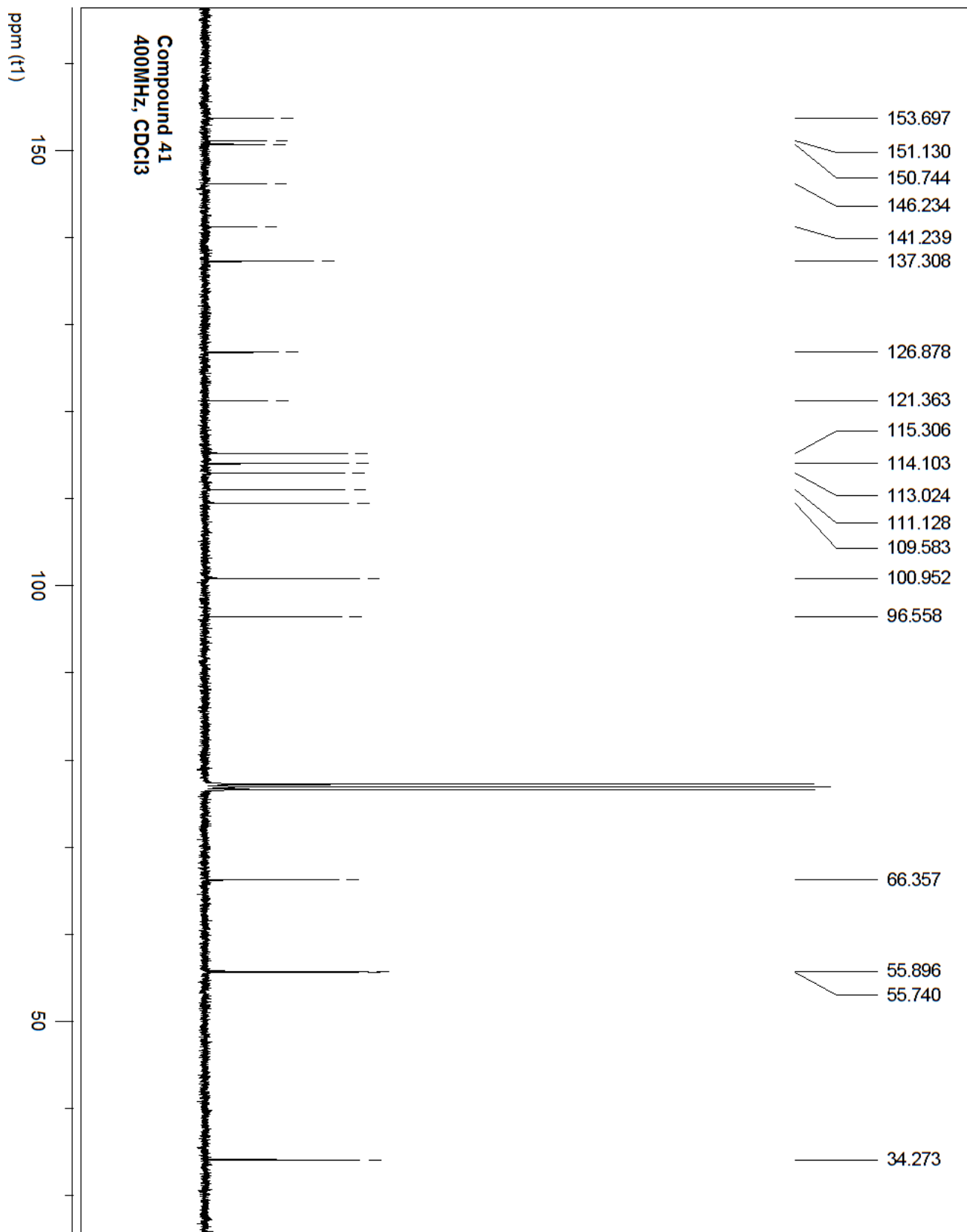
Compound 39
CDCl₃, 400MHz.





Compound 41
CDCl₃, 400MHz

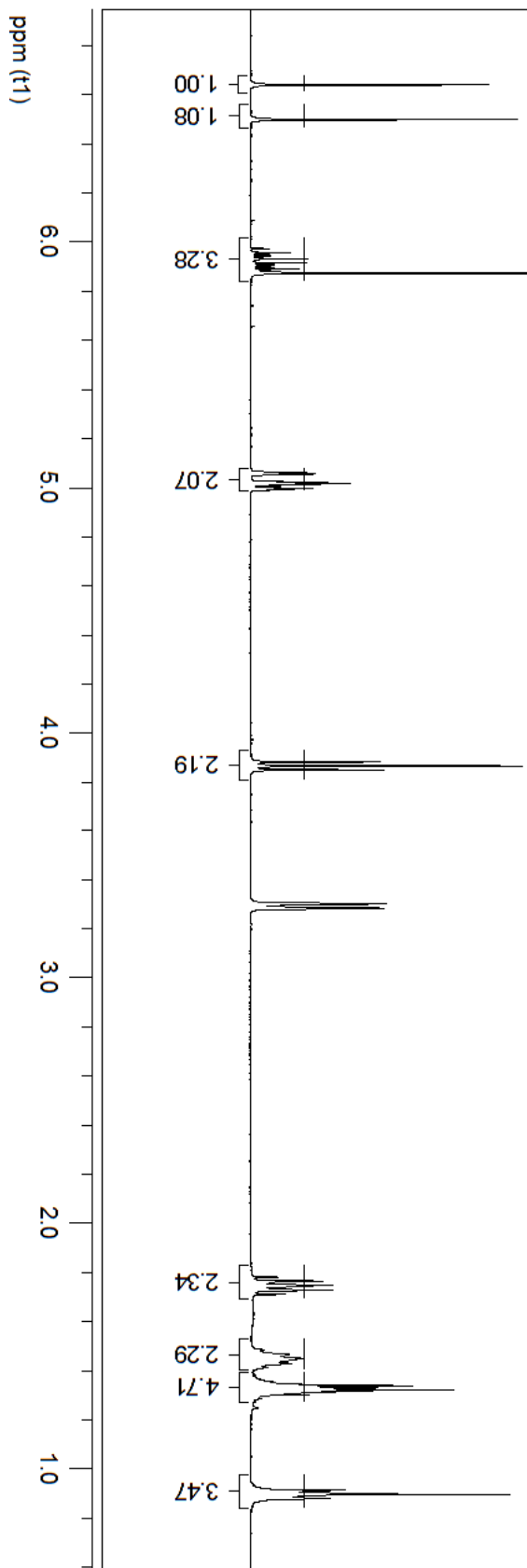


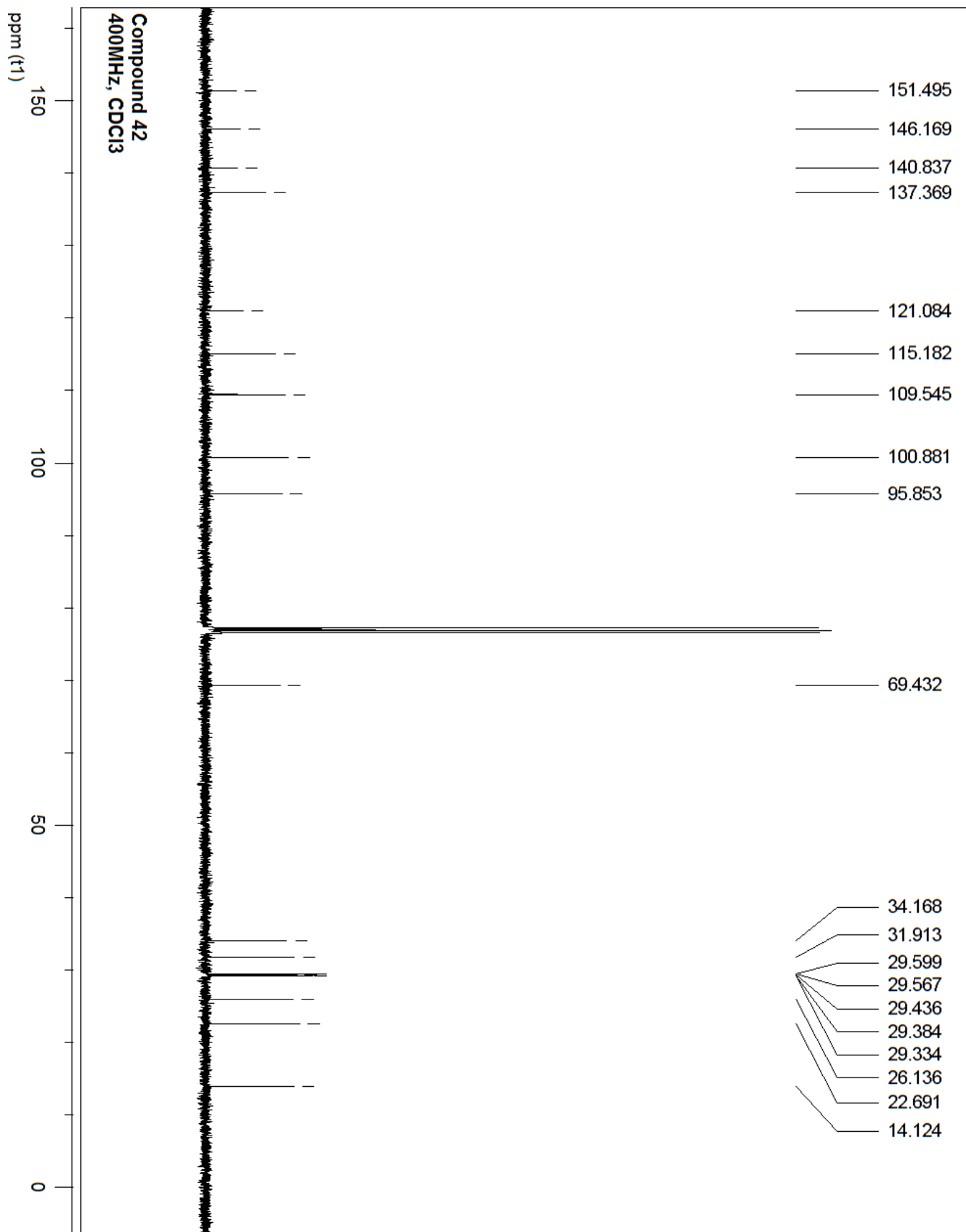


Compound 42
400MHz, CDCl3

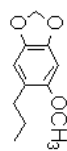


42

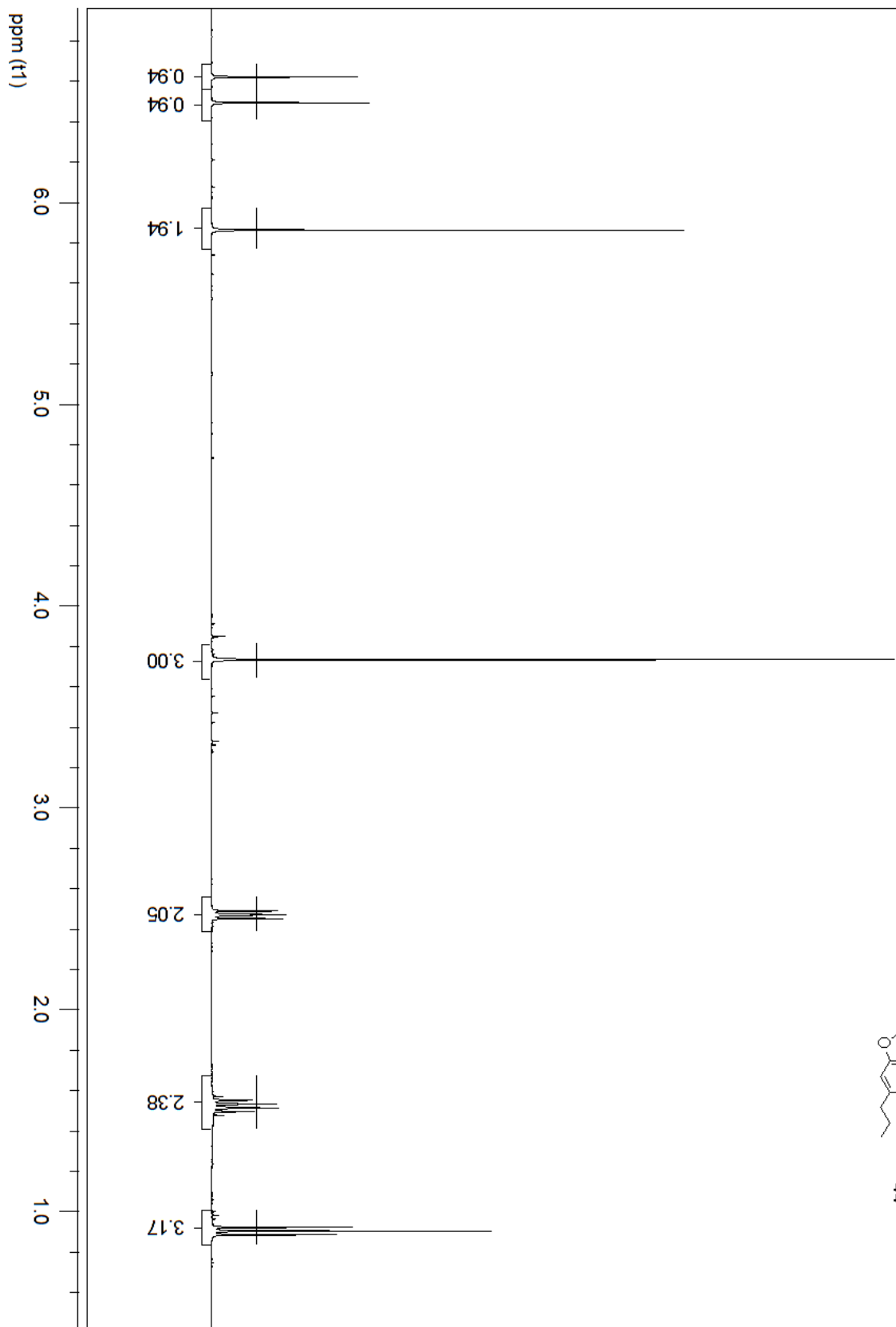


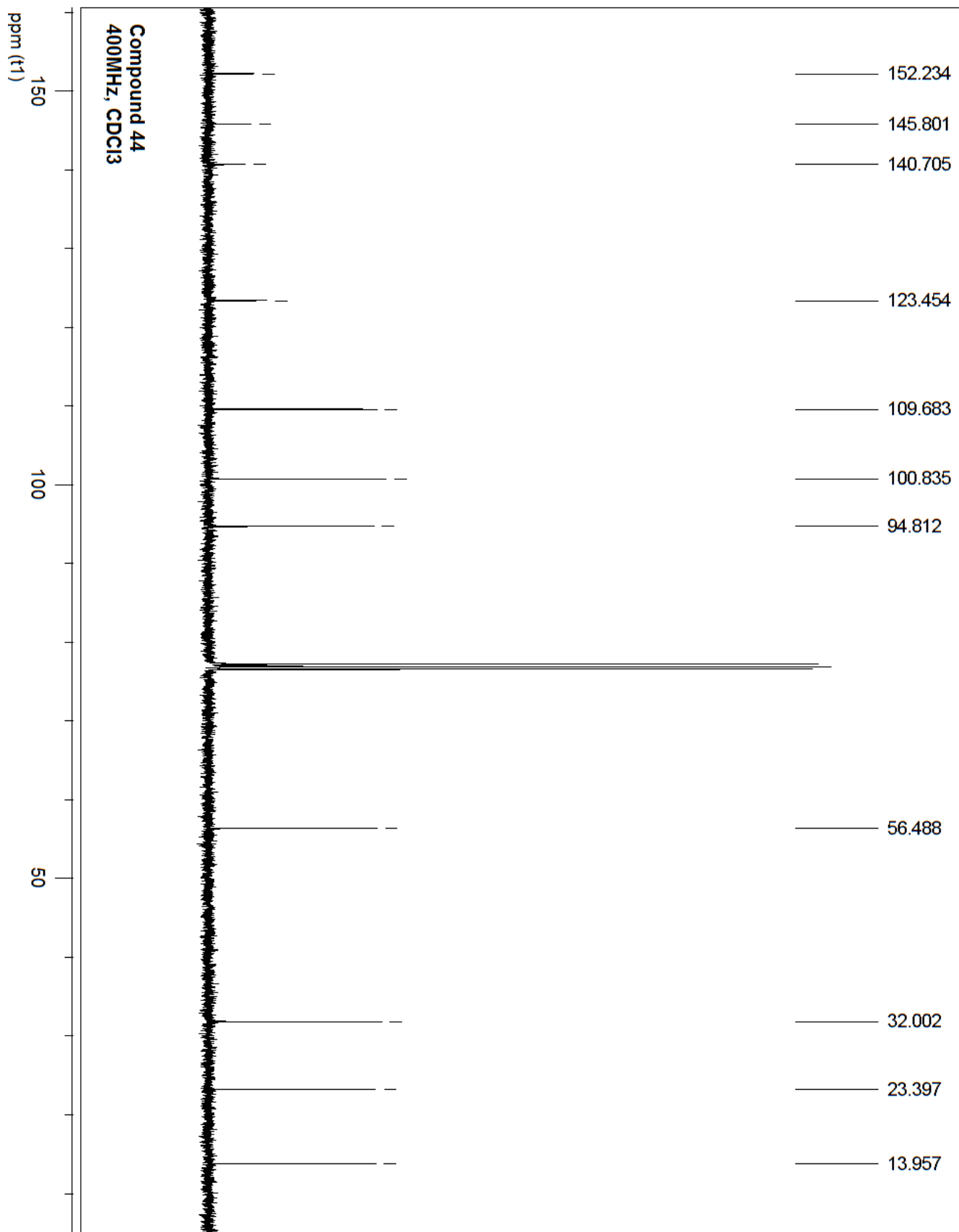


Compound 44
400MHz, CDCl3

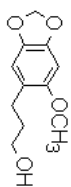


44

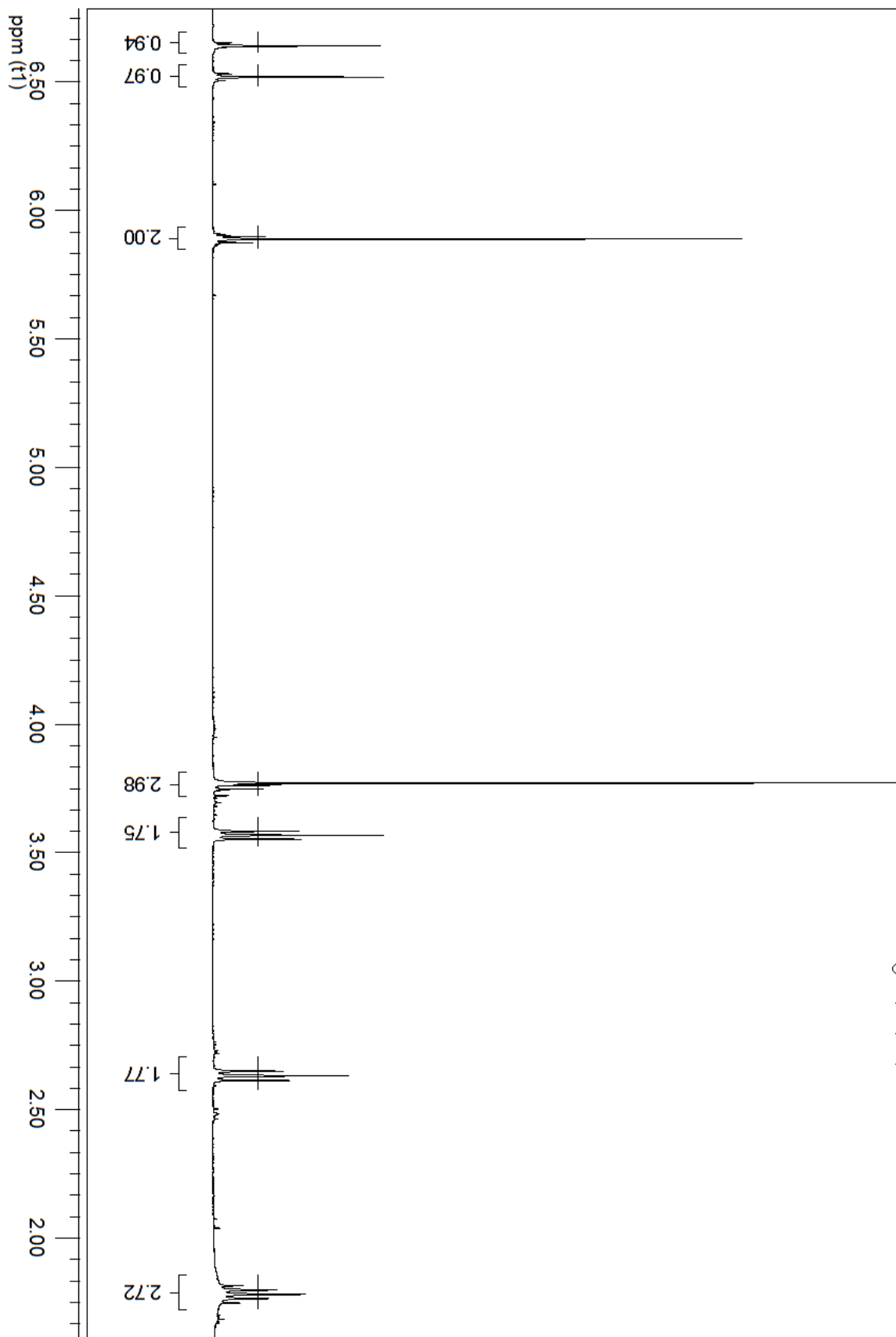




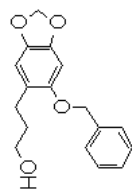
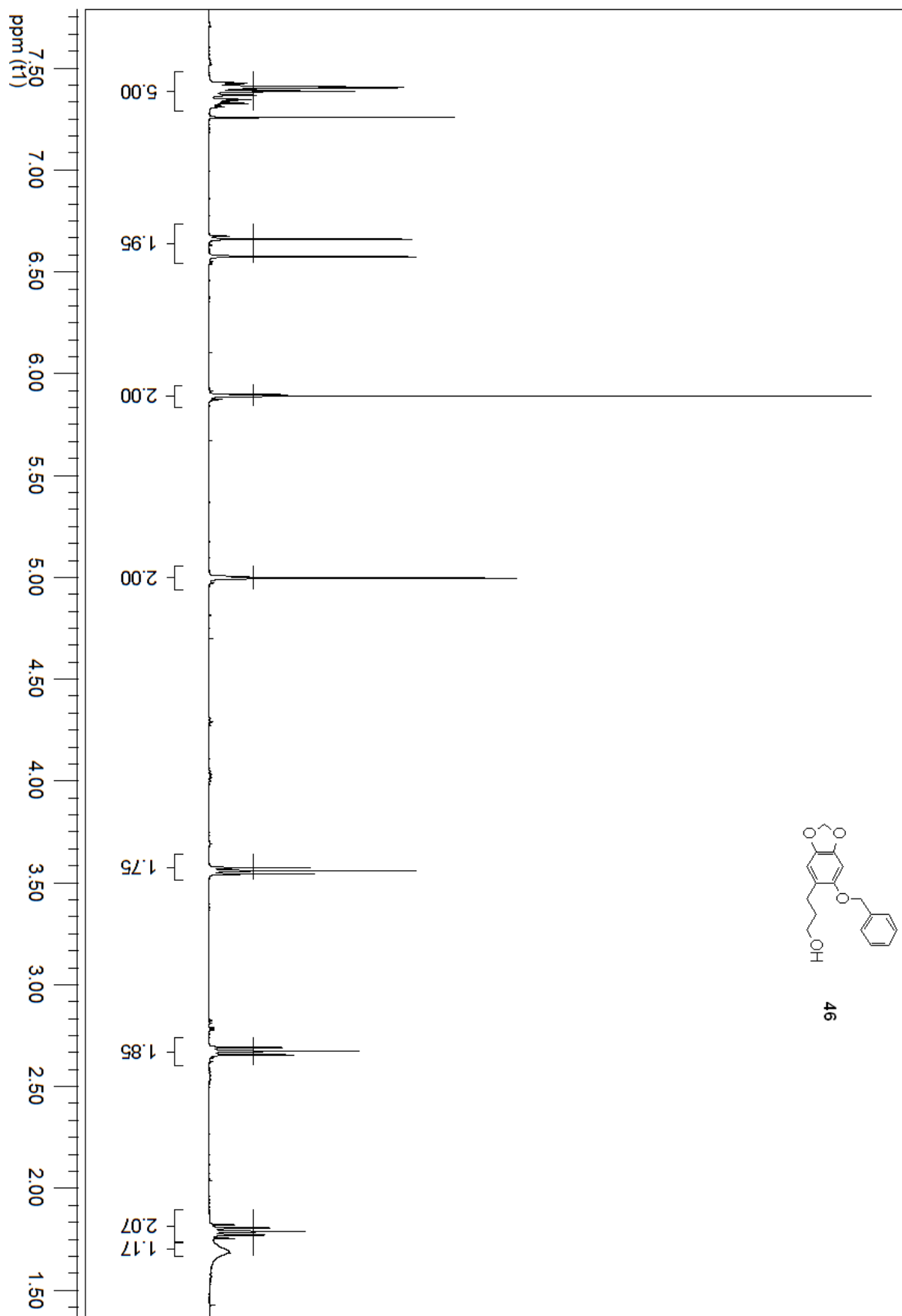
Compound 45
400MHz, CDCl3



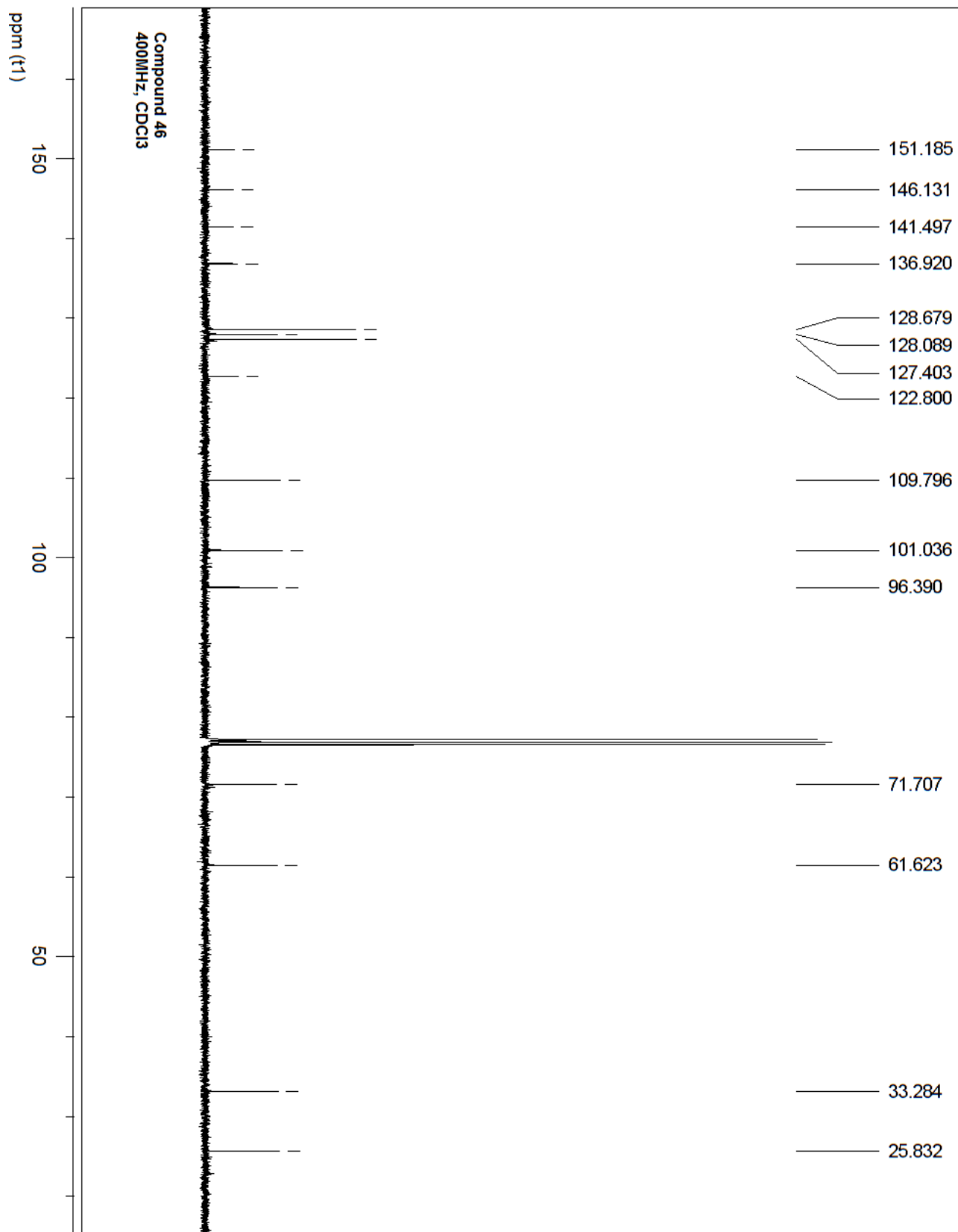
45



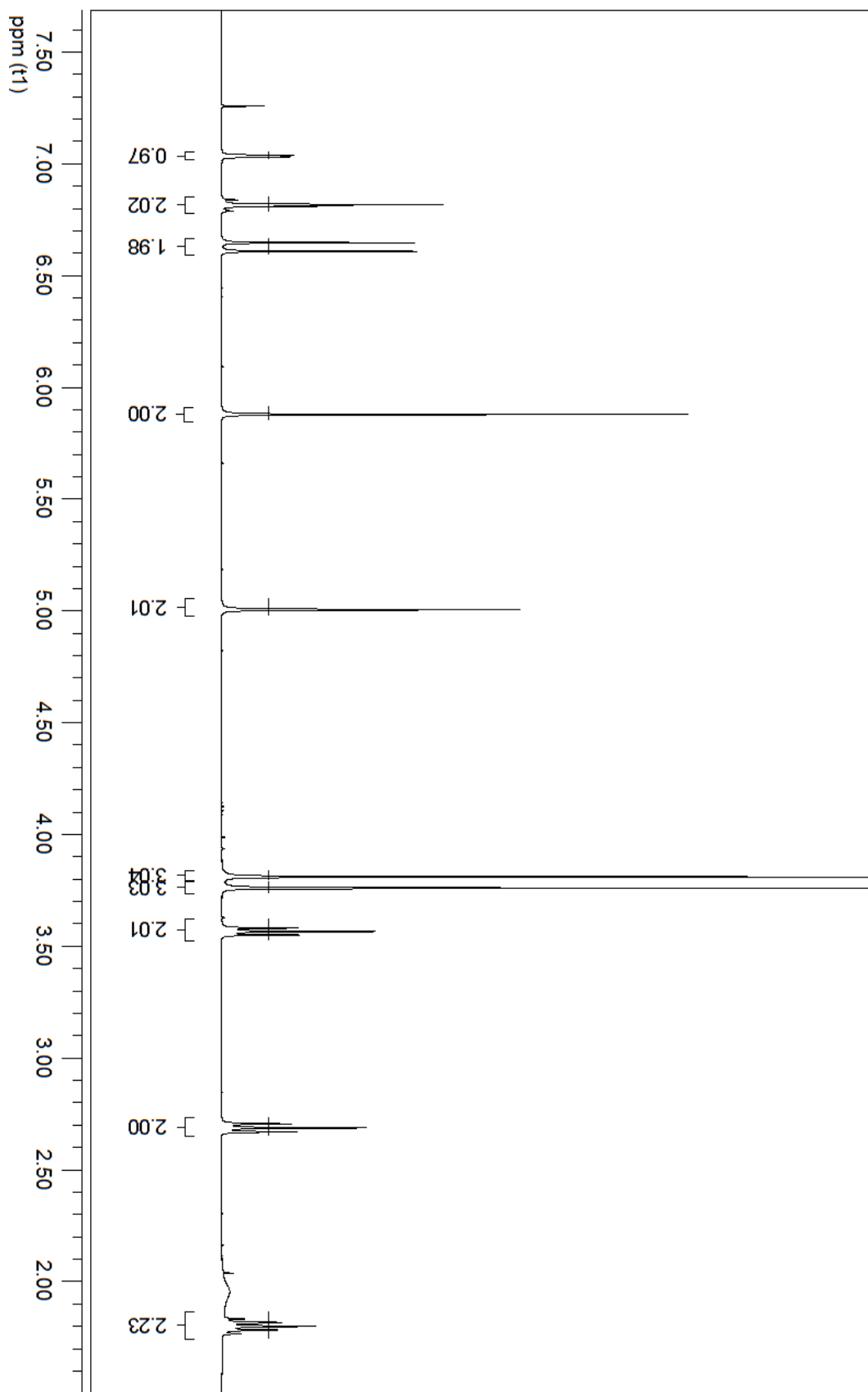
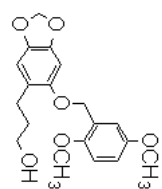
Compound 46
400MHz, CDCl3

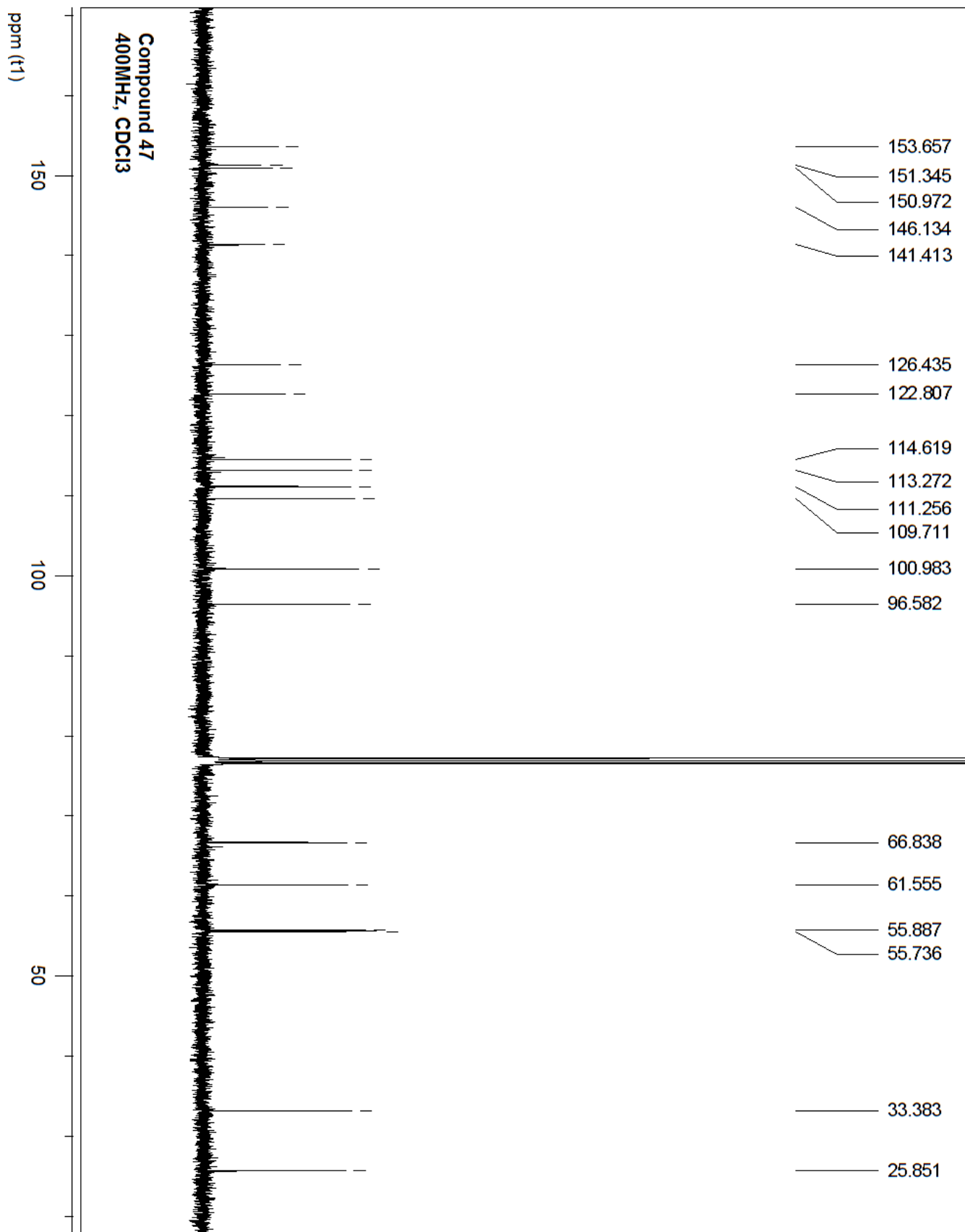


46

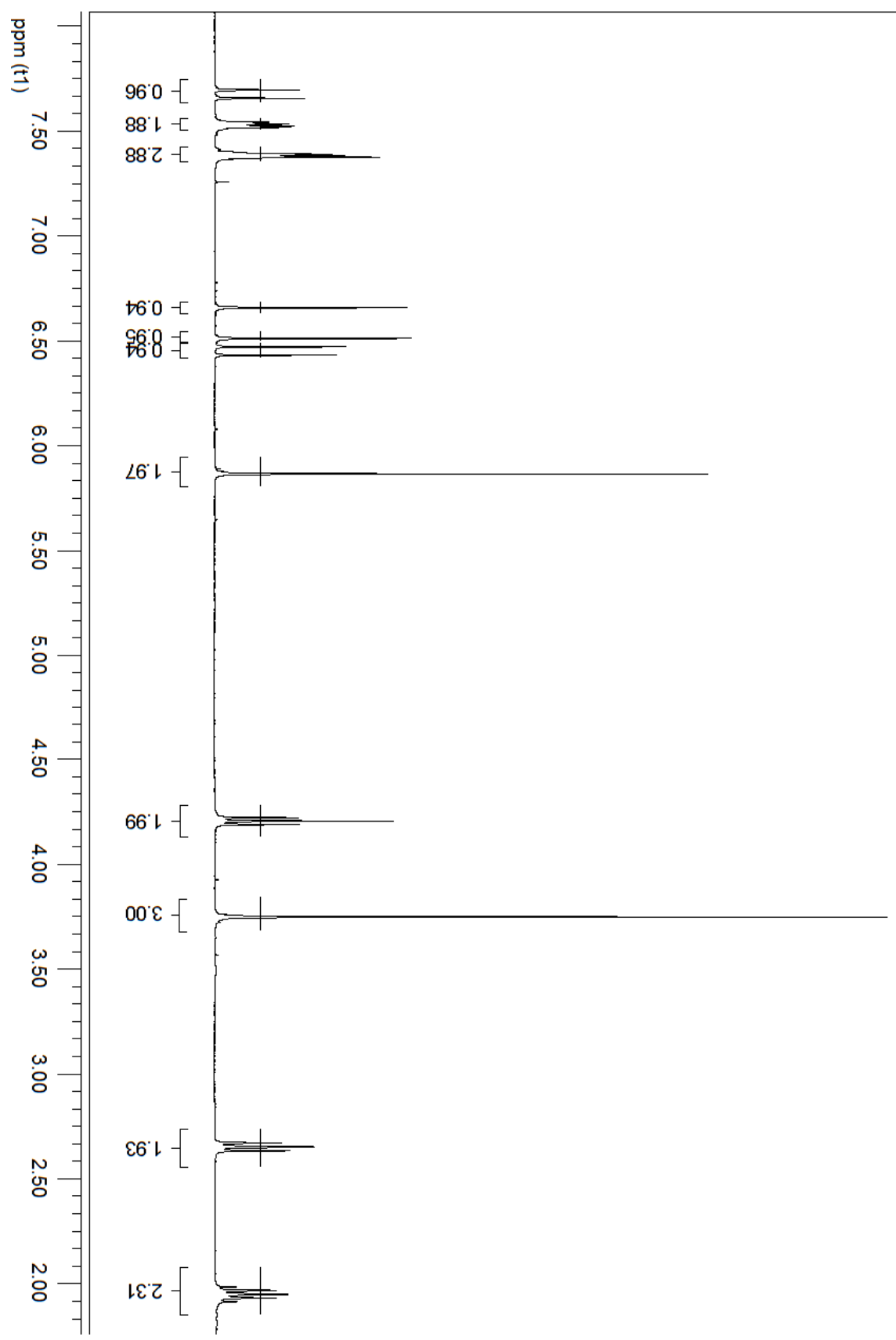
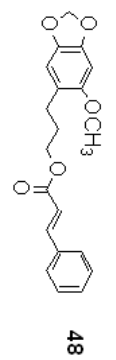


Compound 47
400 MHz, CDCl₃

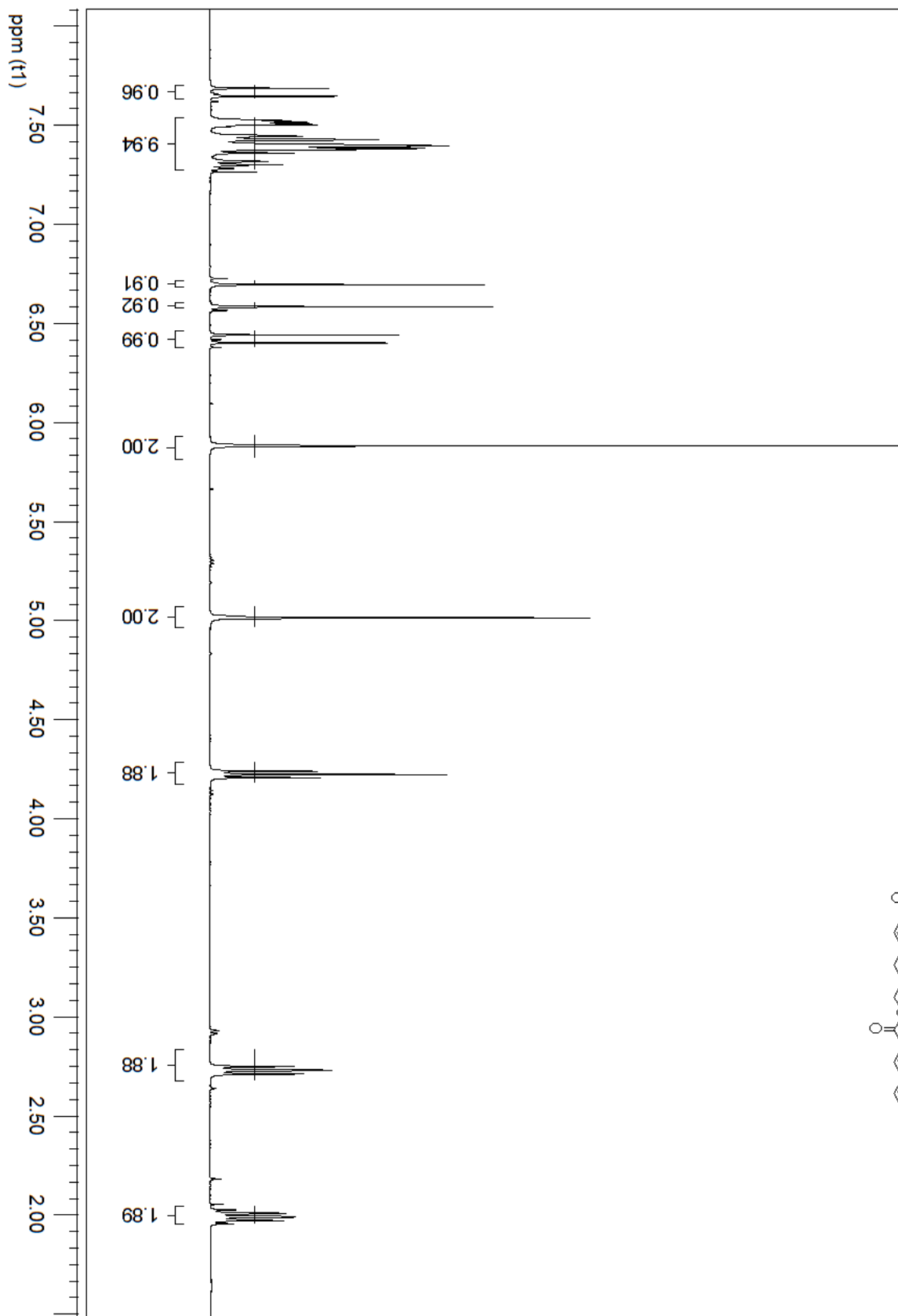
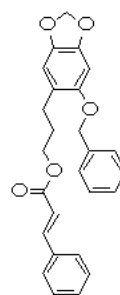


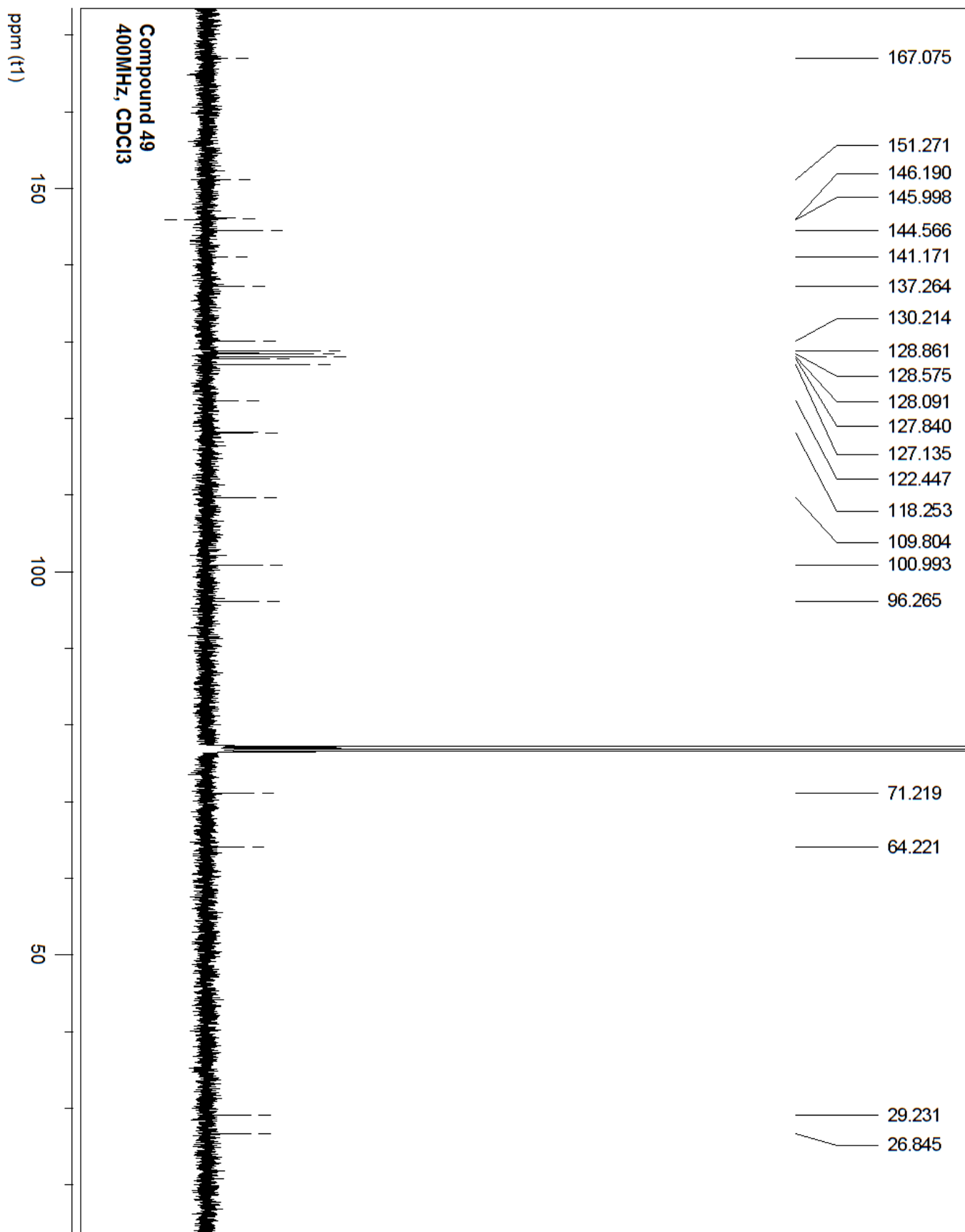


Compound 48
CDCl₃, 400MHz

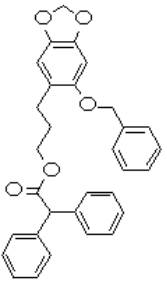


Compound 49
400MHz, CDCl3

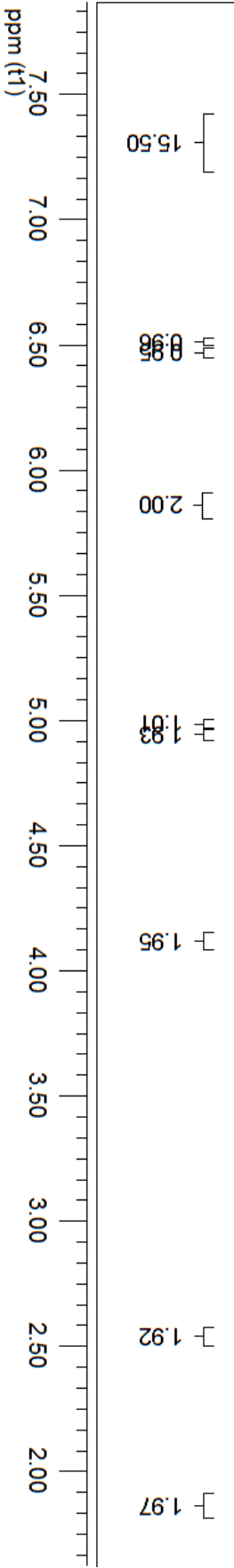


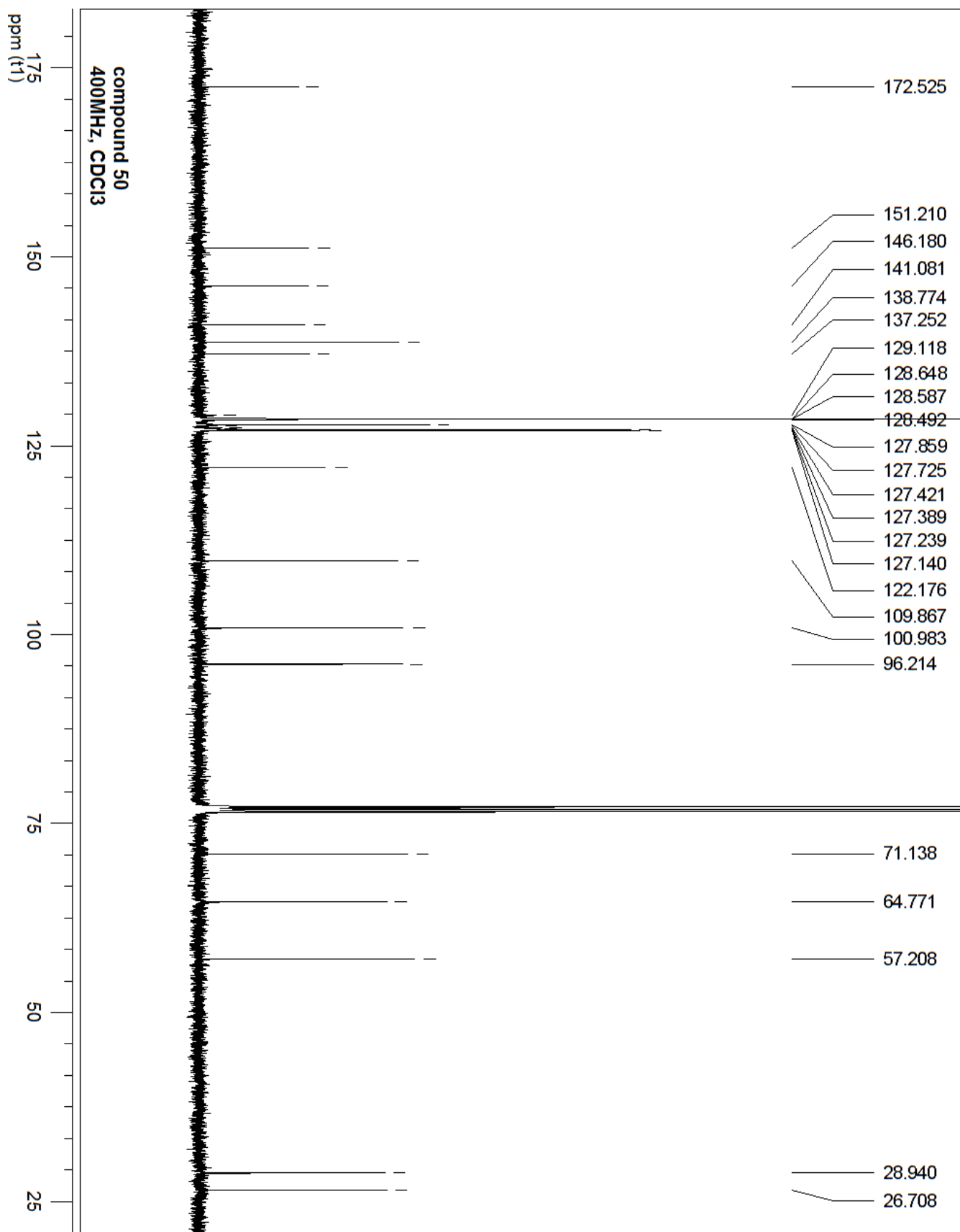


Compound 50
400MHz, CDCl3

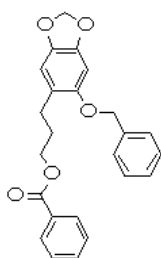


50

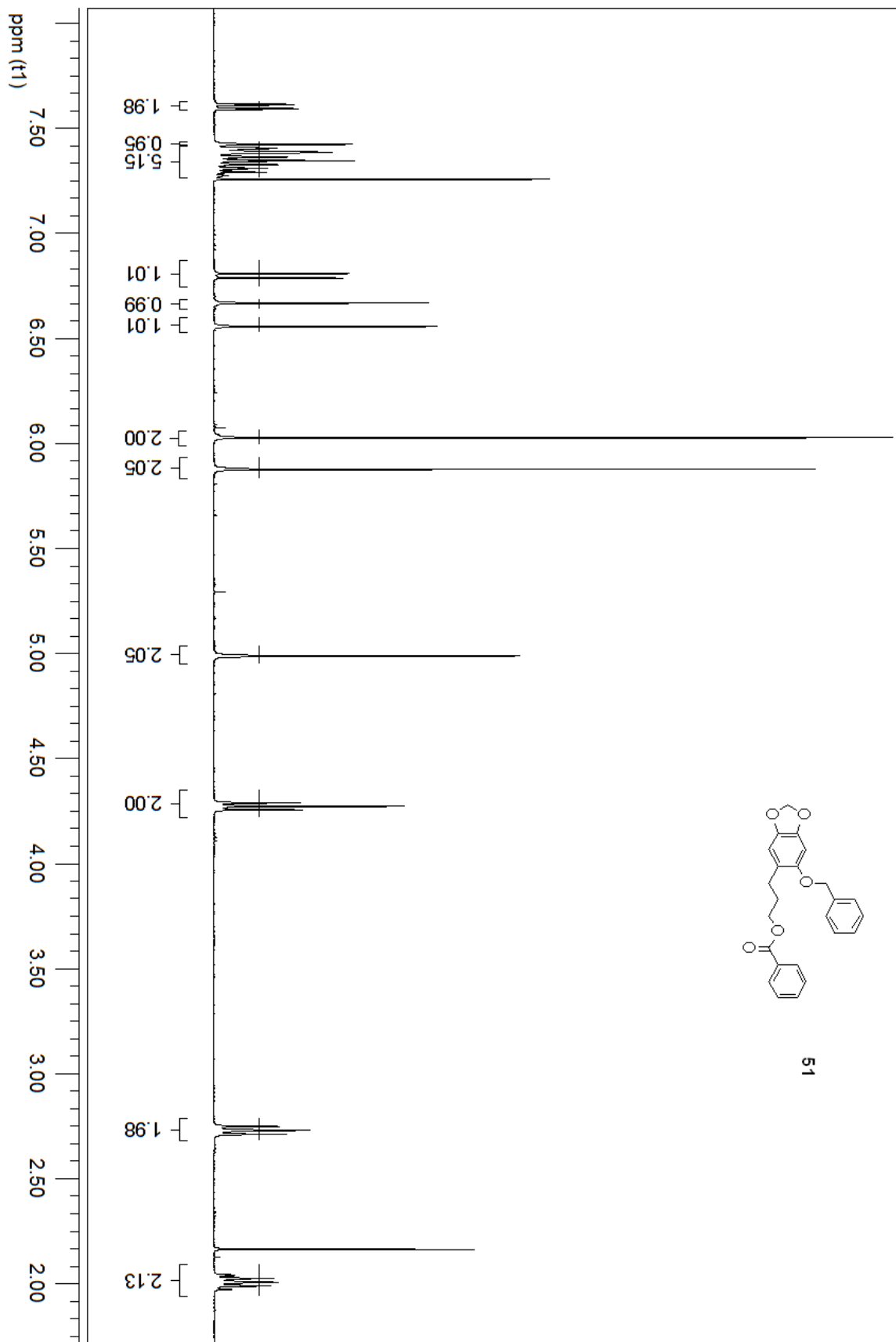


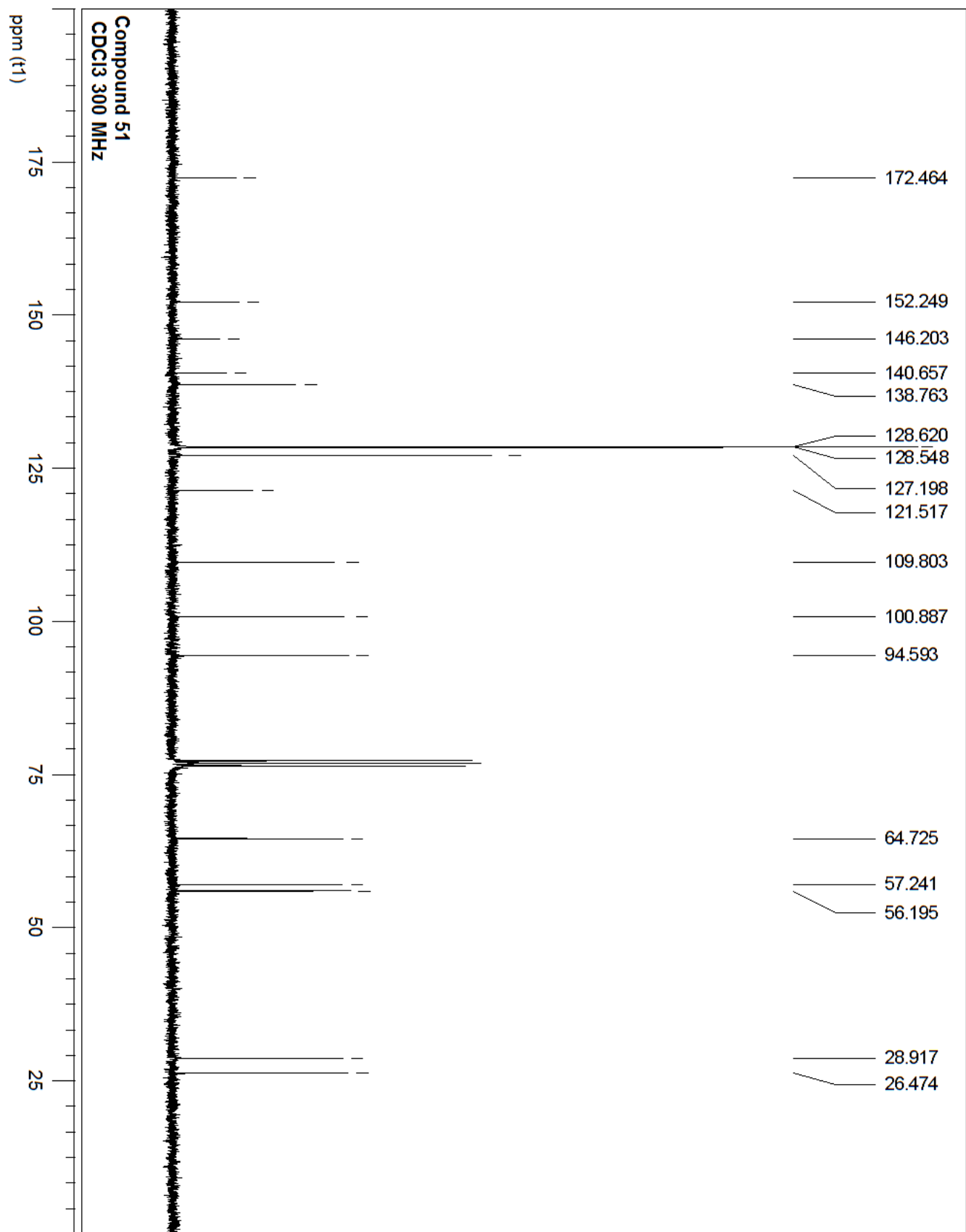


Compound 51
400 MHz, CDCl₃

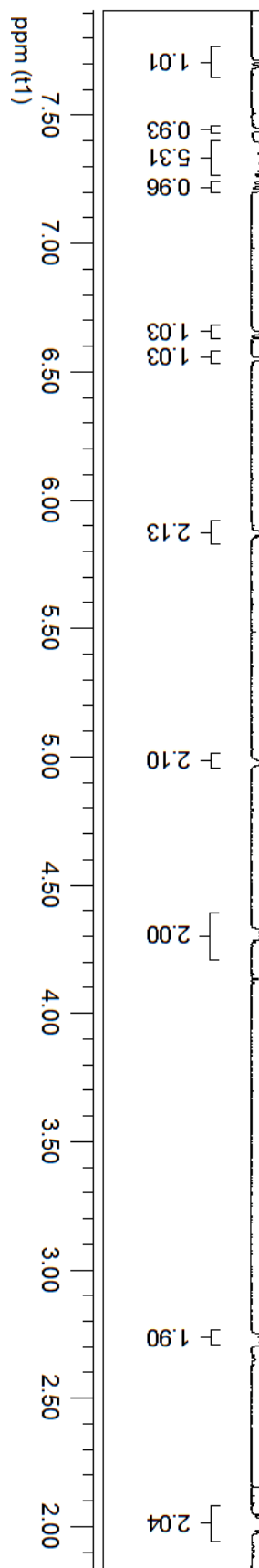
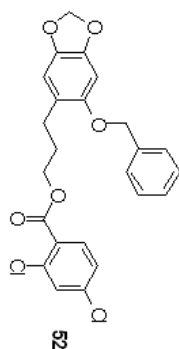


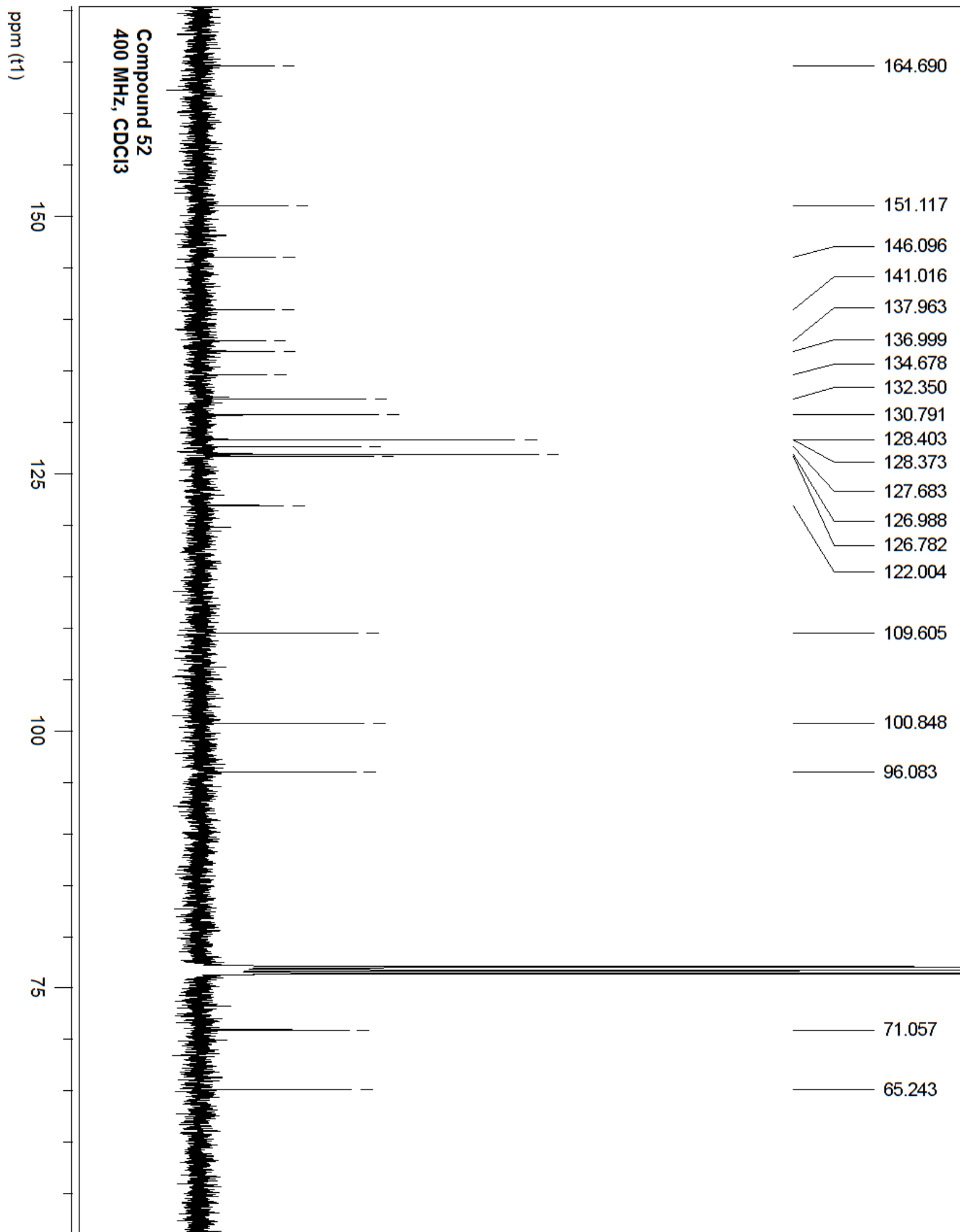
51



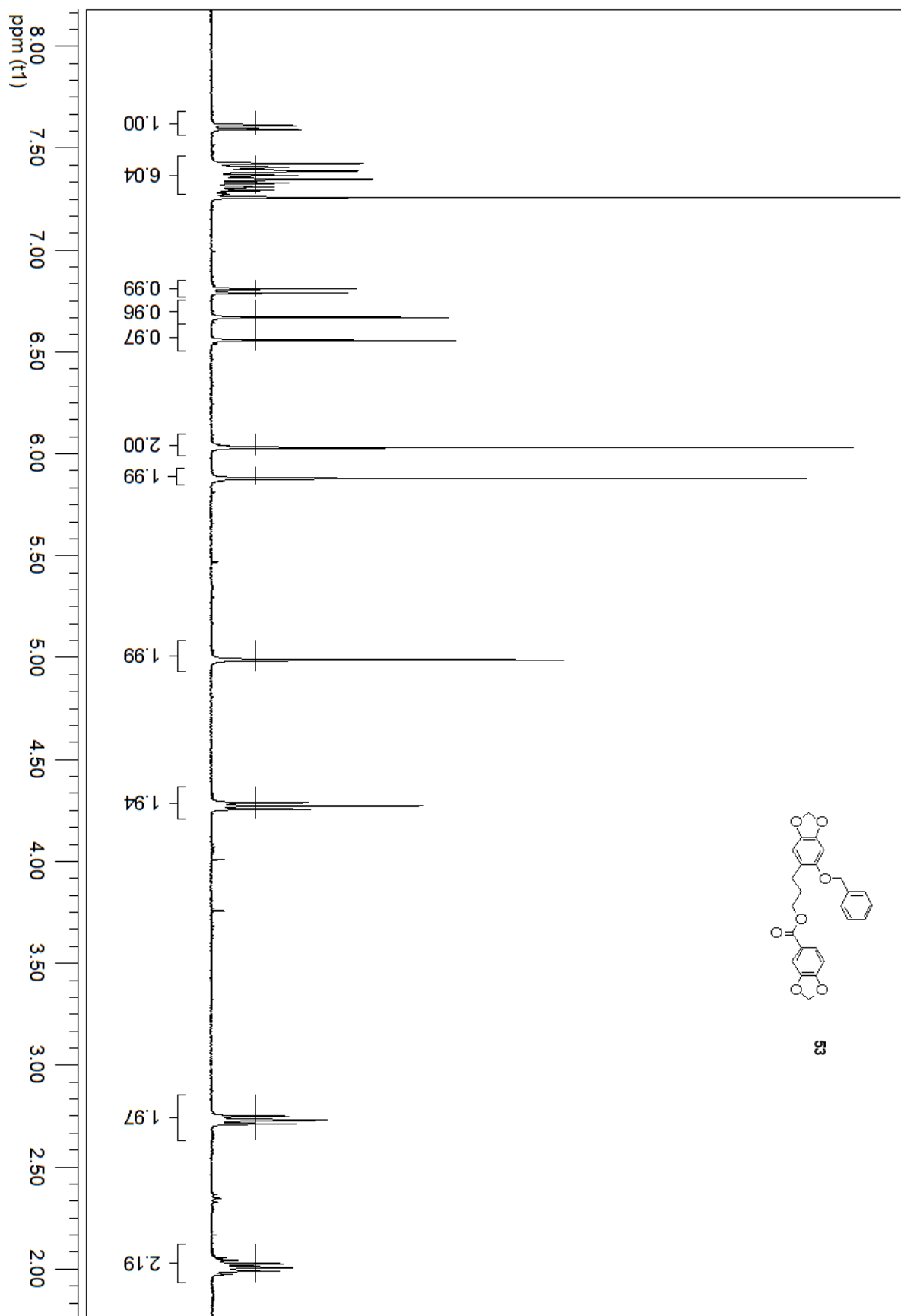


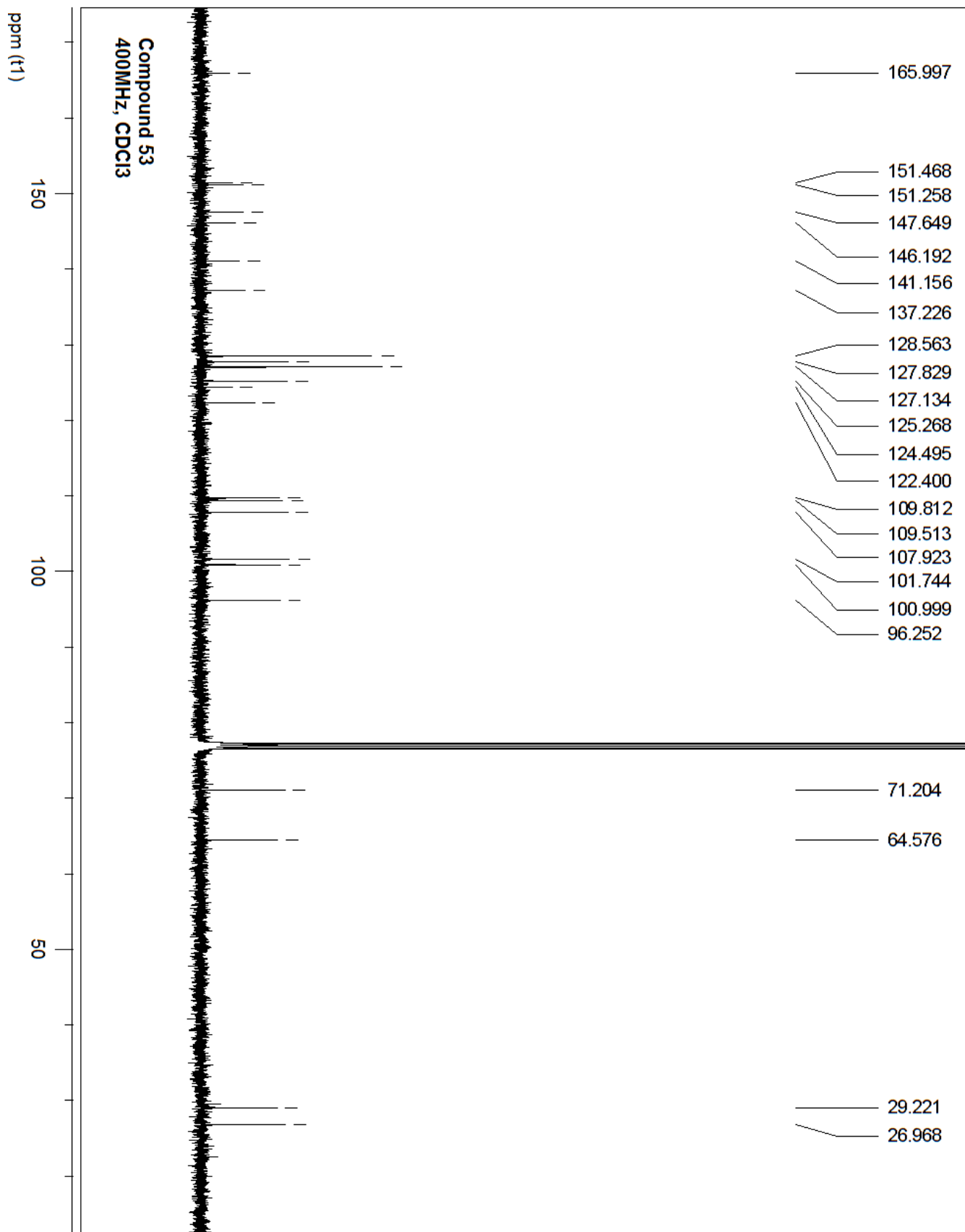
Compound 52
400 MHz, CDCl₃



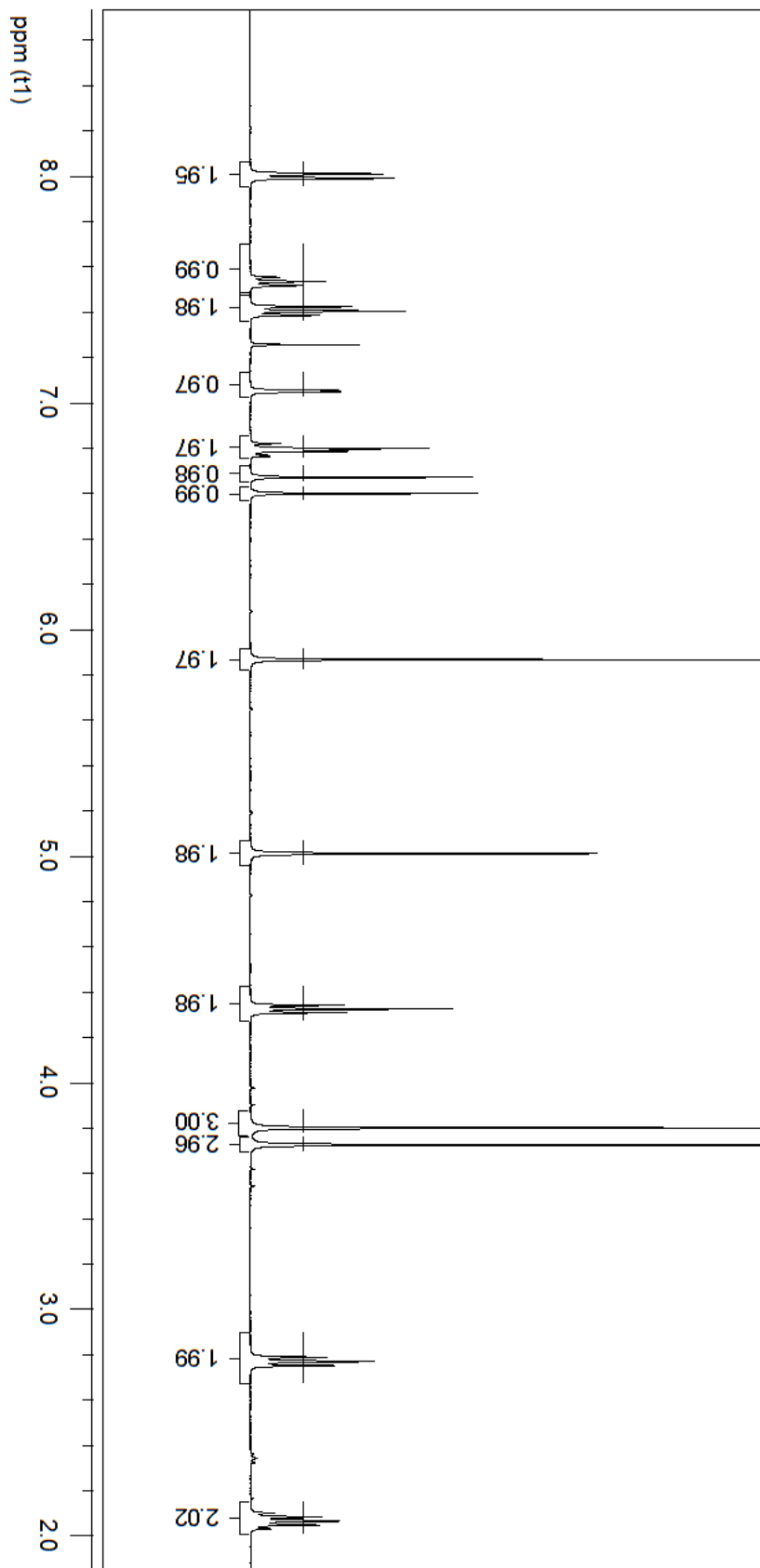
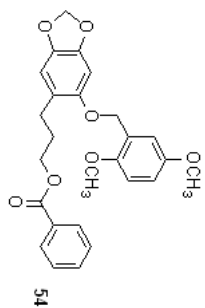


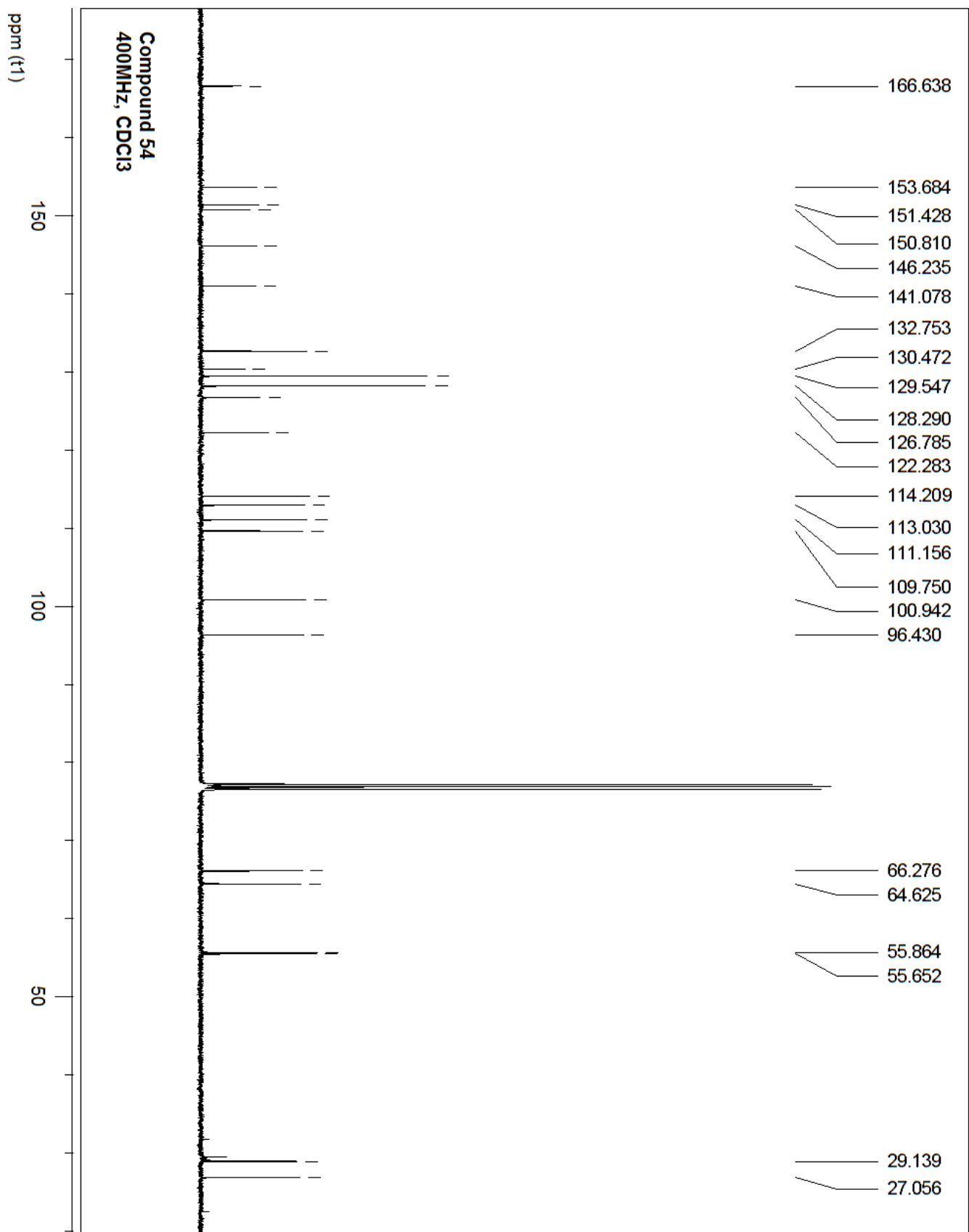
Compound 53
400MHz, CDCl3



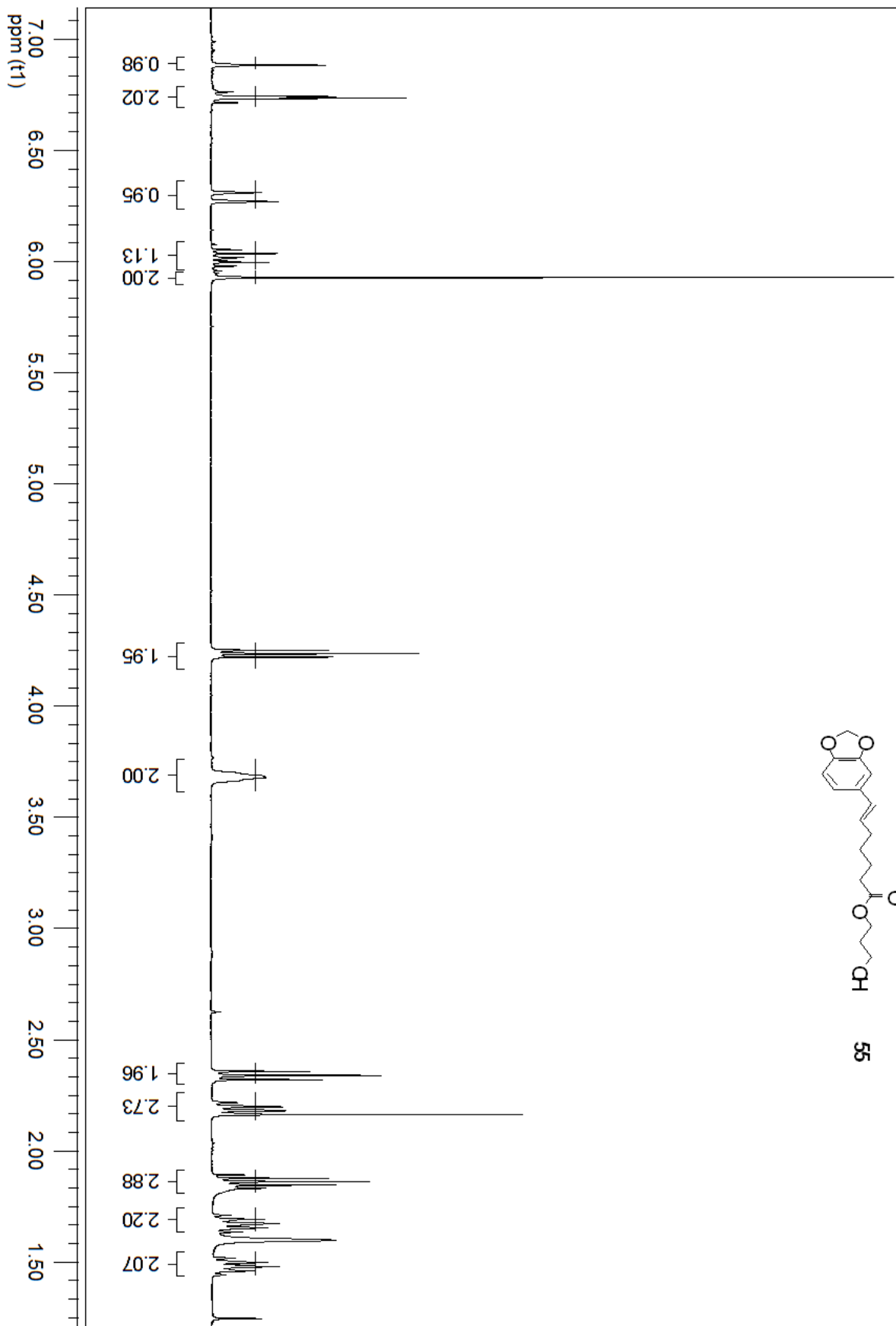
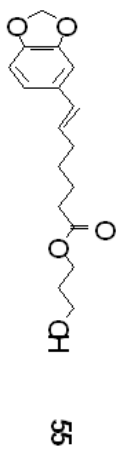


Compound 54
400MHz, CDCl3

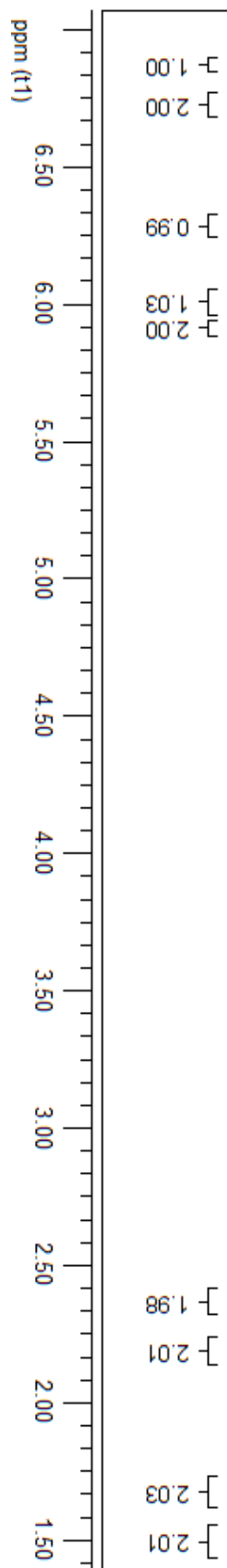
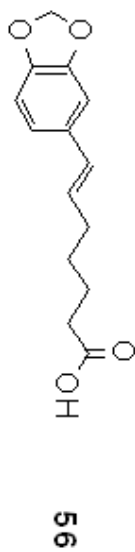




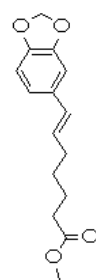
Compound 55
400MHz, CDCl3



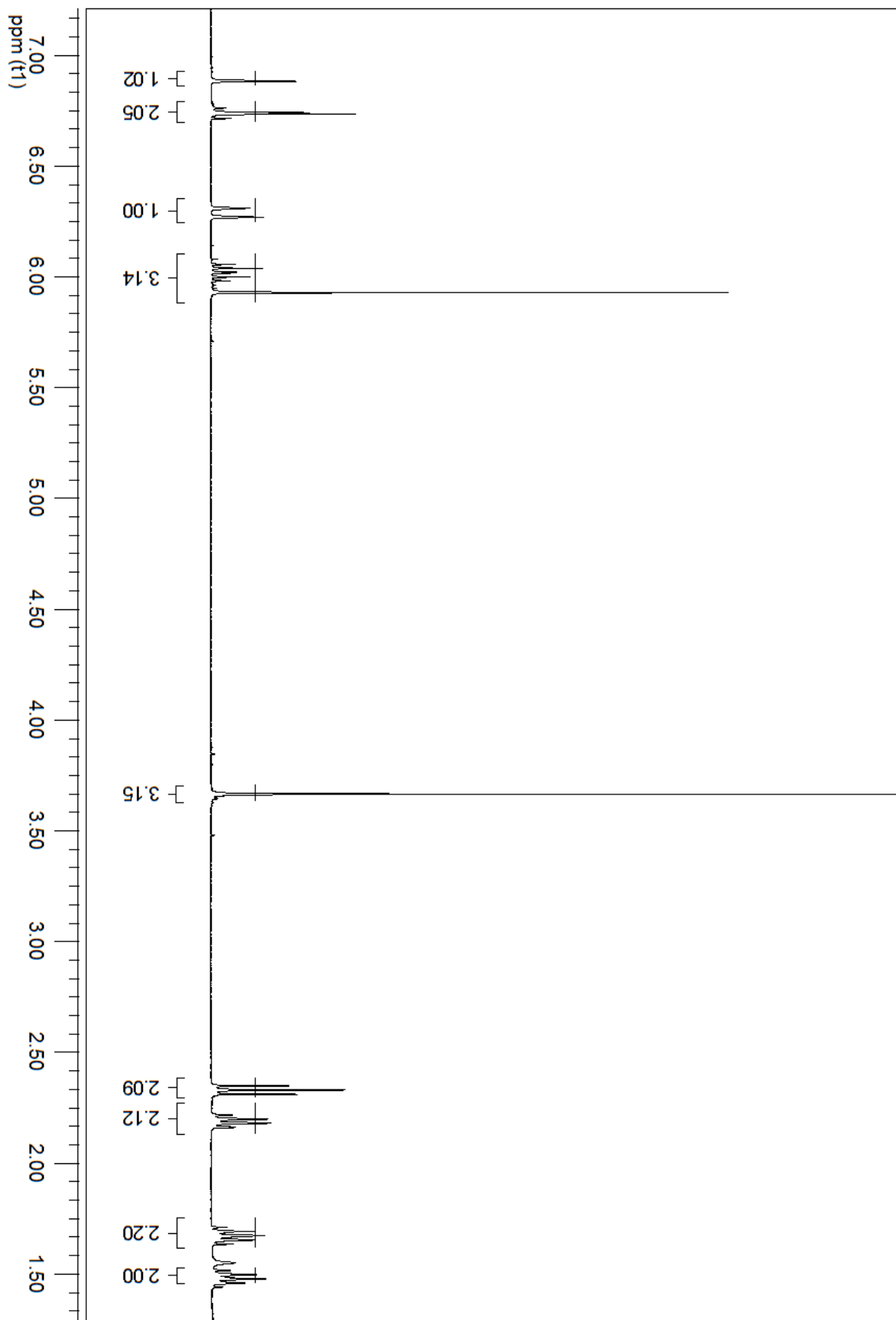
Compound 56
CDCl₃, 400 MHz



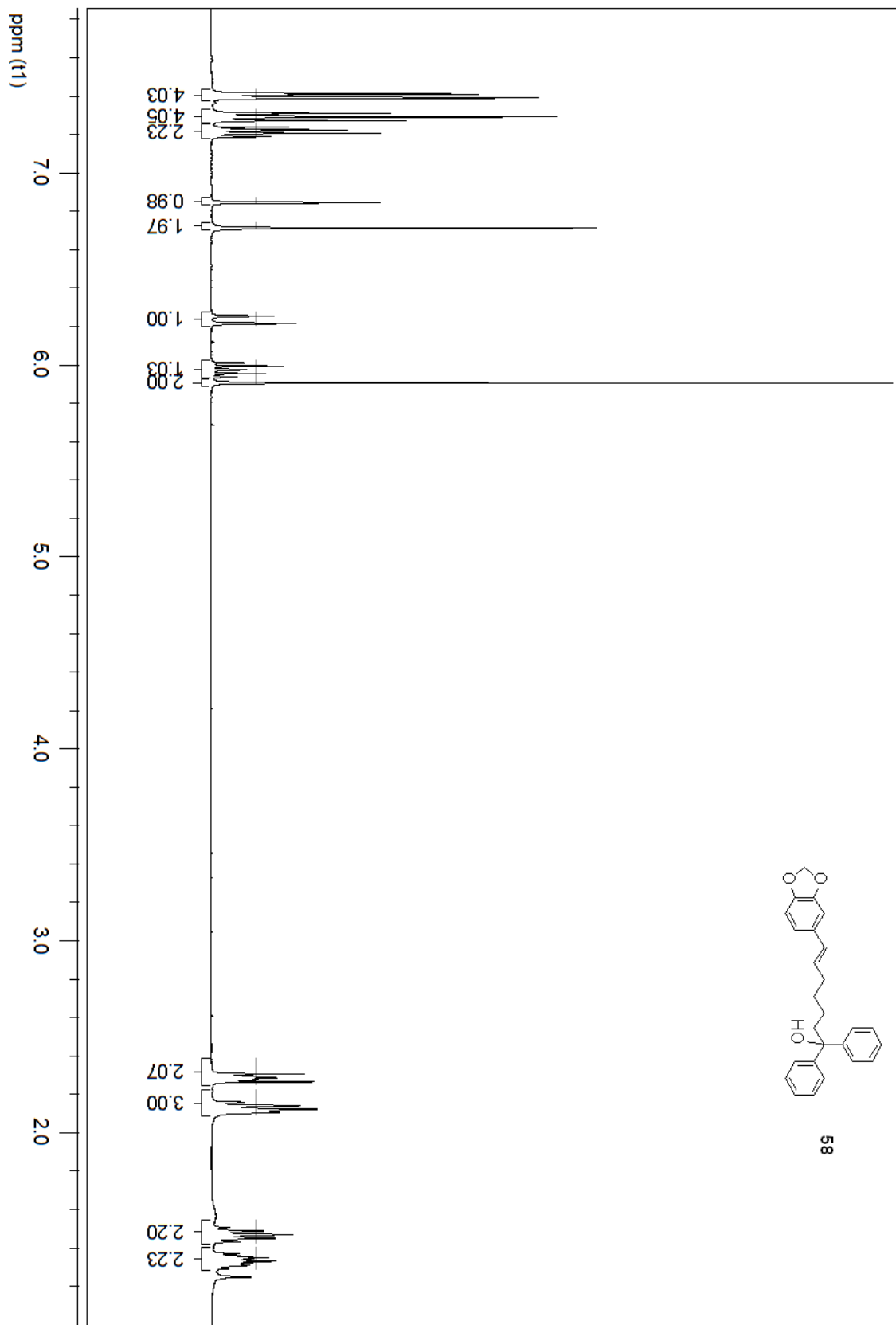
Compound 57
400MHz, CDCl3

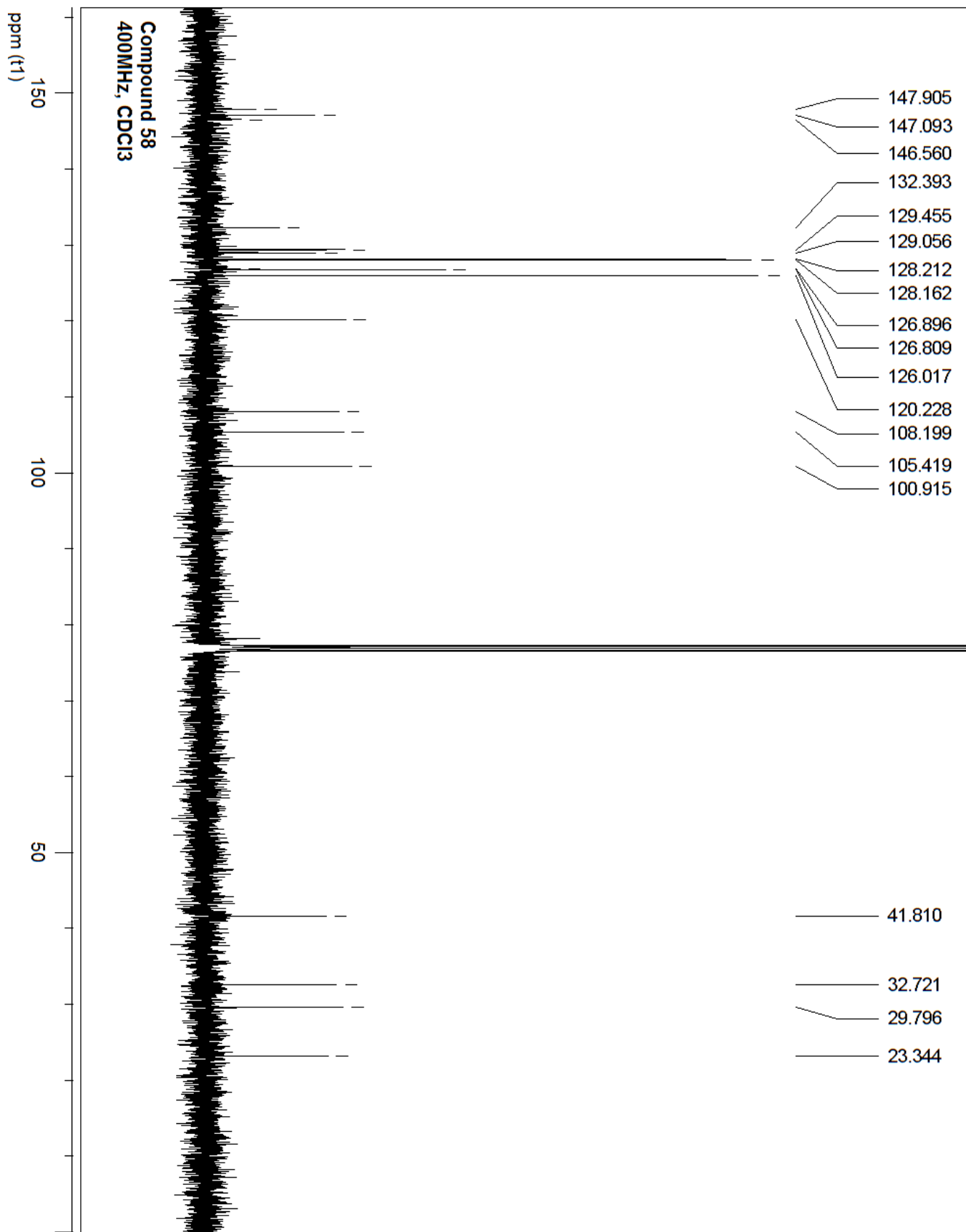


57

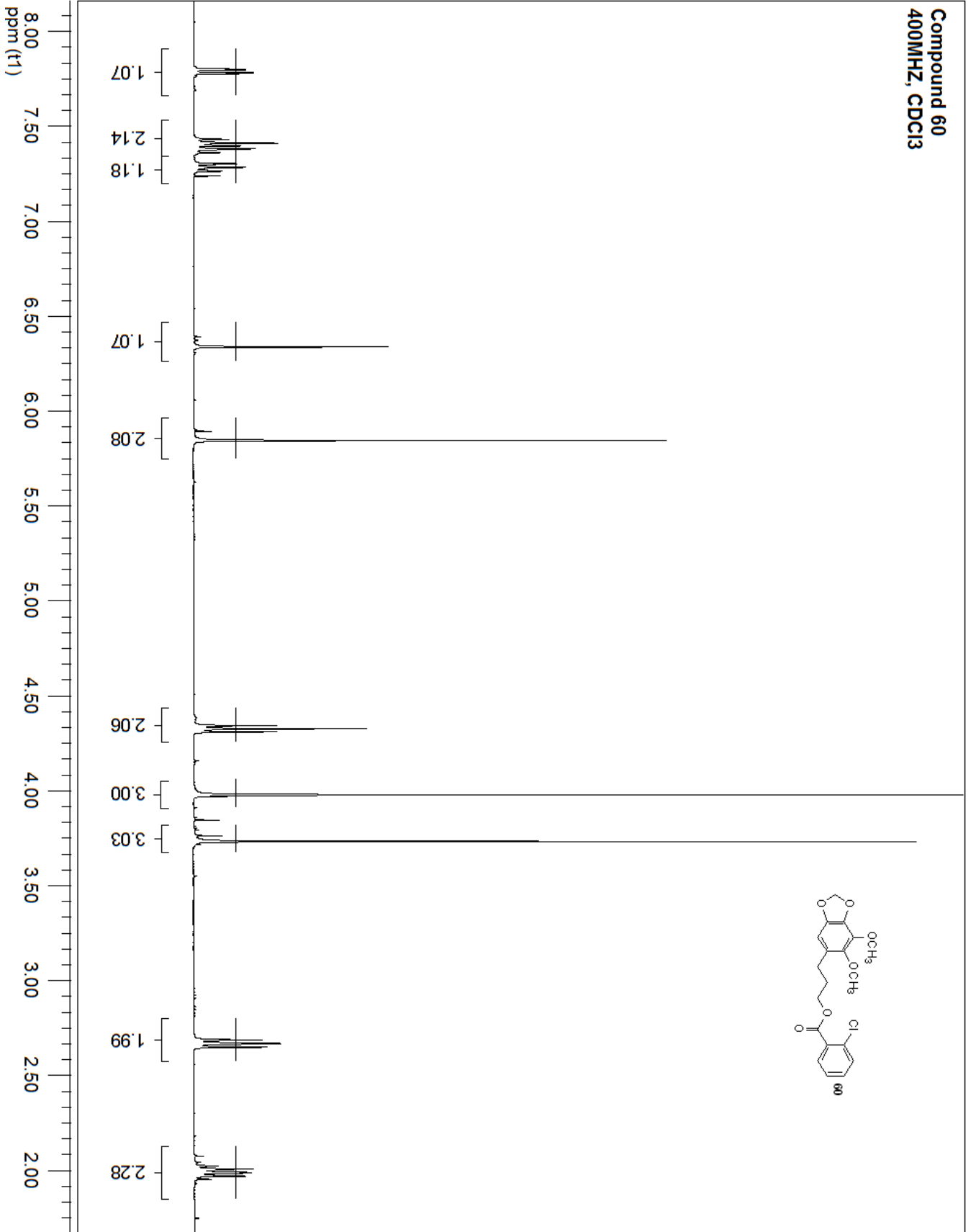


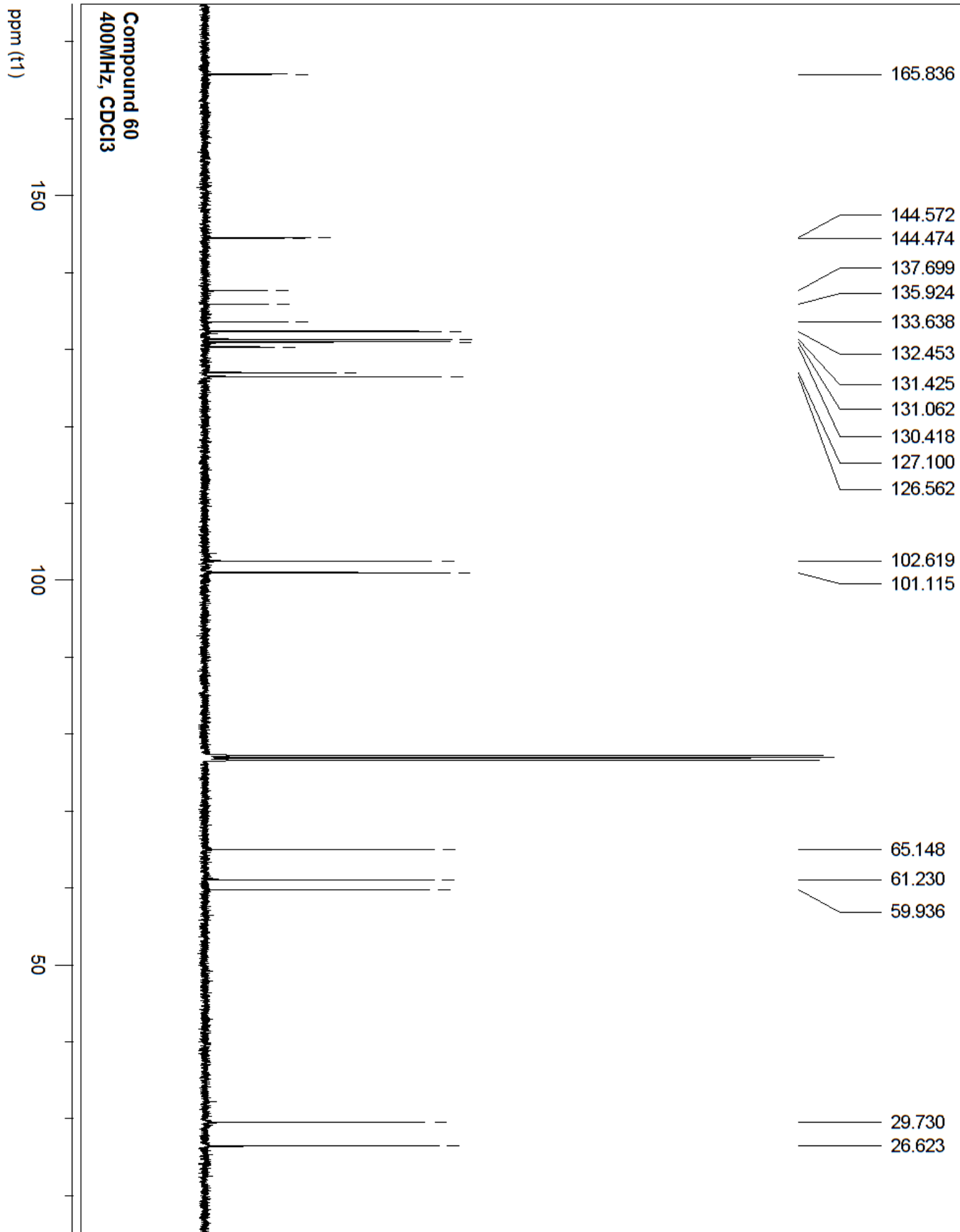
Compound 58
400MHz, CDCl3



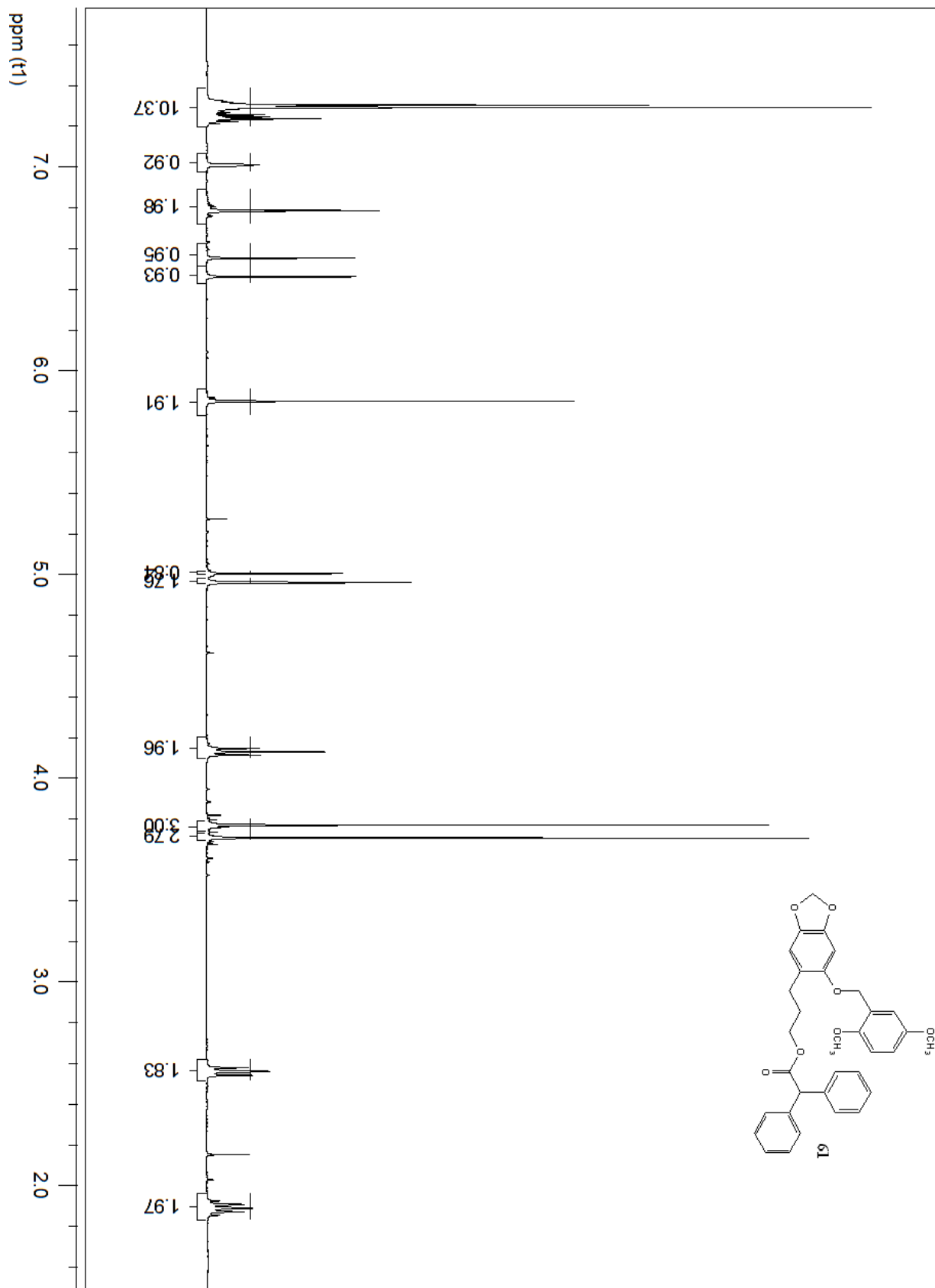


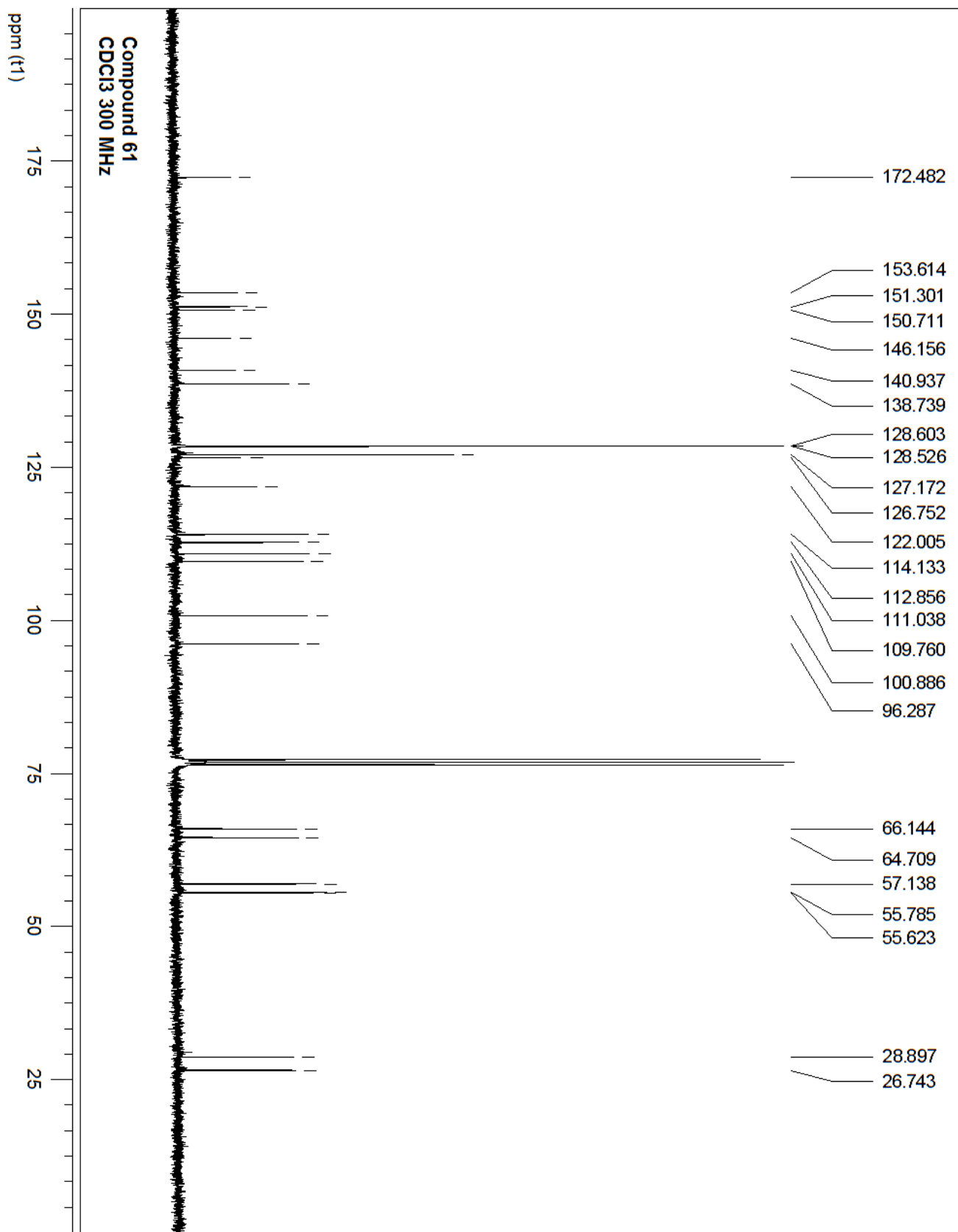
Compound 60
400MHz, CDCl3

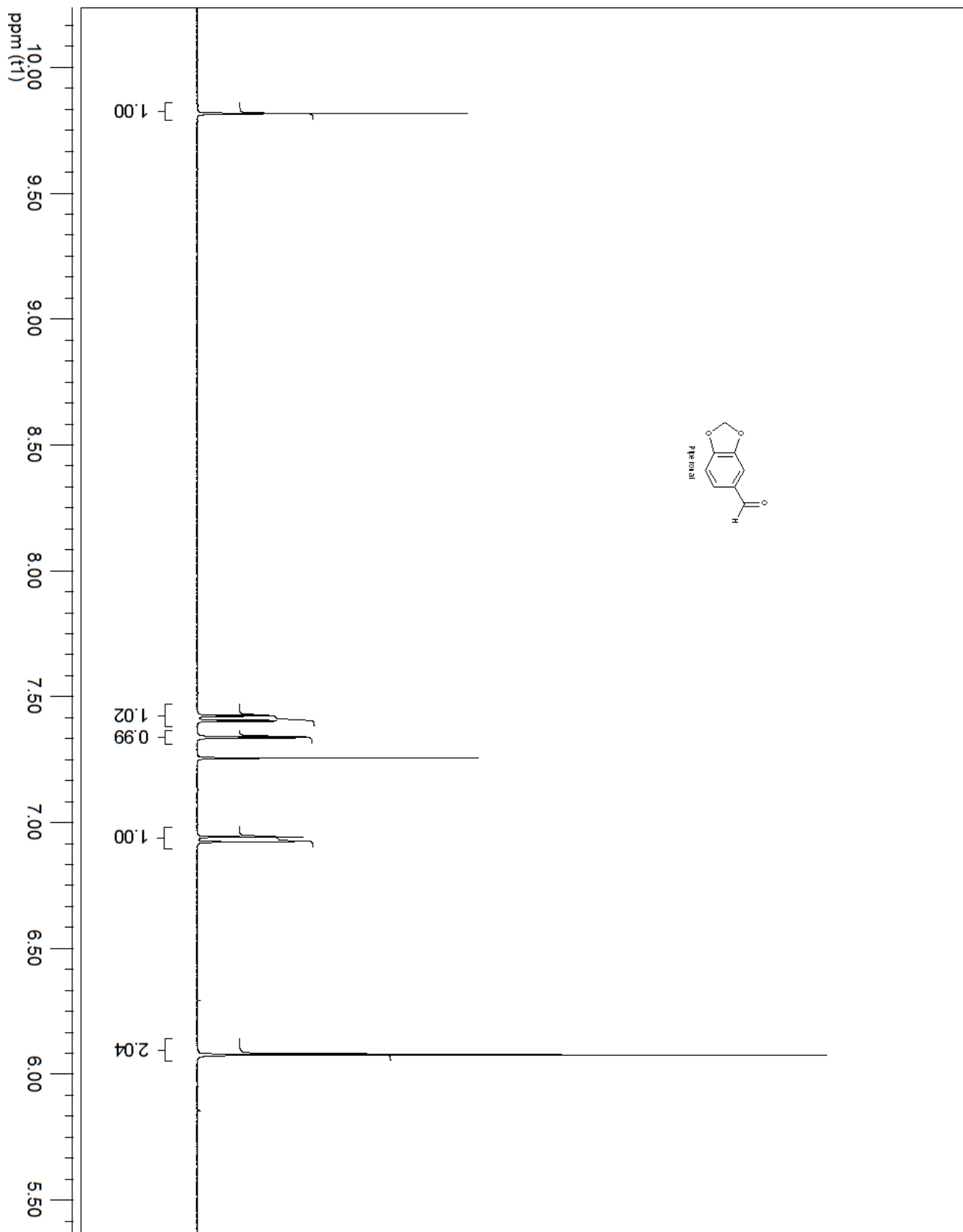




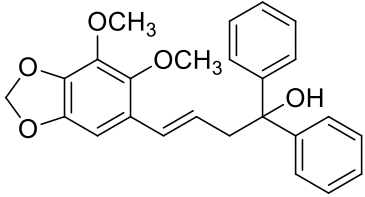
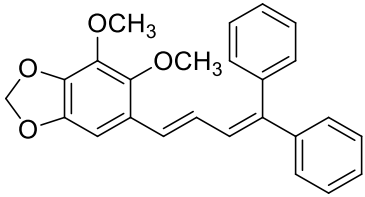
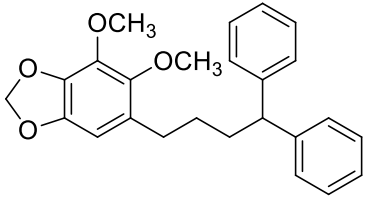
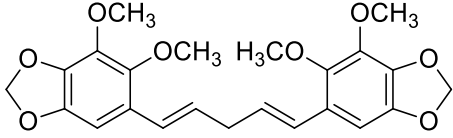
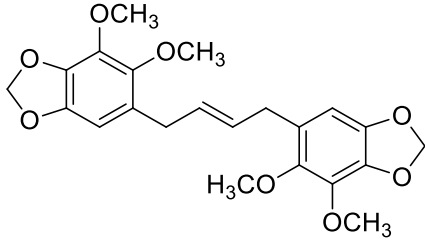
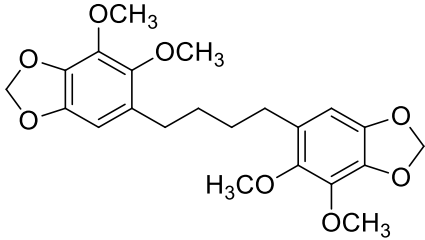
Compound 61
400MHz, CDCl3

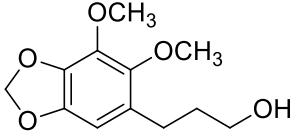
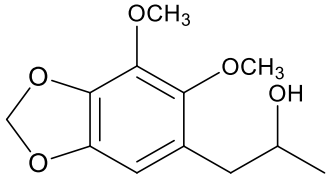
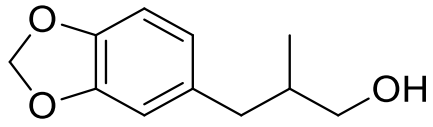
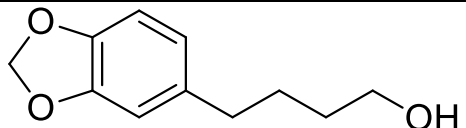
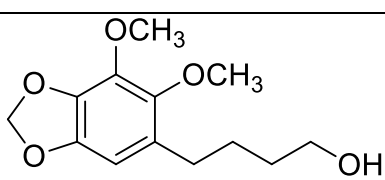
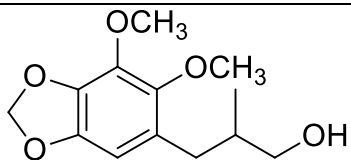
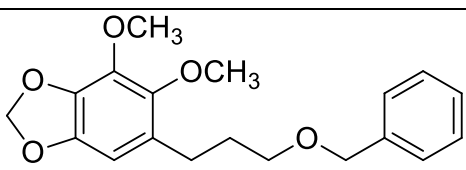
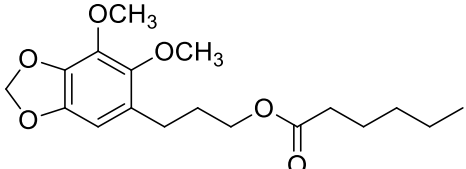
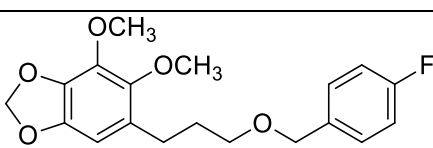


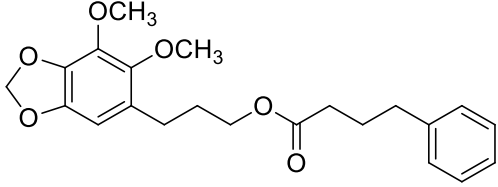
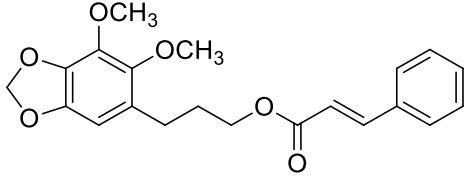
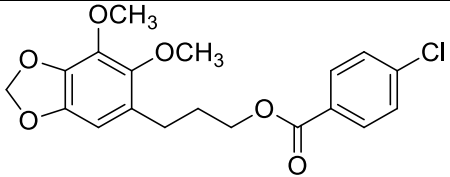
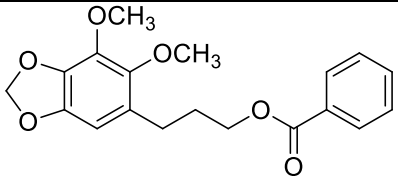
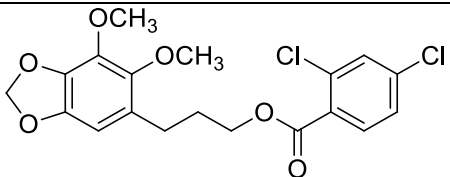
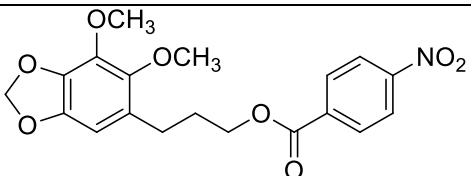
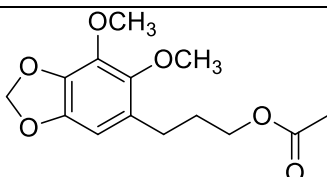
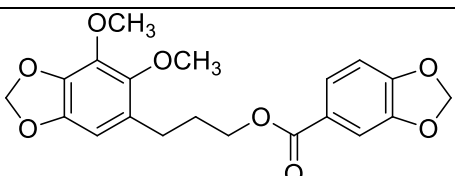


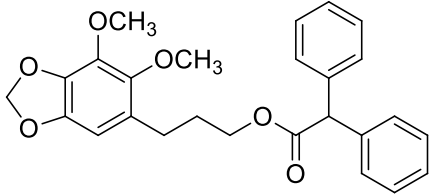
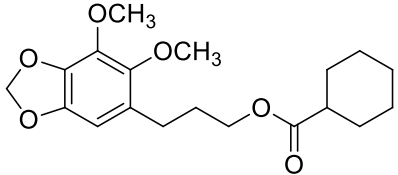
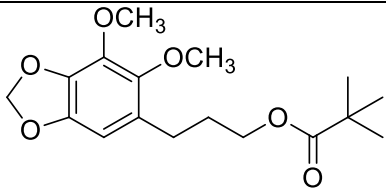
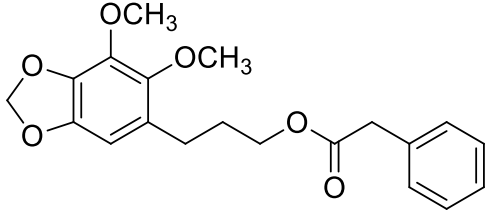
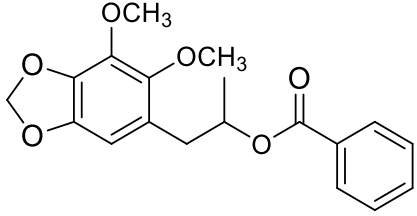
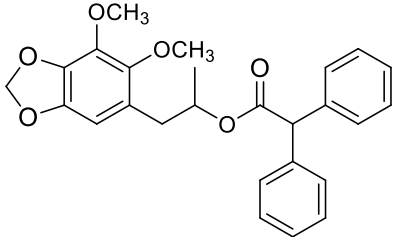
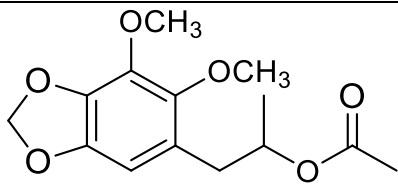


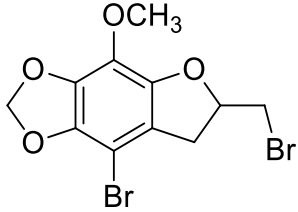
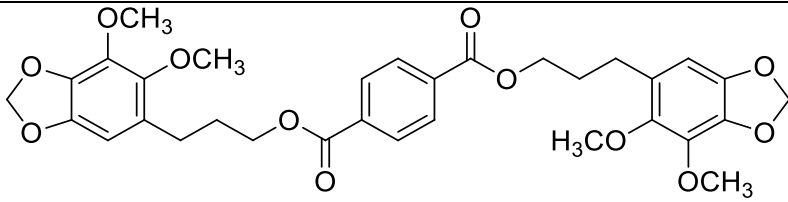
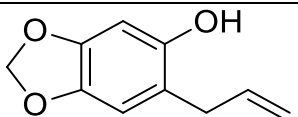
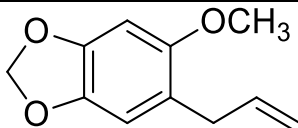
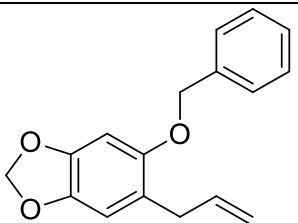
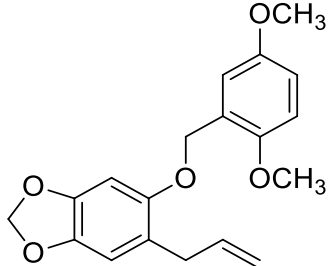
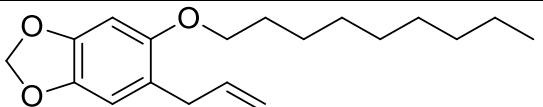
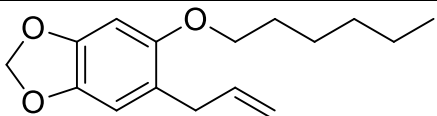
3A. IC₅₀ values for inhibitor activity of CYP3A4

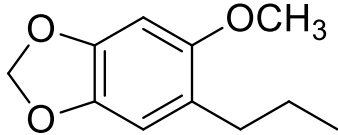
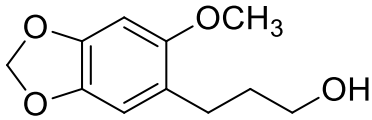
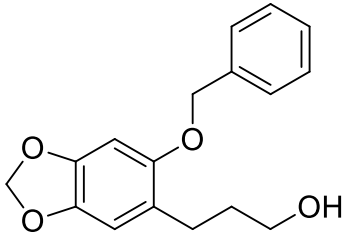
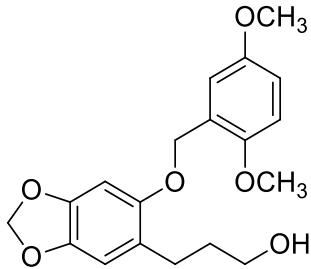
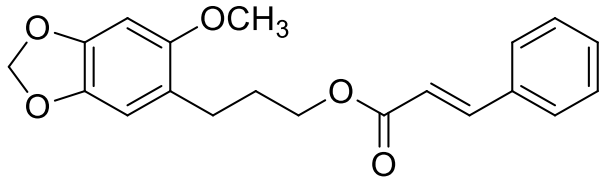
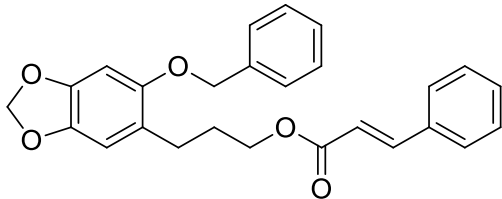
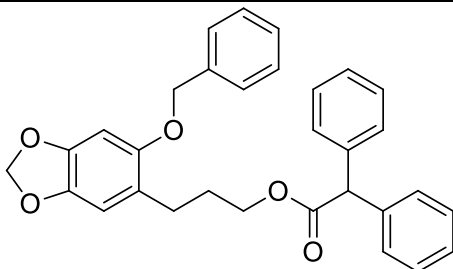
Molecule	IC ₅₀ μM	Activity related to dillapiol
	1.6	5.8
	Non soluble	/
	1.4	6.5
	0.7	13
	1.8	1.1
	0.7	14

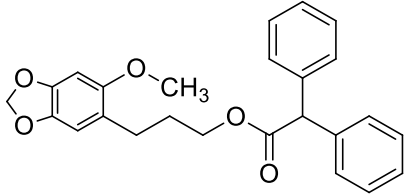
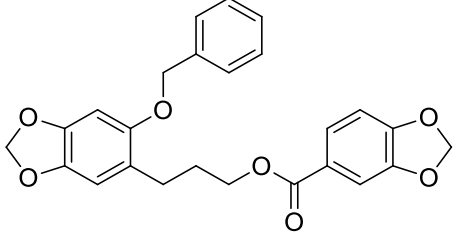
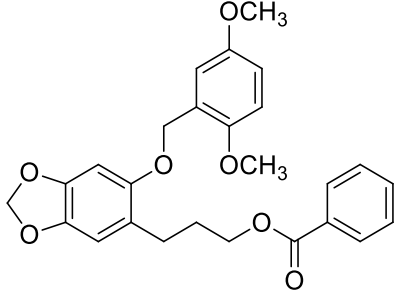
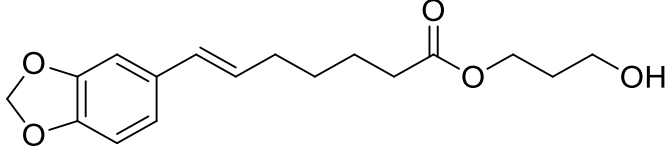
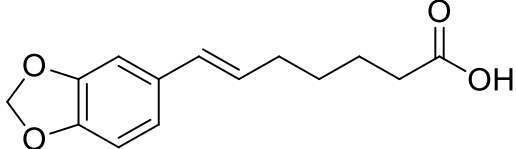
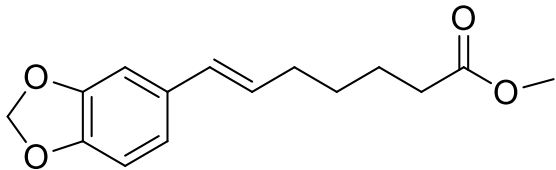
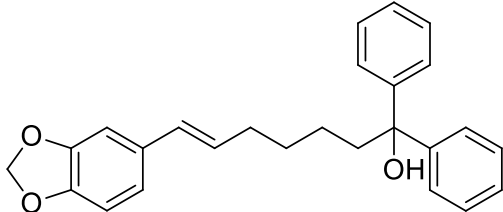
	16	0.6
	>20	/
	>20	/
	>26	/
	11.6	0.8
	>20	/
	6.7	1.4
	3.3	2.8
	10.3	0.9

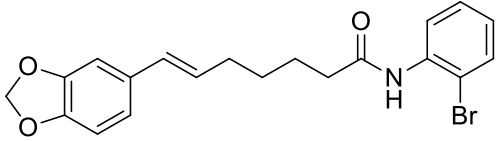
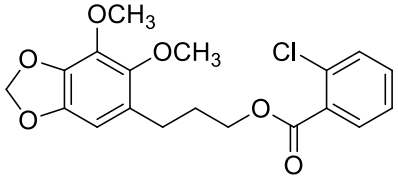
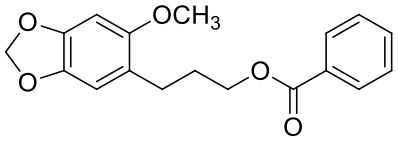
	4.1	2.2
	2.4	3.4
	1.6	5.9
	2.1	4.4
	1.4	6.6
	>13	/
	9.2	1
	2.6	3.5

	0.4	21.2
	1.9	4.8
	2.8	3.3
	1.9	4.8
	3.5	2.6
	0.2	46
	>20	/

	2.7	4
	1.6	5.7
	>28	/
	>16	/
	1.4	6.4
	2.2	4.3
	>>>50	/
	7.4	1.2

	>26	/
	4.1	2.3
	3	3
	1.3	7.1
	4.7	1.9
	8	1.1
	0.6	14

	0.5	19.5
	1.4	6.7
	0.4	25.5
	4.1	2.2
	>26	/
	>20	/
	0.5	17

	5.4	1.7
	5.3	1.8
	2.1	4.4

4A. X-ray analysis for compound 187

checkCIF/PLATON report

Structure factors have been supplied for datablock(s) td011

No syntax errors found. CIF dictionary Interpreting this report

Datablock: td011

Bond precision: C-C = 0.0023 Å Wavelength=0.71073
Cell: a=5.5345(2) b=17.1768(6) c=19.5970(6)
alpha=90 beta=94.122(2) gamma=90
Temperature: 200 K

	Calculated	Reported
Volume	1858.17(11)	1858.17(11)
Space group	P 21/c	P2(1)/c
Hall group	-P 2ybc	?
Moiety formula	C20 H17 Br2 N O S	?
Sum formula	C20 H17 Br2 N O S	C20 H17 Br2 N O S
Mr	479.22	479.23
Dx, g cm ⁻³	1.713	1.713
Z	4	4
Mu (mm ⁻¹)	4.483	4.483
F000	952.0	952.0
F000'	950.58	
h, k, lmax	7, 22, 26	7, 22, 26
Nref	4636	4570
Tmin, Tmax	0.530, 0.611	0.425, 0.638
Tmin'	0.353	


Correction method= MULTI-SCAN

Data completeness= 0.986 Theta(max)= 28.330

R(reflections)= 0.0233(4022) wR2(reflections)= 0.0612(4570)

S = 1.039 Npar= 226

The following ALERTS were generated. Each ALERT has the format
test-name_ALERT_alert-type_alert-level.
Click on the hyperlinks for more details of the test.

 **Alert level C**

PLAT910_ALERT_3_C Missing # of FCF Reflections Below Th(Min)	1
PLAT911_ALERT_3_C Missing # FCF Refl Between THmin & STh/L= 0.600	41

● Alert level G

PLAT005_ALERT_5_G	No _iucr_refine_instructions_details in CIF	?
PLAT007_ALERT_5_G	Note: Number of Unrefined D-H Atoms	1
PLAT793_ALERT_4_G	The Model has Chirality at C7 (Verify)	R
PLAT912_ALERT_4_G	Missing # of FCF Reflections Above STh/L= 0.600	23

0 ALERT level A = Most likely a serious problem - resolve or explain
0 ALERT level B = A potentially serious problem, consider carefully
2 ALERT level C = Check. Ensure it is not caused by an omission or oversight
4 ALERT level G = General information/check it is not something unexpected

0 ALERT type 1 CIF construction/syntax error, inconsistent or missing data
0 ALERT type 2 Indicator that the structure model may be wrong or deficient
2 ALERT type 3 Indicator that the structure quality may be low
2 ALERT type 4 Improvement, methodology, query or suggestion
2 ALERT type 5 Informative message, check

It is advisable to attempt to resolve as many as possible of the alerts in all categories. Often the minor alerts point to easily fixed oversights, errors and omissions in your CIF or refinement strategy, so attention to these fine details can be worthwhile. In order to resolve some of the more serious problems it may be necessary to carry out additional measurements or structure refinements. However, the purpose of your study may justify the reported deviations and the more serious of these should normally be commented upon in the discussion or experimental section of a paper or in the "special_details" fields of the CIF. checkCIF was carefully designed to identify outliers and unusual parameters, but every test has its limitations and alerts that are not important in a particular case may appear. Conversely, the absence of alerts does not guarantee there are no aspects of the results needing attention. It is up to the individual to critically assess their own results and, if necessary, seek expert advice.

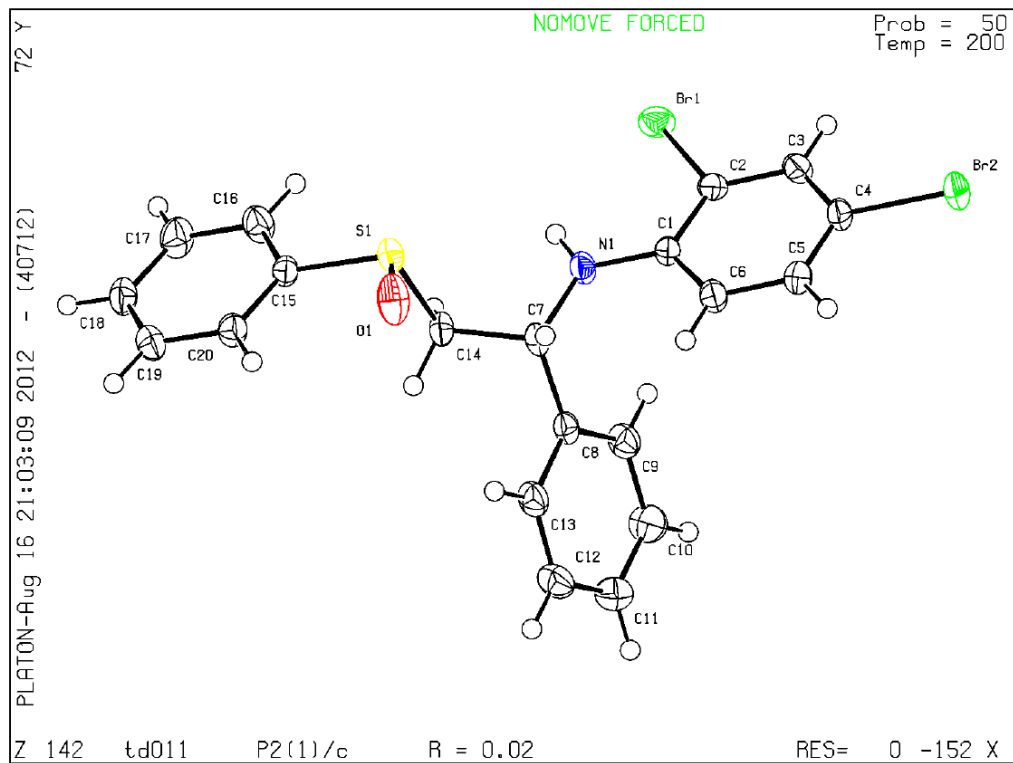
Publication of your CIF in IUCr journals

A basic structural check has been run on your CIF. These basic checks will be run on all CIFs submitted for publication in IUCr journals (*Acta Crystallographica*, *Journal of Applied Crystallography*, *Journal of Synchrotron Radiation*); however, if you intend to submit to *Acta Crystallographica Section C* or *E*, you should make sure that full publication checks are run on the final version of your CIF prior to submission.

Publication of your CIF in other journals

Please refer to the *Notes for Authors* of the relevant journal for any special instructions relating to CIF submission.

PLATON version of 04/07/2012; check.def file version of 28/06/2012



5A. Bioassays results for connexin blocker analogs

Methodology used by Matthew Cooke

MATERIALS AND METHODS

Parachute assay

The parachute assay was used to assess gap junctional intercellular communication as has been previously described²¹⁵. On day 0, 2×10^4 recipient NT2/D1 cells were plated in uncoated optical 96 well plates (Greiner Bio-One 655090). At this time, 5×10^5 donor cells were also plated in a 60 mm tissue culture dish (Corning 430196). On day 1, donor cells were treated for 30 minutes with 4 μ M calcein AM (Sigma-Aldrich C1359) and 10 μ M 1,1'-Dioctadecyl-3,3,3',3'-tetramethylindocarbocyanine perchlorate (DiI) (Sigma-Aldrich 468495, lot 13021HO) in normal growth medium. Donor cells were then washed with PBS, trypsinized for 4 minutes with 0.05% trypsin-EDTA (Gibco 25300, lot 688247) and counted. Donor cells were then seeded on top of recipient cells at a density of 200 cells per well (1:100 donor to recipient ratio) and incubated with treatments and 0.1 μ g/ml Hoechst 33342 trihydrochloride trihydrate (Invitrogen H1399, lot 908746) for 75 minutes in normal growth medium at 37°C prior to imaging. Vehicle concentration was held constant and did not exceed 0.1% total medium. Experiments were imaged on an Opera High Content Screening System (Perkin Elmer) at 20X magnification using the 20xW_UAPO20xW3/340_NA=0.7 objective. Hoechst was excited at a wavelength of 405 nm and its emission was detected at a wavelength of 450 nm. Calcein was excited at a wavelength of 488 nm and its emission was detected at a wavelength of 540 nm. DiI was excited at a wavelength of 561 nm and its emission was detected at a wavelength of 690 nm. Image analysis was performed using Columbus Image Analysis System version 2.3.0 (Perkin Elmer). Replicate

experiments were analyzed with each treatment in replicates of 12 wells and 20 images per well. All plates were controlled with untreated cells, vehicle-treated cells, and cells treated with 10 and 100 μM carbenoxolone disodium salt (C4790, lot 020M1257V).

Zero-calcium dye uptake assay

Uptake of Lucifer Yellow CH dilithium salt (Sigma L0259, lot MKBJ5898V) and propidium iodide (Invitrogen P1304MP, lot 890805) in zero calcium conditions was used to assess hemichannel activity in NT2/D1 cells. On day 0, 2×10^4 NT2/D1 cells were plated in optical 96 well plates (Greiner Bio-One 655090, lot E1110CV) coated with 100 $\mu\text{g}/\text{ml}$ poly-L-lysine hydrobromide (Sigma-Aldrich P1274, lot 030K5101). On day 1, cells were incubated for 5 minutes in either 250 $\mu\text{g}/\text{ml}$ LY or 50 $\mu\text{g}/\text{ml}$ PI in PBS containing 1 mM EGTA. Cells were then washed with PBS and fixed with 3.7% formaldehyde in PBS for 10 minutes. Before imaging, cells were washed and incubated in 0.1 $\mu\text{g}/\text{ml}$ Hoechst 33342 in PBS for 30 minutes at room temperature. LY assays were controlled for dye uptake nonspecific to hemichannels using rhodamine B isothiocyanate dextran, 10,000 MW (Sigma R8881, lot 090M5307V). PI assays were controlled for dye uptake nonspecific to hemichannels using fluorescein isothiocyanate dextran, 10,000 MW (Sigma FD10S, lot 021M5302V). Experiments were imaged on an Opera High Content Screening System (Perkin Elmer) at 20X magnification using the 20xW_UAPO20xW3/340_NA=0.7 objective. Hoechst was excited at a wavelength of 405 nm and its emission was detected at a wavelength of 450 nm. LY was excited at a wavelength of 405 nm and its emission was detected at a wavelength of 600 nm. RD was excited at a wavelength of 561 nm and its emission was detected at a wavelength of 690 nm. PI was excited at a wavelength of 561 nm and its emission

was detected at a wavelength of 690 nm. FITCD was excited at a wavelength of 488 nm and its emission was detected at a wavelength of 540 nm. Image analysis was performed using Columbus Image Analysis System version 2.3.0 (Perkin Elmer). Replicate experiments were analyzed with each treatment in replicates of 12 wells and 20 images per well. Controls included assays performed in medium and 100 μ M carbenoxolone.

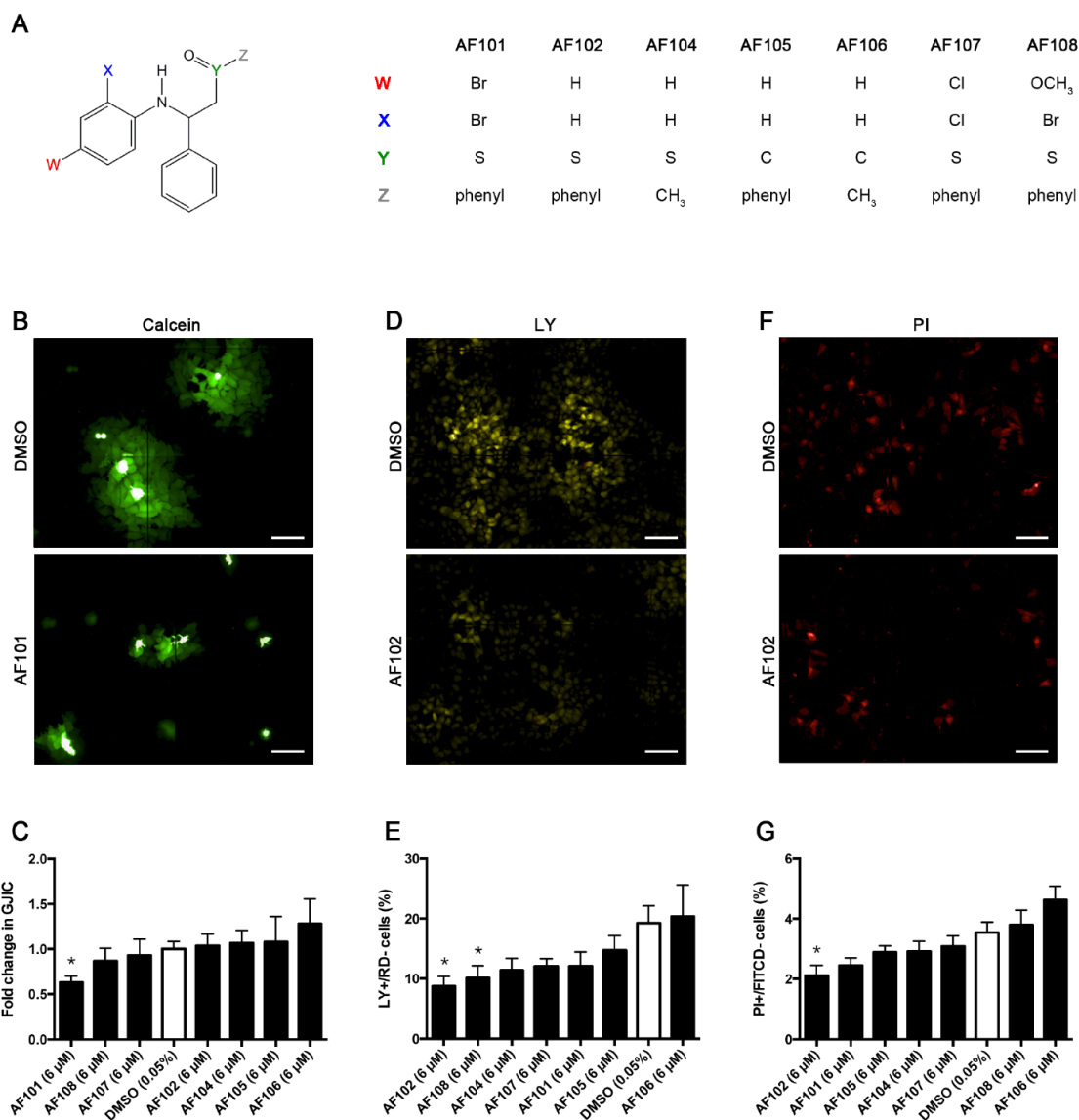


Figure X. AF101 and its derivatives are novel inhibitors of connexin gap junction and hemichannel activity. (A) AF101 is a previously uncharacterized phenolic compound containing three phenyl groups, a secondary amine group, and a phenyl-linked sulfoxide group. Several derivatives of AF101 were synthesized in which substitutions were made for the amine-linked *m*-dibromobenzene group (W and X), the sulfoxide group (Y), and the sulfoxide-linked phenyl group (Z). (B) Representative images depicting the effect of AF101 on gap junctional intercellular communication (GJIC). (C) AF101 (6 μM) was found to significantly decrease GJIC in NT2/D1 cells, as quantified by measuring the mean number of calcein+/DiI- recipient cells

following a one hour incubation with calcein+/DiI+ donor cells. (D) Representative images depicting the effect of AF102 on connexin-mediated lucifer yellow (LY) uptake. (E) AF102 (6 μ M) and AF108 (6 μ M) caused a significantly reduction in anionic hemichannel activity, as quantified by measuring the percentage of LY+/RD- cells following a five minute incubation in calcium-free dye uptake solution. (F) Representative images depicting the effect of AF102 on connexin-mediated propidium iodide (PI) uptake. (G) AF102 (6 μ M) significantly reduced cationic hemichannel activity, as quantified by measuring the percentage of PI+/FITCD- cells following a five minute incubation in calcium-free dye uptake solution. All data shown represents measures taken from 20 fields per well in replicates of six wells per treatment taken from duplicate experiments. * denotes $P < 0.05$ ** denotes $P < 0.01$ from ethanol control, one-way ANOVA, *post-hoc* Fisher's LSD test. Scale bar = 100 μ m.

6A. Spectroscopic data for connexin project analogs

